Physics of Semiconductors and Nanostructures

ECE 4070 / MSE 6050

Spring, 2019

Debdeep Jena (djena@cornell.edu)

ECE & MSE, Cornell University

Course Poster

ECE 4070/MSE 6050, Physics of Semiconductors and Nanostructures: The Physics Enabling Big Data

Cornell University, Spring 2019

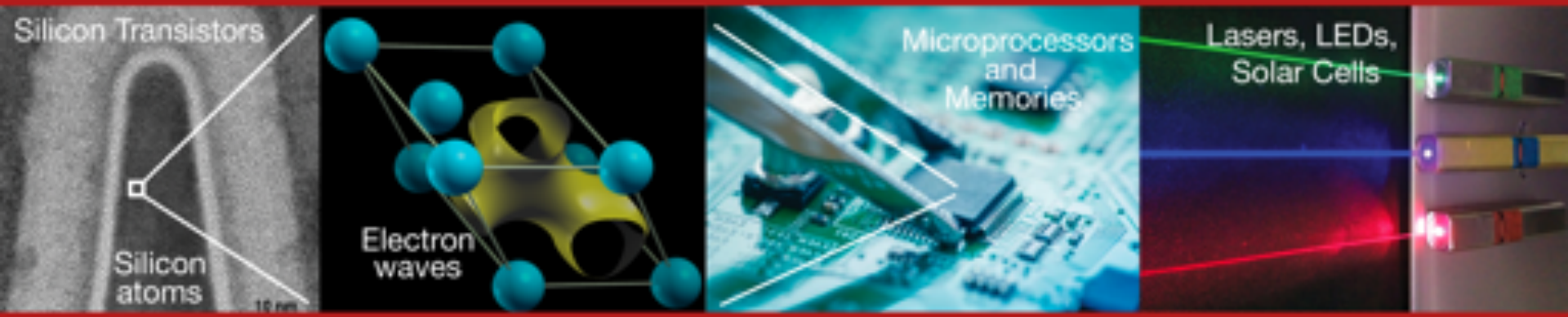

Atoms | Semiconductors | Logic | Memory | Communications

You probably cannnot stop hearing that we are living in the age of "Big Data".
But what exactly is this data? How and where is it created?
How and where is it stored? How is it manipulated to create meaning?
And how are massive chunks of data moved around at the speed of light?

This course is the **red pill** that will show you how deep the physics of "Big Data" goes. Answers to all these questions are tied to the physics of electrons in semiconductor materials.

COURSE CONTENTS:

Solid state physics for semiconductor nanostructures and electronic and photonic devices

+ Quantum mechanics of electrons in crystals
+ Metals, insulators, semiconductors (Silicon, graphene, 2D atomic materials, carbon nanotubes)
+ Lattice dynamics and phonons in 1D, 2D, and 3D materials
+ Electron statistics and quantum transport (Application: Ballistic Transistors, Logic and Memory)
+ Electron-photon interaction, optical interband and intraband processes (Application: LEDs)
+ Semiconductor heterostructures, electron states in 0, 1, and 2D nanostructures
+ Quantum wells, wires, and dots (Application: Semiconductor Lasers)

Lecturer: Debdeep Jena (djena@cornell.edu)
Classes: TR 11:40 am-12:55 pm, Phillips Hall 403

Website: https://djena.engineering.cornell.edu/2019_ece4070_mse6050.htm
Prerequisites: Basic notions of quantum mechanics and statistical physics

Science Fiction turns to Reality

TECHNOLOGY

Microsoft Plumbs Ocean's Depths to Test Underwater Data Center

By JOHN MARKOFF JAN. 31, 2016

Ben Cutler, left, and Norman Whitaker, both of Microsoft Research, with the "Leona Philpot," a prototype underwater data center, at the company's headquarters in Redmond, Wash. Matt Lutton for The New York Times

Scaling of Transistor Sizes: How much longer?

Transistors Will Stop Shrinking in 2021, Moore's Law Roadmap Predicts

By Rachel Courtland

Posted 22 Jul 2016 | 16:00 GMT

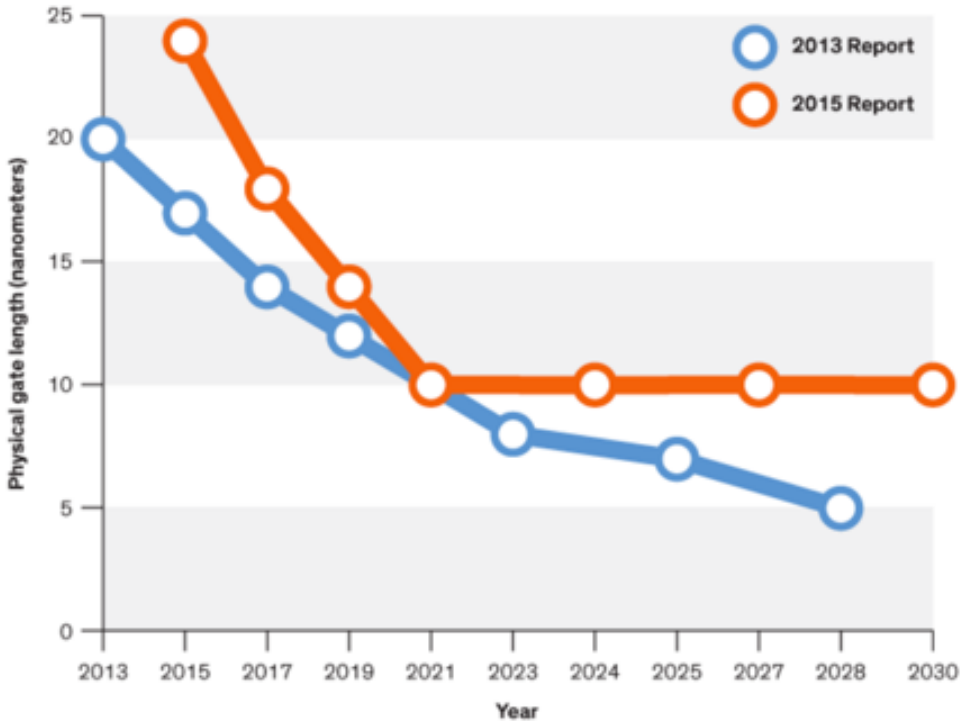

Illustration: Erik Vrielink

The trajectory of transistor feature sizes (the physical gate length of transistors in high-performance logic is shown here) could take a sharp turn in 2021.

~2000 (pre – iPhone era)

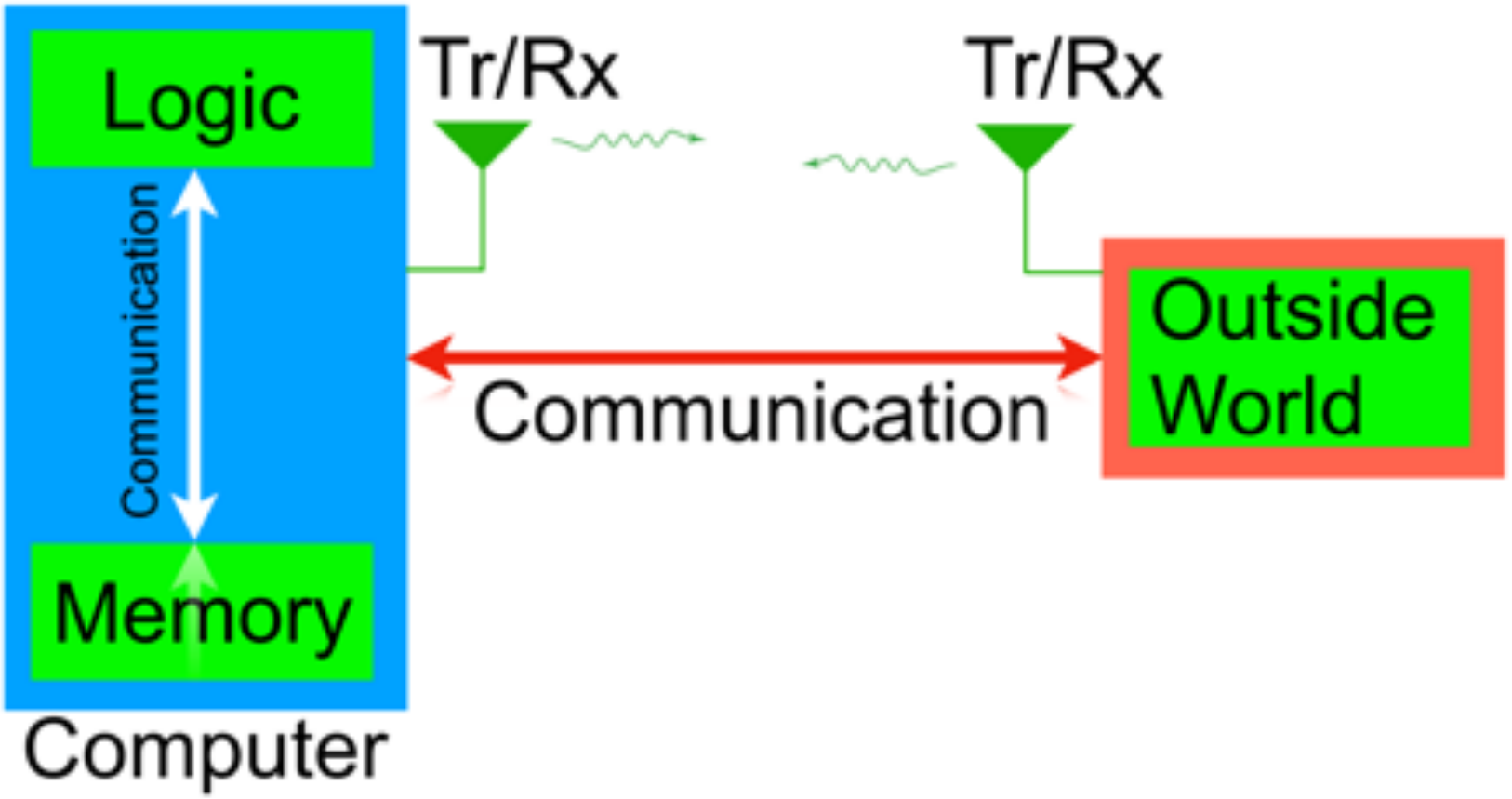

- *3 Pillars of Information systems are: "Computation, Memory, and Communication"*

~Today

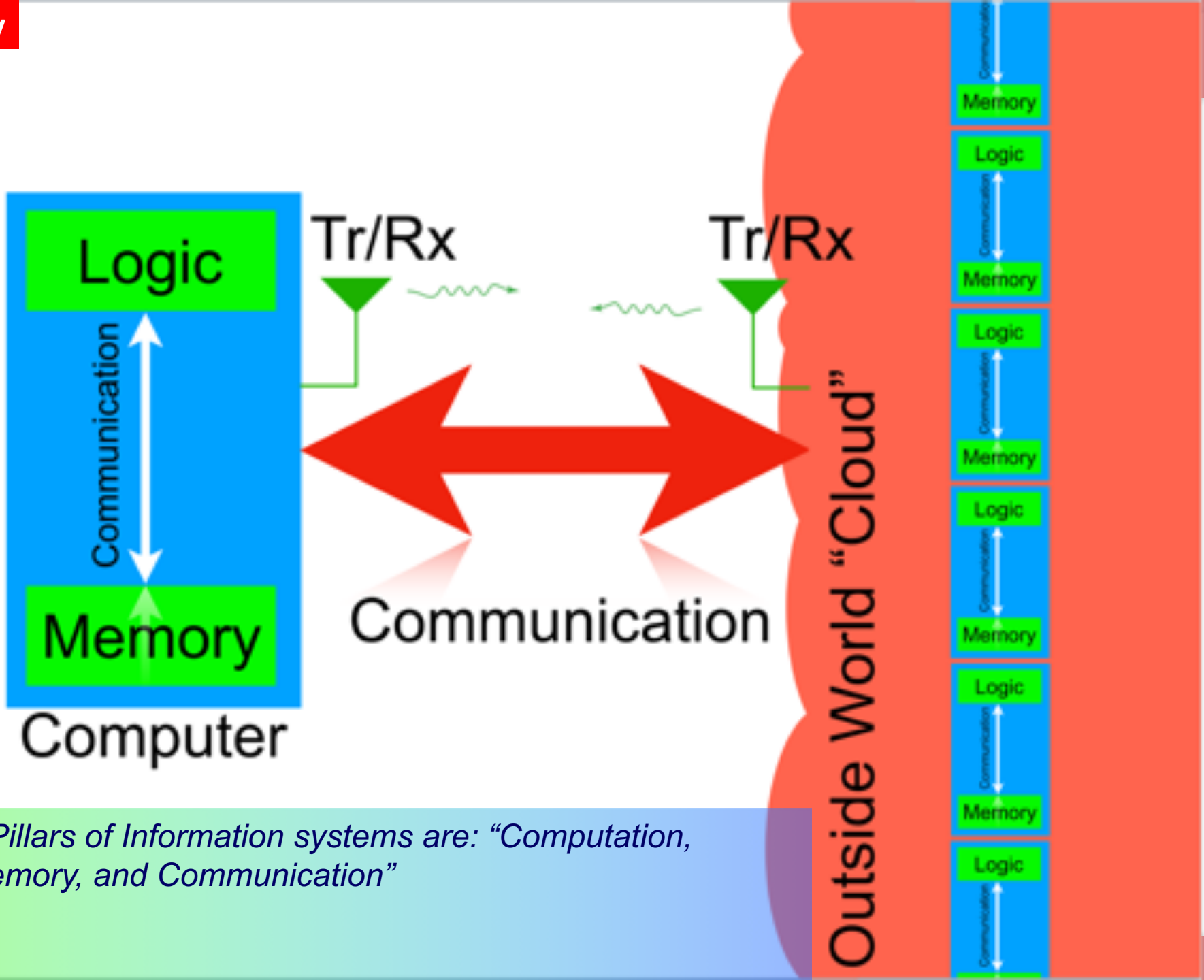

- *3 Pillars of Information systems are: "Computation, Memory, and Communication"*

Course Outline: 4 Modules

- Module I: Fundamentals
  - Chapters 1 - 7
- Module 2: Semiconductor Bands, Doping, and Heterostructures
  - Chapters 8-14
- Module 3: Quantum Electrostatics and Transport in Semiconductors & Devices
  - Chapters 15-24
- Module 4: Photonics with Semiconductors
  - Chapters 25-30

Course Outline: 4 Modules

- Module I: Fundamentals
  - Chapters 1 - 7
- Module 2: Semiconductor Bands, Doping, and Heterostructures
  - Chapters 8-14
- Module 3: Quantum Electrostatics and Transport in Semiconductors & Devices
  - Chapters 15-24
- Module 4: Photonics with Semiconductors
  - Chapters 25-30

The Electron

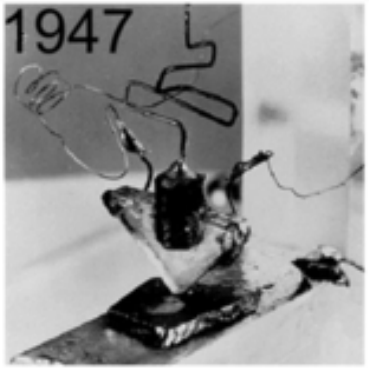

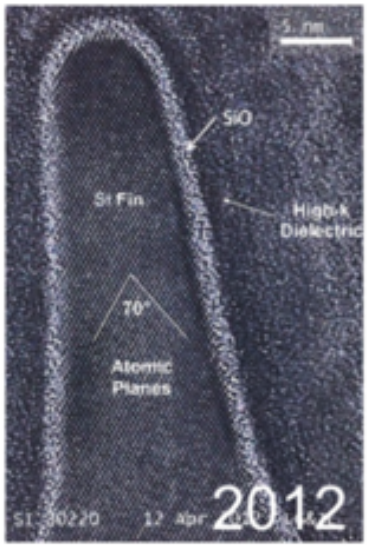

?

The Electron

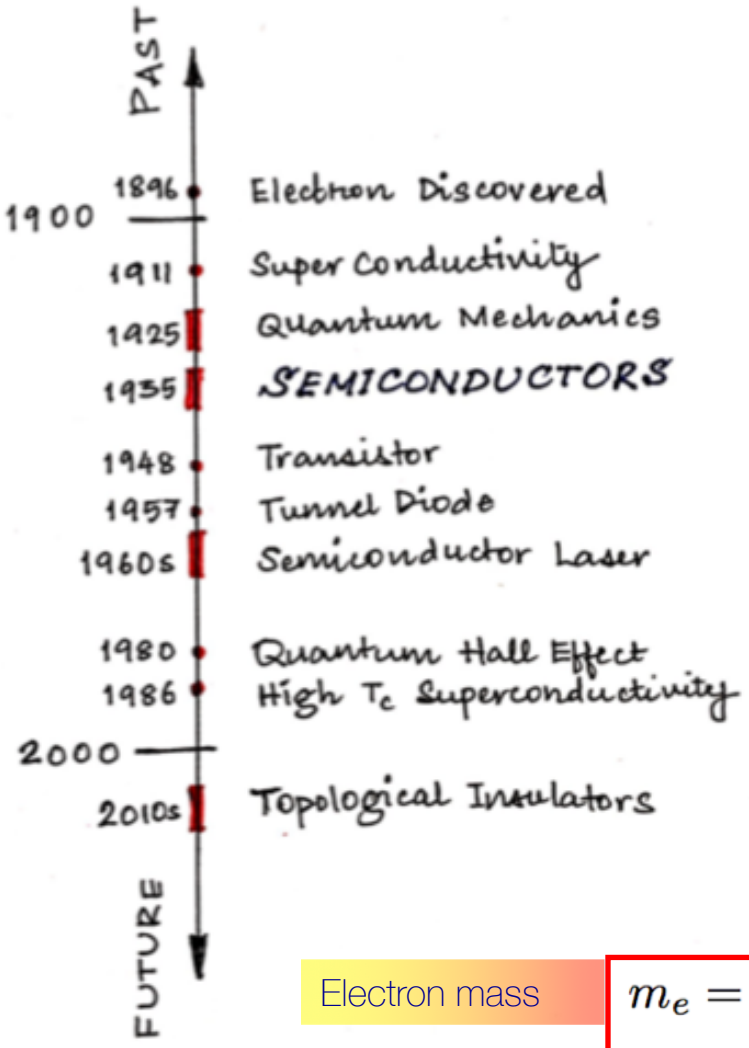

Fig. 1.2 J. J. Thomson discovered the electron in 1896 @ the Cavendish Laboratory. He was awarded the 1906 Nobel prize in Physics. Seven of his students went on to win Nobel prizes.

Electron mass	$m_e = 9.1 \times 10^{-31}$ kg
Electron charge	$q = 1.6 \times 10^{-19}$ Coulomb

Classical Physics

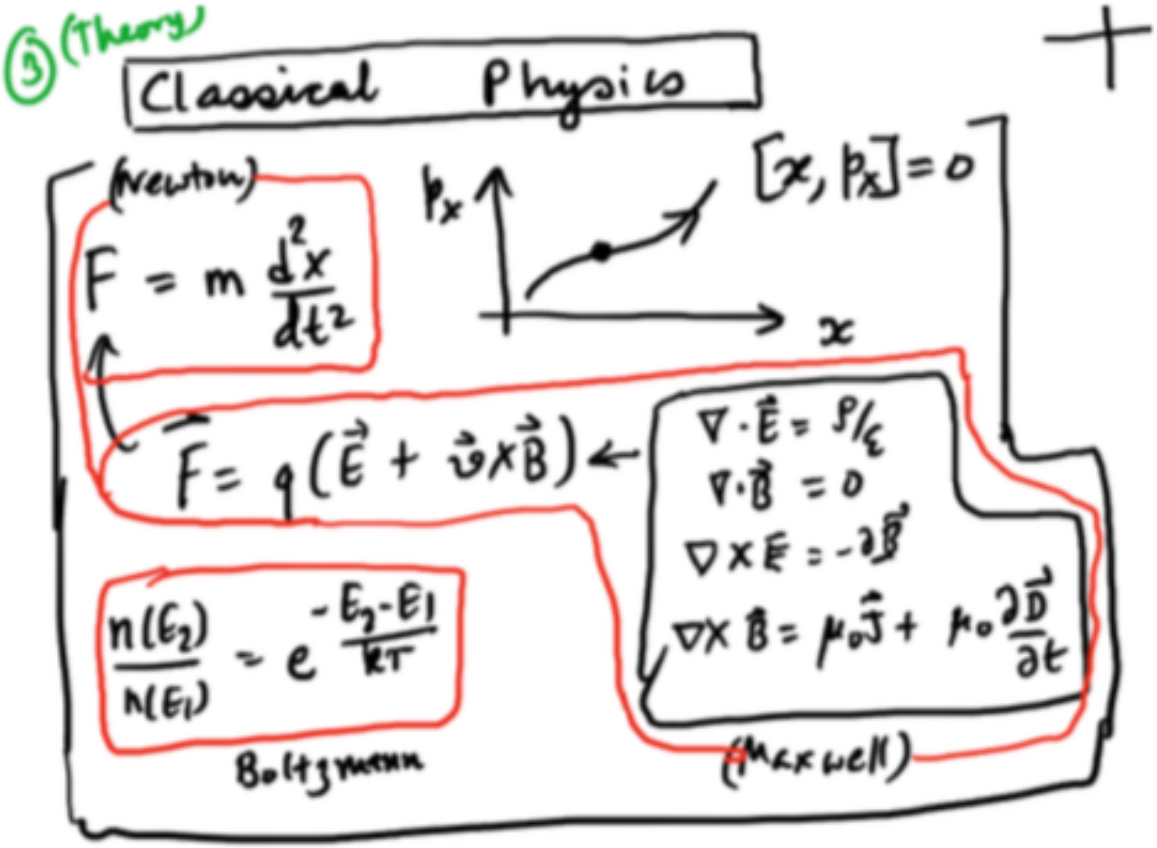

Electrons in the Classical World

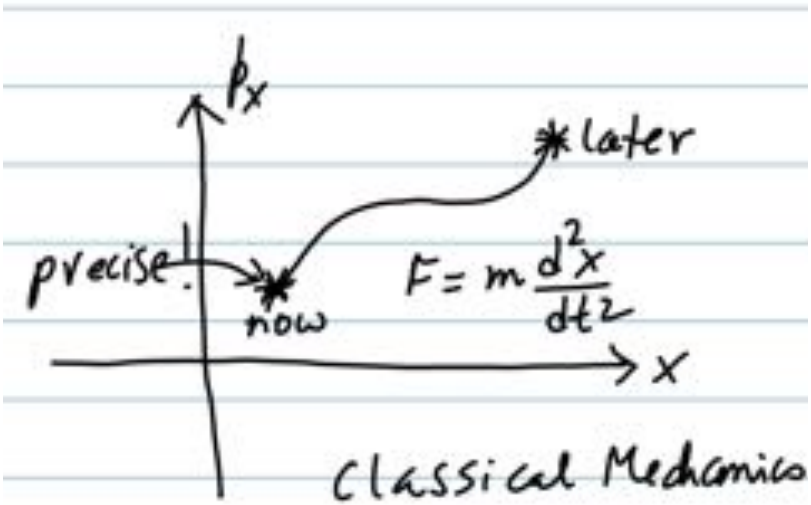

Newton

$$\mathbf{F} = -\nabla V(r) = \frac{d\mathbf{p}}{dt}$$

Path is deterministic

Electron paths in vacuum tubes subject to E and B fields

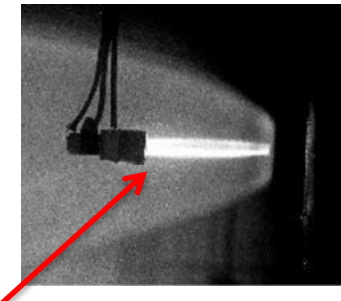

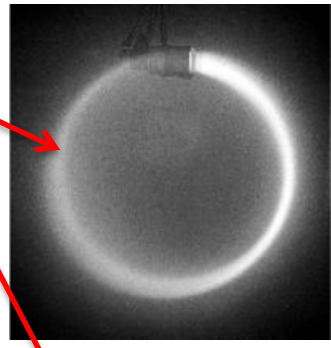

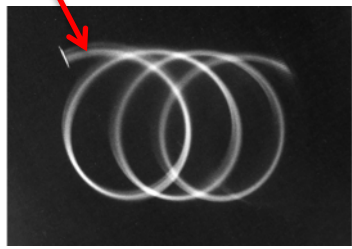

Lorentz

$$\mathbf{F} = q(\mathbf{E} + \mathbf{v} \times \mathbf{B})$$

Path is deterministic

Properties of Metals

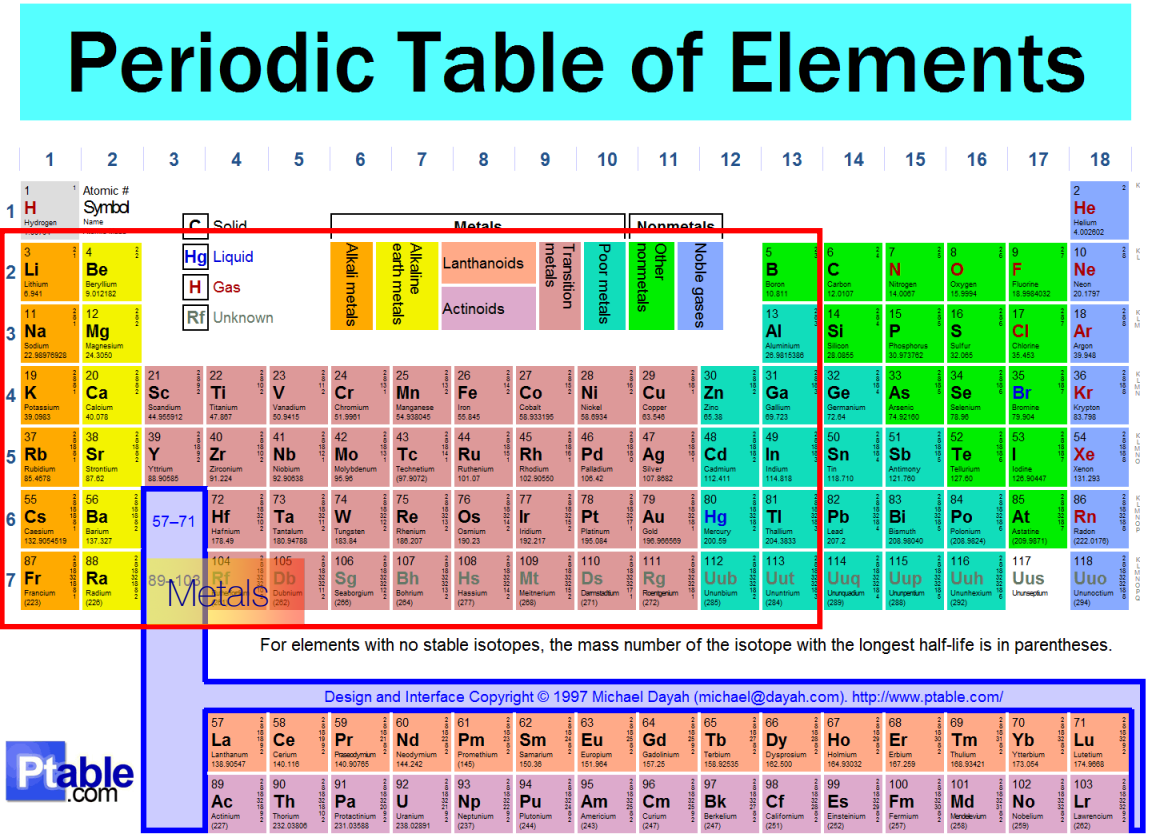

Metals are:

- good conductors of electricity,
- good conductors of heat, and
- reflective and shiny.

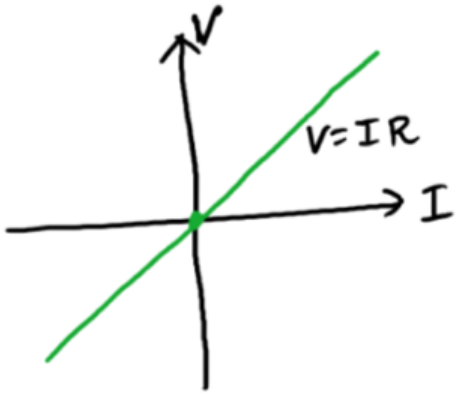

Fig. 2.3 Ohm's law is $V = IR$, or equivalently $J = \sigma E$.

Properties of Metals

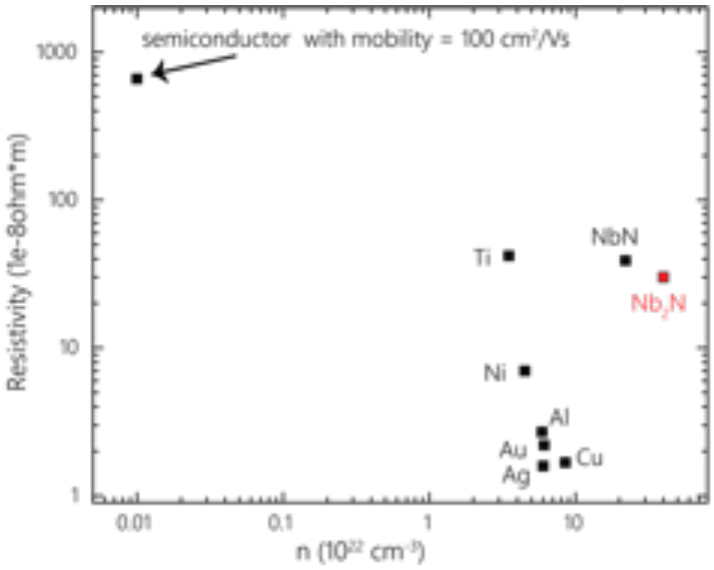

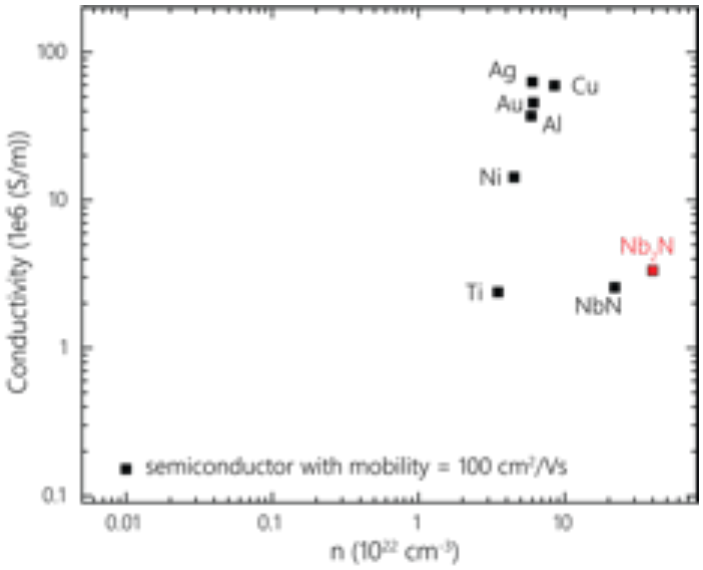

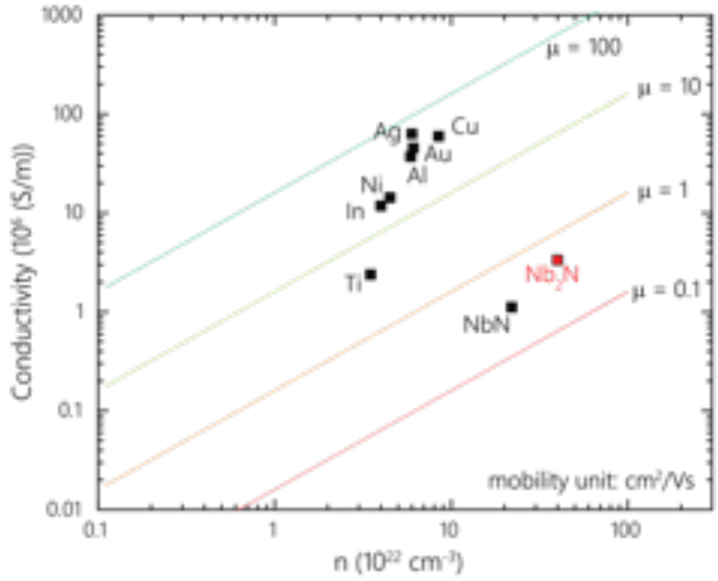

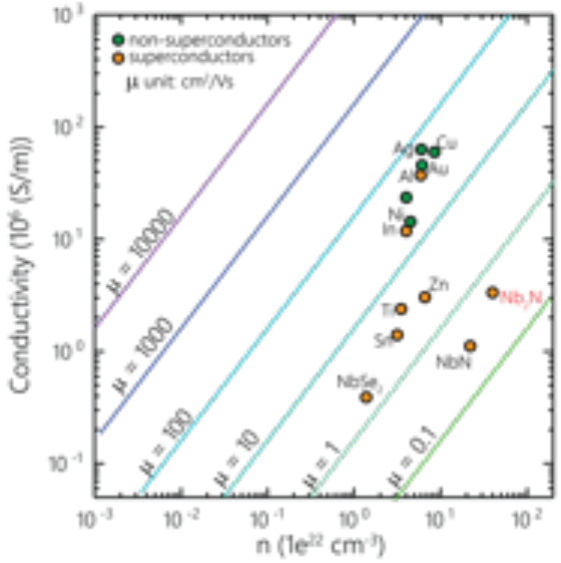

Data compiled by Rusen Yan

Properties of Metals

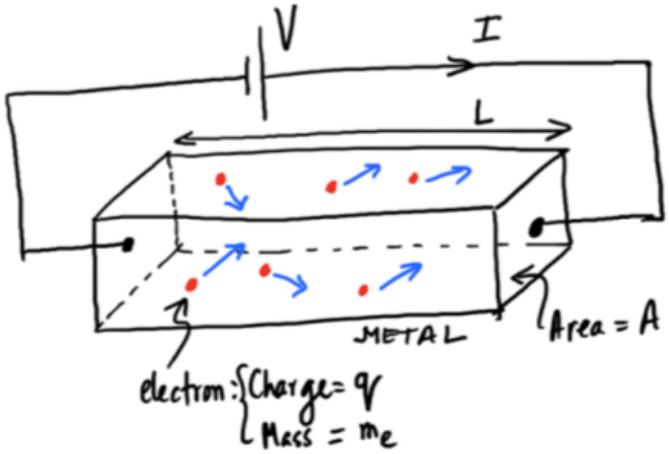

Fig. 2.4 Electron gas moving in response to an electric field in a metal.

Metals are:

- good conductors of electricity,
- good conductors of heat, and
- reflective and shiny.

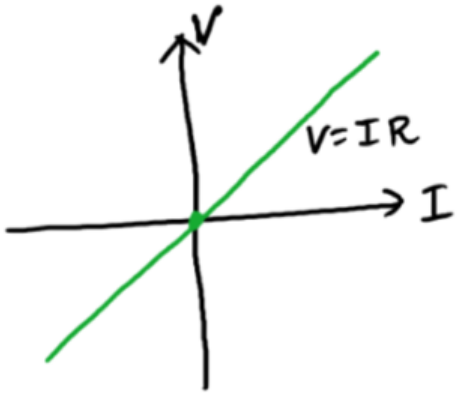

Fig. 2.3 Ohm's law is $V = IR$, or equivalently $J = \sigma E$.

$$J = qnv = \frac{nq^2\tau}{m_e}E = \sigma E \implies \boxed{\sigma = \frac{nq^2\tau}{m_e}}$$

Conductivity

$$\boxed{\mu = \frac{q\tau}{m_e}}$$

Mobility

Properties of Metals

Table 1.1
FREE ELECTRON DENSITIES OF SELECTED METALLIC ELEMENTS[a]

ELEMENT	Z	n (10^{22}/cm^3)	r_s(Å)	r_s/a_0
Li (78 K)	1	4.70	1.72	3.25
Na (5 K)	1	2.65	2.08	3.93
K (5 K)	1	1.40	2.57	4.86
Rb (5 K)	1	1.15	2.75	5.20
Cs (5 K)	1	0.91	2.98	5.62
Cu	1	8.47	1.41	2.67
Ag	1	5.86	1.60	3.02
Au	1	5.90	1.59	3.01
Be	2	24.7	0.99	1.87
Mg	2	8.61	1.41	2.66
Ca	2	4.61	1.73	3.27
Sr	2	3.55	1.89	3.57
Ba	2	3.15	1.96	3.71
Nb	1	5.56	1.63	3.07
Fe	2	17.0	1.12	2.12
Mn (α)	2	16.5	1.13	2.14
Zn	2	13.2	1.22	2.30
Cd	2	9.27	1.37	2.59
Hg (78 K)	2	8.65	1.40	2.65
Al	3	18.1	1.10	2.07
Ga	3	15.4	1.16	2.19
In	3	11.5	1.27	2.41
Tl	3	10.5	1.31	2.48
Sn	4	14.8	1.17	2.22
Pb	4	13.2	1.22	2.30
Bi	5	14.1	1.19	2.25
Sb	5	16.5	1.13	2.14

[a] At room temperature (about 300 K) and atmospheric pressure, unless otherwise noted. The radius r_s of the free electron sphere is defined in Eq. (1.2). We have arbitrarily selected one value of Z for those elements that display more than one chemical valence. The Drude model gives no theoretical basis for the choice. Values of n are based on data from R. W. G. Wyckoff, *Crystal Structures*, 2nd ed., Interscience, New York, 1963.

$$\sigma = \frac{n q^2 \tau}{m_e}$$

Table 1.3
DRUDE RELAXATION TIMES IN UNITS OF 10^{-14} SECOND[a]

ELEMENT	77 K	273 K	373 K
Li	7.3	0.88	0.61
Na	17	3.2	
K	18	4.1	
Rb	14	2.8	
Cs	8.6	2.1	
Cu	21	2.7	1.9
Ag	20	4.0	2.8
Au	12	3.0	2.1
Be		0.51	0.27
Mg	6.7	1.1	0.74
Ca		2.2	1.5
Sr	1.4	0.44	
Ba	0.66	0.19	
Nb	2.1	0.42	0.33
Fe	3.2	0.24	0.14
Zn	2.4	0.49	0.34
Cd	2.4	0.56	
Hg	0.71		
Al	6.5	0.80	0.55
Ga	0.84	0.17	
In	1.7	0.38	0.25
Tl	0.91	0.22	0.15
Sn	1.1	0.23	0.15
Pb	0.57	0.14	0.099
Bi	0.072	0.023	0.016
Sb	0.27	0.055	0.036

[a] Relaxation times are calculated from the data in Tables 1.1 and 1.2, and Eq. (1.8). The slight temperature dependence of n is ignored.

From: Solid State Physics, Ashcroft and Mermin

Properties of Metals

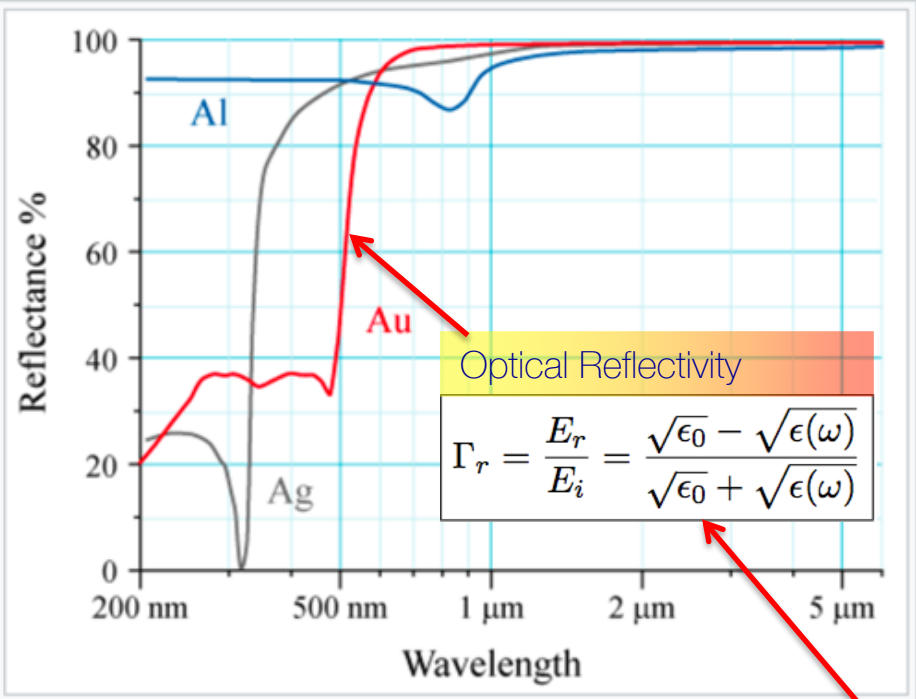

Spectral reflectance curves for aluminium (Al), silver (Ag), and gold (Au) metal mirrors at normal incidence. From Wikipedia

Optical Reflectivity

$$\Gamma_r = \frac{E_r}{E_i} = \frac{\sqrt{\epsilon_0} - \sqrt{\epsilon(\omega)}}{\sqrt{\epsilon_0} + \sqrt{\epsilon(\omega)}}$$

Metals are:

- good conductors of electricity,
- good conductors of heat, and
- reflective and shiny.

$$qE_0 e^{i\omega t} = m_e \frac{dv}{dt} - \frac{m_e v}{\tau}$$

Oscillating electric field

"Optical" Conductivity

$$\sigma(\omega) = \frac{\sigma_0}{1 - i\omega\tau}$$

Dielectric value depends on the frequency

$$\epsilon(\omega) = \epsilon_0[1 + i\frac{\sigma(\omega)}{\omega\epsilon_0}]$$

The classical Drude model

Paul Drude (1900)

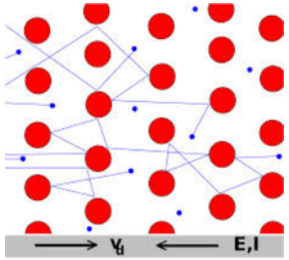

Electrons move and scatter every tau seconds

dc field:

$$m\frac{dv}{dt} = qE - \frac{mv}{\tau} \qquad \text{steady state: } \frac{d}{dt}(...) \to 0 \qquad v = \frac{q\tau}{m}E = \mu E$$

$$J = qnv = \frac{nq^2\tau}{m}E = \sigma E \implies \boxed{\sigma_0 = \frac{nq^2\tau}{m}}$$

dc conductivity

Oscillating field:

$$E(t) = Ee^{i\omega t} \qquad m\frac{dv}{dt} = qEe^{i\omega t} - \frac{mv}{\tau} \qquad v(t) = v(0)e^{i\omega t}$$

$$\sigma(\omega) = \frac{\sigma_0}{1+i\omega\tau} = \underbrace{\frac{\sigma_0}{1+(\omega\tau)^2}}_{\mathrm{Re}(\sigma(\omega))} - i\underbrace{\frac{\omega\tau\sigma_0}{1+(\omega\tau)^2}}_{\mathrm{Im}(\sigma(\omega))}$$

ac conductivity

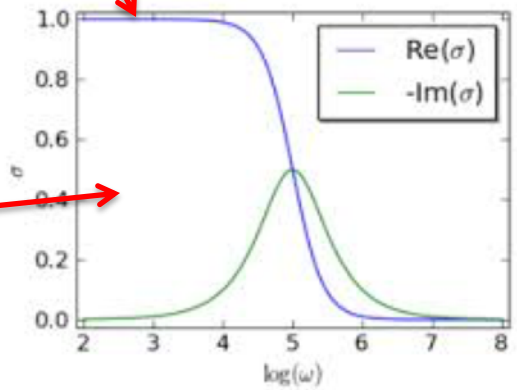

Properties of Metals

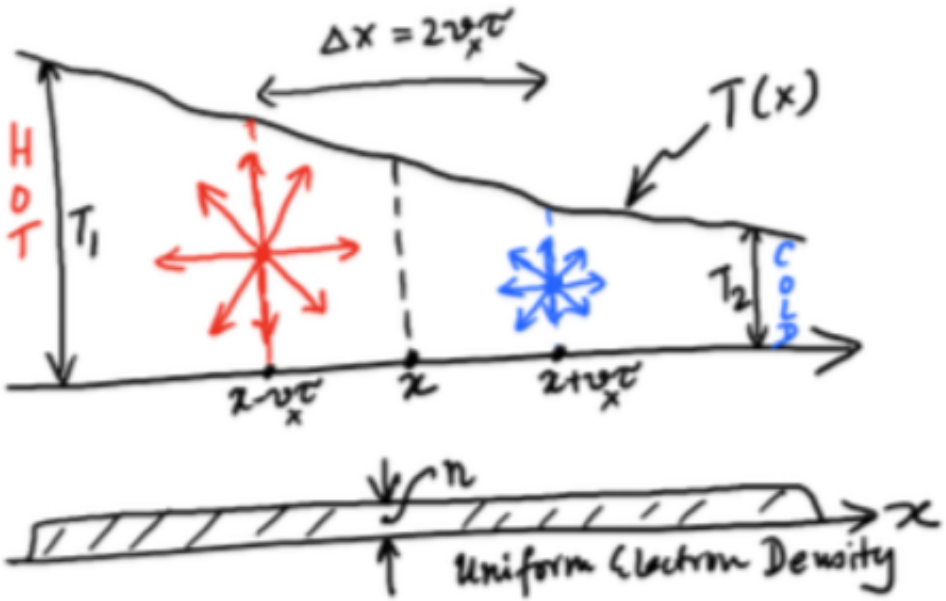

Metals are:

- good conductors of electricity,
- good conductors of heat, and
- reflective and shiny.

$$J_{heat} = \frac{1}{3} c_v v^2 \tau (-\nabla T)$$

Thermal Conductivity

The Weidemann-Franz Law for metals

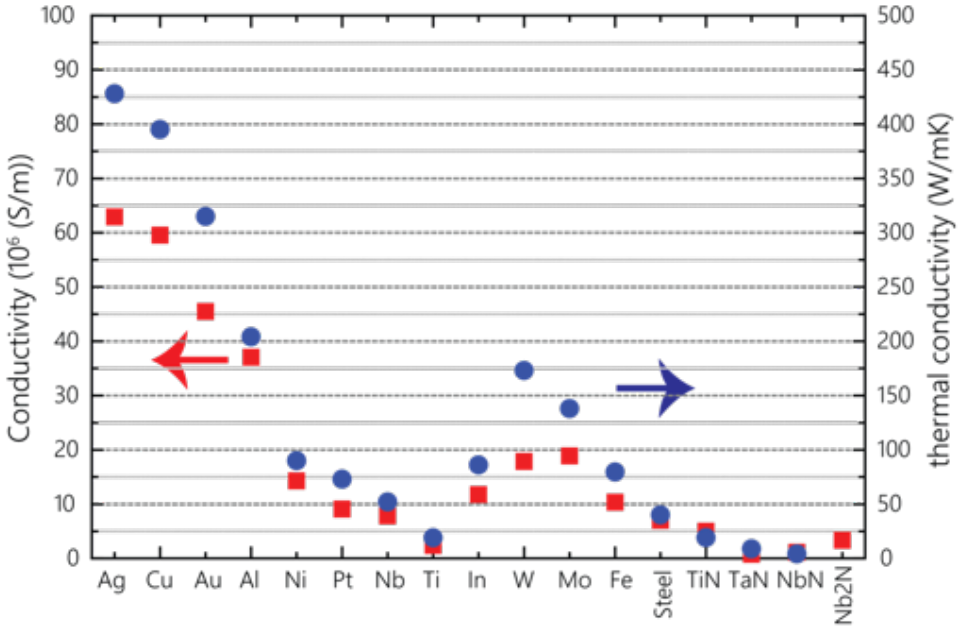

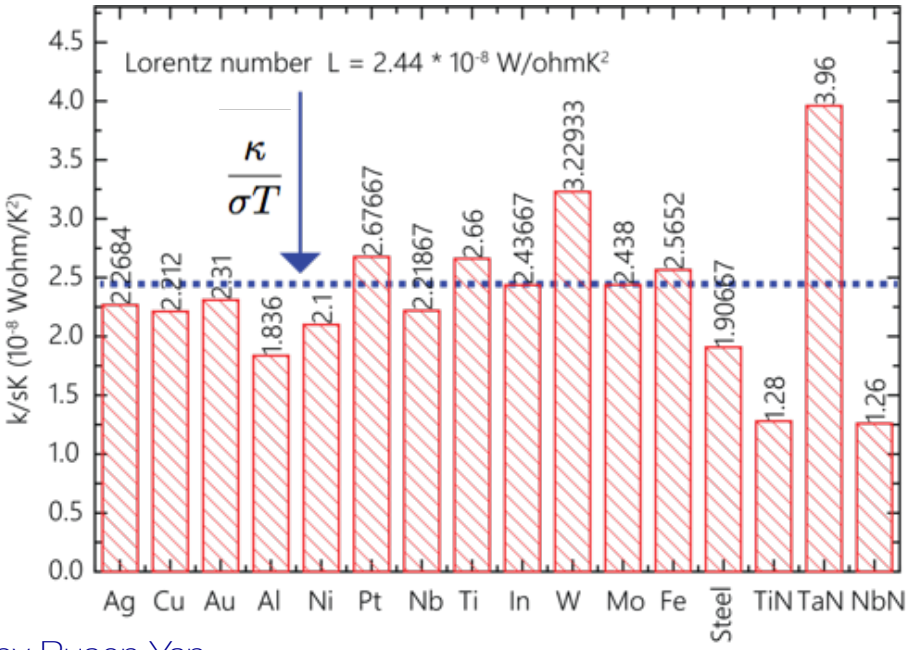

Data compiled by Rusen Yan

$$\frac{\kappa}{\sigma T} = \frac{(\frac{1}{3} c_v v^2 \tau)}{(\frac{nq^2\tau}{m_e})T} = \frac{(\frac{1}{3}\frac{3}{2} n k_B \frac{3k_B T}{m_e} \tau)}{(\frac{nq^2\tau}{m_e})T} = \frac{3}{2}(\frac{k_B}{q})^2 \implies \boxed{\frac{\kappa}{\sigma T} = \frac{3}{2}(\frac{k_B}{q})^2 = \mathcal{L}}$$

Ratio of Boltzmann Constant and Electron Charge, which are fundamental constants and do not depend on the metal.

Electronic specific heat is much smaller than nk_B

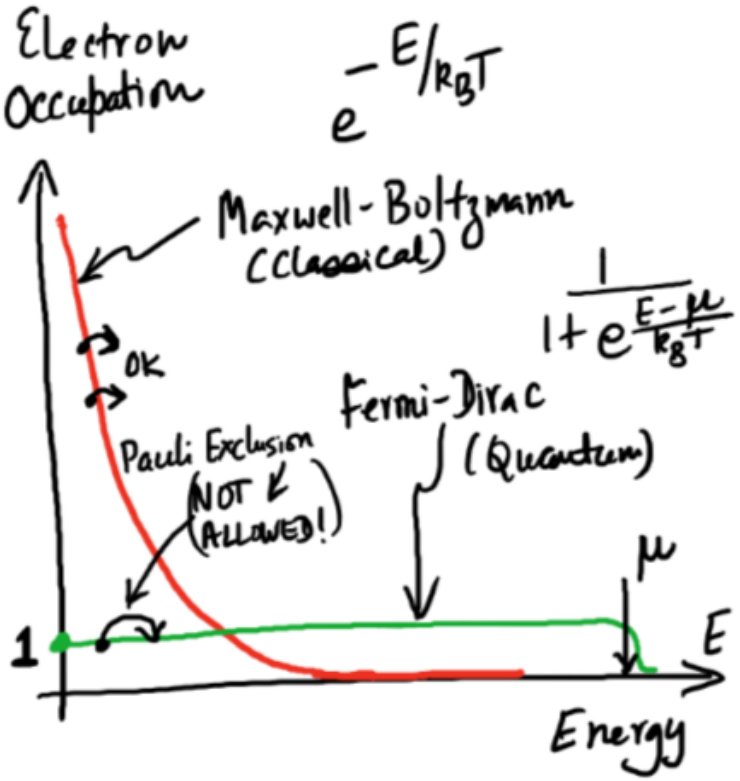

- Classical Mechanics and Thermodynamics is not adequate to explain electron statistics.
- Electrons must follow the Pauli Exclusion principle, and are subject to the laws of quantum mechanics.

Planck's Blackbody Radiation: Birth of 'Quantum'

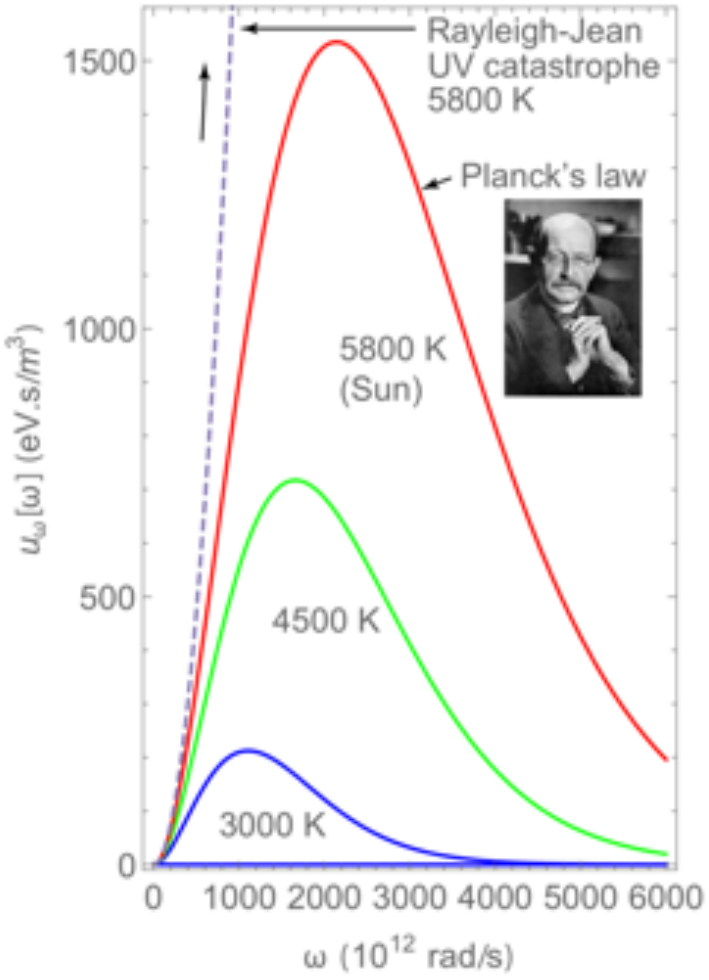

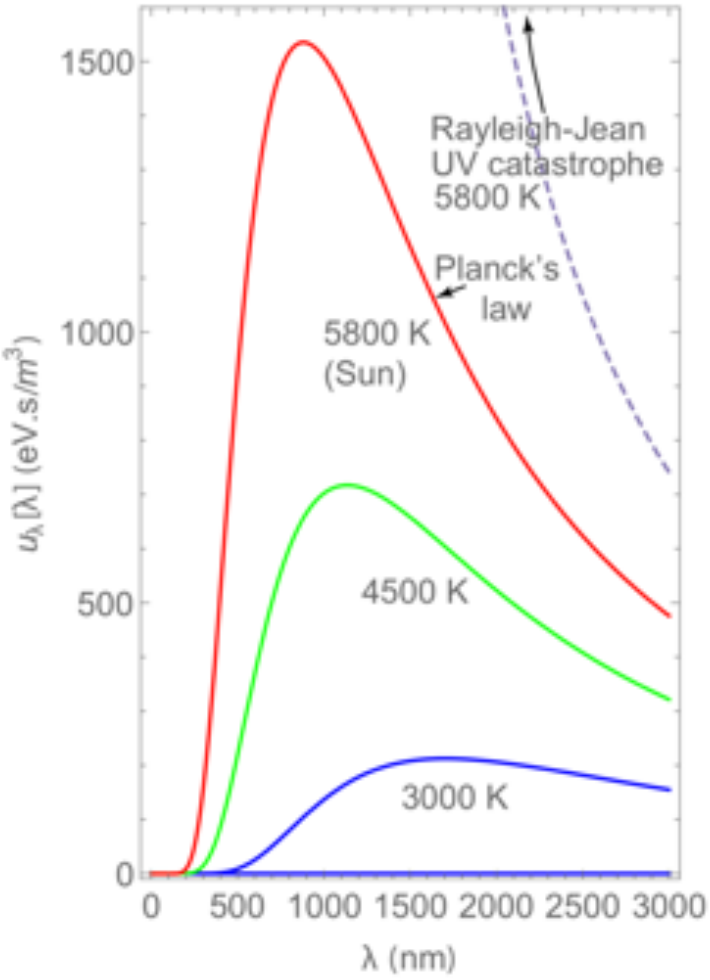

Classical physics unable to explain light spectrum

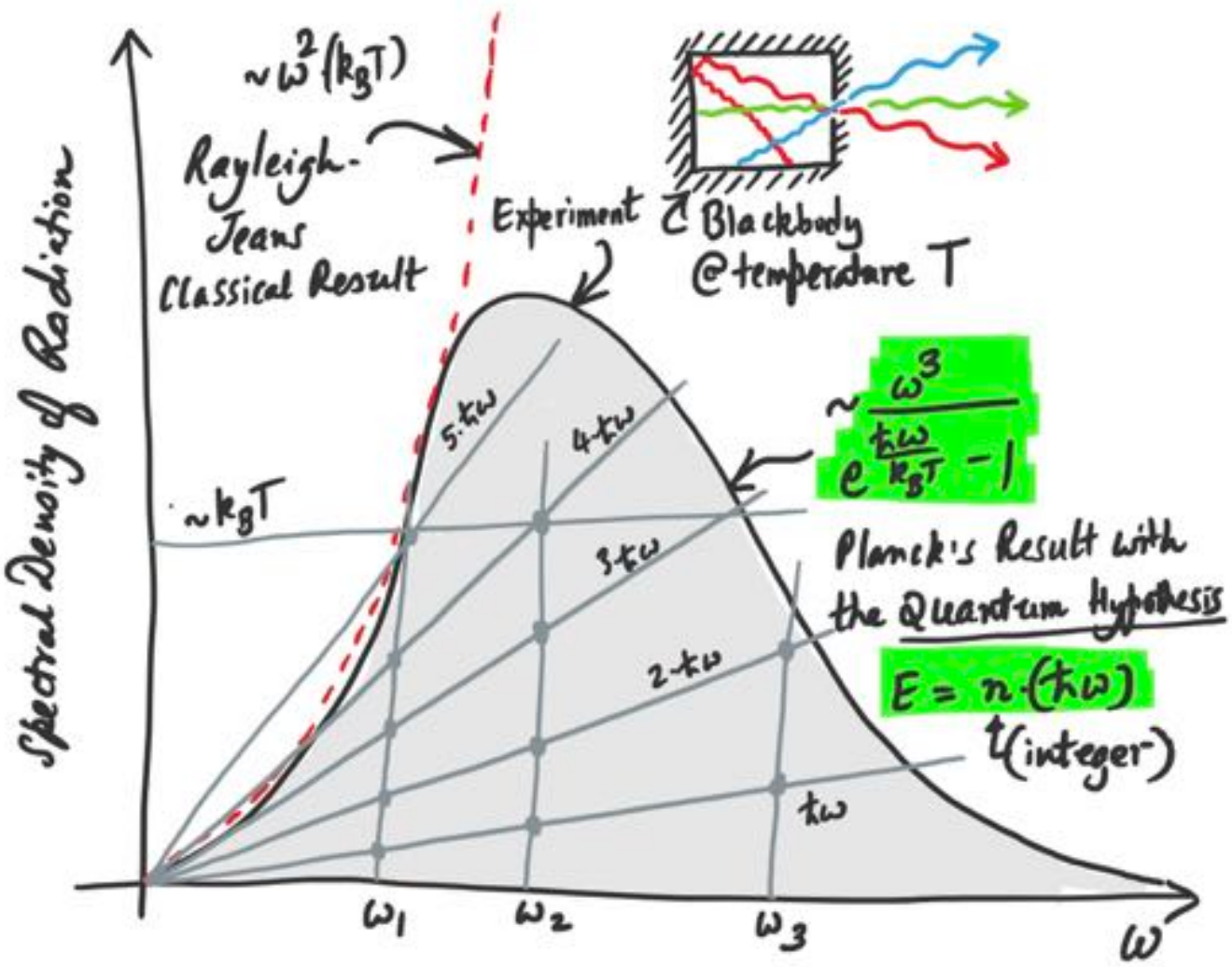

Einstein explains the Photoelectric effect

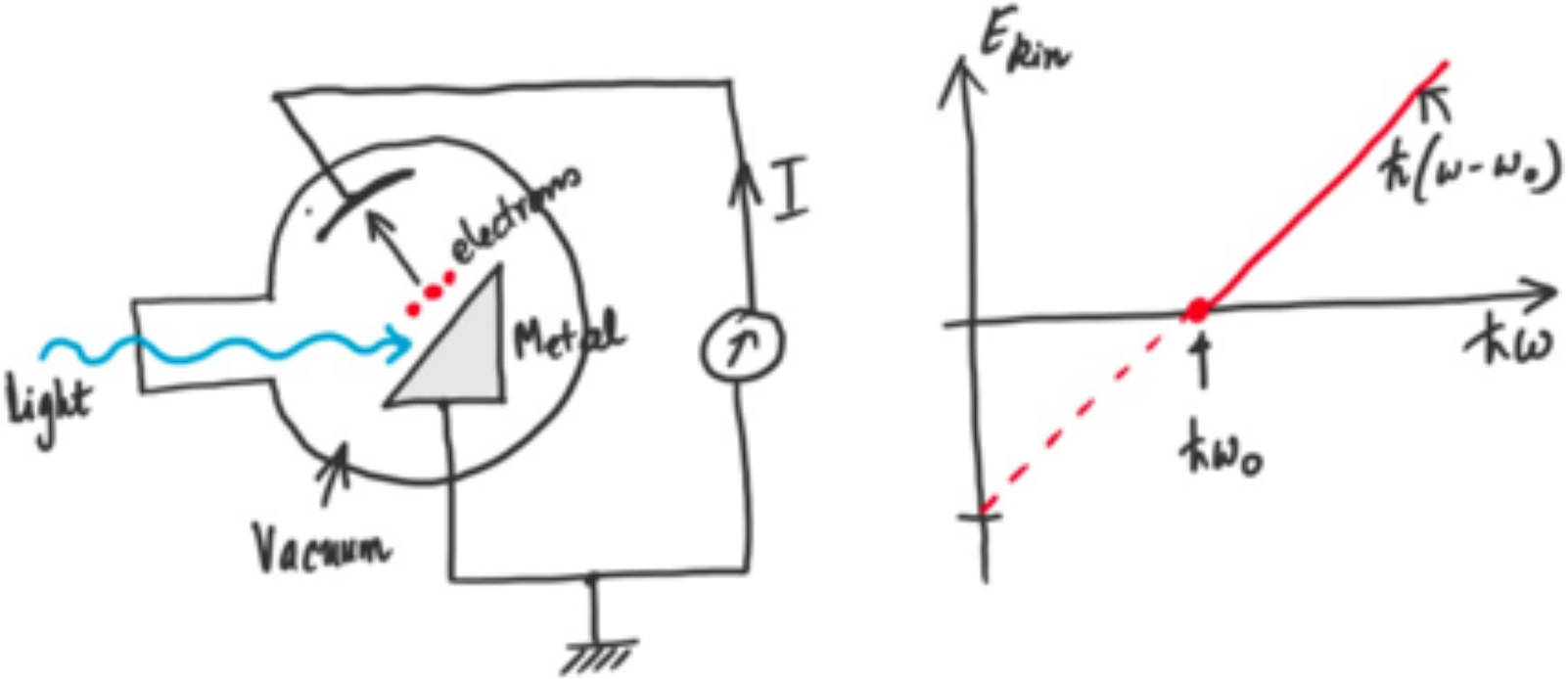

Fig. 3.35 The photoelectric effect.

Experiment: Light is a wave… or a particle?

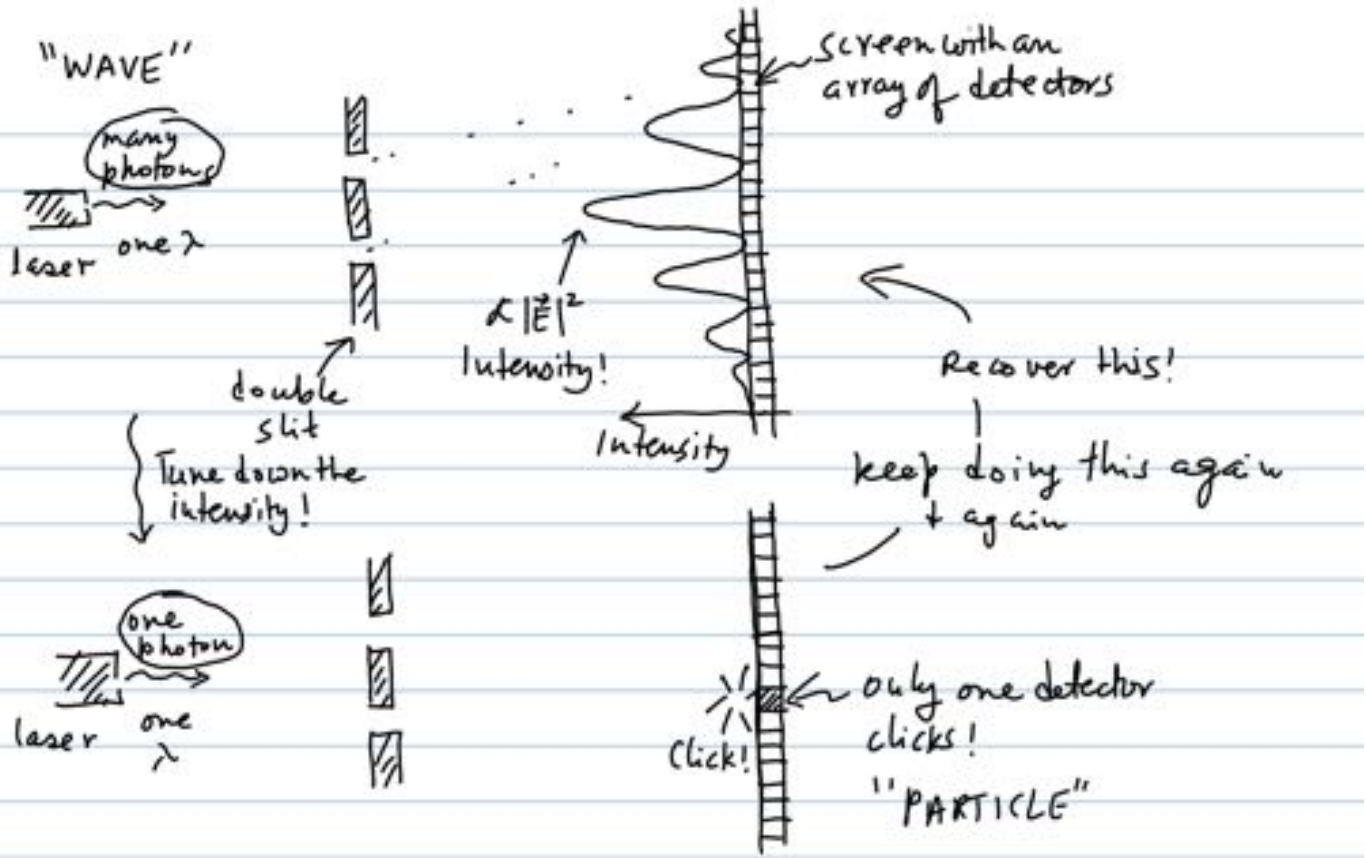

Experiment: Light is a wave… or a particle?

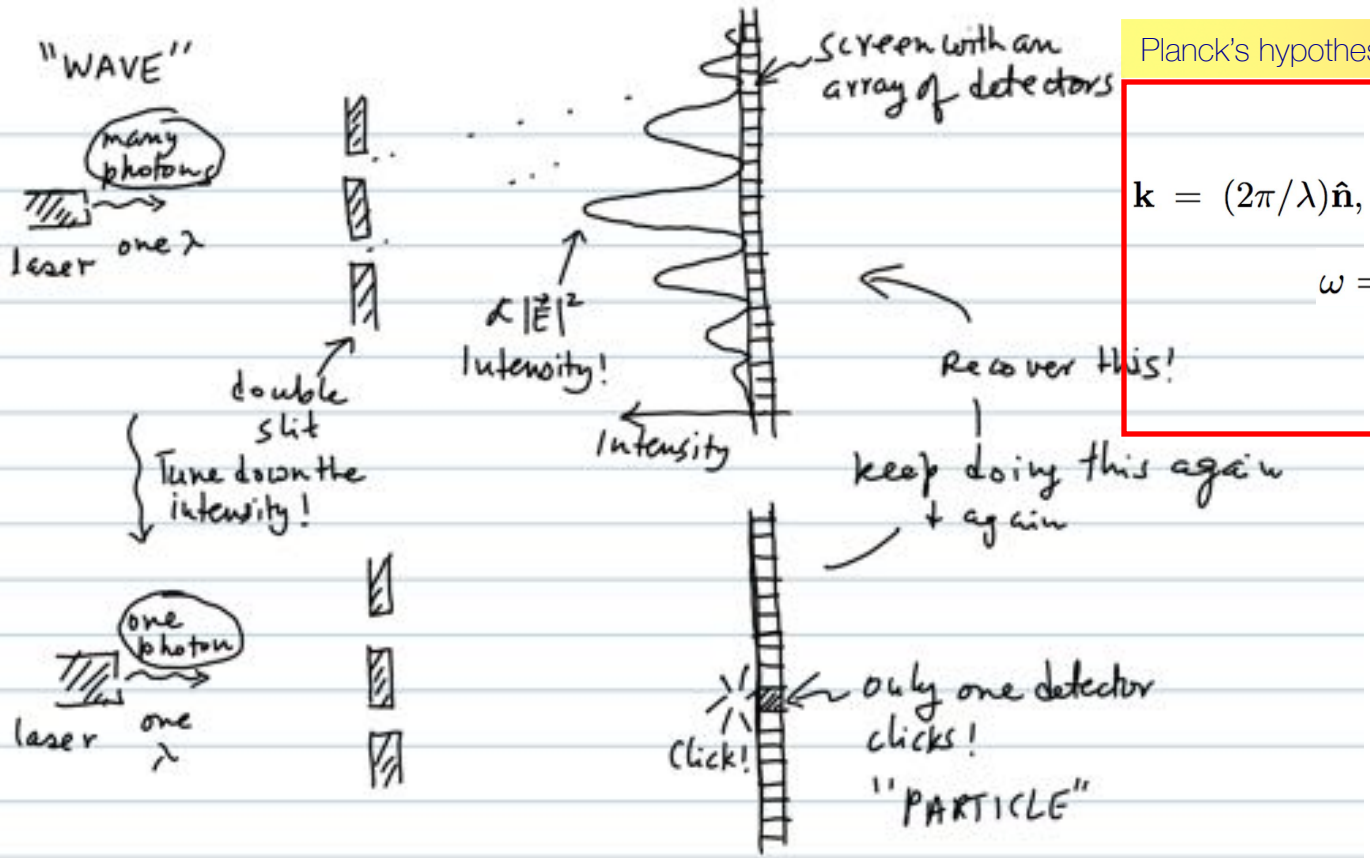

Planck's hypothesis for photons to explain expts:

$$\mathbf{p} = \hbar\mathbf{k}$$

$\mathbf{k} = (2\pi/\lambda)\hat{\mathbf{n}}$, $\hat{\mathbf{n}}$ the direction of propagation

$\omega = c|\mathbf{k}|$ with c the speed of light

$$E = \hbar\omega$$

Einstein: look downstairs!

$$p = mv/\sqrt{1-(v/c)^2}$$

- The only way an object of mass m=0 can have momentum is if its speed v=c, or the speed of light.
- A photon is exactly such an object. No mass, all energy, and a finite momentum!

Bohr's Quantum Theory for Electrons

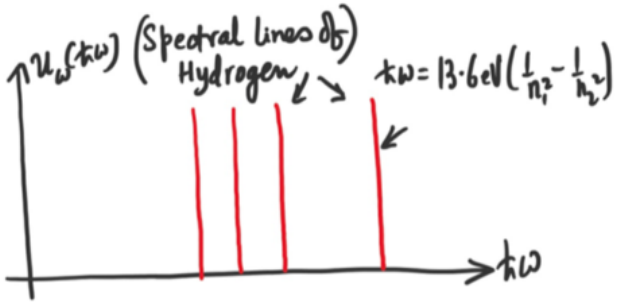

$$E = \frac{p^2}{2m_e} - \frac{q^2}{4\pi\epsilon_0 R}$$

$$\oint p dx = nh \qquad p_n 2\pi R_n = nh \implies p_n R_n = n\hbar.$$

$$\frac{m_e v_n^2}{R_n} = \frac{q^2}{4\pi\epsilon_0 R_n^2} \implies p_n = \frac{q^2 m_e}{4\pi\epsilon_0 \hbar}\cdot\frac{1}{n} = \frac{\hbar}{a_B}\cdot\frac{1}{n}$$

$$R_n = n^2\Big(\underbrace{\frac{4\pi\epsilon_0\hbar^2}{q^2 m_e}}_{a_B}\Big) = n^2 a_B$$

$$E_n = \frac{p_n^2}{2m_e} - \frac{q^2}{4\pi\epsilon_0 R_n} = \frac{1}{2}\frac{\hbar^2}{m_e a_B^2}\frac{1}{n^2} - \frac{\hbar^2}{m_e a_B^2}\frac{1}{n^2} = -\frac{\hbar^2}{2m_e a_B^2}\frac{1}{n^2}$$

$$E_{n_2} - E_{n_1} = \underbrace{\frac{m_e q^4}{2(4\pi\epsilon_0)^2\hbar^2}}_{\text{Ry}=13.6\text{eV}}\left(\frac{1}{n_1^2} - \frac{1}{n_2^2}\right)$$

Particle… or wave?

de Broglie'e hypothesis:
$\lambda = \frac{h}{|\mathbf{p}|}$ holds for objects
with mass too, not just photons.

When electrons are waves:
$qV = E = \frac{p^2}{2m_0}$, but $\lambda = \frac{h}{p}$, which

$$\implies \boxed{\lambda = \frac{h}{\sqrt{2mE}} = \frac{h}{\sqrt{2mqV}}}.$$

You can change the wavelength
of electrons with voltage.

Particle… or wave?

de Broglie'e hypothesis:
$\lambda = \frac{h}{|\mathbf{p}|}$ holds for objects
with mass too, not just photons.

When electrons are waves:
$qV = E = \frac{p^2}{2m_0}$, but $\lambda = \frac{h}{p}$, which

$$\implies \boxed{\lambda = \frac{h}{\sqrt{2mE}} = \frac{h}{\sqrt{2mqV}}}.$$

You can change the wavelength
of electrons with voltage.

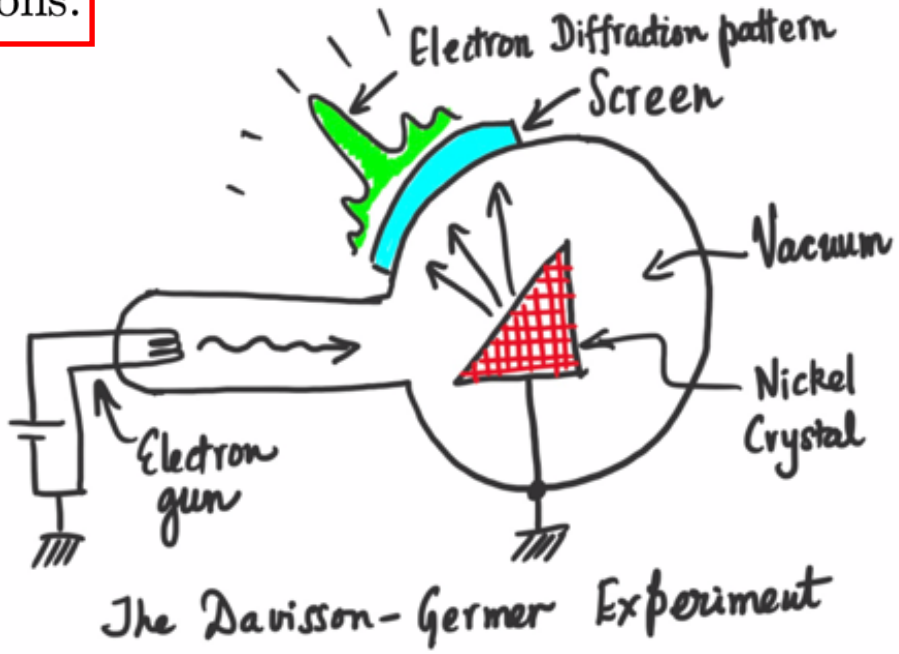

Particle… or wave?

de Broglie'e hypothesis:
$\lambda = \frac{h}{|\mathbf{p}|}$ holds for objects
with mass too, not just photons.

The Diffraction of Electrons by a Crystal of Nickel

By C. J. DAVISSON

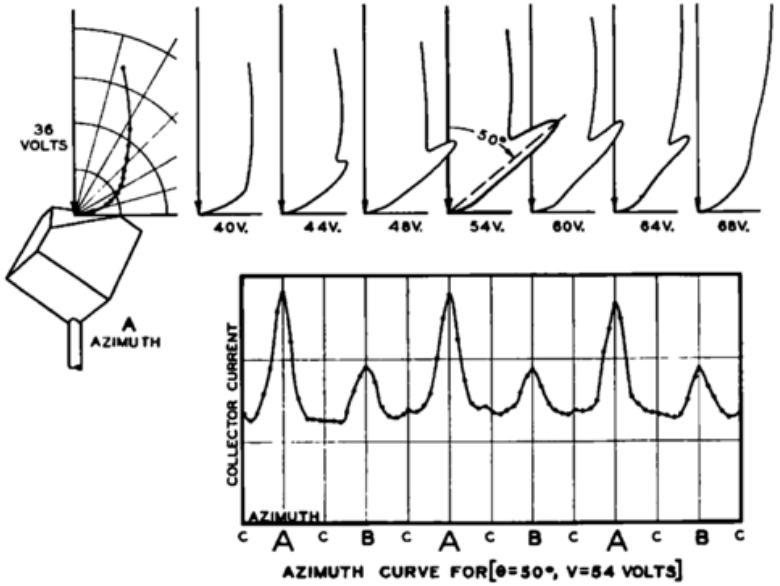

Fig. 3—Curves showing development of diffraction beam in the A-azimuth . . . and variation of intensity with the azimuth at colat. 50° for which beam is strongest in the A-azimuth

When electrons are waves:
$qV = E = \frac{p^2}{2m_0}$, but $\lambda = \frac{h}{p}$, which

$$\implies \boxed{\lambda = \frac{h}{\sqrt{2mE}} = \frac{h}{\sqrt{2mqV}}}.$$

You can change the wavelength of electrons with voltage.

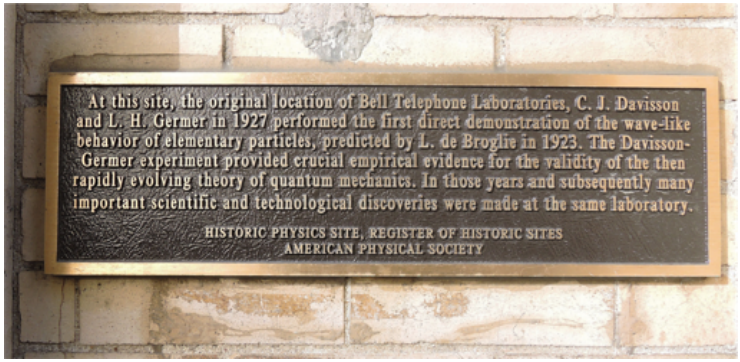

An electron is a particle… or a wave?

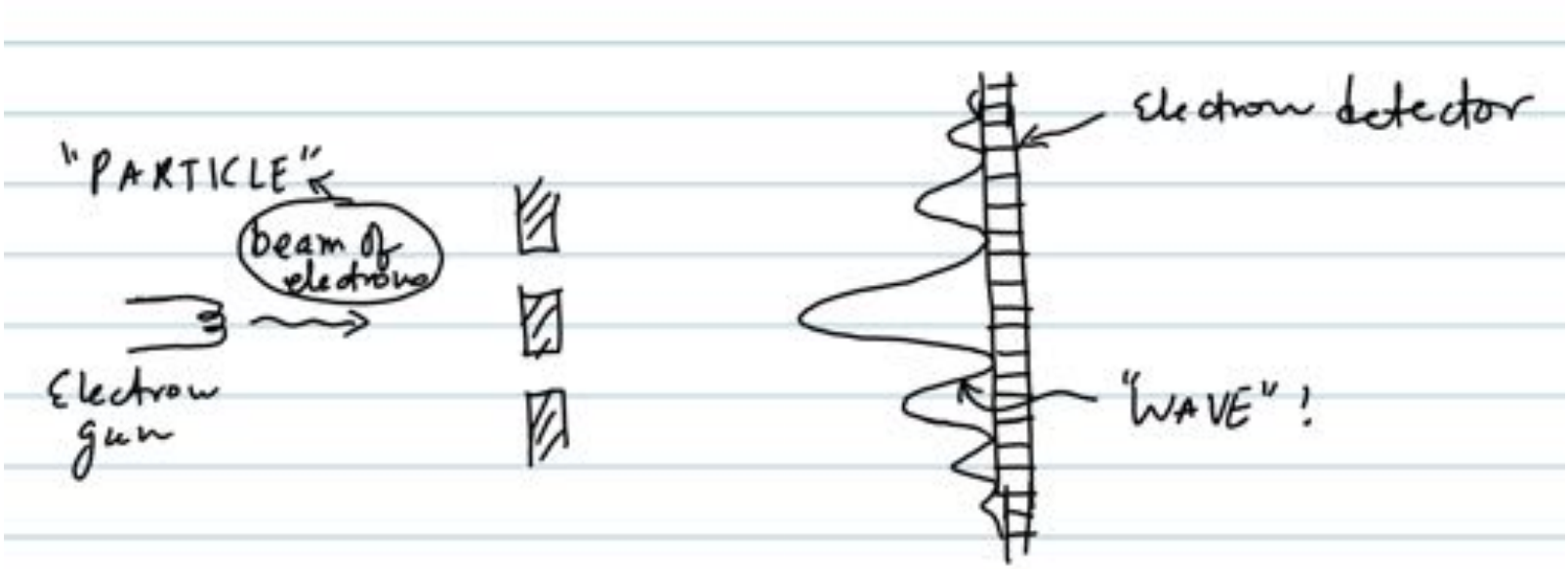

An electron is a particle… or a wave?

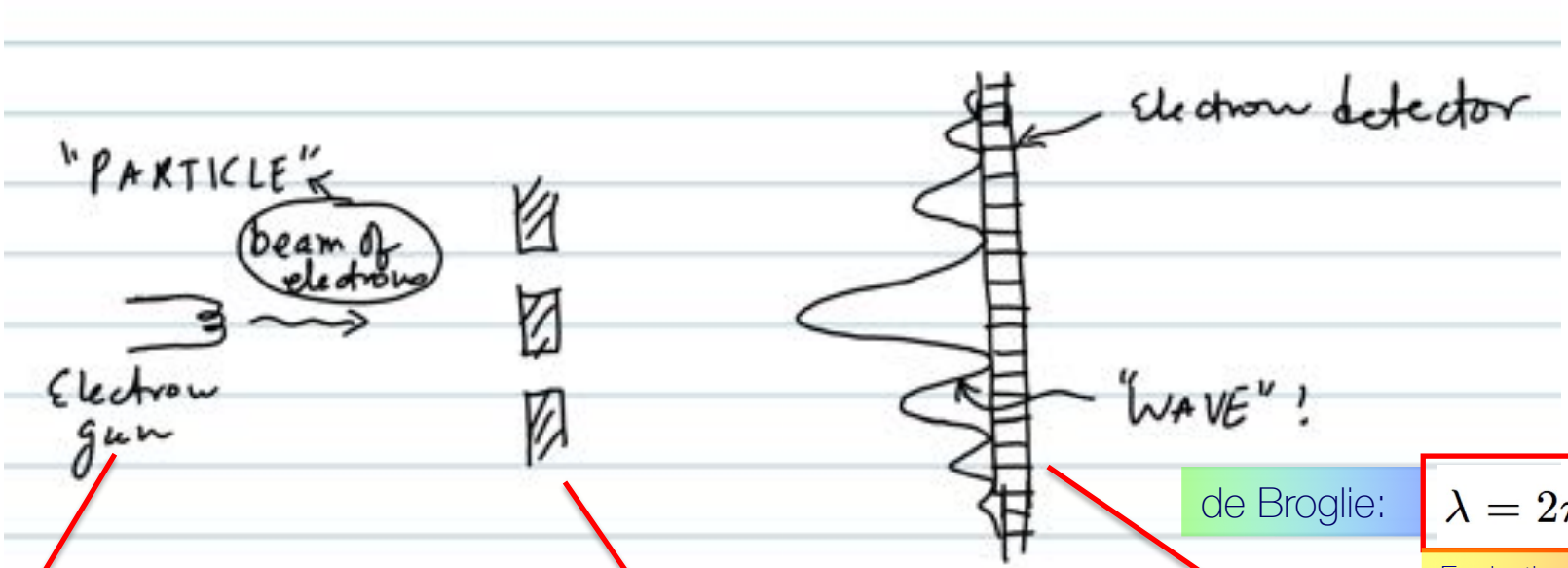

de Broglie: $\lambda = 2\pi\hbar/|\mathbf{p}|$

For both waves, and particles!

Guowang Li (Results from our lab!)

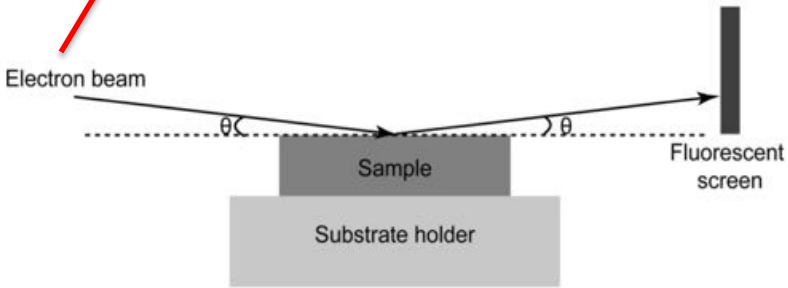

Electron beam incident on a crystal (RHEED)

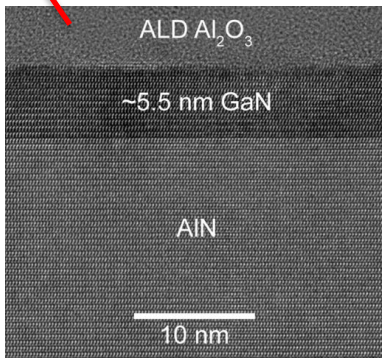

Atomic structure of a crystal (grating!)

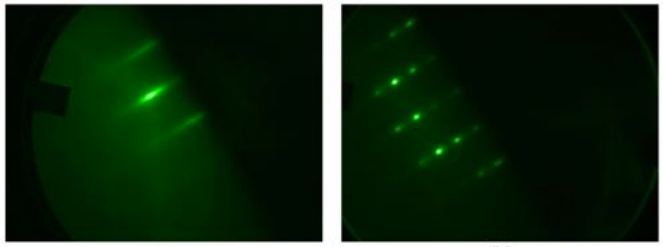

Figure 2.7: RHEED patterns of (a) smooth surface and (b) crystalline but rough of GaN surface.

Electron diffraction pattern on a screen

Wave and particle → need for a wavefunction

Quantum states (electrons, photons) behave as waves AND particles. How do we describe them quantitatively?

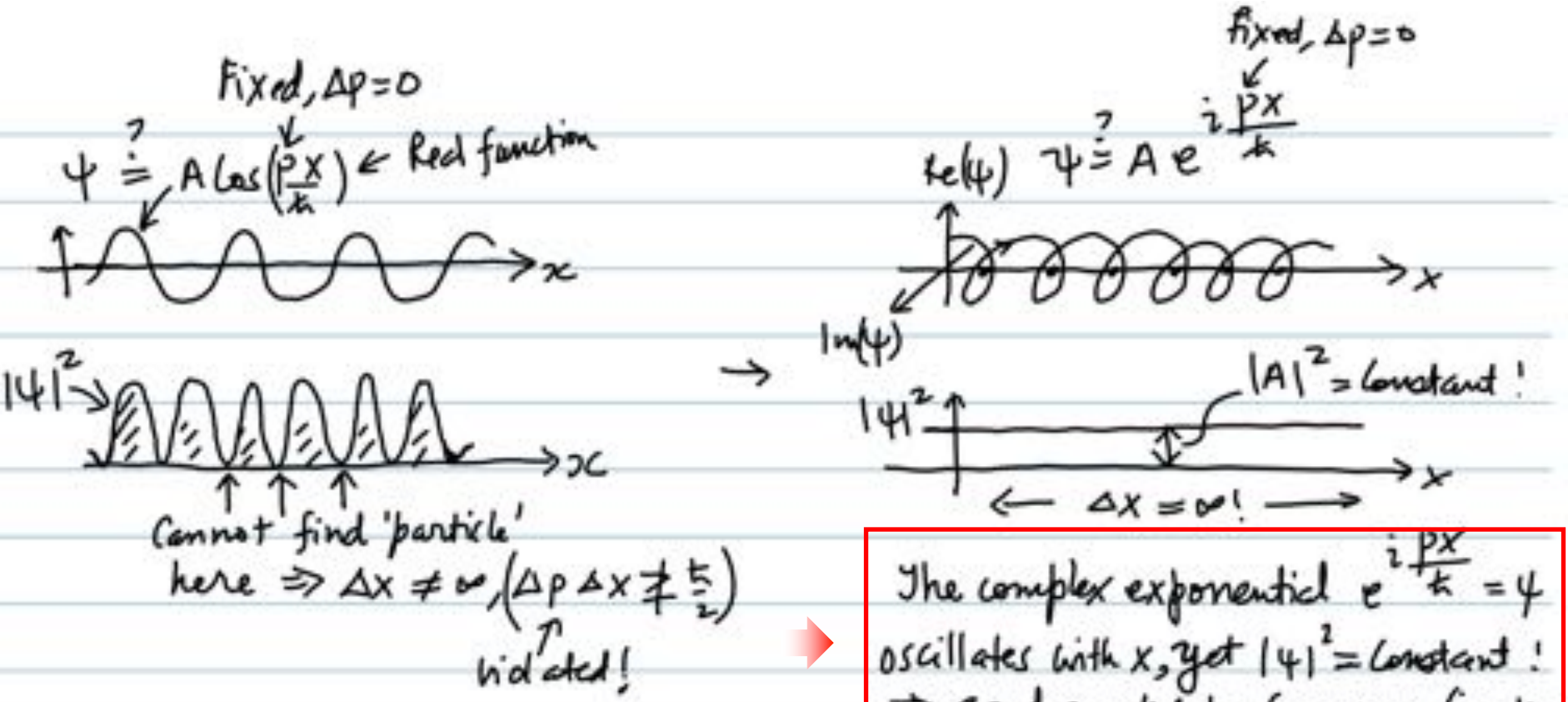

The complex exponential $e^{i\frac{px}{\hbar}} = \psi$ oscillates with x, yet $|\psi|^2$ = Constant!
⇒ good candidate for a wavefunction that respects $\Delta x \Delta p \geq \frac{\hbar}{2}$.

- The state of the free quantum particle cannot be represented by independent 'numbers' (x, p_x).
- We need a function whose amplitude oscillates in space, yet its magnitude never goes to zero.
- The complex exponential e^{ikx} satisfies these requirements, and respects the uncertainty relation.

Constructing wavefunctions: superposition

By linear superposition of complex exponentials, we can create 'particle' like or 'wave' like states as desired for the problem.

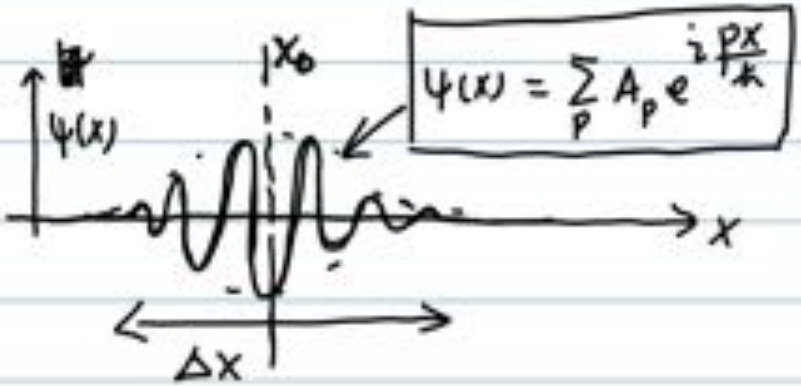

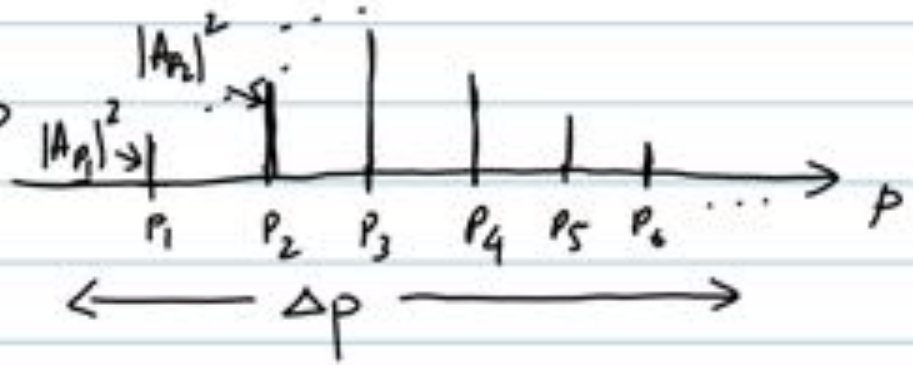

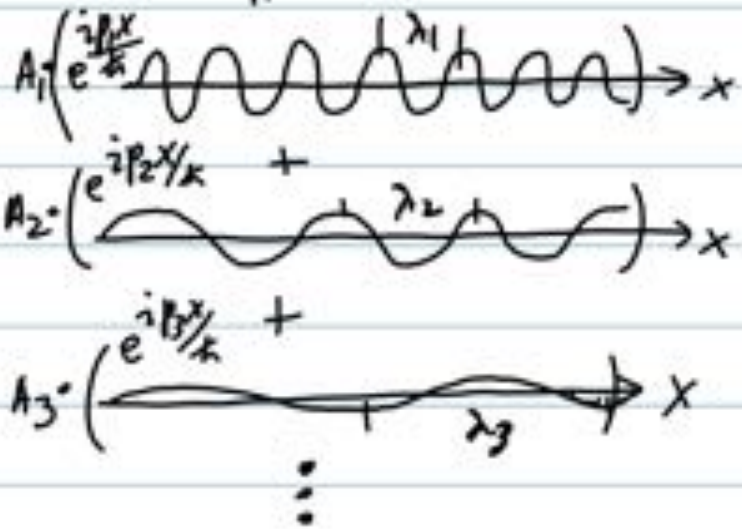

The best we can do to locate a "particle" ⇒ a 'wave packet'.

$\Rightarrow$ $\psi(x) = \sum_p A_p e^{i\frac{px}{\hbar}}$ is an allowed "wavefunction".

- Drawing on Fourier series, we realize that we can create any wavefunction shape to capture the correct physics of the problem. Note the corresponding reciprocal space weight distribution.

Math preliminaries before the physics…

$$\psi_p(x) = Ae^{ipx/\hbar}$$

Wavefunction ties x and p together.
Must respect the uncertainty principle.

$$\hat{p} = -i\hbar\partial/\partial x$$

Obervables are mathematical operators.
They act on the wavefunction to extract info.

$$\hat{p}\psi_p(x) = (\hbar k)\psi_p(x)$$

The states of definite value of an operator are called the eigenstates of that operator.

$$x\hat{p} - \hat{p}x = [x, \hat{p}] = i\hbar.$$

Unlike classical mechanics, some operators fail to commute!

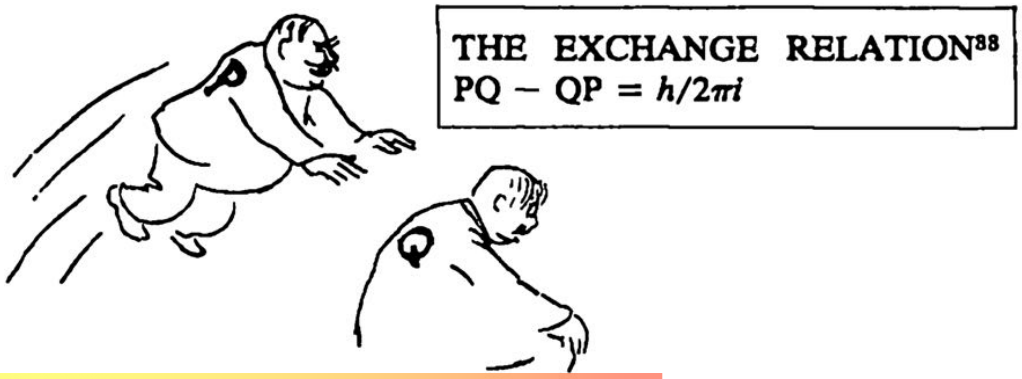

Non-commuting actions…
Ref: Gamow, Thirty years that shook physics.

Definite momentum, and definite location states

A state of definite location x_0:
Must be an eigenstate of operator x, with eigenvalue x_0:

$$x\psi_{x_0}(x) = x_0\psi_{x_0}(x) \implies \psi_{x_0}(x) = \delta(x - x_0)$$

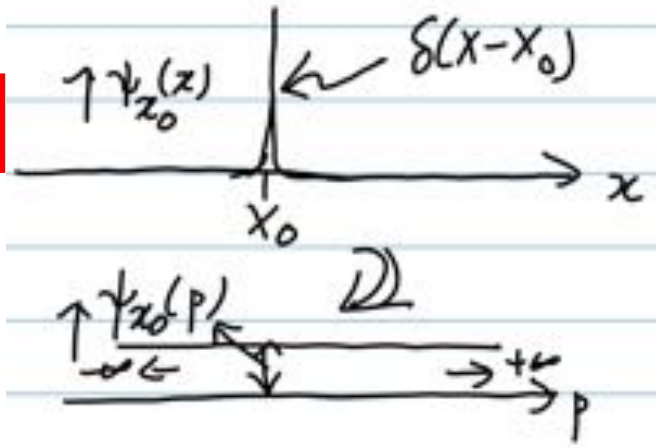

Definite in real space → spread out in momentum

A state of definite momentum p:
Must be an eigenstate of operator –ih(d/dx), with eigenvalue p:

$$\hat{p}_x\psi_p(x) = p_x\psi_p(x) \implies -i\hbar\frac{d}{dx}\psi_p(x) = p_x\psi_p(x)$$

$$\psi_p(x) = Ae^{i\frac{p_x x}{\hbar}} = Ae^{ik_x x}$$

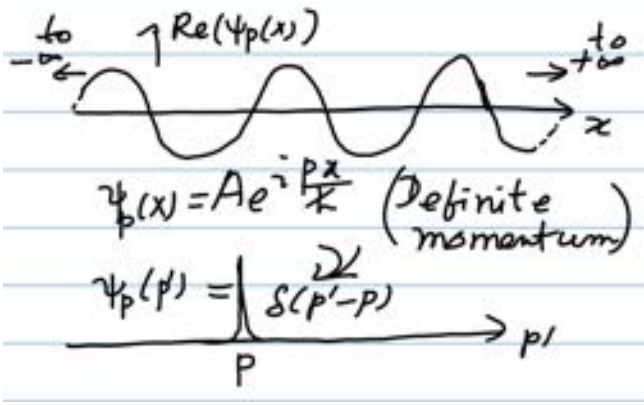

Definite in momentum → spread out in real space

States of definite location and definite momentum are unique in quantum mechanics.

States of definite energy: Schrodinger equation

States of definite energy are not unique, because they depend on the 'potential' V(x)

In classical mechanics, the energy of a particle is:

$$E_{cl} = \frac{p^2}{2m} + V(r)$$

In quantum mechanics, r & p cannot be simultaneously determined because [x,p]=ih. Thus, we must solve an equation to obtain the energy.

Schrodinger

$$[-\frac{\hbar^2}{2m}\frac{\partial^2}{\partial x^2} + V(x)]\psi_E(x) = E\psi_E(x).$$

The Schrodinger equation gives us the prescription to find the states of definite energy.

$$[\underbrace{\frac{\hat{p}^2}{2m} + V(r)}_{\hat{H}}]|\psi\rangle = E|\psi\rangle$$

Quantum states are vectors in the Hilbert space

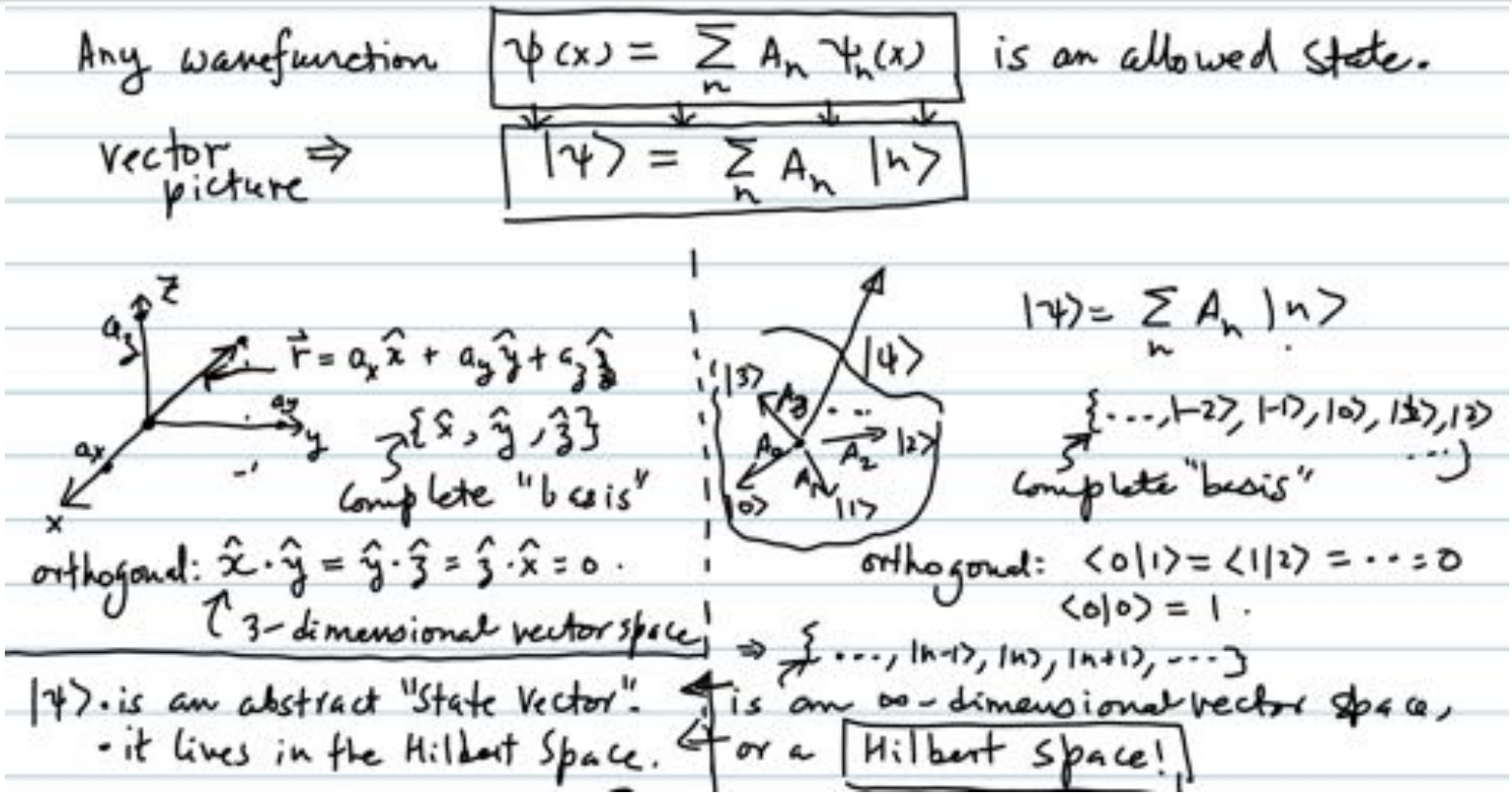

It is useful here to draw an analogy to the decomposition of a vector into specific coordinates. The 'hybrid' state function $\psi(x)$ is pictured as a vector $|\psi\rangle$ in an abstract space. The definite momentum wavefunctions $\psi_n(x)$ are pictured as the 'coordinate' vectors $|n\rangle$ in that space of vectors. This set of vectors is called the basis. Since there are an infinite set of integers $n = 0, \pm1, \pm2, ...$, the vector space is infinite dimensional. It is called the Hilbert space. One may then consider the coefficients A_n as the length of the projections of the state on the basis states. The abstract picture allows great economy of expression by writing $|\psi\rangle = \sum_n A_n|n\rangle$. The orthogonality of the basis states

$$|\psi\rangle = \sum_n A_n|n\rangle \qquad \langle m|n\rangle = \delta_{mn}$$
$$A_n = \langle n|\psi\rangle$$

$$|\psi\rangle = \sum_n \langle n|\psi\rangle|n\rangle = \sum_n |n\rangle\langle n|\psi\rangle$$
$$\sum_n |n\rangle\langle n| = 1$$

By projecting states, get various representations

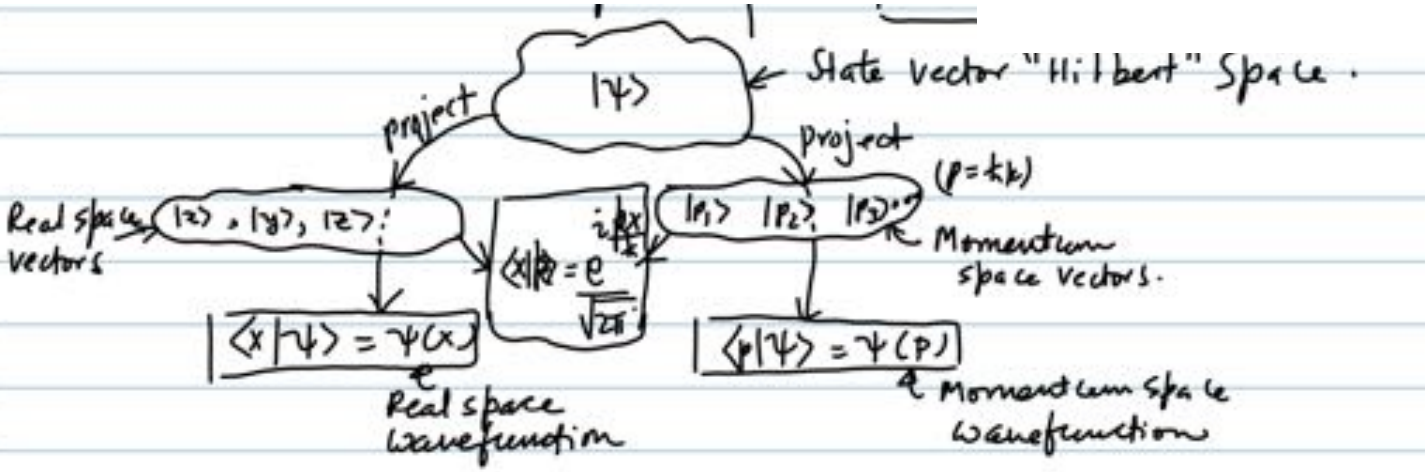

$$|\psi\rangle = \sum_n A_n |n\rangle \Rightarrow A_n = \langle n|\psi\rangle$$

$$\Rightarrow |\psi\rangle = \sum_n \langle n|\psi\rangle |n\rangle = \sum_n |n\rangle\langle n|\psi\rangle$$

($\langle n|\psi\rangle$: a number; same as LHS!)

$$\Rightarrow \boxed{\sum_n |n\rangle\langle n| = 1}$$ "outer product"

Similarly, $\boxed{\int d^3x\, |x\rangle\langle x| = 1}$

$$\langle x|\psi\rangle = \psi(x)$$
$$\langle k|\psi\rangle = \psi(k)$$
$$\langle x|k_x\rangle = \frac{e^{ik_x x}}{\sqrt{2\pi}}$$

$$\langle\psi_2|\psi_1\rangle = \int_{-\infty}^{\infty} dx \langle\psi_2|x\rangle\langle x|\psi_1\rangle = \int_{-\infty}^{\infty} dx \psi_2^\star(x)\psi_1(x)$$

- We can think of the states as vectors.
- The 'inner product' is a complex number generated by projection to the appropriate space.
- This number is the wavefunction – it can be found in real space, momentum space, etc…

The particle in a box

$$V(x) = 0, \quad 0 \le x \le L$$
$$V(x) = \infty, \quad x < 0, x > L$$

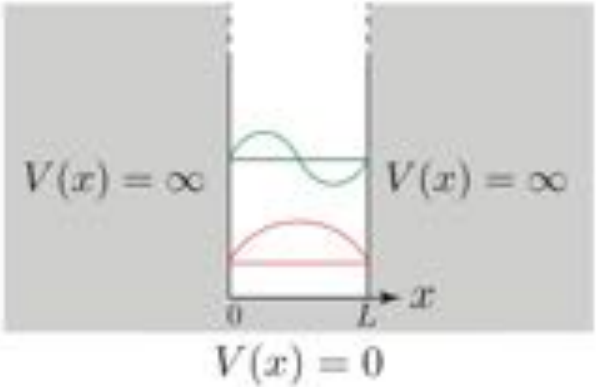

Particle in a box

The major change is that $\psi(x) = 0$ in regions where $V(x) = \infty$.

$$\psi(x) = Ae^{ikx} + Be^{-ikx} \rightarrow \psi(0) = 0 = A + B, \psi(L) = Ae^{ikL} + Be^{-ikL} = 0$$

$$\frac{A}{B} = -e^{-i2kL} = -1 \rightarrow 2kL = 2n\pi \rightarrow \boxed{k_n = n\frac{\pi}{L}}, n = \pm 1, \pm 2, \pm 3, \ldots$$

Note that $n = 0$ is *not allowed*, because then $\psi(x) = 0$ and there is no particle wavefunction after normalization over the length L is

$$\boxed{\psi(n, x) = \sqrt{\frac{2}{L}} \sin(n\frac{\pi}{L}x) = \sqrt{\frac{2}{L}} \sin(k_n x)}$$

Energy spectrum is discrete, zero energy NOT allowed!

$$\boxed{E_n = n^2 \frac{(\pi\hbar)^2}{2m_e L^2} = n^2 \frac{h^2}{8m_e L^2}}$$

The harmonic oscillator

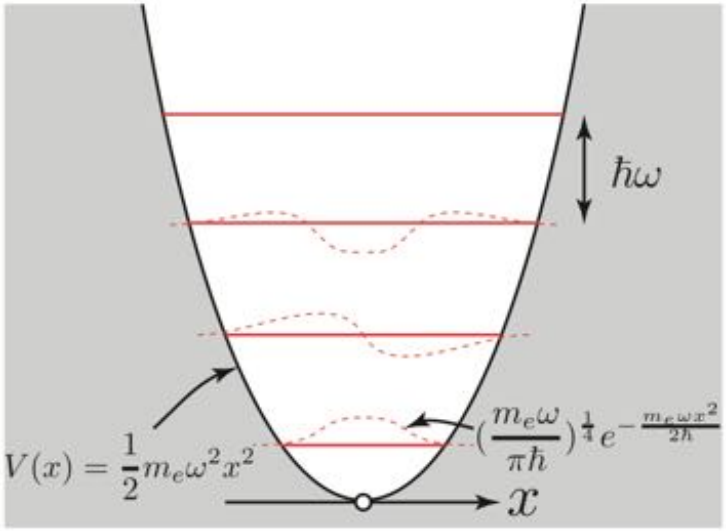

Harmonic Oscillator

$$V(x) = \frac{1}{2}m_e\omega^2x^2$$

$$a = \sqrt{\frac{m\omega}{2\hbar}}(\hat{x} + \frac{i}{m\omega}\hat{p})$$

$$a^\dagger = \sqrt{\frac{m\omega}{2\hbar}}(\hat{x} - \frac{i}{m\omega}\hat{p})$$

$$\hat{x} = \sqrt{\frac{\hbar}{2m\omega}}(a^\dagger + a)$$

$$\hat{p} = i\sqrt{\frac{m\omega\hbar}{2}}(a^\dagger - a)$$

$$\psi_n(x) = \frac{1}{\sqrt{2^n\, n!}} \cdot \left(\frac{m\omega}{\pi\hbar}\right)^{1/4} \cdot e^{-\frac{m\omega x^2}{2\hbar}} \cdot H_n\left(\sqrt{\frac{m\omega}{\hbar}}x\right), \qquad n = 0, 1, 2, \ldots.$$

Can solve the problem using raising and lowering operators

The functions H_n are the Hermite polynomials,

$$H_n(x) = (-1)^n e^{x^2}\frac{d^n}{dx^n}\left(e^{-x^2}\right).$$

The corresponding energy levels are

$$E_n = \hbar\omega\left(n + \frac{1}{2}\right).$$

Energy levels equally spaced
Zero energy NOT allowed!

The hydrogen atom

Energy levels [edit source | edit beta]

The energy levels of hydrogen, including fine structure, are given by the Sommerfeld expression:

$$E_{j\,n} = -m_e c^2 \left[\left(1 + \left[\frac{\alpha}{n - j - \frac{1}{2} + \sqrt{\left(j + \frac{1}{2}\right)^2 - \alpha^2}} \right]^2 \right)^{-1/2} - 1 \right]$$
$$\approx -\frac{m_e c^2 \alpha^2}{2n^2} \left[1 + \frac{\alpha^2}{n^2} \left(\frac{n}{j + \frac{1}{2}} - \frac{3}{4} \right) \right],$$

where α is the fine-structure constant and j is the "total angular momentum" quantum number, which is equal to $|\ell \pm 1/2|$ depending on the direction of the electron spin. The factor in square brackets in the last expression is nearly one; the extra term arises from relativistic effects (for details, see #Features going beyond the Schrödinger solution).

The value

$$\frac{m_e c^2 \alpha^2}{2} = \frac{0.51\,\text{MeV}}{2 \cdot 137^2} = 13.6\,\text{eV}$$

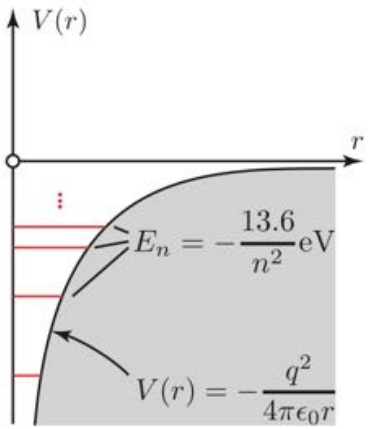

Hydrogen Atom

Wavefunction [edit source | edit beta]

The normalized position wavefunctions, given in spherical coordinates are:

$$\psi_{n\ell m}(r, \vartheta, \varphi) = \sqrt{\left(\frac{2}{na_0}\right)^3 \frac{(n-\ell-1)!}{2n(n+\ell)!}} e^{-\rho/2} \rho^\ell L_{n-\ell-1}^{2\ell+1}(\rho) Y_\ell^m(\vartheta, \varphi)$$

where:

$$\rho = \frac{2r}{na_0},$$

a_0 is the Bohr radius,

$L_{n-\ell-1}^{2\ell+1}(\rho)$ is a generalized Laguerre polynomial of degree $n - \ell - 1$, and

$Y_\ell^m(\vartheta, \varphi)$ is a spherical harmonic function of degree ℓ and order m. Note that the generalized Laguerre polynomials are defined differently by different authors. The usage here is consistent with the definitions used by Messiah,[8] and Mathematica.[9] In other places, the Laguerre polynomial includes a factor of $(n+\ell)!$,[10] or the generalized Laguerre polynomial appearing in the hydrogen wave function is $L_{n+\ell}^{2\ell+1}(\rho)$ instead. [11]

The quantum numbers can take the following values:

$$n = 1, 2, 3, \ldots$$
$$\ell = 0, 1, 2, \ldots, n-1$$
$$m = -\ell, \ldots, \ell.$$

Time-evolution of states: Time-dep. Schr. Eqn.

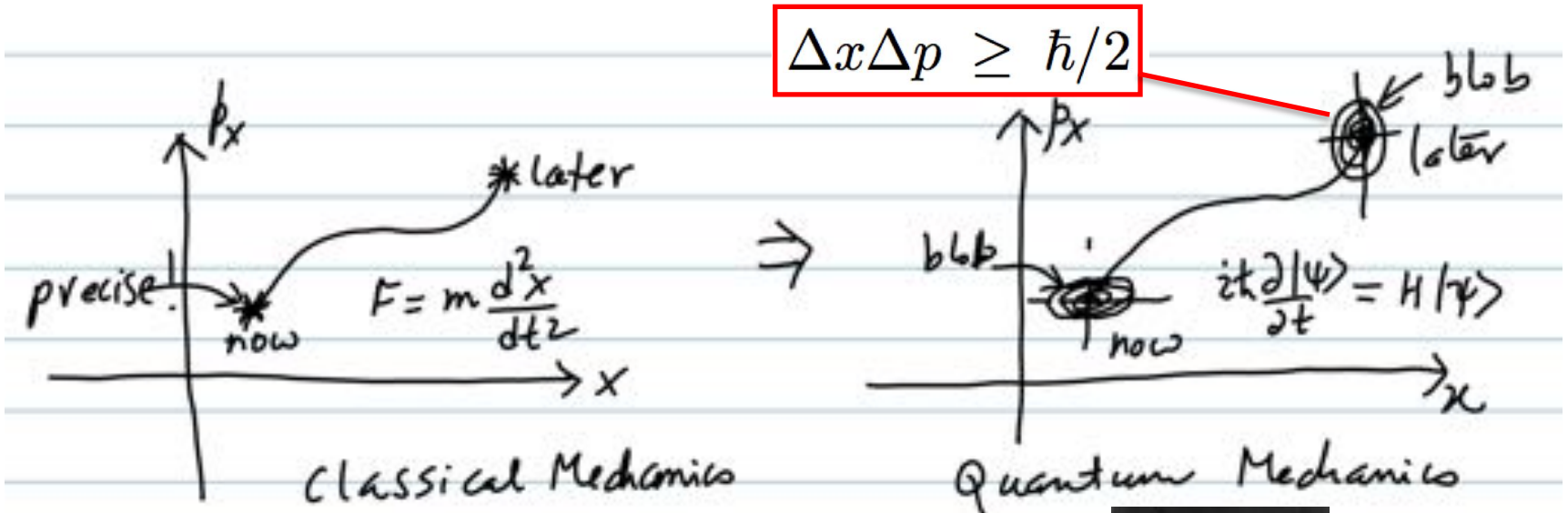

Newton

Schrodinger

$$\mathbf{F} = -\nabla V(r) = \frac{d\mathbf{p}}{dt}$$

Path is deterministic

$$i\hbar\frac{\partial|\psi\rangle}{\partial t} = [\frac{\hat{\mathbf{p}}^2}{2m} + V(\mathbf{r},t)]|\psi\rangle$$

Path respects uncertainty relation

States of definite energy are stationary states

$$i\hbar\frac{\partial\Psi(x,t)}{\partial t} = [\underbrace{-\frac{\hbar^2}{2m}\frac{\partial^2}{\partial x^2} + V(x)}_{\hat{H}}]\Psi(x,t).$$

$$\Psi(x,t) = \chi(t)\psi(x)$$

Try set of solutions that allow the separation of x and t.

$$i\hbar\frac{\dot{\chi}(t)}{\chi(t)} = \frac{\hat{H}\psi(x)}{\psi(x)} = E.$$

$$\Psi_E(x,t) = \psi_E(x)e^{-i\frac{E}{\hbar}t}$$

This means that the amplitude of states of definite energy oscillate with time with frequency E/h

$$|\Psi_E(x,t)|^2 = |\psi_E(x)|^2$$

But observables relate to the probability, which is time independent → this is why they care called stationary states.

$$\frac{d\langle\hat{A}\rangle}{dt} = -\frac{i}{\hbar}\langle[\hat{A},\hat{H}]\rangle$$

Ehrenfrest's theorem for the time evolution of an operator.

- The energy eigenvalues of the time-independent Schrodinger equation are states of definite energy.
- Their probability density does not change with time → they are called stationary states.
- This is analogous to the 1st law of classical mechanics: quantum states of definite energy will continue to remain in those states unless perturbed by a potential.

The classical Drude model

Paul Drude (1900)

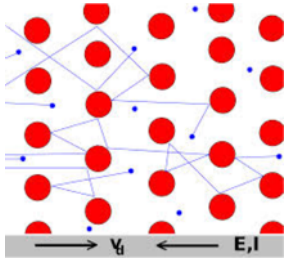

Electrons move and scatter every tau seconds

dc field:

$$m\frac{dv}{dt} = qE - \frac{mv}{\tau} \qquad \text{steady state: } \frac{d}{dt}(...) \to 0 \qquad v = \frac{q\tau}{m}E = \mu E$$

$$J = qnv = \frac{nq^2\tau}{m}E = \sigma E \implies \boxed{\sigma_0 = \frac{nq^2\tau}{m}}$$

dc conductivity

Oscillating field:

$$E(t) = Ee^{i\omega t} \qquad m\frac{dv}{dt} = qEe^{i\omega t} - \frac{mv}{\tau} \qquad v(t) = v(0)e^{i\omega t}$$

$$\sigma(\omega) = \frac{\sigma_0}{1+i\omega\tau} = \underbrace{\frac{\sigma_0}{1+(\omega\tau)^2}}_{\mathrm{Re}(\sigma(\omega))} - i\underbrace{\frac{\omega\tau\sigma_0}{1+(\omega\tau)^2}}_{\mathrm{Im}(\sigma(\omega))}$$

ac conductivity

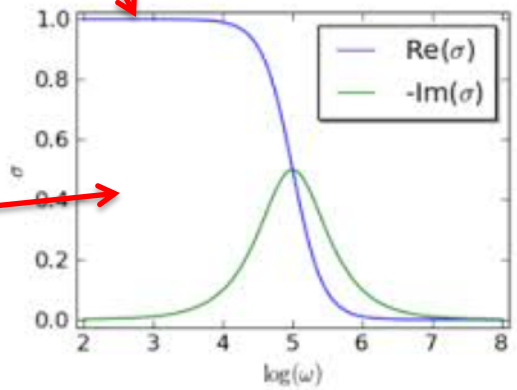

Quantum mechanical current

$$|\Psi(x,t)|^2 = \Psi^\star\Psi$$

Probability density in space and time

$$\frac{\partial|\Psi(x,t)|^2}{\partial t} = \Psi^\star\frac{\partial\Psi}{\partial t} + \frac{\partial\Psi^\star}{\partial t}\Psi$$

Change in probability density with time

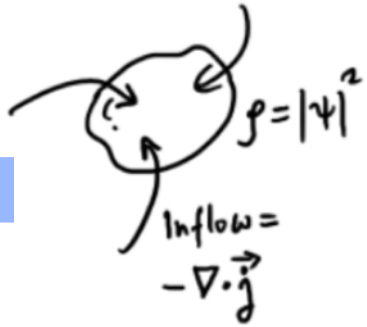

$$\frac{\partial|\Psi(x,t)|^2}{\partial t} = \Psi^\star\frac{(\hat{p}^2/2m + V)\Psi}{i\hbar} + \Psi\frac{(\hat{p}^2/2m + V)\Psi^\star}{-i\hbar}$$

Use time-dependent Schrodinger equation

$$\frac{\partial|\Psi(x,t)|^2}{\partial t} = \frac{1}{2mi\hbar}(\Psi^\star\hat{p}^2\Psi - \Psi\hat{p}^2\Psi^\star)$$

Since $\hat{p} = -i\hbar\nabla_{\mathbf{r}}$

$$\frac{\partial|\Psi(x,t)|^2}{\partial t} = -\nabla_{\mathbf{r}}\cdot\left[\frac{1}{2m}(\Psi^\star\hat{p}\Psi - \Psi\hat{p}\Psi^\star)\right]$$

In the form of a continuity equation → read off the current density!

Continuity equation

$$\partial\rho/\partial t = -\nabla_{\mathbf{r}}\cdot\mathbf{j}$$

$$\mathbf{j} = \frac{1}{2m}(\Psi^\star\hat{\mathbf{p}}\Psi - \Psi\hat{\mathbf{p}}\Psi^\star)$$

Quantum mechanical probability current density

$$\frac{d}{dt}\left(\int_{space} d^3r|\Psi|^2\right) = -\int_{space} d^3r\nabla\cdot\mathbf{j} = -\oint\mathbf{j}\cdot d\mathbf{S} = 0$$

Satisfies the conservation of number of particles

Electric current of quantum states

$$\mathbf{J} = \frac{q}{2m_e}(\Psi^\star \hat{\mathbf{p}} \Psi - \Psi \hat{\mathbf{p}} \Psi^\star)$$

For most semiconductors we know the bandstructure, but not the Bloch functions. Go through the derivation to recast the current in terms of the bandstructure, or the group-velocity (see notes).

$$\mathbf{v}_g(\mathbf{k}) = \nabla_{\mathbf{k}} E(\mathbf{k})/\hbar$$

- Group velocity of electron in state |k>

$$\mathbf{J}_d = \frac{q}{L^d} \sum_{\mathbf{k}} \mathbf{v}_g(\mathbf{k}) f(\mathbf{k})$$

VERY useful result: current in d-dimensions!

$$\mathbf{J}_d = \frac{q g_s g_v}{L^d} \sum_{\mathbf{k}} \mathbf{v}_g(\mathbf{k}) T(\mathbf{k}) [f_L(\mathbf{k}) - f_R(\mathbf{k})]$$

General expression for charge current density in d-dimensions

$$\mathbf{J}_d = \frac{q g_s g_v}{(2\pi)^d} \int d^d\mathbf{k} \times \mathbf{v}_g(\mathbf{k}) T(\mathbf{k}) [f_L(\mathbf{k}) - f_R(\mathbf{k})]$$

Identity crisis: Indistinguishable particles

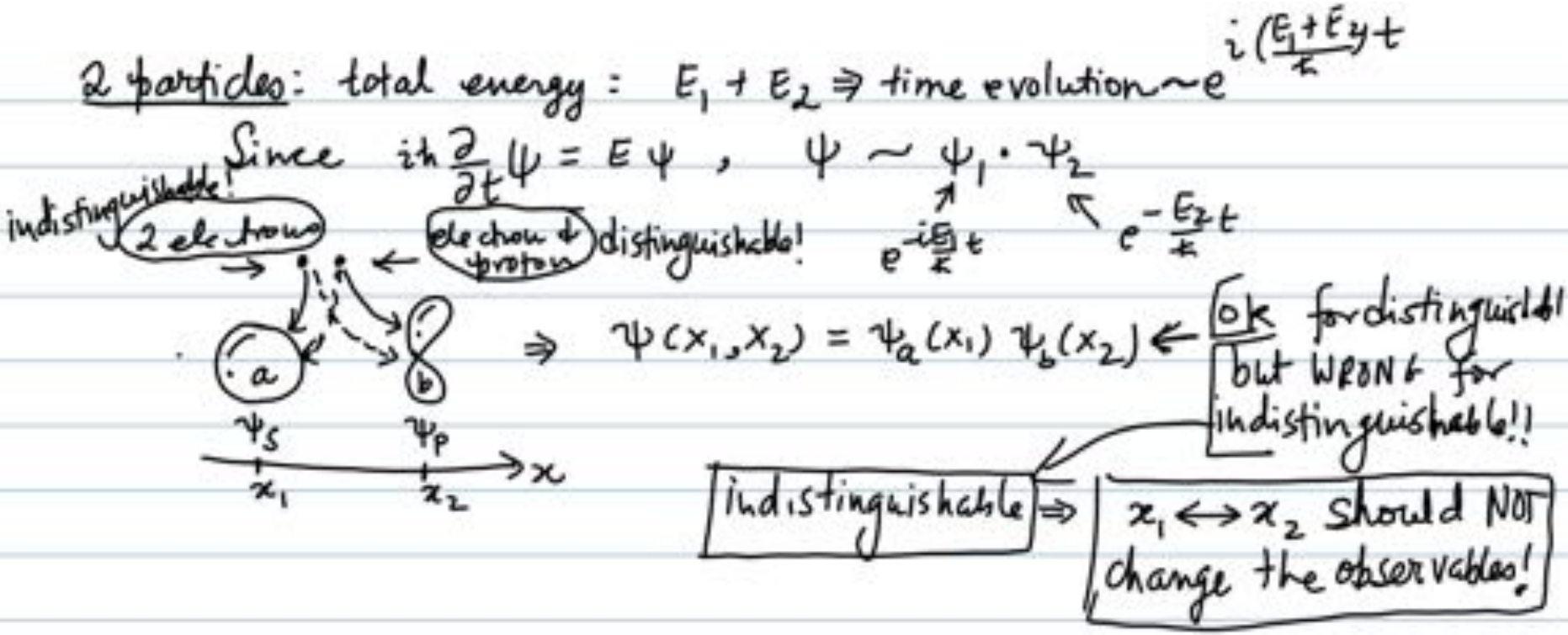

$$\psi(x_1, x_2) = \psi_a(x_1)\psi_b(x_2)$$

This is OK for distinguishable particles such as a proton and an electron.
But NOT OK for indistinguishable particles such as two electrons!
For example, |psi|^2 should not change on swapping $x_1 \leftrightarrow x_2$.
How must we then write the wavefunction for two identical particles?

Pauli Exclusion Explains the Periodic Table

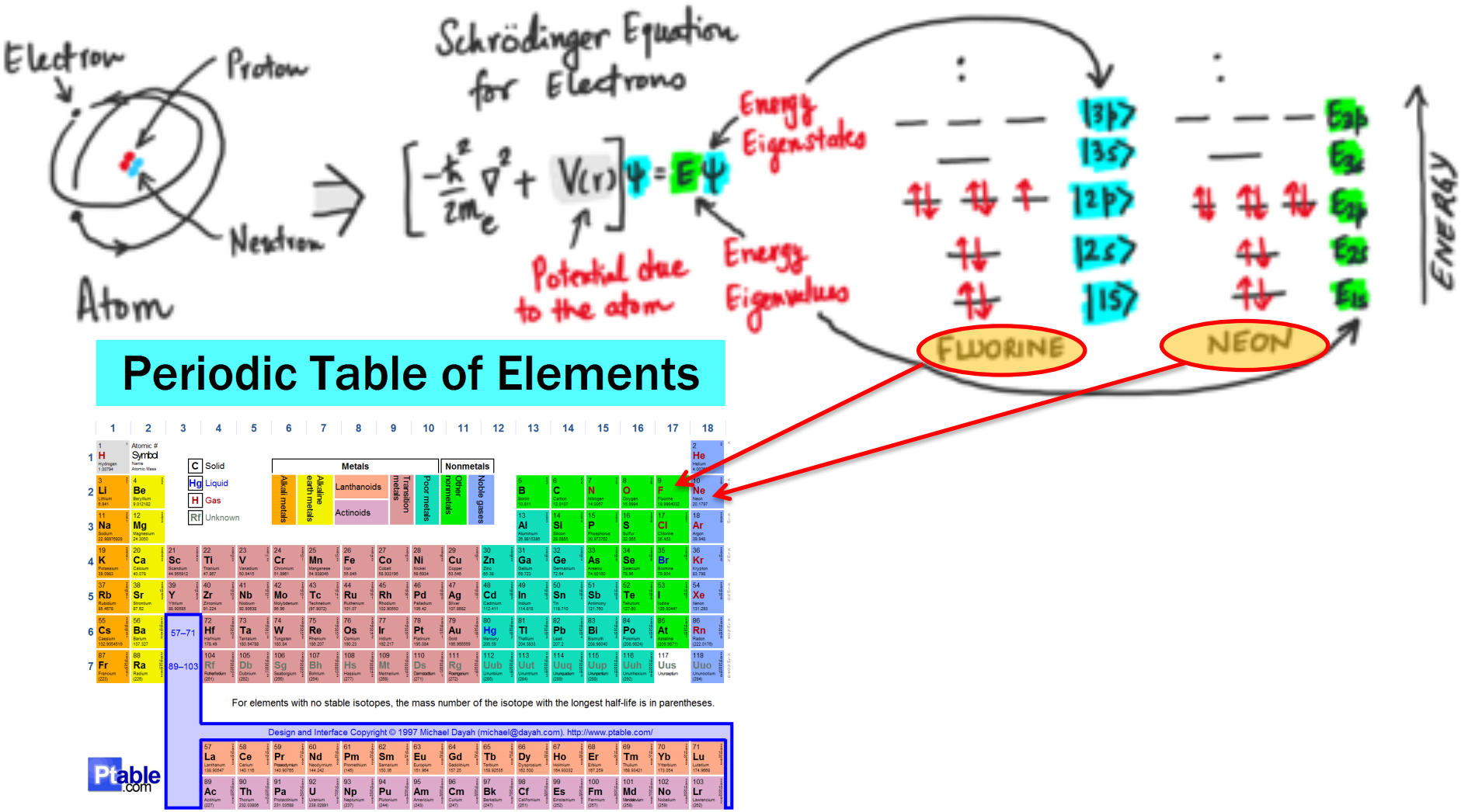

- The restriction that we cannot put two electrons in the same energy state leads to the elements
- The same restriction leads to a periodic variation of the physical properties of the elements.

Resolution of identity crisis: Bosons & Fermions

This is necessary for indistinguishable particles.

$$P(x_2, x_1) = P(x_1, x_2) \rightarrow |\psi(x_2, x_1)|^2 = |\psi(x_1, x_2)|^2.$$

$$\psi(x_1, x_2) = \psi_a(x_1)\psi_b(x_2)$$

$$\psi(x_1, x_2) = \psi_a(x_1)\psi_b(x_2) + \psi_a(x_2)\psi_b(x_1)$$

$$\psi(x_2, x_1) = +\psi(x_1, x_2)$$

$$\psi(x_1, x_1) = +\psi(x_1, x_1)$$

$$f_{BE}(E) = \frac{1}{e^{\frac{E-\mu}{kT}} - 1}$$

The Bose-Einstein distribution!
Particles are called Bosons.
Examples: Photons, Phonons

Bose

$$\psi(x_1, x_2) = \psi_a(x_1)\psi_b(x_2) - \psi_a(x_2)\psi_b(x_1)$$

$$\psi(x_2, x_1) = -\psi(x_1, x_2),$$

$$\psi(x_1, x_1) = -\psi(x_1, x_1) \rightarrow \psi(x_1, x_1) = 0.$$

The Pauli exclusion principle!

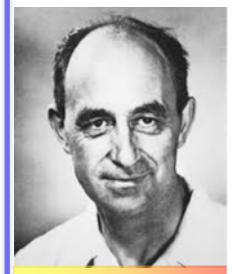

Fermi

$$f_{FD}(E) = \frac{1}{1 + e^{\frac{E-E_F}{kT}}}$$

The Fermi-Dirac distribution!
Particles are called Fermions.
Examples: Electrons, Protons

- Note: Why not $\psi(x_2, x_1) = e^{i\phi}\psi(x_1, x_2)$? Majorana particles → later…

Fermi-Dirac, Bose-Einstein, and Maxwell-Boltzmann

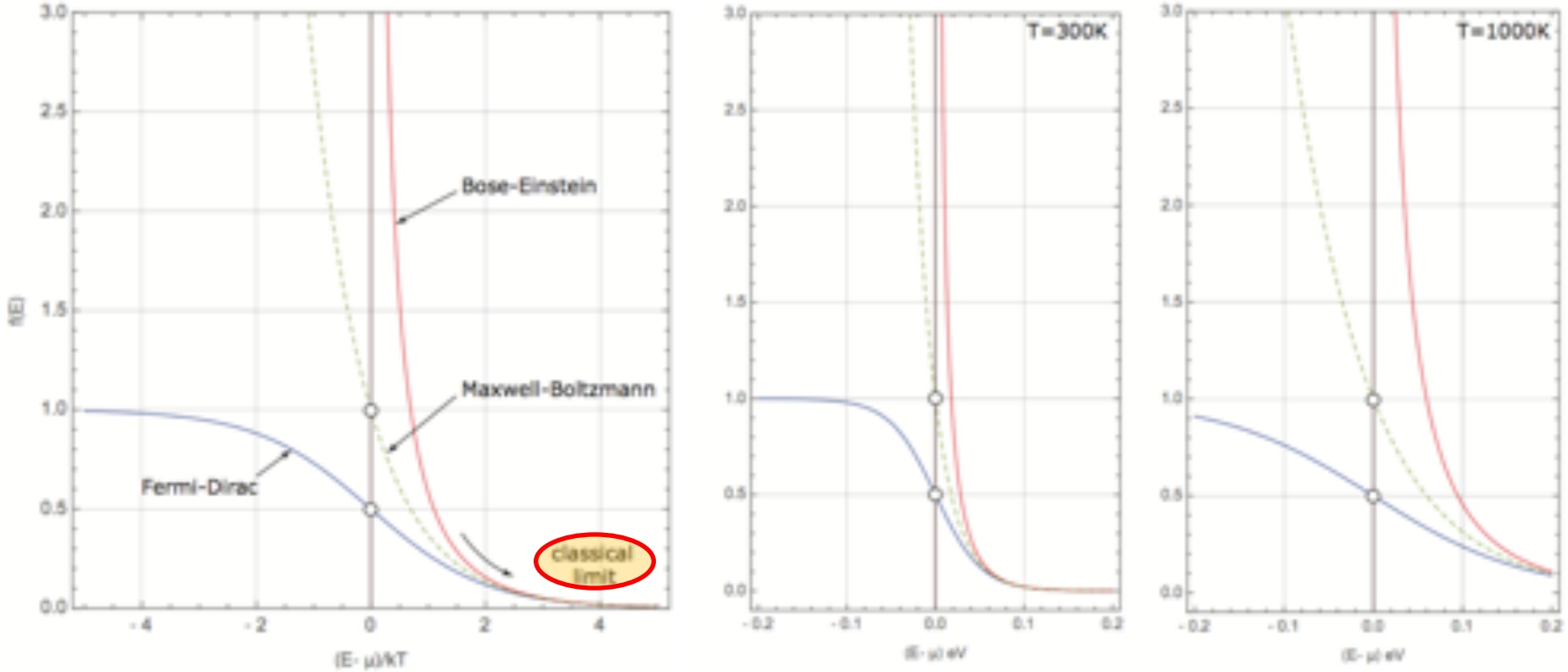

- The Fermi-Dirac and Bose-Einstein distributions asymptotically approach the classical limit at high energies
- Fermi-Dirac occupation function for any energy orbital is less than 1.

Some properties of the Fermi-Dirac Function

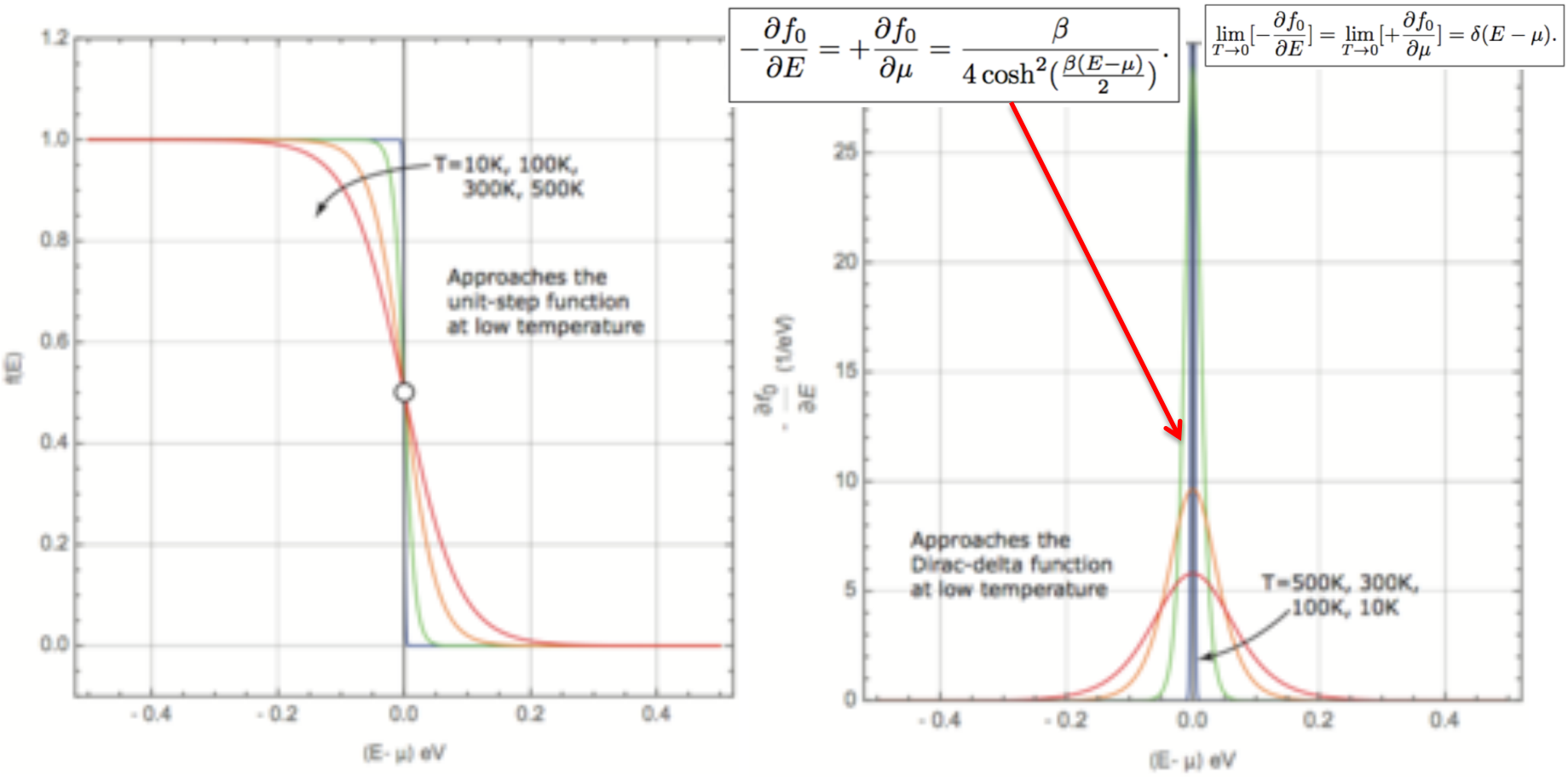

Fig. 4.6 Illustration of the temperature dependence of the Fermi-Dirac distribution, and its derivative.

- The Fermi-function at T=0 K is a step function that is 1 below the Fermi energy, and 0 above.
- The derivative of the Fermi function is of central importance in transport phenomena. Because of the exclusion principle, it defines the energy states that can participate in transport.

The Fermi-Difference Function

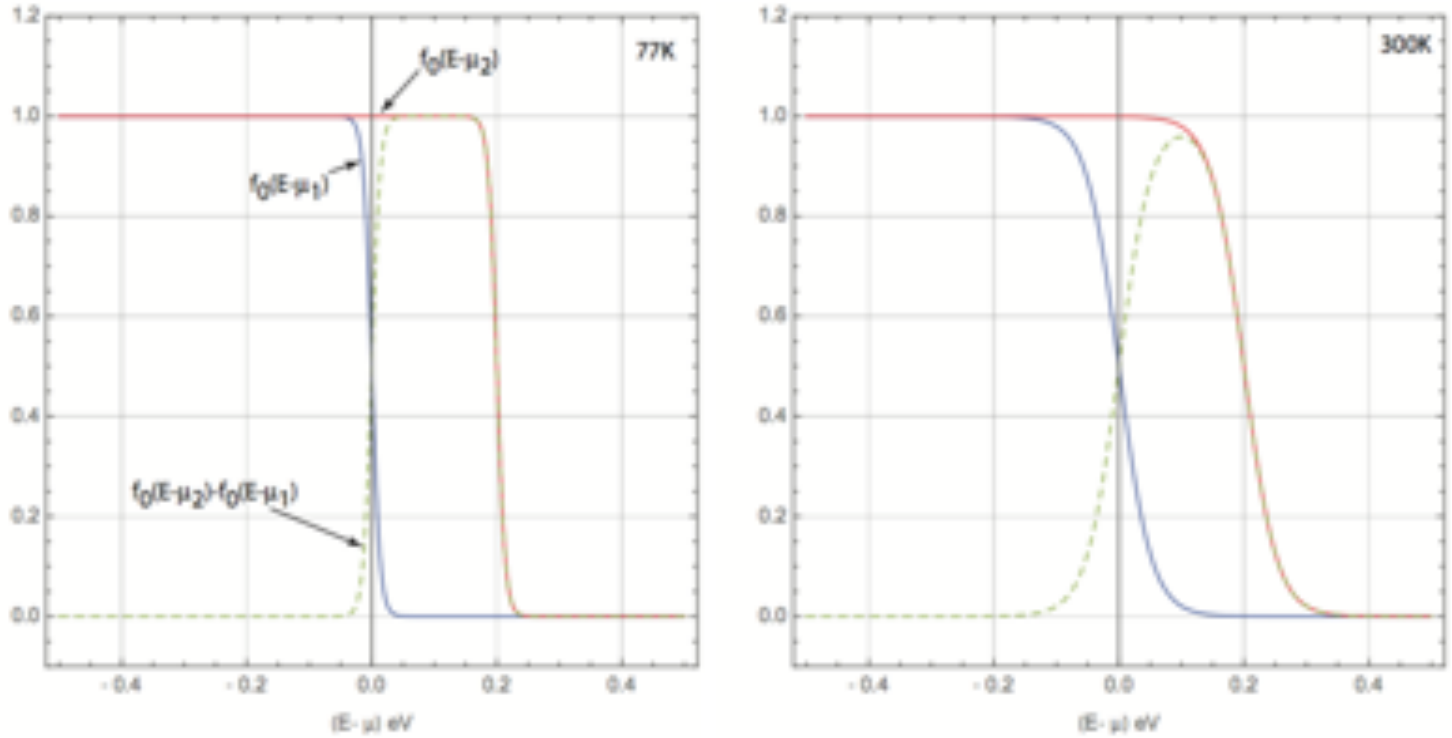

Fig. 4.7 Illustration of the temperature dependence of the Fermi-difference distribution. The difference is a window between $\mu_2 - \mu_1$ that becomes increasingly rectangular as the temperature drops.

$$\int_0^\infty dE[f_0(\mu_1) - f_0(\mu_2)] \approx (\mu_1 - \mu_2).$$

$$f(u) - f(v) = [\underbrace{f(u) + f(v) - 2f(u)f(v)}_{\geq 0}] \times \tanh(\frac{v-u}{2})$$

- Two electrodes with different Fermi levels cause a difference in the Fermi functions for electrons that are in equilibrium with them.
- The Fermi difference function is rectangular, and defines the effect of voltages on transport properties.

Fermi-Dirac Integrals

$$F_j(\eta) = \frac{1}{\Gamma(j+1)} \int_0^\infty du \frac{u^j}{1+e^{u-\eta}}$$

$$\int_0^\infty dE f_0(E-\mu) = \int_0^\infty \frac{dE}{1+e^{\beta(E-\mu)}} = \frac{1}{\beta}\ln(1+e^{\beta\mu}),$$

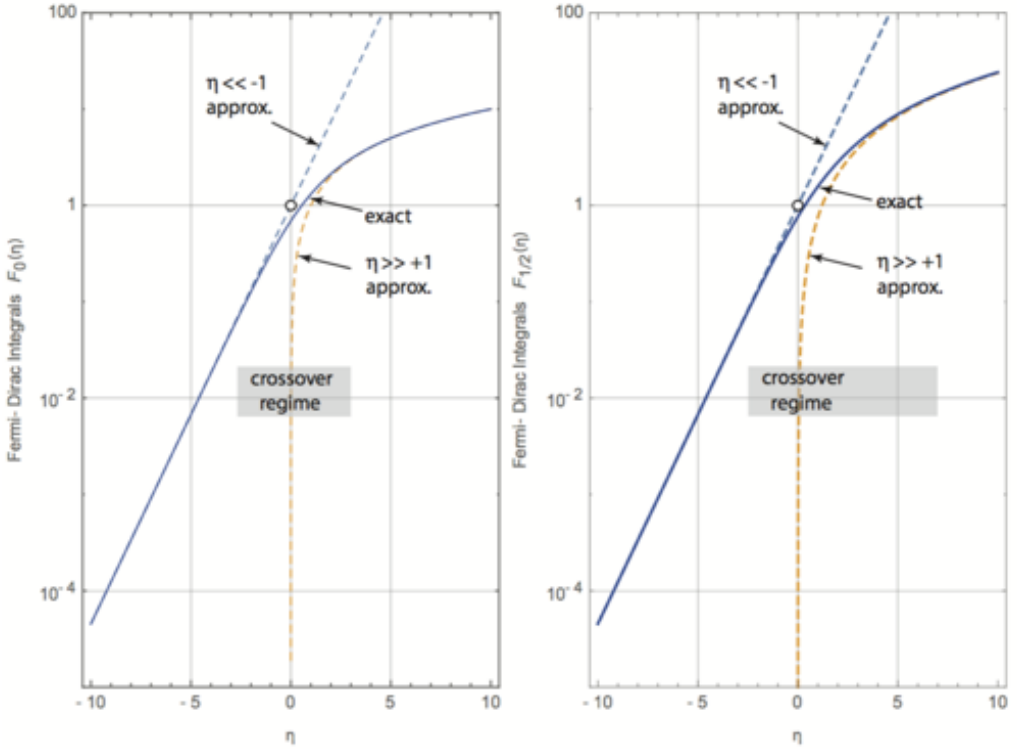

$$F_j(\eta) = \frac{1}{\Gamma(j+1)} \int_0^\infty du \frac{u^j}{1+e^{u-\eta}}, \quad F_j(\eta) \underbrace{\approx}_{\eta<<-1} e^\eta, \quad F_j(\eta) \underbrace{\approx}_{\eta>>1} \frac{\eta^{j+1}}{\Gamma(j+2)}$$

- Fermi-Dirac integrals are of central importance in the physics of semiconductors and nanostructures

Quantum Equipartition of Energy

$$\langle E\rangle_{1d} = \frac{\int_{-\infty}^{+\infty} dv_x \cdot \left(\frac{1}{2}mv_x^2\right) \cdot \frac{1}{e^{\frac{\frac{1}{2}mv_x^2-\mu}{k_BT}}+1}}{\int_{-\infty}^{+\infty} dv_x \cdot \frac{1}{e^{\frac{\frac{1}{2}mv_x^2-\mu}{k_BT}}+1}} = \frac{1}{2}k_BT \cdot \frac{F_{1/2}(\eta)}{F_{-1/2}(\eta)}.$$

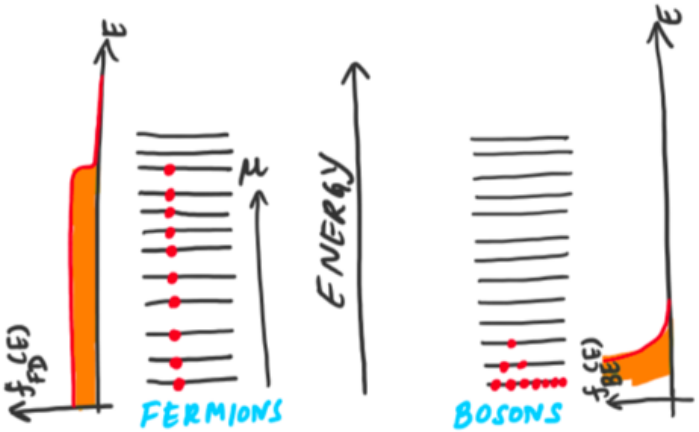

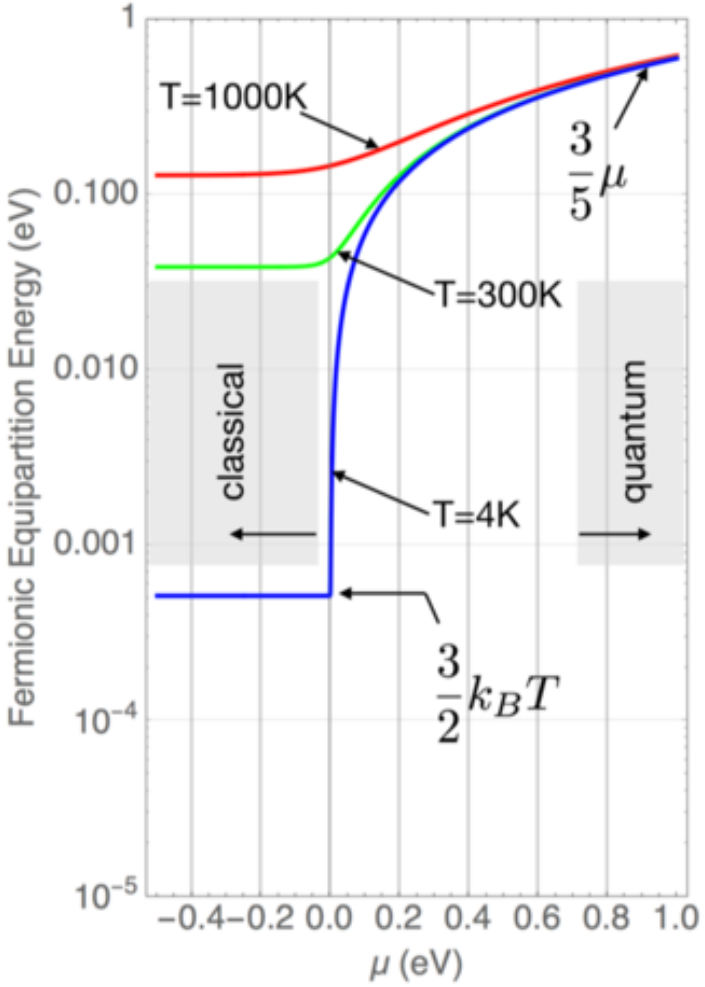

- The equipartition of energy relation is modified from the Maxwell-Boltzmann form

Quantum version of the Equipartition of Energy

$$\langle E\rangle_{1d} = \frac{\int_{-\infty}^{+\infty} dv_x \cdot (\frac{1}{2}mv_x^2) \cdot e^{-\frac{\frac{1}{2}mv_x^2}{k_BT}}}{\int_{-\infty}^{+\infty} dv_x \cdot e^{-\frac{\frac{1}{2}mv_x^2}{k_BT}}} = \frac{1}{2}k_BT.$$

$$\langle E\rangle_{3d} = \frac{\int_{-\infty}^{+\infty} dv_x \int_{-\infty}^{+\infty} dv_y \int_{-\infty}^{+\infty} dv_z \cdot (\frac{1}{2}m(v_x^2+v_y^2+v_z^2)) \cdot e^{-\frac{\frac{1}{2}m(v_x^2+v_y^2+v_z^2)}{k_BT}}}{\int_{-\infty}^{+\infty} dv_x \int_{-\infty}^{+\infty} dv_y \int_{-\infty}^{+\infty} dv_z \cdot e^{-\frac{\frac{1}{2}m(v_x^2+v_y^2+v_z^2)}{k_BT}}} \tag{4.22}$$

$$\langle E\rangle_{3d} = \frac{1}{2}k_BT + \frac{1}{2}k_BT + \frac{1}{2}k_BT = \frac{3}{2}k_BT. \tag{4.23}$$

$$\langle E\rangle_{1d} = \frac{\int_{-\infty}^{+\infty} dv_x \cdot (\frac{1}{2}mv_x^2) \cdot \frac{1}{e^{\frac{\frac{1}{2}mv_x^2-\mu}{k_BT}}+1}}{\int_{-\infty}^{+\infty} dv_x \cdot \frac{1}{e^{\frac{\frac{1}{2}mv_x^2-\mu}{k_BT}}+1}} = \frac{1}{2}k_BT \cdot \frac{F_{1/2}(\eta)}{F_{-1/2}(\eta)}$$

$$\langle E\rangle_{3d} = \frac{3}{2}k_BT \cdot \frac{F_{3/2}(\eta)}{F_{1/2}(\eta)}$$

$$\boxed{\langle E\rangle_{d} = \frac{d}{2}k_BT \cdot \frac{F_{\frac{d}{2}}(\eta)}{F_{\frac{d-2}{2}}(\eta)}}$$

- Fermi-Dirac integrals are of central importance in the physics of semiconductors and nanostructures

Electrons in the quantum world

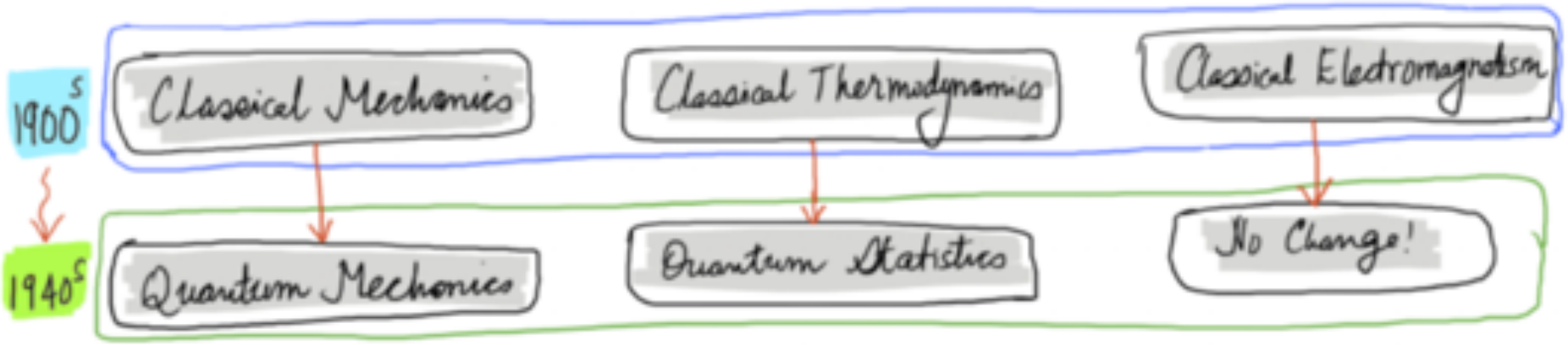

$$-\frac{\hbar^2}{2m_e}\frac{d^2}{dx^2}\psi(x) + V(x)\psi(x) = E\psi(x)$$

$$f_{FD}(E) = \frac{1}{1 + e^{\frac{E-E_F}{kT}}}$$

- solve the Schrodinger equation *exactly* to obtain the wavefunction $\psi(x)$[1],
- the allowed momentum p_x,
- the allowed energy eigenvalues E,
- the quantum current J,
- the Density of States $g(E)$, and
- the *total* energy $\mathcal{U}$, *average* energy u, and energy density u_v of many electrons.

- We will now apply quantum statistics (e.g. the Fermi-Dirac distribution) and quantum mechanics (the Schrodinger equation) to electrons and investigate how properties alien to classical mechanics emerge from these monumental changes.

Free electron in 1 dimension

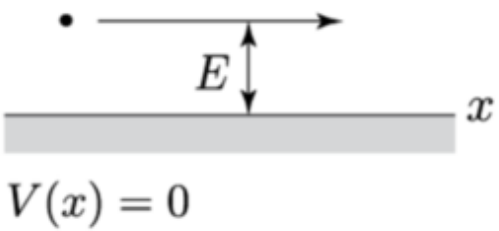

$$-\frac{\hbar^2}{2m_e}\frac{d^2}{dx^2}\psi(x) = E\psi(x)$$

V(x)=0 for the free electron

$$\psi(x) = Ae^{ikx} + Be^{-ikx}$$

Superposition state of a right-and a left-going electron wave.

$$k = \sqrt{\frac{2m_e E}{\hbar^2}} = \frac{2\pi}{\lambda}.$$

De-Broglie relation in action for the free electron.

Free Electron

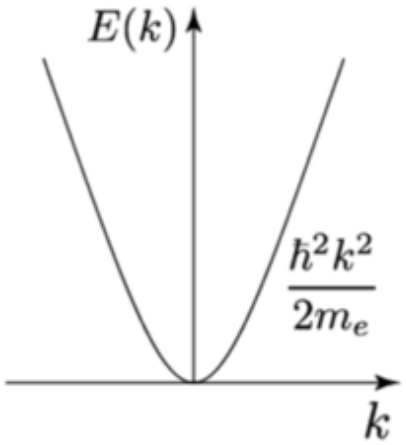

$$E(k) = \frac{\hbar^2 k^2}{2m_e}.$$

Energy is momentum squared by twice mass, all kinetic, no potential.

$$J(+k) = \frac{q}{2m_e}(\psi^\star \hat{p}_x \psi - \psi \hat{p}_x \psi^\star) \Longrightarrow J(+k) = q|A|^2\frac{\hbar k}{m_e}.$$

$$\mathbf{v}_g(\mathbf{k}) = \nabla_{\mathbf{p}} E(\mathbf{p}) = \frac{1}{\hbar}\nabla_{\mathbf{k}} E(\mathbf{k})$$

- The free electron has a parabolic energy distribution. All energies and all momenta are allowed.
- The quantum mechanical current has direct analogy to the classical current.
- We have defined a group velocity for a state as the slope of the energy/momentum curve.

Particle on a Ring: Quantum Confinement

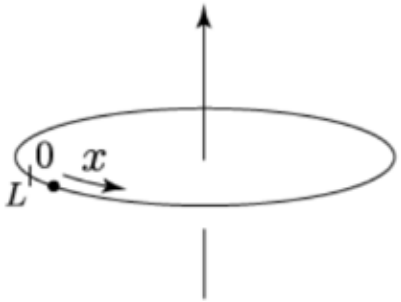

$$\psi(x+L) = \psi(x) \rightarrow e^{ik(x+L)} = e^{ikx} \rightarrow e^{ikL} = 1 \rightarrow kL = 2n\pi$$

Boundary conditions force quantized values of k

$$\psi_n(x) = Ae^{ik_n x}$$

Normalization

$$\boxed{\psi_n(x) = \frac{1}{\sqrt{L}} e^{ik_n x}}$$

$$\boxed{k_n = \frac{2\pi}{L} n}, n = 0, \pm 1, \pm 2, \ldots$$

$$\boxed{p_n = \hbar k_n = \frac{h}{2\pi}\frac{2\pi}{L} n = n\frac{h}{L}}$$

Particle on a ring

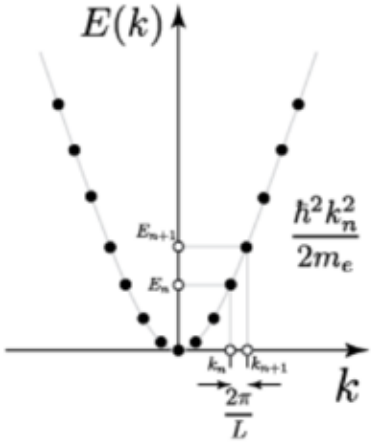

$$\mathbf{L}_n = \mathbf{r} \times \mathbf{p} = \hbar k_n \times \frac{L}{2\pi}\hat{\mathbf{z}} = \frac{2\pi\hbar}{L} n \times \frac{L}{2\pi}\hat{\mathbf{z}} \Longrightarrow \boxed{L_n = n\hbar}$$

$$\boxed{E_n = \frac{\hbar^2 k_n^2}{2m_e} = n^2 \frac{(2\pi\hbar)^2}{2m_e L^2} = n^2 \frac{h^2}{2m_e L^2}}$$

- Particle on a ring has a parabolic energy distribution.
- Discrete energies and momenta are allowed.
- The quantum mechanical current has direct analogy to the classical current.

Quantum Confinement & Density of States

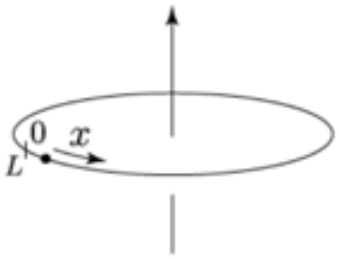

Particle on a ring

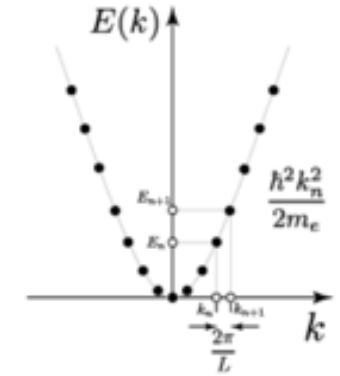

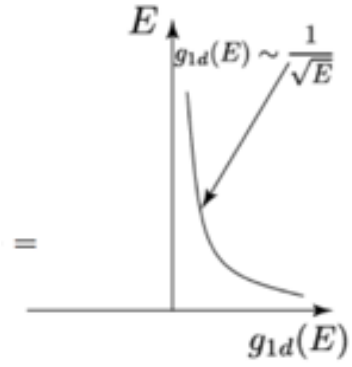

$$E_n = \frac{\hbar^2 k_n^2}{2m_e} = n^2 \frac{(2\pi\hbar)^2}{2m_e L^2} = n^2 \frac{h^2}{2m_e L^2}$$

- The smaller the circle, the larger the allowed energies ($L \downarrow \Longrightarrow E_n \uparrow$), and
- The smaller the mass, the larger the allowed energies ($m \downarrow \Longrightarrow E_n \uparrow$).

$$g_s g_v \frac{2dk}{\frac{2\pi}{L}} = G_{1d}(E)dE \Longrightarrow g_{1d}(E) = \frac{G_{1d}}{L} = \frac{2g_s g_v}{2\pi \frac{dE}{dk}} \Longrightarrow$$

$$g_{1d}(E) = \frac{g_s g_v}{2\pi} \left(\frac{2m_e}{\hbar^2}\right)^{\frac{1}{2}} \frac{1}{\sqrt{E}}$$

The Density of States is the number of quantum states allowed between energies E and E + dE

- Quantum confinement can be used to engineer the energy levels of nanostructures.
- The Density of states can be expressed in momentum or in energy space.

Fermi Energy, Fermi velocity & their quantum origin

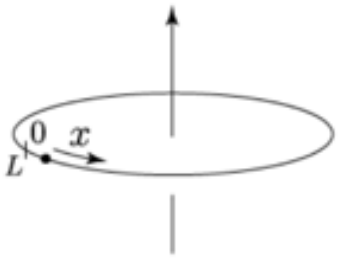

$$E_n = \frac{\hbar^2 k_n^2}{2m_e} = n^2 \frac{(2\pi\hbar)^2}{2m_e L^2} = n^2 \frac{h^2}{2m_e L^2}$$

The Fermi energy is a remarkable consequence of the exclusion principle!

Many-Electron Effect:

$$\frac{g_s g_v \times 2k_F}{\frac{2\pi}{L}} = N \Longrightarrow \boxed{k_F = \frac{\pi}{2}n} \Longrightarrow \boxed{E_F = \frac{\hbar^2 \pi^2 n^2}{8m_e}}$$

Particle on a ring

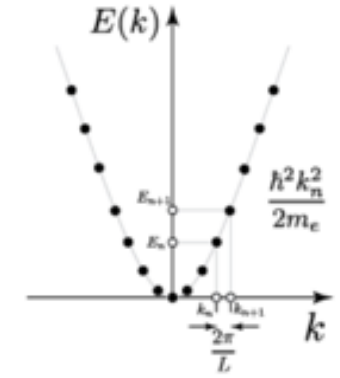

$$n \sim 10^8/\text{cm} \qquad E_F \sim 10 \text{ eV} \qquad T \sim 10^5 \text{ K}$$

$$\lambda_F \sim 0.4 \text{ nm} \qquad v_F = \frac{\hbar k_F}{m_e} = \frac{hn}{4m_e} \sim 5 \times 10^7 \text{ cm/s}$$

Typical values for metals

$$\mathcal{U} = \int_0^{E_F} dE \cdot E \cdot G_{1d}(E) \Longrightarrow u_{1d} = \frac{\mathcal{U}}{N} = \frac{\int_0^{E_F} dE \cdot E \cdot G_{1d}(E)}{\int_0^{E_F} dE \cdot G_{1d}(E)} = \frac{1}{3}E_F$$

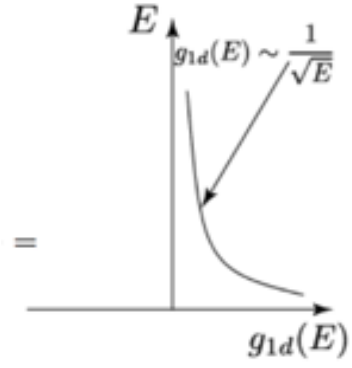

$$\boxed{u_v(1d) = \frac{1}{3}nE_F}$$

- Because of the Pauli exclusion principle and the Fermi-Dirac distribution, the presence of many electrons in a metal gain significant energy and velocity even at T=0 K. This is a most remarkable consequence of quantum theory!

Temperature-dependence of Carrier Density

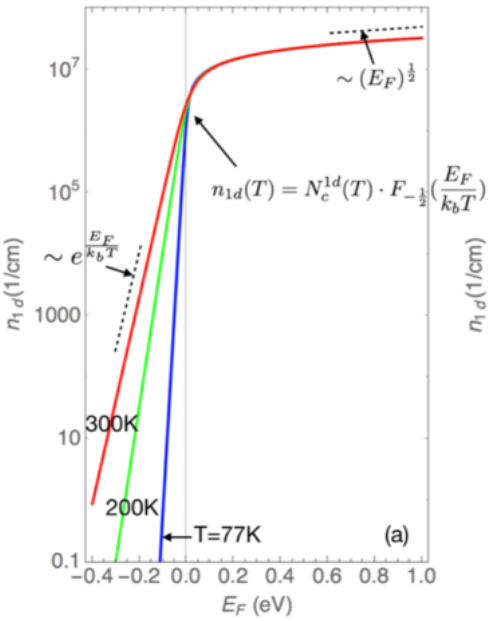

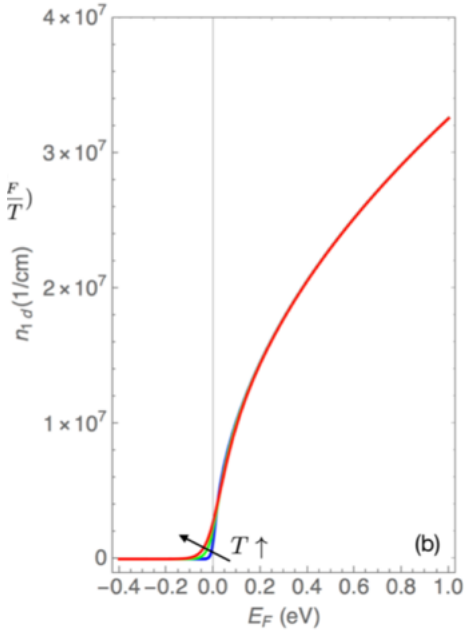

$$n_{1d}(T) = \frac{g_s g_v}{L}\sum_k f(k) = \frac{g_s g_v}{L}\int_{-\infty}^{+\infty}\frac{dk}{\frac{2\pi}{L}}\frac{1}{1+e^{\frac{\frac{\hbar^2k^2}{2m_e}-E_F^{1d}(T)}{k_bT}}} \qquad (5.22)$$

The dimensionless variables $u = (\frac{\hbar^2k^2}{2m_e})/k_bT$ and $\eta = E_F^{1d}(T)/k_bT$ convert the carrier density at any temperature to

$$n_{1d}(T) = \underbrace{g_s g_v(\frac{2\pi m_e k_b T}{h^2})^{\frac{1}{2}}}_{N_c^{1d}} F_{-\frac{1}{2}}(\frac{E_F}{k_bT}) = N_c^{1d}F_{-\frac{1}{2}}(\eta), \qquad (5.23)$$

From Ballistic conductance to Ohm's Law

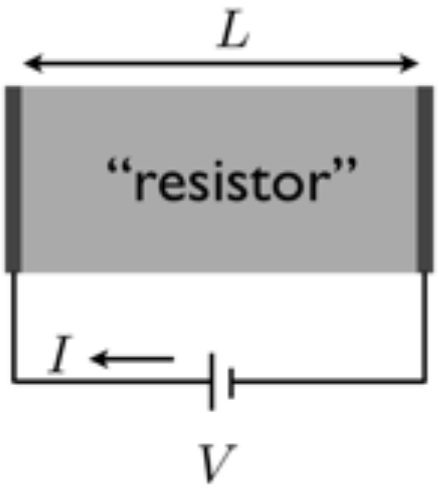

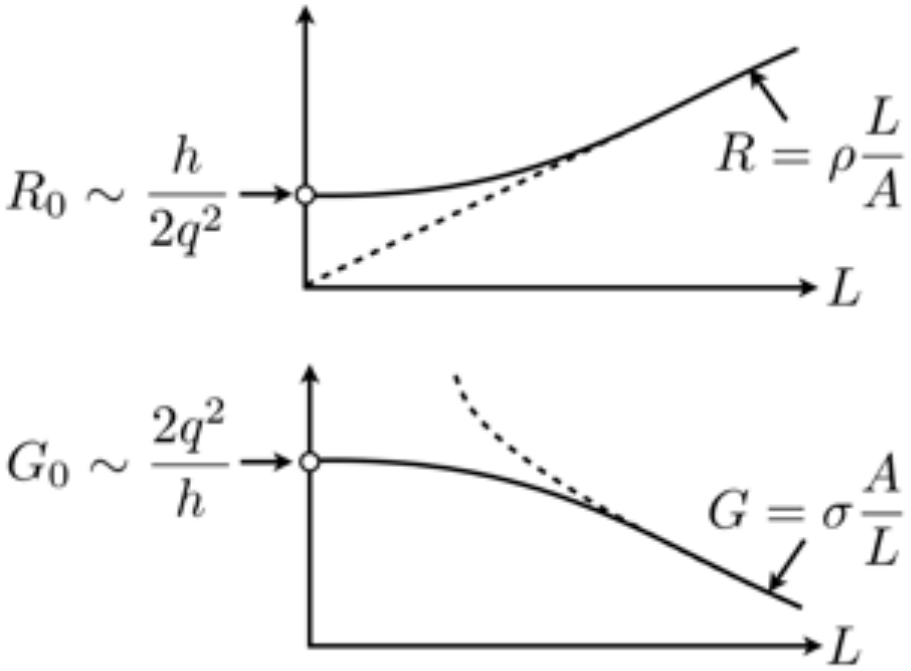

$$R = \frac{h}{2q^2} \cdot \frac{1}{M} \cdot (1 + \frac{L}{\lambda_{mfp}})$$

For $L >> \lambda_{mfp}$ and 3D: $M \sim k_F^2 A$
$\rightarrow R \sim \frac{h}{2q^2} \cdot \frac{1}{k_F^2 A} \cdot \frac{L}{\lambda_{mfp}}$ (Ohm's Law)

For $L << \lambda_{mfp}$ and 3D: $M \sim k_F^2 A$
$\rightarrow R \sim \frac{h}{2q^2} \cdot \frac{1}{k_F^2 A}$ (Sharvin resistance)

“Ballistic” Transport & Quantized Conductance

Experiments:

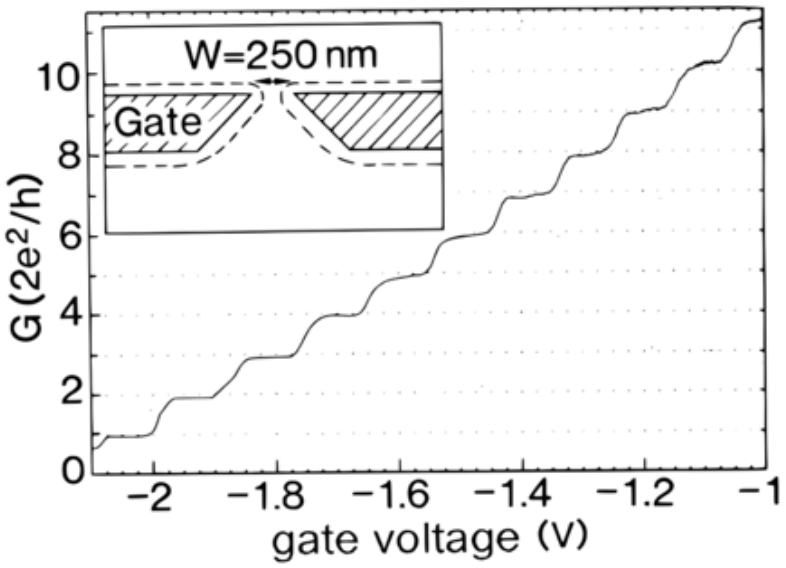

FIG. 44 Point contact conductance as a function of gate voltage at 0.6 K, demonstrating the conductance quantization in units of $2e^2/h$. The data are obtained from the two-terminal resistance after subtraction of a background resistance. The constriction width increases with increasing voltage on the gate (see inset). Taken from B. J. van Wees et al., Phys. Rev. Lett. **60**, 848 (1988).

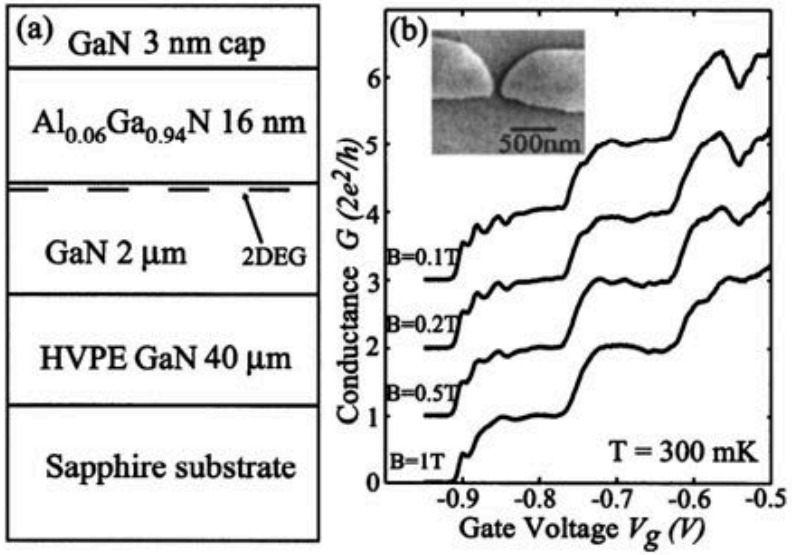

FIG. 1. (a) Schematic layer structure of the heterostructure. (b) improvement of plateau quantization with the application of a small magnetic field. Linear conductance $G(V_g)$ is plotted at magnetic field B=0.1 T, 0.2 T, 0.5 T, and 1 T. Traces are shifted vertically for clarity. Inset: micrograph of the QPC. The gap between the two split gates is 80 nm at its narrowest point. All experimental data shown in this letter were measured at 300 mK.

Appl. Phys. Lett. 86, 073108 (2005);

‘Ohmic’ Contacts as Fermi Fillers

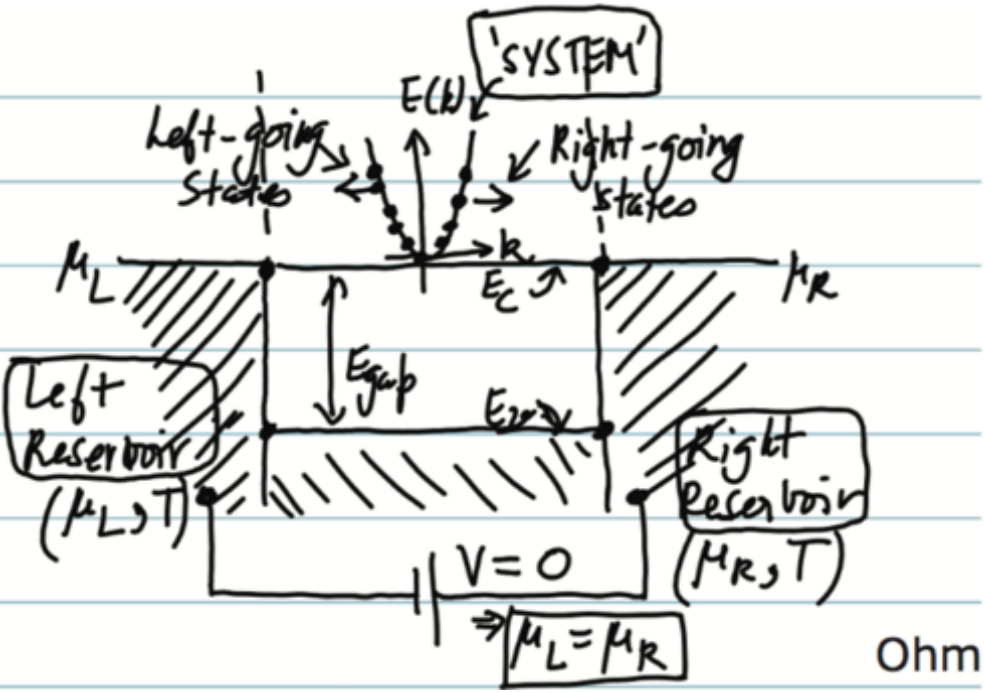

Ohmic

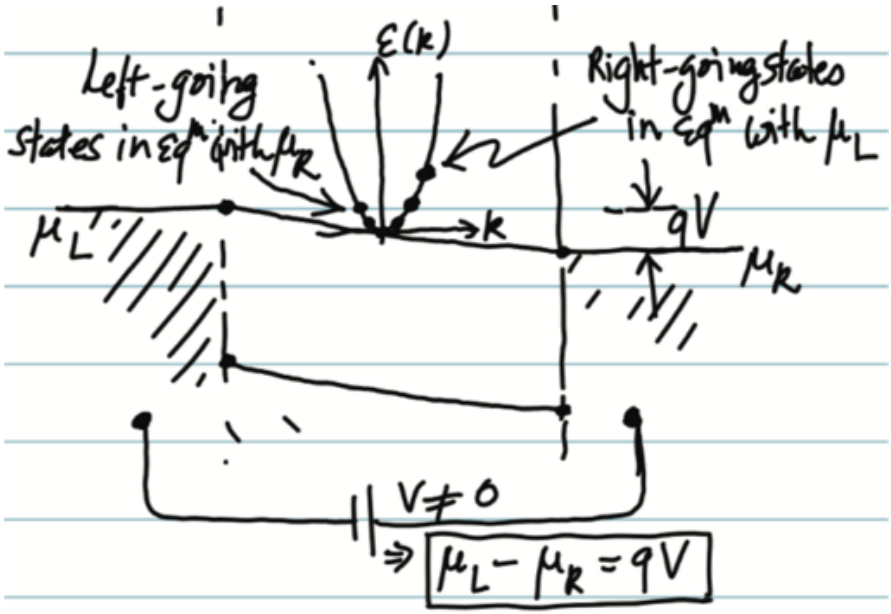

"Ballistic" Transport & Quantized Conductance

Many electrons:

$$\mathbf{F} = \hbar d\mathbf{k}/dt$$

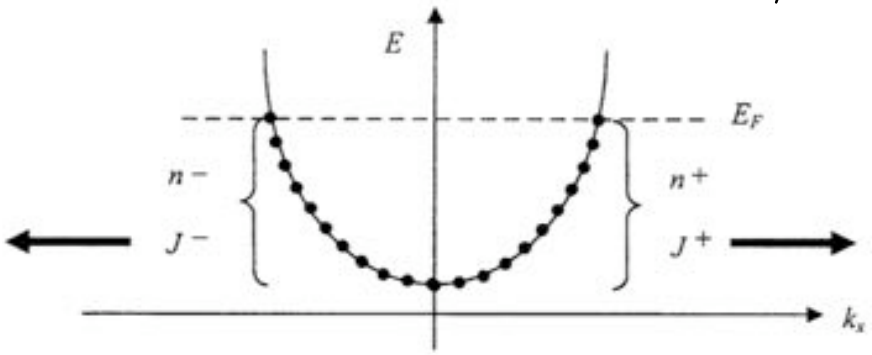

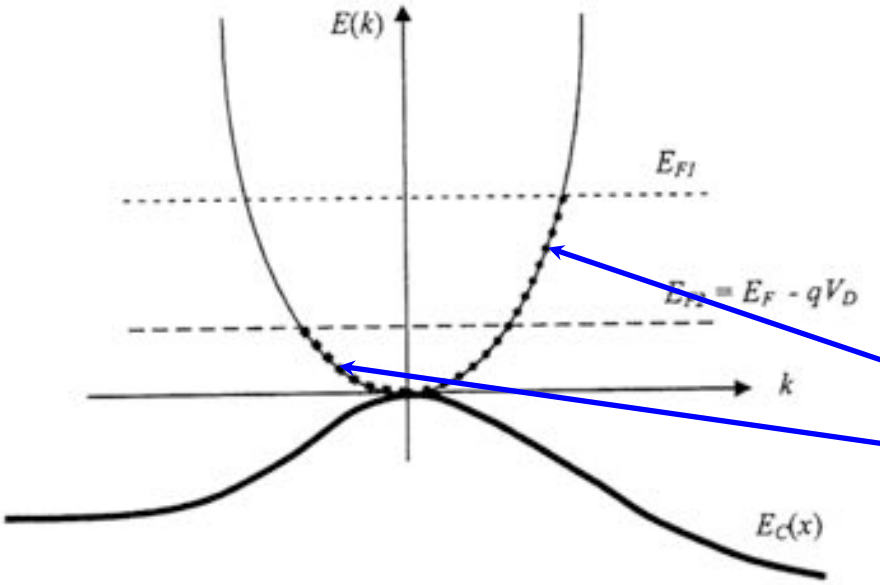

Most general expression for 'Current Density' in 'd' dimensions:

$$\mathbf{J_d} = q \times \frac{g_s g_v}{L^d} \sum_k \mathbf{v_g}(k) f(k), \text{ where}$$

g_s = spin degeneracy

g_v = valley degeneracy

$\mathbf{v_g} = \frac{1}{\hbar}\nabla\mathcal{E}(\mathbf{k})$ is the group velocity

$f(k)$ is the Fermi-Dirac function

Example: 1D current flow at $T = 0$ K :

$$J_1 = I = I^{\rightarrow} - I^{\leftarrow}$$

$$I^{\rightarrow} = \frac{2q}{h} E_{F1}$$

$$I^{\leftarrow} = \frac{2q}{h} E_{F2}$$

$$\rightarrow I = I^{\rightarrow} - I^{\leftarrow} = \frac{2q^2}{h} V_D$$

Quantum of conductance

Ballistic Transport in 1 Dimension

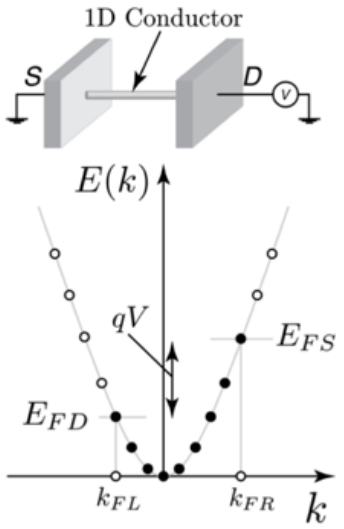

Fig. 5.5 Quantum picture of current flow in the 1D k-space due to a difference in the occupation functions of right-going and left-going eigenstates. The left contact is called the source, and the right contact the drain.

$$n_{1d}(T) = \frac{g_s g_v}{L}\sum_k f(k) = \frac{g_s g_v}{L}\int_{-\infty}^{+\infty}\frac{dk}{\frac{2\pi}{L}}\frac{1}{1+e^{\frac{\frac{\hbar^2k^2}{2m_e}-E_F^{1d}(T)}{k_bT}}} \qquad (5.22)$$

The dimensionless variables $u = (\frac{\hbar^2k^2}{2m_e})/k_bT$ and $\eta = E_F^{1d}(T)/k_bT$ convert the carrier density at any temperature to

$$n_{1d}(T) = \underbrace{g_s g_v(\frac{2\pi m_e k_b T}{h^2})^{\frac{1}{2}}}_{N_c^{1d}} F_{-\frac{1}{2}}(\frac{E_F}{k_bT}) = N_c^{1d}F_{-\frac{1}{2}}(\eta), \qquad (5.23)$$

$$\eta_s = \frac{E_{FS}}{k_bT},\ \eta_d = \frac{E_{Fd}}{k_bT},\ \text{and}\ v_d = \frac{qV}{k_bT}$$

$$E_{Fs} - E_{Fd} = qV$$

$$\eta_s - \eta_d = v_d$$

$$\eta_s - \eta_d = v_d,\ \text{and}\ n_{1d} = \frac{1}{2}N_c^{1d}(T)[F_{-\frac{1}{2}}(\eta_s) + F_{-\frac{1}{2}}(\eta_d)]$$

$$J^{1d} = J_R^{1d} - J_L^{1d} = \frac{qg_sg_v}{2\pi\hbar}(k_BT)\ln(\frac{1+e^{\eta_s}}{1+e^{\eta_d}}).$$

Ballistic Transport in 1 Dimension

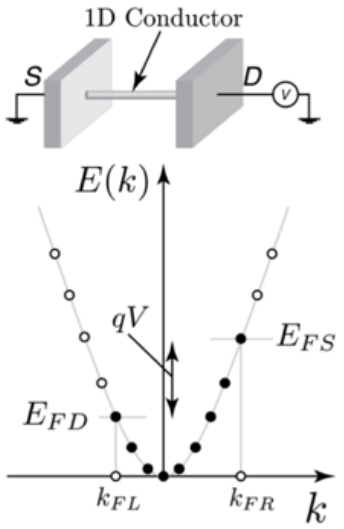

Fig. 5.5 Quantum picture of current flow in the 1D k-space due to a difference in the occupation functions of right-going and left-going eigenstates. The left contact is called the source, and the right contact the drain.

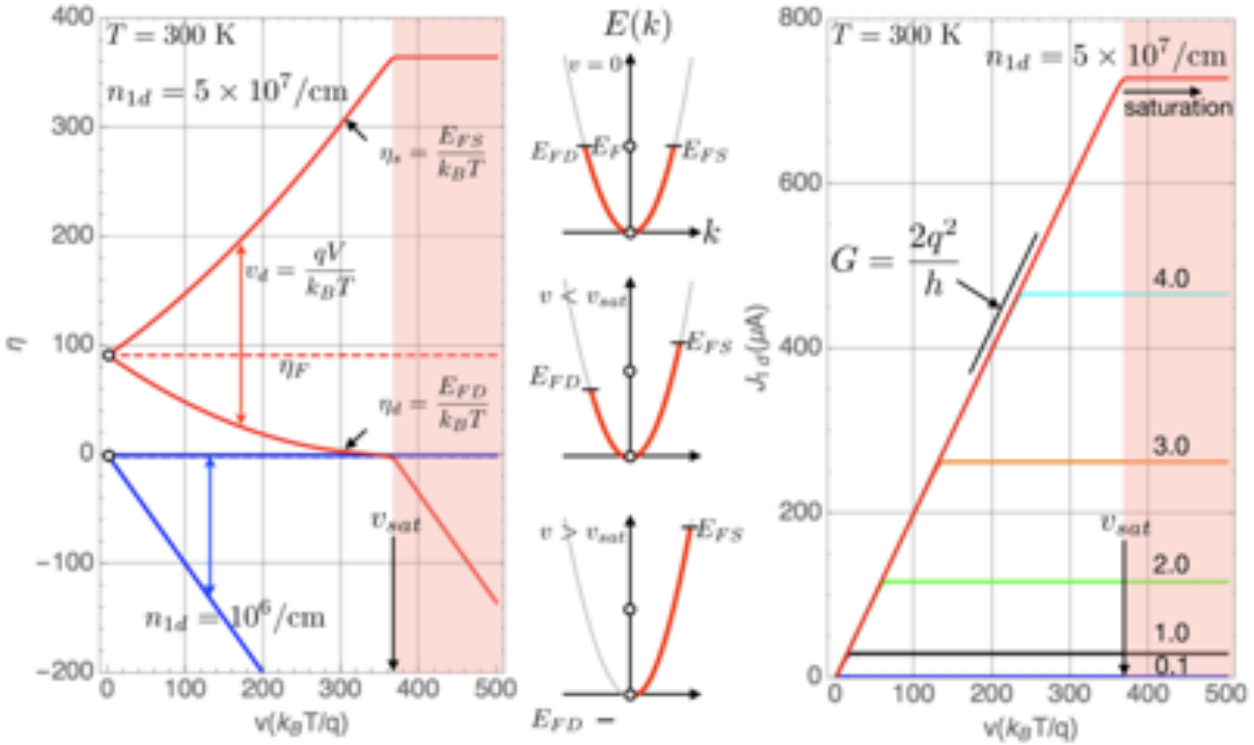

Fig. 5.8 The left plot shows the calcuated normalized Fermi level $\eta_F = E_F/k_BT$ at $V = 0$, and the split normalized Fermi levels η_s and η_d for nonzero normalized voltages $v_d = qV/k_BT$ for two values of 1D electron density at 300 K. The red curves are for $n_{1d} = 5 \times 10^7$/cm, and the blue for $n_{1d} = 10^6$/cm. The right plot shows the resulting quantum mechanical current flowing in response to the voltage for six values of 1D electron densities ranging from $0.1 - 5.0 \times 10^7$/cm. For example, at a 1D electron density of $n_{1d} = 10^7$/cm, the maximum (or saturation) current is ~ 70 μA. The middle $E(k)$ figures show the changes in the corresponding occupied electron states for $n_{1d} = 5 \times 10^7$/cm for three different voltages.

$$\eta_s - \eta_d = v_d, \text{ and } n_{1d} = \frac{1}{2} N_c^{1d}(T)[F_{-\frac{1}{2}}(\eta_s) + F_{-\frac{1}{2}}(\eta_d)]$$

$$J^{1d} = J_R^{1d} - J_L^{1d} = \frac{q g_s g_v}{2\pi\hbar}(k_B T)\ln\left(\frac{1+e^{\eta_s}}{1+e^{\eta_d}}\right).$$

Generalizing Ballistic Transport in d-Dimensions

$$\eta_s - \eta_d = v_d, \text{ and } n_{1d} = \frac{1}{2} N_c^{1d}(T)[F_{-\frac{1}{2}}(\eta_s) + F_{-\frac{1}{2}}(\eta_d)]$$

$$J^{1d} = J_R^{1d} - J_L^{1d} = \frac{q g_s g_v}{2\pi\hbar}(k_B T)\ln\left(\frac{1+e^{\eta_s}}{1+e^{\eta_d}}\right).$$

$$J_{1d} = \frac{q^2}{h} \cdot N_c^{0d} \cdot \frac{k_b T}{q} \cdot [F_0(\frac{E_{Fs} - E_c}{k_b T}) - F_0(\frac{E_{Fs} - E_c - qV}{k_b T})]$$

where $N_c^{0d} = g_s g_v = g_s g_v(\frac{2\pi m_e k_b T}{h^2})^0$

$$J_d = \frac{q^2}{h} \cdot N_c^{d-1} \cdot \frac{k_b T}{q} \cdot [F_{\frac{d-1}{2}}(\frac{E_{Fs} - E_c}{k_b T}) - F_{\frac{d-1}{2}}(\frac{E_{Fs} - E_c - qV}{k_b T})].$$

$$n_d = N_c^d F_{\frac{d-2}{2}}(\eta), \text{ where } N_c^d = g_s g_v(\frac{2\pi m_e k_b T}{h^2})^{\frac{d}{2}}$$

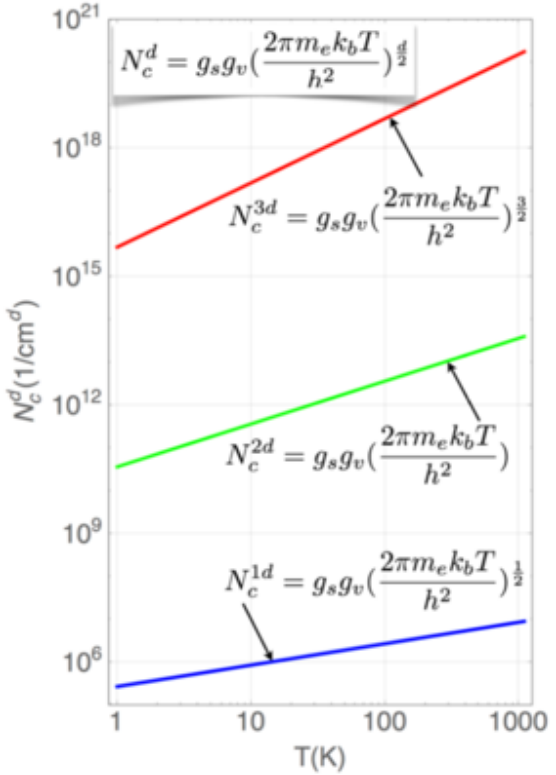

Fig. 5.5 The free electron band edge DOS N_c^d for $d = 1,2,3$ in units of $1/\text{cm}$ for 1d, $1/\text{cm}^2$ for 2d, and $1/\text{cm}^3$ for 3d.

Electrons in 2D

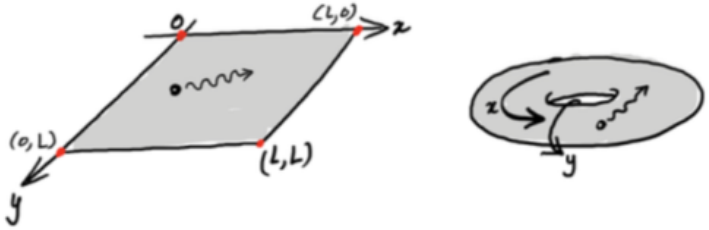

Fig. 5.5 Periodic boundary conditions in 2D leads to a Torus.

$$\psi(\mathbf{r}) = \frac{1}{\sqrt{L^2}} e^{i(k_x x + k_y y)} = \frac{1}{\sqrt{A}} e^{i\mathbf{k}\cdot\mathbf{r}}$$

$$\mathbf{k} = (k_{n_x}, k_{n_y}) = \frac{2\pi}{L}(n_x, n_y) \implies \mathbf{p} = \hbar\mathbf{k}, |\mathbf{p}| = \frac{h}{L}\sqrt{n_x^2 + n_y^2}$$

$$E(k_x, k_y) = \frac{\hbar^2}{2m_e}(k_{n_x}^2 + k_{n_y}^2) = E(n_x, n_y) = (n_x^2 + n_y^2)\frac{h^2}{2m_e L^2} = \frac{\hbar^2|\mathbf{k}|^2}{2m_e}$$

$$g_s g_v \frac{2\pi k dk}{(\frac{2\pi}{L})^2} = G_{2d}(E)dE \implies \frac{G_{2d}(E)}{L^2} = g_{2d}(E) = \frac{g_s g_v m_e}{2\pi\hbar^2}\Theta(E)$$

$$g_s g_v \frac{\pi k_F^2}{(\frac{2\pi}{L})^2} = N \implies k_F = \sqrt{\frac{4\pi n}{g_s g_v}}$$

If $g_s = 2$ and $g_v = 1$

$$k_F = \sqrt{2\pi n}$$

$n \sim 10^{12}/\text{cm}^2$ $\quad k_F \sim 2.5 \times 10^8/\text{m}$ $\quad \lambda_F = \frac{2\pi}{k_F} \sim 25$ nm

$n \sim 10^{16}/\text{cm}^2$ $\quad \lambda_F \sim 0.25$ nm

Electrons in 2D

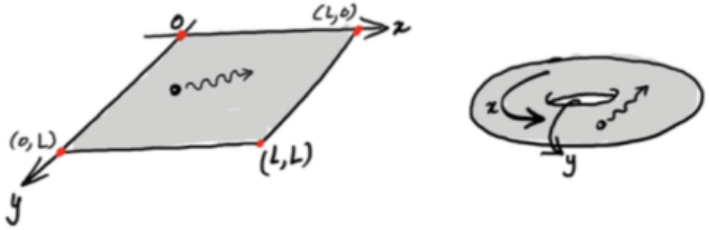

Fig. 5.5 Periodic boundary conditions in 2D leads to a Torus.

$$n = \int_0^\infty dE \cdot g_{2d}(E) \cdot f(E) = \frac{g_s g_v m_e k_B T}{2\pi\hbar^2} \ln(1+e^{\frac{E_F}{k_B T}}) \implies \boxed{E_F = k_B T \ln(e^{\frac{n}{n_q}} - 1)}$$

$$\mathcal{U} = \int_0^\infty dE \cdot E \cdot G_{2d}(E) \cdot f(E) \implies \boxed{u_{2d} = \frac{\mathcal{U}}{N} = \frac{\int_0^\infty dE \cdot E \cdot G_{2d}(E) \cdot f(E)}{\int_0^\infty dE \cdot G_{2d}(E) \cdot f(E)} = \frac{1}{2} E_F}$$

$$\boxed{u_v(2d) = \frac{1}{2} n E_F}$$

$$\boxed{\mathbf{J}(\mathbf{k}) = \frac{q}{2m_e}(\psi^\star \hat{\mathbf{p}} \psi - \psi \hat{\mathbf{p}} \psi^\star) = q \cdot \frac{1}{A} \cdot \frac{\hbar \mathbf{k}}{m_e} = q(\frac{1}{A}) \mathbf{v}_g(\mathbf{k})}$$

Quantum Mechanical Current

Electrons in 2D

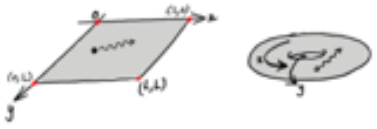

Fig. 5.9 Periodic boundary conditions in 2D leads to a Torus.

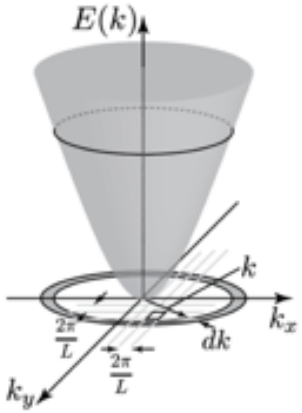

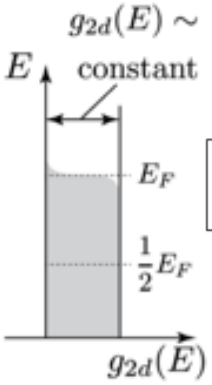

$$g_{2d}(E) = \frac{g_s g_v m_e}{2\pi\hbar^2}\Theta(E).$$

Fig. 5.10 Energy eigenvalues and density of states for free electrons in 2 dimensions.

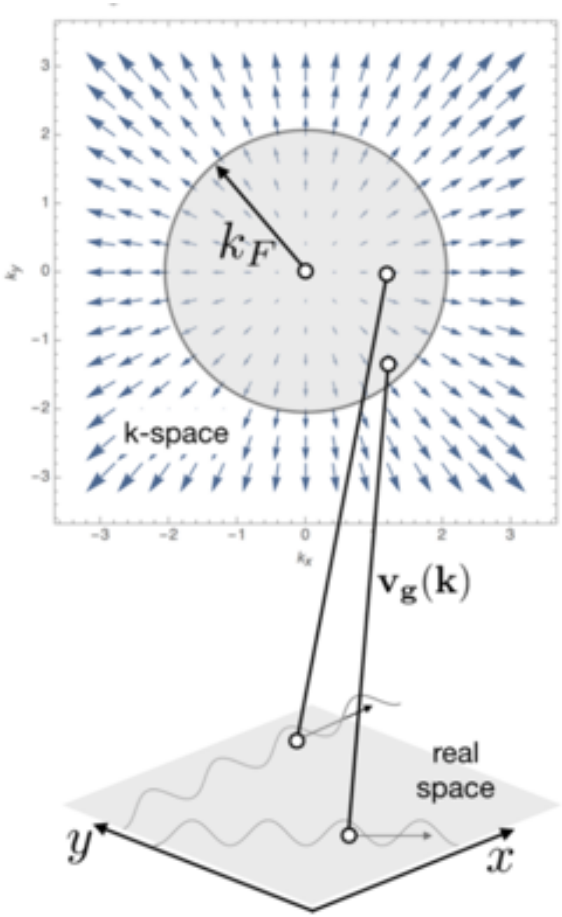

Fig. 5.13 Group velocity of 2D electrons in the $\mathbf{k}-$space, and its relation to transport in real space.

Electrons in 2D

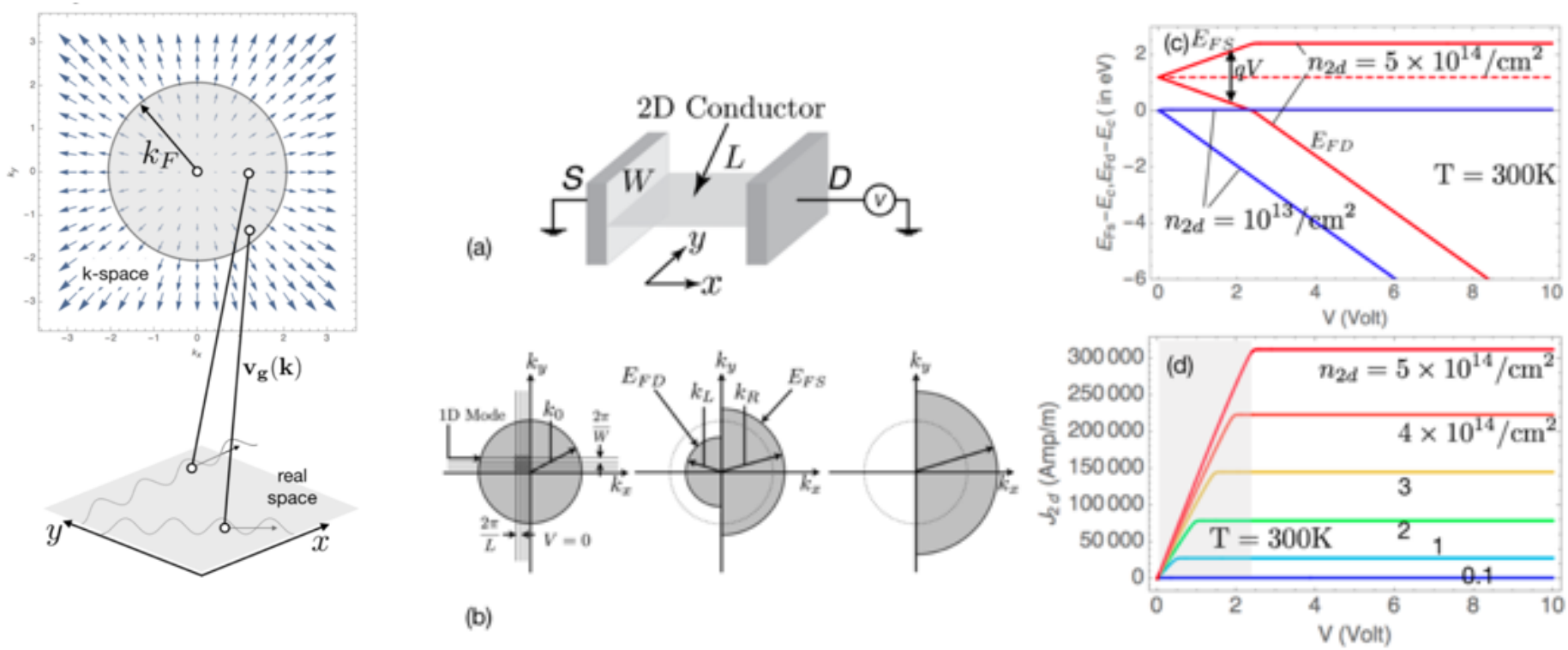

Fig. 5.13 Group velocity of 2D electrons in the **k**−space, and its relation to transport in real space.

Electrons in 3D

$$\psi(\mathbf{r}) = \frac{1}{\sqrt{L^3}} e^{i(k_x x + k_y y + k_z z)} = \frac{1}{\sqrt{V}} e^{i\mathbf{k}\cdot\mathbf{r}}$$

$$\mathbf{k} = (k_{n_x}, k_{n_y}, k_{n_z}) = \frac{2\pi}{L}(n_x, n_y, n_z) \implies \mathbf{p} = \hbar\mathbf{k}, |\mathbf{p}| = \frac{h}{L}\sqrt{n_x^2 + n_y^2 + n_z^2}$$

$$E(k_x, k_y, k_z) = \frac{\hbar^2}{2m_e}(k_{n_x}^2 + k_{n_y}^2 + k_{n_z}^2) = (n_x^2 + n_y^2 + n_z^2)\frac{h^2}{2m_e L^2} = \frac{\hbar^2 |\mathbf{k}|^2}{2m_e}$$

$$g_s g_v \frac{4\pi k^2 dk}{(\frac{2\pi}{L})^3} = G_{3d}(E)dE \implies \frac{G_{3d}(E)}{L^3} = g_{3d}(E) = \frac{g_s g_v}{4\pi^2}(\frac{2m_e}{\hbar^2})^{\frac{3}{2}}\sqrt{E}$$

$$g_s g_v \frac{\frac{4}{3}\pi k_F^3}{(\frac{2\pi}{L})^3} = N \implies k_F = (\frac{6\pi^2 n}{g_s g_v})^{\frac{1}{3}}$$

If $g_s = 2$ and $g_v = 1$

$$k_F = (3\pi^2 n)^{\frac{1}{3}}$$

3D Fermi Wavevector

$n \sim 10^{24}/\text{cm}^3$ $\quad k_F \sim 3 \times 10^{10}/\text{m}$ $\quad \lambda_F \sim 0.2$ nm

Electrons in 3D

$$n = \int_0^\infty dE \cdot g_{3d}(E) \cdot f(E) = \frac{g_s g_v}{4\pi^2} \left(\frac{2m_e}{\hbar^2}\right)^{\frac{3}{2}} \int_0^\infty dE \cdot \sqrt{E} \cdot f(E) = n_{3d} F_{\frac{1}{2}}(\eta)$$

$$\mathcal{U} = \int_0^\infty dE \cdot E \cdot G_{3d}(E) \cdot f(E) \implies \boxed{u_{3d} = \frac{\mathcal{U}}{N} = \frac{\int_0^\infty dE \cdot E \cdot G_{3d}(E) \cdot f(E)}{\int_0^\infty dE \cdot G_{3d}(E) \cdot f(E)} = \frac{3}{5} E_F}$$

$$\boxed{u_v(3d) = \frac{3}{5} n E_F}$$

Average energy density of a 3D Fermi Gas

Electrons in 3D

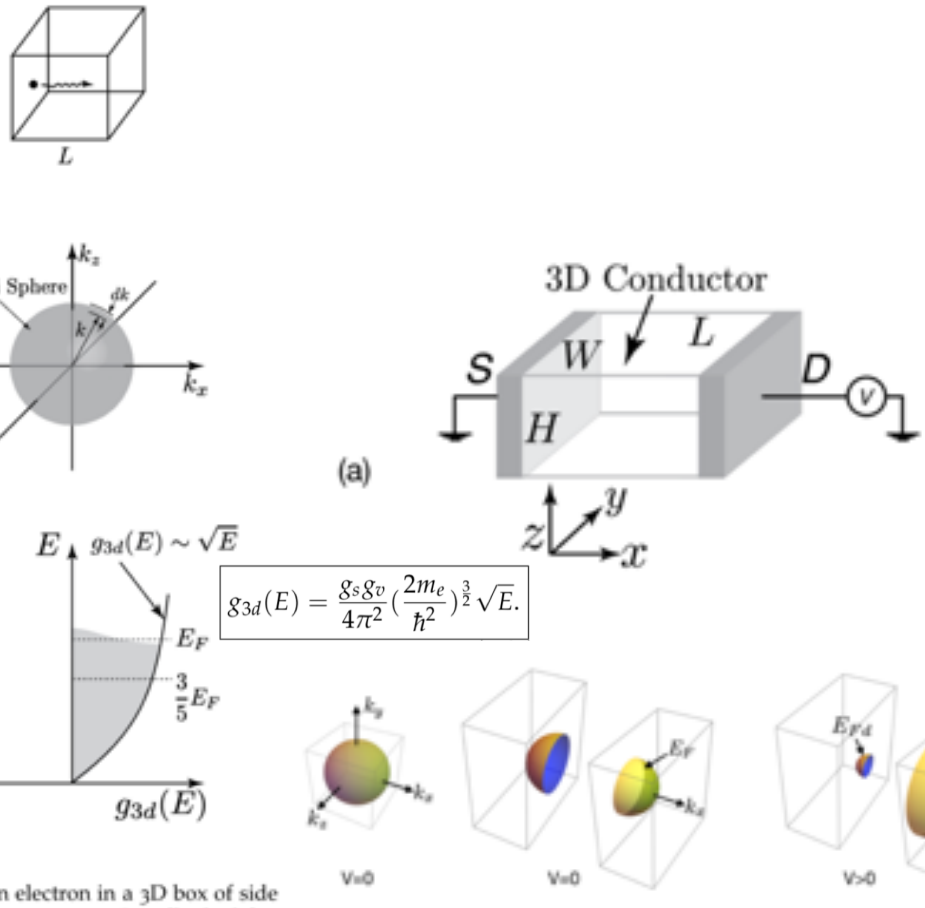

Fig. 5.15 An electron in a 3D box of side L can have wavevectors $\mathbf{k} = (k_x, k_y, k_z) = \frac{2\pi}{L}(n_x, n_y, n_z)$ which form a discrete grid in the 3D **k**-space. When N electrons are filled in the box, the **k**-states are filled inside the Fermi sphere such that the states on the Fermi sphere surface have energy E_F. The density of states for free electrons in 3 dimensions showing the $\sqrt{E}$ dependence, the Fermi level, and the average energy of the electron distribution.

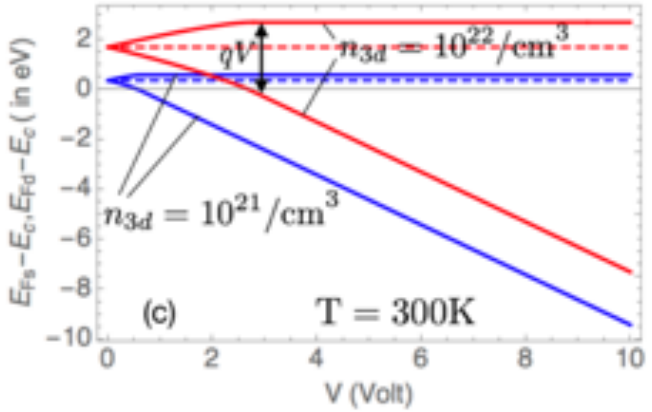

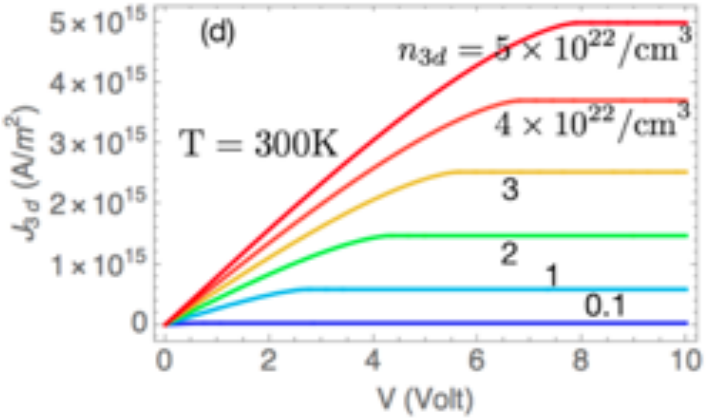

Ballistic Transport in 1, 2, and 3 Dimensions

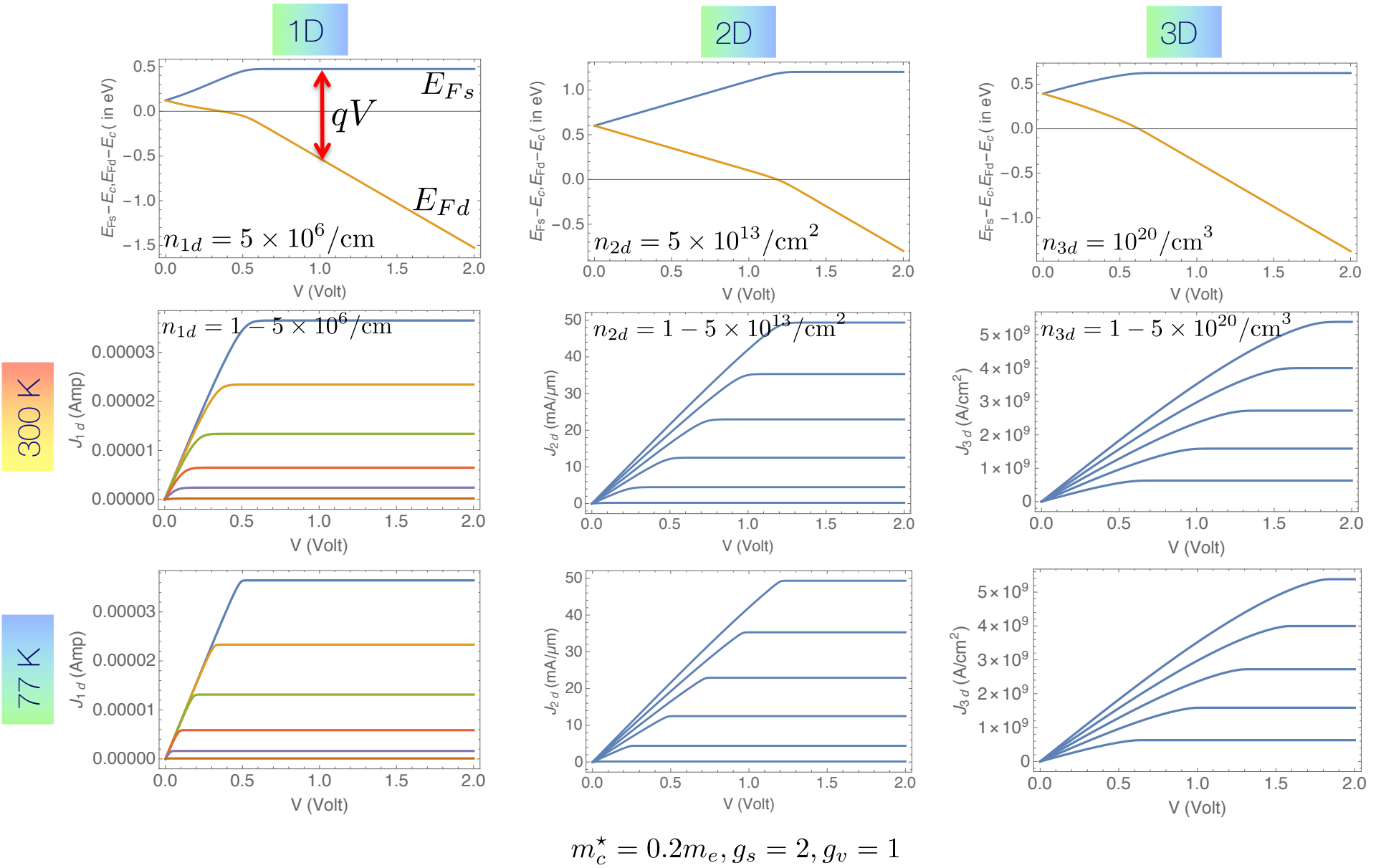

$$m_c^\star = 0.2 m_e, g_s = 2, g_v = 1$$

Semiconductor Physics Summary

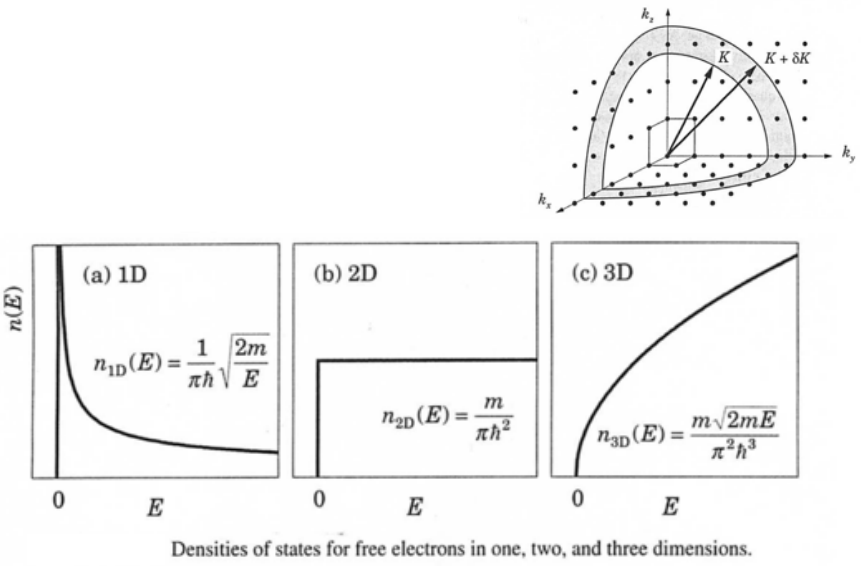

Densities of states for free electrons in one, two, and three dimensions.

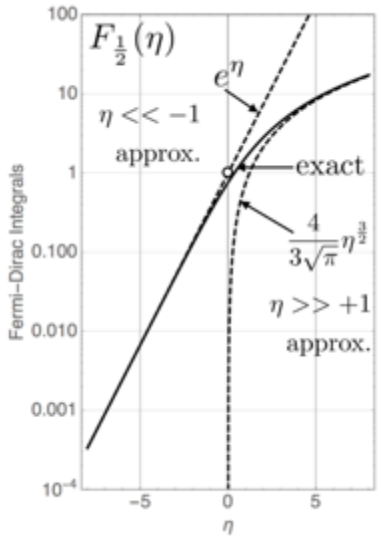

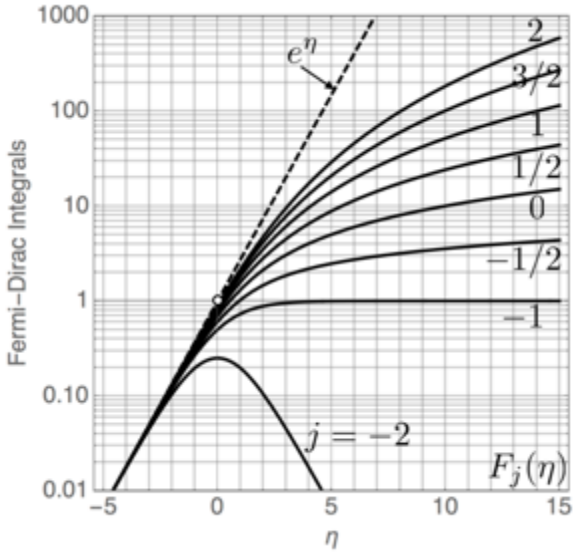

	0 Dimension	1 Dimension	2 Dimensions	3 Dimensions	d Dimensions
Conduction Bandstructure	E_c	$E_c + \frac{\hbar^2 k^2}{2m^*}$	$E_c + \frac{\hbar^2}{2m^*}(k_x^2 + k_y^2)$	$E_c + \frac{\hbar^2}{2m^*}(k_x^2 + k_y^2 + k_z^2)$	$E_c + \frac{\hbar^2}{2m^*}(k_1^2 + \ldots + k_d^2)$
Conduction Band DOS $g_c^d(E)$	$g_c(E) = \delta(E - E_{cm})$	$g_c(E) = \frac{4\sqrt{2}}{h}(m^*)^{\frac{1}{2}}\frac{1}{\sqrt{E - E_c}}$	$g_c(E) = \frac{4\pi}{h^2}m^* H(E - E_c)$	$g_c(E) = \frac{4\pi}{h^3}(2m^*)^{\frac{3}{2}}\sqrt{E - E_c}$	$g_c(E) = \frac{4\pi^{\frac{d}{2}}}{h^d\Gamma(\frac{d}{2})}(2m^*)^{\frac{d}{2}}(E - E_c)^{\frac{d}{2}-1}$
Conduction Band-Edge Effective DOS N_c^d	$g_c\delta(\cdot)$	$g_c\delta(\frac{2\pi m^* k_B T}{h^2})\frac{1}{2}$	$g_c\delta(\frac{2\pi m^* k_B T}{h^2})$	$g_c\delta(\frac{2\pi m^* k_B T}{h^2})\frac{3}{2}$	$g_c\delta(\frac{2\pi m^* k_B T}{h^2})\frac{d}{2}$
Electron Density n_d	–	$N_c^{1D}F_{-\frac{1}{2}}(\frac{E_F - E_c}{k_B T})$	$N_c^{2D}F_0(\frac{E_F - E_c}{k_B T})$	$N_c^{3D}F_{\frac{1}{2}}(\frac{E_F - E_c}{k_B T})$	$N_c^{dD}F_{\frac{d}{2}-1}(\frac{E_F - E_c}{k_B T})$
Source Fermi Level E_{Fs} under bias V	–	$n_{1d} = \frac{1}{2}N_c^{1D}F_{-\frac{1}{2}}(\frac{E_F - E_c}{k_B T}) + F_{-\frac{1}{2}}(\frac{E_F - E_c - qV}{k_B T})$	$n_{2d} = \frac{1}{2}N_c^{2D}F_0(\frac{E_F - E_c}{k_B T}) + F_0(\frac{E_F - E_c - qV}{k_B T})$	$n_{3d} = \frac{1}{2}N_c^{3D}F_{\frac{1}{2}}(\frac{E_F - E_c}{k_B T}) + F_{\frac{1}{2}}(\frac{E_F - E_c - qV}{k_B T})$	$n_d = \frac{1}{2}N_c^{dD}F_{\frac{d}{2}-1}(\frac{E_F - E_c}{k_B T}) + F_{\frac{d}{2}-1}(\frac{E_F - E_c - qV}{k_B T})$
Ballistic Electron Current Density J_d at voltage V	–	$\frac{q}{h}\cdot N_c^{1D}\cdot\frac{k_B T}{2}\cdot[F_0(\frac{E_F - E_c}{k_B T}) - F_0(\frac{E_F - E_c - qV}{k_B T})]$	$\frac{q}{h}\cdot N_c^{2D}\cdot\frac{k_B T}{2}\cdot[F_{\frac{1}{2}}(\frac{E_F - E_c}{k_B T}) - F_{\frac{1}{2}}(\frac{E_F - E_c - qV}{k_B T})]$	$\frac{q}{h}\cdot N_c^{3D}\cdot\frac{k_B T}{2}\cdot[F_1(\frac{E_F - E_c}{k_B T}) - F_1(\frac{E_F - E_c - qV}{k_B T})]$	$\frac{q}{h}\cdot N_c^{d-1}\cdot\frac{k_B T}{2}\cdot[F_{\frac{d}{2}}(\frac{E_F - E_c}{k_B T}) - F_{\frac{d}{2}}(\frac{E_F - E_c - qV}{k_B T})]$
Valence Bandstructure	E_v	$E_v - \frac{\hbar^2 k^2}{2m^*}$	$E_v - \frac{\hbar^2}{2m^*}(k_x^2 + k_y^2)$	$E_v - \frac{\hbar^2}{2m^*}(k_x^2 + k_y^2 + k_z^2)$	$E_v - \frac{\hbar^2}{2m^*}(k_1^2 + \ldots + k_d^2)$
Valence Band DOS $g_v^d(E)$	$g_v\delta(E - E_{vm})$	$g_v(\frac{4\sqrt{2}}{h})(m^*)^{\frac{1}{2}}\frac{1}{\sqrt{E_v - E}}$	$g_v(\frac{4\pi}{h^2})m^* H(E_v - E)$	$g_v(\frac{4\pi}{h^3})(2m^*)^{\frac{3}{2}}\sqrt{E_v - E}$	$\frac{g_v 4\pi^{\frac{d}{2}}}{h^d\Gamma(\frac{d}{2})}(2m^*)^{\frac{d}{2}}(E_v - E)^{\frac{d}{2}-1}$
Valence Band-Edge Effective DOS N_v^d	–	$g_v\delta(\frac{2\pi m^* k_B T}{h^2})\frac{1}{2}$	$g_v\delta(\frac{2\pi m^* k_B T}{h^2})$	$g_v\delta(\frac{2\pi m^* k_B T}{h^2})\frac{3}{2}$	$g_v\delta(\frac{2\pi m^* k_B T}{h^2})\frac{d}{2}$
Hole Density p_d	–	$N_v^{1D}F_{-\frac{1}{2}}(\frac{E_v - E_F}{k_B T})$	$N_v^{2D}F_0(\frac{E_v - E_F}{k_B T})$	$N_v^{3D}F_{\frac{1}{2}}(\frac{E_v - E_F}{k_B T})$	$N_v^{dD}F_{\frac{d}{2}-1}(\frac{E_v - E_F}{k_B T})$
Source Fermi Level E_{Fs} under bias V	–	$p_{1d} = \frac{1}{2}N_v^{1D}F_{-\frac{1}{2}}(\frac{E_v - E_F}{k_B T}) + F_{-\frac{1}{2}}(\frac{E_v - E_F - qV}{k_B T})$	$p_{2d} = \frac{1}{2}N_v^{2D}F_0(\frac{E_v - E_F}{k_B T}) + F_0(\frac{E_v - E_F - qV}{k_B T})$	$p_{3d} = \frac{1}{2}N_v^{3D}F_{\frac{1}{2}}(\frac{E_v - E_F}{k_B T}) + F_{\frac{1}{2}}(\frac{E_v - E_F - qV}{k_B T})$	$p_d = \frac{1}{2}N_v^{dD}F_{\frac{d}{2}-1}(\frac{E_v - E_F}{k_B T}) + F_{\frac{d}{2}-1}(\frac{E_v - E_F - qV}{k_B T})$
Ballistic Hole Current Density J_d	–	$\frac{q}{h}\cdot N_v^{1D}\cdot\frac{k_B T}{2}\cdot[F_0(\frac{E_v - E_F}{k_B T}) - F_0(\frac{E_v - E_F - qV}{k_B T})]$	$\frac{q}{h}\cdot N_v^{2D}\cdot\frac{k_B T}{2}\cdot[F_{\frac{1}{2}}(\frac{E_v - E_F}{k_B T}) - F_{\frac{1}{2}}(\frac{E_v - E_F - qV}{k_B T})]$	$\frac{q}{h}\cdot N_v^{3D}\cdot\frac{k_B T}{2}\cdot[F_1(\frac{E_v - E_F}{k_B T}) - F_1(\frac{E_v - E_F - qV}{k_B T})]$	$\frac{q}{h}\cdot N_v^{d-1}\cdot\frac{k_B T}{2}\cdot[F_{\frac{d}{2}}(\frac{E_v - E_F}{k_B T}) - F_{\frac{d}{2}}(\frac{E_v - E_F - qV}{k_B T})]$

Physics of Semiconductor Nanostructures Summary

Table 1: Quantum Electronic, Photonic, and Statistical Properties of Conduction and Valence Band Electrons in Semiconductor Nanostructures.

- E_c is the band edge, and m_c^* the effective mass of the conduction band. E_v is the band edge, and m_v^* the effective mass of the valence band.
- For low dimensions, E_c and E_v, and the bandgap $E_g = E_c - E_v$ include the quantum confinement energies if present.
- h is Planck's constant, $\hbar = \frac{h}{2\pi}$, k_b is the Boltzmann constant, and q the electron charge.
- g_s is the spin degeneracy, and g_v the valley degeneracy.
- $F_j(\eta) = \frac{1}{\Gamma(j+1)} \int_0^\infty d\varepsilon \frac{\varepsilon^j}{1+e^{\varepsilon-\eta}}$ is the Fermi-Dirac integral of order j, and $\Gamma(...)$ is the Gamma function.
- E_f is the Fermi level at equilibrium. E_{fs} is the source quasi-Fermi level and E_{fd} the drain quasi-Fermi level.
- Similarly, F_n is the conduction band quasi-Fermi level and F_p is the valence band quasi-Fermi level.
- $h\nu$ is the photon energy of frequency ν, and L_x, L_y, L_z are the dimensions of the semiconductor nanostructure.
- A and B are the Einstein A and B coefficients, $\lambda_0 = c/\nu$ the wavelength of the photon in vacuum, and n the refractive index of the semiconductor.
- $f_c(E_2) = 1/[1 + e^{\frac{E_2 - F_n}{k_b T}}]$ is the Fermi-Dirac occupation function of state $E_2 = E_c + \frac{\hbar^2 k^2}{2m_c^*}$ in the conduction band.
- $f_v(E_1) = 1/[1 + e^{\frac{E_1 - F_p}{k_b T}}]$ is the Fermi-Dirac occupation function of state $E_1 = E_v - \frac{\hbar^2 k^2}{2m_v^*}$ in the valence band.
- $E_2 - E_1 = h\nu = E_g + \frac{\hbar^2 k^2}{2m_r^*}$ is the energy of the photon emitted when the electron transitions from $E_2 \to E_1$ radiatively.
- The Einstein A and B coefficients are related by $\frac{A}{B} = \frac{8\pi n^3 \nu^3 h}{c^3}$.
- The photon density is $\rho_\nu = I_\nu/(c/n)$ in eV/cm^3, c/n is the speed of light in a media of refractive index n, and $I_\nu = E_0^2/2\eta$ in W/cm^2 is the Poynting energy density with electric field amplitude E_0 and wave impedance η.

Prelim 1 for ECE 4070 / MSE 6050

- Tuesday March 5th 2019
- Time: 7:30 – 9:00 pm
- In Phillips Hall 219 (Note: different from class location!)

- No restrictions on books/notes/calculators/computers etc.
- Bring pen/pencil – exam books will be provided.
- Questions: conceptual, no heavy number crunching will be needed.
- Previous year questions fairly representative of what to expect.
- Topics covered: Chapters 1-5 from the Notes.

Exams and Grades:
An assignment every 1.5 weeks. Total of 6-8 homework assignments per semester. Exams: 2 Evening Prelim Exams and 1 Final Exam. Here is the approximate breakup of scores that will go towards your final grade:
35% Assignments
15% Prelim 1 [Tuesday March 5th, 2019]
20% Prelim 2 [Thursday April 11th, 2019]
30% Final [Wednesday May 15th, 2019]

Energy Bands of Si, Ge, and GaAs for Reference

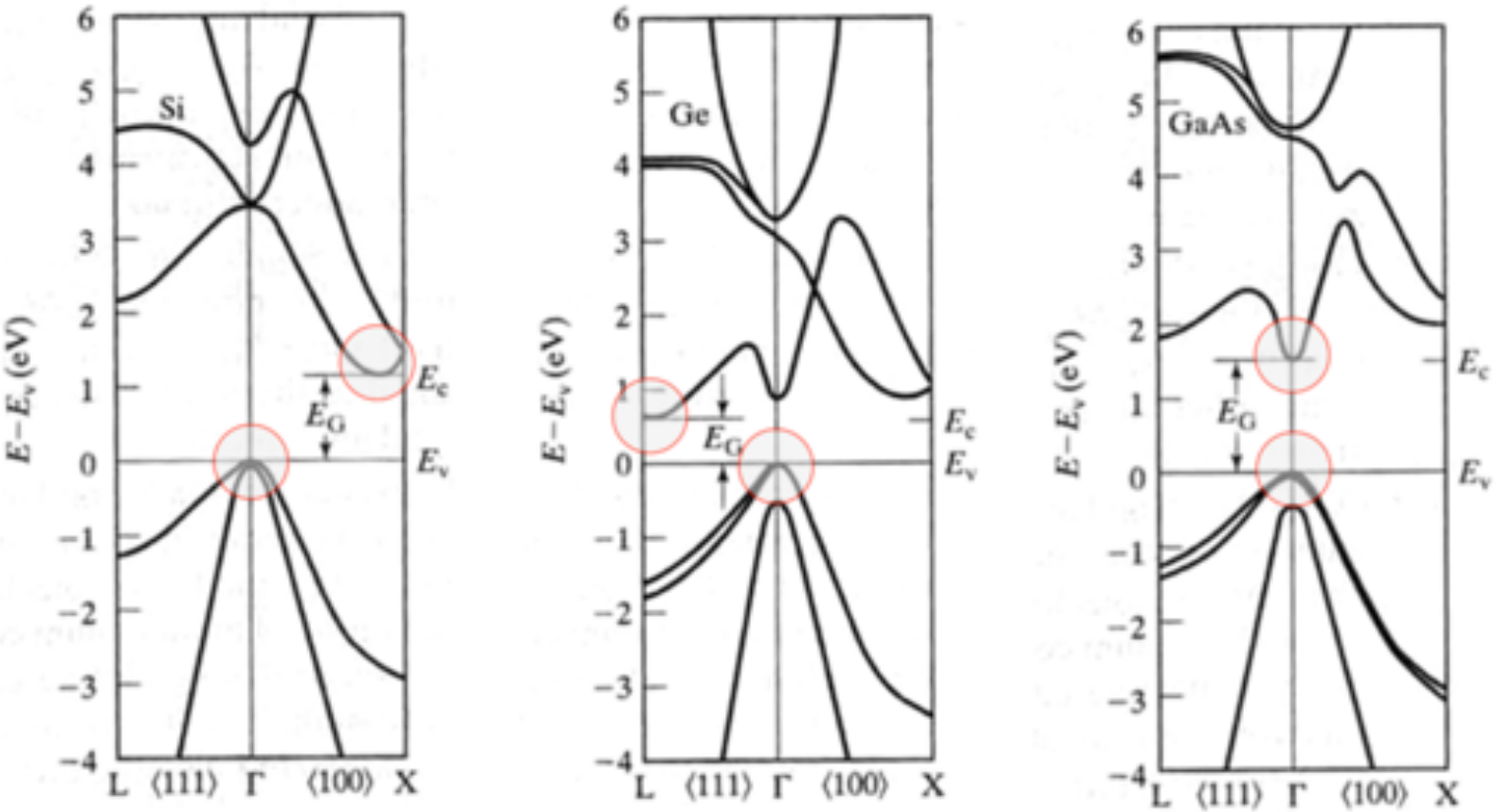

ECE 4070 / MSE 6050
Energy Bandstructures of the most common Semiconductors

Semiconductors: Quantum Energy Eigenvalues

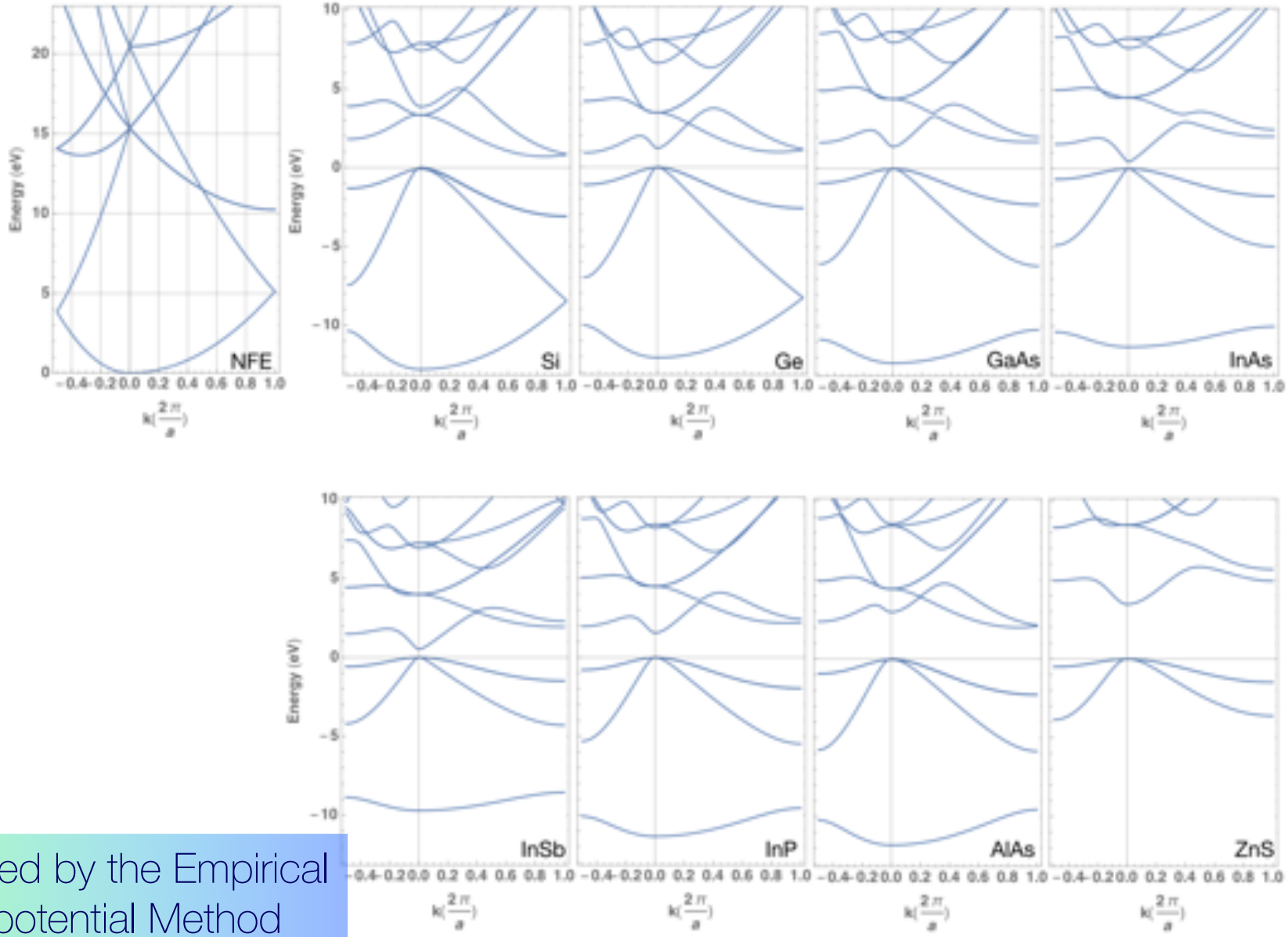

- Calculated by the Empirical Pseudopotential Method

The Nearly Free Electron Model for Any FCC Lattice

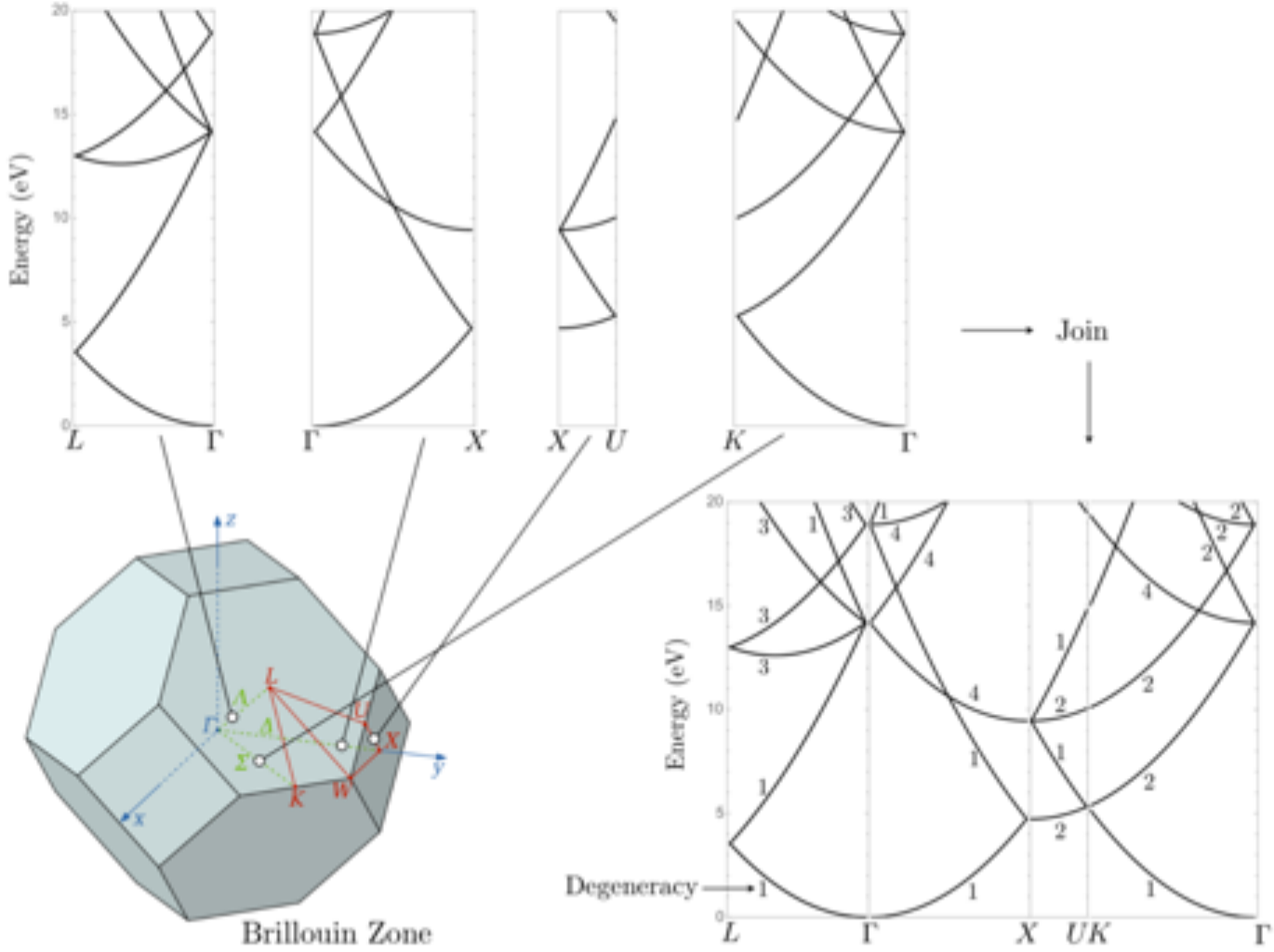

Fig. 9.5 Nearly Free Electron Bandstructure for the FCC Lattice. Silicon, Ge, GaAs, Diamond, and many semiconductors have a FCC real-space lattice with 2-atom bases. The nearly free electron bandstructure shown here is representative of all semiconductors that share the same real-space lattice.

Electrons in a Crystal are not Exactly Free…

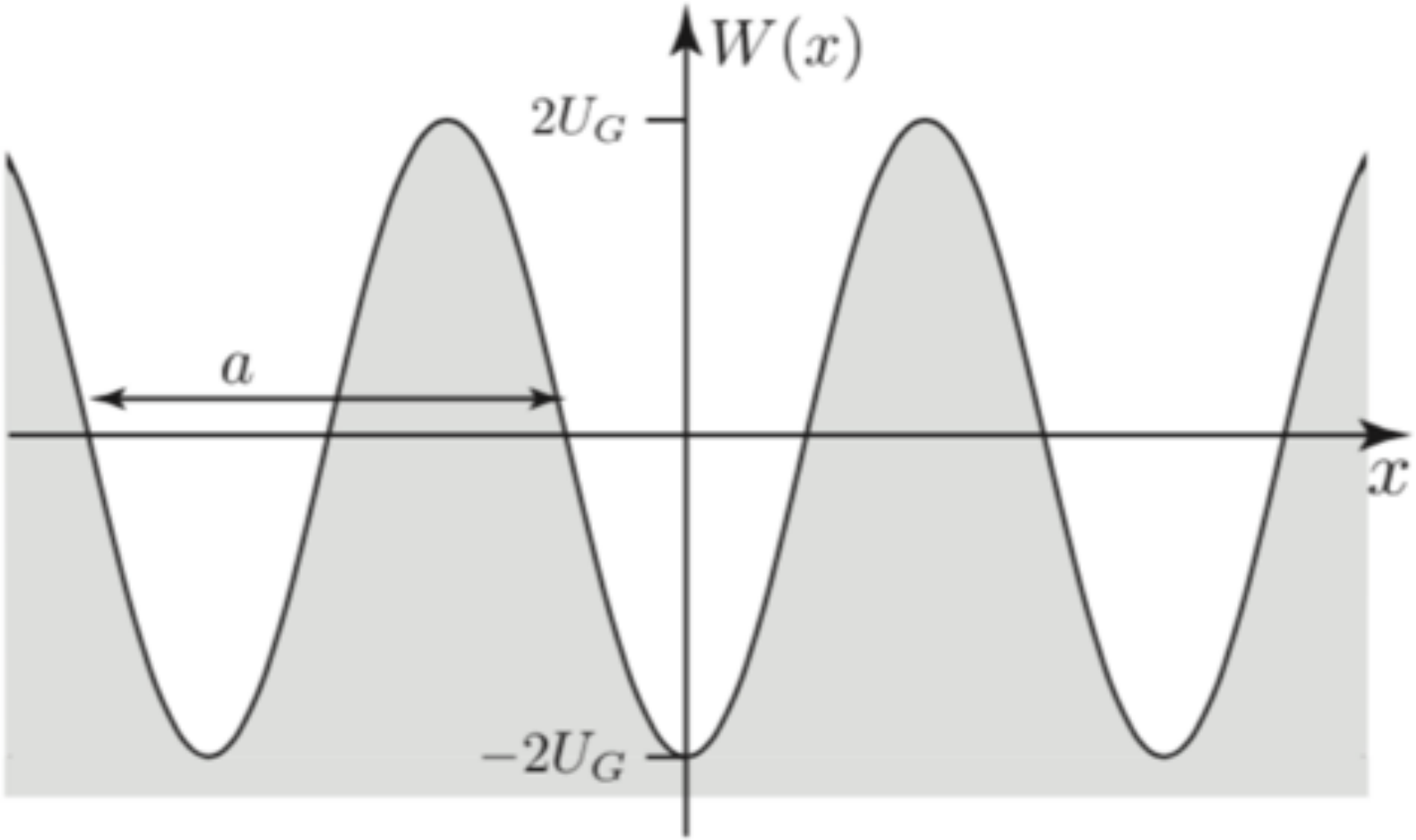

- The Periodic Potential for electrons in a crystal

Electrons in a Crystal are not Exactly Free…

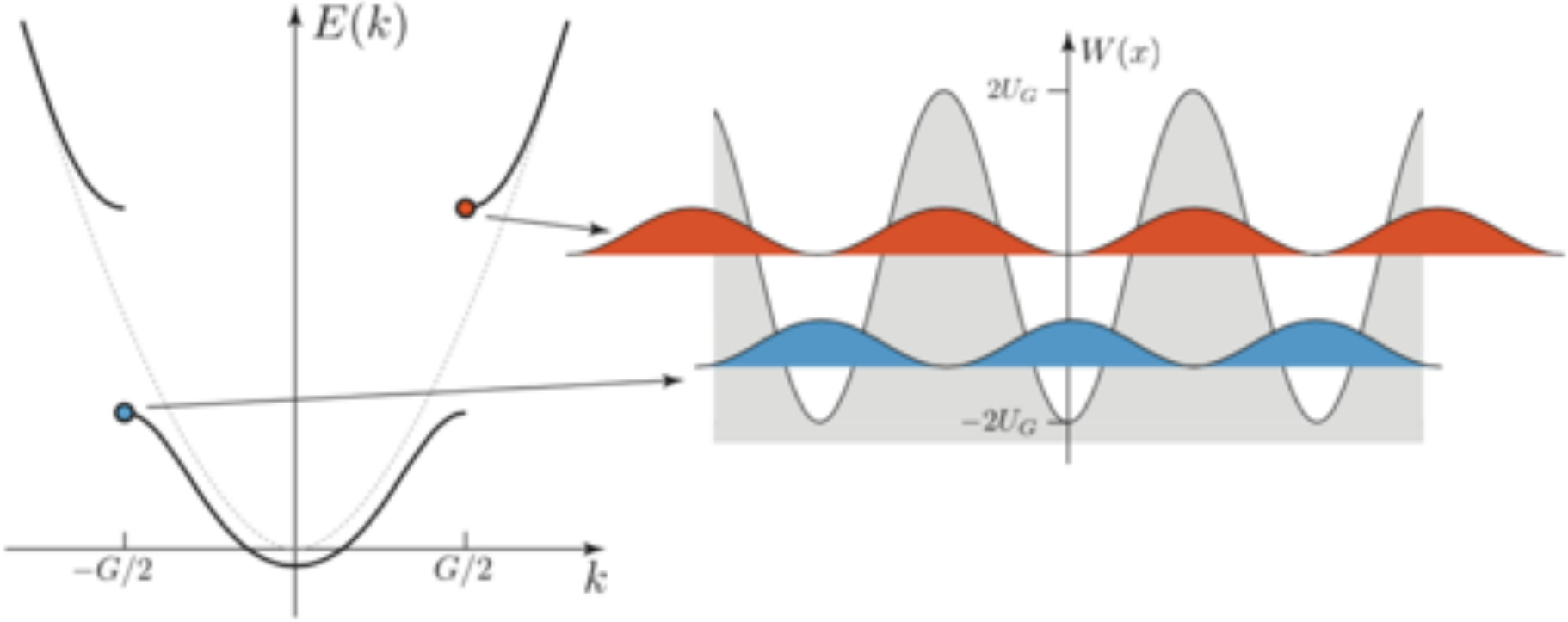

- The Periodic Potential in a crystal causes standing waves for electrons.
- It splits the allowed energies into bands separated by gaps

Electrons in a Crystal are not Exactly Free…

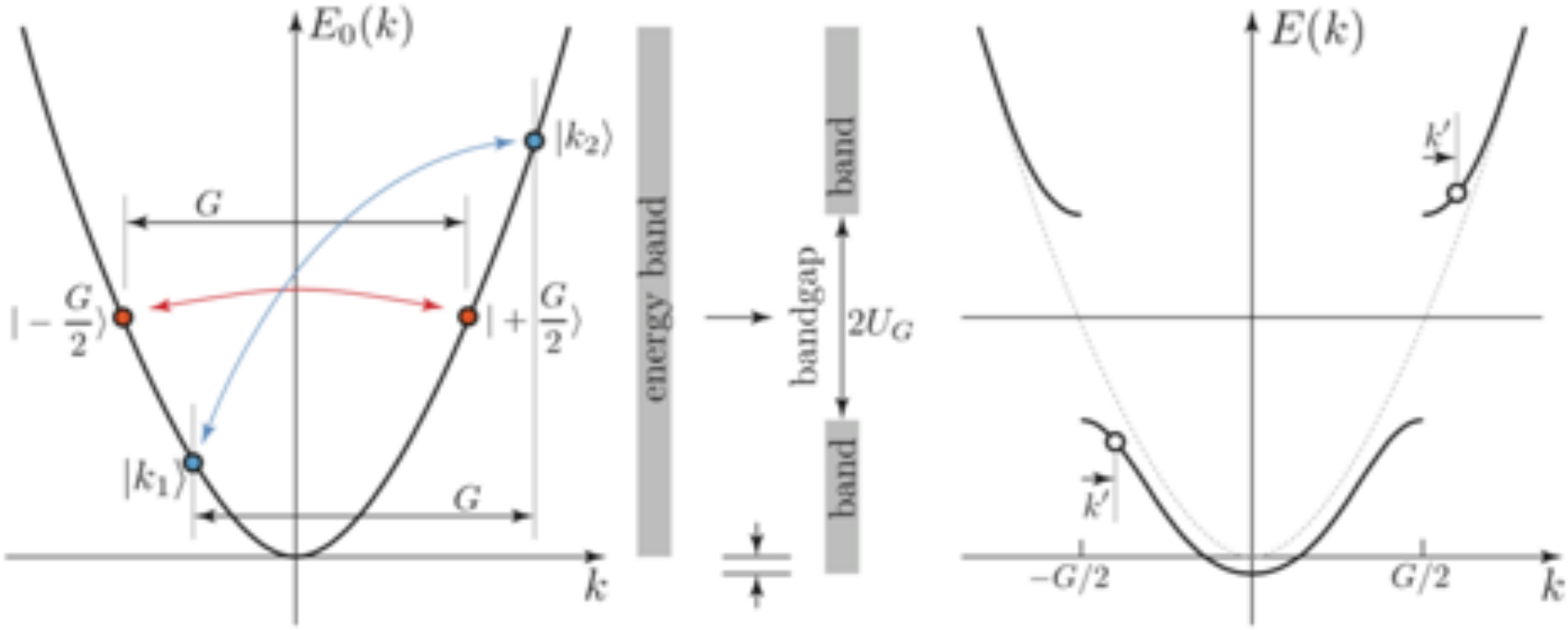

Fig. 8.3 Bandgap opening in the energy spectrum of a free electron upon perturbation by a periodic potential.

- The Periodic Potential in a crystal causes standing waves for electrons.
- It splits the allowed energies into bands separated by gaps
- To explain the quantitative details, we must learn perturbation theory of quantum mechanics

Background: The expansion principle

Fourier

We learn early on that *any* well-behaved[1] function $f(x)$ can be expressed as a sum over a *complete* set of trigonometric functions (or complex exponentials) by the Fourier theorem $f(x) = \sum_k a_k e^{ikx}$. Note that *any* complete set of eigenfunctions $[\ldots, e^{ikx}, \ldots]$ works! To find the Fourier coefficients, we use the 'filtering' property of complex exponentials $a_{k_n} = \int dx f(x) e^{-ik_n x}$. If we tweak the function $f(x) \rightarrow f(x) + \delta(x) = h(x)$, then $h(x) = \sum_k a_k' e^{ikx}$ is still a valid expansion; the Fourier coefficients will be tweaked from $a_k \rightarrow a_k'$. But note that the perturbed function can still be expanded in terms of the *original* complete set of eigenfunctions. This idea leads to the Expansion Principle in quantum mechanics.

Be sure to understand and appreciate this powerful statement!

In quantum mechanics, any quantum state 'vector' $|\Psi\rangle$ may be expanded as a linear superposition of the eigenvectors of *any* Hermitian operator $|\Psi\rangle = \sum_n a_n |n\rangle$. This is the Expansion Principle of quantum mechanics. For most problems, the Hermitian operator of choice is the Hamiltonian operator $\hat{H} = (\hat{\mathbf{p}}^2/2m_0) + V(\mathbf{r})$, but it need not be. We choose the Hamiltonian operator since there exist a few problems for which we know the set of *exact* eigenvectors $[\ldots, |n-1\rangle, |n\rangle, |n+1\rangle, \ldots]$. These sets of eigenvectors are *complete*. We also discussed in chapter 2 that this choice of eigenstates are *stationary*, which makes life easier.

Background: Operators = Matrices

$$|\Psi\rangle = \sum_n a_n |n\rangle$$

$$|\Psi\rangle = \begin{bmatrix} a_1 \\ a_2 \\ a_3 \\ \vdots \end{bmatrix} = \begin{bmatrix} \langle 1|\Psi\rangle \\ \langle 2|\Psi\rangle \\ \langle 3|\Psi\rangle \\ \vdots \end{bmatrix}$$

State vector

$$\langle\Psi| = \begin{bmatrix} a_1^\star & a_2^\star & a_3^\star & \cdots \end{bmatrix}$$

Conjugate vector

$$\langle\Psi|\Psi\rangle = 1 \qquad \sum_n |a_n|^2 = 1$$

Normalization of state vector

$$\langle m|n\rangle = \delta_{mn}$$

orthogonality

$$\sum_n |n\rangle\langle n| = 1$$

Completeness (discrete)

$$\int dx |x\rangle\langle x| = 1$$

Completeness (continuous)

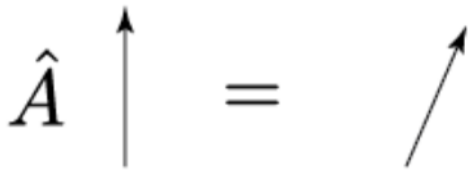

$$\hat{A}|\Psi\rangle = |\Phi\rangle$$

$$[A][\Psi] = [\Phi]$$

Fig. 6.3 Three ways of saying the same thing. The operator $\hat{A}$ rotates a state vector $|\Psi\rangle$ into $|\Phi\rangle$. The pictorial depiction is equivalent to the algebraic operator equation, which in turn is equivalent to the matrix form $[A][\Psi] = [\Phi]$.

Background: Operators = Matrices

$|\Psi\rangle = \sum_n a_n |n\rangle$

$$|\Psi\rangle = \begin{bmatrix} a_1 \\ a_2 \\ a_3 \\ \vdots \end{bmatrix} = \begin{bmatrix} \langle 1|\Psi\rangle \\ \langle 2|\Psi\rangle \\ \langle 3|\Psi\rangle \\ \vdots \end{bmatrix}$$

State vector

$$\langle\Psi| = \begin{bmatrix} a_1^\star & a_2^\star & a_3^\star & \cdots \end{bmatrix}$$

Conjugate vector

$$\langle\Psi|\Psi\rangle = 1 \qquad \sum_n |a_n|^2 = 1$$

Normalization of state vector

$$\langle m|n\rangle = \delta_{mn}$$

orthogonality

$$\sum_n |n\rangle\langle n| = 1$$

Completeness (discrete)

$$\int dx |x\rangle\langle x| = 1$$

Completeness (continuous)

Consider now an operator $\hat{A}$ acts on the state vector $|\Psi\rangle$. It will try to 'rotate' the state vector in the Hilbert state to a state $|\Phi\rangle$, which is written as $\hat{A}|\Psi\rangle = |\Phi\rangle$

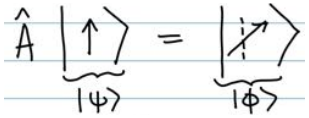

By the expansion principle, we can expand the new state $|\Phi\rangle = \sum_m b_m |m\rangle$. Then, if we project this state on $|m\rangle$, we have

$$\langle m|\Phi\rangle = \langle m|\hat{A}|\Psi\rangle \rightarrow b_m = \sum_n a_n \langle m|\hat{A}|n\rangle = \sum_n A_{mn} a_n. \qquad (11.6)$$

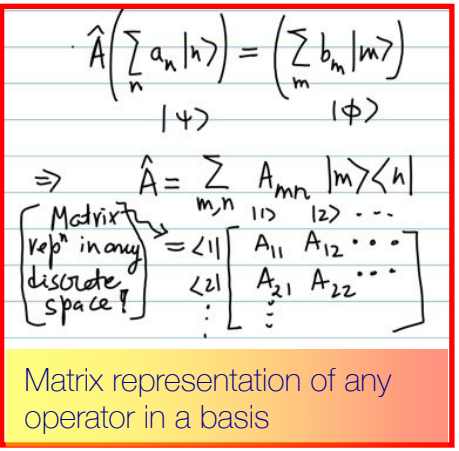

Matrix representation of any operator in a basis

We see that the operator is equivalent to a *matrix* $\hat{A} \equiv A_{mn}$. The elements of the equivalent matrix are the terms $A_{mn} = \langle m|\hat{A}|n\rangle$, obtained by the operator acting on eigenstates on both sides. They are called matrix elements for this reason.

Background: Hamiltonian Operator as a Matrix

$$\hat{H}|n\rangle = E_n|n\rangle$$

For eigenstates

The most important operator is the Hamiltonian operator, which 'extracts' the energy of the state it is acting on. If the state happens to be an eigenstate, the Hamiltonian operator extracts its energy eigenvalue: $\hat{H}|n\rangle = E_n|n\rangle$. Visualize $\hat{H}|n\rangle$ as a new vector whose 'direction' is the same as the eigenvector $|n\rangle$, but the length determined by the eigenvalue E_n. So the action of the Hamiltonian operator leaves the 'direction' of the eigenvector $|n\rangle$ unaffected.

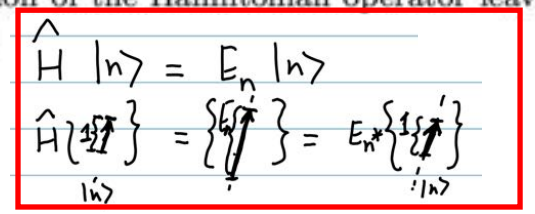

$$|\Psi\rangle = \sum_n a_n|n\rangle$$

not an eigenstate

$$\hat{H}\sum_n a_n|n\rangle = E\sum_n a_n|n\rangle$$

$$\sum_n \langle m|\hat{H}|n\rangle a_n = Ea_m$$

$$\begin{aligned} H_{11}a_1 + H_{12}a_2 + H_{13}a_3 \ldots &= Ea_1 \\ H_{21}a_1 + H_{22}a_2 + H_{23}a_3 \ldots &= Ea_2 \\ H_{31}a_1 + H_{32}a_2 + H_{33}a_3 \ldots &= Ea_3 \\ \vdots &= \vdots \end{aligned}$$

$$\begin{bmatrix} H_{11} & H_{12} & H_{13} & \ldots \\ H_{21} & H_{22} & H_{23} & \ldots \\ H_{31} & H_{32} & H_{33} & \ldots \\ \vdots & \vdots & \vdots & \ddots \end{bmatrix} \begin{bmatrix} a_1 \\ a_2 \\ a_3 \\ \vdots \end{bmatrix} = E \begin{bmatrix} a_1 \\ a_2 \\ a_3 \\ \vdots \end{bmatrix}$$

Matrix form of Schrodinger eqn.

The strangest property of matrices is that they do not necessarily *commute*. Which is to say that in general for square matrices, $AB \neq BA$. As a mathematical object, therefore they are quite distinct from real or complex numbers. Matrices thus form the natural objects for non-commutative algebra. Therefore they are central to the tenets of quantum mechanics, which is built upon the non-commutativity of operators.

Background: Spectral decomposition of H

$$\begin{bmatrix} H_{11} & H_{12} & H_{13} & \dots \\ H_{21} & H_{22} & H_{23} & \dots \\ H_{31} & H_{32} & H_{33} & \dots \\ \vdots & \vdots & \vdots & \ddots \end{bmatrix} \begin{bmatrix} a_1 \\ a_2 \\ a_3 \\ \vdots \end{bmatrix} = E \begin{bmatrix} a_1 \\ a_2 \\ a_3 \\ \vdots \end{bmatrix}$$

Map to equivalent problem in matrix algebra

$$\begin{bmatrix} H_{11}-E & H_{12} & H_{13} & \dots \\ H_{21} & H_{22}-E & H_{23} & \dots \\ H_{31} & H_{32} & H_{33}-E & \dots \\ \vdots & \vdots & \vdots & \ddots \end{bmatrix} \begin{bmatrix} a_1 \\ a_2 \\ a_3 \\ \vdots \end{bmatrix} = 0.$$

Eigenvalue problem of a matrix

$$A[x] = \lambda[x] \rightarrow [A - \lambda I][x] = 0$$

Solve, form diagonal matrix with e'vals

$$D = \begin{bmatrix} \lambda_1 & 0 & \cdots \\ 0 & \lambda_2 & \cdots \\ \vdots & \vdots & \ddots \end{bmatrix}$$

Form unitary transformation matrix with e'vectors

$$U = \begin{bmatrix} [x_1] & [x_2] & \cdots \end{bmatrix}$$

$$A = UDU^{-1}$$

$$A = UDU^{-1}$$

Spectral decomposition of matrix A

$$\begin{bmatrix} H_{11} & H_{12} & H_{13} & \dots & H_{1N} \\ H_{21} & H_{22} & H_{23} & \dots & H_{2N} \\ H_{31} & H_{32} & H_{33} & \dots & H_{3N} \\ \vdots & \vdots & \vdots & \ddots & \vdots \\ H_{N1} & H_{N2} & H_{N3} & \dots & H_{NN} \end{bmatrix} = U \begin{bmatrix} E_1 & 0 & 0 & \dots & 0 \\ 0 & E_2 & 0 & \dots & 0 \\ 0 & 0 & E_3 & \dots & 0 \\ \vdots & \vdots & \vdots & \ddots & \vdots \\ 0 & 0 & 0 & \dots & E_N \end{bmatrix} U^{-1}$$

Spectral decomposition of the Hamiltonian operator (diagonalization)

Property of Traces of matrices

$$\mathrm{Tr}[AB] = \mathrm{Tr}[BA]$$

$$\mathrm{Tr}[U^{-1}UD] = \mathrm{Tr}[D] = \sum_n E_n$$

Trace of the Hamiltonian matrix = Sum of the eigenvalues

Background: Spectral decomposition enables…

$$A = UDU^{-1}$$

$$A^2 = UD(U^{-1}U)DU^{-1} = UD^2U^{-1} = U \begin{bmatrix} \lambda_1^2 & 0 & \cdots \\ 0 & \lambda_2^2 & \cdots \\ \vdots & \vdots & \ddots \end{bmatrix} U^{-1}.$$

$$A^N = UD^NU^{-1}$$

Functions of matrices

$$e^A = 1 + A + \frac{1}{2!}A^2 + \ldots = Ue^DU^{-1} = U \begin{bmatrix} e^{\lambda_1} & 0 & 0 & \ldots \\ 0 & e^{\lambda_2} & 0 & \ldots \\ 0 & 0 & e^{\lambda_3} & \ldots \\ \vdots & \vdots & \vdots & \ddots \end{bmatrix} U^{-1}$$

Baker-Hausdorff formulae

$$e^A e^B = e^{(B+[A,B]+\frac{1}{2!}[A,[A,B]]+\ldots)} e^A \neq e^B e^A$$

$$e^A B e^{-A} = B + [A,B] + \frac{1}{2!}[A,[A,B]] + \frac{1}{3!}[A,[A,[A,B]]] + \ldots$$

Jacobi formula

$$\mathrm{Det}[e^A] = e^{\mathrm{Trace}[A]}$$

Consider 2 state vectors

$$|\Psi\rangle = \begin{bmatrix} a_1 \\ a_2 \\ \vdots \end{bmatrix} \qquad |\Phi\rangle = \begin{bmatrix} b_1 \\ b_2 \\ \vdots \end{bmatrix}$$

Inner product is a number

$\langle\Phi|\Psi\rangle = \sum_n a_n b_n^\star$, we get a *number*

Trace is invariant!

$\mathrm{Tr}[|\Psi\rangle\langle\Phi|] = \mathrm{Tr}[\langle\Phi|\Psi\rangle] = \sum_n a_n b_n^\star$

Outer product is the density matrix

$$|\Psi\rangle\langle\Phi| = \begin{bmatrix} a_1 \\ a_2 \\ \vdots \\ a_N \end{bmatrix} \begin{bmatrix} b_1^\star & b_2^\star & \ldots & b_N^\star \end{bmatrix} = \begin{bmatrix} a_1 b_1^\star & a_1 b_2^\star & a_1 b_3^\star & \ldots & a_1 b_N^\star \\ a_2 b_1^\star & a_2 b_2^\star & a_2 b_3^\star & \ldots & a_2 b_N^\star \\ a_3 b_1^\star & a_3 b_2^\star & a_3 b_3^\star & \ldots & a_3 b_N^\star \\ \vdots & \vdots & \vdots & \ddots & \vdots \\ a_N b_1^\star & a_N b_2^\star & a_N b_3^\star & \ldots & a_N b_N^\star \end{bmatrix}$$

Evaluation of Matrices

```
(* The Eigenvalues and Eigenfunctions of a 2x2 matrix *)
H2 = {{h11, h12}, {h12, h22}};
Print["H2=", MatrixForm[H2]]
Print["EigenSystem[H2]=", MatrixForm[Eigensystem[H2]]]
```

$$H2=\begin{pmatrix} h11 & h12 \\ h12 & h22 \end{pmatrix}$$

$$\text{EigenSystem}[H2]=\begin{pmatrix} \frac{1}{2}\left(h11+h22-\sqrt{h11^2+4\,h12^2-2\,h11\,h22+h22^2}\right) & \frac{1}{2}\left(h11+h22+\sqrt{h11^2+4\,h12^2-2\,h11\,h22+h22^2}\right) \\ \left\{-\frac{h11-h22-\sqrt{h11^2+4\,h12^2-2\,h11\,h22+h22^2}}{2\,h12},\ 1\right\} & \left\{-\frac{h11-h22+\sqrt{h11^2+4\,h12^2-2\,h11\,h22+h22^2}}{2\,h12},\ 1\right\} \end{pmatrix}$$

```
M = {{1, 1, 0}, {0, 2, 0}, {0, 1, 1}};
Print["M=", MatrixForm[M]]
Print["EigenSystem[M]=", MatrixForm[Eigensystem[M]]]
```

$$M=\begin{pmatrix} 1 & 1 & 0 \\ 0 & 2 & 0 \\ 0 & 1 & 1 \end{pmatrix}$$

$$\text{EigenSystem}[M]=\begin{pmatrix} 2 & 1 & 1 \\ \{1,1,1\} & \{0,0,1\} & \{1,0,0\} \end{pmatrix}$$

```
H5 = {{E0, -t, 0, 0, -t}, {-t, E0, -t, 0, 0}, {0, -t, E0, -t, 0}, {0, 0, -t, E0, -t}, {-t, 0, 0, -t, E0}};
Print["H5=", MatrixForm[H5]]
Print["EigenSystem[H5]=", MatrixForm[Eigensystem[H5]]]
```

$$H5=\begin{pmatrix} E0 & -t & 0 & 0 & -t \\ -t & E0 & -t & 0 & 0 \\ 0 & -t & E0 & -t & 0 \\ 0 & 0 & -t & E0 & -t \\ -t & 0 & 0 & -t & E0 \end{pmatrix}$$

$$\text{EigenSystem}[H5]=\begin{pmatrix} E0-2t & \frac{1}{2}\left(2\,E0+t-\sqrt{5}\,t\right) & \frac{1}{2}\left(2\,E0+t-\sqrt{5}\,t\right) & \frac{1}{2}\left(2\,E0+t+\sqrt{5}\,t\right) & \frac{1}{2}\left(2\,E0+t+\sqrt{5}\,t\right) \\ \{1,1,1,1,1\} & \left\{\frac{1}{4}\left(-1+\sqrt{5}\right),\frac{1}{4}\left(1-\sqrt{5}\right),-1,0,1\right\} & \left\{-1,\frac{1}{4}\left(1-\sqrt{5}\right),\frac{1}{4}\left(-1+\sqrt{5}\right),1,0\right\} & \left\{\frac{1}{4}\left(-1-\sqrt{5}\right),\frac{1}{4}\left(1+\sqrt{5}\right),-1,0,1\right\} & \left\{-1,\frac{1}{4}\left(1+\sqrt{5}\right),\frac{1}{4}\left(-1-\sqrt{5}\right),1,0\right\} \end{pmatrix}$$

Fig. 6.4 Examples of 2x2, 3x3, and 5x5 Matrix eigenvalue and eigenfunction calculations in Mathematica. The 2x2 Hamiltonian is general and one of the most important in all of quantum mechanics. The 3x3 matrix is a numerical example, and the 5x5 matrix of a 5-site circular ring tight-binding Hamiltonian model. Note that the eigenvectors (or eigenfunction coefficients a_n are evaluated for each eigenvalue, which is *very* nice.

Background: Green's Function Matrices

construct operators of the form $\hat{A} = \sum a_n |n\rangle\langle n|$

$$(E - \hat{H}^0)|\psi\rangle = 0$$

Time independent Schrodinger equation

$$\hat{G}(E) = \sum_n \frac{|n\rangle\langle n|}{E - E_n}$$

Definition of the Green's function operator
E_n is the eigenvalue of state |n>

$$\hat{G}(E)|m\rangle = \sum_n \frac{|n\rangle\langle n|}{E - E_n}|m\rangle = \sum_n \frac{|n\rangle}{E - E_n}\langle n|m\rangle = \frac{1}{E - E_m}|m\rangle$$

Action of G(E) on a state |m>

$$\hat{G}(E)(E - \hat{H}^0)|\psi\rangle = \sum_n \frac{|n\rangle\langle n|}{E - E_n}(E - \hat{H}^0)|\psi\rangle = \sum_n |n\rangle\langle n|\psi\rangle = |\psi\rangle$$

Action of G(E) on the Schrodinger equation yields identity

$$\hat{G}(E) = (E - \hat{H}^0)^{-1}$$

Green's function operator is the inverse operator of $(E\text{-}H_0)$

Formal solution of the perturbation problem using Green's functions: elegant, but analytically not too useful…

$$(E - \hat{H}^0)|\psi\rangle = 0 \quad \rightarrow \quad \hat{H}^0 \rightarrow \hat{H}^0 + \hat{W} \quad \Rightarrow \quad (E - \hat{H}^0 - \hat{W})|\phi\rangle = 0$$

Perturbation W changes the Hamiltonian

$$|\psi\rangle \rightarrow |\phi\rangle$$

Eigenstates have changed because of the perturbation W

$$\underbrace{(E - \hat{H}^0)}_{\hat{G}^{-1}(E)}[1 - \underbrace{(E - \hat{H}^0)^{-1}}_{\hat{G}(E)}\hat{W}]|\phi\rangle = \hat{G}^{-1}[1 - \hat{G}\hat{W}]|\phi\rangle = 0$$

$$\hat{G}^{-1}(1 - \hat{G}\hat{W})|\phi\rangle = \hat{G}^{-1}|\psi\rangle \implies |\phi\rangle = (1 - \hat{G}\hat{W})^{-1}|\psi\rangle$$

Using G(E), we can write the new eigenstate in terms of the old (known) eigenstates and eigenvalues

$$|\phi\rangle = (1 + \hat{G}\hat{W} + \hat{G}\hat{W}\hat{G}\hat{W} + \hat{G}\hat{W}\hat{G}\hat{W}\hat{G}\hat{W} + ...)|\psi\rangle$$

Lippmann-Schwinger equation, or Dyson equation

Time-independent perturbation theory

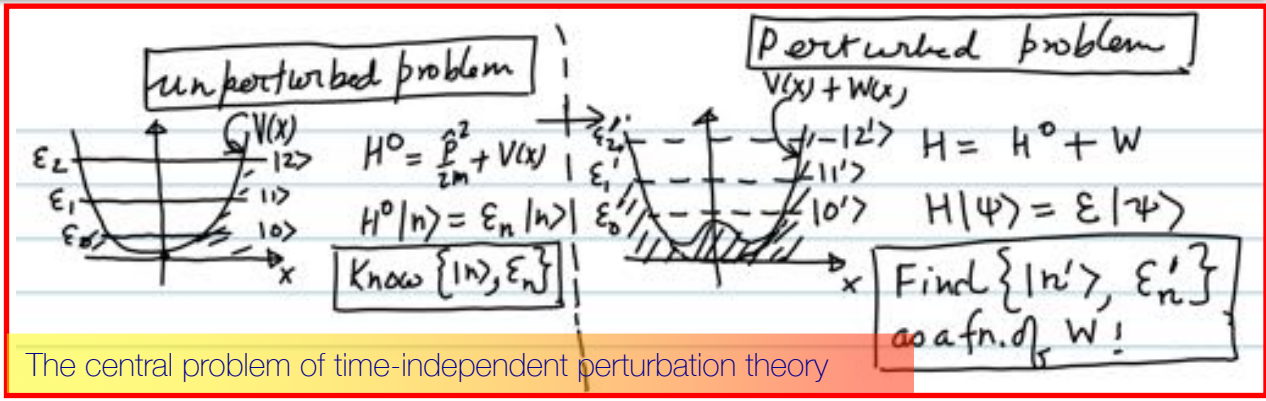

The central problem of time-independent perturbation theory

$$H^0|n\rangle = \mathcal{E}_n^0|n\rangle$$

Unperturbed (solved) problem: We know the eigenvalues & eigenstates

$$H = H^0 + W$$

Perturbed Hamiltonian, new eigenstates

$$(H^0 + W)|\psi\rangle = \mathcal{E}|\psi\rangle$$

Expansion principle!

$$|\psi\rangle = \sum_n a_n|n\rangle$$

$$a_n = \langle n|\psi\rangle$$

$$|\psi\rangle = \sum_{n=1}^{n=N} a_n|n\rangle$$

$$\begin{bmatrix} H_{11} & H_{12} & \dots & H_{1N} \\ H_{21} & H_{22} & \dots & H_{2N} \\ \vdots & \vdots & & \vdots \\ H_{N1} & H_{N2} & \dots & H_{NN} \end{bmatrix} \times \begin{bmatrix} a_1 \\ a_2 \\ \vdots \\ a_N \end{bmatrix} = \mathcal{E} \begin{bmatrix} a_1 \\ a_2 \\ \vdots \\ a_N \end{bmatrix}$$

Matrix solution of the perturbation problem: diagonalize & get solns.

Matrix elements include the perturbation

$$H_{mn} = \langle m|H|n\rangle$$

Degenerate perturbation theory

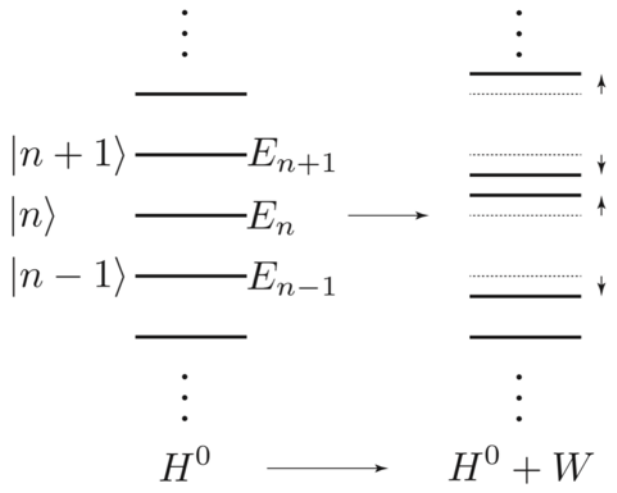

$$\sum_n a_n \langle m|(\hat{H}^0 + W)|n\rangle = E a_m.$$

$$\begin{bmatrix} E_1 + W_{11} & W_{12} & W_{13} & \dots & W_{1N} \\ W_{21} & E_2 + W_{22} & W_{23} & \dots & W_{2N} \\ W_{31} & W_{32} & E_3 + W_{33} & \dots & W_{3N} \\ \vdots & \vdots & \vdots & \ddots & \vdots \\ W_{N1} & W_{N2} & W_{N3} & \dots & E_N + W_{NN} \end{bmatrix} \begin{bmatrix} a_1 \\ a_2 \\ a_3 \\ \vdots \\ a_N \end{bmatrix} = E \begin{bmatrix} a_1 \\ a_2 \\ a_3 \\ \vdots \\ a_N \end{bmatrix}$$

$$\begin{bmatrix} H^0_{11} + W_{11} & H^0_{12} + W_{12} & H^0_{13} + W_{13} & \dots & H^0_{1N} + W_{1N} \\ H^0_{21} + W_{21} & H^0_{22} + W_{22} & H^0_{23} + W_{23} & \dots & H^0_{2N} + W_{2N} \\ H^0_{31} + W_{31} & H^0_{32} + W_{32} & H^0_{33} + W_{33} & \dots & H^0_{3N} + W_{3N} \\ \vdots & \vdots & \vdots & \ddots & \vdots \\ H^0_{N1} + W_{N1} & H^0_{N2} + W_{N2} & H^0_{N3} + W_{N3} & \dots & H^0_{NN} + W_{NN} \end{bmatrix} \begin{bmatrix} a_1 \\ a_2 \\ a_3 \\ \vdots \\ a_N \end{bmatrix} = E \begin{bmatrix} a_1 \\ a_2 \\ a_3 \\ \vdots \\ a_N \end{bmatrix}$$

Time-independent perturbation theory

$$\begin{bmatrix} H_{11} & H_{12} & \dots & H_{1N} \\ H_{21} & H_{22} & \dots & H_{2N} \\ \vdots & \vdots & & \vdots \\ H_{N1} & H_{N2} & \dots & H_{NN} \end{bmatrix} \times \begin{bmatrix} a_1 \\ a_2 \\ \vdots \\ a_N \end{bmatrix} = \mathcal{E} \begin{bmatrix} a_1 \\ a_2 \\ \vdots \\ a_N \end{bmatrix} \Rightarrow \begin{vmatrix} H_{11}-\mathcal{E} & H_{12} & \dots & H_{1N} \\ H_{21} & H_{22}-\mathcal{E} & \dots & H_{2N} \\ \vdots & \vdots & & \vdots \\ H_{N1} & H_{N2} & \dots & H_{NN}-\mathcal{E} \end{vmatrix} = 0$$

Solve these for solutions to the perturbation problem. Exact solution is an infinite matrix! How to truncate?

$$|m\rangle \leftrightarrow |n\rangle$$

$$|\mathcal{E}_m - \mathcal{E}_n|$$

$$W_{mn} = \langle m|W|n\rangle$$

$$\Delta\mathcal{E}_{ix} = \frac{|W_{ix}|^2}{\mathcal{E}_x - \mathcal{E}_i}$$

Strength of interaction between states depends on:

- Their energy separation
- The matrix element between them
- (Matrix element)^2/Energy difference

Example: 2-Level system

Matrix to be diagonalized

$$\begin{vmatrix} H_{11}-\mathcal{E} & H_{12} \\ H_{21} & H_{22}-\mathcal{E} \end{vmatrix} = 0$$

Eigenvalues

$$\mathcal{E}_\pm = \frac{1}{2}(H_{11}+H_{22}) \pm \sqrt{\frac{1}{4}(H_{11}-H_{22})^2 + |H_{12}|^2}$$

Eigenstate coefficients

$$|\psi\rangle = a_1|1\rangle + a_2|2\rangle$$

$$a_1 = \frac{H_{12}}{\sqrt{|H_{12}|^2 + (\mathcal{E}-H_{11})^2}}$$

$$a_2 = \frac{\mathcal{E}-H_{11}}{\sqrt{|H_{12}|^2 + (\mathcal{E}-H_{11})^2}}$$

Analytical time-independent perturbation theory

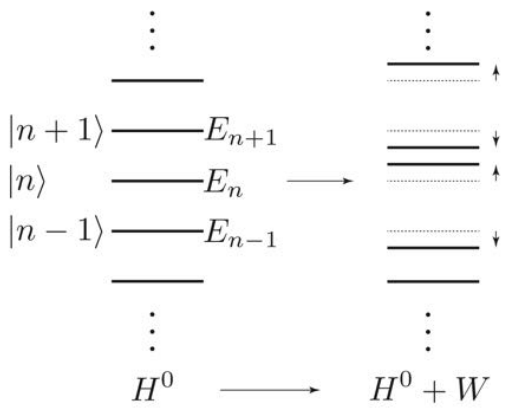

$$H^0|u\rangle = \mathcal{E}_u|u\rangle$$

$$|u\rangle \rightarrow |u\rangle + |\phi\rangle = |\psi\rangle$$

Select out an unperturbed state u

$$[H^0 + \underbrace{H^D + W'}_{perturbation, W}]|\psi\rangle = \mathcal{E}|\psi\rangle$$

$$|\psi\rangle = |u\rangle + \underbrace{\sum_{m\neq u}\sum_{n\neq m}|m\rangle\frac{\langle m|W|n\rangle}{\mathcal{E}-\mathcal{E}'_m}\langle n|\psi\rangle}_{|\phi\rangle}$$

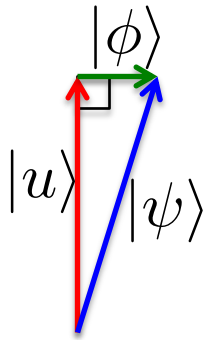

$$\mathcal{E} \approx \mathcal{E}_u + \underbrace{\langle u|W|u\rangle}_{\Delta\mathcal{E}^{(1)}} + \underbrace{\sum_{m\neq u}\frac{|\langle m|W|u\rangle|^2}{\mathcal{E}-\mathcal{E}'_m}}_{\Delta\mathcal{E}^{(2)}}$$

Eigenvalues and eigenstates after perturbation

$$|\phi\rangle \approx \sum_{m\neq u}\frac{\langle m|W|u\rangle}{\mathcal{E}-\mathcal{E}'_m}|m\rangle$$

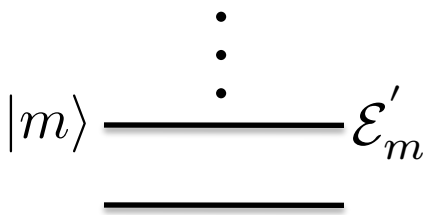

Define…

$$\mathcal{E}'_u = \mathcal{E}_u + \langle u|W|u\rangle$$
$$\mathcal{E}'_m = \mathcal{E}_m + \langle m|W|m\rangle$$

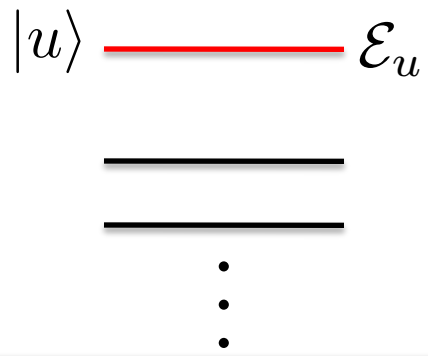

Iff this condition holds, in rhs… $\mathcal{E} \rightarrow \mathcal{E}_u$

$$|\Delta\mathcal{E}^{(1)} + \Delta\mathcal{E}^{(2)}| \approx |\mathcal{E} - \mathcal{E}'_u| << |\mathcal{E}_m - \mathcal{E}_u|$$

$$\mathcal{E} \approx \mathcal{E}'_u + \sum_{m\neq u}\frac{|\langle m|W|u\rangle|^2}{\mathcal{E}-\mathcal{E}'_m}$$

recursive

Brillouin-Wigner (BW) Perturbation theory

$$\mathcal{E} \approx \mathcal{E}'_u + \sum_{m\neq u}\frac{|\langle m|W|u\rangle|^2}{\mathcal{E}_u-\mathcal{E}'_m}$$

Rayleigh-Schrodinger (RS) Perturbation theory

Level repulsion and Avoided Crossing

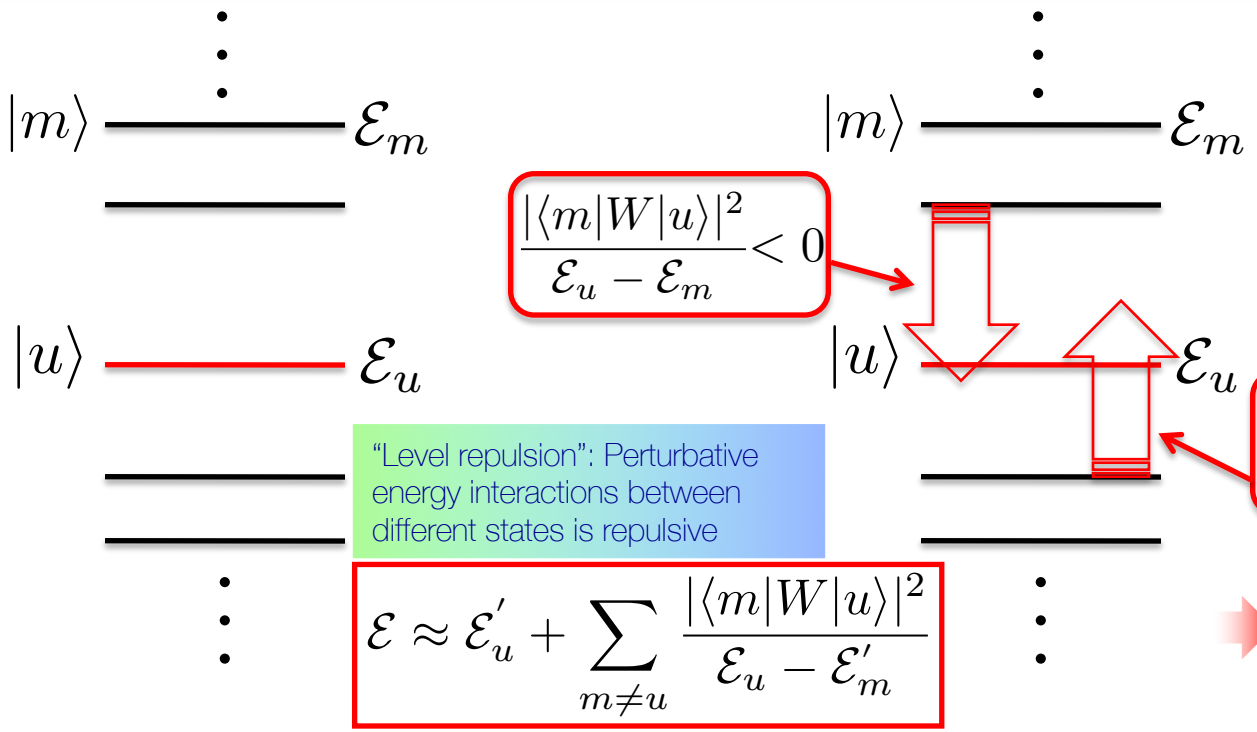

"Level repulsion": Perturbative energy interactions between different states is repulsive

$$\mathcal{E} \approx \mathcal{E}'_u + \sum_{m \neq u} \frac{|\langle m|W|u\rangle|^2}{\mathcal{E}_u - \mathcal{E}'_m}$$

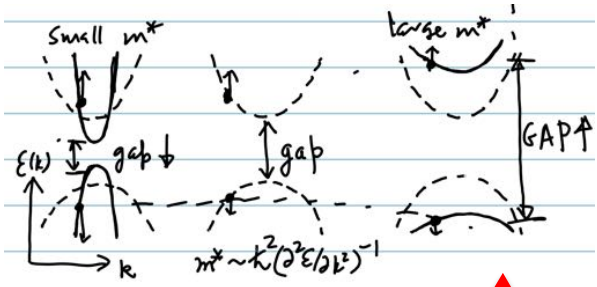

Responsible for "curvature" of bands, and effective masses of band-edge electron states. Small bandgap semiconductors have small band-edge effective masses.

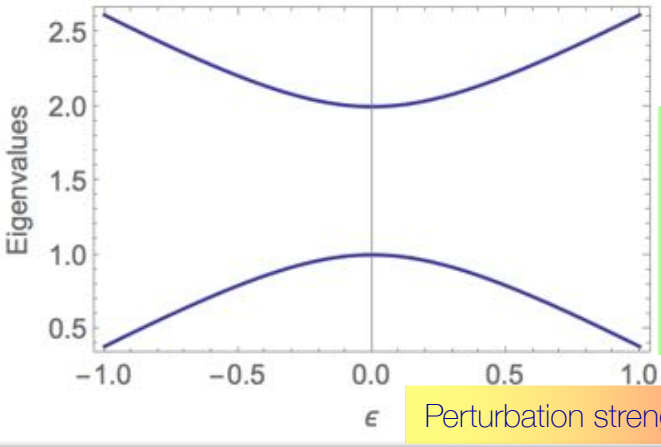

"Avoided Crossing":
Two unperturbed states that are not degenerate cannot be made degenerate (cross) by perturbation. This is because the interaction is repulsive in energy eigenvalues.

This observation holds independent of the sign of the perturbation, because the 2nd order energy correction has the square of the matrix element.

Perturbation Theory Example: Particle in a Box

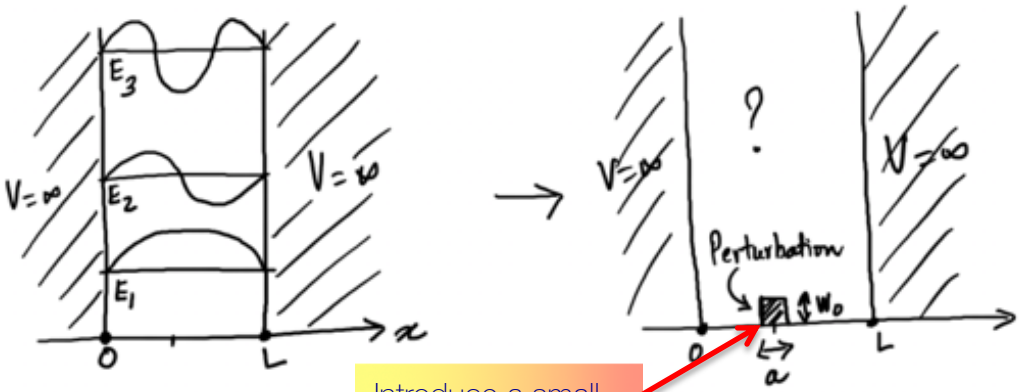

Introduce a small perturbation to the particle in a box.

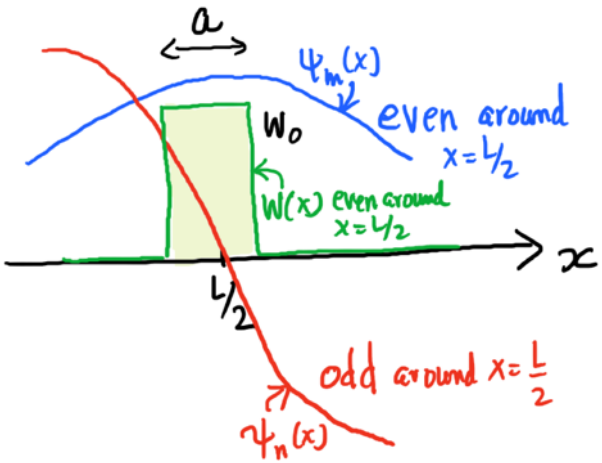

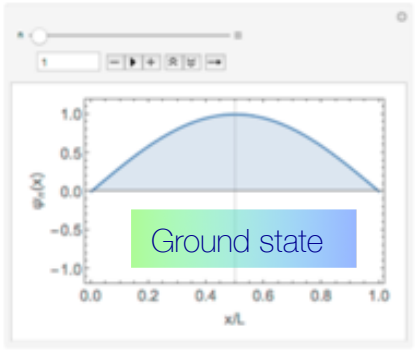

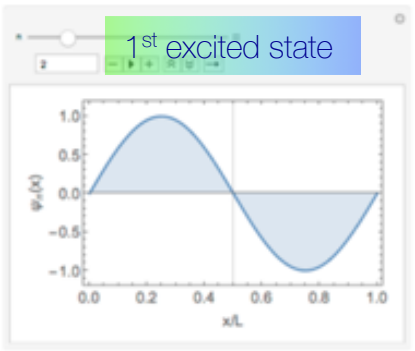

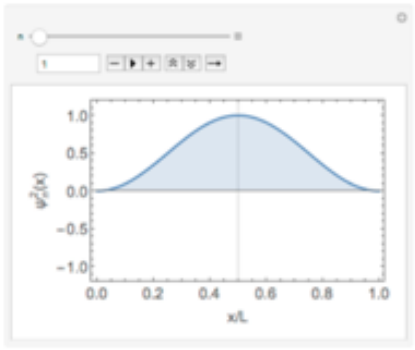

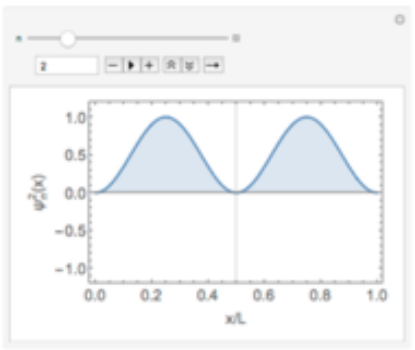

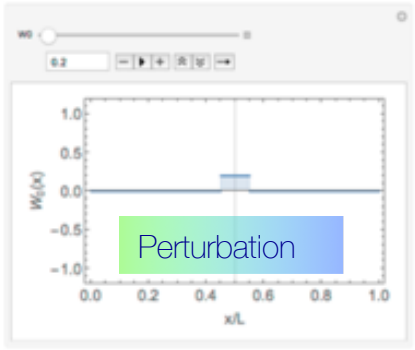

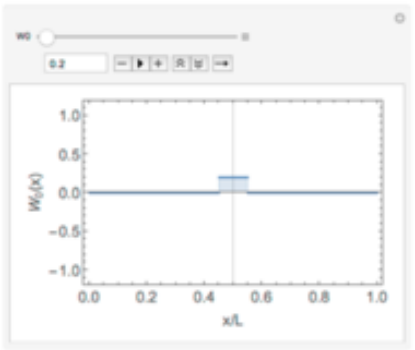

States with maximum wavefunction at the center will be perturbed the most.
States with low energy will be perturbed more than states of high energy.

Perturbation Theory Example: Particle in a Box

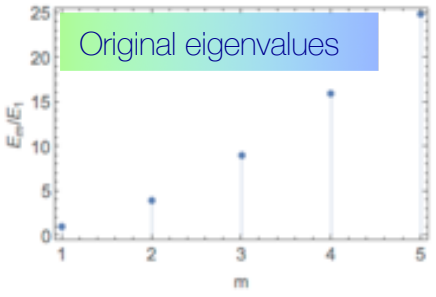

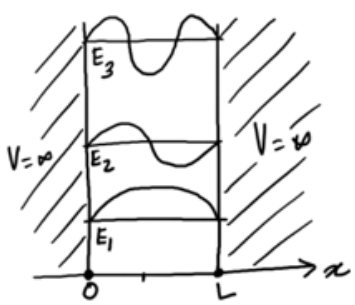

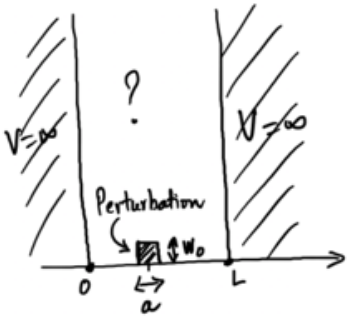

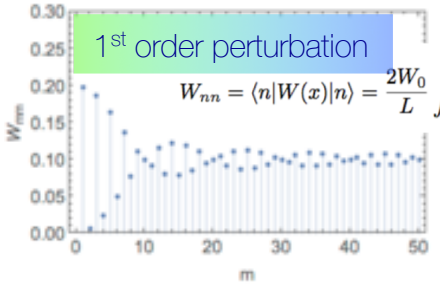

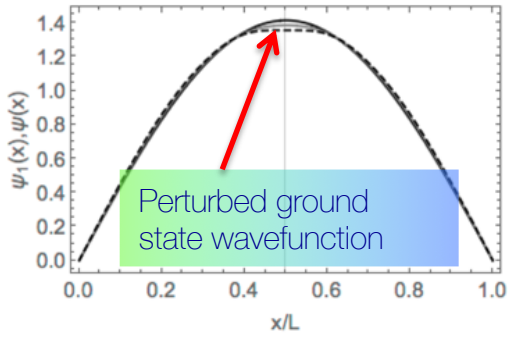

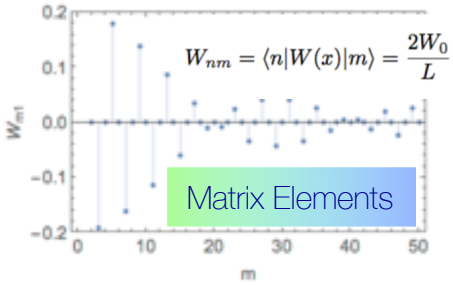

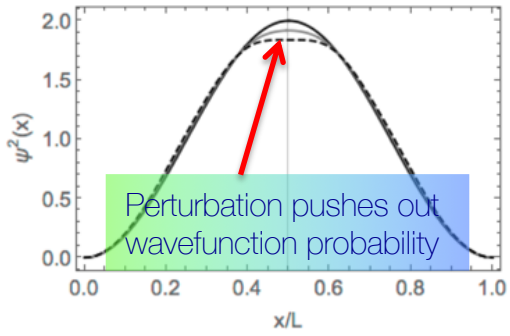

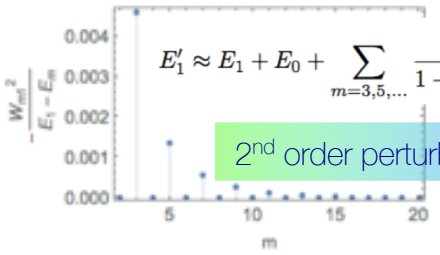

$$|\psi\rangle = |1\rangle + \sum_{m=3,5,\ldots} \frac{E_0}{E_1(1-m^2-\frac{E_0}{E_1})}|m\rangle$$

$$\implies \psi(x) = \psi_1(x) + \sum_{m=3,5,\ldots} \frac{E_0}{E_1(1-m^2-\frac{E_0}{E_1})}\psi_m(x)$$

$$\hat{H}^0 + W = \begin{array}{c} \\ \langle 1| \\ \langle 2| \\ \langle 3| \end{array} \begin{array}{c} \begin{array}{ccc} |1\rangle & |2\rangle & |3\rangle \end{array} \\ \begin{pmatrix} E_1+E_0 & 0 & E_0 \\ 0 & E_2 & 0 \\ E_0 & 0 & E_3+E_0 \end{pmatrix} \end{array}$$

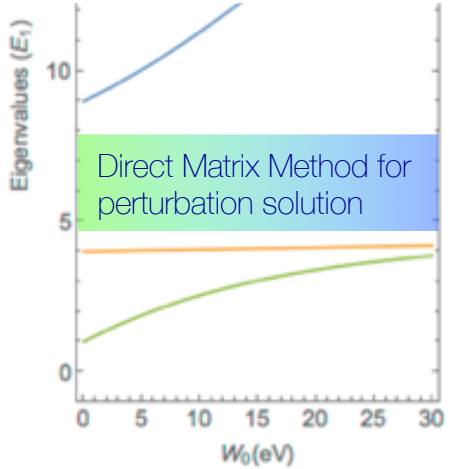

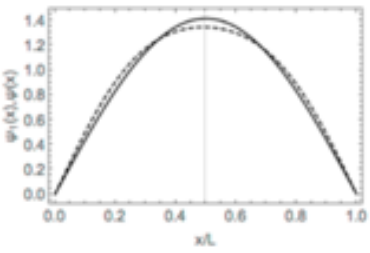

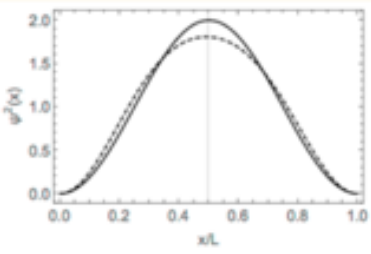

A Periodic Potential for the Electron on a Ring

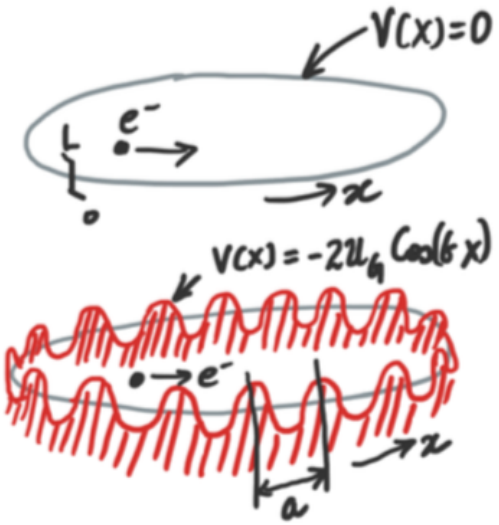

Fig. 8.2 The electron on a ring experiences a periodic potential.

Fig. 8.5 Rudolph Peierls while working with Heisenberg was the first to produce the famous energy dispersion of a free electron perturbed by a periodic potential. His plot is reproduced in Figure 8.6

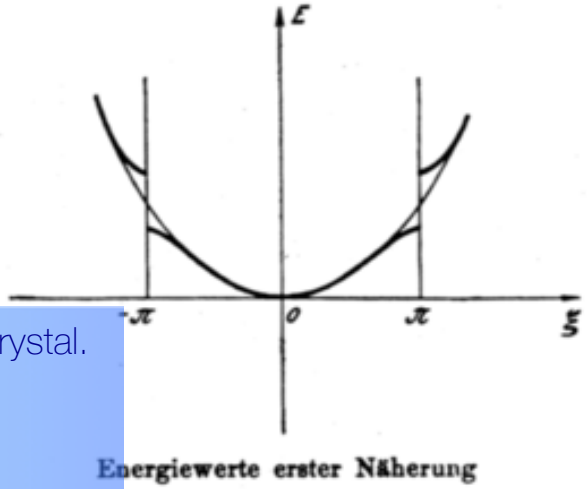

Fig. 8.6 Rudy Peierls' iconic plot of the energy dispersion of a free electron in a periodic potential from his 1930 paper.

- The central problem of the physics of semiconductors is that of an electron in a crystal.
- A crystal is a periodic array of atoms.
- The quantum mechanical electron experiences a periodic potential V(x+a) = V(x).
- What are the allowed eigenvalues and eigenfunctions?
- All answers to semiconductor physics are hidden in the solution of this problem.

Example: Opening of a bandgap in a crystal

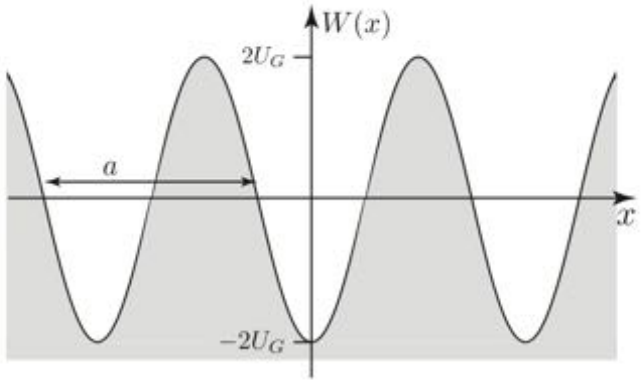

FIGURE 13.1: A periodic potential $W(x) = -2U_G\cos(Gx)$ acts as a perturbation to the free electron.

Unperturbed problem is the 'electron on a ring': E'states, E'Vals:

$$\langle x|k\rangle = \psi(x,k) = \frac{1}{\sqrt{L}}e^{ikx} \qquad E_0(k) = \frac{\hbar^2 k^2}{2m_0}$$

$$\langle k_m|k_n\rangle = \int dx\langle k_m|x\rangle\langle x|k_n\rangle = \int dx\psi^\star(x,k_m)\psi(x,k_n) = \frac{1}{L}\int_0^L dx e^{i2\pi(n-m)x} = \delta_{n,m}$$

unperturbed E'states are orthogonal

$$W(x) = -2U_G\cos(Gx) = -U_G(e^{iGx} + e^{-iGx})$$

Perturbation potential

$$\langle k_2|W(x)|k_1\rangle = -\frac{U_G}{L}\int_0^L dx e^{i(k_1-k_2)x}(e^{iGx} + e^{-iGx}) = -U_G\delta_{k_1-k_2,\pm G}$$

Perturbing potential only couples state k with k+G, k-G with strength $-U_G$

States most strongly perturbed: +G/2, -G/2.
F= E_0(G/2) is their unperturbed energy.

$$E_0(G/2) = \hbar^2G^2/8m_0 = F$$

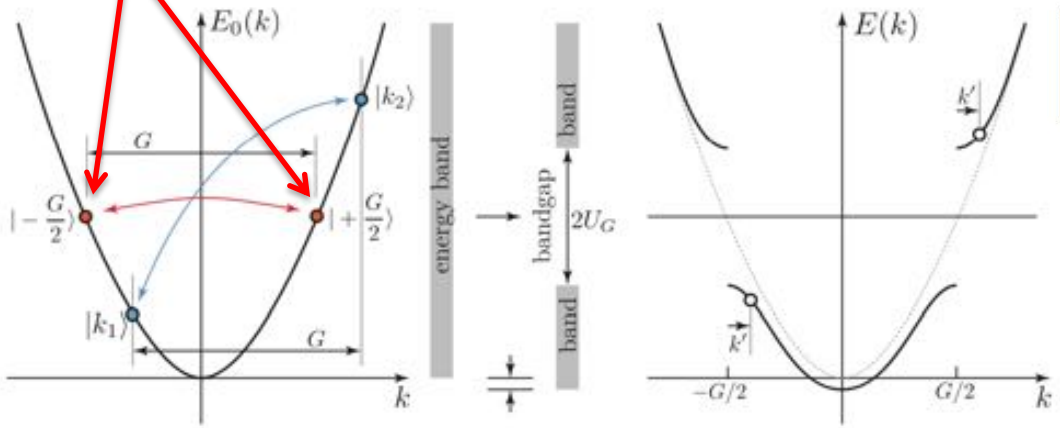

$$\begin{bmatrix} H_{11} & H_{12} \\ H_{21} & H_{22} \end{bmatrix}$$

$$\hat{H}^0 + W = \begin{matrix} \\ \langle +\frac{G}{2}| \\ \langle -\frac{G}{2}| \end{matrix} \begin{matrix} \begin{matrix} |+\frac{G}{2}\rangle & |-\frac{G}{2}\rangle \end{matrix} \\ \begin{pmatrix} F & -U_G \\ -U_G & F \end{pmatrix} \end{matrix}$$

Form the 2-state Hamiltonian

$$E_\pm = \frac{H_{11}+H_{22}}{2} \pm \sqrt{(\frac{H_{11}-H_{22}}{2})^2 + |H_{12}|^2}$$

$$\begin{bmatrix} a_1 \\ a_2 \end{bmatrix}_\pm = \begin{bmatrix} \frac{H_{12}}{\sqrt{|H_{12}|^2+(E_\pm-H_{11})^2}} \\ \frac{E_\pm-H_{11}}{\sqrt{|H_{12}|^2+(E_\pm-H_{11})^2}} \end{bmatrix}$$

Solve to get the eigenvalues and the eigenfunctions

Bandgap, band-edge states, effective masses

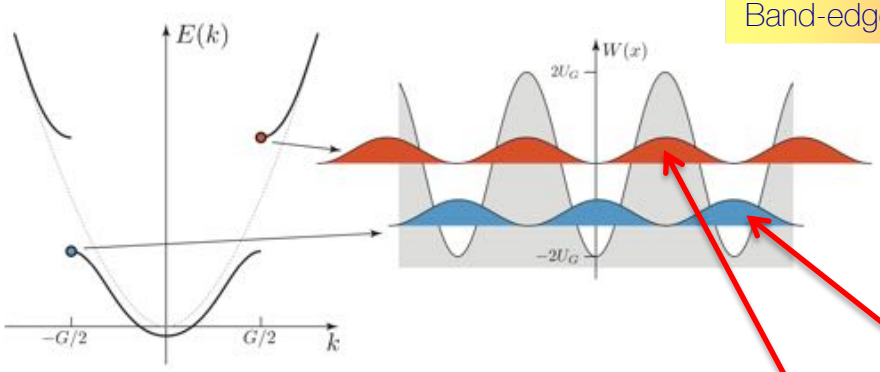

FIGURE 13.3: Probability pileups of band-edge states.

Band-edge states

$$\hat{H}^0 + W = \begin{array}{c} \\ \langle +\frac{G}{2}| \\ \langle -\frac{G}{2}| \end{array} \begin{array}{c} \begin{array}{cc} |+\frac{G}{2}\rangle & |-\frac{G}{2}\rangle \end{array} \\ \begin{pmatrix} F & -U_G \\ -U_G & F \end{pmatrix} \end{array}$$

$$(F-E)^2 - U_G^2 = 0$$

$$E_\pm = F \pm U_G$$

$$E_+ - E_- = 2U_G$$

Bandgap at +/- G/2

Perturbed eigenstates

$$|\psi\rangle = \sum_n a_n |n\rangle \qquad |\pm\rangle = a_{1\pm}|+\frac{G}{2}\rangle + a_{2\pm}|-\frac{G}{2}\rangle$$

$$a_{1+} = -1/\sqrt{2} \quad a_{2+} = +1/\sqrt{2}, \quad a_{1-} = -1/\sqrt{2} \quad a_{2-} = -1/\sqrt{2}.$$

$$\langle x|+\rangle = \psi_+(x) = (-\frac{1}{\sqrt{2}})\cdot(\frac{e^{i\frac{G}{2}x}}{\sqrt{L}}) + (+\frac{1}{\sqrt{2}})\cdot(\frac{e^{-i\frac{G}{2}x}}{\sqrt{L}}) = -i\sqrt{\frac{2}{L}}\sin(\frac{G}{2}x).$$

$$\langle x|-\rangle = \psi_-(x) = (-\frac{1}{\sqrt{2}})\cdot(\frac{e^{i\frac{G}{2}x}}{\sqrt{L}}) + (-\frac{1}{\sqrt{2}})\cdot(\frac{e^{-i\frac{G}{2}x}}{\sqrt{L}}) = -\sqrt{\frac{2}{L}}\cos(\frac{G}{2}x).$$

$$|\psi_+(x)|^2 = (2/L)\sin^2(Gx/2) \qquad |\psi_-(x)|^2 = (2/L)\cos^2(Gx/2)$$

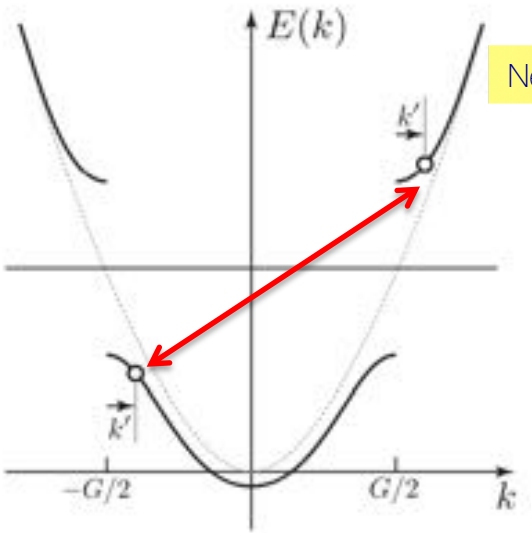

Near band-edge states

2-state Hamiltonian for states near +G/2 and –G/2

$$\hat{H}^0 + W = \begin{array}{c} \\ \langle +\frac{G}{2}+k'| \\ \langle -\frac{G}{2}+k'| \end{array} \begin{array}{c} \begin{array}{cc} |+\frac{G}{2}+k'\rangle & |-\frac{G}{2}+k'\rangle \end{array} \\ \begin{pmatrix} E_0(+\frac{G}{2}+k') & -U_G \\ -U_G & E_0(-\frac{G}{2}+k') \end{pmatrix} \end{array}$$

$$E_\pm(k') \approx (F \pm U_G) + (1 \pm \frac{2F}{U_G})\frac{\hbar^2 k'^2}{2m_0}$$

$$E_c(k') \approx E_c(0) + \frac{\hbar^2 k'^2}{2m_c^\star}$$

$$E_v(k') \approx E_v(0) + \frac{\hbar^2 k'^2}{2m_v^\star}$$

Conduction band
Valence band

Bandgap, band-edge states, effective masses

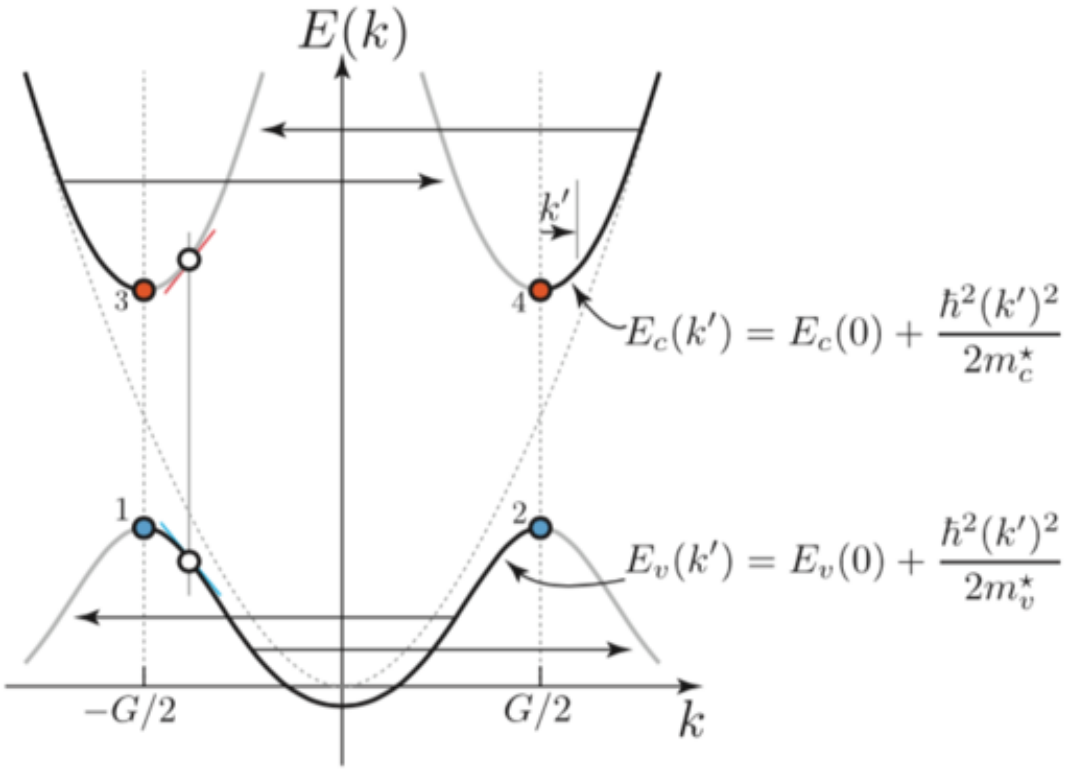

$$E_c(k') = E_c(0) + \frac{\hbar^2 (k')^2}{2m_c^\star}$$

$$E_v(k') = E_v(0) + \frac{\hbar^2 (k')^2}{2m_v^\star}$$

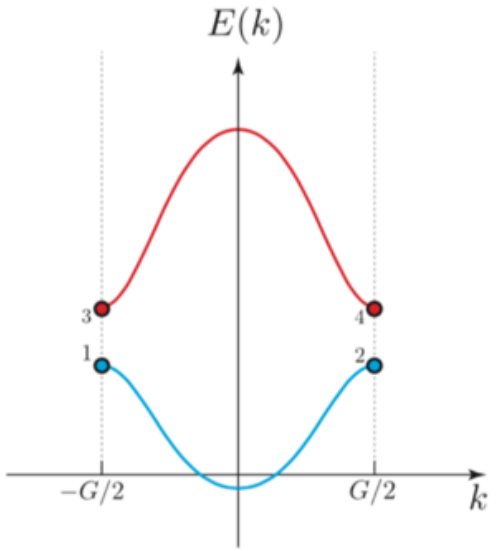

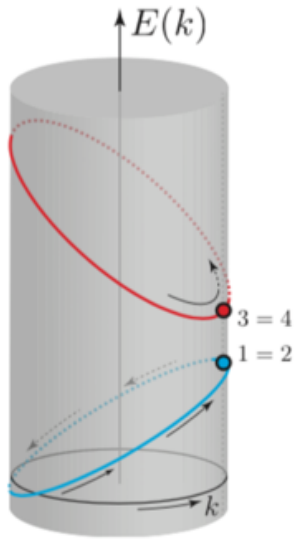

Fig. 8.17 1D bandstructure plotted in a periodic *k*-space.

- The effective mass at any k is proportional to the curvature of the energy band at that k
- States at the Brillouin Zone edges 1=2 and 3=4.
- After the opening of the bandgap, E(k+G) = E(k), the allowed energies are periodic in k-space.

Bands, Gaps, Metals vs Insulators

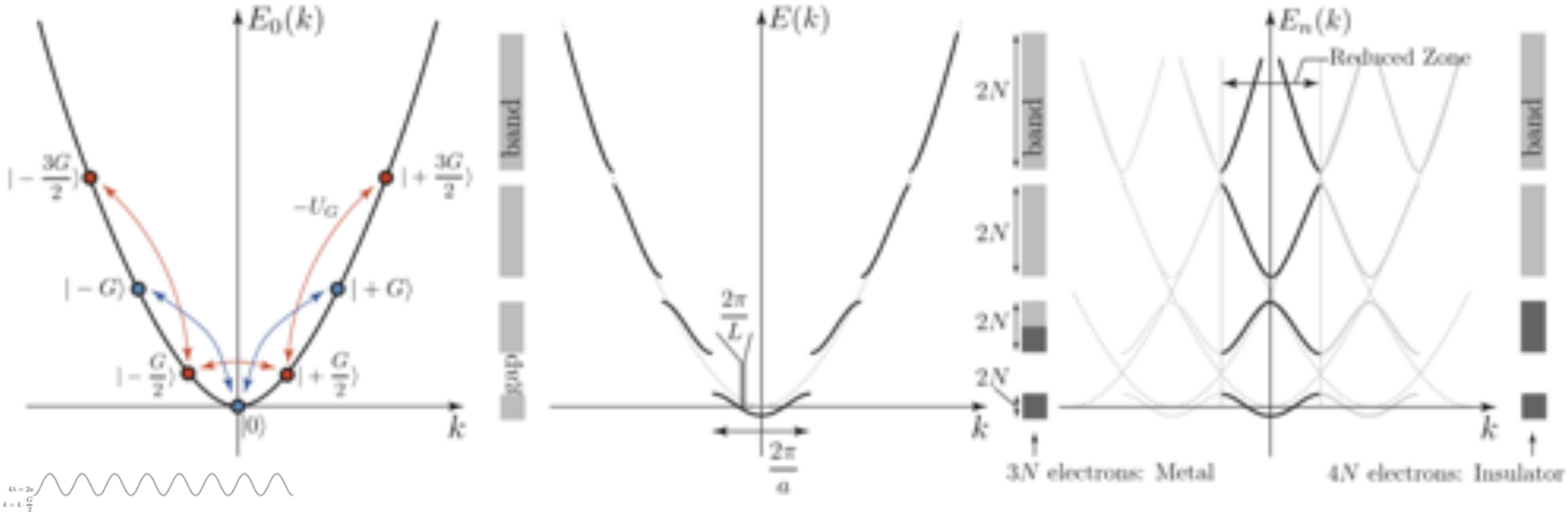

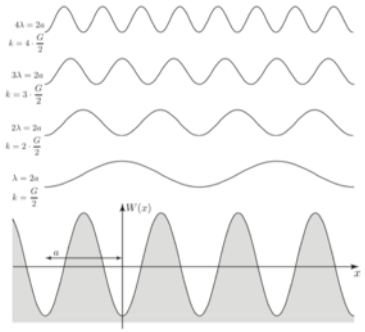

Fig. 8.10 Energy gaps open at $k = n \cdot \frac{G}{2}$, which is identical to the conditions when the electron wavelengths become resonant with twice the lattice constant, i.e. $n\lambda = 2a$. This is analogous to Bragg's law of diffraction for a wave incident at an angle θ on a crystal of period d, when the law reads $n\lambda = 2d\sin\theta$.

Because the width of each band in the $k-$space is $G = \frac{2\pi}{a}$, and the separation between two allowed states is $\frac{2\pi}{L}$ where L is the macroscopic length, **the number of states in each band is $N = L/a$, equal to the number of atoms in the crystal.** Since each allowed state can hold 2 electrons of opposite spin, **each band can hold 2N electrons.** We can plot all energies within $-\frac{G}{2} \leq k \leq +\frac{G}{2}$ and index them as $E_n(k)$ where n indicates a reciprocal lattice vector. Because of the opening of the bandgaps, when an electron in an allowed band moves in response to $F = \hbar\frac{dk}{dt}$, it cannot jump to the higher band when its $k \to \pm\frac{G}{2}$ under moderate forces[5]. In that case, the electron remains in the same band, but enters it from $k = -\frac{G}{2}$. This is because they are actually the same point in the reduced zone scheme.

Fig. 8.1 Alan Wilson in 1930s explained how the number of electrons and periodic arrangement of atoms decides if a solid is a metal, a semiconductor, or an insulator. The idea is similar to the formation of open and closed shells for electrons in atoms periodically as the electron number increases.

Bandgap, band-edge states, effective masses

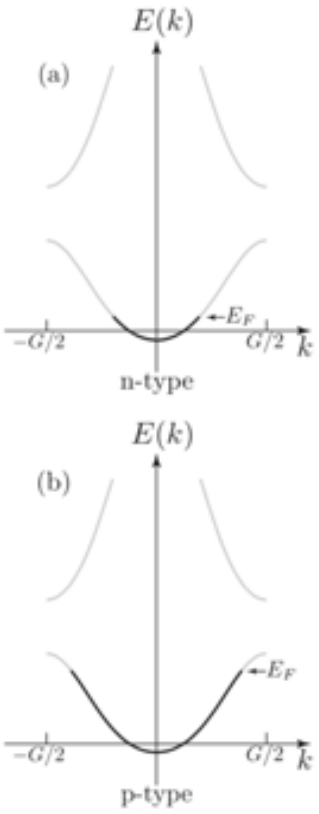

Fig. 8.11 The band theory developed by Peierls for the first time offered an explanation for a positive measured Hall coefficient. Though the particles conducting the electric current are all electrons, the Hall effect shows a positive sign for some metals and doped semiconductors. This is because the Fermi level is near the top of a band, the effective mass is negative, and the transport can be thought of as due to the superposition of a filled band with zero conductivity, with positively charged holes at the top of the band.

$$v_g = \frac{1}{\hbar}\frac{\partial E(k)}{\partial k}$$

Group velocity of state k = slope of the band at that k

$$J = q\frac{g_s}{L}\sum_k v_g(k) f(k)$$

Quantum current carried by electrons in a band

$$J_{filled} = q\frac{g_s}{L}\sum_k v_g(k) f(k) = 0$$

Current carried by a filled (or empty) band is zero

Filled bands carry no net current.

$$J = \underbrace{(-q)}_{\text{hole charge}} \frac{g_s}{L}\sum_k v_g(k) \underbrace{[1-f(k)]}_{\text{hole occupation probability}}$$

- Current is carried in an almost filled band by HOLES.
- Holes behave as POSITIVE charges.
- Hole conduction causes a POSITIVE sign in the Hall Effect.
- Holes behave as POSITIVE charges in Field Effect.

Metals, Insulators and Semimetals

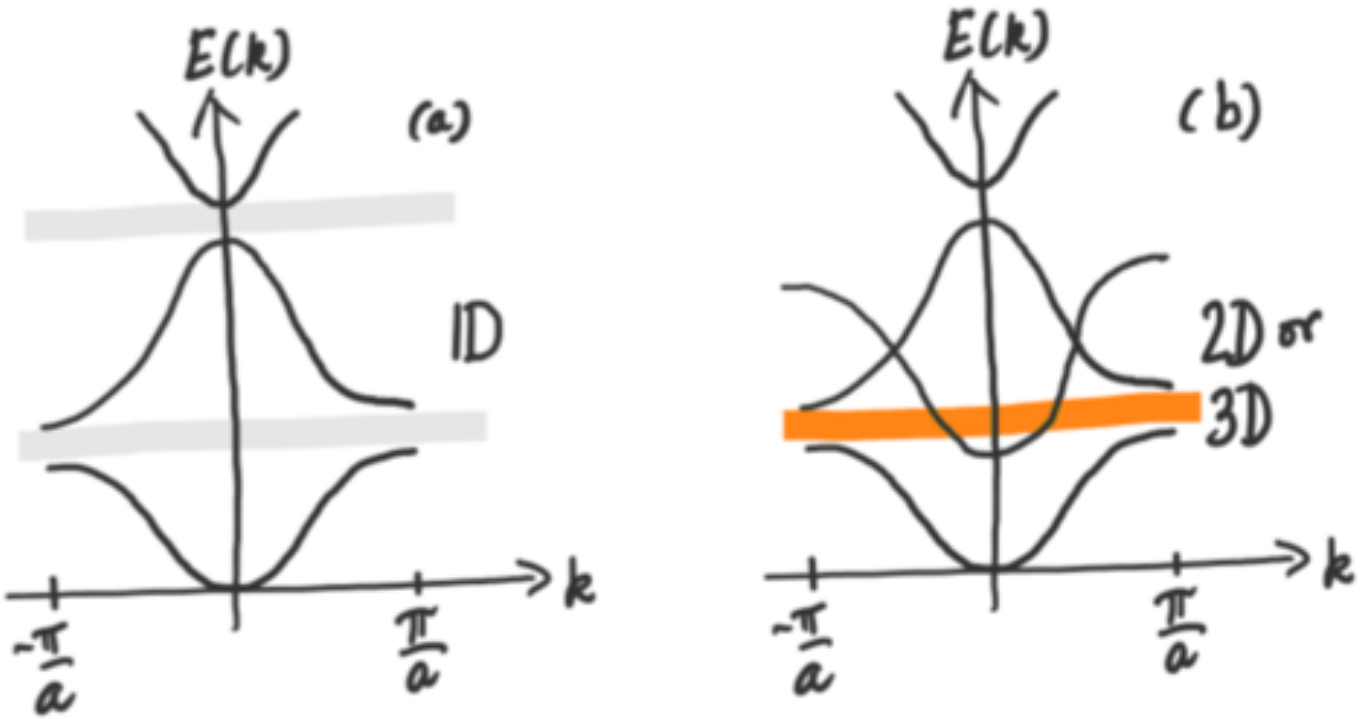

Fig. 8.17 Impossibility of band overlaps in 1D, and possible overlaps in 2 and 3D crystals.

Higher order interactions and Bloch Theorem

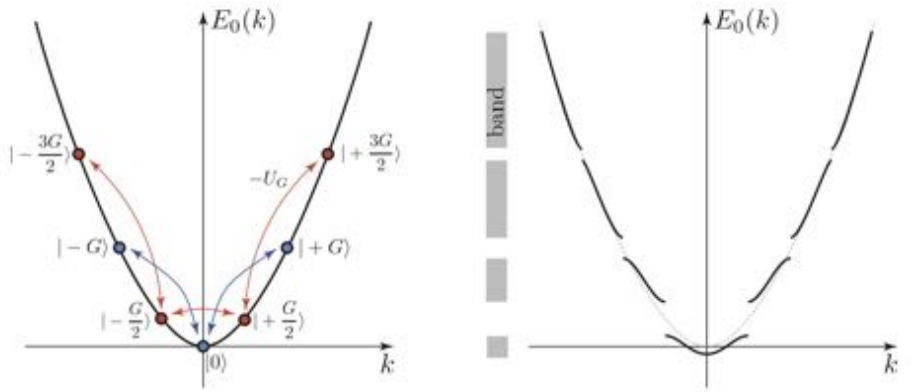

FIGURE 13.4: Indirect coupling via intermediate states. Each coupling has a strength $-U_G$.

$$\hat{H}^0 + W = \begin{array}{c} \\ \langle -G| \\ \langle 0| \\ \langle +G| \end{array} \begin{array}{c} \begin{array}{ccc} |-G\rangle & 0 & |+G\rangle \end{array} \\ \begin{pmatrix} 4F & -U_G & 0 \\ -U_G & 0 & -U_G \\ 0 & -U_G & 4F \end{pmatrix} \end{array}$$

3-level intxn

$|-G\rangle \leftrightarrow |0\rangle \leftrightarrow |+G\rangle$

E'vals

$$4F,\ 2F \pm \sqrt{4F^2 + 2U_G^2}$$

same e'vals!

$$E \approx E_u + \langle u|W|u\rangle + \sum_{m \neq u} \frac{|\langle m|\hat{W}|u\rangle|^2}{E - E'_m}$$

$|-G\rangle \leftrightarrow |0\rangle \leftrightarrow |+G\rangle$

BW $\quad E \approx 0 + 0 + \dfrac{U_G^2}{E - 4F} + \dfrac{U_G^2}{E - 4F} = -\dfrac{2U_G^2}{E - 4F}$

$|-G/2\rangle \leftrightarrow |+G/2\rangle$

BW $\quad E \approx F + \dfrac{U_G^2}{E - F} \implies E \approx F \pm U_G$

Same gap at matrix method

$|-G\rangle \leftrightarrow |0\rangle \leftrightarrow |+G\rangle$

RS $\quad E \approx 0 + 0 + \dfrac{U_G^2}{0 - 4F} + \dfrac{U_G^2}{0 - 4F} = -\dfrac{U_G^2}{2F}$

Limited applicability

Glimpses of the Bloch Theorem

Perturbation strength

$$|k'\rangle \approx |k\rangle + \frac{\langle k+G|W|k\rangle}{E(k) - E(k+G)}|k+G\rangle + \frac{\langle k-G|W|k\rangle}{E(k) - E(k-G)}|k-G\rangle$$

$$\psi_{k'}(x) = \langle x|k'\rangle \approx \frac{e^{ikx}}{\sqrt{L}} - \frac{U_G}{E(k) - E(k+G)}\frac{e^{i(k+G)x}}{\sqrt{L}} - \frac{U_G}{E(k) - E(k-G)}\frac{e^{i(k-G)x}}{\sqrt{L}}$$

$$\psi_{k'}(x) \approx e^{ikx} \cdot \underbrace{\left[\frac{1}{\sqrt{L}} - \left(\frac{U_G}{E(k) - E(k+G)}\right)\frac{e^{iGx}}{\sqrt{L}} - \left(\frac{U_G}{E(k) - E(k-G)}\right)\frac{e^{-iGx}}{\sqrt{L}}\right]}_{u_k(x)}$$

The wavefunction in a periodic potential: Is in the form of a Bloch function!

$$\psi_k(x) \approx e^{ikx}u_k(x) \qquad u_k(x+a) = u_k(x)$$

because $e^{\pm iGa} = 1$

However, note that the Bloch function is an EXACT result, meaning a non-perturbative one. But it is useful to see that perturbation theory hints at its existence.

Bloch Functions of Electrons in Periodic Potentials

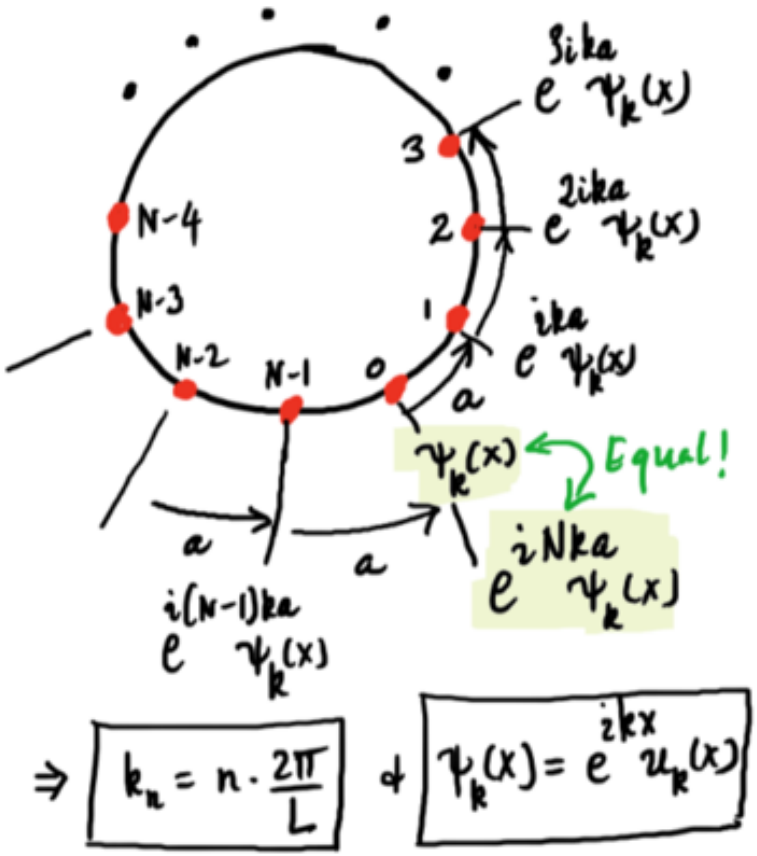

$\Rightarrow$ $k_n = n \cdot \frac{2\pi}{L}$ & $\psi_k(x) = e^{ikx} u_k(x)$

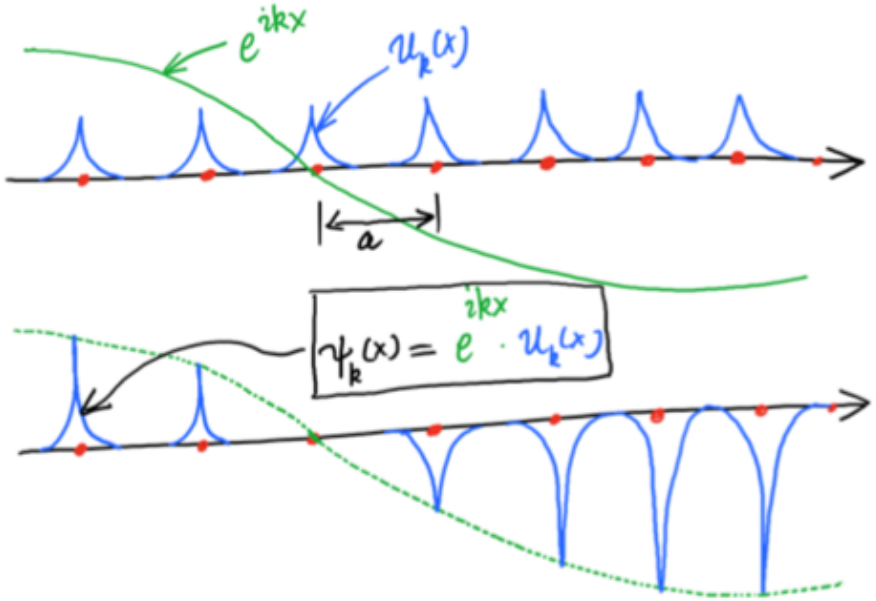

Fig. 9.2 The Bloch function is a plane wave modulated by a function periodic in the lattice constant.

Fig. 9.1 Bloch functions

$$\psi_k(x) = e^{ikx} u_k(x), \quad \text{where} \quad u_k(x+a) = u_k(x)$$

Bloch Functions of Electrons in Periodic Potentials

$$\boxed{\psi_k(x) = e^{ikx}u_k(x)}, \text{ where } \boxed{u_k(x+a) = u_k(x)}$$

$$e^{ikx} \rightarrow e^{ikx}\underbrace{(1 + \sum c_G(k)e^{iGx})}_{u_k(x)}$$

$$\langle k'|V(x)|k\rangle = \int_0^L dx \cdot e^{i(k'-k)x} \cdot \underbrace{[V(x)u^{\star}_{k'}(x)u_k(x)]}_{\sum_G c_G e^{iGx}} = \sum_G c_G \delta_{k'-k,G}$$

The most general Matrix Element for Bloch States of Electrons in Crystals

[1] "When I started to think about it, I felt that the main problem was to explain how the electrons could sneak by all the ions in a metal so as to avoid a mean free path of the order of atomic distances. Such a distance was much too short to explain the observed resistances... To make my life easy, I began by considering wave functions in a one-dimensional periodic potential. By straight Fourier analysis *I found to my delight that the wave differed from the plane wave of free electrons only by a periodic modulation* $[\psi_k(x) = e^{ikx}u_k(x)]$. This was so simple that I didn't think it could be much of a discovery, but when I showed it to Heisenberg he said right away: 'That's it!' Well that wasn't quite it yet, and my calculations were only completed in the summer when I wrote my thesis on *The Quantum Mechanics of Electrons in Crystal Lattices*." [F. Bloch 1976]

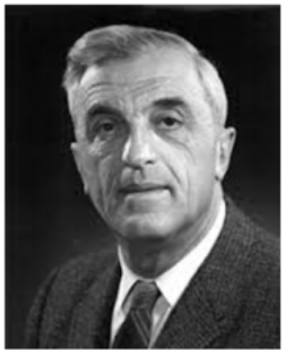

Fig. 8.12 Felix Bloch showed mathematically that electron waves can propagate in a crystal with no scattering, by introducing a wavefunction that electrons experiencing a periodic potential must satisfy. Bloch was awarded the Nobel Prize in physics in 1952 for his work on nuclear magnetic resonance.

The Nearly Free Electron Bandstructure Model

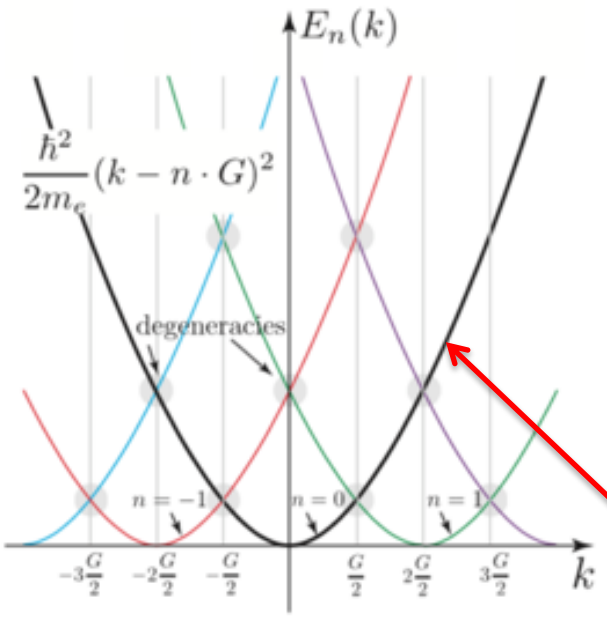

Fig. 8.13 The nearly free electron bandstructure. The model is where there is a lattice, but no crystal potential. Bloch theorem ensures that the allowed energy bands are exactly the same of a free electron, but repeated in the $k-$space by reciprocal lattice vectors, $E_n(k) = \frac{\hbar^2}{2m_e}(k - nG)^2$ where $n = 0, \pm 1, \pm 2, \ldots$. Note the points of degeneracies: these points can be split to open gaps by a periodic potential.

nearly free electron model

the periodic potential $V(x) = 0$ is turned off, but the lattice periodicity remains.

Bloch functions $\psi(x) = e^{ikx} \sum_G c_G e^{iGx}$

$$-\frac{\hbar^2}{2m_e}\frac{\partial^2}{\partial x^2}\psi(x) = E\psi(x)$$

$$\sum_G c_G e^{iGx} \frac{\hbar^2 (k+G)^2}{2m_e} = E \sum_G c_G e^{iGx}$$

the **nearly free electron (NFE) bandstructure**

$$E_n(k) = \frac{\hbar^2}{2m_e}(k - nG)^2 \text{ where } n = 0, \pm 1, \pm 2, \ldots$$

As shown in Figure 8.13, the NFE bandstructure consists of copies of the free electron bandstructure translated by nG in the $k-$axis, where $G = \frac{2\pi}{a}$ and $n = 0, \pm 1, \pm 2, \ldots$. This is a direct consequence of periodicity of the lattice.

Bandgap, band-edge states, effective masses

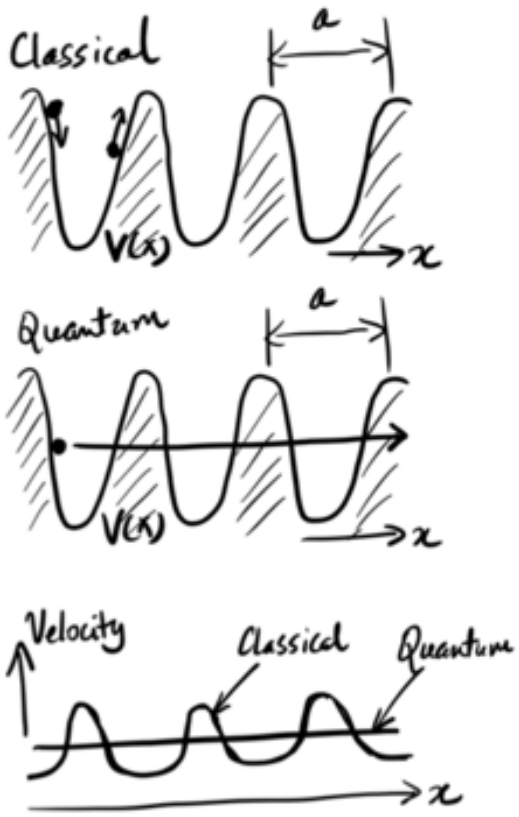

Fig. 9.7 Classical vs. Quantum pictures of a particle in a periodic potential. The Bloch state maintains the same velocity in spite of a rapidly varying periodic potential of the crystal - this is impossible in classical mechanics.

$$\langle \psi_{\mathbf{k}} | \frac{\hat{\mathbf{p}}}{m_e} | \psi_{\mathbf{k}} \rangle = \mathbf{v}(\mathbf{k}) = \frac{1}{\hbar} \nabla_{\mathbf{k}} E(\mathbf{k}).$$

$$\mathbf{F} = \hbar \frac{d\mathbf{k}}{dt}.$$ **F** is an **external** force, **k** is the **crystal momentum**.

Bandgap, band-edge states, effective masses

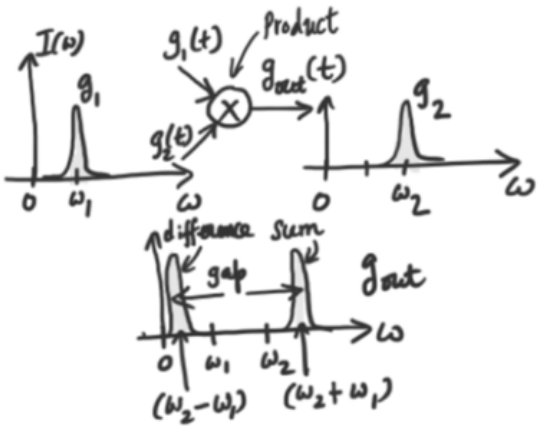

Fig. 8.14 Mixing of electronic signals produces sum and difference frequencies. The problem of electron wave propagation in a crystal is an analogous problem.

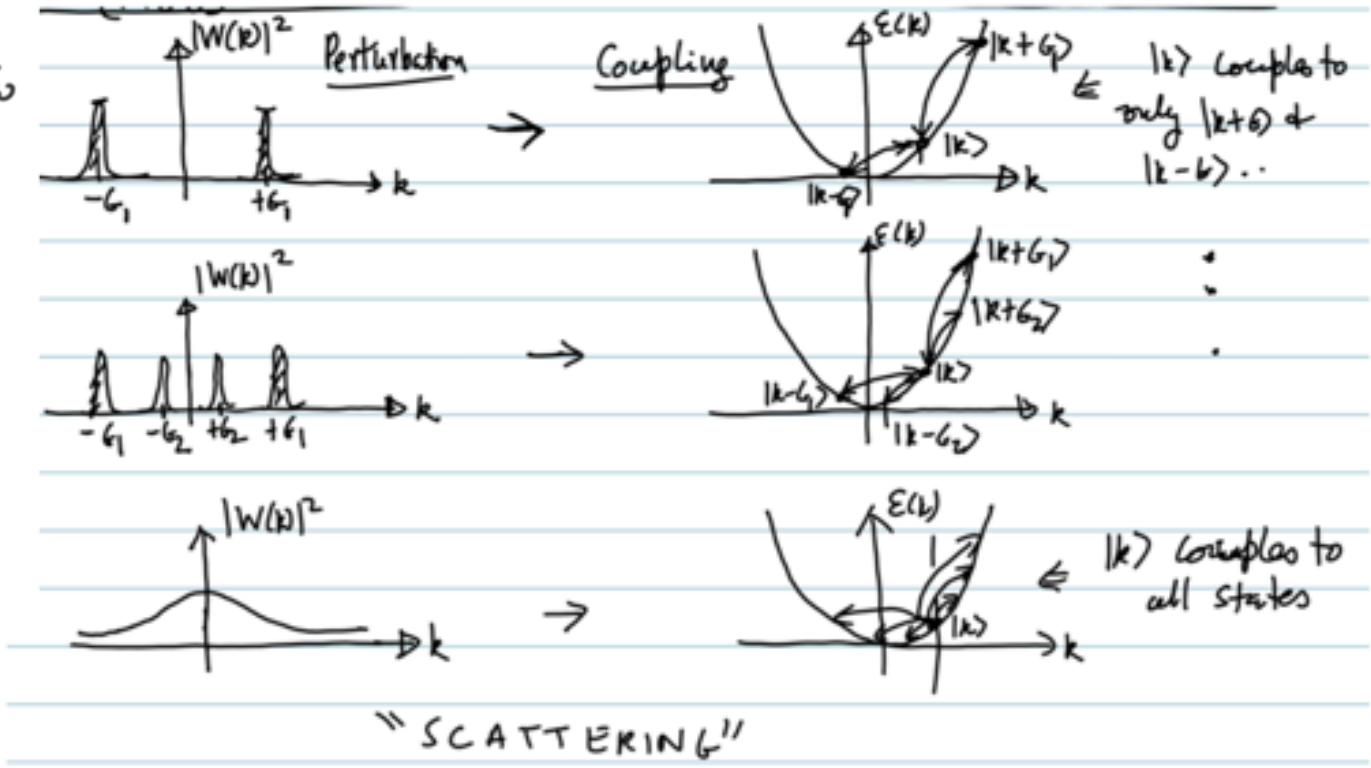

Fig. 8.15 Periodic potentials only scatter states separated by specific G values, and thus open bandgaps at specific k values because they have spectral weight only for specific k's. Non-periodic potentials on the other hand can scatter a state $|k\rangle$ into several states depending on the weight of the potential in the $k-$space.

Bandgap, band-edge states, effective masses

$$\frac{\hbar^2}{2m_e}(k+G)^2 c_G + \sum_{G'} \mathcal{V}_{G-G'} c_{G'} = E_G(k) c_G.$$

→ **Exact Bandstructure**, Chapter 12

$$E_G(k) = \frac{\hbar^2}{2m_e}(k+G)^2, \text{ and } \psi_G(x) = \frac{1}{\sqrt{L}} e^{i(k+G)x} = e^{ikx} \cdot \underbrace{\left(\frac{1}{\sqrt{L}} e^{iGx}\right)}_{u(x)} \quad (9.9)$$

→ **Empty lattice bandstructure, Brillouin zones**, this Chapter

$$\psi_k(x) = \sum_{n=1}^{N} \frac{e^{ikna}}{\sqrt{N}} \phi(x-na) \implies \psi_k(x+a) = e^{ika}\psi_k(x). \quad (9.10)$$

→ **The tight binding model**, Chapter 10.

$$\left[\frac{(\hat{\mathbf{p}}+\hbar\mathbf{k})^2}{2m_e} + V\right] u_{\mathbf{k}} = E(\mathbf{k}) u_{\mathbf{k}}.$$

$$\left[-\frac{\hbar^2}{2m_e}\nabla^2 + V\right] u_{\mathbf{k}} + \left(\frac{\hbar}{m_e}\mathbf{k}\cdot\hat{\mathbf{p}}\right) u_{\mathbf{k}} = \left[E(\mathbf{k}) - \frac{\hbar^2|\mathbf{k}|^2}{2m_e}\right] u_{\mathbf{k}}.$$

→ The '$\mathbf{k}\cdot\mathbf{p}$' approximation, Chapter 11.

Some consequences of symmetry on E(k)

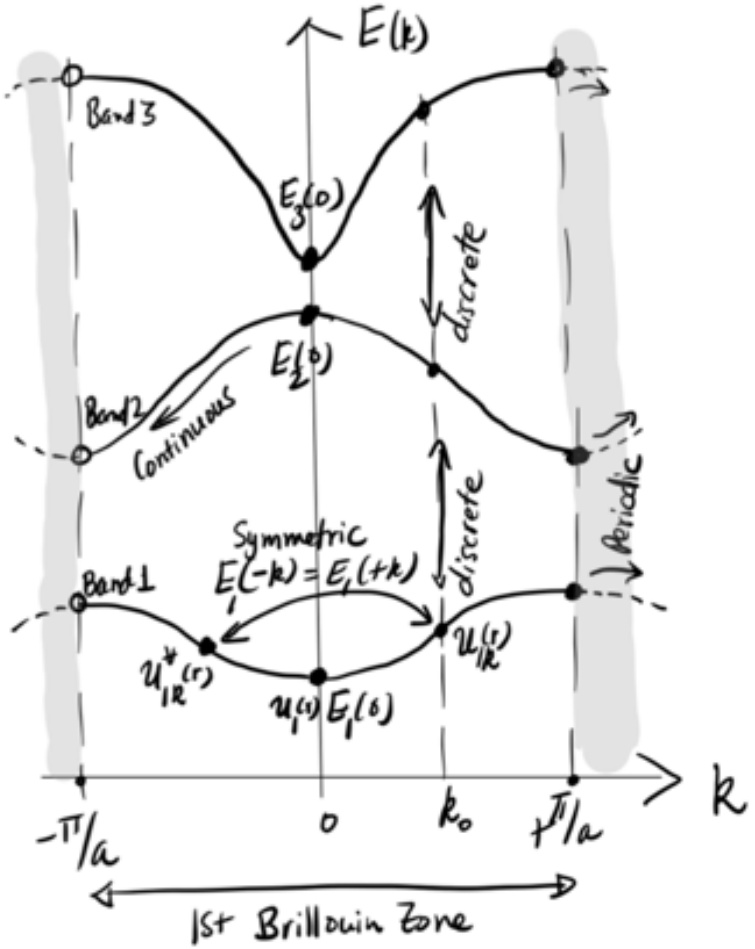

Fig. 9.14 Properties energy bands must satisfy for Bloch states in crystals.

Table 9.2 Symmetries of Bloch Eigenvalues.

Time Reversal ($t \rightarrow -t$) $E_{n,\uparrow}(\mathbf{k}) \rightarrow E_{n,\downarrow}(-\mathbf{k})$ $E_{n,\downarrow}(\mathbf{k}) \rightarrow E_{n,\uparrow}(-\mathbf{k})$
Inversion ($\mathbf{r} \rightarrow -\mathbf{r}$) $E_{n,\uparrow}(\mathbf{k}) \rightarrow E_{n,\uparrow}(-\mathbf{k})$ $E_{n,\downarrow}(\mathbf{k}) \rightarrow E_{n,\downarrow}(-\mathbf{k})$
TR & Inversion $E_n(\mathbf{k}) = E_n(-\mathbf{k})$
Lattice periodicity $E_n(\mathbf{k}+\mathbf{G}) = E_n(\mathbf{k})$

Electron group velocity

$$\mathbf{F} = \hbar \frac{d\mathbf{k}}{dt}.$$ **F** is an **external** force, **k** is the **crystal momentum**.

$$\langle \psi_{\mathbf{k}} | \frac{\hat{\mathbf{p}}}{m_e} | \psi_{\mathbf{k}} \rangle = \mathbf{v}(\mathbf{k}) = \frac{1}{\hbar} \nabla_{\mathbf{k}} E(\mathbf{k}).$$

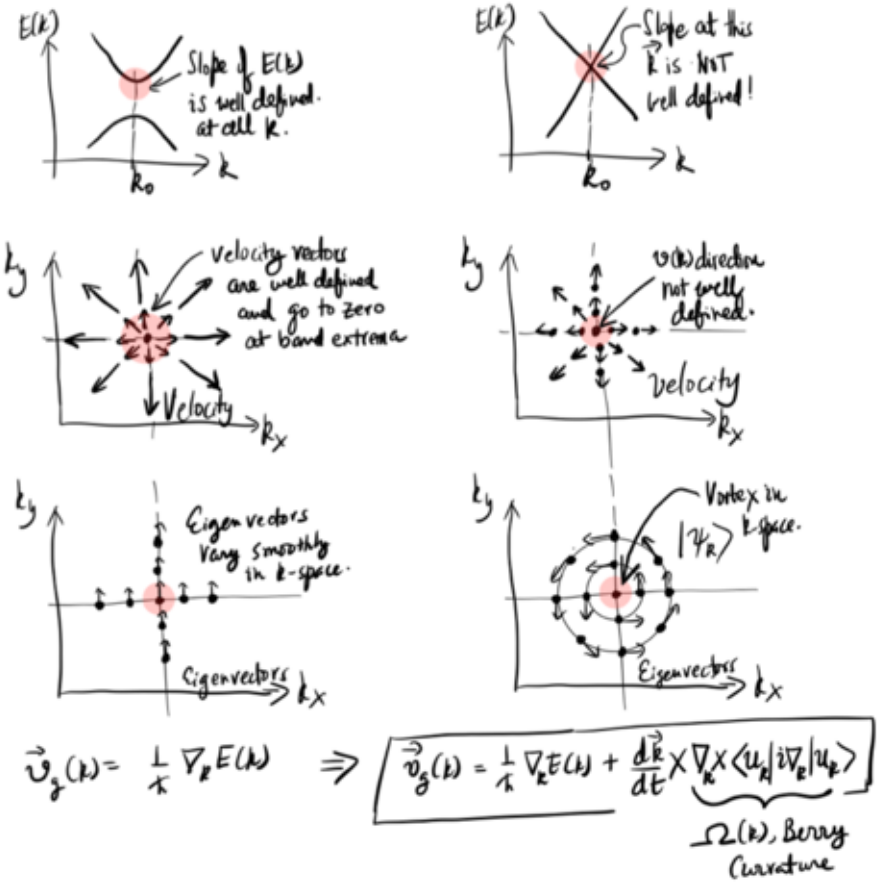

$$\mathbf{v}(\mathbf{k}) = \frac{1}{\hbar} \nabla_{\mathbf{k}} E(\mathbf{k}) - \frac{\mathbf{F}}{\hbar} \times \mathbf{\Omega}_{\mathbf{k}}.$$

Bloch Functions of Electrons in Periodic Potentials

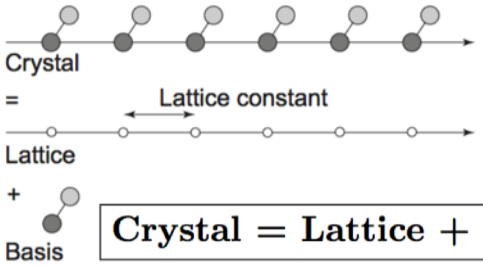

$$\textbf{Crystal} = \textbf{Lattice} + \textbf{Basis}.$$

$$e^{ikx} \rightarrow e^{ikx}\underbrace{(1 + \sum c_G(k)e^{iGx})}_{u_k(x)}$$

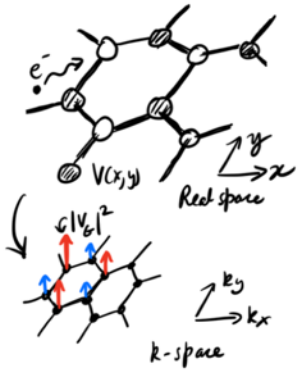

Real Space

$$\Omega_r = \mathbf{a_1} \cdot \mathbf{a_2} \times \mathbf{a_3}$$

$$\mathbf{R} = n_1\mathbf{a_1} + n_2\mathbf{a_2} + n_3\mathbf{a_3}$$

Wigner-Seitz cell

Reciprocal Space or k-space

Fig. 9.12 The crystal potential in the **k**−space is **concentrated** at the reciprocal lattice points **G**.

$$\mathbf{b_1} = 2\pi\frac{\mathbf{a_2} \times \mathbf{a_3}}{\mathbf{a_1} \cdot \mathbf{a_2} \times \mathbf{a_3}}, \mathbf{b_2} = 2\pi\frac{\mathbf{a_3} \times \mathbf{a_1}}{\mathbf{a_1} \cdot \mathbf{a_2} \times \mathbf{a_3}}, \mathbf{b_3} = 2\pi\frac{\mathbf{a_1} \times \mathbf{a_2}}{\mathbf{a_1} \cdot \mathbf{a_2} \times \mathbf{a_3}}.$$

$$\mathbf{G} = m_1\mathbf{b_1} + m_2\mathbf{b_2} + m_3\mathbf{b_3}$$

Brillouin Zone

$|\psi_{\mathbf{k}}(\mathbf{r}+\mathbf{R})|^2 = |\psi_{\mathbf{k}}(\mathbf{r})|^2$: **The Bloch wavefunction *squared* repeats in every Wigne**

$|\psi_{\mathbf{k}+\mathbf{G}}(\mathbf{r})|^2 = |\psi_{\mathbf{k}}(\mathbf{r})|^2$: **The Bloch wavefunction *squared* repeats in every BZ.**

Crystals in 1D, 2D, and 3D

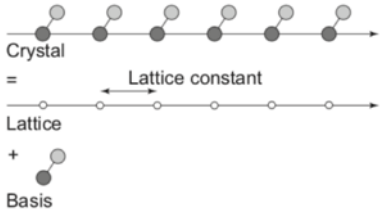

Fig. 9.10 Crystal = Lattice + Basis.

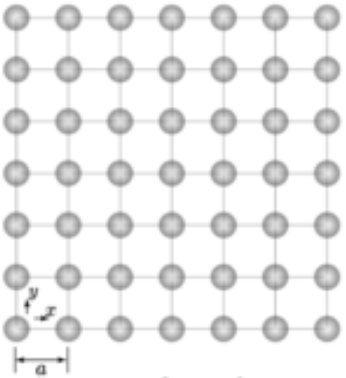

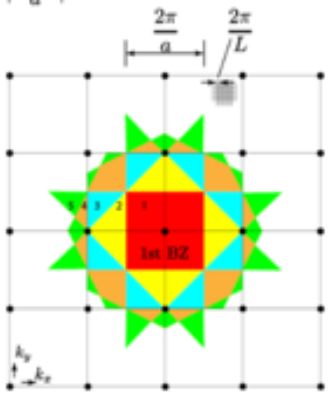

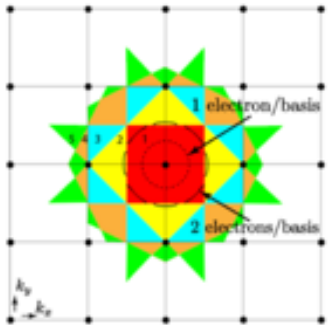

Fig. 9.13 A 2D crystal (top) and its reciprocal lattice points (middle), defining the **Brillouin Zones** of a 2D square lattice. The bottom figure indicates that the 1st BZ is filled up to the dashed line constant-energy contour for monovalent atoms with $N = 1$, and spills over to the 2nd BZ shown as solid line constant energy contours for divalent atoms with $N = 2$.

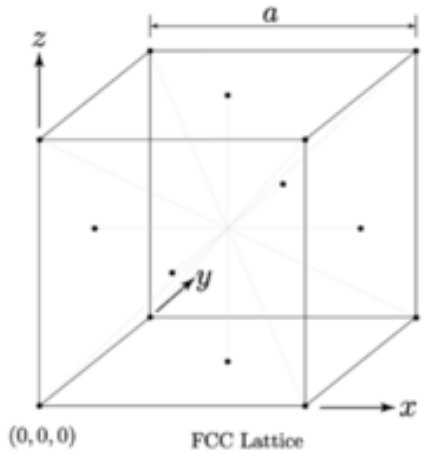

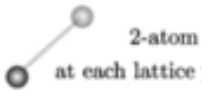

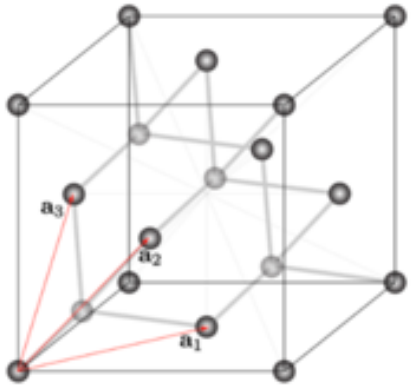

Crystal structure of Silicon, Diamond, GaAs, etc...

Fig. 9.11 The FCC lattice, a 2-atom basis, and the crystal of Silicon, Diamond, GaAs, InP, and a wide variety of semiconductors. The three arrows from $(0, 0, 0)$ to the face center lattice sites are the primitive lattice vectors.

2D Bravais Lattices

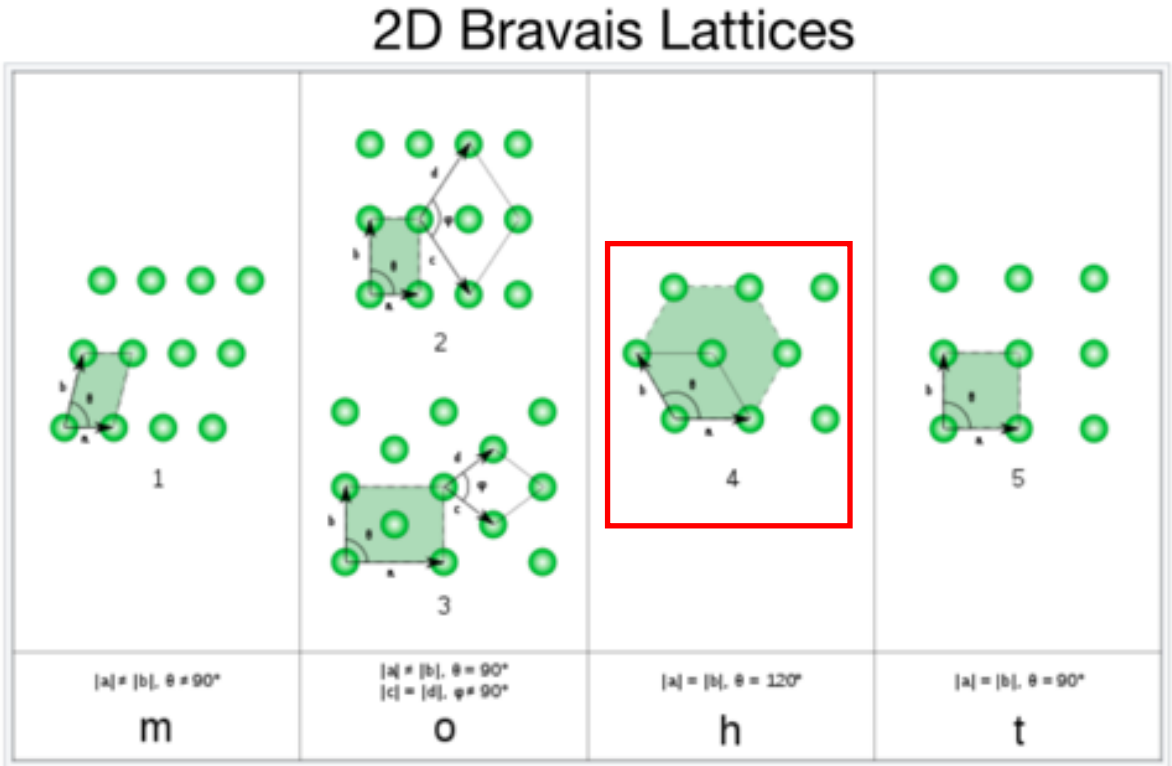

1 – oblique (monoclinic), 2 – rectangular (orthorhombic), 3 – centered rectangular (orthorhombic), 4 – hexagonal, and 5 – square (tetragonal).

Crystal family	Point group (Schönflies notation)	5 Bravais lattices	
		Primitive	Centered
Monoclinic	C_2	Oblique	
Orthorhombic	D_2	Rectangular	Centered rectangular
Hexagonal	D_6	Hexagonal	
Tetragonal	D_4	Square	

Crystal family	Area	Axial distances (edge lengths)	Axial angle
Monoclinic	$ab \sin\theta$	$a \neq b$	$\theta \neq 90°$
Orthorhombic	ab	$a \neq b$	$\theta = 90°$
Hexagonal	$\frac{\sqrt{3}}{2}a^2$	$a = b$	$\theta = 120°$
Tetragonal	a^2	$a = b$	$\theta = 90°$

Fig. 9.21 Bravais Lattices in 2D from Wikipedia.

3D Bravais Lattices

Crystal Family	Lattice System	Schönflies	14 Bravais Lattices			
			Primitive (P)	Base-centered (C)	Body-centered (I)	Face-centered (F)
Triclinic		C_i				
Monoclinic		C_{2h}				
Orthorhombic		D_{2h}				
Tetragonal		D_{4h}	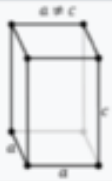			
Hexagonal	Rhombohedral	D_{3d}	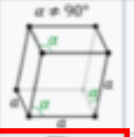			
	Hexagonal	D_{6h}	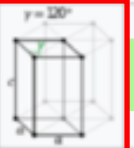			
Cubic		O_h	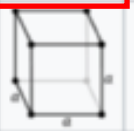			

GaN, AlN

Si, Ge, GaAs

The first measured crystal structure: FCC!

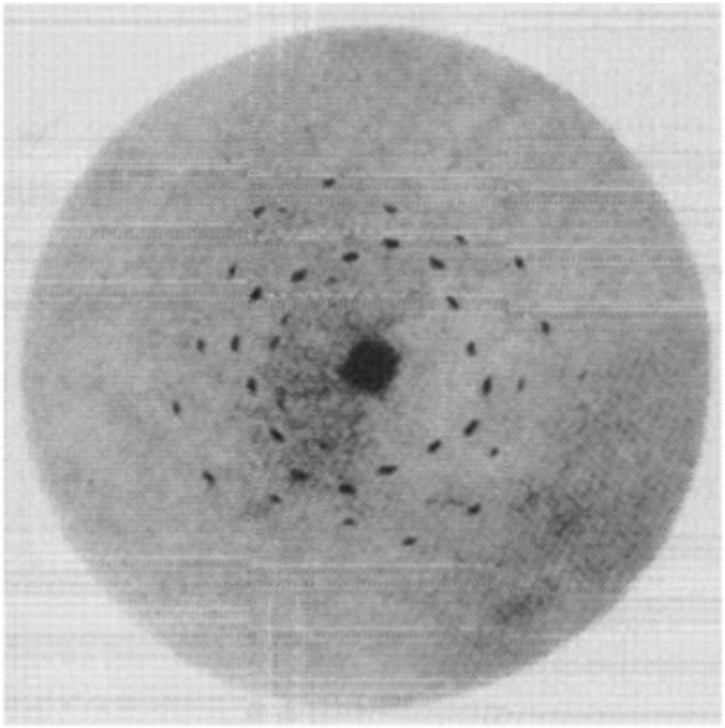

Fig. 9.16 The famous 'Fig 5', showing the diffraction spots observed by Max von Laue in Munich due to Roentgen's X-Rays bouncing off a crystal of ZnS, a semiconductor.

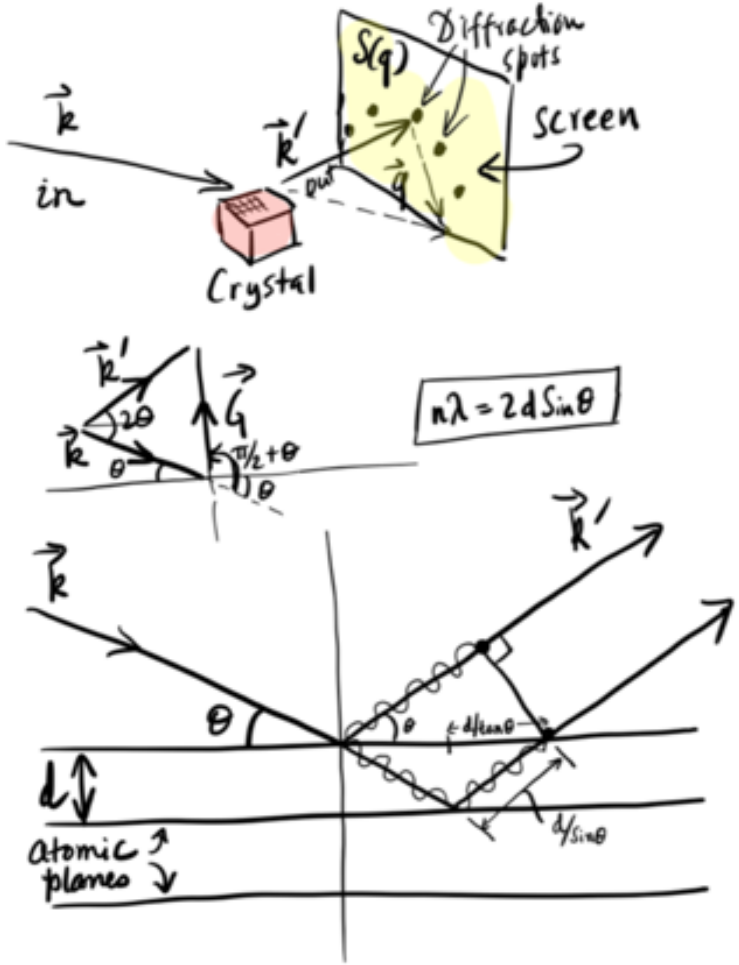

Fig. 9.18 Bragg Law for diffraction of X-Rays from a crystal.

TEM images of semiconductor crystals

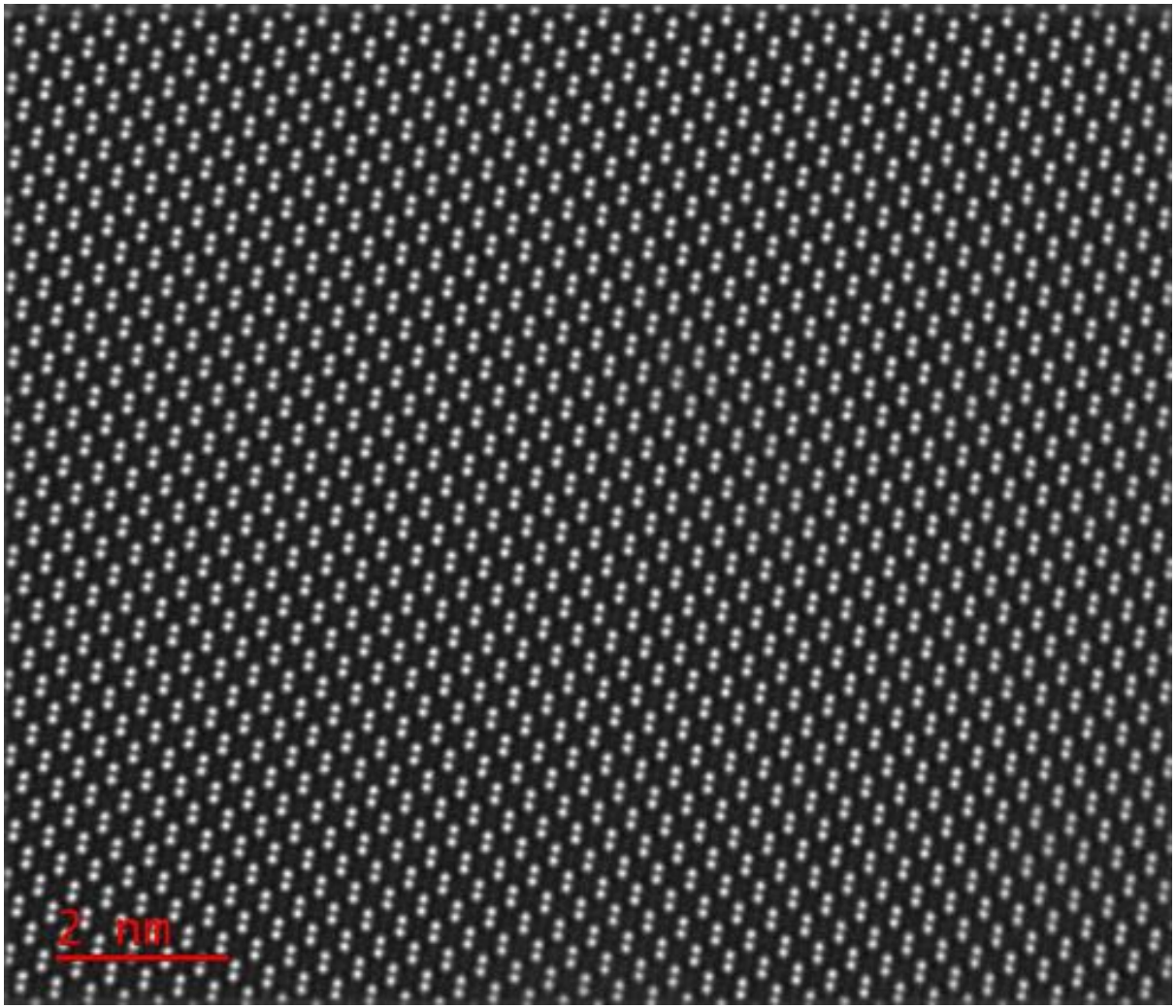

Silicon Crystal

TEM images of semiconductor crystals

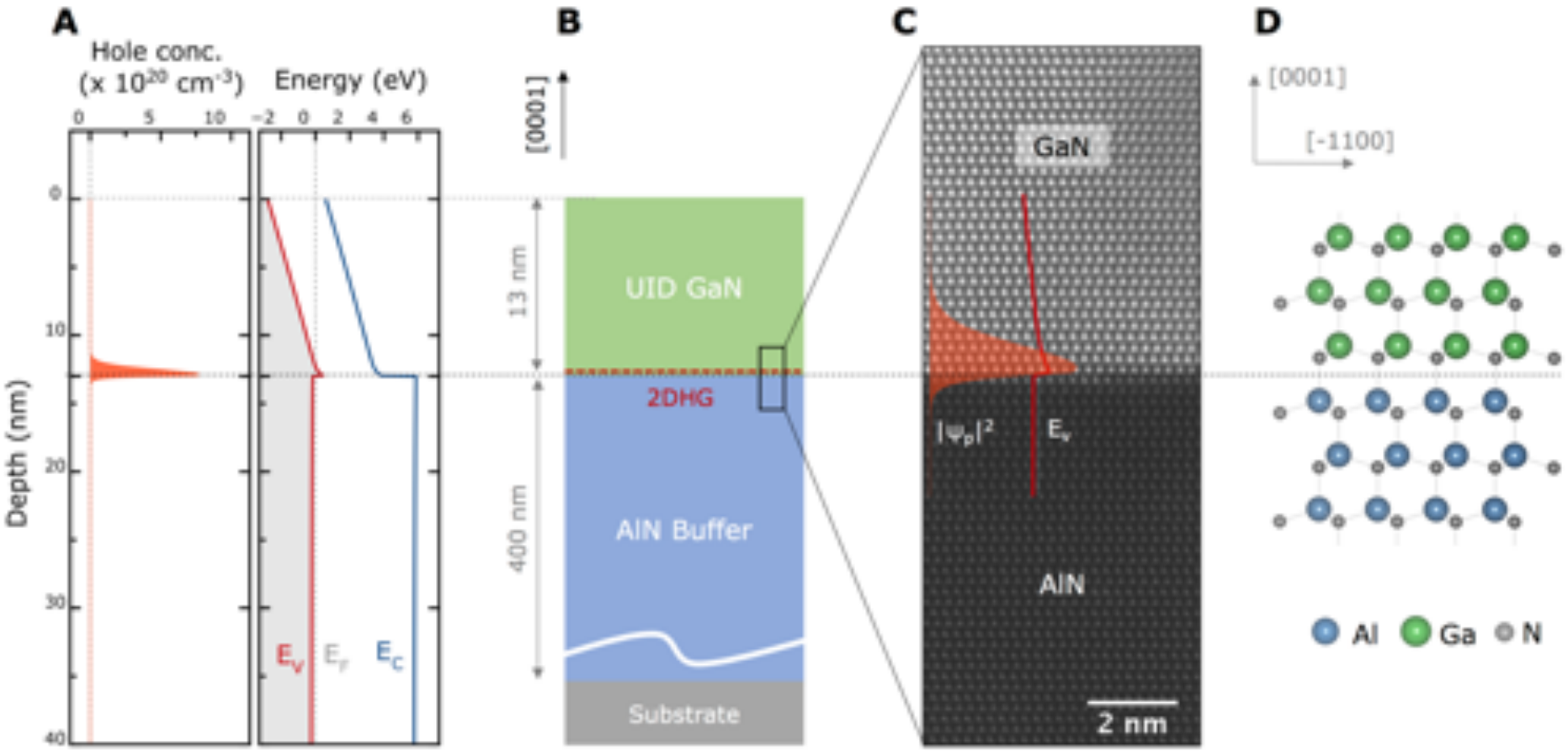

GaN/AlN Quantum Well
Grown/Imaged @ Cornell

Face-Centered Cubic Lattice

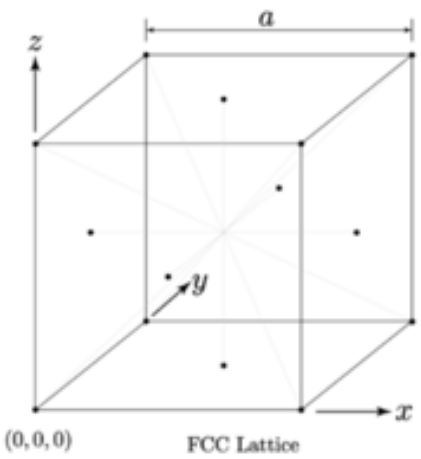

+

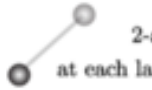

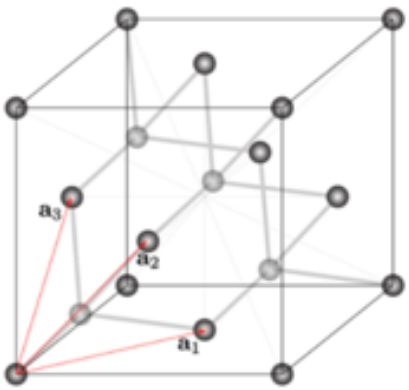

Crystal structure of Silicon, Diamond, GaAs, etc...

1st step in bandstructure calculation: Determine **primitive lattice vectors, $\mathbf{a}_1, \mathbf{a}_2, \mathbf{a}_3$**

primitive lattice vectors for Silicon-like crystals are $\mathbf{a}_1 = a(\frac{1}{2}, \frac{1}{2}, 0)$, $\mathbf{a}_2 = a(0, \frac{1}{2}, \frac{1}{2})$, and $\mathbf{a}_3 = a(\frac{1}{2}, 0, \frac{1}{2})$.

$$\Omega_u = \mathbf{a}_1 \cdot \mathbf{a}_2 \times \mathbf{a}_3 = a(\frac{1}{2}, \frac{1}{2}, 0) \cdot a(0, \frac{1}{2}, \frac{1}{2}) \times a(\frac{1}{2}, 0, \frac{1}{2})$$
$$= a(\frac{1}{2}, \frac{1}{2}, 0) \cdot a^2(\frac{1}{4}, \frac{1}{4}, -\frac{1}{4}) = a^3(\frac{1}{8} + \frac{1}{8}) = \boxed{\frac{a^3}{4}}.$$

FCC Primitive cell volume

Now the greatest importance of the Wigner-Seitz cell is recognized when we move from the real space to the wavevector, or $\mathbf{k}-$space. Corresponding to the three real space primitive lattice vectors are the three **primitive reciprocal lattice vectors** given by

$$\mathbf{b}_1 = 2\pi \frac{\mathbf{a}_2 \times \mathbf{a}_3}{\mathbf{a}_1 \cdot \mathbf{a}_2 \times \mathbf{a}_3}, \mathbf{b}_2 = 2\pi \frac{\mathbf{a}_3 \times \mathbf{a}_1}{\mathbf{a}_1 \cdot \mathbf{a}_2 \times \mathbf{a}_3}, \mathbf{b}_3 = 2\pi \frac{\mathbf{a}_1 \times \mathbf{a}_2}{\mathbf{a}_1 \cdot \mathbf{a}_2 \times \mathbf{a}_3}. \quad (9.43)$$

With an integer triplet (m_1, m_2, m_3), the vectors

$$\mathbf{G} = m_1\mathbf{b}_1 + m_2\mathbf{b}_2 + m_3\mathbf{b}_3 \quad (9.44)$$

define the **reciprocal space lattice**, just as the real-space lattice of the crystal.

2nd step in bandstructure calculation: Convert real space points to reciprocal space

The Nearly Free Electron Model for Any FCC Lattice

3rd step in bandstructure calculation: Calculate the Nearly Free Electron Bandstructure for various reciprocal lattice vector bands (typical Gmax<4).

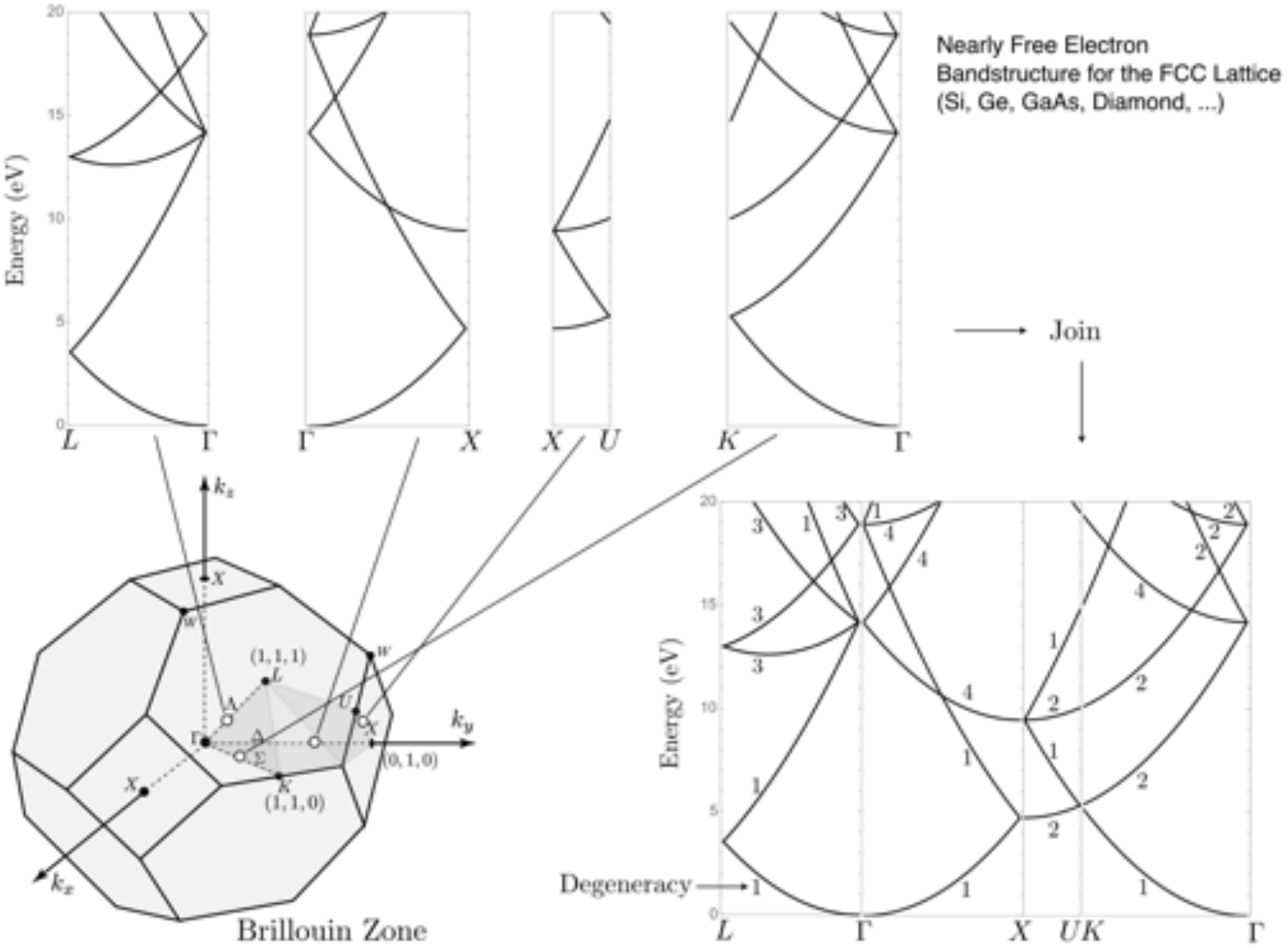

The Nearly Free Electron Model for Any HCP Lattice

3rd step in bandstructure calculation: Calculate the Nearly Free Electron Bandstructure for various reciprocal lattice vector bands (typical Gmax<4).

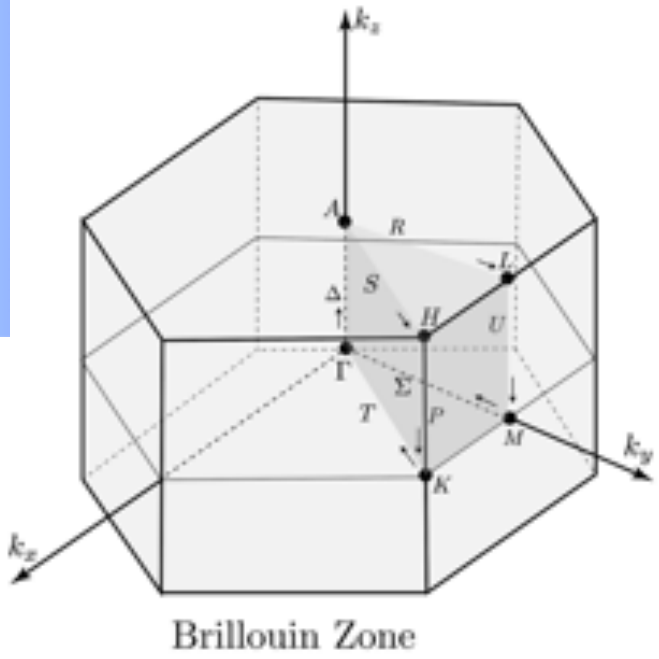

Brillouin Zone

Nearly Free Electron Bandstructure for the HCP Lattice (GaN, AlN, InN, ZnO, ZnS, ...)

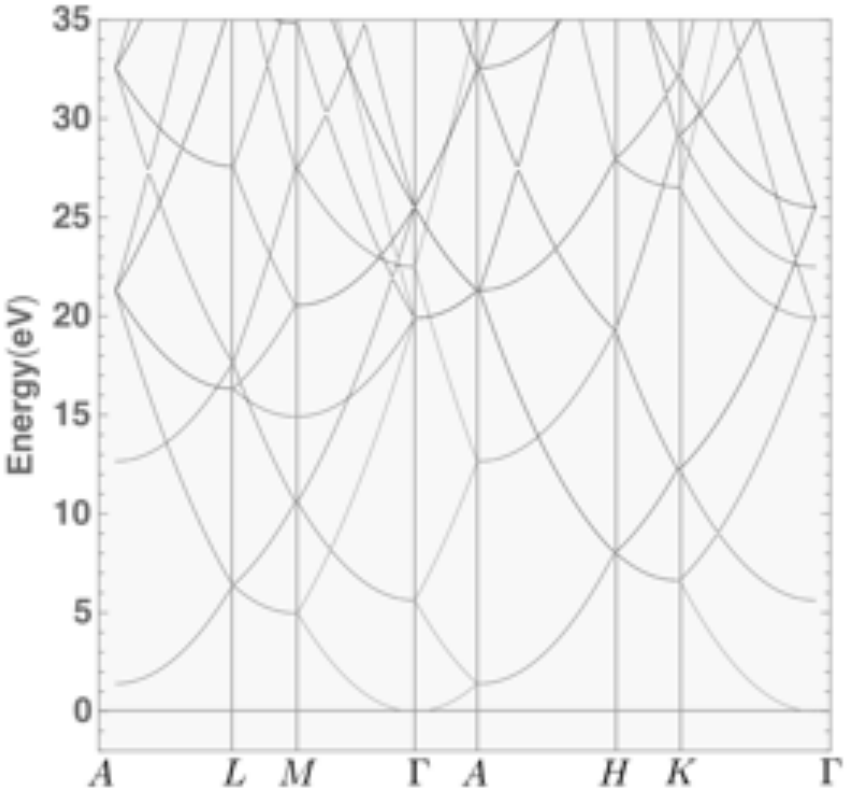

Semiconductors, Semimetals, Metals, Insulators

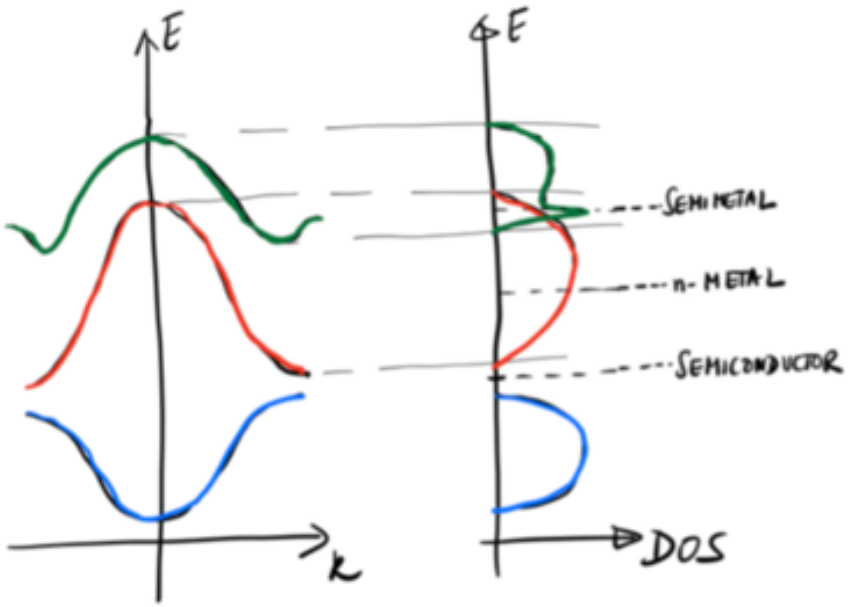

Fig. 9.26 Semiconductors, Metals, and Semimetals differ primarily by the density of states at their Fermi level, $g(E_F)$. The Fermi level is determined by counting the total valence electrons/basis of a crystal and using the rule that each filled band holds $2N$ electrons.

Bloch State: Current with Scattering

$$\mathbf{F} = \hbar\frac{d\mathbf{k}}{dt} - \frac{\hbar\Delta\mathbf{k}}{\tau_\mathbf{k}}$$

$$J = q\frac{g_s g_v}{L}\sum_k v_g(k)f(k) = q\frac{g_s g_v}{L}\sum_k v_g(k)f(\mathbf{k}(0) - \frac{\mathbf{F}\tau_\mathbf{k}}{\hbar})$$

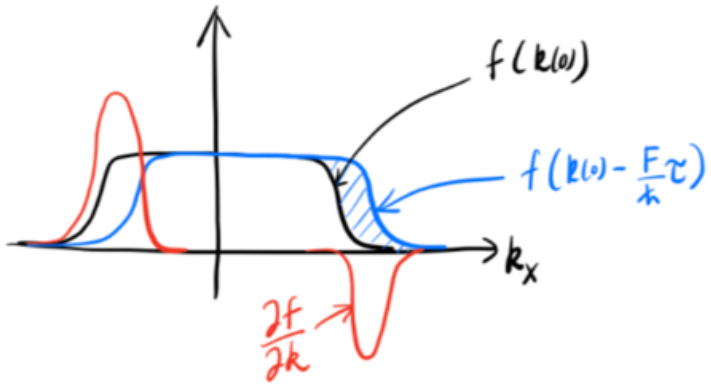

$$f(\mathbf{k}(0) - \tfrac{\mathbf{F}\tau_\mathbf{k}}{\hbar}) \approx f(\mathbf{k}(0)) - \tfrac{\mathbf{F}\tau_\mathbf{k}}{\hbar}\cdot\nabla_\mathbf{k} f(\mathbf{k}(0))$$

$$J = q\frac{g_s g_v}{L}\sum_k v_g(k)f(\mathbf{k}(0) - \frac{\mathbf{F}\tau_\mathbf{k}}{\hbar})$$

$$\approx \underbrace{q\frac{g_s g_v}{L}\sum_k v_g(k)f(\mathbf{k}(0))}_{0} + q\frac{g_s g_v}{L}\frac{\mathbf{F}}{\hbar}\cdot\sum_k v_g(k)\tau_\mathbf{k}(-\nabla_\mathbf{k} f(\mathbf{k}(0))),$$

Fig. 9.25 The occupation function shifts from the equilibrium Fermi-Dirac value upon the application of an external force. The sketch indicates $f(\mathbf{k})$, $f(\mathbf{k} - \frac{\mathbf{F}}{\hbar}\tau)$, and $\nabla_\mathbf{k} f(\mathbf{k})$.

$$n = \frac{g_s g_v}{L^d}\sum_k f(k)$$

$$\mathcal{L}_q = \frac{\kappa}{\sigma T} = \frac{g_s g_v \ln(\frac{N_c}{n})k_b \int \frac{d^d k}{(2\pi)^d} v^2 \tau E \frac{\partial f}{\partial E}}{T\cdot q^2 \cdot g_s g_v \int \frac{d^d k}{(2\pi)^d} v^2 \tau \frac{\partial f}{\partial E}} \underbrace{\rightarrow}_{\text{semi-classical approx.}} \sim (\frac{k_b}{q})^2$$

$$J \approx \frac{nq^2}{m^\star}\underbrace{(\frac{2}{d}\frac{\sum_k E_\mathbf{k}\tau_\mathbf{k}(-\frac{\partial f(k)}{\partial E_\mathbf{k}})}{\sum_k f(k)})}_{\langle\tau\rangle} E = \underbrace{\frac{nq^2\langle\tau\rangle}{m^\star}}_{\sigma} E = qn\underbrace{\frac{q\langle\tau\rangle}{m^\star}}_{\mu} E,$$

Energy Bands of Si, Ge, and GaAs for Reference

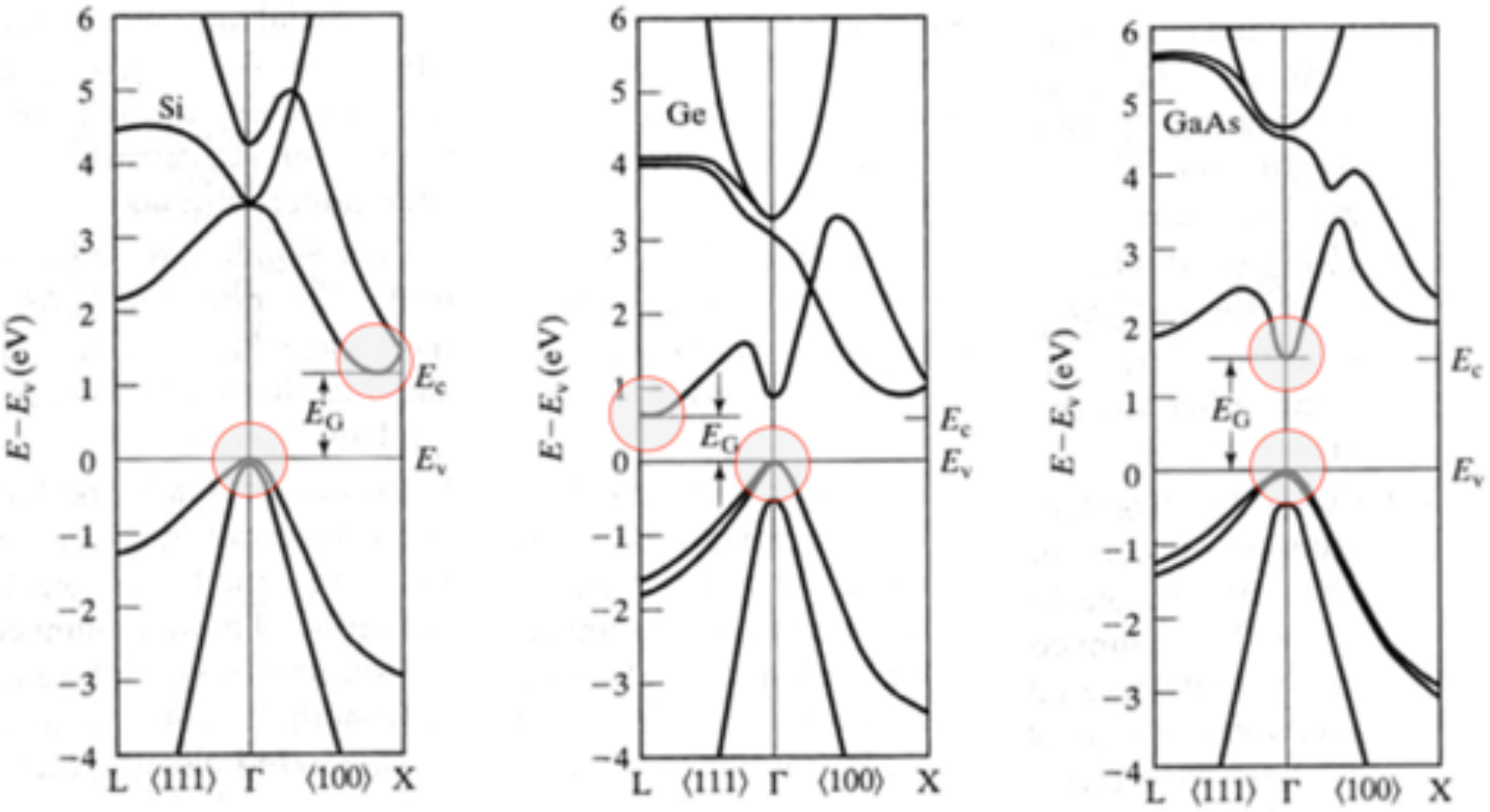

ECE 4070 / MSE 6050
Energy Bandstructures of the most common Semiconductors

The elements that form semiconductors

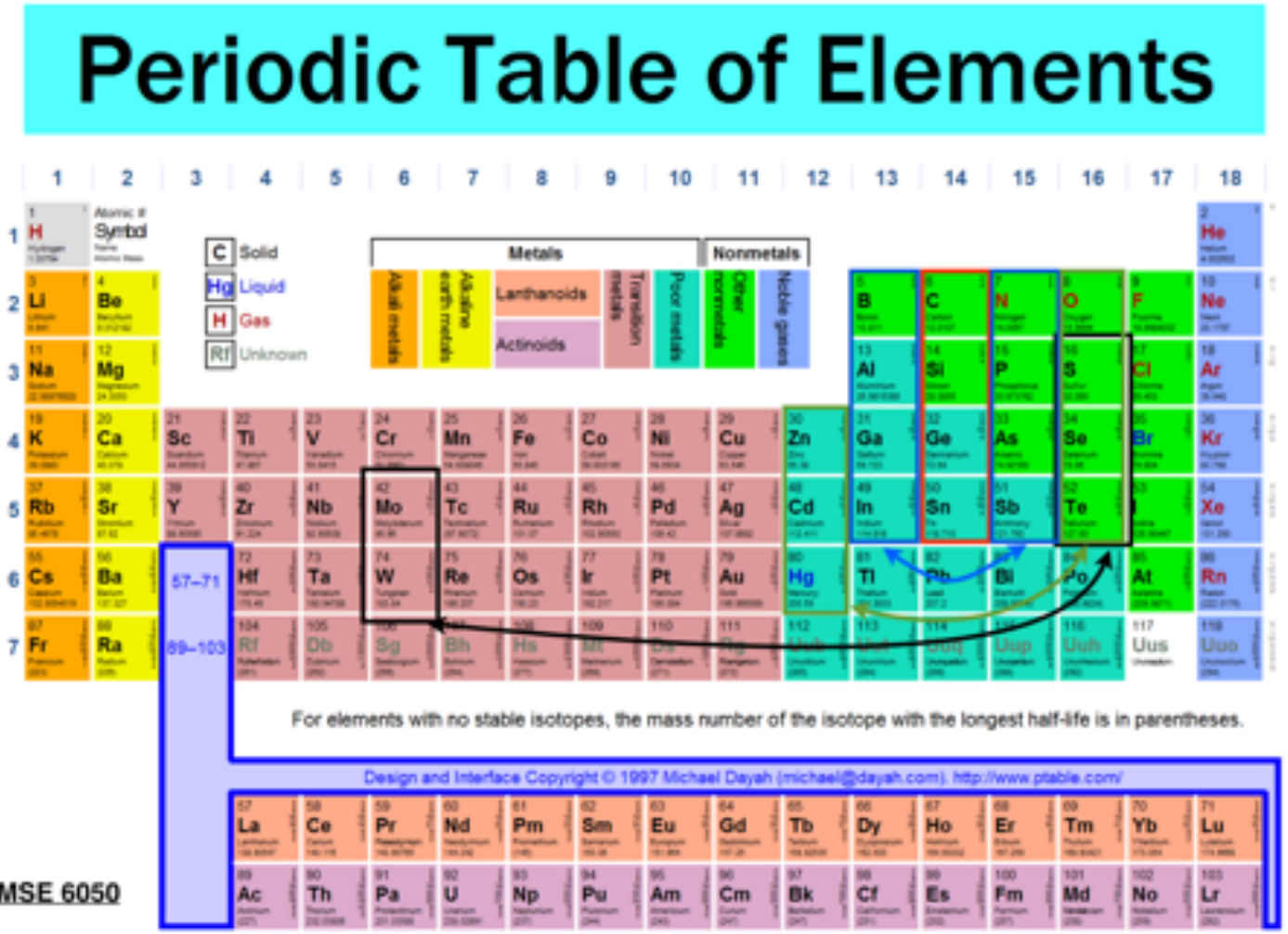

ECE 4070 / MSE 6050

Some common Semiconductor Families:

- Group IV: Diamond, Silicon, Ge, ...
- Group III-V: GaAs, InP, InSb,GaN, ...
- Group II-VI: ZnO, MgO, CdSe, HgTe...
- 2D Materials: Graphene, MoS_2, GaSe, ...

Metals and the Fermi-Surface Database

Semiconductor Orbital Structures

Group IV

C:$[1s^2](2s^2 2p^2) \leftarrow 4$

Si:$[1s^2][2s^2][2p^6](3s^2 3p^2) \leftarrow 4$

Ge:$[1s^2][2s^2][2p^6][3s^2][3p^6][3d^{10}](4s^2 4p^2) \leftarrow 4$

Group III

B:$[1s^2](2s^2 2p^1) \leftarrow 3$

Al: $[1s^2][2s^2][2p^6](3s^2 3p^1) \leftarrow 3$

Ga:$[1s^2][2s^2][2p^6][3s^2][3p^6][3d^{10}](4s^2 4p^1) \leftarrow 3$

[Core electrons] (Valence electrons)

Group V

N:$[1s^2](2s^2 2p^3) \leftarrow 5$

P: $[1s^2][2s^2][2p^6](3s^2 3p^3) \leftarrow 5$

As:$[1s^2][2s^2][2p^6][3s^2][3p^6][3d^{10}](4s^2 4p^3) \leftarrow 5$

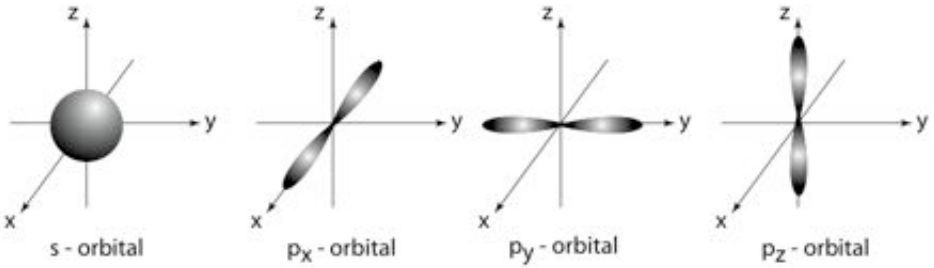

Semiconductor Crystal Structures

Which electrons have to be included in band structure calculations?

In principle all, but the inner core electrons are strongly bound and their spatial extension is so small, that no significant overlap of the wavefunctions occur.

In silicon (Si), the 1s, 2s and 2p electrons are inner core electrons.

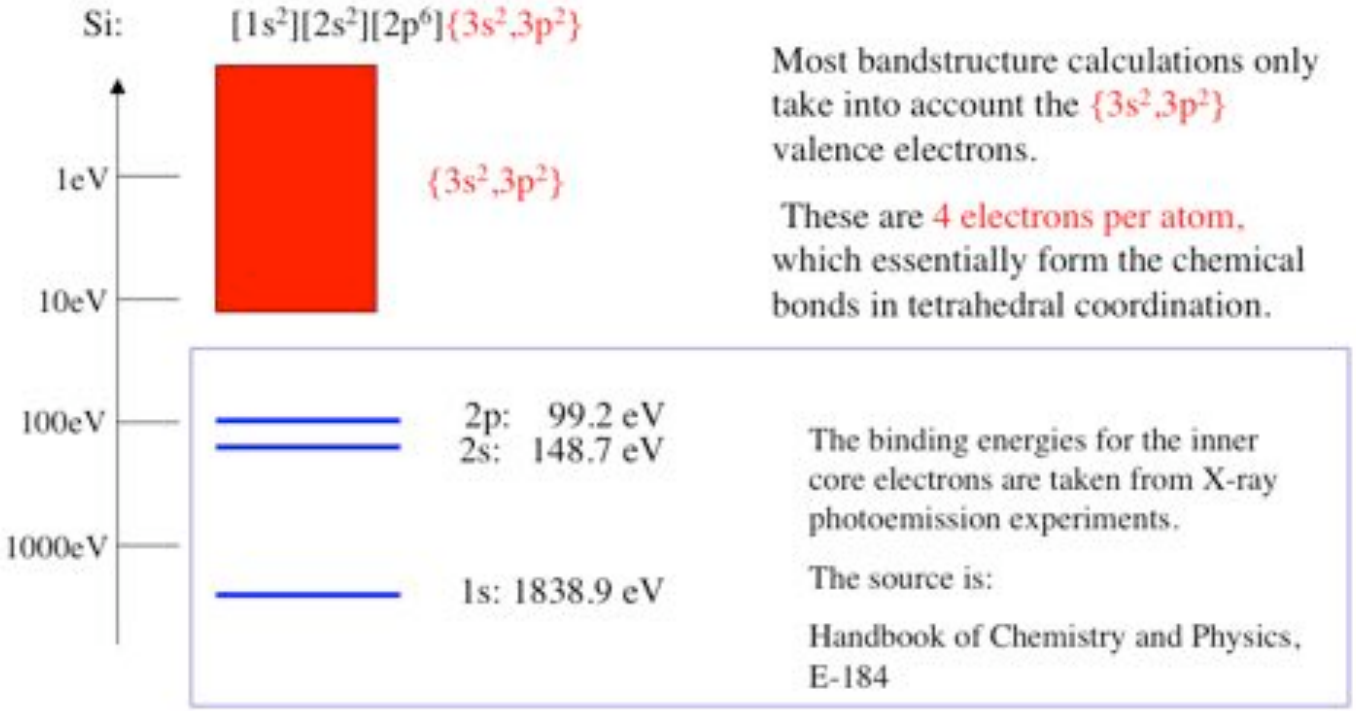

Most bandstructure calculations only take into account the $\{3s^2,3p^2\}$ valence electrons.

These are 4 electrons per atom, which essentially form the chemical bonds in tetrahedral coordination.

The binding energies for the inner core electrons are taken from X-ray photoemission experiments.

The source is:

Handbook of Chemistry and Physics, E-184

(Denninger)

Semiconductor Crystal Structures

Each band can hold 2 electrons per unit cell.

The factor 2 is the spin-multiplicity.

Valence band area

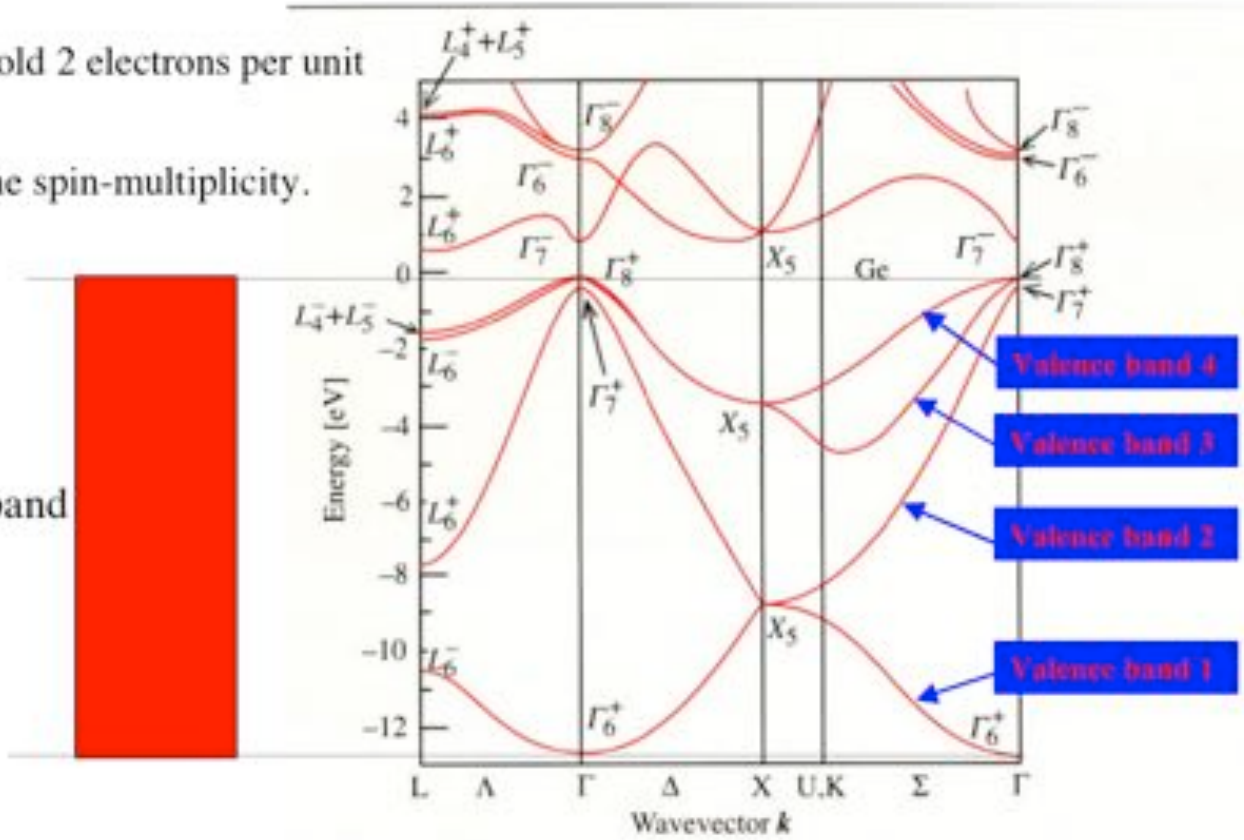

Valence bands: 4 bands

2 atoms per unit cell 4 electrons per atom

8 electrons in 4 bands

(Denninger)

Tight-Binding (or LCAO) Bandstructure

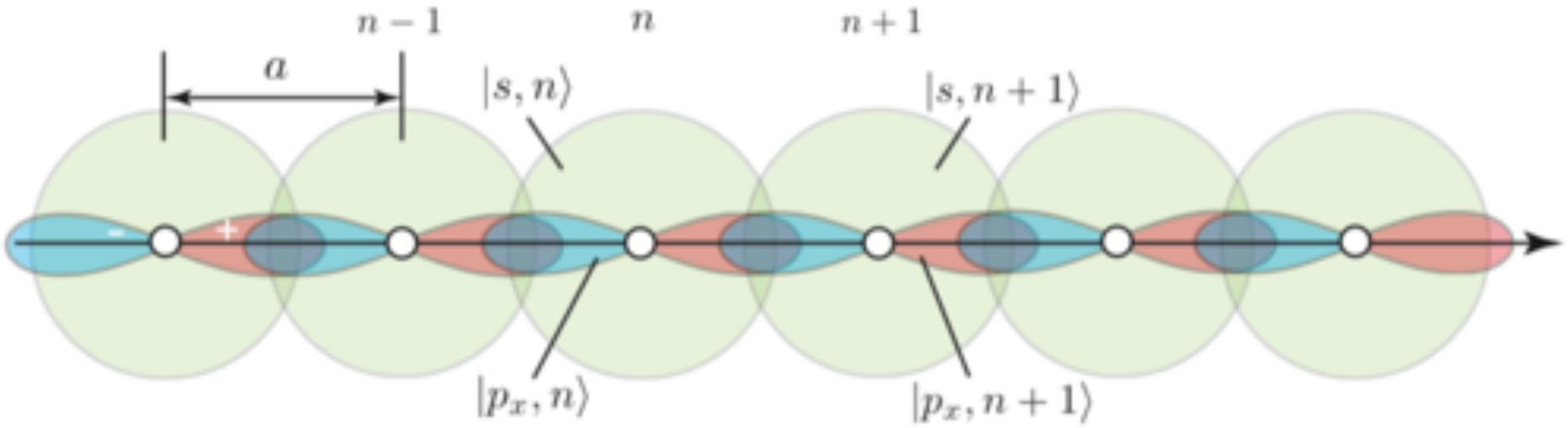

$$|\psi\rangle = \sum_{m=1}^{N} \frac{e^{i\mathbf{k}\cdot\mathbf{R}_m}}{\sqrt{N}} |m\rangle \qquad \hat{H} \sum_{m=1}^{N} e^{i\mathbf{k}\cdot\mathbf{R}_m} |m\rangle = E(\mathbf{k}) \sum_{m=1}^{N} e^{i\mathbf{k}\cdot\mathbf{R}_m} |m\rangle$$

$$\boxed{E(\mathbf{k}) = \frac{\sum_{n,m=1}^{N} e^{i\mathbf{k}\cdot(\mathbf{R}_m - \mathbf{R}_n)} \langle n|\hat{H}|m\rangle}{\sum_{n,m=1}^{N} e^{i\mathbf{k}\cdot(\mathbf{R}_m - \mathbf{R}_n)} \langle n|m\rangle}}$$

$$E(k) = \frac{E_0 - 2t_1\cos(ka) - 2t_2\cos(2ka) - 2t_3\cos(3ka)\ldots}{1 + 2s_1\cos(ka) + 2s_2\cos(2ka) + 2s_3\cos(3ka)\ldots} \approx E_0 - 2t_1\cos(ka)$$

Example: A 1D Crystal with 1 Orbital per Primitive Cell

Consider a 1D lattice of atoms:

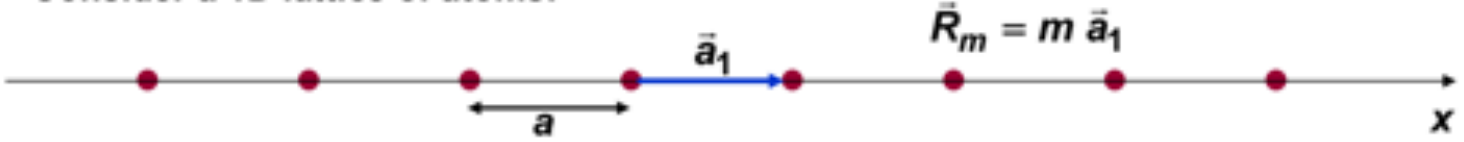

Each atom has the energy levels as shown

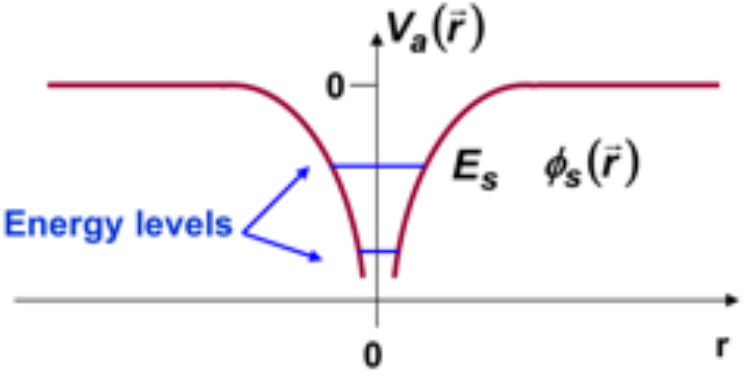

- The electrons in the lowest energy level(s) are well localized and do not take part in bonding with neighboring atoms
- The electrons in the outermost s-orbital participate in bonding

The crystal has the Hamiltonian: $\hat{H} = -\frac{\hbar^2}{2m}\nabla^2 + \sum_m V_a\left(\vec{r} - \vec{R}_m\right)$

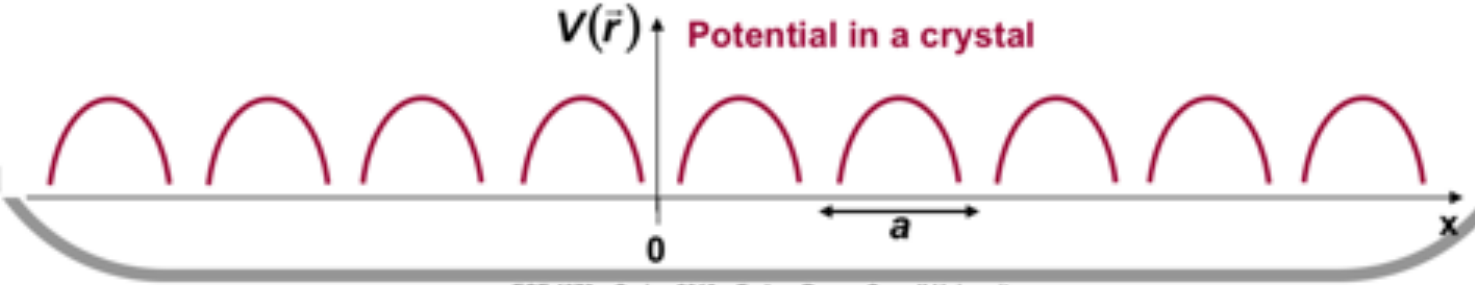

ECE 4070 – Spring 2010 – Farhan Rana – Cornell University

Tight Binding Approach for a 1D Crystal

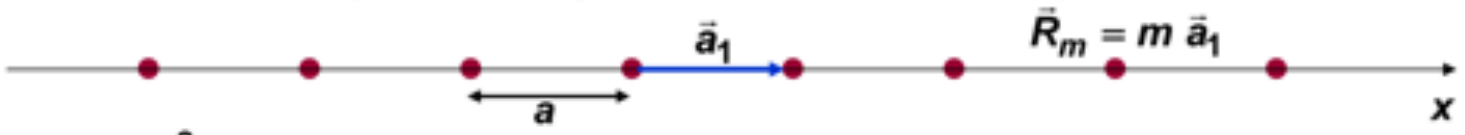

$$\hat{H} = -\frac{\hbar^2}{2m}\nabla^2 + \sum_m V_a\left(\vec{r} - \vec{R}_m\right) \longrightarrow \text{Periodic potential}$$

We assume that the solution is of the LCAO form: $\psi(\vec{r}) = \sum_m c_m\, \phi_s\left(\vec{r} - \vec{R}_m\right)$

And assume that orbitals on different atoms are approx. orthogonal:

$$\left\langle \phi_s\left(\vec{r} - \vec{R}_n\right) \middle| \phi_s\left(\vec{r} - \vec{R}_m\right) \right\rangle = \delta_{n\,m}$$

- If we have *N* atoms in the lattice, then our solution is made up of *N* different s-orbitals that are sitting on the *N* atoms

- In principle one can take the assumed solution, as written above, plug it in the Schrodinger equation, get an *N*x*N* matrix and solve it (just as we did in the case of molecules). But one can do better .....

We know from Bloch's theorem that the solution must satisfy the following:

$$\left|\psi\left(\vec{r} + \vec{R}\right)\right|^2 = \left|\psi(\vec{r})\right|^2$$

$$\psi\left(\vec{r} + \vec{R}\right) = e^{i\,\vec{k}\,.\,\vec{R}}\psi(\vec{r})$$

Tight Binding Approach for a 1D Crystal

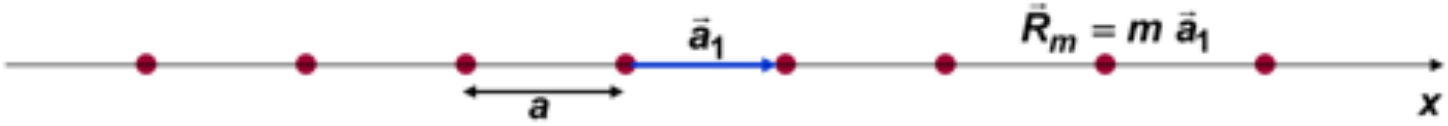

Consideration 1:

For the solution: $\psi(\vec{r}) = \sum_m c_m\, \phi_s(\vec{r} - \vec{R}_m)$

to satisfy:

$$|\psi(\vec{r} + \vec{R})|^2 = |\psi(\vec{r})|^2$$

one must have the same value of $|c_m|^2$ for all m (i.e. all coefficients must have the same weight).

So we can write without loosing generality: $c_m = \frac{e^{i\,\theta_m}}{\sqrt{N}} \longrightarrow \int |\psi(\vec{r})|^2 d^3\vec{r} = 1$

Consideration 2:

For the solution: $\psi(\vec{r}) = \sum_m \frac{e^{i\,\theta_m}}{\sqrt{N}}\, \phi_s(\vec{r} - \vec{R}_m)$

to satisfy:

$$\psi(\vec{r} + \vec{R}) = e^{i\,\vec{k}\,.\,\vec{R}}\psi(\vec{r})$$

one must have the phase value equal to: $\theta_m = \vec{k}\,.\,\vec{R}_m$

ECE 4070 – Spring 2010 – Farhan Rana – Cornell University

Tight Binding Approach for a 1D Crystal

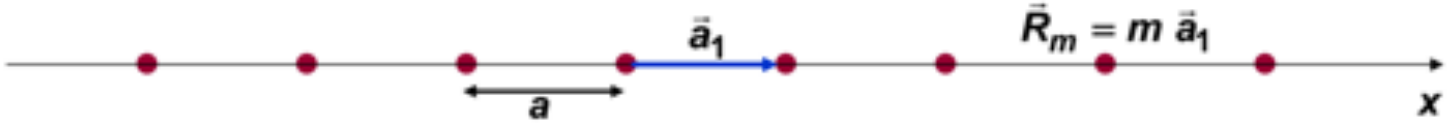

Consideration 2 (contd…):

Proof:

$$\psi(\vec{r}) = \sum_m \frac{e^{i\theta_m}}{\sqrt{N}} \phi_s(\vec{r} - \vec{R}_m) = \sum_m \frac{e^{i\vec{k}\cdot\vec{R}_m}}{\sqrt{N}} \phi_s(\vec{r} - \vec{R}_m)$$

For the Bloch condition we get:

$$\psi(\vec{r} + \vec{R}) = \sum_m \frac{e^{i\vec{k}\cdot\vec{R}_m}}{\sqrt{N}} \phi_s(\vec{r} + \vec{R} - \vec{R}_m) = \sum_m \frac{e^{i\vec{k}\cdot\vec{R}_m}}{\sqrt{N}} \phi_s(\vec{r} - (\vec{R}_m - \vec{R}))$$

Let:

$$\vec{R}_m - \vec{R} = \vec{R}_p$$

$$\Rightarrow \psi(\vec{r} + \vec{R}) = \sum_p \frac{e^{ik\cdot(\vec{R}_p + \vec{R})}}{\sqrt{N}} \phi_s(\vec{r} - \vec{R}_p) = e^{i\vec{k}\cdot\vec{R}} \sum_p \frac{e^{i\vec{k}\cdot\vec{R}_p}}{\sqrt{N}} \phi_s(\vec{r} - \vec{R}_p)$$

$$= e^{i\vec{k}\cdot\vec{R}}\,\psi(\vec{r})$$

Tight Binding Approach for a 1D Crystal

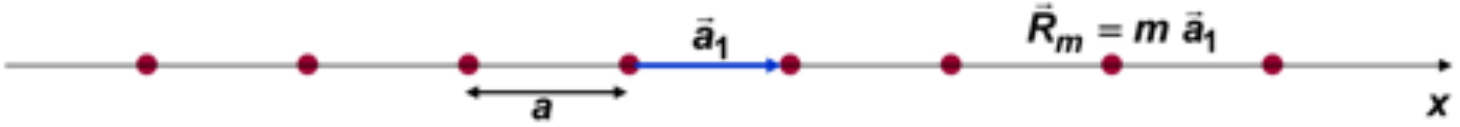

So we can write the solution as:

$$\psi_{\vec{k}}(\vec{r}) = \sum_m \frac{e^{i\,\vec{k}\,.\,\vec{R}_m}}{\sqrt{N}}\,\phi_s(\vec{r} - \vec{R}_m)$$

And we know that it is a Bloch function because:

$$\psi_{\vec{k}}(\vec{r} + \vec{R}) = e^{i\,\vec{k}\,.\,\vec{R}}\psi_{\vec{k}}(\vec{r})$$

All that remains to be found is the energy of this solution – so we plug it into the Schrodinger equation:

$$\hat{H}\,|\psi_{\vec{k}}(\vec{r})\rangle = E(\vec{k})\,|\psi_{\vec{k}}(\vec{r})\rangle$$

$$\Rightarrow \sum_m \frac{e^{i\,\vec{k}\,.\,\vec{R}_m}}{\sqrt{N}}\,\hat{H}\,|\phi_s(\vec{r} - \vec{R}_m)\rangle = E(\vec{k})\sum_m \frac{e^{i\,\vec{k}\,.\,\vec{R}_m}}{\sqrt{N}}\,|\phi_s(\vec{r} - \vec{R}_m)\rangle$$

Tight Binding Approach for a 1D Crystal

$\vec{R}_m = m\,\vec{a}_1$

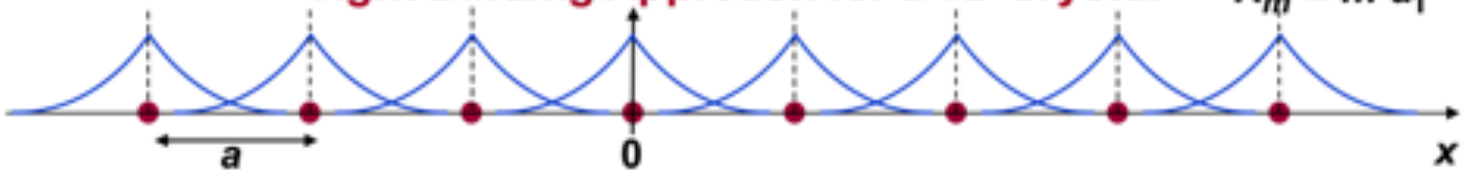

$$\Rightarrow \sum_m \frac{e^{i\vec{k}\cdot\vec{R}_m}}{\sqrt{N}} \hat{H} \left|\phi_s(\vec{r}-\vec{R}_m)\right\rangle = E(\vec{k}) \sum_m \frac{e^{i\vec{k}\cdot\vec{R}_m}}{\sqrt{N}} \left|\phi_s(\vec{r}-\vec{R}_m)\right\rangle$$

Multiply this equation with $\langle\phi_s(\vec{r})|$ and:

- keep the energy matrix elements for orbitals that are nearest neighbors and
- assume that the orbitals on different atoms are orthogonal

$$\frac{e^{i\vec{k}\cdot\vec{R}_1}}{\sqrt{N}} \langle\phi_s(\vec{r})|\hat{H}\left|\phi_s(\vec{r}-\vec{R}_1)\right\rangle + \frac{1}{\sqrt{N}} \langle\phi_s(\vec{r})|\hat{H}\left|\phi_s(\vec{r})\right\rangle + \frac{e^{i\vec{k}\cdot\vec{R}_{-1}}}{\sqrt{N}} \langle\phi_s(\vec{r})|\hat{H}\left|\phi_s(\vec{r}-\vec{R}_{-1})\right\rangle$$

$$= E(\vec{k}) \frac{1}{\sqrt{N}} \langle\phi_s(\vec{r})|\phi_s(\vec{r})\rangle$$

$$\Rightarrow -V_{ss\sigma} \frac{e^{i\vec{k}\cdot\vec{a}_1}}{\sqrt{N}} + \frac{1}{\sqrt{N}} E_s - \frac{e^{-i\vec{k}\cdot\vec{a}_1}}{\sqrt{N}} V_{ss\sigma} = E(\vec{k}) \frac{1}{\sqrt{N}}$$

$$\Rightarrow E(\vec{k}) = E_s - 2V_{ss\sigma} \cos(\vec{k}\cdot\vec{a}_1)$$

Tight-Binding Bandstructure

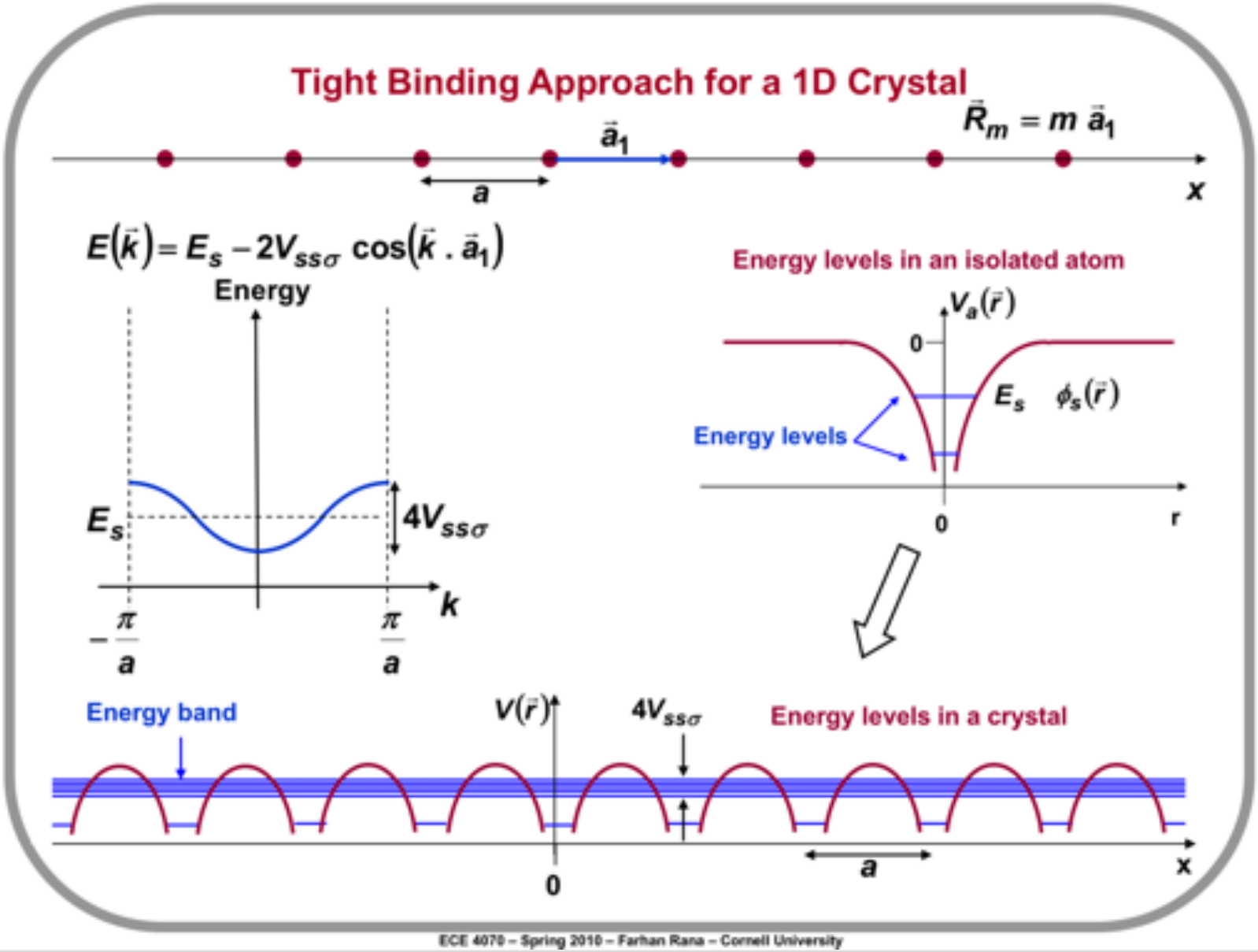

Tight Binding Approach for a 1D Crystal

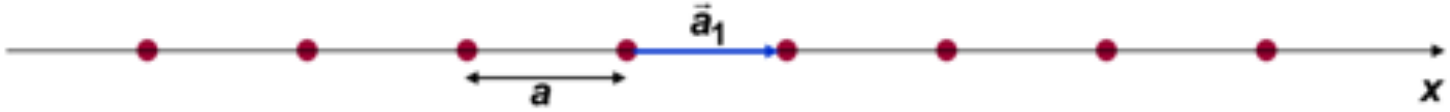

$$E(\vec{k}) = E_s - 2V_{ss\sigma}\cos(\vec{k}\,.\,\vec{a}_1)$$

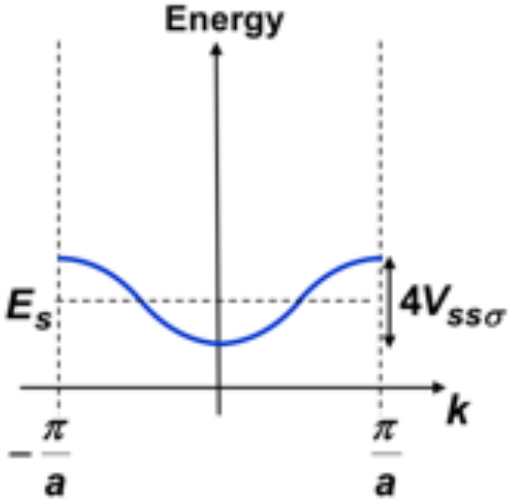

- Number of quantum states at the starting point = 2 x number of orbitals used in the LCAO solution = $2N$
- Number of quantum states at the ending point = 2 x energy levels per band for an N atom crystal = $2N$

$\Rightarrow$ Initial number of quantum states = Final number of quantum states

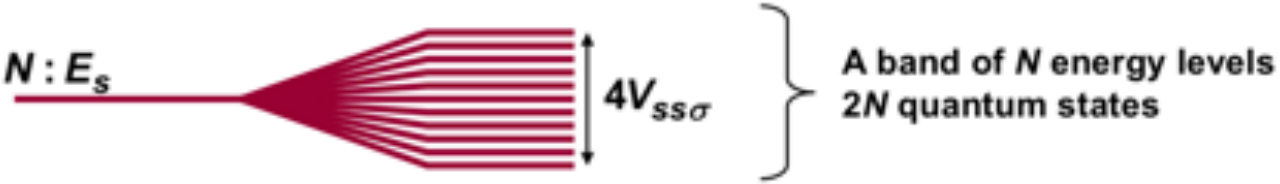

ECE 4070 – Spring 2010 – Farhan Rana – Cornell University

Atomic Orbitals and their Overlaps

Atomic Orbitals

- Wavefunction amplitudes of the atomic s and p orbitals in the angular directions are plotted
- The s-orbital is spherically symmetric
- The p-orbitals have +ve and –ve lobes and are oriented along x-axis, y-axis, and z-axis

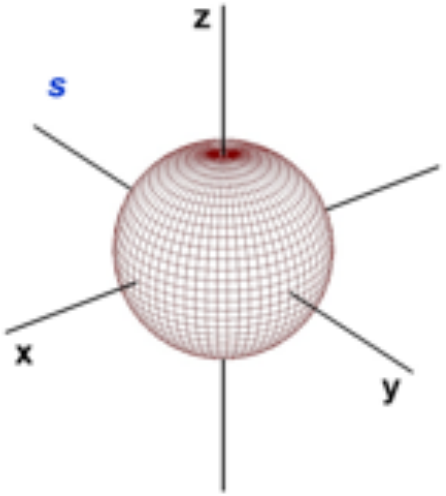

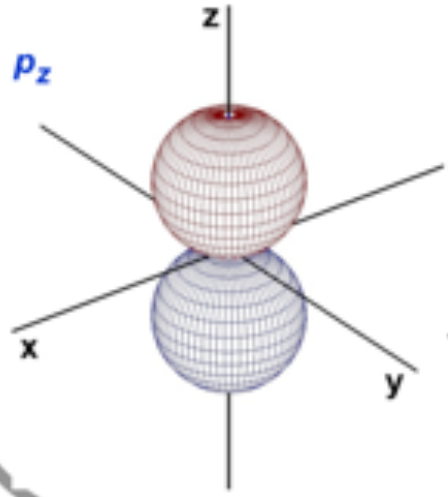

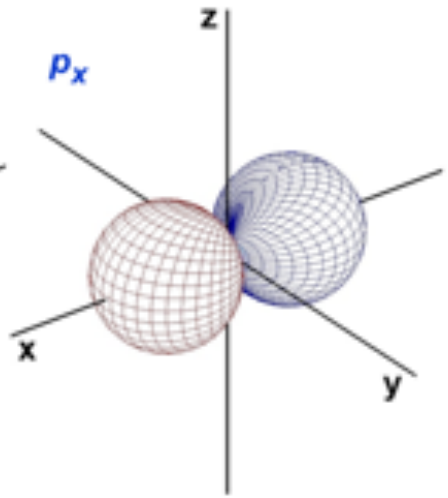

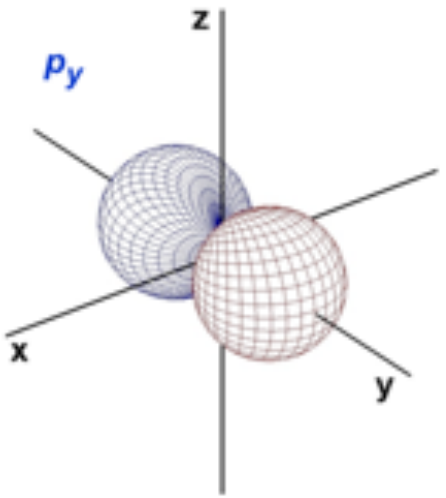

ECE 4070 – Spring 2010 – Farhan Rana – Cornell University

Atomic Orbitals and their Overlaps

Orbitals and Bonding

There are two main types of co-valent bonds: sigma bonds (or σ-bonds) and pi-bonds (or π-bonds)

(1) Sigma bonds (or σ-bonds):

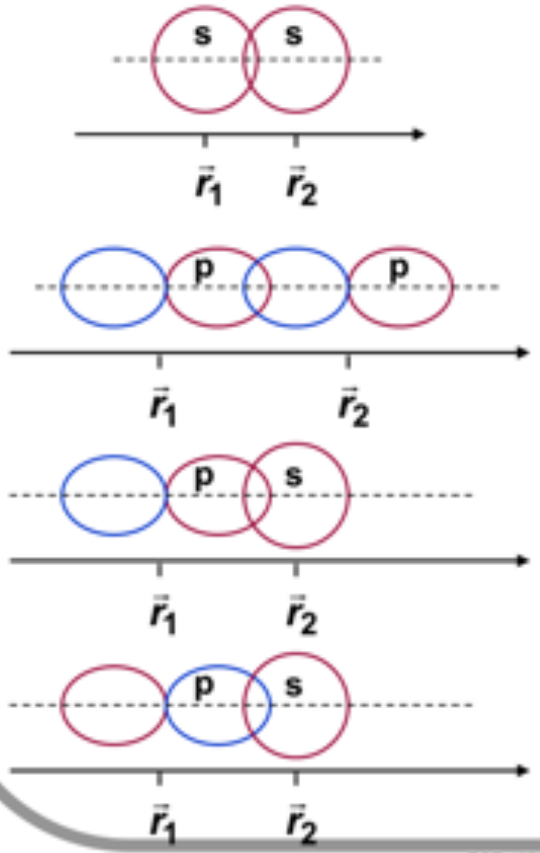

s-s σ-bond
(Example: Hydrogen molecule, semiconductors)

$$\langle \phi_s(\vec{r}-\vec{r}_1)|\,\hat{H}\,|\phi_s(\vec{r}-\vec{r}_2)\rangle \approx -V_{ss\sigma}$$

p-p σ-bond
(Example: Semiconductors)

$$\langle \phi_p(\vec{r}-\vec{r}_1)|\,\hat{H}\,|\phi_p(\vec{r}-\vec{r}_2)\rangle \approx V_{pp\sigma}$$

s-p σ-bond
(Example: Semiconductors)

$$\langle \phi_p(\vec{r}-\vec{r}_1)|\,\hat{H}\,|\phi_s(\vec{r}-\vec{r}_2)\rangle \approx -V_{sp\sigma}$$

s-p σ-bond
(Example: Semiconductors)

$$\langle \phi_p(\vec{r}-\vec{r}_1)|\,\hat{H}\,|\phi_s(\vec{r}-\vec{r}_2)\rangle \approx V_{sp\sigma}$$

ECE 4070 – Spring 2010 – Farhan Rana – Cornell University

Orbitals and Bonding

What about this situation?

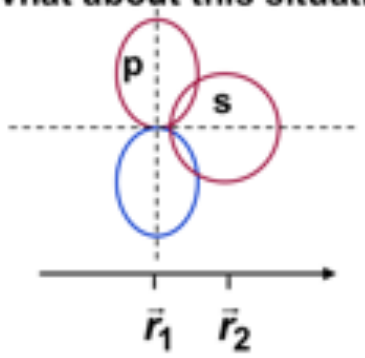

$$\langle \phi_p(\vec{r}-\vec{r}_1) | \hat{H} | \phi_s(\vec{r}-\vec{r}_2) \rangle \approx 0$$

The Hamiltonian is up-down symmetric
The s-orbital is up-down symmetric
The p-orbital is up-down anti-symmetric
⇒ The matrix element is zero! No bonding possible

What about this situation? What should be the matrix element?

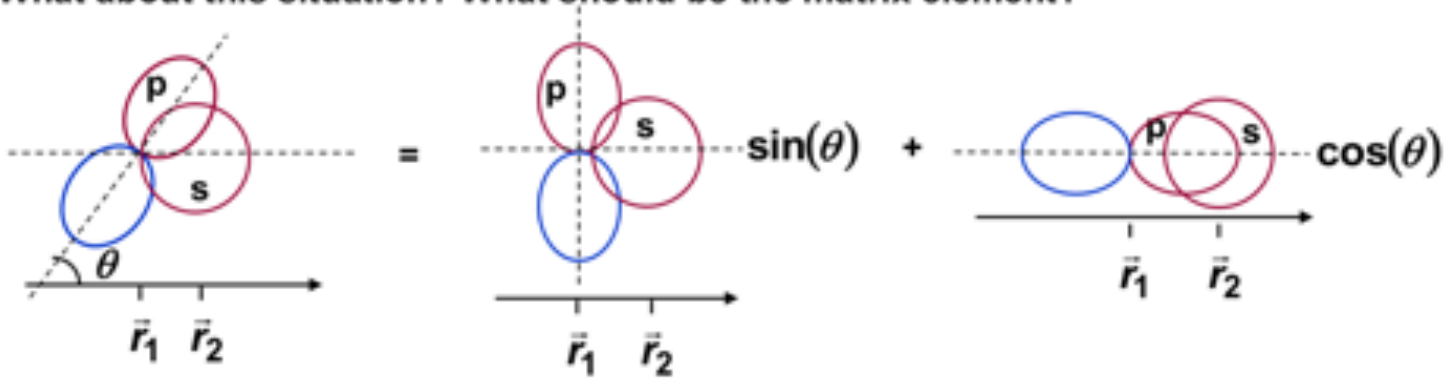

$$\langle \phi_p(\vec{r}-\vec{r}_1) | \hat{H} | \phi_s(\vec{r}-\vec{r}_2) \rangle \approx 0 \,.\, \sin(\theta) + \left(-V_{sp\sigma}\right).\cos(\theta)$$
$$= -V_{sp\sigma}\cos(\theta)$$

ECE 4070 – Spring 2010 – Farhan Rana – Cornell University

Orbitals and Bonding

(2) Pi bonds (or π-bonds):

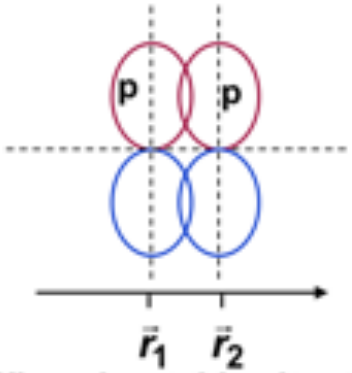

p-p π-bond

(Example: graphene, carbon nanotubes, conjugated conducting molecules)

$$\left\langle \phi_p(\vec{r}-\vec{r}_1) \middle| \hat{H} \middle| \phi_p(\vec{r}-\vec{r}_2) \right\rangle \approx -V_{pp\pi}$$

What about this situation? What should be the matrix element?

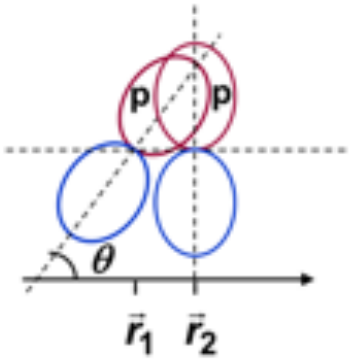

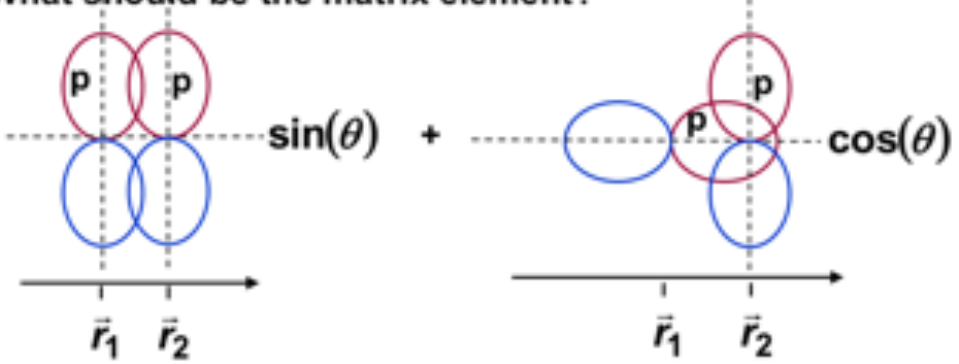

$$\left\langle \phi_p(\vec{r}-\vec{r}_1) \middle| \hat{H} \middle| \phi_p(\vec{r}-\vec{r}_2) \right\rangle \approx \left(-V_{pp\pi}\right).\sin(\theta)+0\,.\cos(\theta)$$
$$= -V_{pp\pi}\sin(\theta)$$

ECE 4070 – Spring 2010 – Farhan Rana – Cornell University

Tight Binding vs NFEA for a 1D Crystal

LCAO – Tight Binding

$$E(\vec{k}) = E_s - 2V_{ss\sigma}\cos(\vec{k}\cdot\vec{a}_1)$$

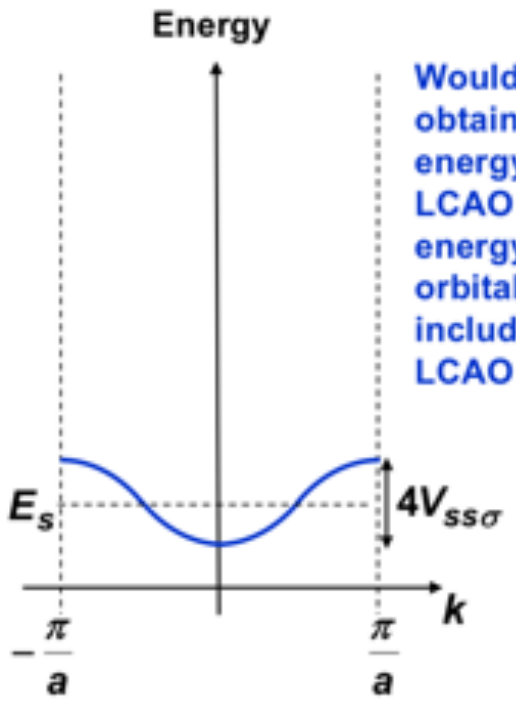

Would have also obtained the higher energy bands in LCAO if higher energy atomic orbitals were also included in the LCAO solution

Nearly Free Electron Approach (NFEA)

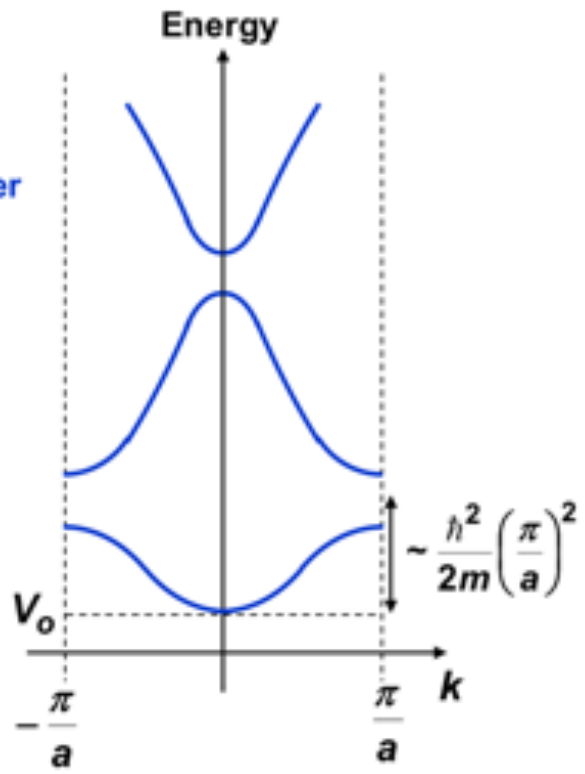

The energy matrix elements are of the order of: $V_{ss\sigma} \sim \frac{\hbar^2}{m}\frac{1}{a^2}$

Example: A 1D Crystal with 2 Orbitals per Primitive Cell

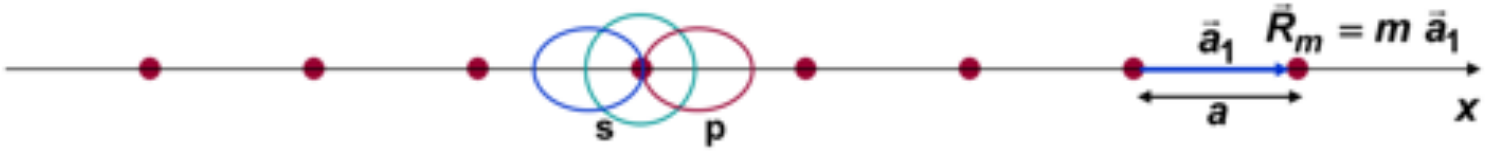

Each atoms now has a s-orbital and a p-orbital that contributes to energy band formation

$$\phi_s(\vec{r}) \rightarrow E_s$$
$$\phi_p(\vec{r}) \rightarrow E_p$$

We write the solution in the form:

$$\psi_{\vec{k}}(\vec{r}) = \sum_m \frac{e^{j\,\vec{k}\,.\,\vec{R}_m}}{\sqrt{N}} \left[c_s(\vec{k})\,\phi_s(\vec{r}-\vec{R}_m) + c_p(\vec{k})\,\phi_p(\vec{r}-\vec{R}_m) \right]$$

Verify that it satisfies: $\psi_{\vec{k}}(\vec{r}+\vec{R}) = e^{j\,\vec{k}\,.\,\vec{R}}\,\psi_{\vec{k}}(\vec{r})$

And plug it into the Schrodinger equation:

$$\hat{H}\,|\psi_{\vec{k}}(\vec{r})\rangle = E(\vec{k})\,|\psi_{\vec{k}}(\vec{r})\rangle$$

Tight Binding Approach for a 1D Crystal

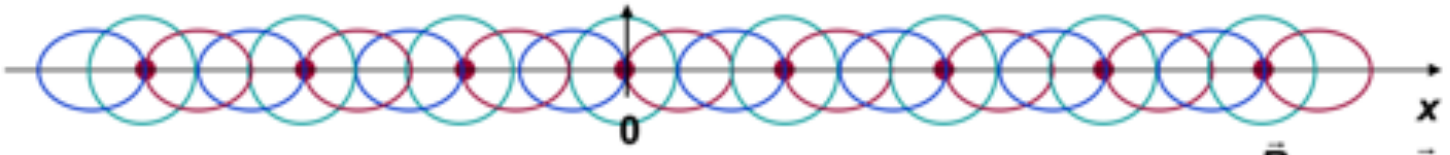

$\vec{R}_m = m\,\vec{a}_1$

$$\hat{H}\left|\psi_{\vec{k}}(\vec{r})\right\rangle = E(\vec{k})\left|\psi_{\vec{k}}(\vec{r})\right\rangle$$

Step 1:

Multiply the equation with $\left\langle\phi_s(\vec{r})\right|$ and:

- keep the energy matrix elements for orbitals that are nearest neighbors and
- assume that the orbitals on different atoms are orthogonal

$$\left[E_s - 2V_{ss\sigma}\cos(\vec{k}.\vec{a}_1)\right]c_s(\vec{k}) + 2i\,V_{sp\sigma}\sin(\vec{k}.\vec{a}_1)c_p(\vec{k}) = E(\vec{k})c_s(\vec{k})$$

Step 2:

Multiply the equation with $\left\langle\phi_p(\vec{r})\right|$ and:

- keep the energy matrix elements for orbitals that are nearest neighbors and
- assume that the orbitals on different atoms are orthogonal

$$\left[E_p + 2V_{pp\sigma}\cos(\vec{k}.\vec{a}_1)\right]c_p(\vec{k}) - 2i\,V_{sp\sigma}\sin(\vec{k}.\vec{a}_1)c_s(\vec{k}) = E(\vec{k})c_p(\vec{k})$$

Tight Binding Approach for a 1D Crystal

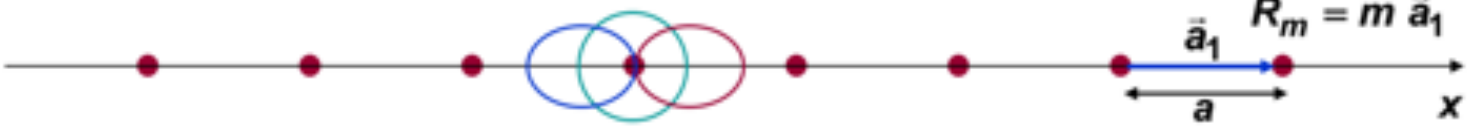

We can write the two equations in matrix form:

$$\begin{bmatrix} E_s - 2V_{ss\sigma}\cos(\vec{k}.\vec{a}_1) & 2i\,V_{sp\sigma}\sin(\vec{k}.\vec{a}_1) \\ -2i\,V_{sp\sigma}\sin(\vec{k}.\vec{a}_1) & E_p + 2V_{pp\sigma}\cos(\vec{k}.\vec{a}_1) \end{bmatrix} \begin{bmatrix} c_s(\vec{k}) \\ c_p(\vec{k}) \end{bmatrix} = E(\vec{k}) \begin{bmatrix} c_s(\vec{k}) \\ c_p(\vec{k}) \end{bmatrix}$$

For each value of wavevector one obtains two eigenvalues – corresponding to two energy bands

For $\vec{k} = 0$ we get:

$$E(\vec{k}=0) = E_p + 2V_{pp\sigma}$$

$$\begin{bmatrix} c_s(\vec{k}=0) \\ c_p(\vec{k}=0) \end{bmatrix} = \begin{bmatrix} 0 \\ 1 \end{bmatrix}$$

Bloch function is made of only p-orbitals

$$E(\vec{k}=0) = E_s - 2V_{ss\sigma}$$

$$\begin{bmatrix} c_s(\vec{k}=0) \\ c_p(\vec{k}=0) \end{bmatrix} = \begin{bmatrix} 1 \\ 0 \end{bmatrix}$$

Bloch function is made of only s-orbitals

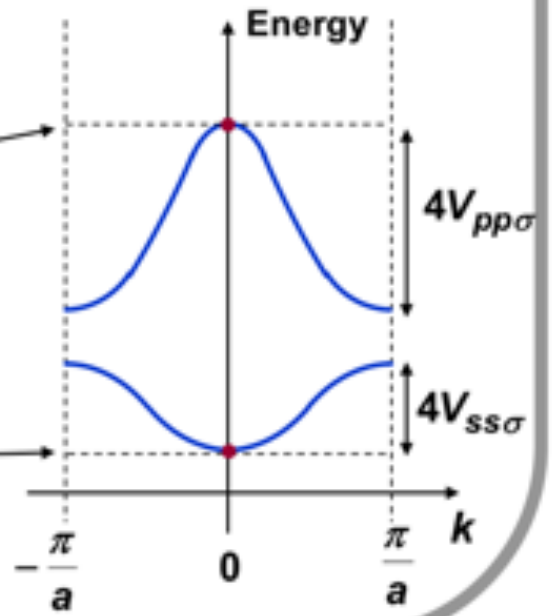

Tight Binding Approach for a 1D Crystal

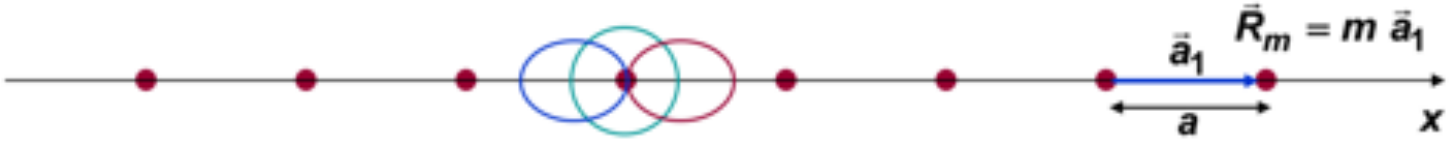

For $\vec{k} = \frac{\pi}{2a}\hat{x}$ we get:

$$E\left(\vec{k} = \frac{\pi}{2a}\hat{x}\right) = ?$$

$$\begin{bmatrix} c_s\left(\vec{k} = \frac{\pi}{2a}\hat{x}\right) \\ c_p\left(\vec{k} = \frac{\pi}{2a}\hat{x}\right) \end{bmatrix} = \begin{bmatrix} ? \\ ? \end{bmatrix}$$

Bloch function is made of both s- and p-orbitals

$$E\left(\vec{k} = \frac{\pi}{2a}\right) = ?$$

$$\begin{bmatrix} c_s\left(\vec{k} = \frac{\pi}{2a}\hat{x}\right) \\ c_p\left(\vec{k} = \frac{\pi}{2a}\hat{x}\right) \end{bmatrix} = \begin{bmatrix} ? \\ ? \end{bmatrix}$$

Bloch function is made of both s- and p-orbitals

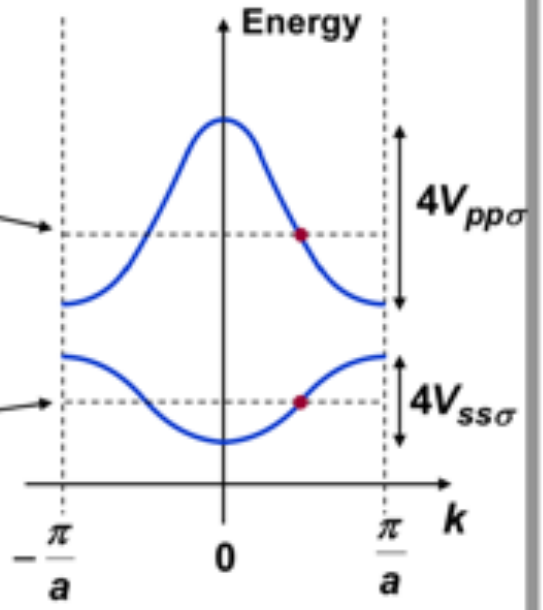

ECE 4070 – Spring 2010 – Farhan Rana – Cornell University

Tight Binding Approach for a 1D Crystal

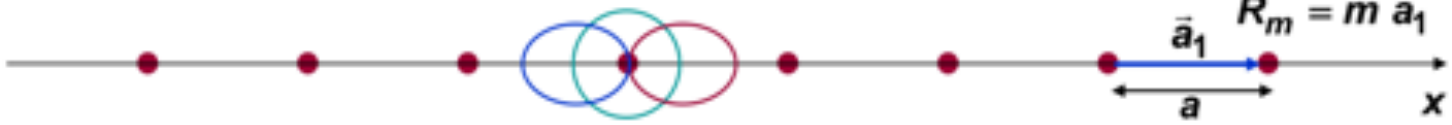

For $\vec{k} = \frac{\pi}{a}\hat{x}$ we get:

$$E\left(\vec{k} = \frac{\pi}{a}\hat{x}\right) = E_p - 2V_{pp\sigma}$$

$$\begin{bmatrix} c_s\left(\vec{k} = \frac{\pi}{a}\hat{x}\right) \\ c_p\left(\vec{k} = \frac{\pi}{a}\hat{x}\right) \end{bmatrix} = \begin{bmatrix} 0 \\ 1 \end{bmatrix}$$

Bloch function is made of only p-orbitals

$$E\left(\vec{k} = \frac{\pi}{a}\hat{x}\right) = E_s + 2V_{ss\sigma}$$

$$\begin{bmatrix} c_s\left(\vec{k} = \frac{\pi}{a}\hat{x}\right) \\ c_p\left(\vec{k} = \frac{\pi}{a}\hat{x}\right) \end{bmatrix} = \begin{bmatrix} 1 \\ 0 \end{bmatrix}$$

Bloch function is made of only s-orbitals

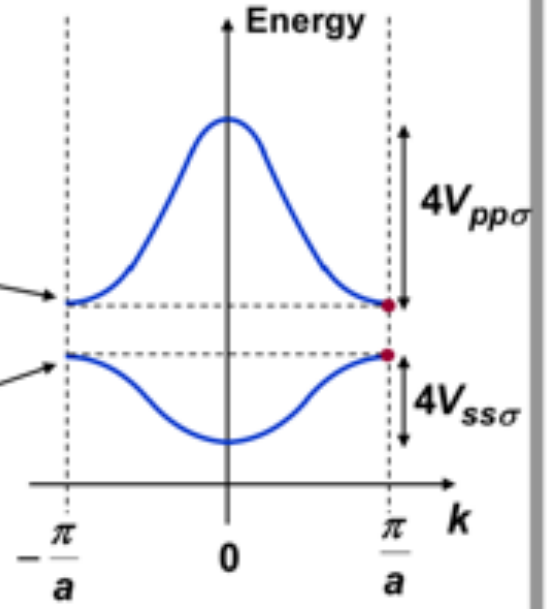

A Simple Example: 2D Graphene and Boron Nitride

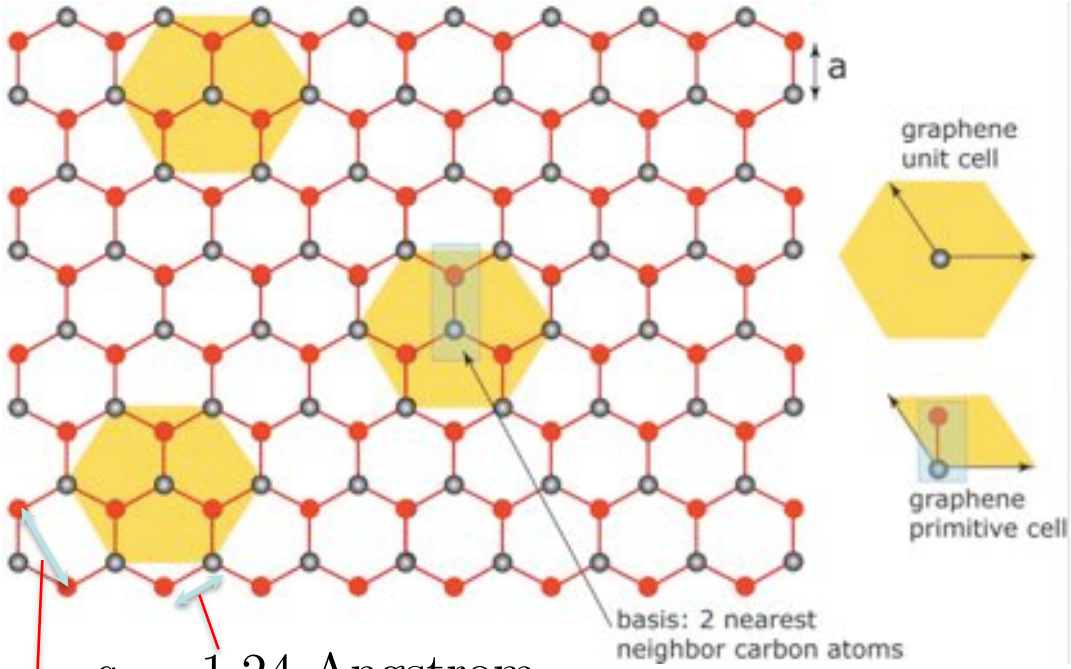

a_{cc}=1.24 Angstrom

$a = \sqrt{3}a_{cc} = 2.15$ Angstrom (lattice constant)

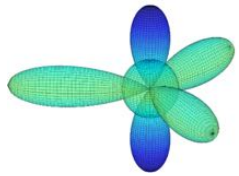

sp^2 hybridization

Orbital figs from Pulfrey

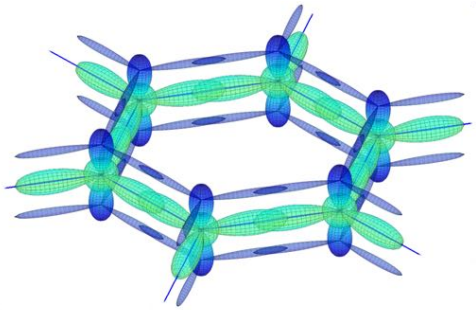

Hopping energy: $\gamma_0 \approx 3$ eV

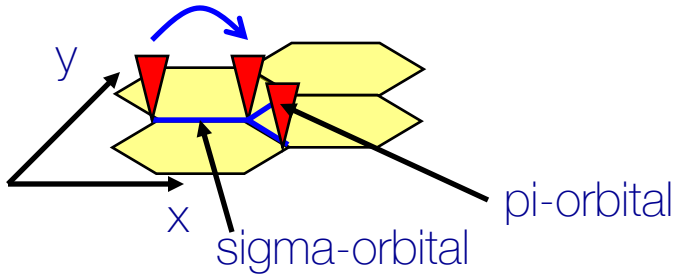

Real-space picture

- Sigma-orbitals hold the atoms together.
  (3 electrons/carbon atom, one left over)

- Pi-orbitals are responsible for conduction.
  (1 electron/carbon atom)

A Simple Example: 2D Graphene and Boron Nitride

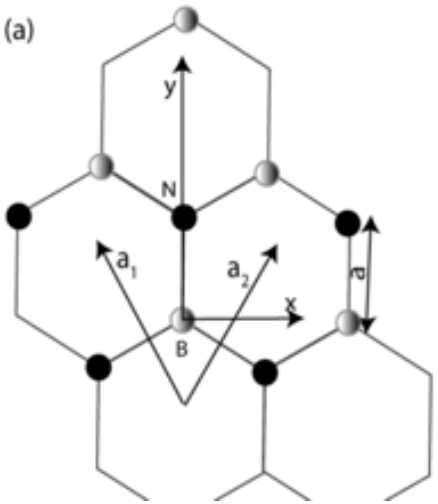

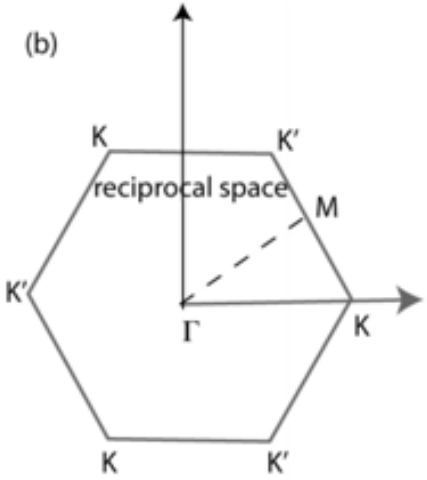

Find the real space lattice vectors

$$\mathbf{a_1} = (\frac{\sqrt{3}}{2}, \frac{3}{2}) \qquad \mathbf{a_2} = (-\frac{\sqrt{3}}{2}, \frac{3}{2})$$

Write down the tight-binding Hamiltonian Matrix

$$\mathcal{H} = \begin{pmatrix} \epsilon_B & h(k) \\ h(k)^\star & \epsilon_N \end{pmatrix}$$

hopping energy to each neighbor with phase factor

on-site energies of each atom in basis

$$h(k) = -t\left[1 + e^{i\mathbf{k}\cdot\mathbf{a_1}} + e^{i\mathbf{k}\cdot\mathbf{a_2}}\right]$$

Find the eigenvalues of the Hamiltonian to get the bandstructure

$$\mathcal{E}_{\pm}(k_x, k_y) = A \pm \sqrt{B^2 + t^2\left[1 + 4\cos(3k_x a/2)\cos(\sqrt{3}k_y a/2) + 4\cos^2(\sqrt{3}k_y a/2)\right]}$$

$$A = (\epsilon_B + \epsilon_N)/2 \qquad B = (\epsilon_B - \epsilon_N)/2$$

A Simple Example: 2D Graphene and Boron Nitride

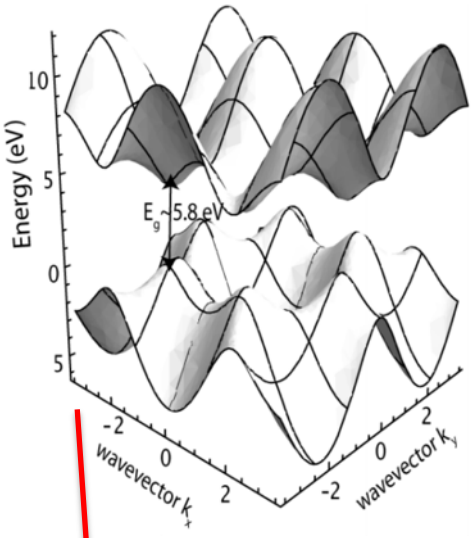

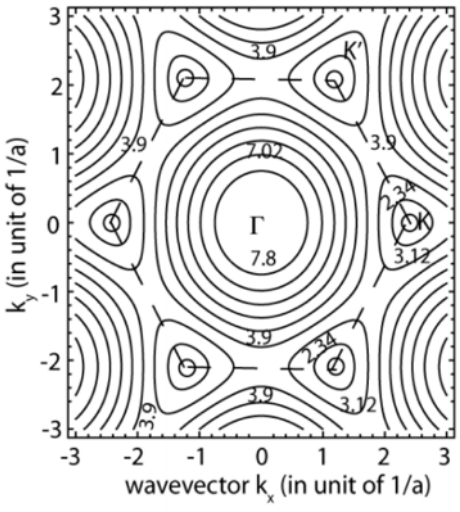

Find the real space lattice vectors

$$\mathbf{a_1} = (\frac{\sqrt{3}}{2}, \frac{3}{2}) \qquad \mathbf{a_2} = (-\frac{\sqrt{3}}{2}, \frac{3}{2})$$

Write down the tight-binding Hamiltonian Matrix

$$\mathcal{H} = \begin{pmatrix} \epsilon_B & h(k) \\ h(k)^\star & \epsilon_N \end{pmatrix}$$

hopping energy to each neighbor with phase factor

on-site energies of each atom in basis

$$h(k) = -t\left[1 + e^{i\mathbf{k}\cdot\mathbf{a_1}} + e^{i\mathbf{k}\cdot\mathbf{a_2}}\right]$$

Find the eigenvalues of the Hamiltonian to get the bandstructure

$$\mathcal{E}_\pm(k_x, k_y) = A \pm \sqrt{B^2 + t^2\left[1 + 4\cos(3k_x a/2)\cos(\sqrt{3}k_y a/2) + 4\cos^2(\sqrt{3}k_y a/2)\right]}$$

$$A = (\epsilon_B + \epsilon_N)/2 \qquad B = (\epsilon_B - \epsilon_N)/2$$

A Simple Example: 2D Graphene and Boron Nitride

Find the eigenvalues of the Hamiltonian to get the bandstructure

$$\mathcal{E}_{\pm}(k_x, k_y) = A \pm \sqrt{B^2 + t^2\left[1 + 4\cos(3k_x a/2)\cos(\sqrt{3}k_y a/2) + 4\cos^2(\sqrt{3}k_y a/2)\right]}$$

$$A = (\epsilon_B + \epsilon_N)/2 \qquad B = (\epsilon_B - \epsilon_N)/2$$

$$E_g = \mathcal{E}_+ - \mathcal{E}_- = 2B = 5.8 \text{ eV}$$

$$\epsilon_B \sim +2.9 \text{ eV}, \epsilon_N \sim -2.9 \text{ eV}$$

$$E_g{=}5.8 \text{ eV}, \; t{=}2.92 \text{ eV}, \; a \sim 0.15 \text{ nm}$$

Find the conduction and valence band structures and effective masses

$$\mathcal{E}_c(k) = E_g + \frac{\hbar^2 k^2}{2m^\star}, \qquad \text{(conduction band)}$$

$$\mathcal{E}_v(k) = -\frac{\hbar^2 k^2}{2m^\star}, \qquad \text{(valence band)}$$

$$m^\star = \frac{2\hbar^2 E_g}{9a^2 t^2} \sim 0.6 m_0$$

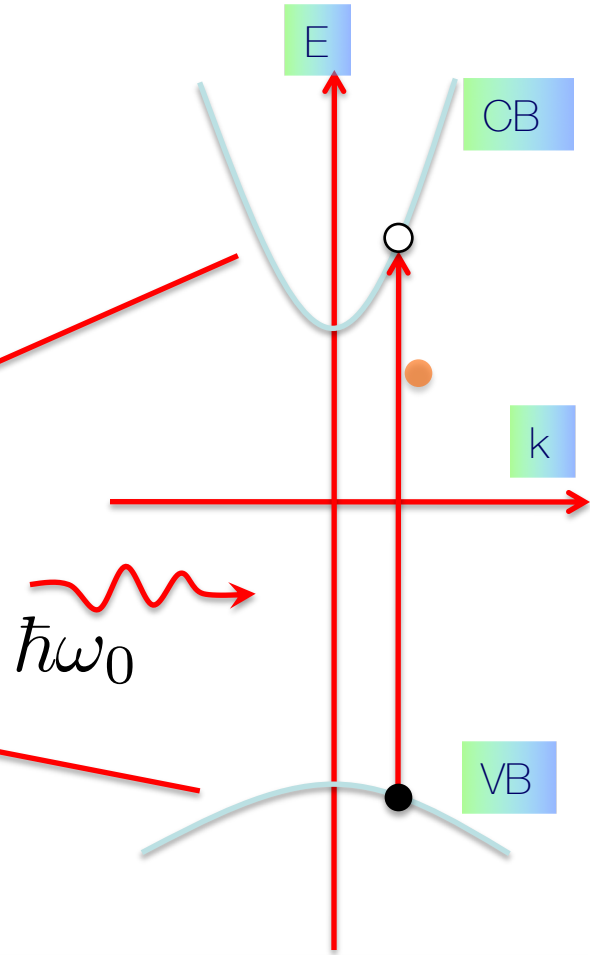

A Simple Example: 2D Graphene Bonds and Bands

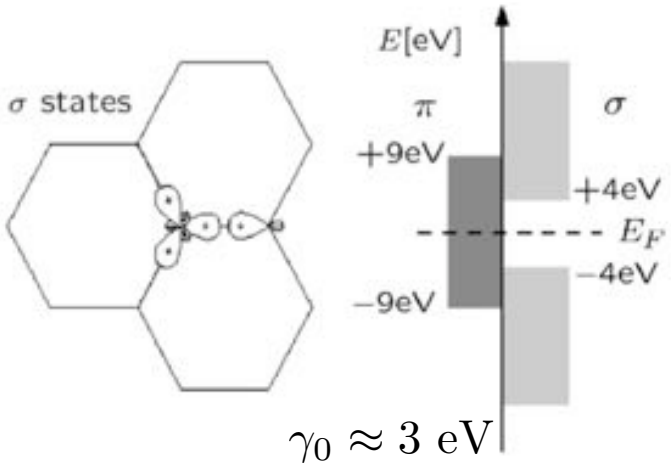

$\gamma_0 \approx 3$ eV

For 2D Graphene, because the on-site energies are the SAME, the gap is ZERO!

BN is the compound semiconductor counterpart of Graphene; the broken symmetry opens a very large bandgap.

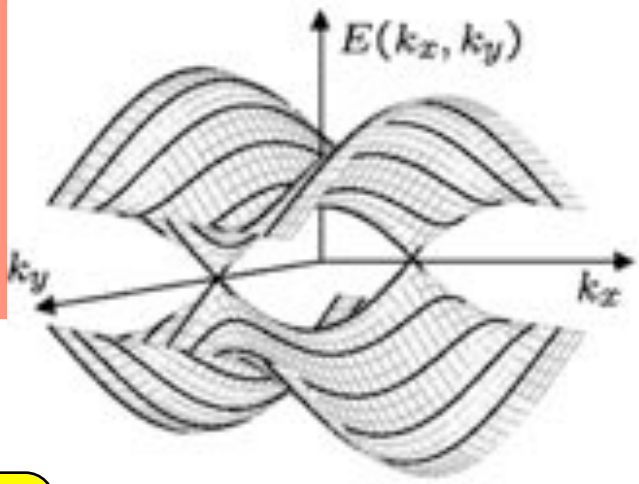

$$\mathcal{E}(k_x, k_y) = \mathcal{E}_F \pm \gamma_0 \sqrt{1 + 4\cos(\frac{\sqrt{3}k_x a}{2})\cos(\frac{k_y a}{2}) + 4\cos^2(\frac{k_y a}{2})}$$

- Expand around the Dirac point

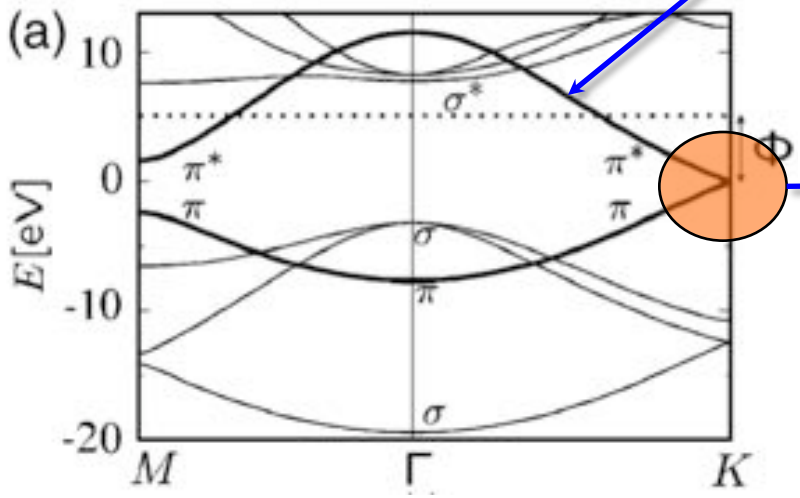

$$\mathcal{E}(k_x, k_y) \approx \hbar v_F \sqrt{k_x^2 + k_y^2}$$

$v_F \sim 10^8 \mathrm{cm/s}$

$g_{spin} = 2$

$g_{valley} = 2$

Conical!
Linear dispersion

- Reviews of Modern Physics, 79 677 (2007).

A Simple Example: 2D Graphene Bonds and Bands

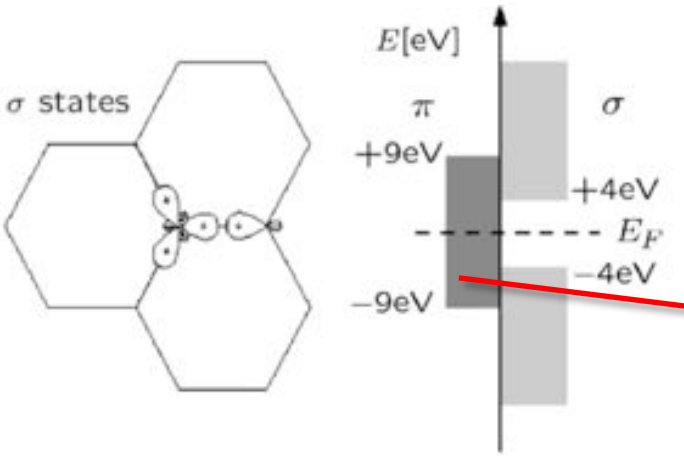

$$\mathcal{E}(k_x, k_y) = \mathcal{E}_F \pm \gamma_0 \sqrt{1 + 4\cos(\frac{\sqrt{3}k_x a}{2})\cos(\frac{k_y a}{2}) + 4\cos^2(\frac{k_y a}{2})}$$

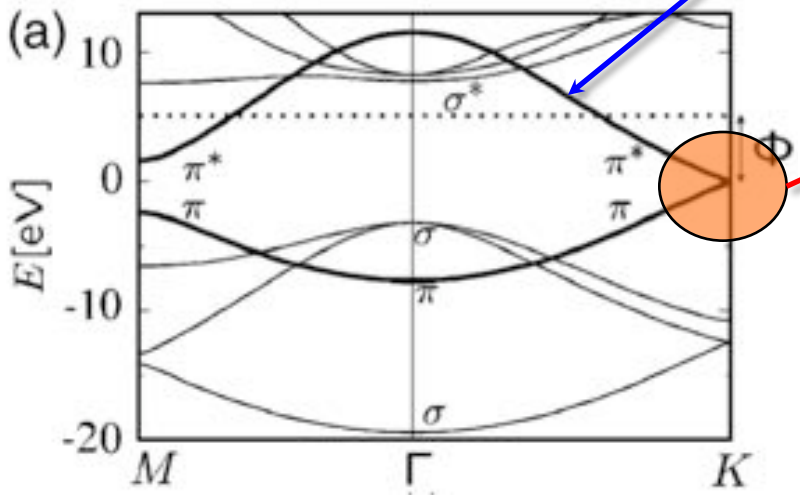

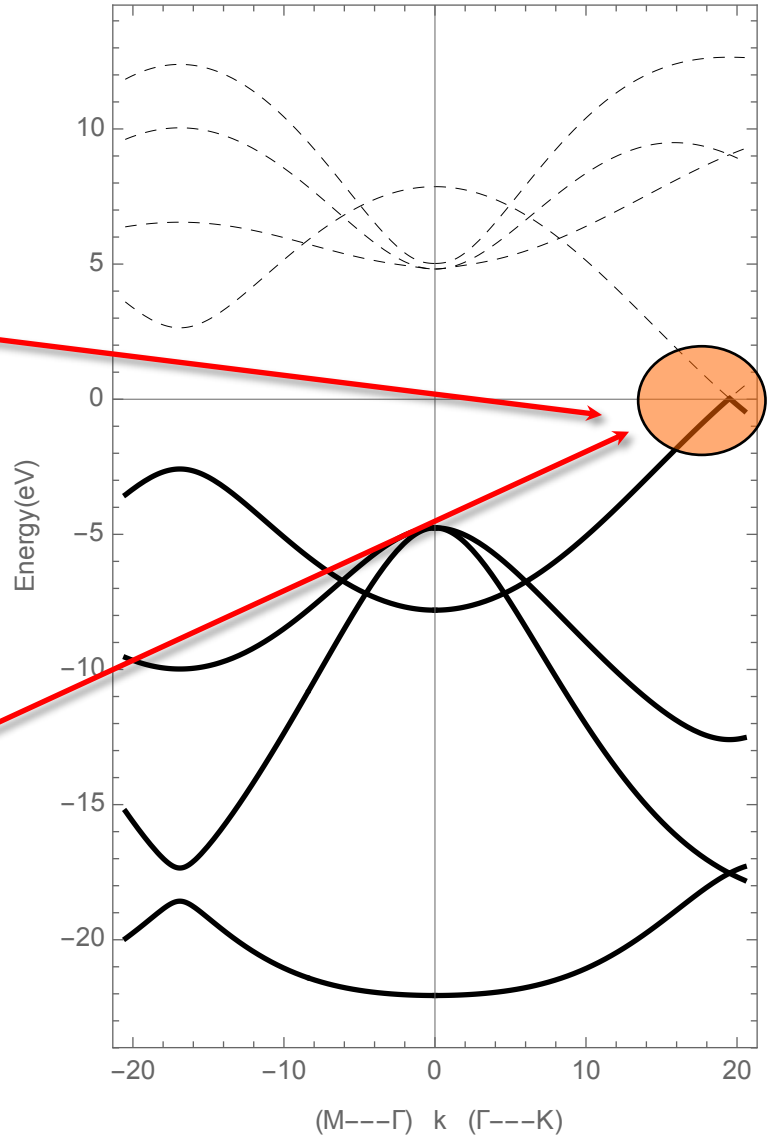

A Simple Example: 2D Graphene Bonds and Bands

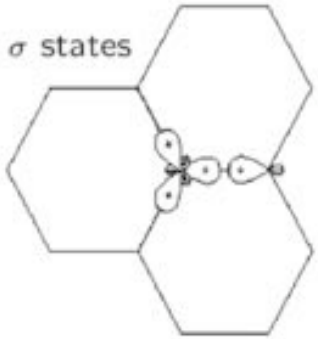

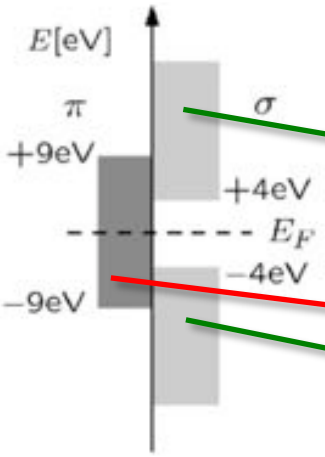

$$\mathcal{E}(k_x, k_y) = \mathcal{E}_F \pm \gamma_0 \sqrt{1 + 4\cos(\frac{\sqrt{3}k_x a}{2})\cos(\frac{k_y a}{2}) + 4\cos^2(\frac{k_y a}{2})}$$

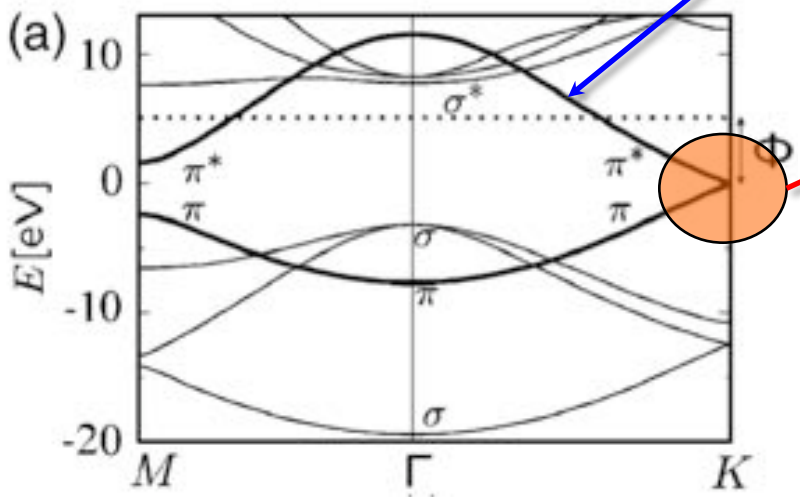

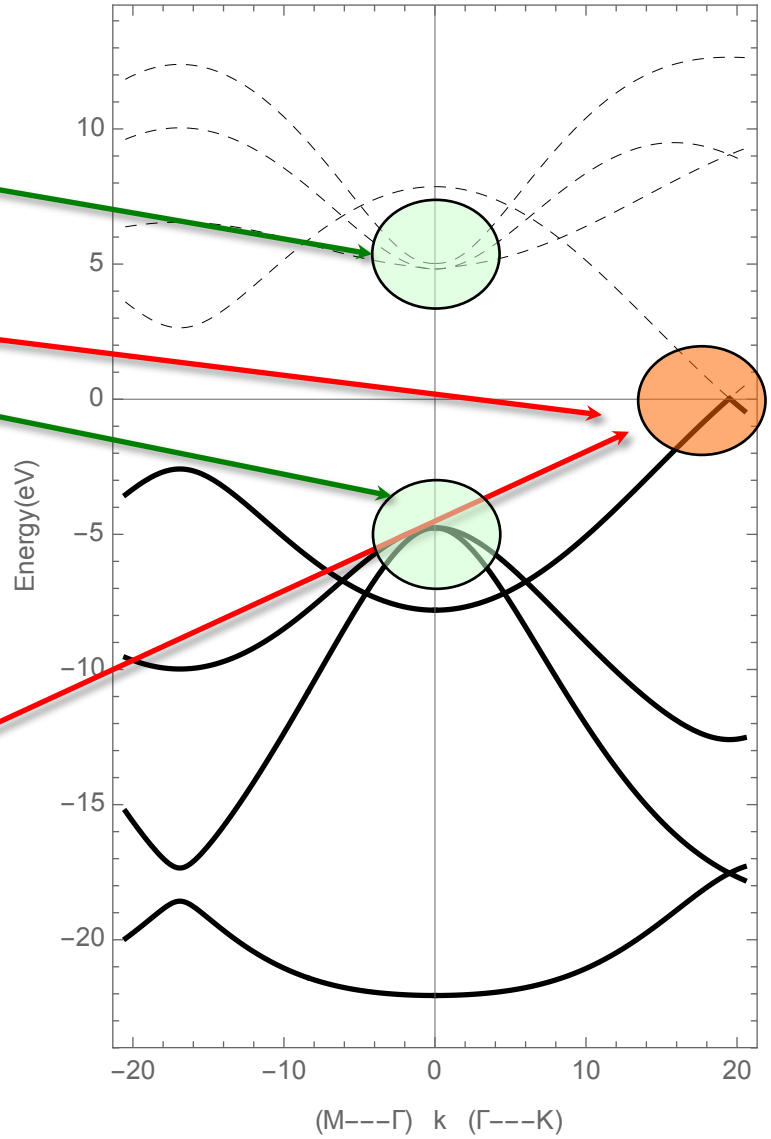

Comparison of NFE, Tight-Binding, and True Bands

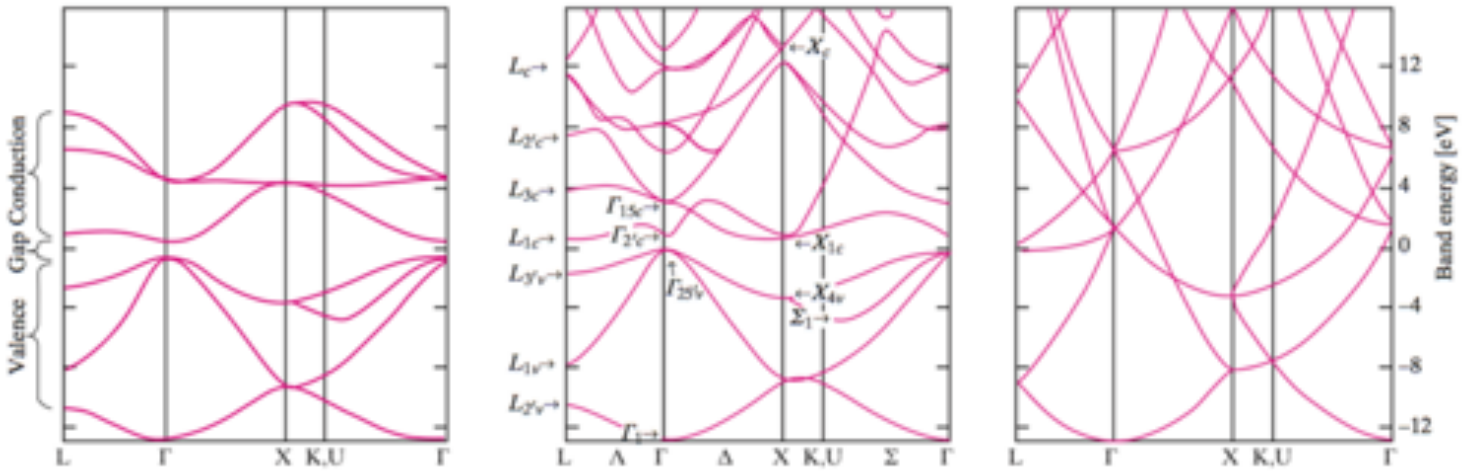

Fig. 2.25. A comparison between the band structure of Ge calculated by (**a**) the tight-binding method, (**b**) the empirical pseudopotential method, and (**c**) the nearly free electron model [Ref. 2.24, p. 79]

From Cardona and Yu

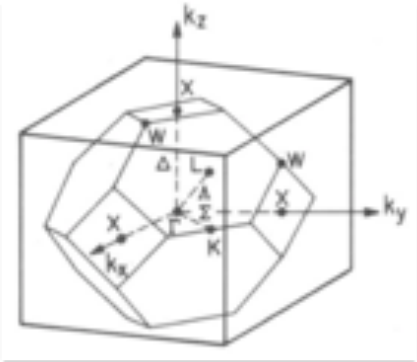

ECE 4070 / MSE 6050
Comparison of Bandstructures
NFE, Tight-Binding (LCAO) & EPM
(Germanium, representative of Si,...)

The Tight-Binding (or LCAO) Matrix for FCC Crystals

$H =$

ε_{1s}	0	0	0	$-V_{sss}g_0(k)$	$\frac{V_{sps}}{\sqrt{3}}g_1(k)$	$\frac{V_{sps}}{\sqrt{3}}g_2(k)$	$\frac{V_{sps}}{\sqrt{3}}g_3(k)$
0	ε_{2p_1}	0	0	$-\frac{V_{sps}}{\sqrt{3}}g_1(k)$	$V_1 g_0(k)$	$V_2 g_3(k)$	$V_2 g_2(k)$
0	0	ε_{2p_2}	0	$-\frac{V_{sps}}{\sqrt{3}}g_2(k)$	$V_2 g_3(k)$	$V_1 g_0(k)$	$V_2 g_1(k)$
0	0	0	ε_{2p_3}	$-\frac{V_{sps}}{\sqrt{3}}g_3(k)$	$V_2 g_2(k)$	$V_2 g_1(k)$	$V_1 g_0(k)$
				ε_{2s}	0	0	0
	Hermitian			0	ε_{3p_1}	0	0
				0	0	ε_{3p_2}	0
				0	0	0	ε_{3p_3}

$g_0(k) = e^{ik_x a/4} + e^{ik_y a/4} + e^{ik_z a/4} + e^{-ik_x a/4}$ $\quad g_1(k) = e^{ik_x a/4} - e^{ik_y a/4} - e^{ik_z a/4} + e^{-ik_x a/4}$

$g_2(k) = e^{ik_x a/4} - e^{ik_y a/4} + e^{ik_z a/4} - e^{-ik_x a/4}$ $\quad g_3(k) = e^{ik_x a/4} + e^{ik_y a/4} - e^{ik_z a/4} - e^{-ik_x a/4}$

$V_1 = \frac{1}{3}V_{sps} - \frac{2}{3}V_{pps}$ $\quad V_2 = \frac{1}{3}V_{sps} + \frac{1}{3}V_{pps}$

Atoms to Crystals

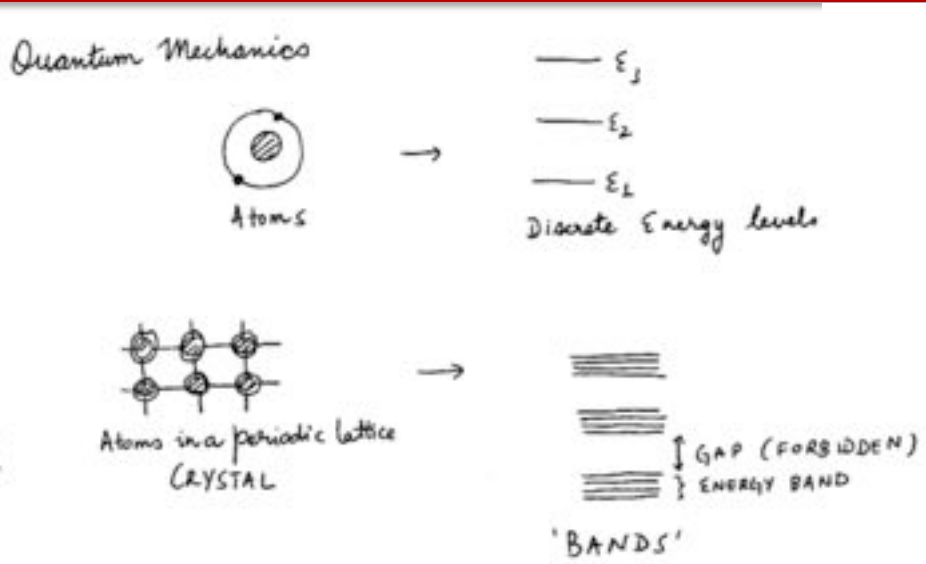

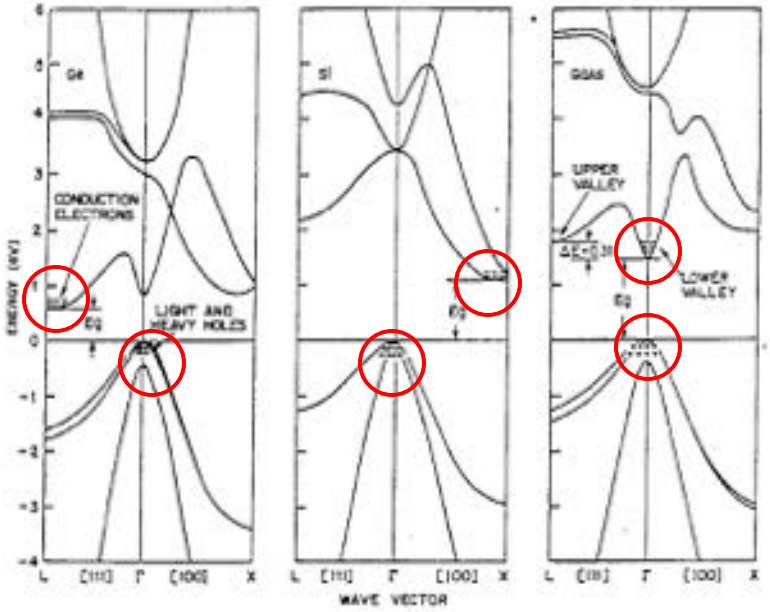

Indirect Direct

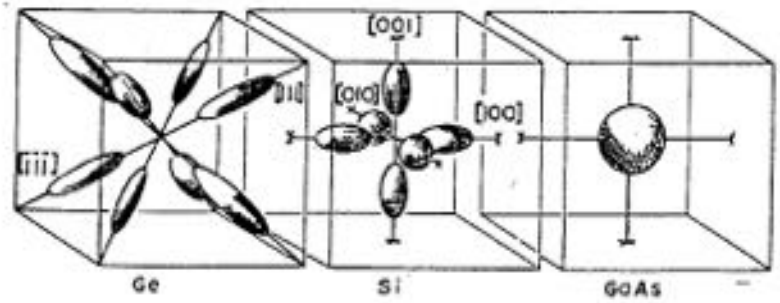

Crystal → Bandstructure

Typical 3D semiconductor crystal structures

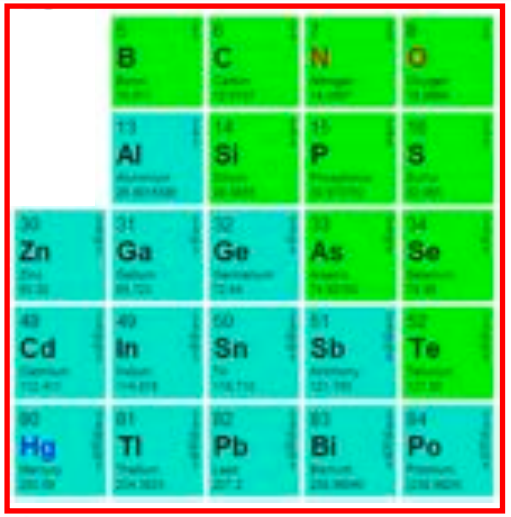

Due to the covalent bond structure (the bonding orbitals are s-p hybrids), most common semiconductors are found in three distinct structures:

i) The diamond lattice type: e.g. Si, Ge

ii) The zinkblende type: e.g. GaAs, InP

iii) The wurtzite type (hexagonal): e.g. GaN, ZnO

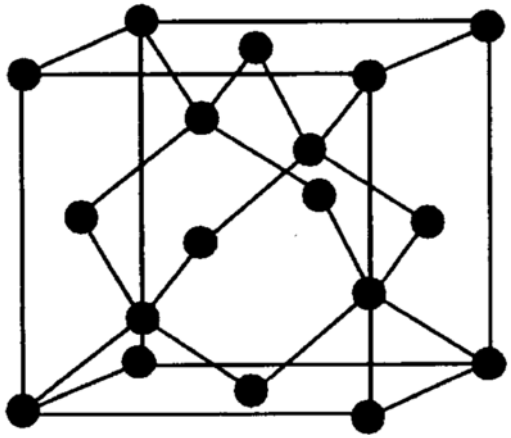

Fig. 1.2 Diamond lattice structure.

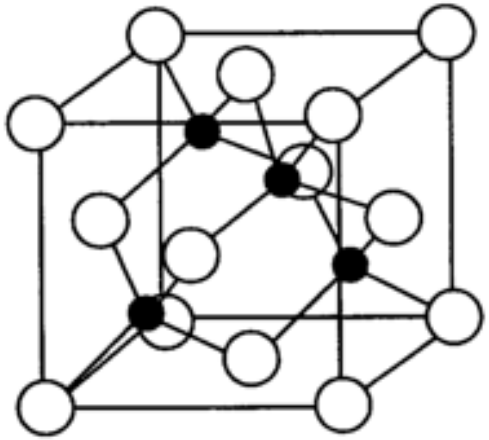

(a)

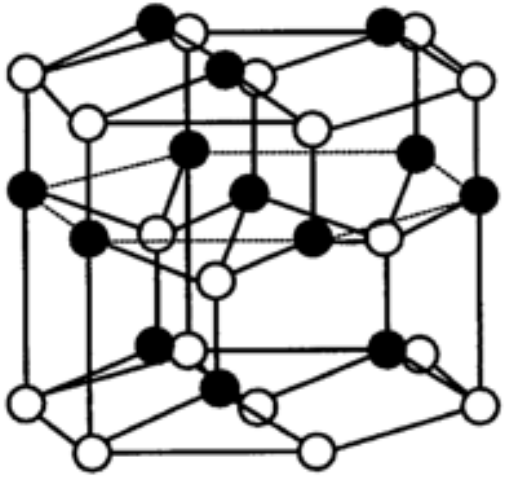

(b)

Fig. 1.3 (s) Zincblende lattice structure and (b)Wurtzite lattice structure. (○) A atom, (●) B atom.

(Denninger,Oda)

Nearly free electron bandstructure, k-space points

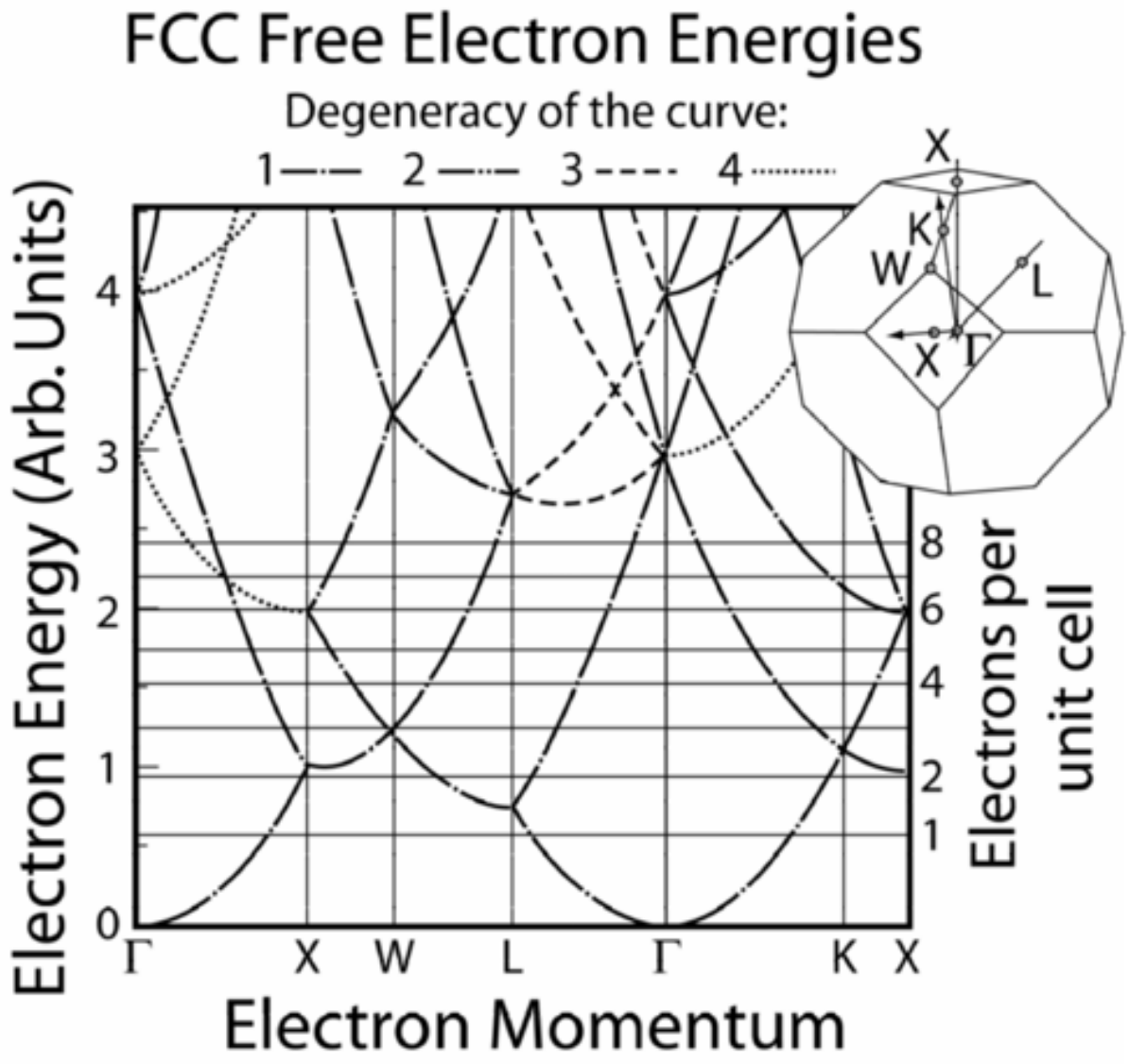

(Rockett)

Orbital overlaps and bonds in semiconductors

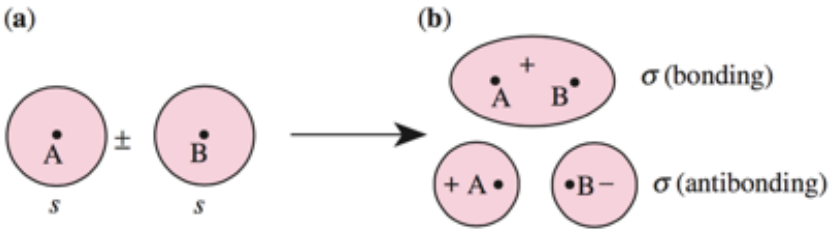

Fig. 2.17a,b. Overlap of two s orbitals to form bonding and antibonding σ orbitals

$$V_{ss\sigma}$$

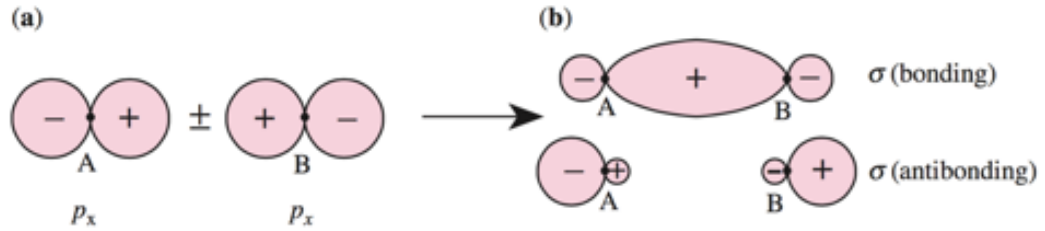

Fig. 2.18a,b. Overlap of two p_x orbitals along the x axis to form bonding and antibonding σ orbitals

$$V_{pp\sigma}$$

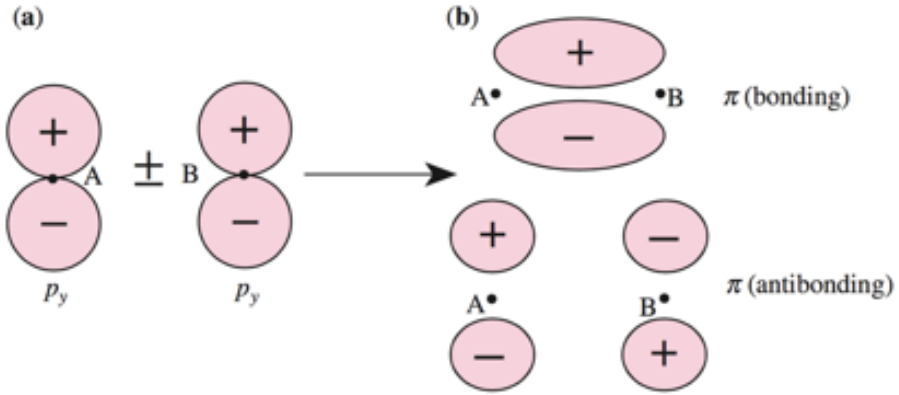

Fig. 2.19a,b. Overlap of two p_y orbitals to form bonding and antibonding π orbitals

$$V_{pp\pi}$$

(Cardona/Yu)

Orbital overlaps and bonds in semiconductors

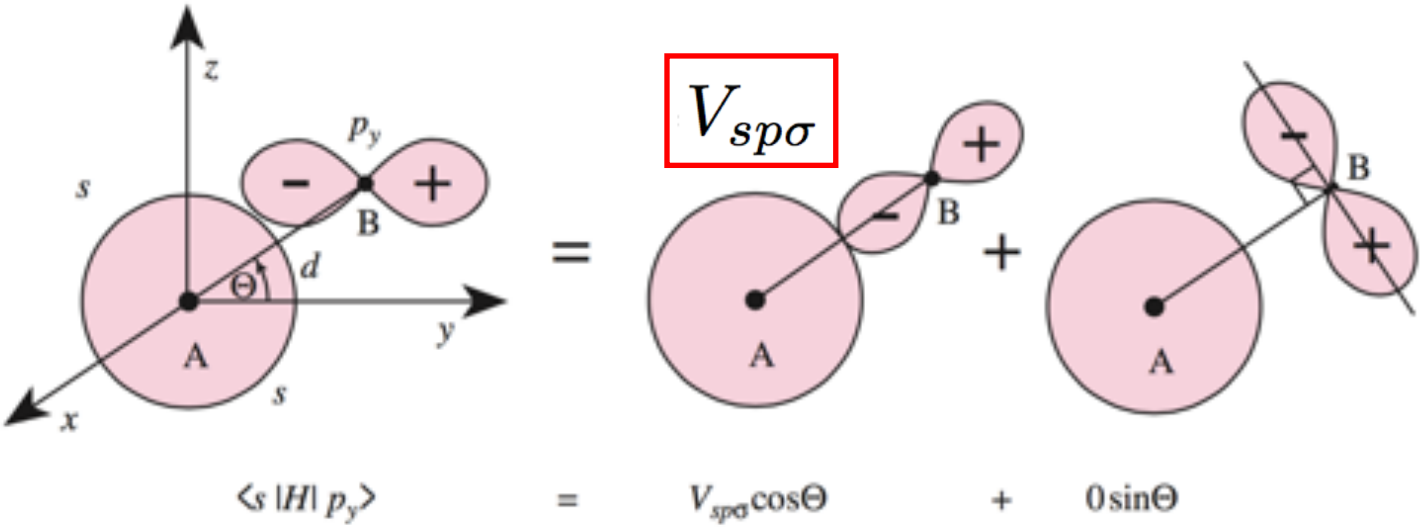

$$\langle s\,|H|\,p_y\rangle = V_{sp\sigma}\cos\Theta + 0\sin\Theta$$

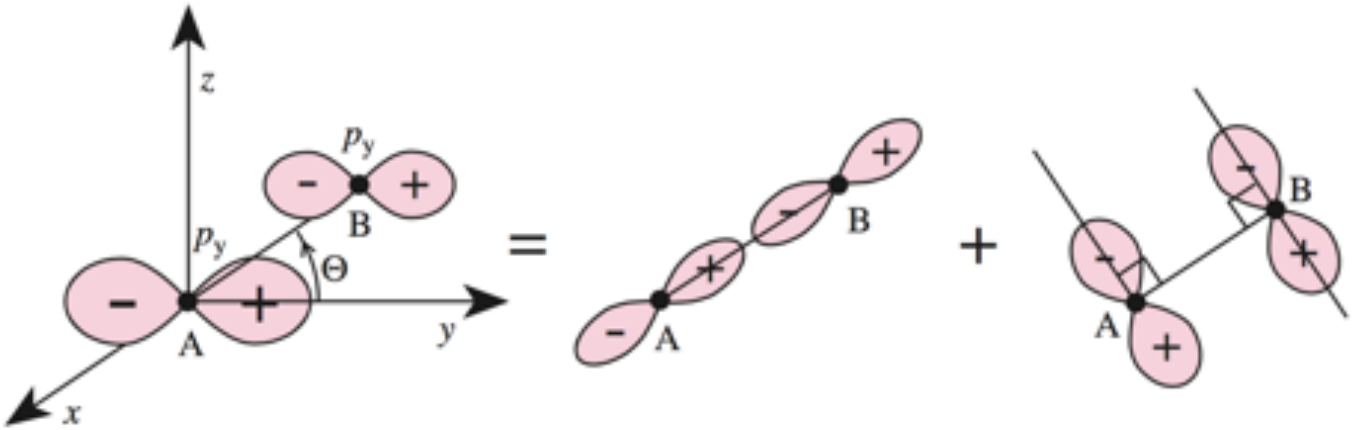

$$\langle p_y\,|H|\,p_y\rangle = V_{pp\sigma}\cos^2\Theta + V_{pp\pi}\sin^2\Theta$$

(Cardona/Yu)

Tight-Binding Bandstructure Matrix

$$\mathbf{a}_1 = \tfrac{a}{4}(1,1,1),\ \mathbf{a}_2 = \tfrac{a}{4}(-1,-1,1),\ \mathbf{a}_3 = \tfrac{a}{4}(-1,1,-1),\ \mathbf{a}_4 = \tfrac{a}{4}(1,-1,-1)$$

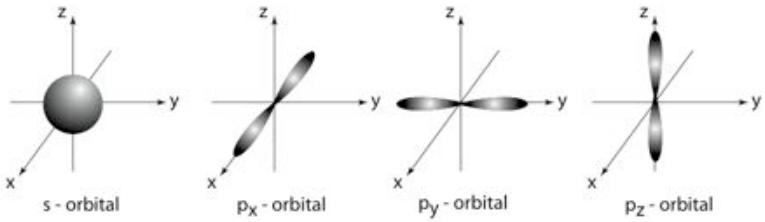

$$V_0 = V_{ss\sigma},$$
$$V_1 = \tfrac{1}{\sqrt{3}} V_{sp\sigma},$$
$$V_2 = \tfrac{1}{3} V_{pp\sigma} - \tfrac{2}{3} V_{pp\pi}$$
$$V_3 = \tfrac{1}{3} V_{pp\sigma} + \tfrac{1}{3} V_{pp\pi}$$

$$g_0(\mathbf{k}) = e^{i\mathbf{k}\cdot\mathbf{a}_1} + e^{i\mathbf{k}\cdot\mathbf{a}_2} + e^{i\mathbf{k}\cdot\mathbf{a}_3} + e^{i\mathbf{k}\cdot\mathbf{a}_4},$$
$$g_1(\mathbf{k}) = e^{i\mathbf{k}\cdot\mathbf{a}_1} - e^{i\mathbf{k}\cdot\mathbf{a}_2} - e^{i\mathbf{k}\cdot\mathbf{a}_3} + e^{i\mathbf{k}\cdot\mathbf{a}_4},$$
$$g_2(\mathbf{k}) = e^{i\mathbf{k}\cdot\mathbf{a}_1} - e^{i\mathbf{k}\cdot\mathbf{a}_2} + e^{i\mathbf{k}\cdot\mathbf{a}_3} - e^{i\mathbf{k}\cdot\mathbf{a}_4},$$
$$g_3(\mathbf{k}) = e^{i\mathbf{k}\cdot\mathbf{a}_1} + e^{i\mathbf{k}\cdot\mathbf{a}_2} - e^{i\mathbf{k}\cdot\mathbf{a}_3} - e^{i\mathbf{k}\cdot\mathbf{a}_4}$$

$$\begin{array}{c|cccccccc}
 & |s^A\rangle & |p_x^A\rangle & |p_y^A\rangle & |p_z^A\rangle & |s^B\rangle & |p_x^B\rangle & |p_y^B\rangle & |p_z^B\rangle \\
\hline
\langle s^A| & E_s^A & 0 & 0 & 0 & -V_0 g_0(\mathbf{k}) & V_1 g_1(\mathbf{k}) & V_1 g_2(\mathbf{k}) & V_1 g_3(\mathbf{k}) \\
\langle p_x^A| & 0 & E_p^A & 0 & 0 & -V_1 g_1(\mathbf{k}) & V_2 g_0(\mathbf{k}) & V_3 g_3(\mathbf{k}) & V_3 g_2(\mathbf{k}) \\
\langle p_y^A| & 0 & 0 & E_p^A & 0 & -V_1 g_2(\mathbf{k}) & V_3 g_3(\mathbf{k}) & V_2 g_0(\mathbf{k}) & V_3 g_1(\mathbf{k}) \\
\langle p_z^A| & 0 & 0 & 0 & E_p^A & -V_1 g_3(\mathbf{k}) & V_3 g_2(\mathbf{k}) & V_3 g_1(\mathbf{k}) & V_2 g_0(\mathbf{k}) \\
\langle s^B| & \text{c.c.} & \text{c.c.} & \text{c.c.} & \text{c.c.} & E_s^B & 0 & 0 & 0 \\
\langle p_x^B| & \text{c.c.} & \text{c.c.} & \text{c.c.} & \text{c.c.} & 0 & E_p^B & 0 & 0 \\
\langle p_y^B| & \text{c.c.} & \text{c.c.} & \text{c.c.} & \text{c.c.} & 0 & 0 & E_p^B & 0 \\
\langle p_z^B| & \text{c.c.} & \text{c.c.} & \text{c.c.} & \text{c.c.} & 0 & 0 & 0 & E_p^B
\end{array}$$

Tight-Binding Bandstructure

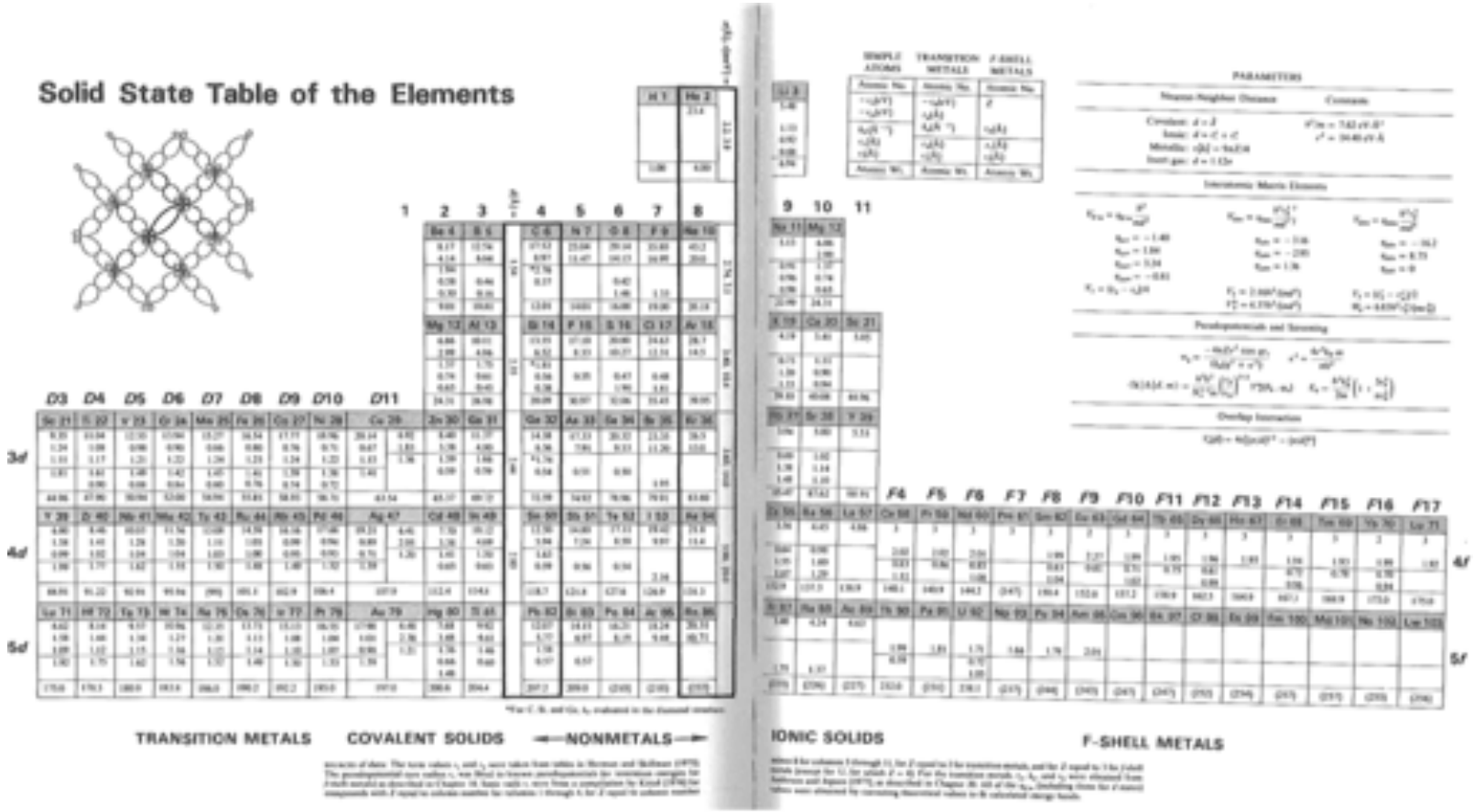

ECE 4070 / MSE 6050

The Solid-State Table for Elements.
Provides the tight-binding
parameters for chemical bonds.

From Harrison

Semiconductor Bandstructures

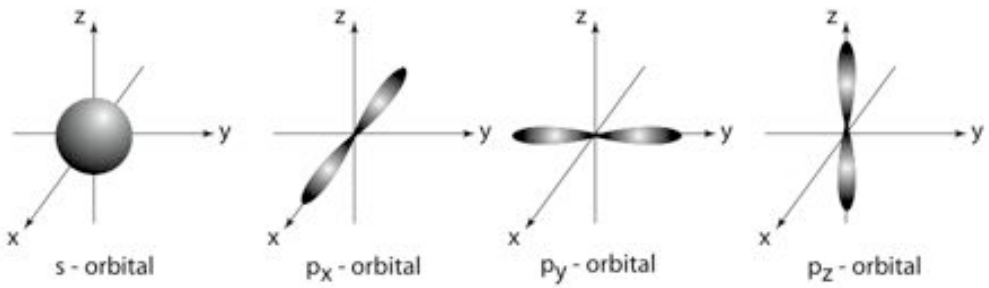

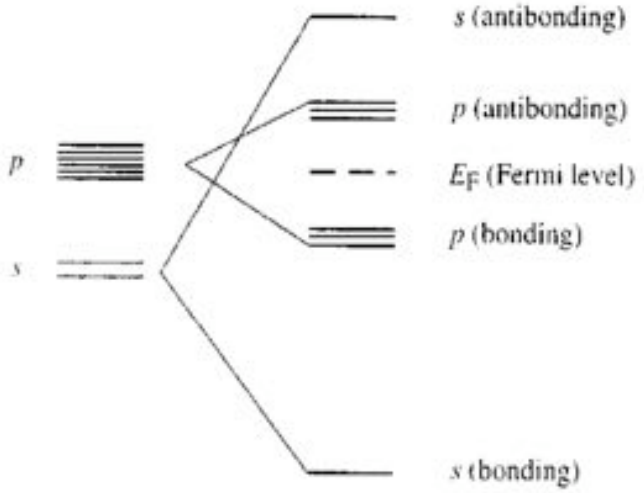

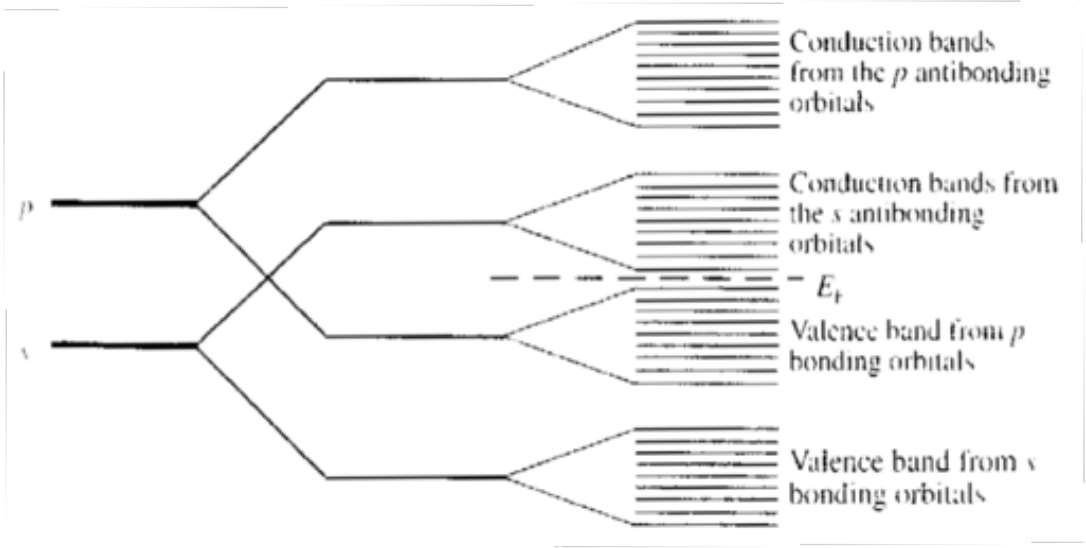

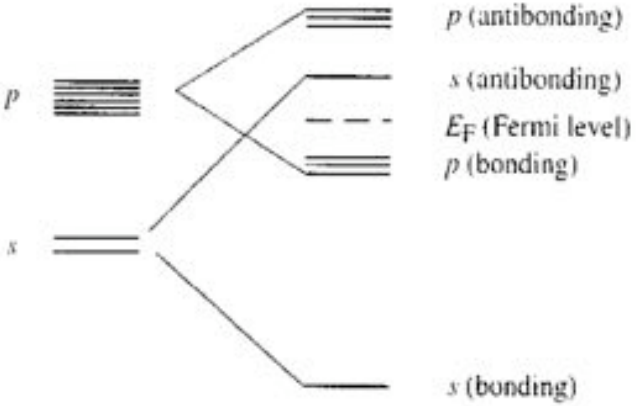

Origin of s and p 'contents' in semiconductor bandstructure

Tight Binding Solution for GaAs

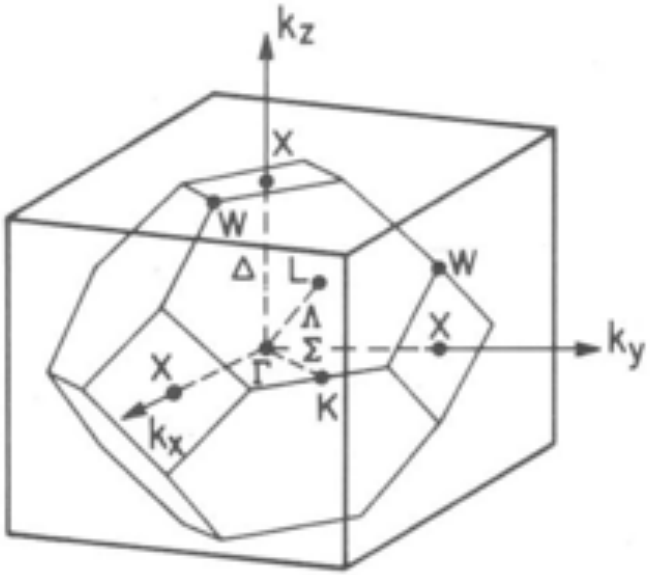

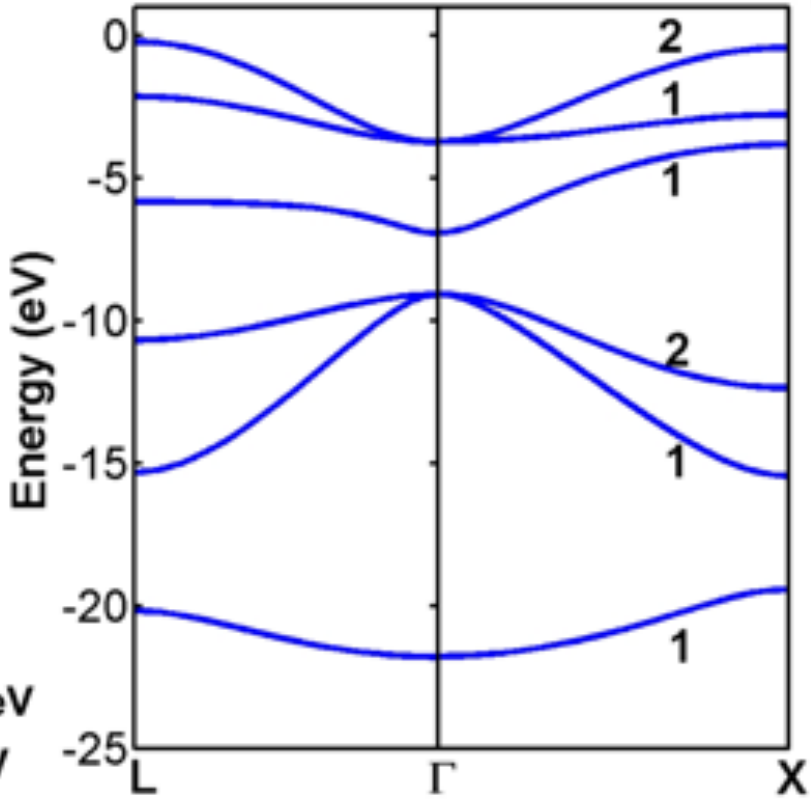

Tight Binding Solution

Parameter values for GaAs:

$E_{SG} = -11.37$ eV $E_{SA} = -17.33$ eV

$E_{PG} = -4.90$ eV $E_{PA} = -7.91$ eV

$V_{ss\sigma} = 1.70$ eV $V_{pp\sigma} = 3.44$ eV

$V_{sp\sigma} = 2.15$ eV $V_{pp\pi} = 0.89$ eV

Tight Binding Solution for GaAs: States at the Γ-Point

At the Γ-point:

$$g_0(\vec{k}=0)=4$$

$$g_1(\vec{k})=g_2(\vec{k})=g_3(\vec{k})=0$$

⇒ Energy eigenvalues can be found analytically

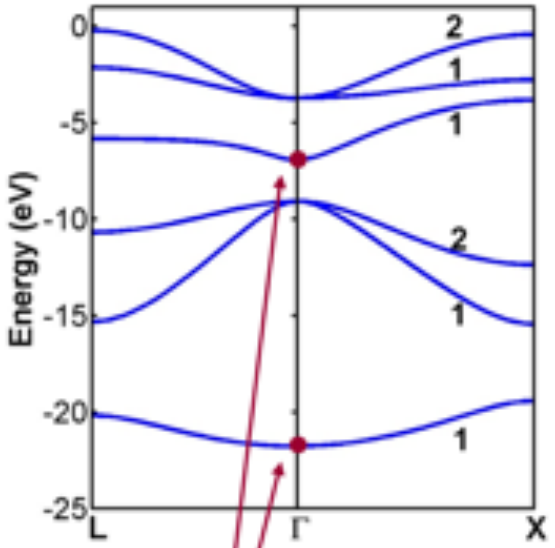

Two of the eigenvalues at the Γ-point are:

$$E_{5,1}(\vec{k}=0)=\left(\frac{E_{SG}+E_{SA}}{2}\right)\pm\sqrt{\left(\frac{E_{SG}-E_{SGA}}{2}\right)^2+(4V_{ss\sigma})^2}$$

The Bloch function of the lowest energy band and of the conduction band at Γ-point are made up of ONLY s-orbitals from the Ga and As atoms

$$\psi_{c,\vec{k}=0}(\vec{r})=\sum_m \frac{1}{\sqrt{N}}\left[c_1\left|\phi_1(\vec{r}-\vec{R}_m)\right\rangle+c_5\left|\phi_5(\vec{r}-\vec{R}_m-\vec{d}_2)\right\rangle\right]$$

Tight Binding Solution for GaAs: States at the Γ-Point

Six remaining eigenvalues at the Γ-point are:

$$E_{\substack{678\\234}}(\vec{k}=0)=\left(\frac{E_{PG}+E_{PA}}{2}\right)\pm\sqrt{\left(\frac{E_{PG}-E_{PA}}{2}\right)^2+(4V_1)^2}$$

Each eignevalue above is triply degenerate

The Bloch function of the highest three energy bands and of the three valence bands at Γ-point are made up of ONLY p-orbitals from the Ga and As atoms

$$\psi_{v,\vec{k}=0}(\vec{r})=\sum_m \frac{1}{\sqrt{N}}\left[\sum_{j=2}^{4} c_j\left|\phi_j(\vec{r}-\vec{R}_m)\right\rangle + \sum_{j=6}^{8} c_j\left|\phi_j(\vec{r}-\vec{R}_m-\vec{d}_2)\right\rangle\right]$$

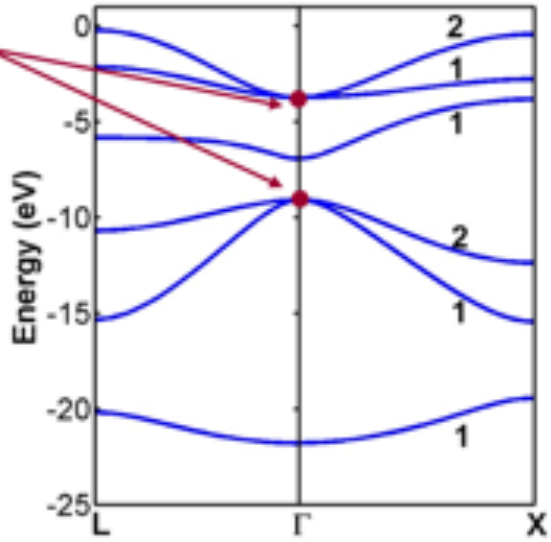

Semiconductor Bandstructures

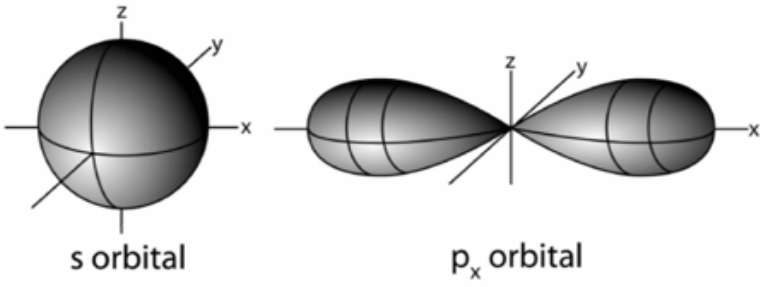

$$\psi_s = \frac{2a_0^{-3/2}}{\sqrt{\pi}}\left(1-\frac{r}{2a_0}\right)e^{-r/2a_0} \qquad \psi_{px} = \frac{2a_0^{-3/2}}{\sqrt{\pi/3}}\left(1-\frac{r}{2a_0}\right)e^{-r/2a_0}\cos\theta$$

Figure 5.1: Shows the shape of the s and p_x orbitals and the equations that describe them. a_0 is the atomic orbital size, r is the radius from the nucleus, and θ is the angle in the x,y plane.

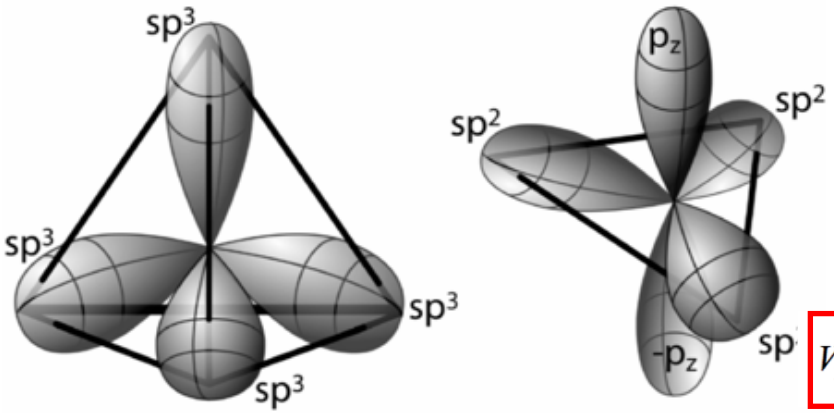

$$V_2 \approx 4.4\frac{\hbar^2}{md^2}\,\text{eV}$$

Figure 5.2: Shows the symmetry of the hybridized sp^3 and sp^2 molecular orbitals. The sp^2 orbitals lie in a plane perpendicular to the p_z orbitals and are equal lengths. The sp^3 orbitals are all equivalent to each other and stretch to corners of a tetrahedron.

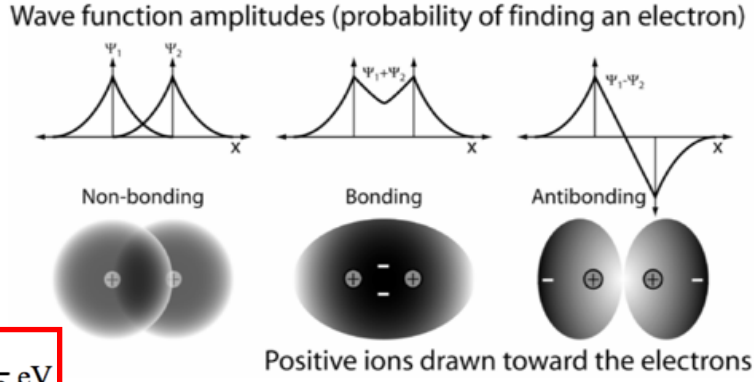

Figure 5.3: A schematic diagram illustrating the basis of cohesion in solids resulting from symmetric and antisymmetric combinations of atomic orbitals. The center of electron charge lies between the positive ions for a symmetric bonding orbital and outside of the positive ions for an antisymmetric orbital combination.

Origin of s and p 'contents' in semiconductor bandstructure

(Rockett)

Semiconductor Bandstructures

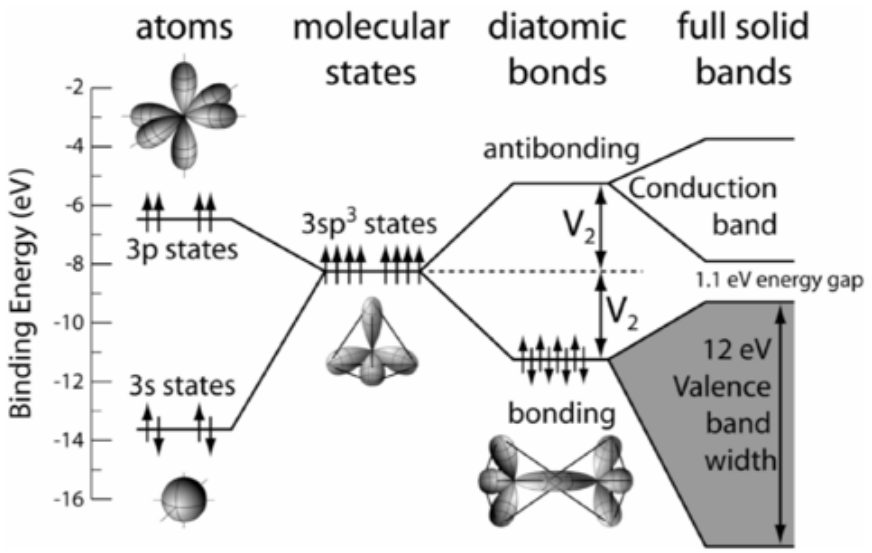

Figure 5.4: A schematic diagram of the evolution of bonding of Si atoms. The filled 3s and partially filled 3p atomic orbitals of two atoms combine to form half-filled sp^3 hybrid molecular orbitals. These combine to form bonding and antibonding orbtials. As more atoms collect atoms collect to create a bulk solid, bands form.

Silicon

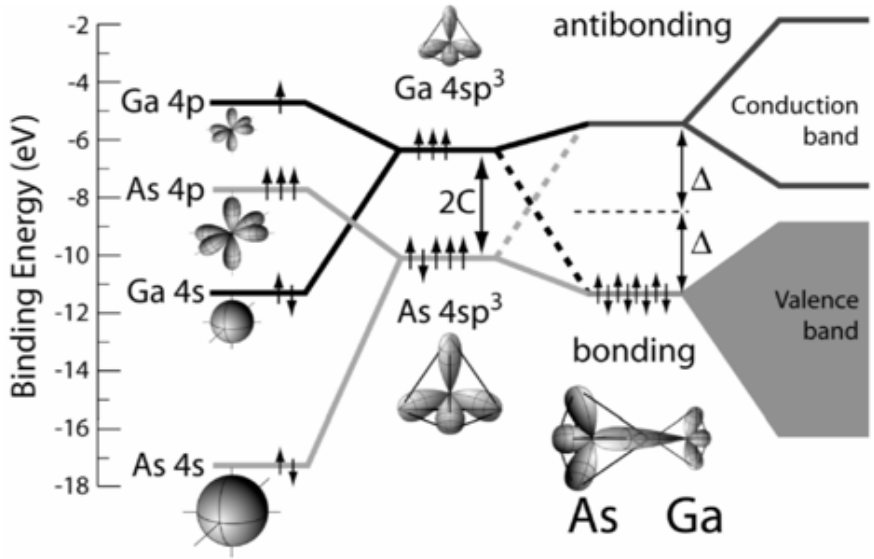

Figure 5.5: Shows the evolution of atomic orbital energies to form bonds and ultimately bands. The geometries of the atomic and hybrid orbitals are shown schematically as insets.

GaAs

(Rockett)

Semiconductor Bandstructures

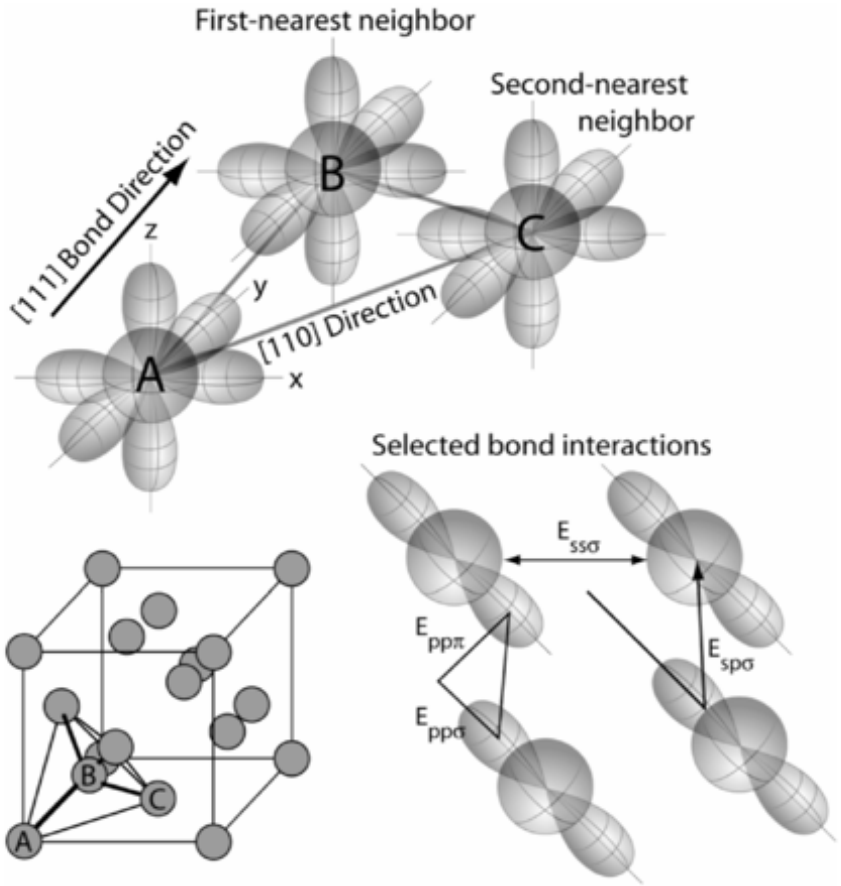

Figure 5.6: A schematic diagram showing the interactions of selected atomic orbitals and the geometry of these orbitals with respect to the crystal lattice in a zincblende or diamond structure material.

Table 5.3: **Energy Gaps and Lattice Parameters**

Semiconductor Class	Semiconductor	Lattice Parameter	Energy Gap, eV (at 20°C)	E_c (eV)	E_v (eV)
Cubic		nm			
IV	C (diamond)	0.35597	5.5		
IV	Si	0.54307	1.12 (indirect)	4.05	5.17
IV	Ge	0.56754	0.67 (indirect)	4.0	4.67
IV	a-Sn	0.64912	0.08		
III-V	GaP	0.54505	2.26 (indirect)	3.8	6.1
III-V	GaAs	0.56532	1.42	4.07	5.49
III-V	GaSb	0.609593	0.726	4.06	4.79
III-V	InP	0.58687	1.344	4.38	5.72
III-V	InAs	0.60583	0.354	4.9	5.25
III-V	InSb	0.6479	0.17	4.59	4.76
II-VI	ZnSe (cubic)	0.567	2.58	4.1	6.7
I-VII	CuBr	5.69	2.94	4.35	7.29
I-III-VI_2	$CuInSe_2$	0.578	0.98	4.0	5.0
II-IV-V_2	$ZnGeAs_2$	0.567	0.85		
Hexagonal					
III-V	AlN	0.3111 (a) 0.4978 (c)	5.9	0.6	6.5
III-V	GaN	0.3190 (a) 0.5189 (c)	3.45	4.0	7.4
III-V	InN	0.3533 (a) 0.5693 (c)	0.7 (note values vary greatly)		
II-VI	ZnS	0.3814 (a) 0.6258 (c)	3.911		
II-VI	CdSe	0.4299 (a) 0.7010 (c)	1.751 eV		

E_c (the electron affinity) and E_v (electron affinity + energy gap) measured with respect to the vacuum level. Lattice parameters in nm.

Chemical bonding, Lattice Constants, Band edges, and Band Gaps for various Semiconductors

(Rockett)

Semiconductor Bandstructures

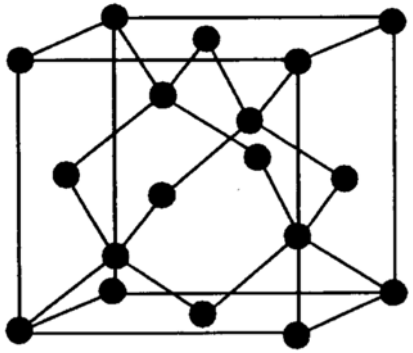

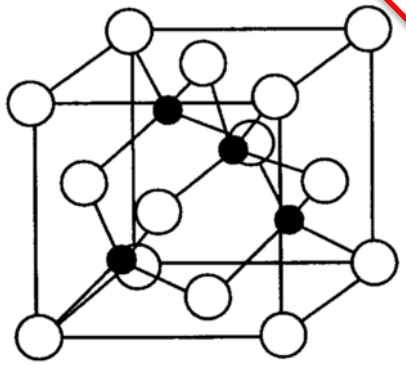

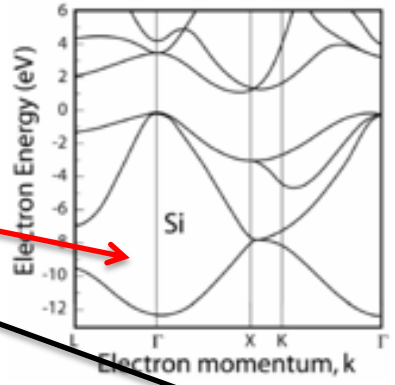

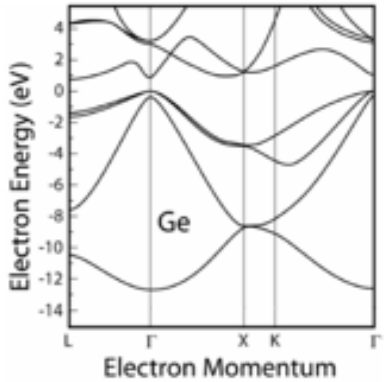

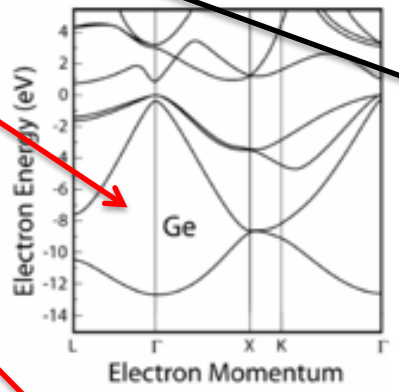

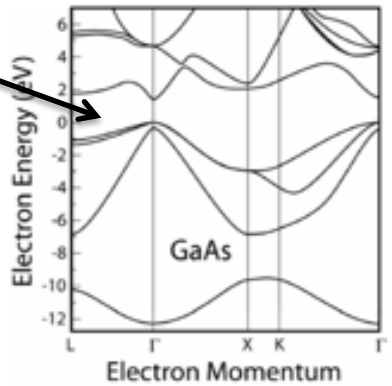

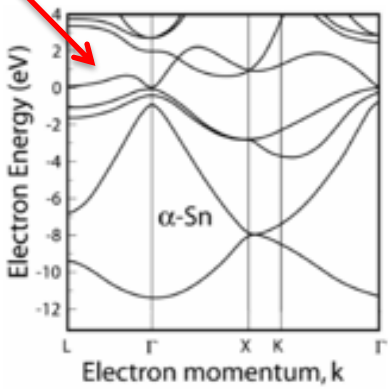

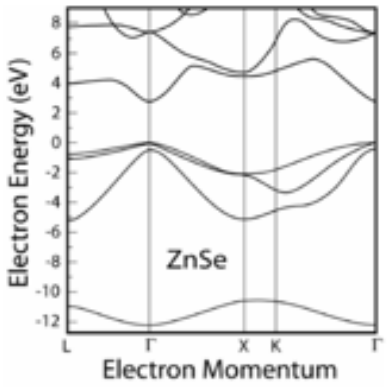

Bandstructures of
Elemental and Compound Semiconductors

Semiconductor Bandstructures

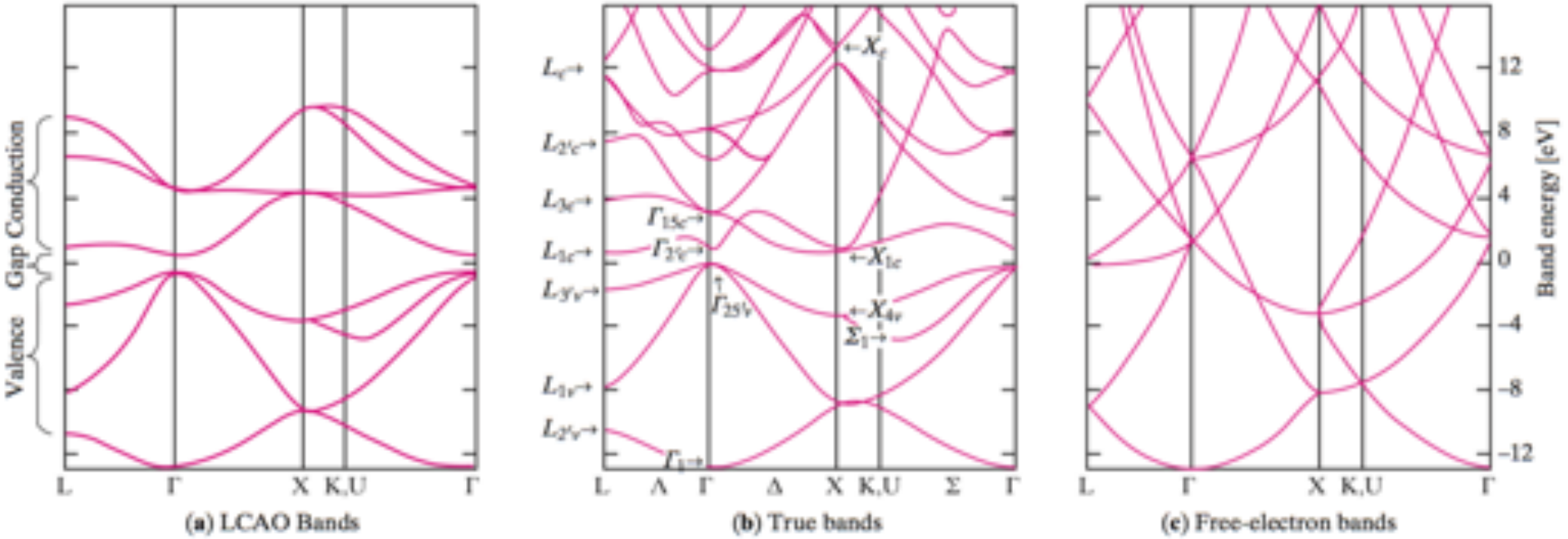

Fig. 2.25. A comparison between the band structure of Ge calculated by (**a**) the tight-binding method, (**b**) the empirical pseudopotential method, and (**c**) the nearly free electron model [Ref. 2.24, p. 79]

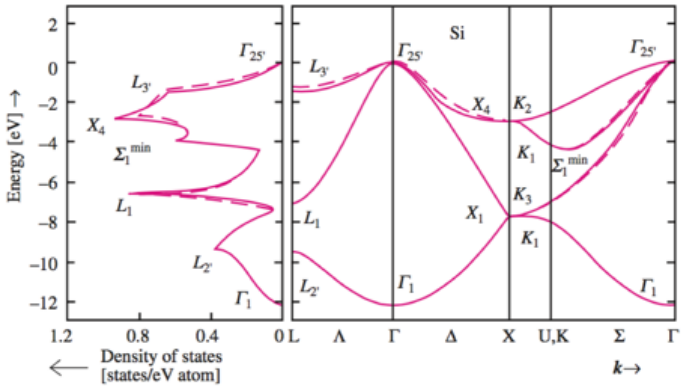

Fig. 2.24. The valence band structure and density of states (see Sect. 4.3.1 for definition) of Si calculated by the tight-binding method (*broken curves*) and by the empirical pseudopotential method (*solid lines*) [2.25]

Electron clouds in semiconductors

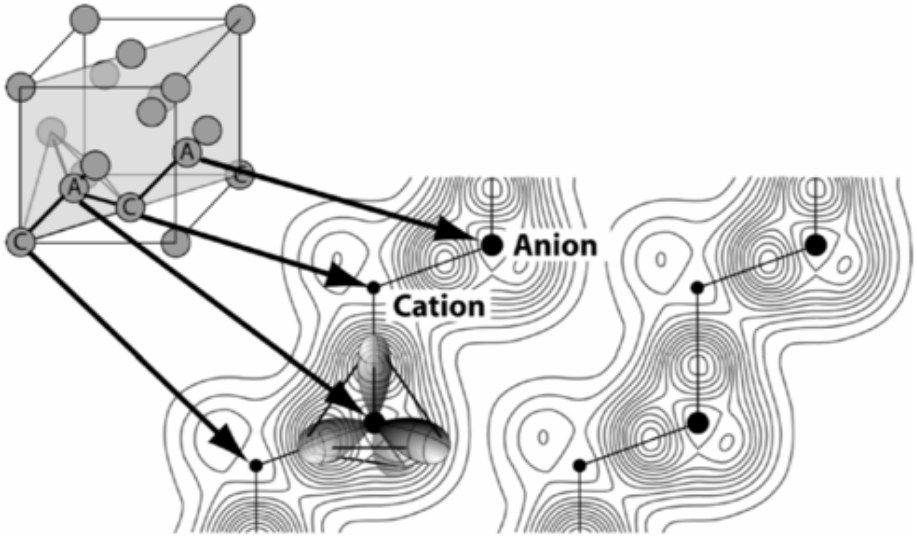

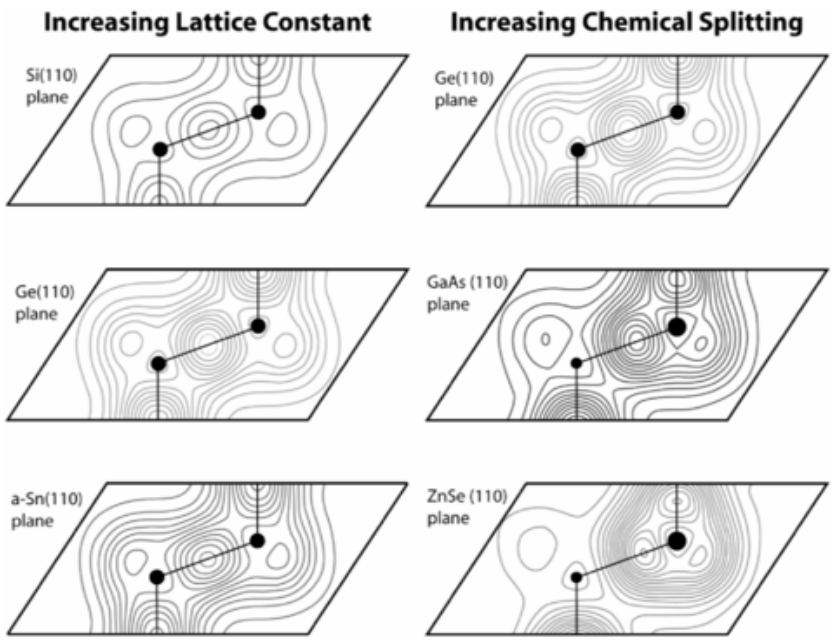

Electron wavefunction squared = probability density of finding electrons

(Rockett)

Measurement of Semiconductor Bandstructures

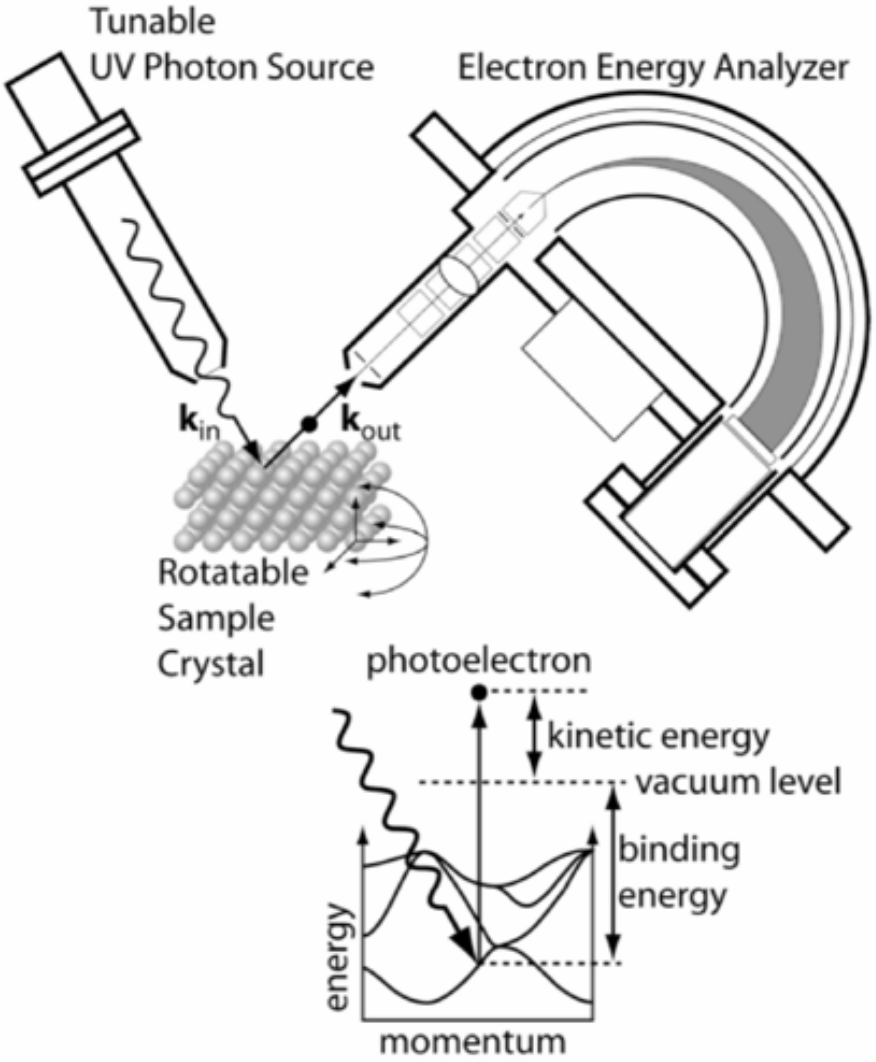

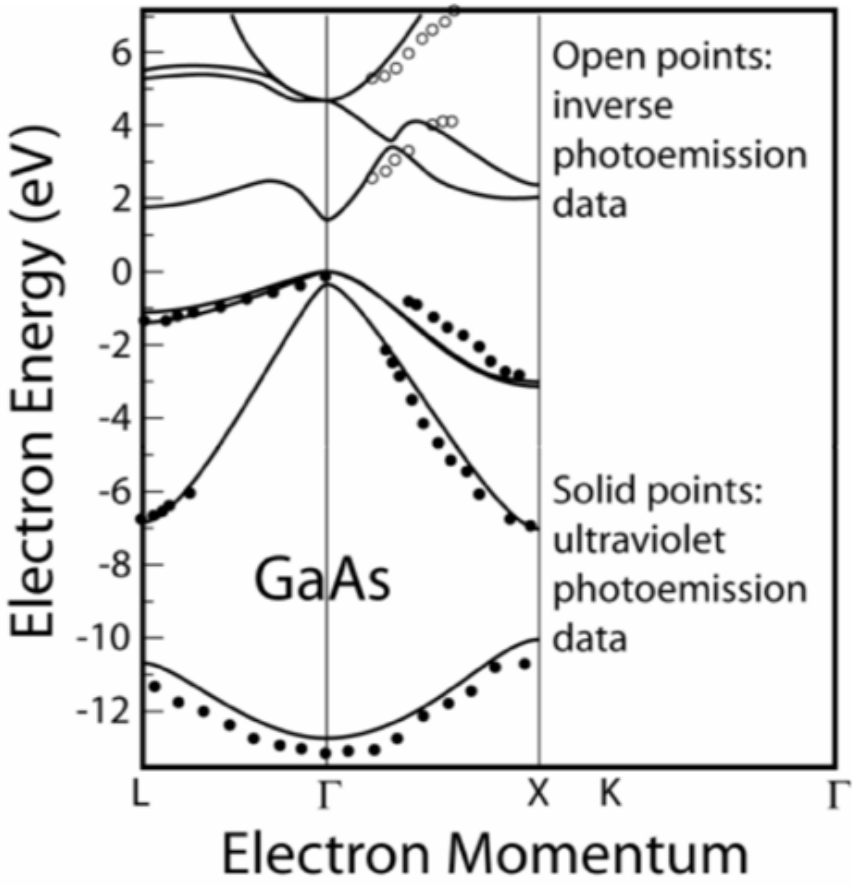

Angle-Resolved Photo-Emission Spectroscopy (ARPES)

(Rockett)

Semiconductor Bandstructures

Free electron vs. real bandstructure

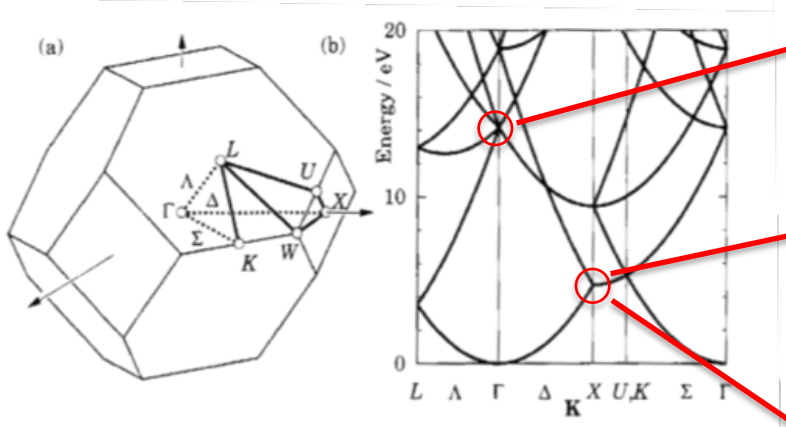

FIGURE 2.15. (a) Brillouin zone for a face-centred cubic crystal, showing the notation for special points and directions. Solid lines are on the surface with broken lines inside the zone. (b) Band structure in the free-electron model, showing the effect of folding back the parabola into the reduced zone.

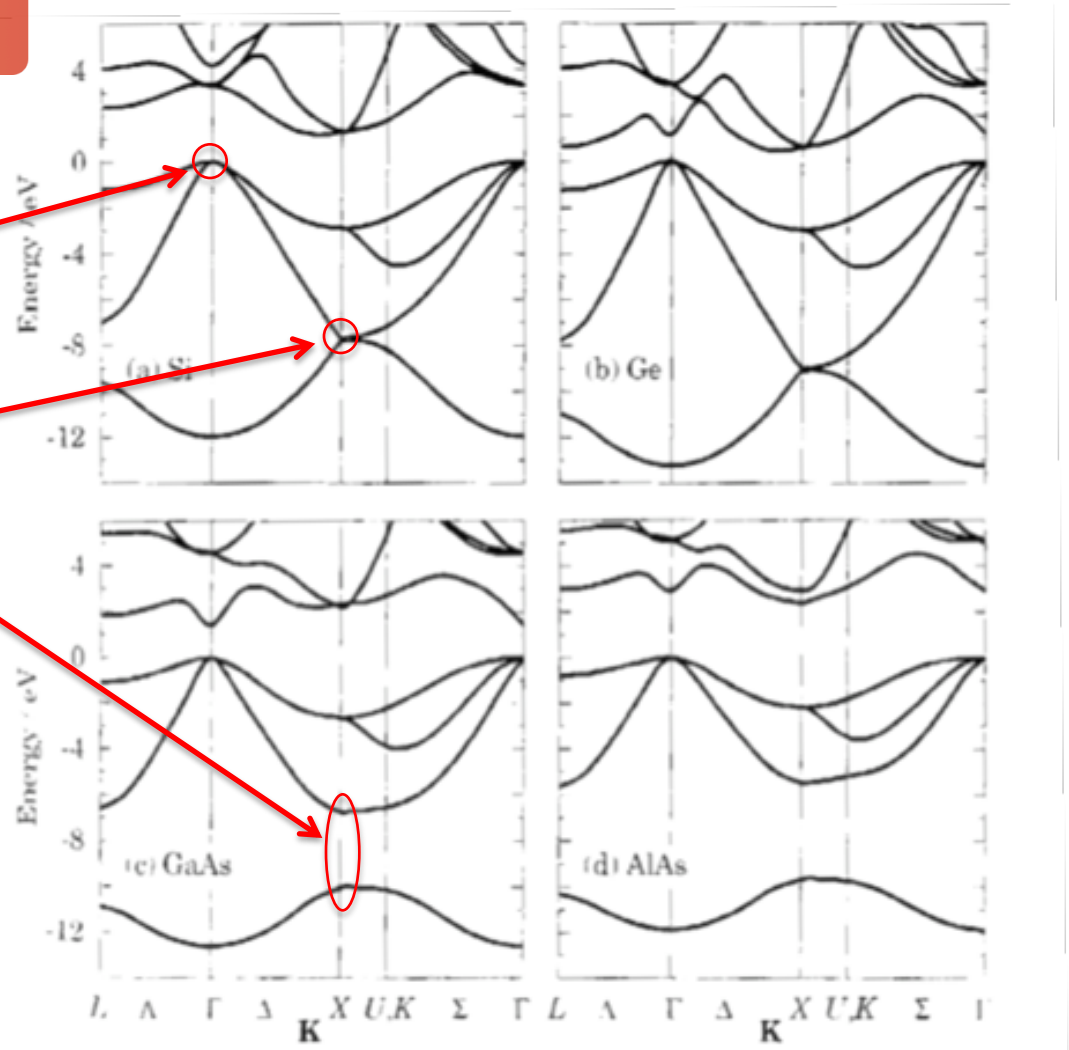

FIGURE 2.16. Band structure of four common semiconductors: silicon, germanium, gallium arsenide, and aluminium arsenide. The calculations do not include the spin–orbit coupling. [Results kindly supplied by Prof. G. P. Srivastava, University of Exeter.]

Energy Bands of Si, Ge, and GaAs for Reference

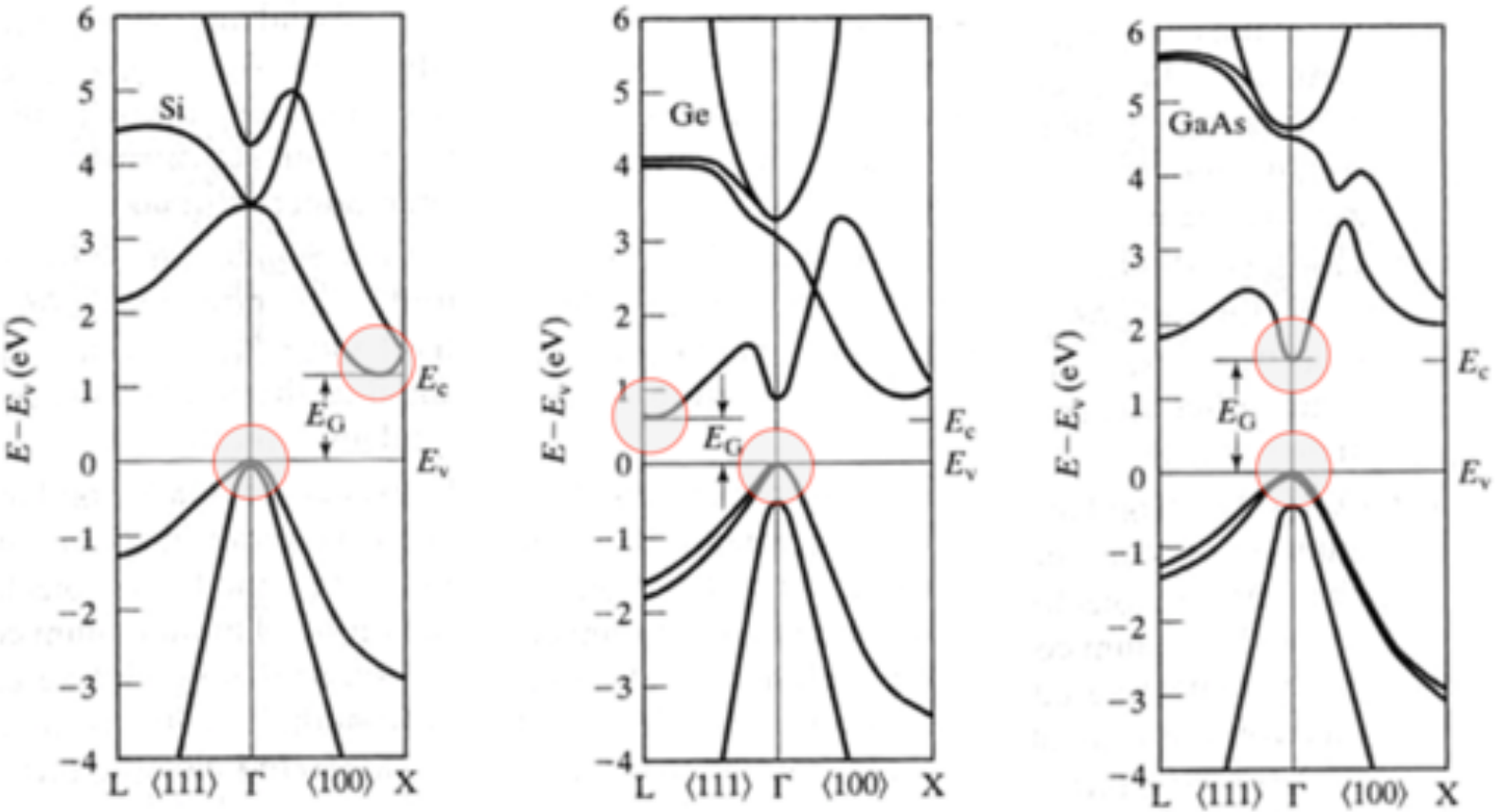

ECE 4070 / MSE 6050
Energy Bandstructures of the most common Semiconductors

A Timely Note About This Course!

> Semiconductor electronics requires for its foundation primarily wave mechanics and statistics. However, crystallography, thermodynamics, and chemistry also have a share in it and, quite generally, "it is incredible what miserable quantities of thought and mathematics are needed to provide even the simplest tools for daily use in semiconductor physics" (from a conversation of W. Schottky with the author).

ECE 4070 / MSE 6050

- If you are finding the course tough at this point, you are in hallowed company.
- That is the nature of the subject - solve problems and think about them (do not let go), you will learn it.
- We have developed a rich range of powerful tools, but the only way to learn their power is to apply them.
- The transition from "no idea" to "completely understand" is very quick in this subject (if you put in the effort) - I am here to help.

Walter Schottky

Eberhard Spenke

Prelim 2 for ECE 4070 / MSE 6050

- Thursday April 11th 2019
- Time: 7:30 – 9:00 pm
- In Phillips Hall 219 (Note: different from class location!)

- No restrictions on books/notes/calculators/computers etc.
- Bring pen/pencil – exam books will be provided.
- The questions will be conceptual, no heavy number crunching will be needed.
- Questions from previous years are fairly representative of what to expect.
- Topics: Chapters 1-9 from the Notes, and suggested Slides.

Exams and Grades:
An assignment every 1.5 weeks. Total of 6-8 homework assignments per semester. Exams: 2 Evening Prelim Exams and 1 Final Exam. Here is the approximate breakup of scores that will go towards your final grade:
35% Assignments
15% Prelim 1 [Tuesday March 5th, 2019]
20% Prelim 2 [Thursday April 11th, 2019]
30% Final [Wednesday May 15th, 2019]

Tight-Binding Bandstructure

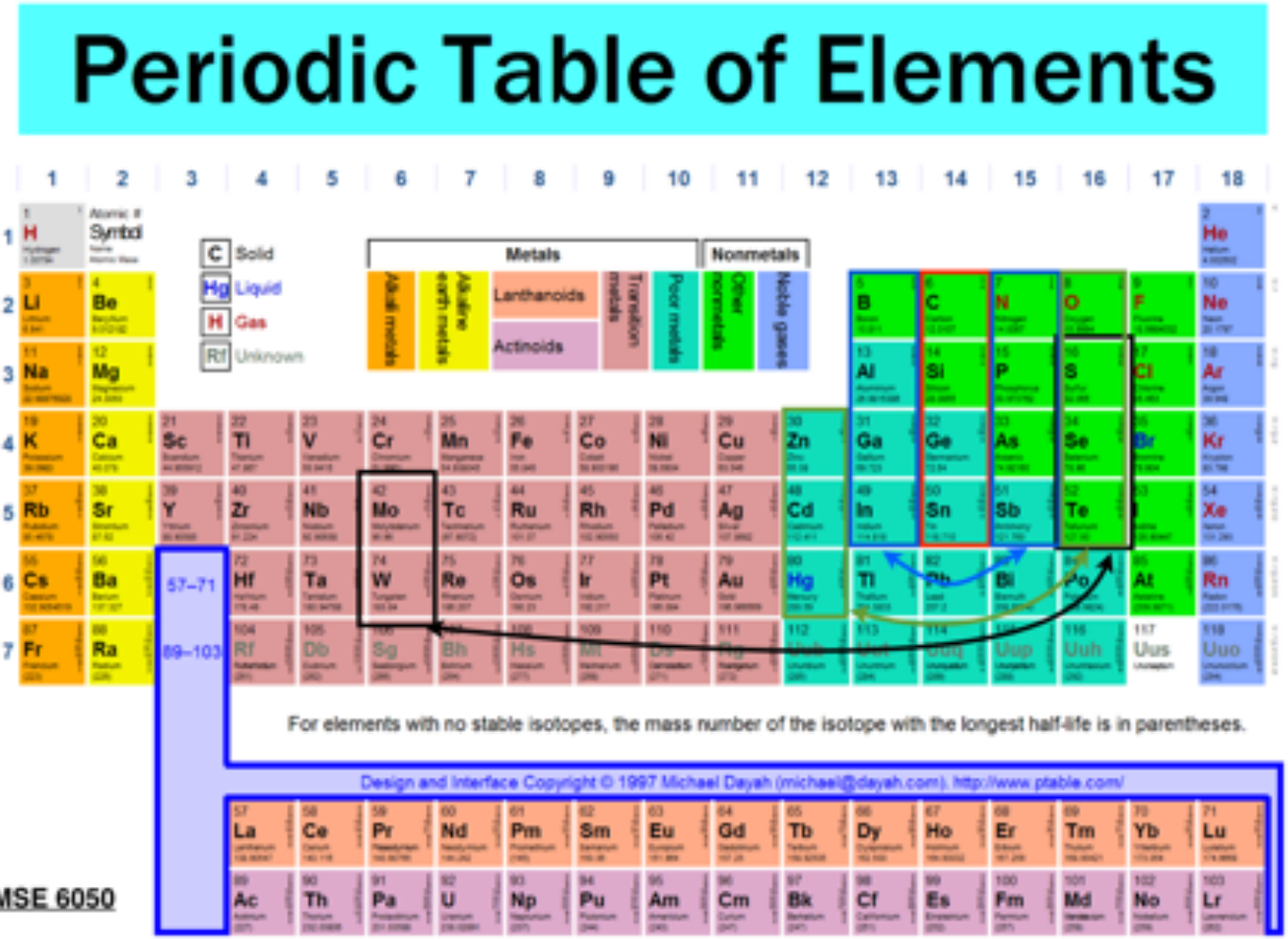

ECE 4070 / MSE 6050

Some common Semiconductor Families:

- Group IV: Diamond, Silicon, Ge, ...
- Group III-V: GaAs, InP, InSb,GaN, ...
- Group II-VI: ZnO, MgO, CdSe, HgTe...
- 2D Materials: Graphene, MoS_2, GaSe, ...

Tight-Binding Bandstructure

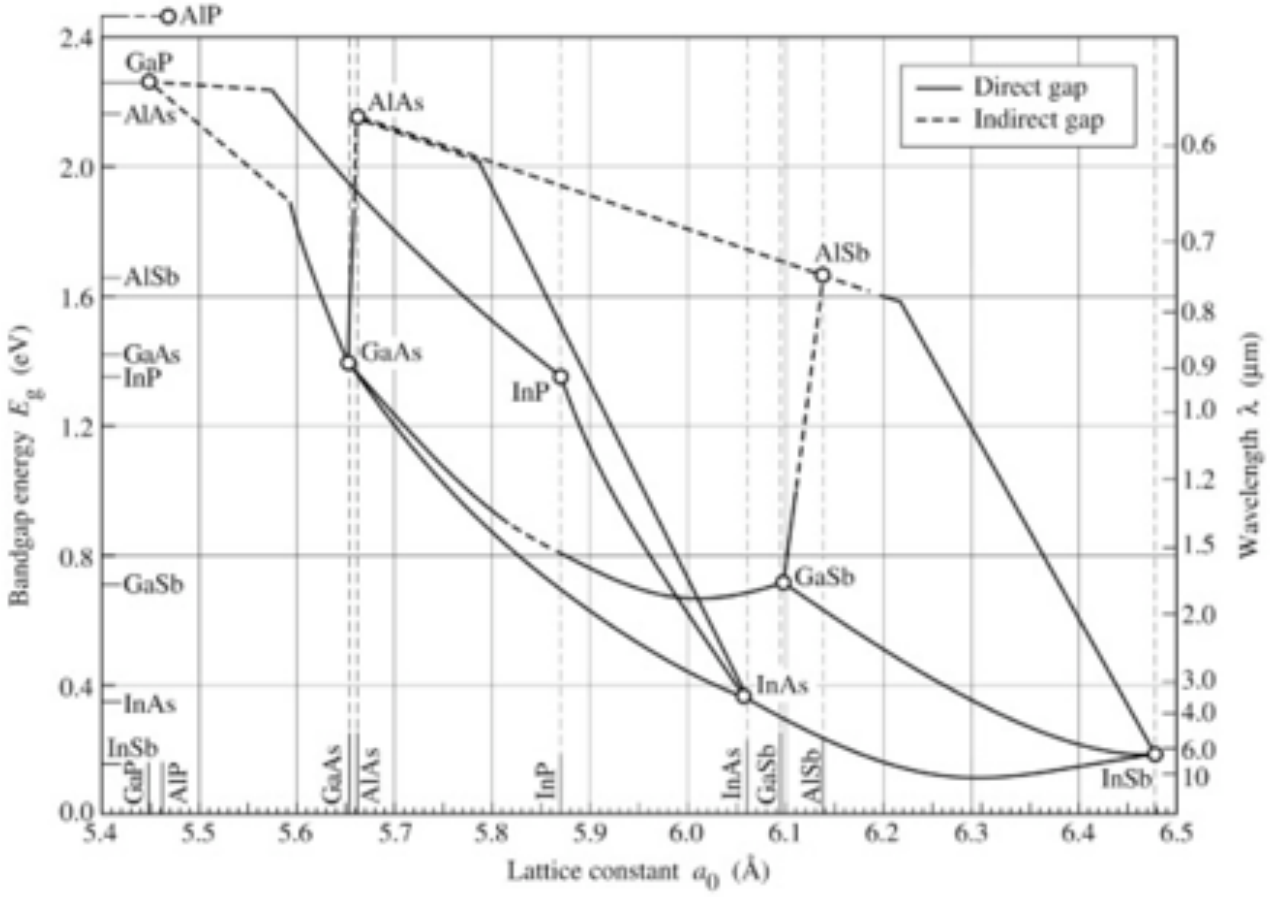

Fig. 7.6. Bandgap energy and lattice constant of various III-V semiconductors at room temperature (adopted from Tien, 1988).

ECE 4070 / MSE 6050

- A wide variety of bandgaps and lattice constant semiconductors are available.

Tight-Binding Bandstructure

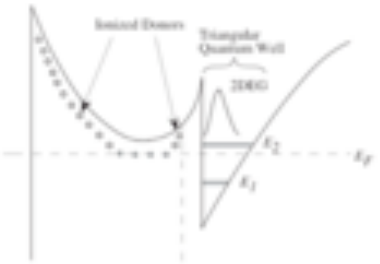

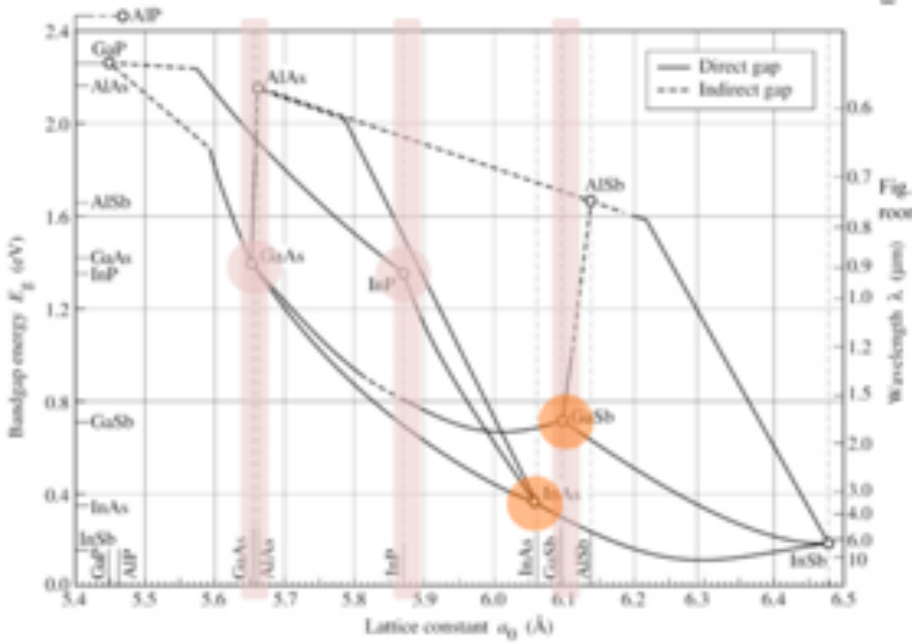

Fig. 7.6. Bandgap energy and lattice constant of various III-V semiconductors at room temperature (adopted from Tien, 1988).

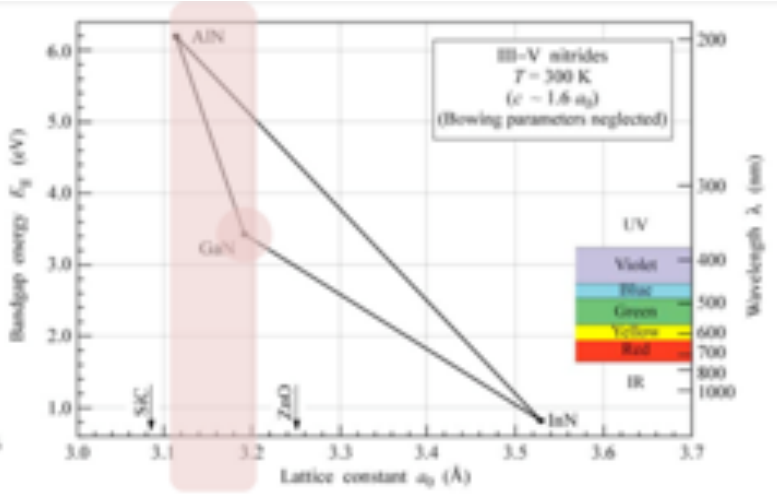

Fig. 12.12. Bandgap energy versus lattice constant of III–V nitride semiconductors at room temperature.

Major HFET families:

- *GaAs-based (AlGaAs/GaAs) (strain-free, or pseudomorphic)*
- *InP based (InGaAs channels)*
- *6.1 Angstrom/narrow gap channels (generally grown metamorphically on GaAs)*
- *GaN-based (AlGaN/GaN and AlN/GaN) (typically pseudomorphic)*

ECE 4070 / MSE 6050

- Semiconductors can be grown on top of each other.

Compound Semiconductor Heterostructures: Strain

Lattice-Matching, Strain

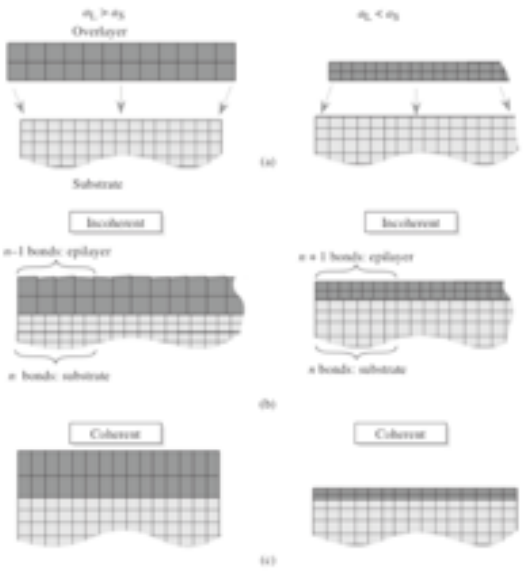

Figure 1.16: (a) The conceptual exercise in which an overlayer with one lattice constant is placed without distortion on a substrate with a different lattice constant. (b) Dislocations are generated at positions where the interface bonding is lost. (c) The case is shown where the overlayer is distorted so that no dislocation is generated.

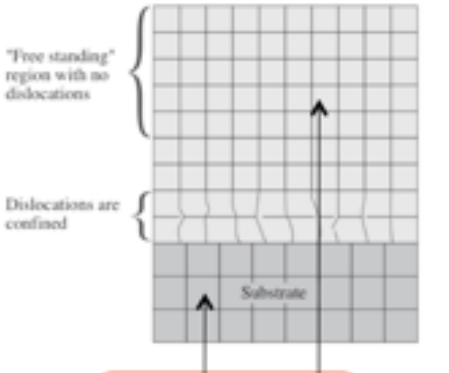

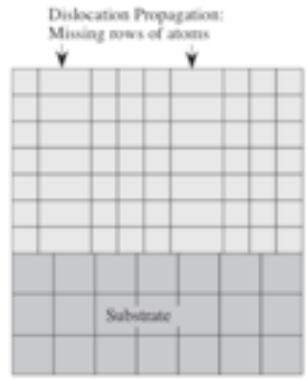

$$\epsilon = \frac{a_S - a_L}{a_L}$$

$$d_c \cong \frac{a_S}{2|\epsilon|}$$

Critical thickness for coherent strained growth

Example: AlN on GaN, d_c~7 nm

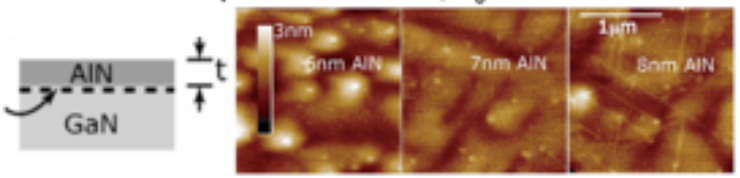

FIG. 1. (Color online) AFM images showing $2\times2\ \mu m^2$ scans of the AlN surfaces after growth.

APPLIED PHYSICS LETTERS **90**, 182112 (2007)

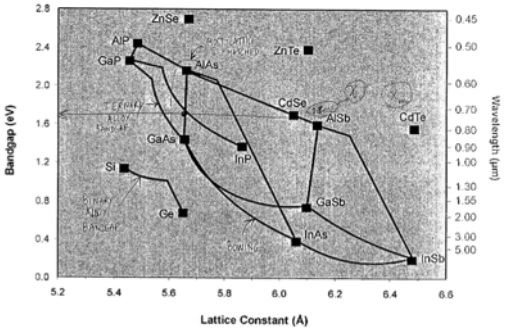

Compound semiconductors: Heterostructures

Semiconductor Heterostructures

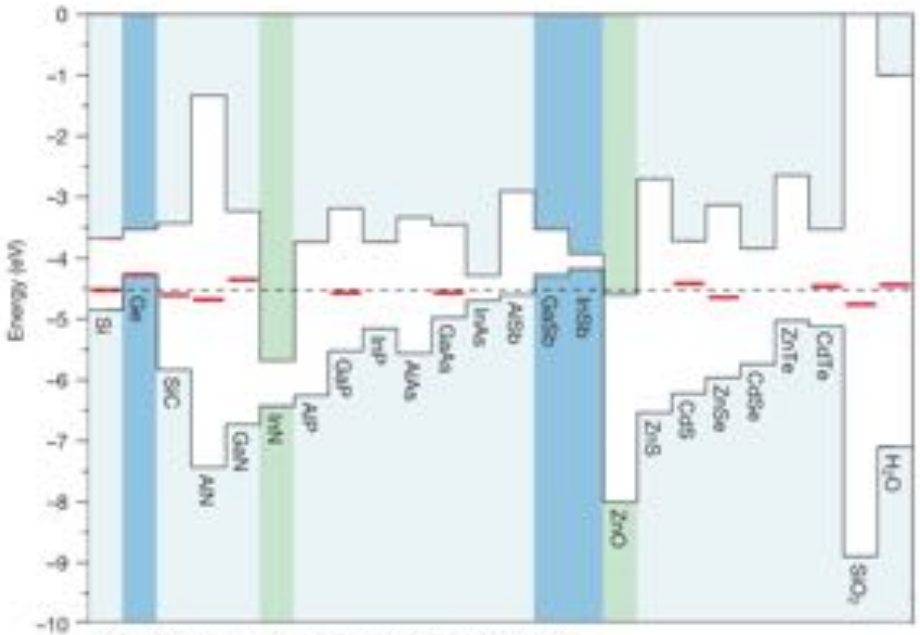

Nature, vol 423, p 626 (2003)

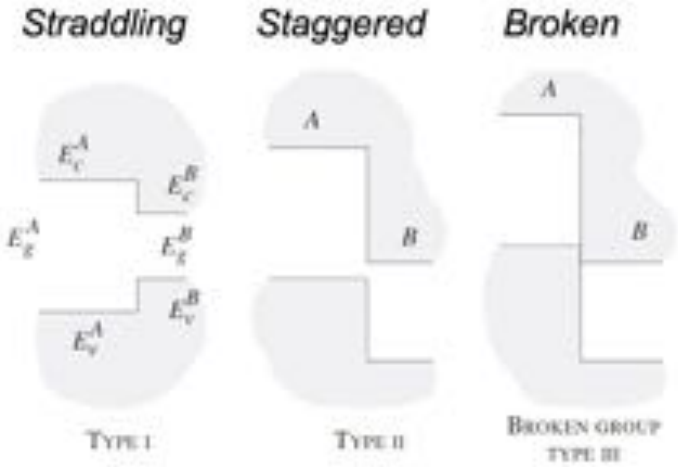

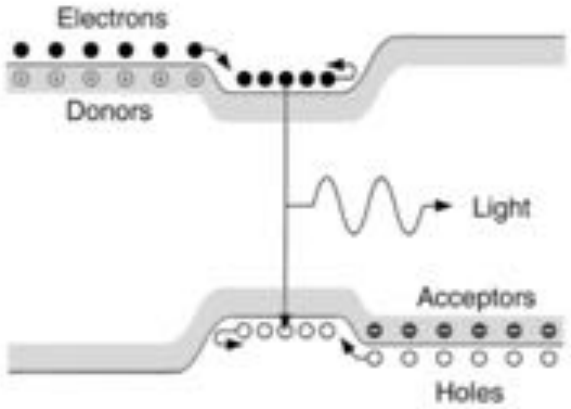

Semiconductor bands line up with each other in 3 ways.

Based on the lineups, one can create

- *Barriers*
- *Wells*
- *Quasi-Electric fields*

For both electrons and holes independently with suitable material choices.

Example –
Double Heterostructure LED/Laser

Compound semiconductor heterostructure band offsets

Straddling Gap

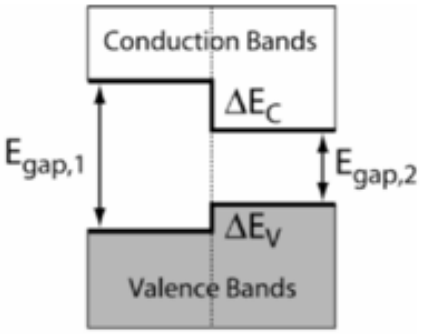

Offset Gap

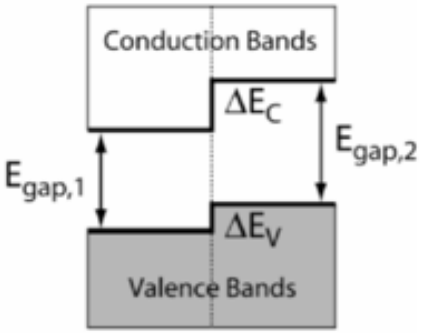

Broken Gap

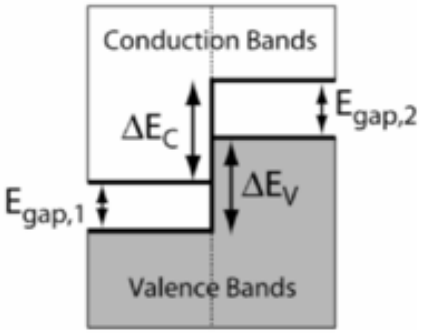

$$\Delta E_V(A:B)+\Delta E_V(B:C)+\Delta E_V(C:A)=0$$

Transitivity of band offsets

The Common Anion Rule: When the anion (the electron accepting atom such as As in GaAs and InAs) is in common across a semiconductor heterojunction, the change in the conduction band edge is greater than the change in the valence band edge across the semiconductor heterojunction. Mathematically, $\Delta E_V < \Delta E_C$.

The Common Cation Rule: When the cation (e.g. Ga in GaAs or GaSb) is in common across the junction, the valence band edge energies scale with the anion electronegativities. For example, the valence band edge of phosphide semiconductors will lie below those for arsenides which will lie below those of antimonides. Mathematically, $E_V(CA_1) < E_V(CA_2) < E_V(CA_3)$, where C designates a cation, and A_1, A_2, and A_3 designate three anions with decreasing electronegativities.

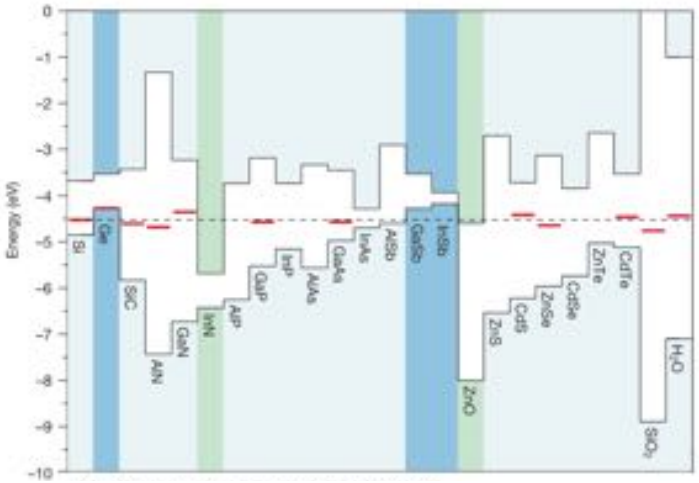

(Rockett)

Quasi electric fields in semiconductor heterostructures

Semiconductor Heterostructures & Quasi-Electric Fields

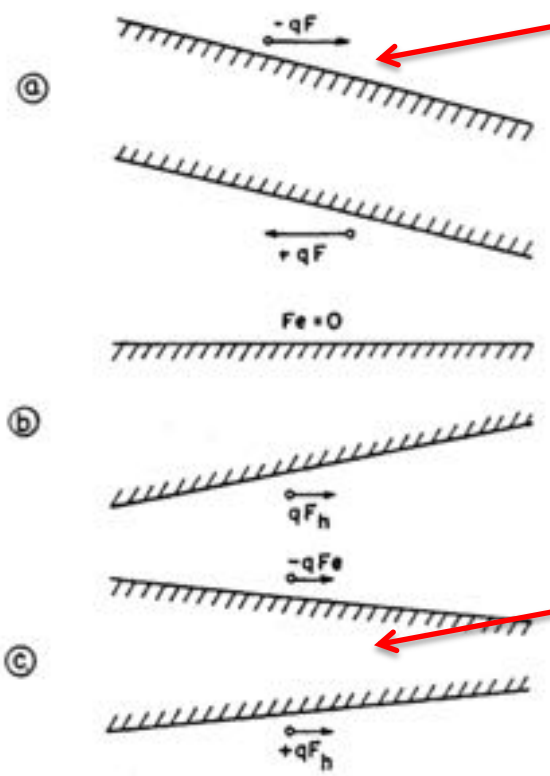

Equal force on electrons and holes

> . . . a drift field may also be generated through a variation of the energy gap itself, by making the base region from a nonstoichiometric mixed crystal of different semiconductors with different energy gaps (for example, Ge-Si), with a composition that varies continuously through the base. (Translated from Krömer, 1954)

Forces different for electrons and holes

Rev. Mod. Phy., vol 73, p 783 (2001)

FIG. 1. Quasielectric fields: (a) A true electric field simply tilts the bands; (b) quasielectric fields, with no force on electrons, but a force on holes; (c) quasielectric fields forcing electrons and holes in the same direction. From Kroemer, 1957a.

The Nobel Prize in Physics 2000

"for basic work on information and communication technology"

"for developing semiconductor heterostructures used in high-speed- and opto-electronics"

"for his part in the invention of the integrated circuit"

Zhores I. Alferov
1/4 of the prize
Russia
A.F. Ioffe Physico-Technical Institute
St. Petersburg, Russia
b. 1930

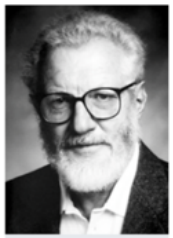

Herbert Kroemer
1/4 of the prize
Federal Republic of Germany
University of California
Santa Barbara, CA, USA
b. 1928

Jack S. Kilby
1/2 of the prize
USA
Texas Instruments
Dallas, TX, USA
b. 1923
d. 2005

GaN based Visible LEDs and Lasers

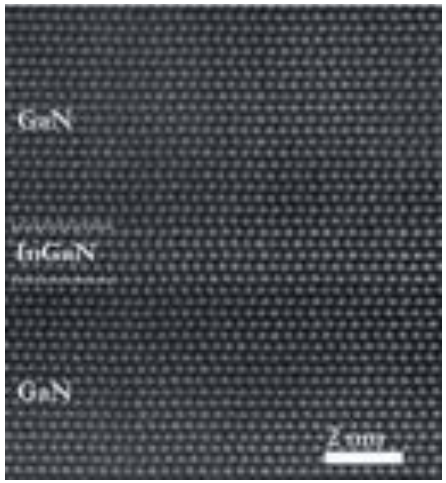

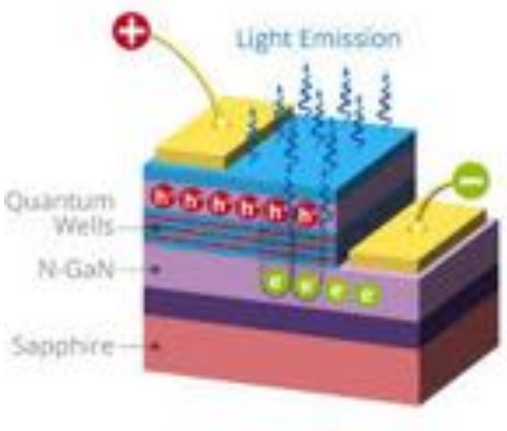

The Nobel Prize in Physics 2014
Isamu Akasaki, Hiroshi Amano, Shuji Nakamura

Share this: 2.5K

The Nobel Prize in Physics 2014

Photo: A. Mahmoud
Isamu Akasaki
Prize share: 1/3

Photo: A. Mahmoud
Hiroshi Amano
Prize share: 1/3

Photo: A. Mahmoud
Shuji Nakamura
Prize share: 1/3

The Nobel Prize in Physics 2014 was awarded jointly to Isamu Akasaki, Hiroshi Amano and Shuji Nakamura *"for the invention of efficient blue light-emitting diodes which has enabled bright and energy-saving white light sources"*.

- Science of light

How to make a Semiconductor Light Emitter

REVIEWS OF MODERN PHYSICS, VOLUME 87, OCTOBER–DECEMBER 2015

Nobel Lecture: Background story of the invention of efficient blue InGaN light emitting diodes*

Shuji Nakamura

University of California, Santa Barbara, California, USA

(published 5 October 2015)

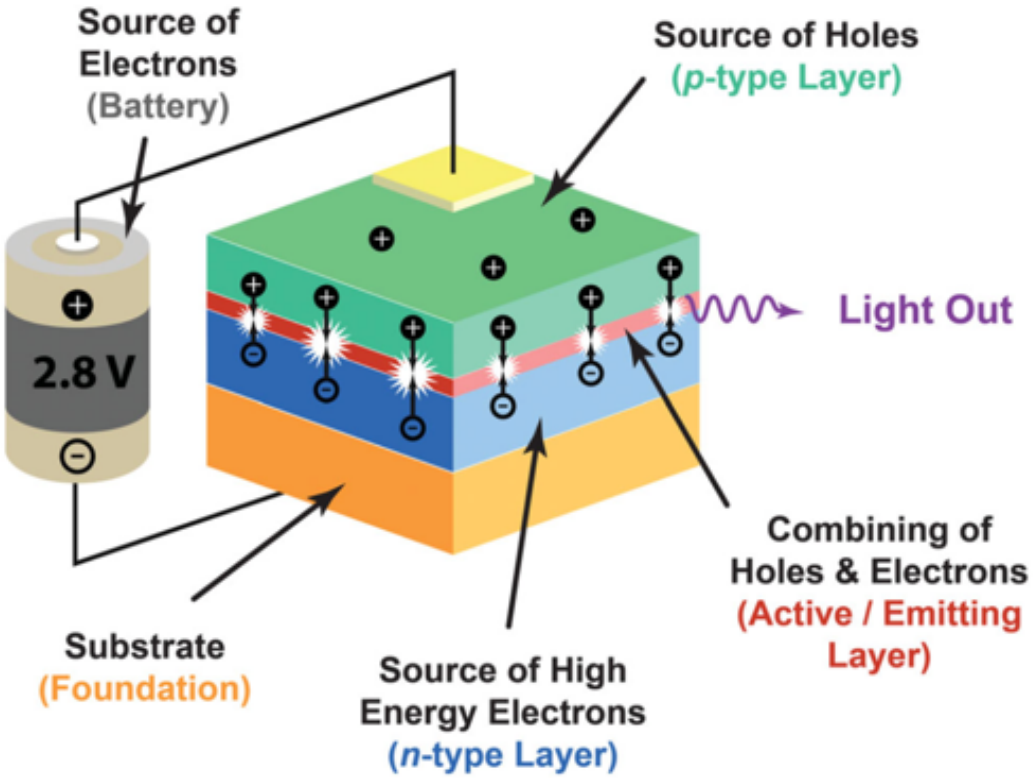

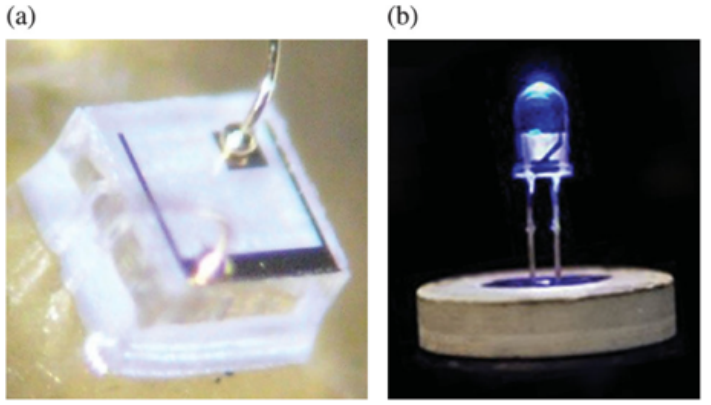

FIG. 2 (color). (a) Image of a blue GaN LED with attached gold wire contacts (size of diode 0.4×0.4 mm^2) and (b) the same LED packaged as a commercial product. From Nakamura, Mukai, and Senoh, 1994.

How to make white light with semiconductors

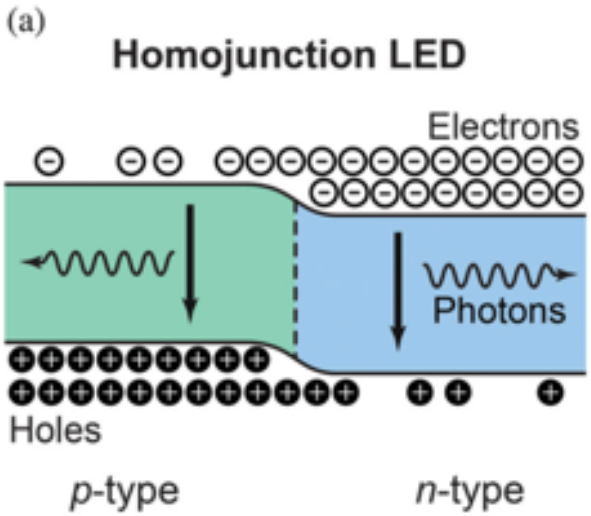

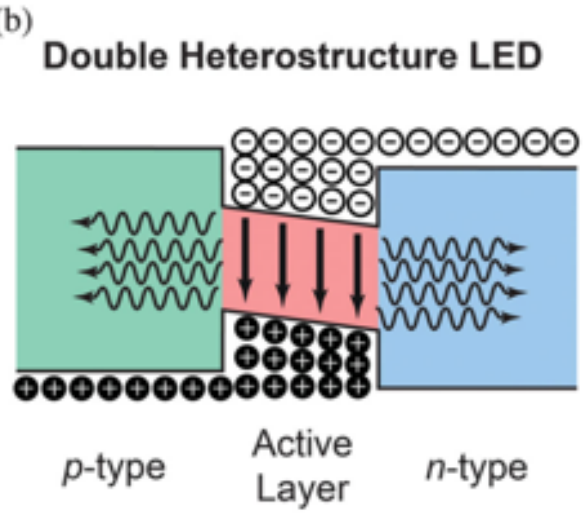

$$\text{IQE} = \frac{\text{Light generated}}{\text{Electrons injected}} = \frac{R_{\text{radiative}}}{R_{\text{radiative}} + R_{\text{nonradiative}}} = \frac{Bn^2}{An + Bn^2 + Cn^3}.$$

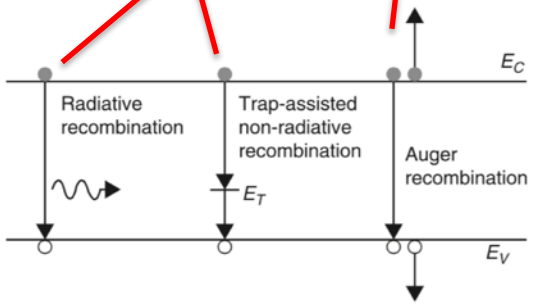

LED Blue + **Phosphor** Blue → Yellow = **White Light** Blue + Yellow & **White LED**

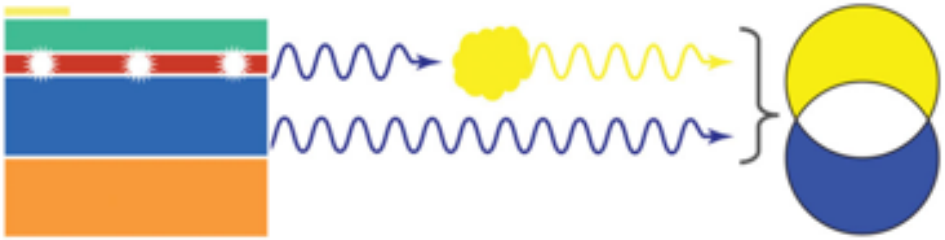

Solid state lighting: The lighting of the future

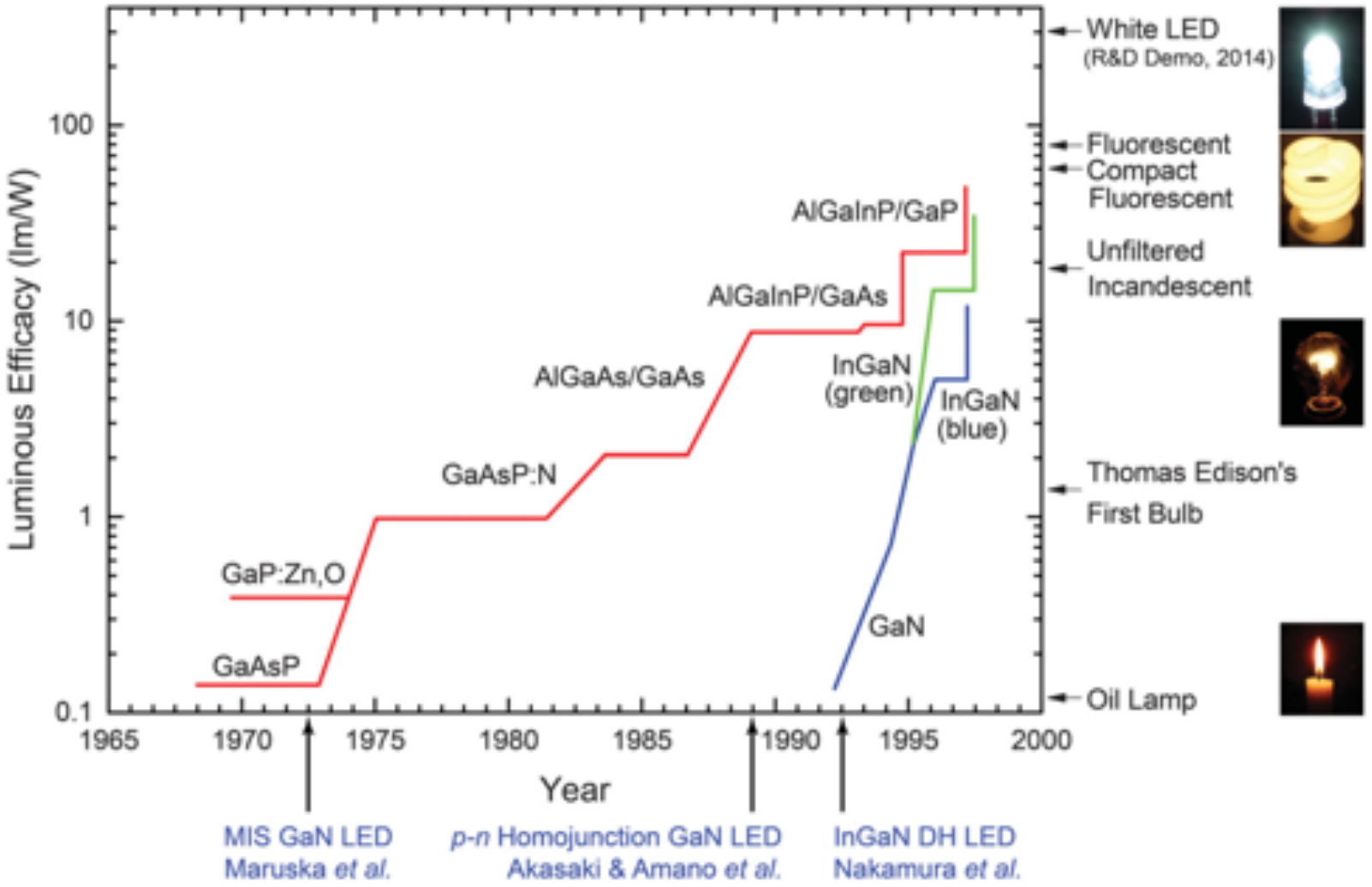

Effect of Defects and Quantum Wells on Efficiency

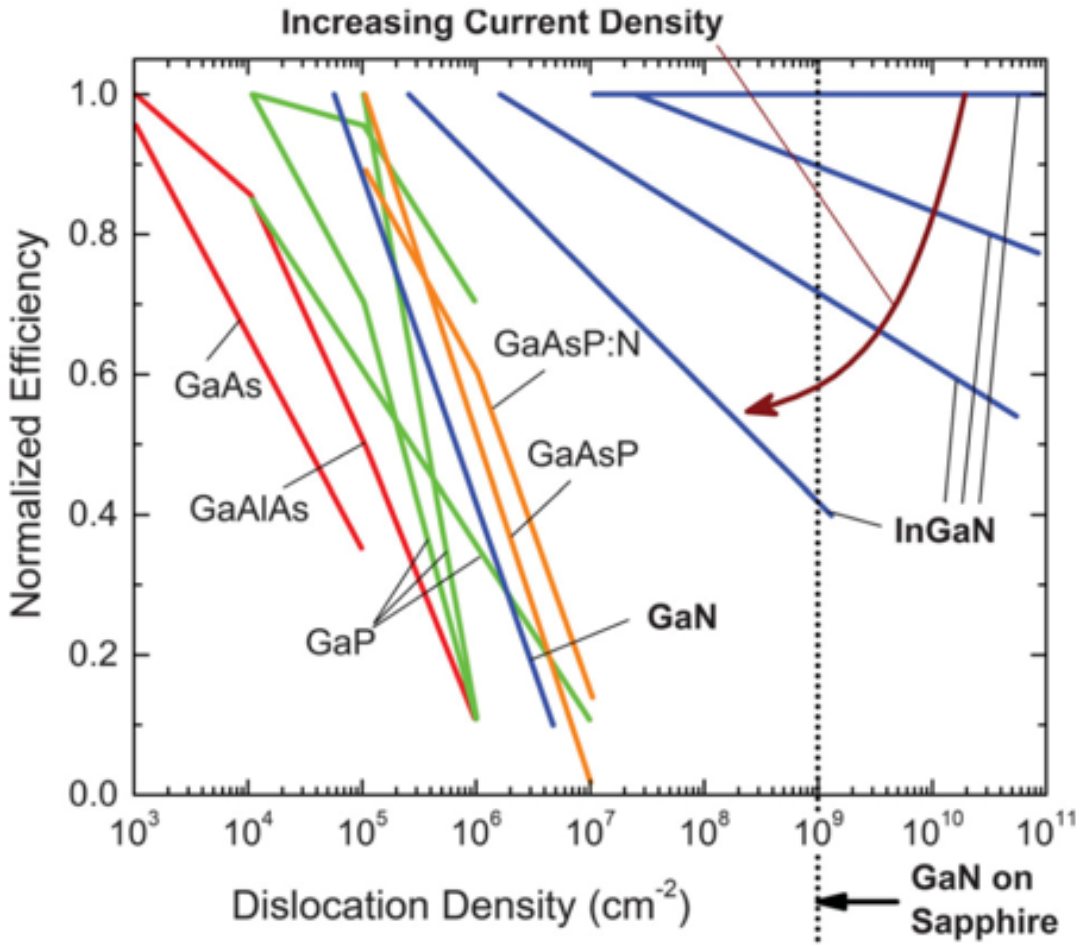

FIG. 13 (color). Dependence of LED efficiency on dislocation density for various semiconductor materials. From Lester *et al.*, 1995, Chichibu *et al.*, 1996, and Nakamura, 1998.

Lasers outperform LEDs in efficiency!

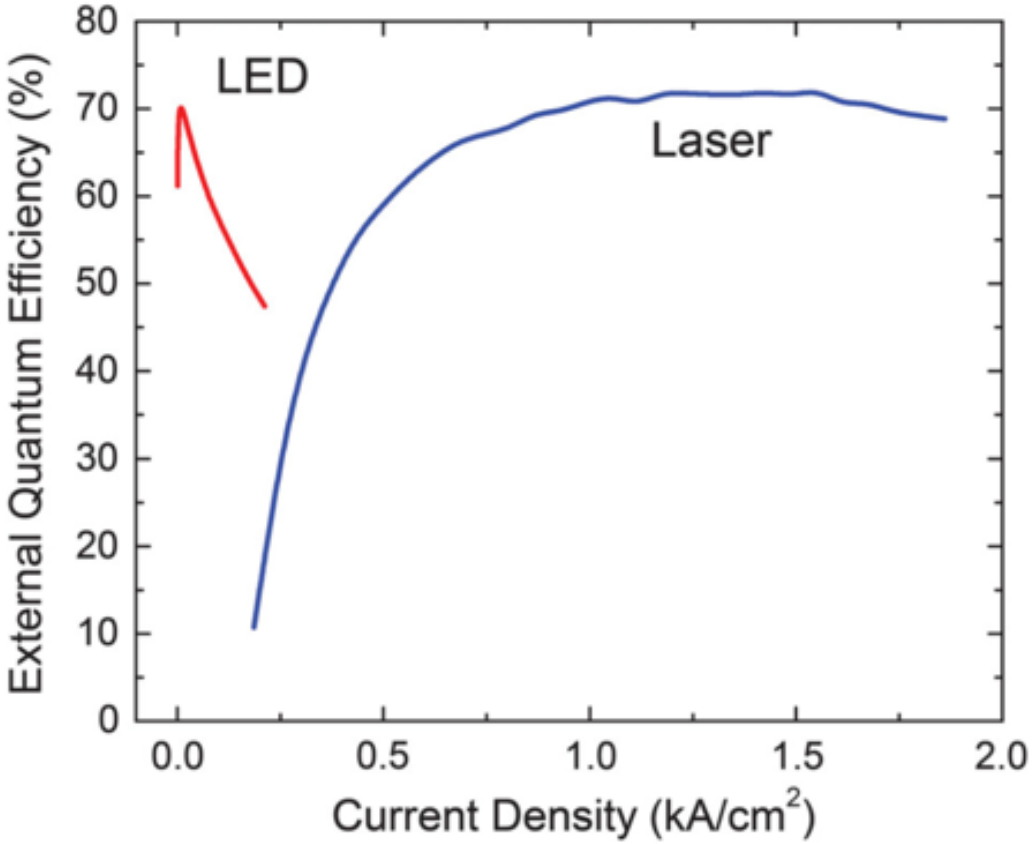

FIG. 17 (color). Comparison of external quantum efficiency (EQE) of a commercial LED and laser with increasing current density. From Pourhashemi *et al.*, 2013.

Lasers outperform LEDs in efficiency!

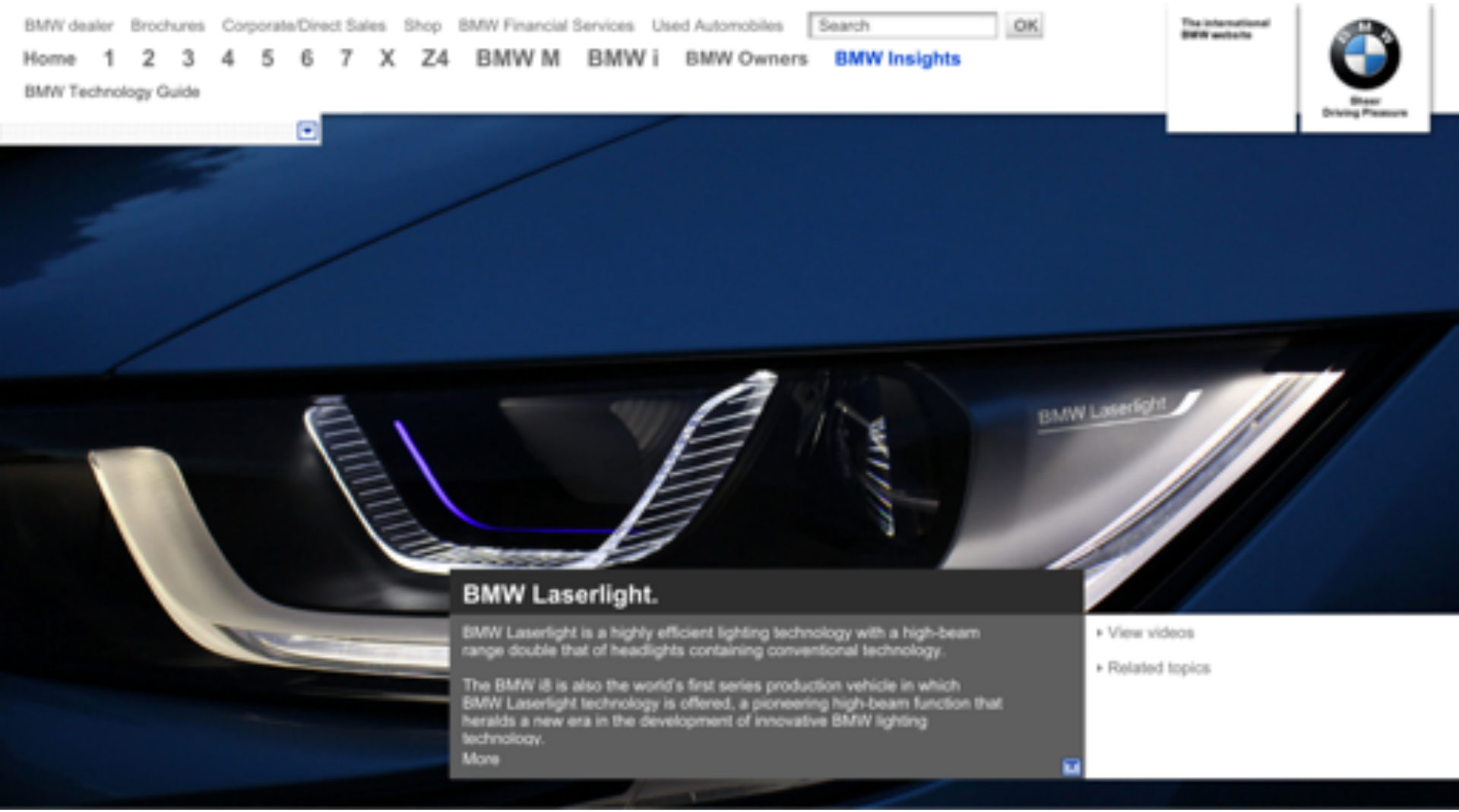

Compound semiconductors: Heterostructures

Nobel Lecture: Quasielectric fields and band offsets: teaching electrons new tricks*

Herbert Kroemer

Electrical and Computer Engineering Department, University of California, Santa Barbara, California 93106-9560

(Published 22 October 2001)

I. INTRODUCTION

Heterostructures, as I use the word here, may be defined as heterogeneous semiconductor structures built from two or more different semiconductors, in such a way that the transition region or interface between the different materials plays an essential role in any device action. Often, it may be said that the interface is the device.

The participating semiconductors all involve elements from the central portion of the periodic table of the elements (Table I). In the center is silicon, the backbone of modern electronics. Below Si is germanium. Although Ge is rarely used by itself, Ge-Si alloys with a composition-dependent position play an increasingly important role in today's heterostructure technology. In fact, historically this was the first heterostructure device system proposed, although it was also the system that took longest to bring to practical maturity, largely because of the 4% mismatch between the lattice constants of Si and Ge.

Silicon plays the same central role in electronic metallurgy that steel plays in structural metallurgy. But just

Similar to the III-V compounds, every element shown in column II may be used together with every element in column VI to create II-VI compounds, and again alloying is possible to create a continuous range of the latter.

II. BAND DIAGRAMS AND QUASIELECTRIC FORCES

Whenever I teach my semiconductor device physics course, one of the central messages I try to get across early is the importance of energy-band diagrams. I often put this in the form of "Kroemer's Lemma of Proven Ignorance":

> If, in discussing a semiconductor problem, you cannot draw an *Energy-Band-Diagram*, this shows that you don't know what you are talking about,

with the corollary

> If you can draw one, but don't, then your audience won't know what you are talking about.

Nowhere is this more true than in the discussion of heterostructures, and much of the understanding of the latter is based on one's ability to draw their band diagrams—and knowing what they mean.

- Rev. Mod. Phys., vol 73, pg. 783 (2001)

Effective Mass Approximation

• Effective Mass Approximation MAPS the complicated problem of
•Electrons in a complicated crystal + heterostructure potential … to …
the simplest of all quantum mech problems: The particle in a box

PHYSICAL REVIEW VOLUME 97, NUMBER 4 FEBRUARY 15, 1955

Motion of Electrons and Holes in Perturbed Periodic Fields

J. M. Luttinger* and W. Kohn†
Bell Telephone Laboratories, Murray Hill, New Jersey
(Received October 13, 1954)

A new method of developing an "effective-mass" equation for electrons moving in a perturbed periodic structure is discussed. This method is particularly adapted to such problems as arise in connection with impurity states and cyclotron resonance in semiconductors such as Si and Ge. The resulting theory generalizes the usual effective-mass treatment to the case where a band minimum is not at the center of the Brillouin zone, and also to the case where the band is degenerate. The latter is particularly striking, the usual Wannier equation being replaced by a set of coupled differential equations.

The Nobel Prize in Chemistry 1998

Walter Kohn

1/2 of the prize

USA

University of California
Santa Barbara, CA, USA

Joaquin M. Luttinger

• Developed by Luttinger & Kohn and refined since then…
• Real power of the EMA is exercised in understanding the electronic properties of Quantum Heterostructures.

Effective Mass Approximation

• Effective Mass Approximation MAPS the complicated problem of Electrons in a complicated crystal + heterostructure potential … to … the simplest of all quantum mech problems: The particle in a box

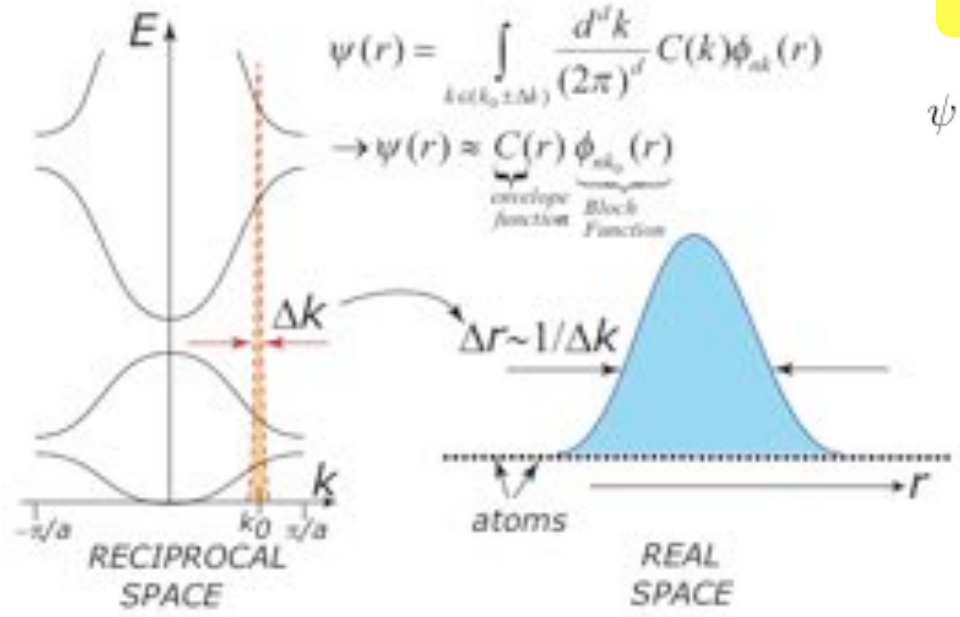

Wave packet

$$\psi(x) = \sum_n \sum_k C(k)\phi_{nk}(x) = \sum_n \int \frac{dk}{2\pi} C(k)\phi_{nk}(x)$$

Over small number of k-states

$$\psi(x) \approx \phi_{n0}(x) \int \frac{dk}{2\pi} C(k)e^{ikx} = \underbrace{\phi_{n0}}_{Bloch} \cdot \underbrace{C(x)}_{envelope}$$

Effective Mass Approximation

$$\psi(x) \approx \phi_{n0}(x) \int \frac{dk}{2\pi} C(k) e^{ikx} = \underbrace{\phi_{n0}}_{Bloch} \cdot \underbrace{C(x)}_{envelope}$$

$$H_0\psi(x) = \int \frac{dk}{2\pi} C(k) E_n(k) \phi_{nk}(x) \approx \phi_{n0}(x) \int \frac{dk}{2\pi} C(k) E_n(k) e^{ikx}$$

$$E_n(k) = \sum a_m k^m$$ Energy "operator"

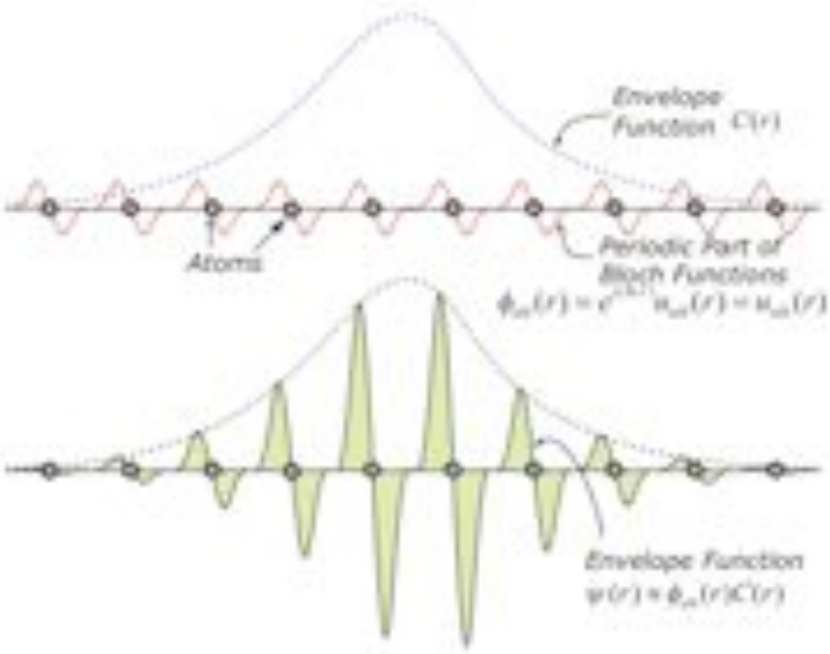

$$H\psi(x) \approx \phi_{n0}(x) \sum_m \int \frac{dk}{2\pi} C(k) k^m e^{ikx}$$

$$\int \frac{dk}{2\pi} k^m C(k) e^{ikx} \leftrightarrow (-i\frac{d}{dx})^m C(x)$$

$$H\psi(x) \approx \phi_{n0}(x) E_n(-i\nabla) C(x)$$

$$[E_n(-i\nabla) + V(r)]C(r) = EC(r)$$

Density of States

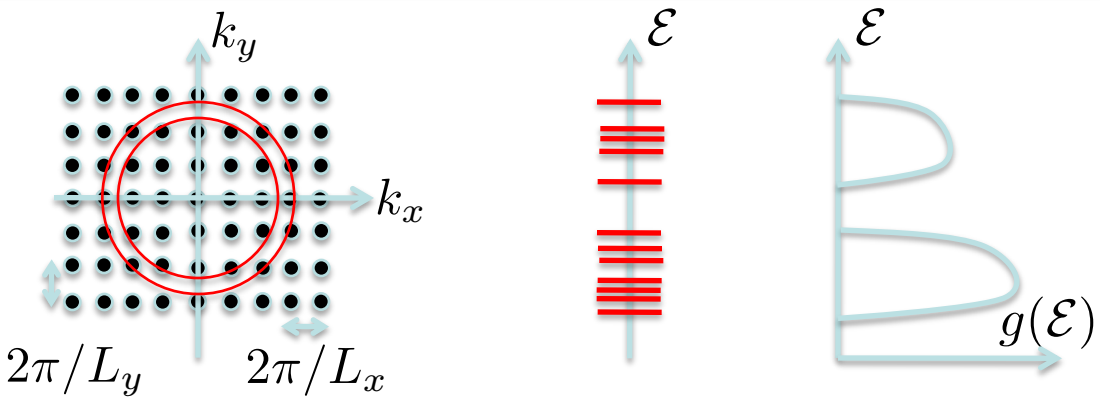

DOS: $\boxed{g(\mathcal{E}) = g_s \cdot \sum_{\mathbf{k}} \delta[\mathcal{E} - \mathcal{E}(\mathbf{k})]}$

Valid for electrons, photons, phonons...

Important result: $\boxed{\sum_{\mathbf{k}}(...) \rightarrow \int \frac{d^d\mathbf{k}}{(2\pi)^d}(...)}$

If we know the energy dispersion $\mathcal{E}(\mathbf{k})$, we can find the DOS using this prescription.

Free Electron: $\mathcal{E}(\mathbf{k}) = \frac{\hbar^2|\mathbf{k}|^2}{2\mathbf{m_0}}$

Free electron in 3D: $g(\mathcal{E}) = g_s \cdot \frac{1}{(2\pi)^2}\left(\frac{2m_0}{\hbar^2}\right)^{\frac{3}{2}}\sqrt{\mathcal{E}}$

Effective Mass Approximation

Application: Bulk Semiconductors

- 3D (Bulk)

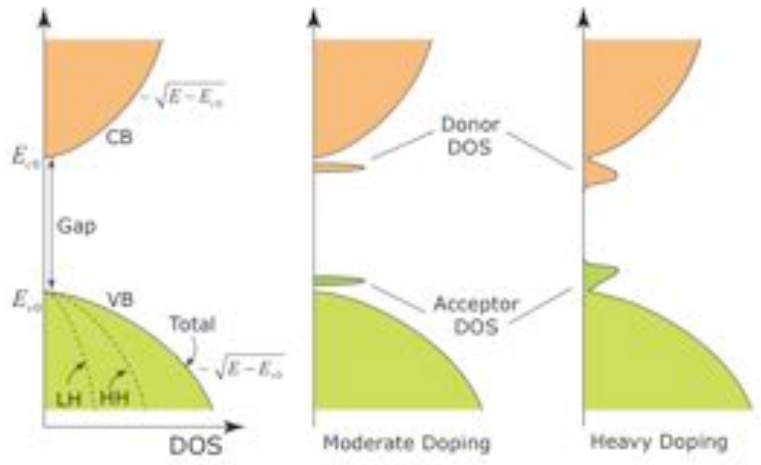

$$[-\frac{\hbar^2}{2m^\star}\nabla^2 + V_{imp}(r)]C(r) = [E - E_c(r)]C(r)$$

$$C(r) = \frac{1}{\sqrt{V}}e^{i\vec{k}\cdot\vec{r}}$$

$$E(k) = E_{c0}(r) + \frac{\hbar^2 k^2}{2m^\star} = E_{c0}(r) + \frac{\hbar^2}{2}(\frac{k_x^2}{m_{xx}^\star} + \frac{k_y^2}{m_{yy}^\star} + \frac{k_z^2}{m_{zz}^\star})$$

$$g_{3D}(E) = \frac{1}{2\pi^2}(\frac{2m^\star}{\hbar^2})^{3/2}\sqrt{E - E_{c0}}$$

$$n = \int_0^\infty dE f_{FD}(E) g_{3D}(E) = N_C^{3D} F_{1/2}(\frac{E_C - E_F}{k_B T}) \approx N_C^{3D} e^{-\frac{E_C - E_E}{k_B T}}$$

Effective Mass Approximation

$$E_n(k) \approx E_c(r) + \frac{\hbar^2 k^2}{2m^\star} \rightarrow E_n(-i\nabla) \approx E_c(r) - \frac{\hbar^2}{2m^\star}\nabla^2$$

$$[-\frac{\hbar^2}{2m^\star}\nabla^2 + V_{imp}(r)]C(r) = [E - E_c(r)]C(r)$$

Central Result of Effective Mass Approximation

"Particle-in-a-box" problem with:
Real mass -> Effective mass,
Real wavefunction -> Envelope function
Crystal potential -> Band-edge potential + Impurity potentials, etc

Example: Shallow donor states

$$E_n = -\frac{m_e q^4}{2(4\pi\epsilon_0)^2\hbar^2}\frac{1}{n^2}$$

$$[-\frac{\hbar^2}{2m^\star}\nabla^2 - \frac{e^2}{4\pi\epsilon r}]C(r) = (E - E_c)C(r)$$

$$E - E_c = E_\infty \frac{m^\star}{\epsilon_r^2}$$

$$a_B^\star = a_B \frac{\epsilon_r}{m^\star}$$

$$C(r) \sim e^{-r/r_0}$$

Carrier Statistics (Electrons/Holes)

ENERGY distribution of electrons : (3)

Determined by the FERMI-DIRAC DISTRIBUTION FN.

$$f(\varepsilon) = \frac{1}{1 + \exp\left(\frac{\varepsilon - E_F}{kT}\right)}$$

E_F: FERMI ENERGY

ELECTRON density in the conduction band:

$$n = \int_{E_c}^{\infty} dE \; g_c(\varepsilon) \, f(\varepsilon)$$

$$n = N_c \, F_{1/2}(\eta)$$

EFFECTIVE DOS $N_c = 2\left(\frac{m^* kT}{2\pi\hbar^2}\right)^{3/2}$

FERMI-DIRAC INTEGRAL $F_j(\eta) = \frac{1}{\Gamma(j+1)} \int_0^{\infty} dx \frac{x^j}{1 + e^{x-\eta}}$ order j

$$F_{1/2}(\eta) = \frac{2}{\sqrt{\pi}} \int_0^{\infty} dx \frac{x^{1/2}}{1 + e^{x-\eta}}$$

$$\eta = \frac{E_F - E_c}{kT}$$

For Non-Degenerate semiconductors, $\eta \ll -1$ ⇒ BOLTZMANN APPROX.

$\Rightarrow F_{1/2}(\eta) \approx e^{\eta}$ ($\uparrow$ true for any order $F_j(\eta) \approx e^{\eta}$) $\Rightarrow$

$$n \approx N_c \exp\left(\frac{E_F - E_c}{kT}\right)$$

USED VERY OFTEN!

Semiconductor carrier statistics

Carrier Statistics (Electrons/Holes)

$$p = N_v \exp\left(\frac{E_v - E_F}{kT}\right)$$

$$\Rightarrow \quad np = n_i^2 = \left(\underbrace{\sqrt{N_c N_v}\exp\left(-\frac{E_g}{2kT}\right)}_{n_i}\right)^2$$

SEMICONDUCTOR

n_i ↑ Intrinsic Carrier Concentration.

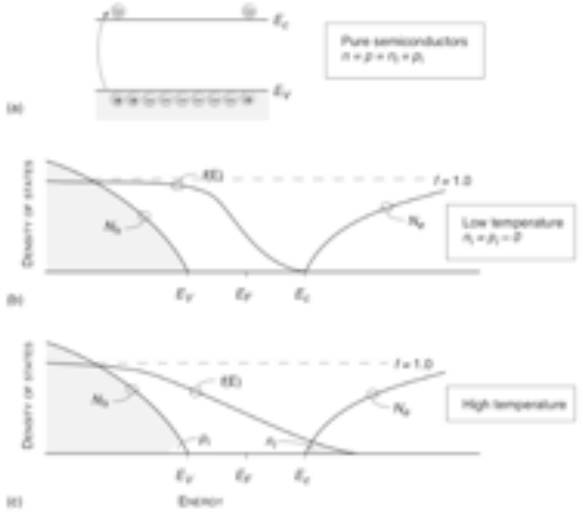

Where is the Fermi Level E_F? → BASIC UNDERLYING PRINCIPLE: CHARGE NEUTRALITY

WILL DETERMINE THE FERMI LEVEL E_F! - MORE LATER.

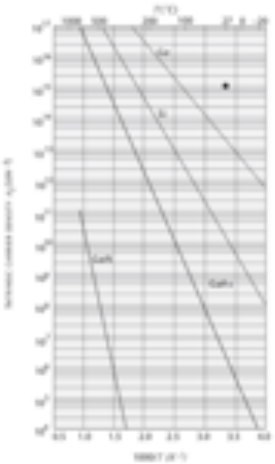

Intrinsic Semiconductor:

$$n = p = n_i = \sqrt{N_c N_v}\exp\left(-\frac{E_g}{2RT}\right)$$

$$E_F = E_i = \frac{E_c + E_v}{2} + \frac{kT}{2}\ln\left(\frac{N_v}{N_c}\right)$$

↑ 'Intrinsic' Fermi-Level.

Semiconductor carrier statistics

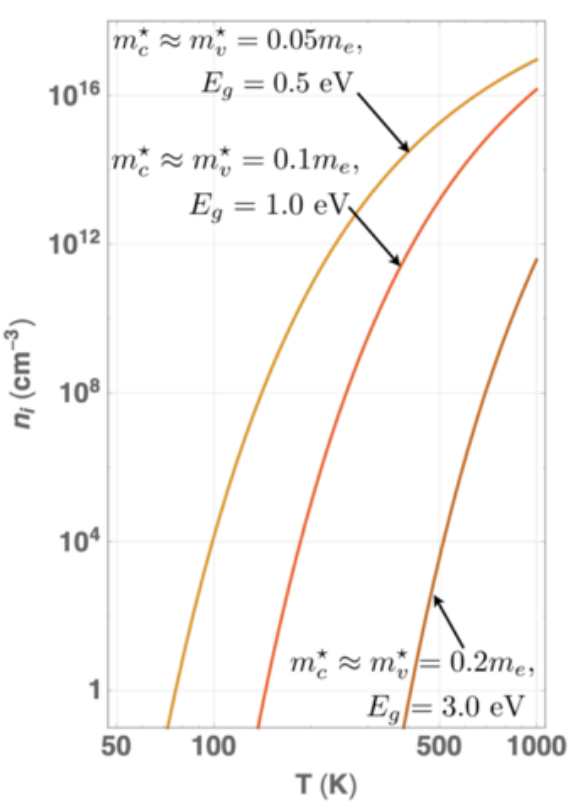

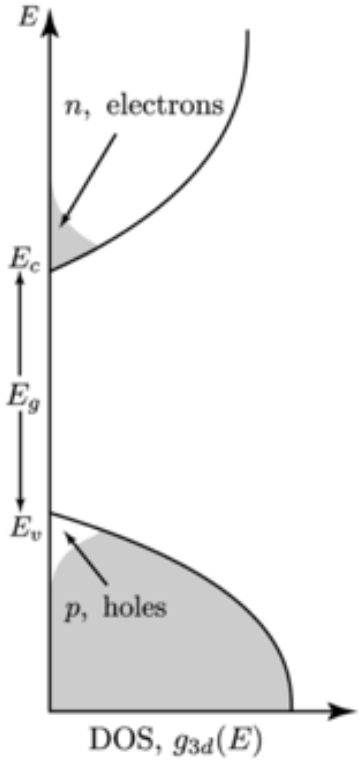

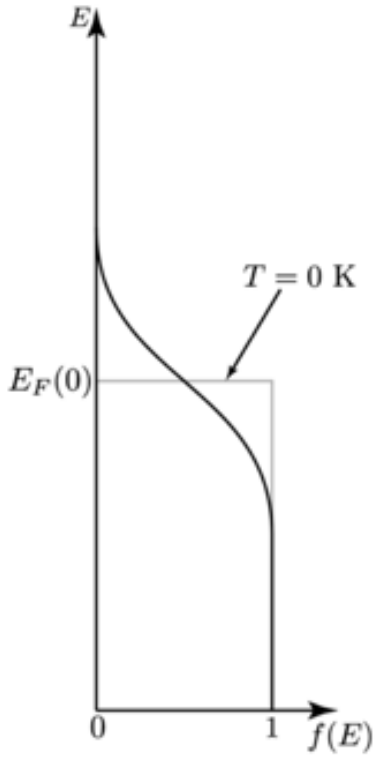

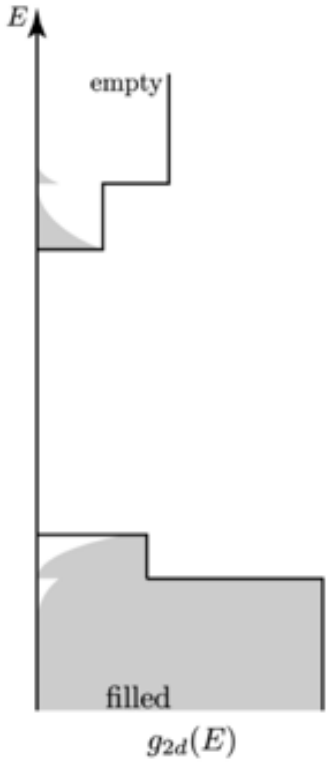

Semiconductor carrier statistics

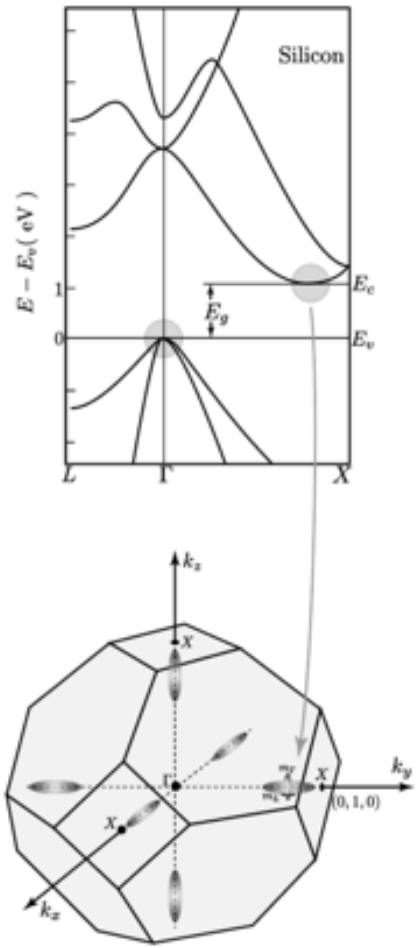

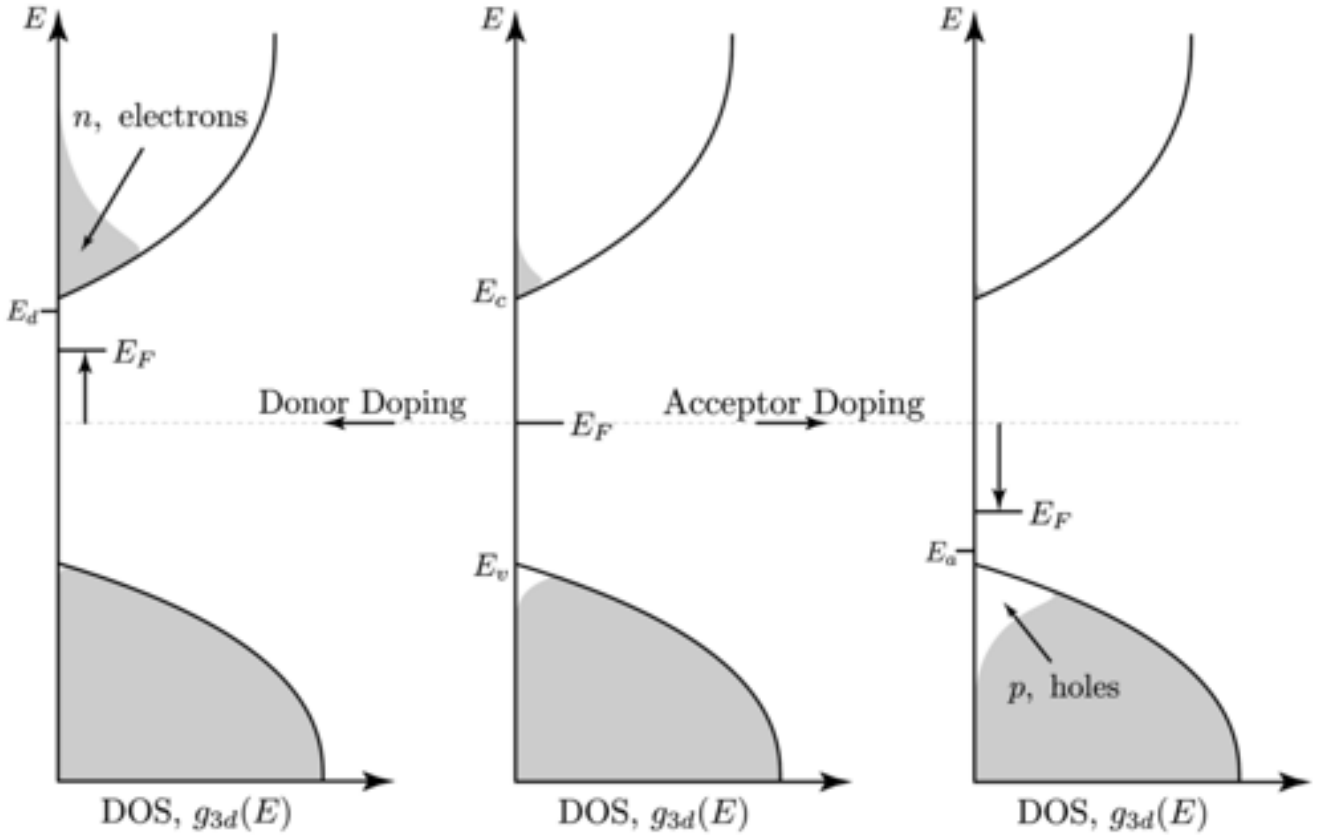

Fig. 14.3 Conduction band minima of Silicon showing the $g_v = 6$ valleys along the six $\Gamma - X$ directions, and the origin of the DOS effective mass $(m_L m_T^2)^{\frac{1}{3}}$.

$$E_F = \frac{1}{2}(E_c + E_v) + k_b T \ln\left(\frac{n}{N_c} \cdot \frac{N_v}{p}\right)$$

Semiconductor carrier statistics

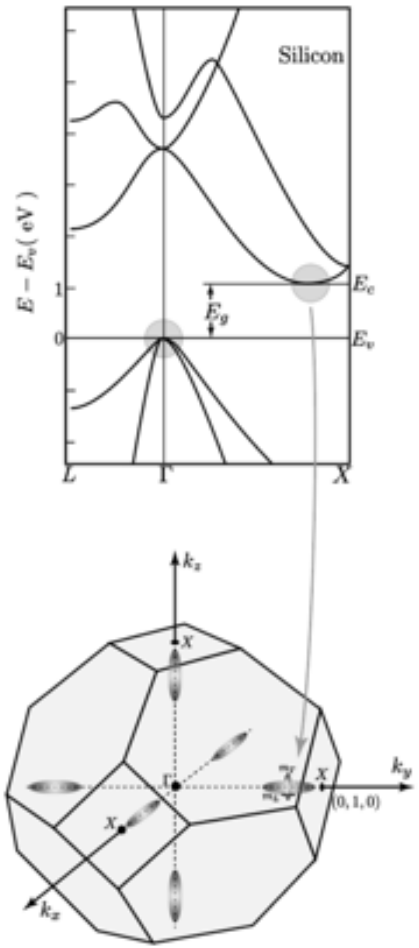

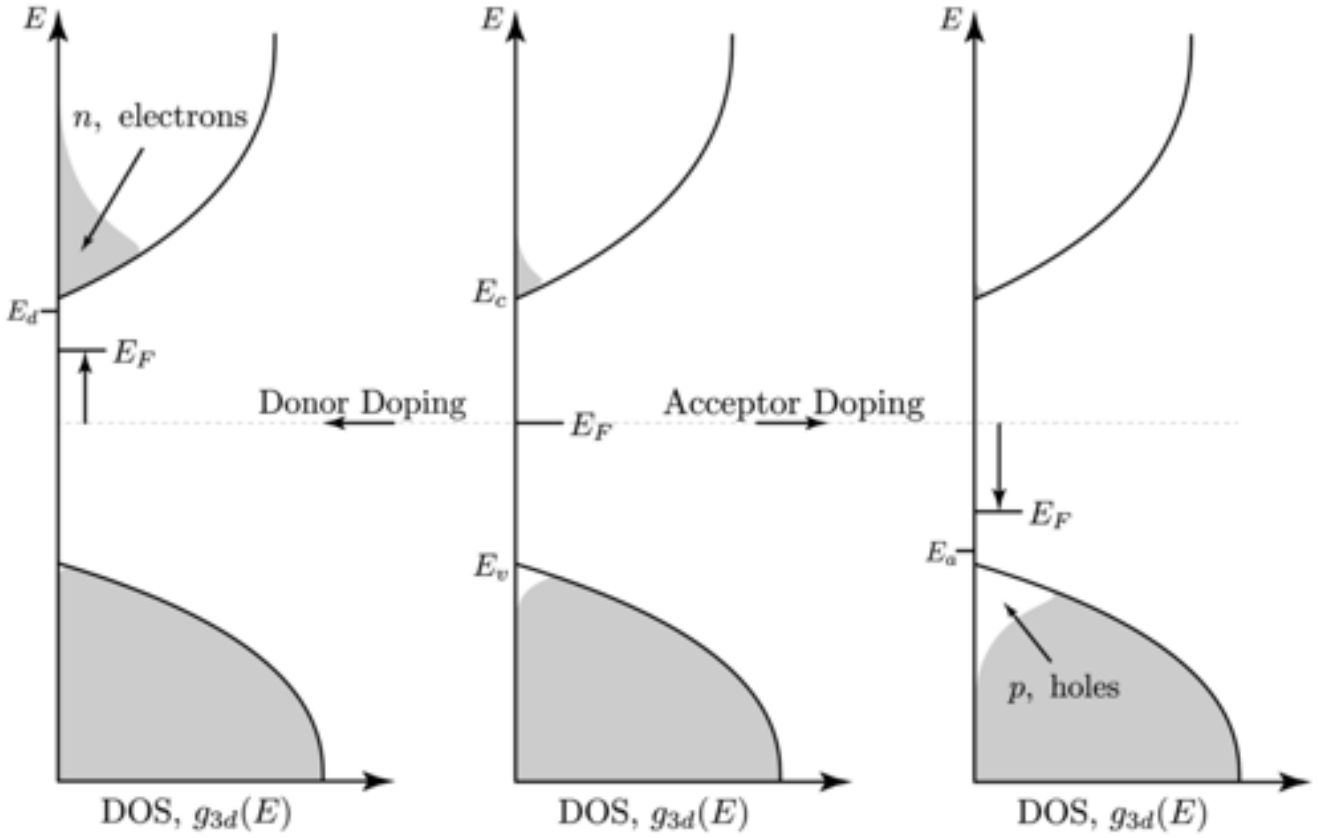

Fig. 14.3 Conduction band minima of Silicon showing the $g_v = 6$ valleys along the six $\Gamma - X$ directions, and the origin of the DOS effective mass $(m_L m_T^2)^{\frac{1}{3}}$.

$$E_F = \frac{1}{2}(E_c + E_v) + k_b T \ln\left(\frac{n}{N_c} \cdot \frac{N_v}{p}\right)$$

Semiconductor doping

SEMICONDUCTOR
↓
INTRINSIC – PURE
↓
EXTRINSIC – DOPED – p-type
n-type
↓
COMPENSATED – DOPED – p + n type.

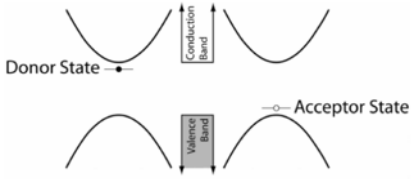

DOPANT: ATOM that replaces an atom of the intrinsic semiconductor

- DONOR: ATOM with an EXTRA electron than the atom it replaces; the extra electron can be 'DONATED' to the cond. band.
- ACCEPTOR: ATOM with one less electron than the atom it replaces; it can accept one electron from the Valence band (same as forming a hole in VB).

$N_D^+ = N_D\left[1 - \frac{1}{1 + \frac{1}{g_e}\exp\left(\frac{E_d - E_F}{kT}\right)}\right]$

$N_D^- = \frac{N_D}{1 + g_e \exp\left(\frac{E_d - E_F}{kT}\right)}$

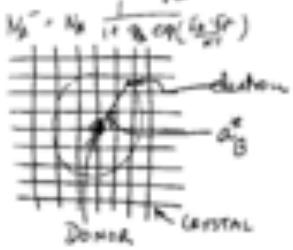

'Shallow' donor ionization energy

$E_c - E_d \approx \frac{m_e^*}{\epsilon_r^2} R_H < kT$ to be shallow

13.6 eV, Hydrogen atom ionization energy.

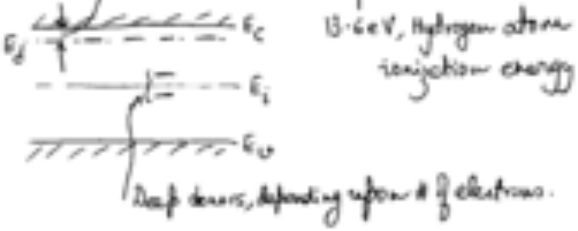

'Effective Bohr radius'

$a_B^* \approx \frac{\epsilon_r}{m_e^*} a_B^0$

0.53 Å, H-atom Bohr radius

Typically: $a_B^* >> a_B^0$.

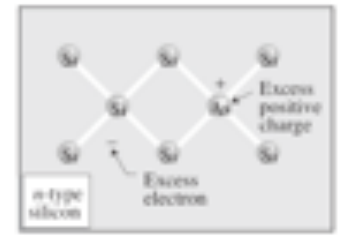

Arsenic (As) atom donates one electron to the conduction band to produce an n-type silicon

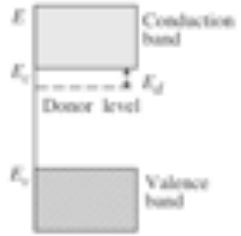

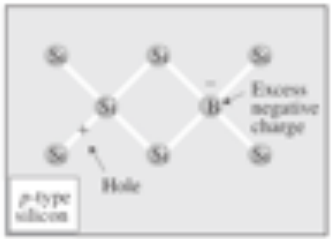

One electron taken from the valence band to complete the bonding of the boron atom → hole

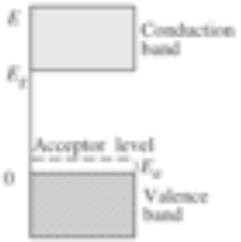

EXAMPLE: n-doped semiconductor:

$n = p + N_d^+$, $np = n_i^2$

Shallow donor $\Rightarrow N_D^+ \simeq N_D \Rightarrow$ $n \approx \frac{\sqrt{(N_d)^2 + 4n_i^2} + N_d}{2}$

If $N_d >> n_i$, $n \simeq N_D$ ⇒ as many electrons in CB as # of donors!

Semiconductor carrier statistics

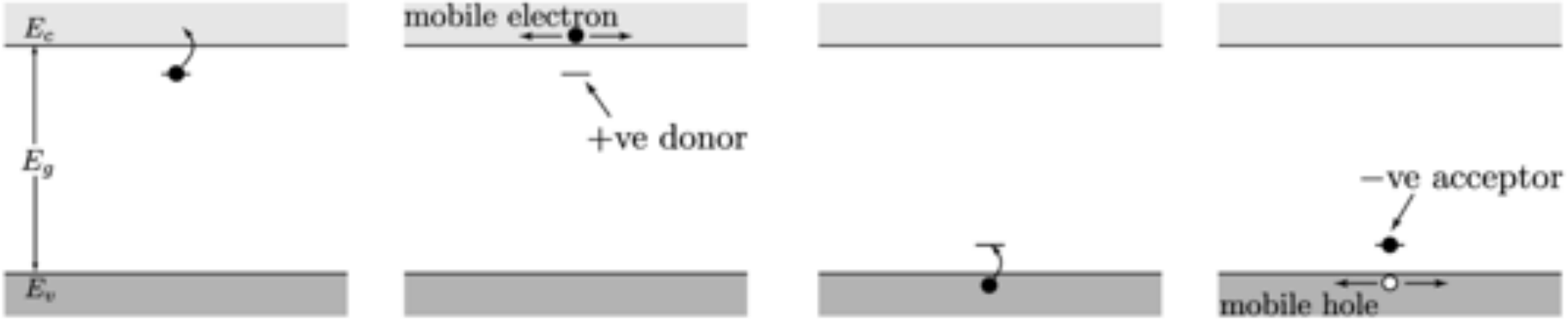

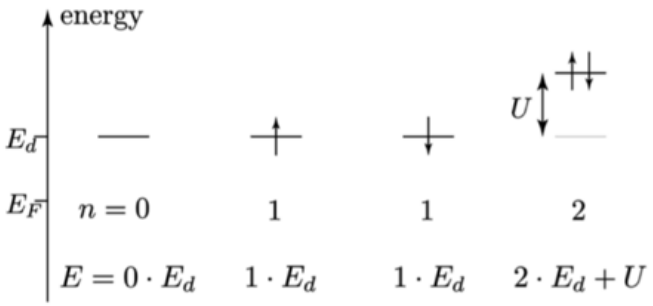

$$\frac{N_D^+}{N_D} = \frac{1}{1 + 2 \cdot e^{\frac{E_F - E_d}{k_b T}}}, \quad \frac{N_A^-}{N_A} = \frac{1}{1 + 2 \cdot e^{\frac{E_a - E_F}{k_b T}}}$$

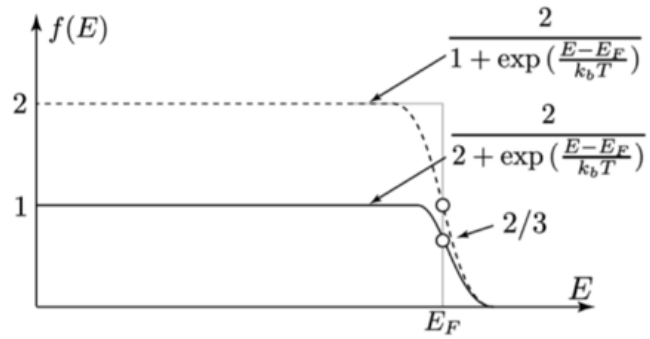

$$\underbrace{N_v F_{\frac{1}{2}}\left(\frac{E_v - E_F}{k_b T}\right)}_{p} + \underbrace{\frac{N_D}{1 + 2 \cdot e^{\frac{E_F - E_d}{k_b T}}}}_{N_D^+} = \underbrace{N_c F_{\frac{1}{2}}\left(\frac{E_c - E_F}{k_b T}\right)}_{n} + \underbrace{\frac{N_A}{1 + 2 \cdot e^{\frac{E_a - E_F}{k_b T}}}}_{N_A^-} \quad (14.$$

Carrier Statistics in Doped Semiconductors

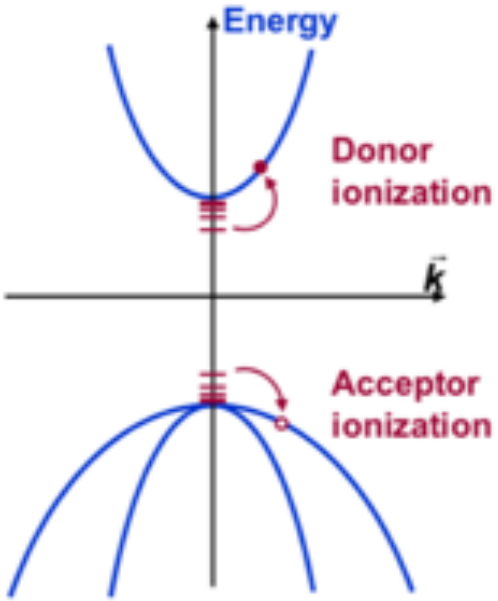

Consider a semiconductor that is doped with both donor and acceptor impurity atoms

- The total charge must be zero:

$$N_d^+ - N_a^- + p - n = 0$$

The above equation can be used to find the position of the equilibrium Fermi level since every term depends on the Fermi level position (one equation in one unknown)

$$N_d^+ = \frac{N_d}{1+2\,e^{-(E_d-E_f)/KT}}$$

$$N_a^- = \frac{N_a}{1+2\,e^{(E_a-E_f)/KT}}$$

ECE 407 – Spring 2009 – Farhan Rana – Cornell University

Semiconductor carrier statistics

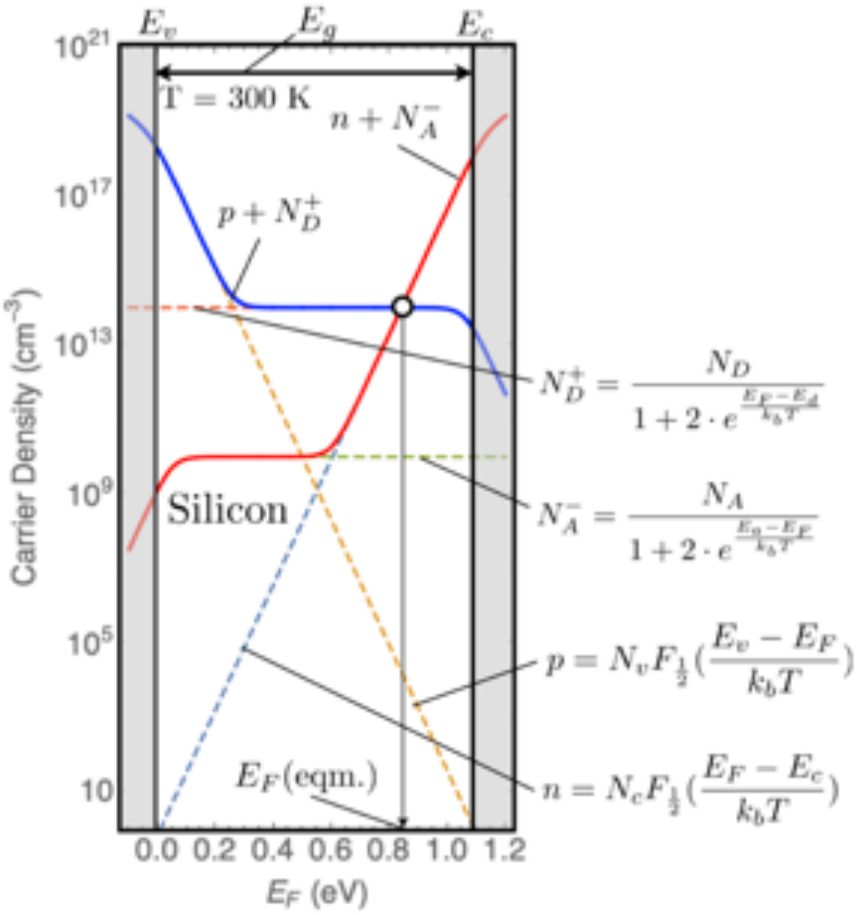

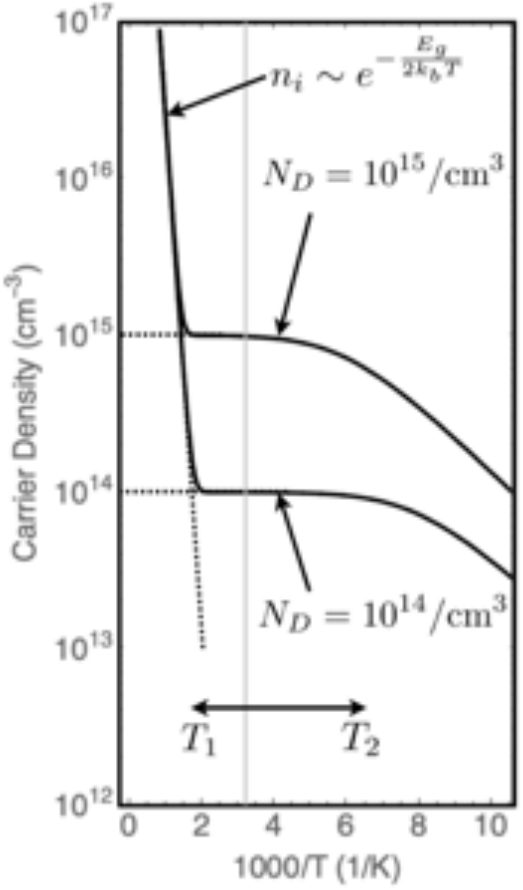

Graphical Solution for Locating the Fermi Level

Charge Neutrality: $n + N_A^- = p + N_D^+$

↙

Solve to find the Fermi Level

↙

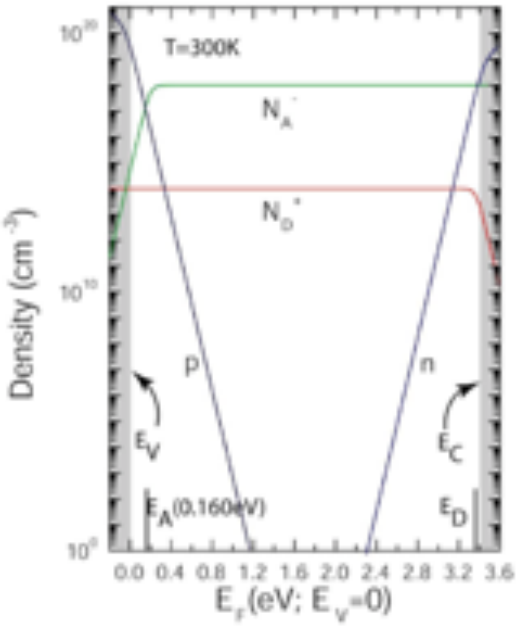

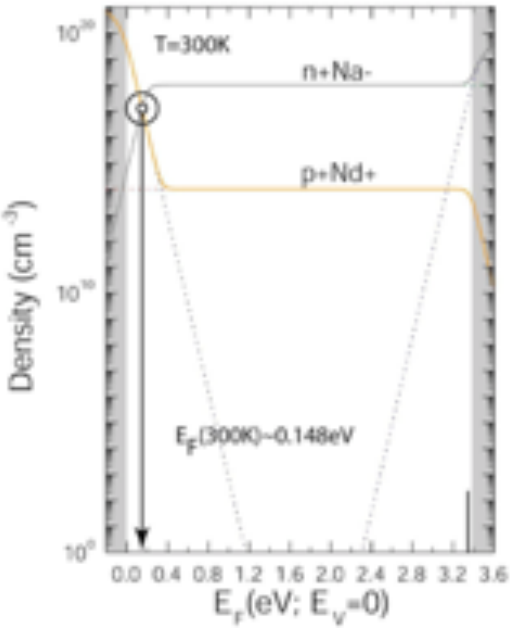

Example for GaN (N_A=10^{18}/cm^3, N_D=10^{14}/cm^3)

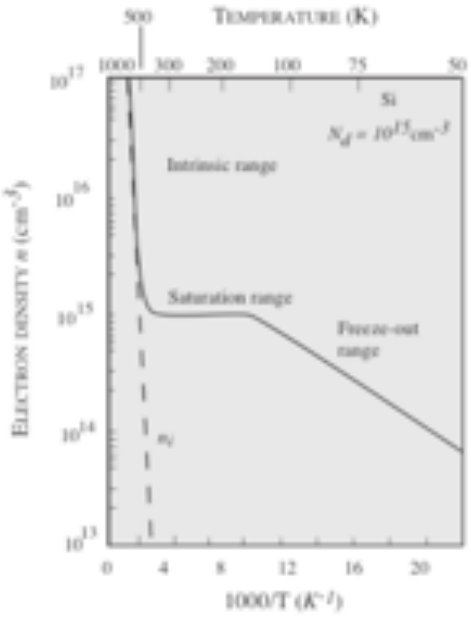

Temperature dependence of mobile carrier density in doped Silicon

Semiconductor doping

Controlling resistivity of semiconductors by doping

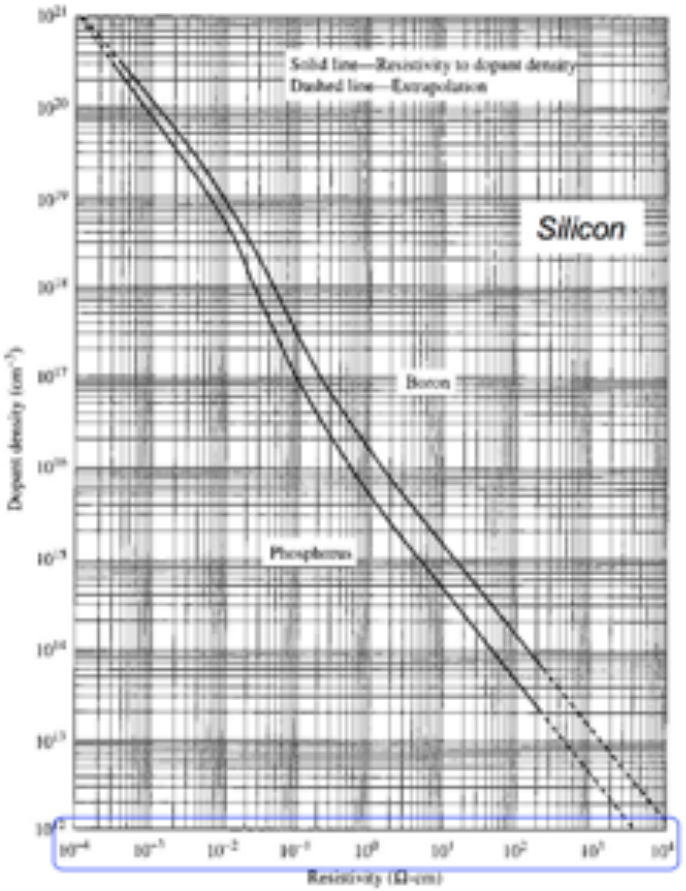

FIGURE 1.15 Dopant density versus resistivity at 23°C (296 K) for silicon

Resistivity of
- *Metals ~ 10^{-6} Ohm-cm*
- *SiO_2 (insulator) ~ 10^{14} Ohm-cm*

Various methods of "Doping"

Traditional Bulk Semiconductors -
- *Impurity doping (bulk, uniform)*
- *Impurity doping (graded, delta-doping)*

(Since '50s)

Impurity + Heterostructures -
- *Modulation Doping*

(Since '80s)

Polar Semiconductor Heterostructures –
- *Polarization-induced doping*

(Since late '90s)

Other "Dynamic" methods –
- *Electrostatic gating*
- *Optical excitation*
- *Thermal excitation*

These are the various methods for Creating mobile carriers in the conduction & valence bands

Effect of Doping and Temperature

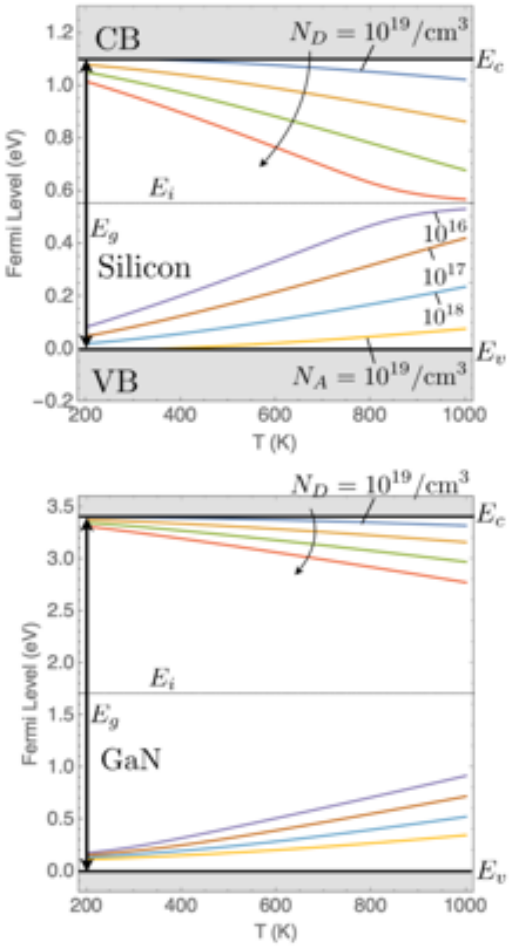

Fig. 14.7 Location of the Fermi level E_F in Silicon and GaN as a function of temperature for various donor and acceptor doping densities.

Band Diagrams

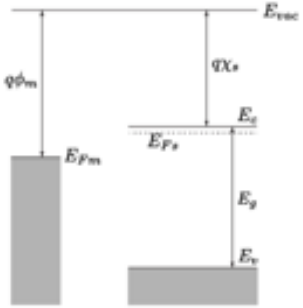

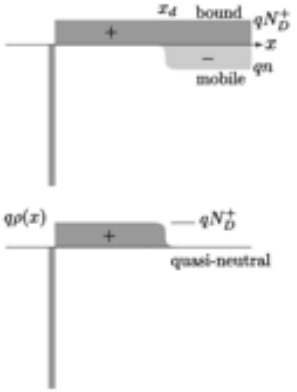

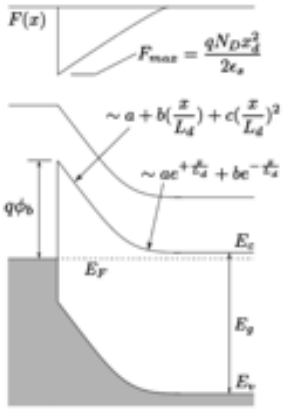

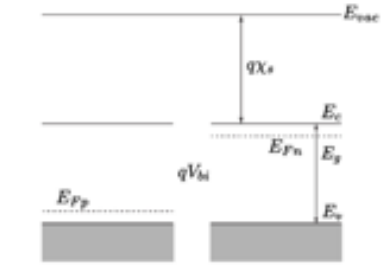

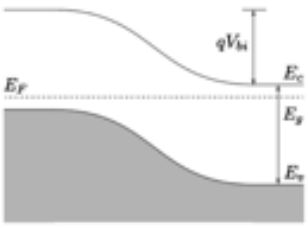

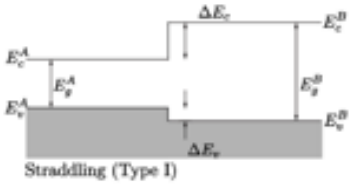

Straddling (Type I)

Staggered (Type II)

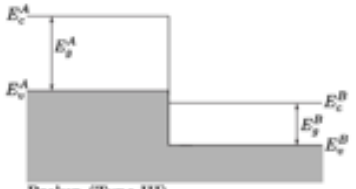

Broken (Type III)

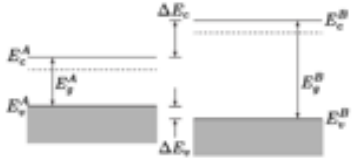

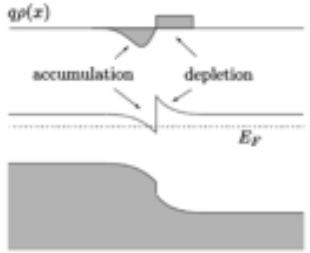

Band Alignments: 3D semiconductors

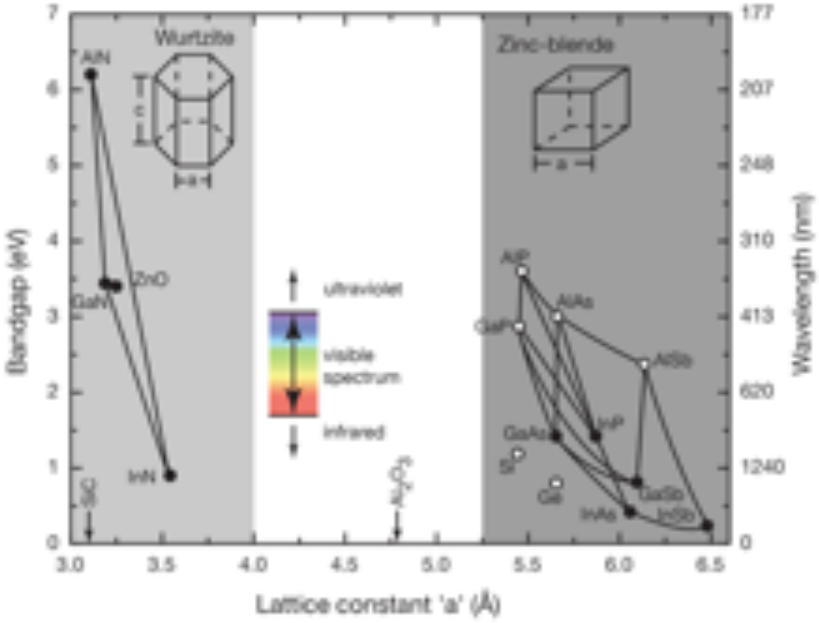

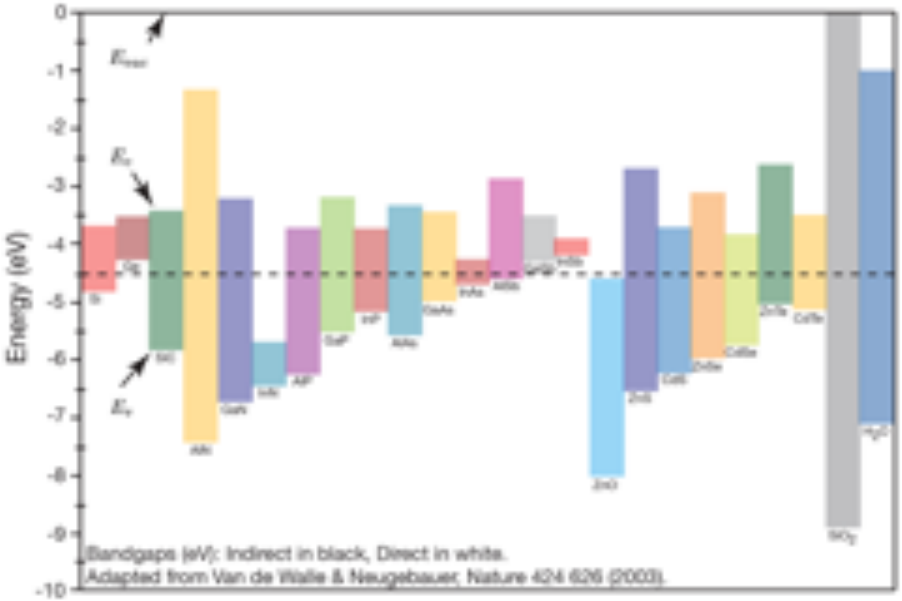

Fig. 14.13 Bandgaps vs lattice constants, and band alignments of 3D semiconductors.

Band Alignments: 2D semiconductors

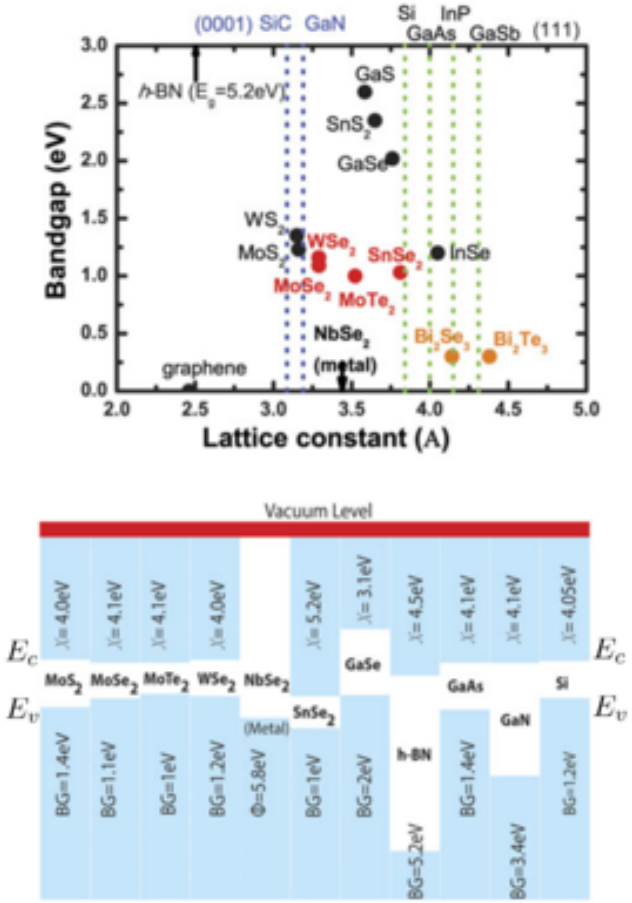

Fig. 14.14 Bandgaps vs lattice constants, and band alignments of 2D semiconductors. From J. Mater. Res. 31, 900 (2016).

The Schottky Diode

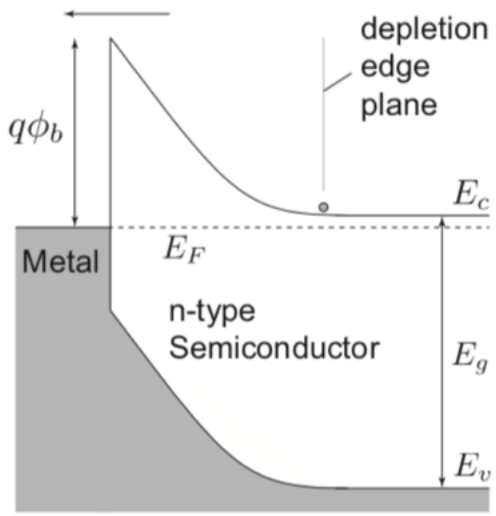

Fig. 16.1 Schottky Diode.

$$J = A^\star T^2 e^{-\frac{q\phi_b}{k_b T}} \left(e^{\frac{qV}{k_b T}} - 1\right)$$

$$A^\star = \frac{4\pi q k_b^2 m_c^\star}{h^3}$$

Richardson constant

$$J = J_0\left(e^{\frac{qV}{k_b T}} - 1\right)$$

Metal-Semiconductor Junctions: Current Flow

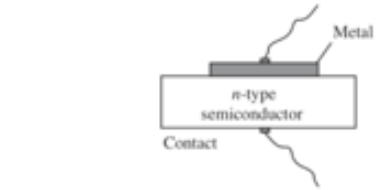

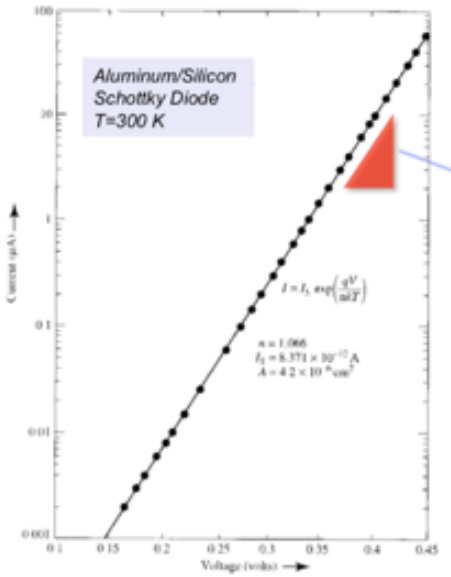

FIGURE 3.10 Measured values of current (plotted on a logarithmic scale) versus voltage for an aluminum-silicon Schottky barrier. Values for $I_0 = J_0 A$ and n are obtained from an empirical fit of the data to Equation 3.3.17.

$$S = \frac{kT}{q}\ln(10)$$

$$= 60 \text{ mV/decade at } 300 \text{ K}$$

*This is a **FUNDAMENTAL** limit of voltage control of currents that are limited by **Thermionic Emission** over barriers*

q x Voltage == Energy of electrons. Therefore, this is also the fundamental limit Of 'energy efficiency' of switching devices That operate using Thermionic Emission currents

Fig. 16.2 Walter Schottky was an early investigator of the metal-semiconductor junction. A semiconductor research institute in Munich is named after him.

Fig. 16.3 Owen Richardson was awarded the 1928 Physics Nobel prize for thermionic emission; the Richardson constant is named after him.

The Schottky Diode

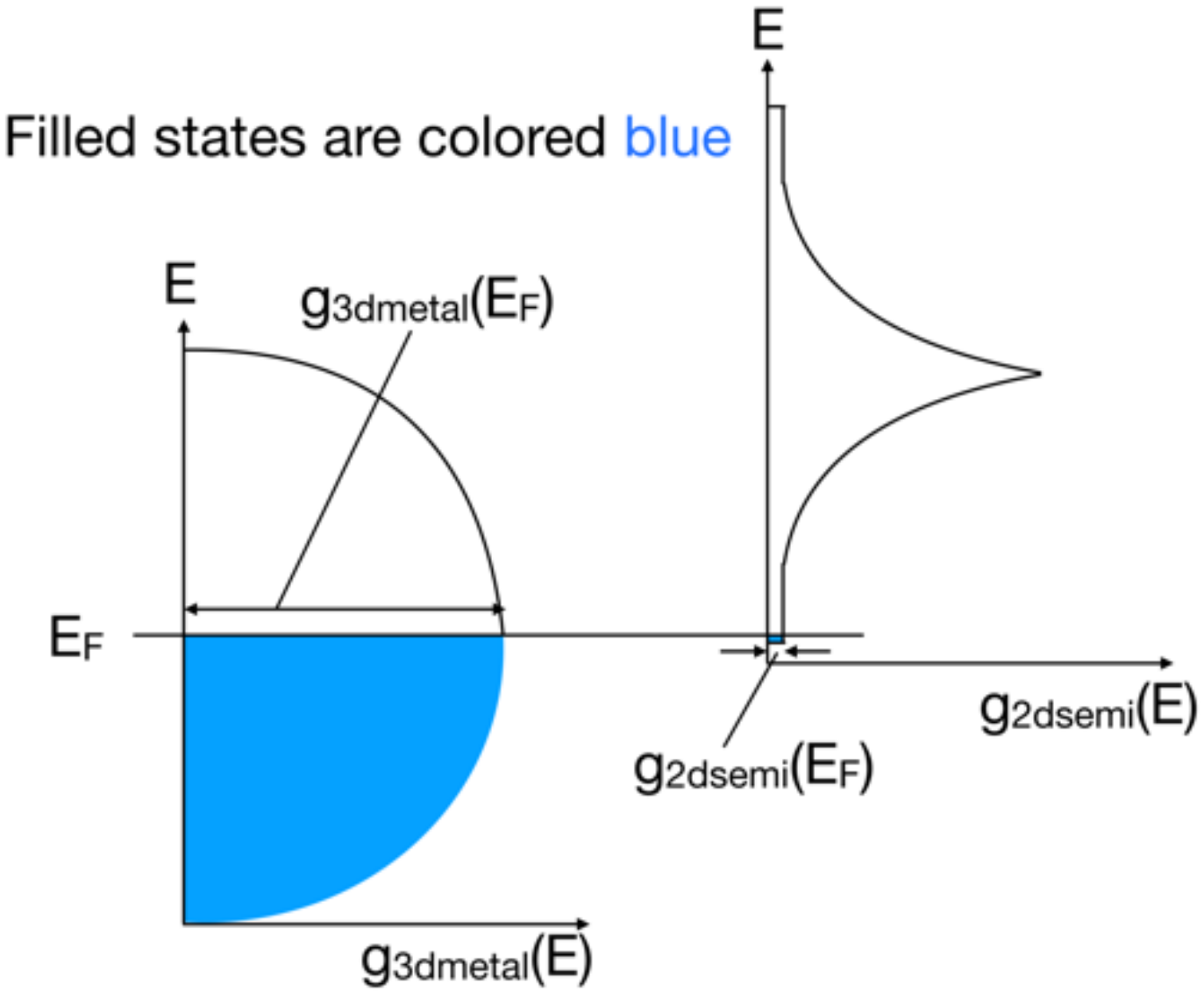

The Schottky Diode Rectifier

Metal-Semiconductor Junctions: Current Flow

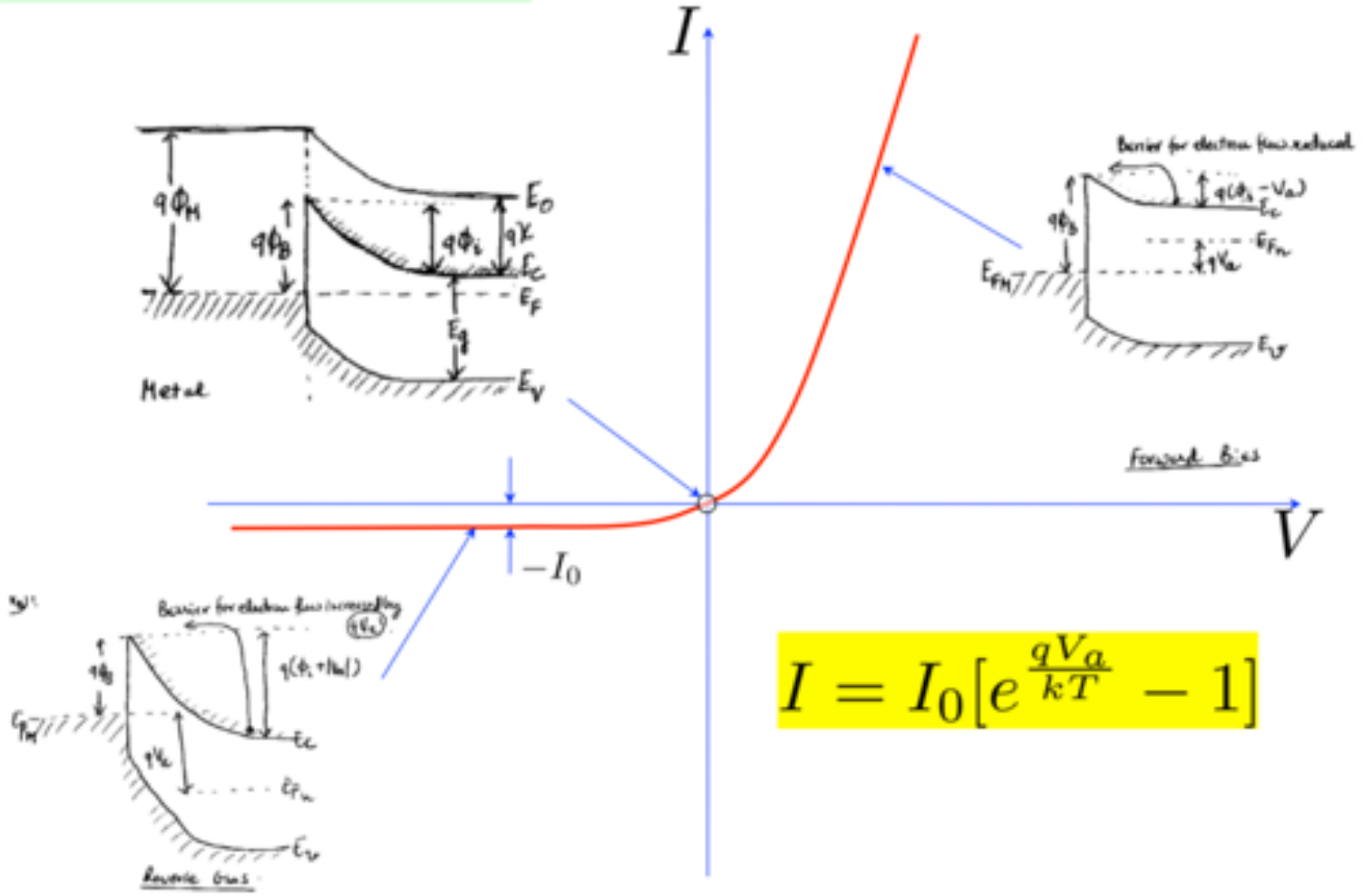

Various kinds of Metal-Semiconductor Junctions

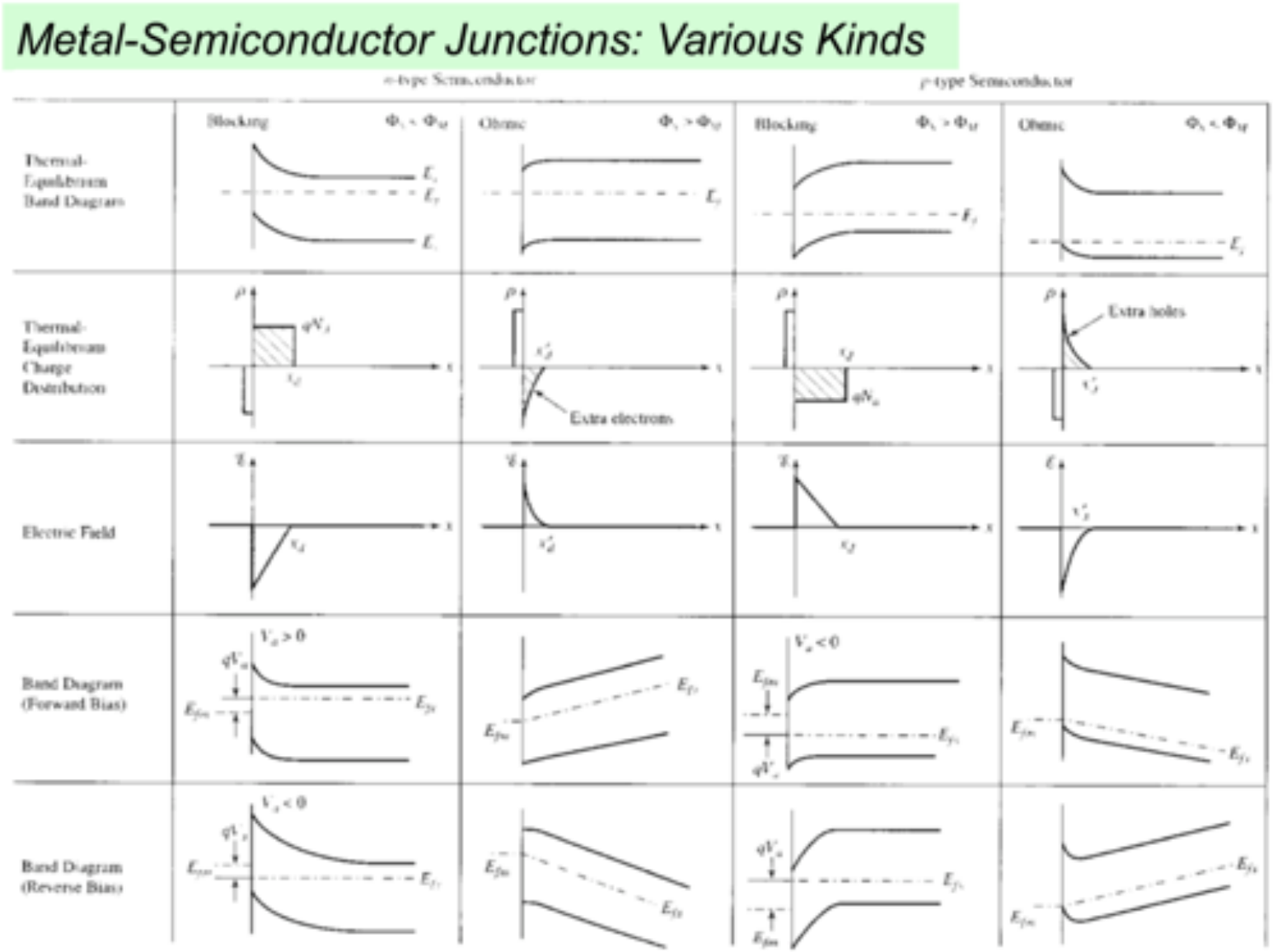

Energy Band Diagrams

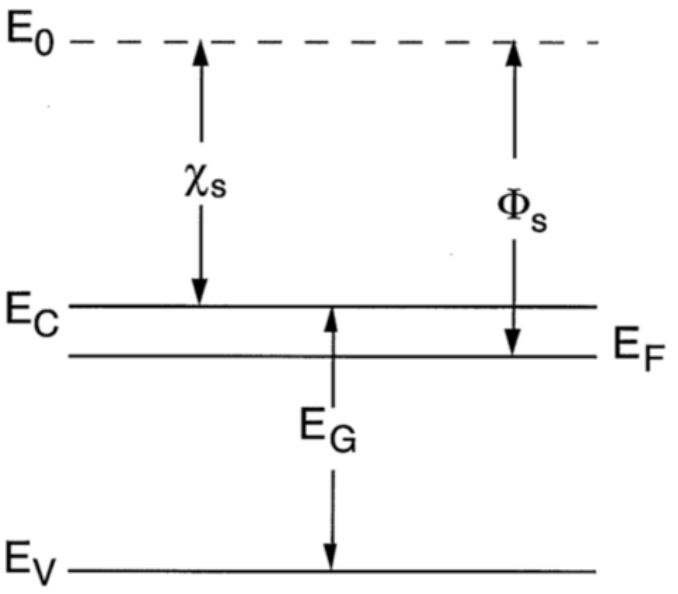

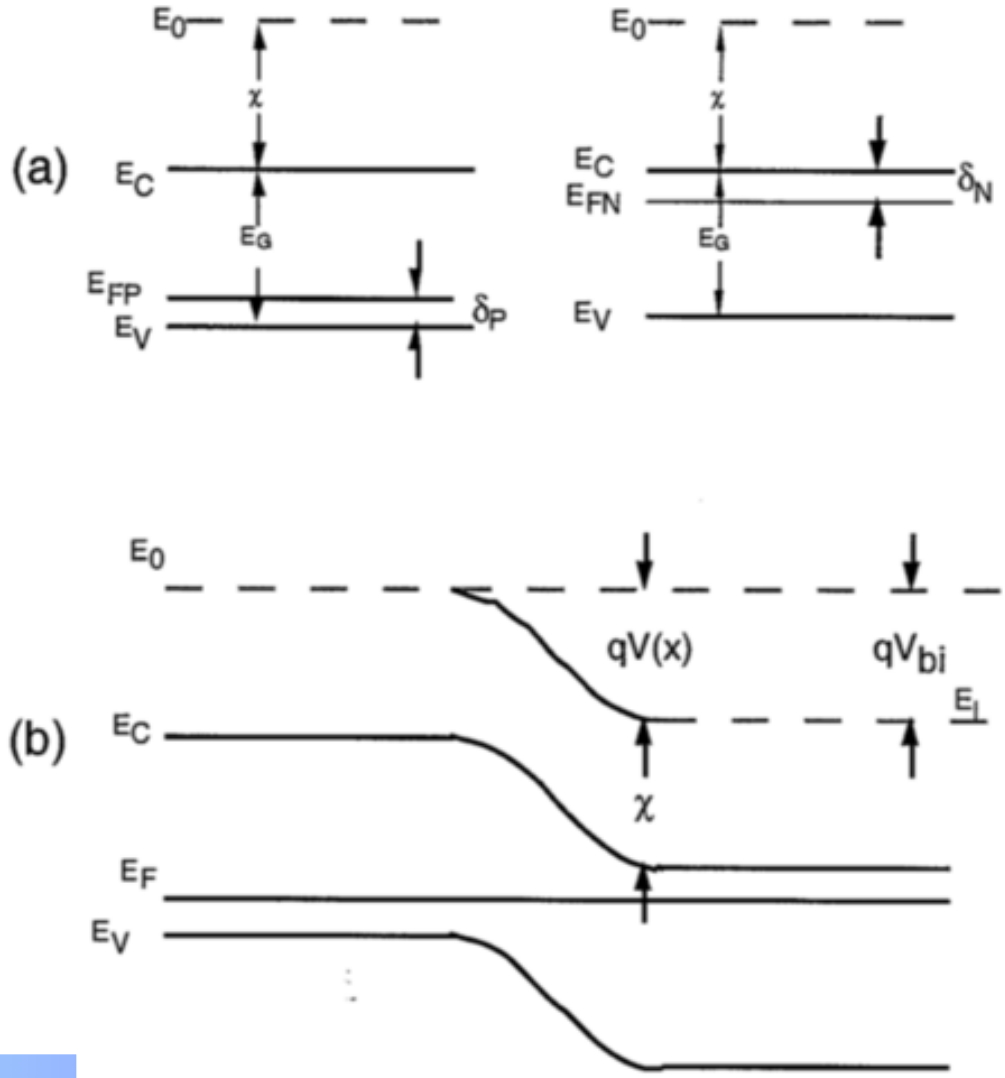

Energy Band Diagrams

Heterojunction Energy Band Diagrams

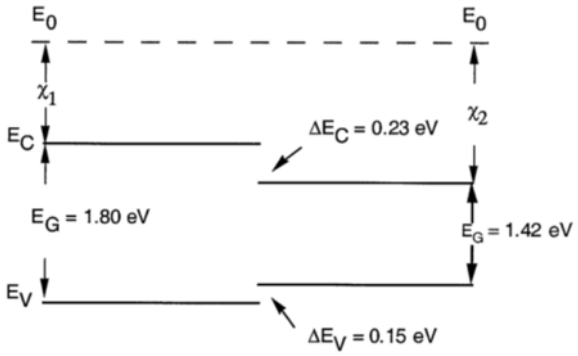

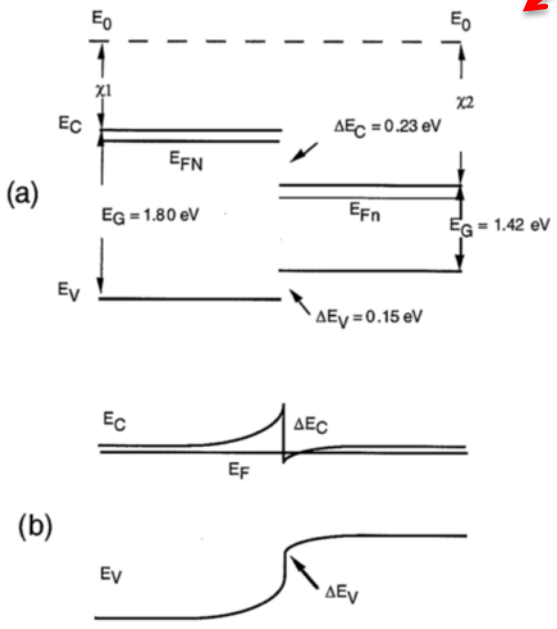

$Al_{0.3}Ga_{0.7}As$ GaAs

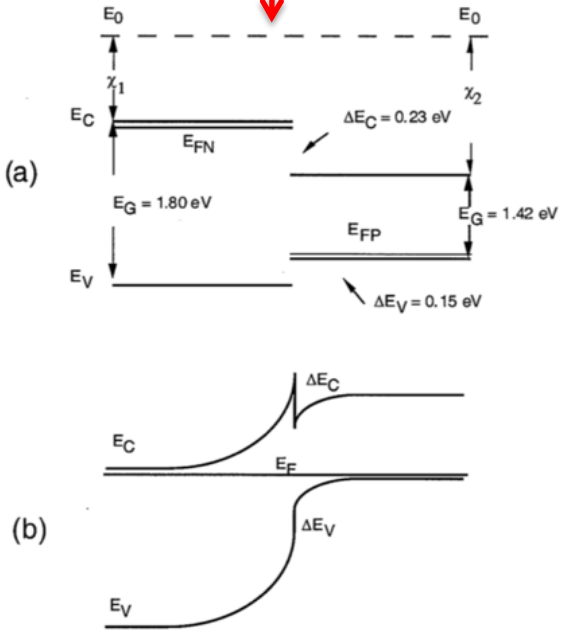

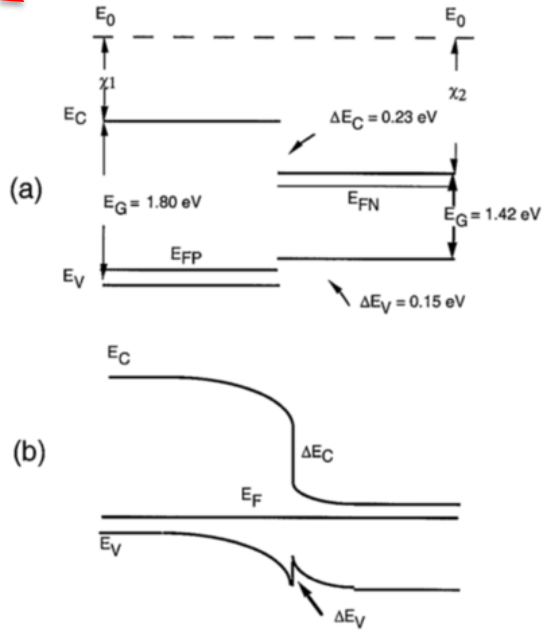

Energy Band Diagrams

Heterojunction Energy Band Diagrams

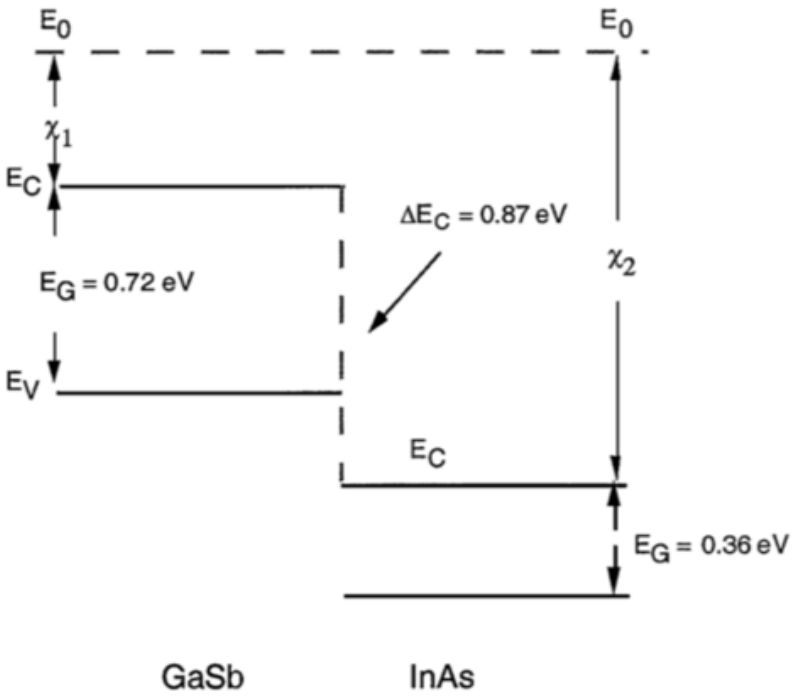

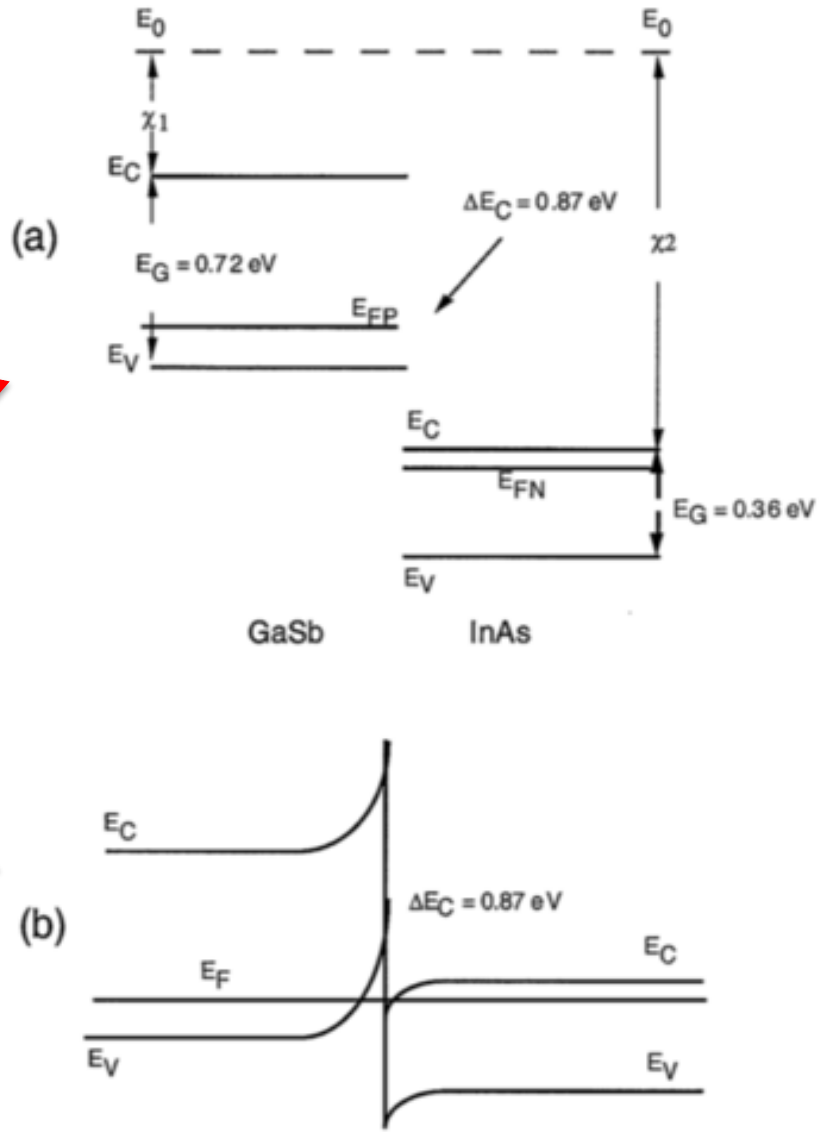

Energy Band Diagrams

Graded Heterojunction Energy Band Diagrams

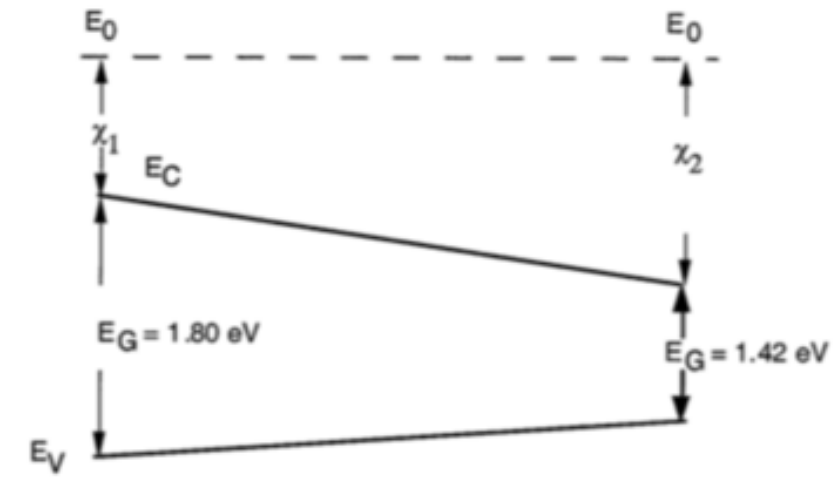

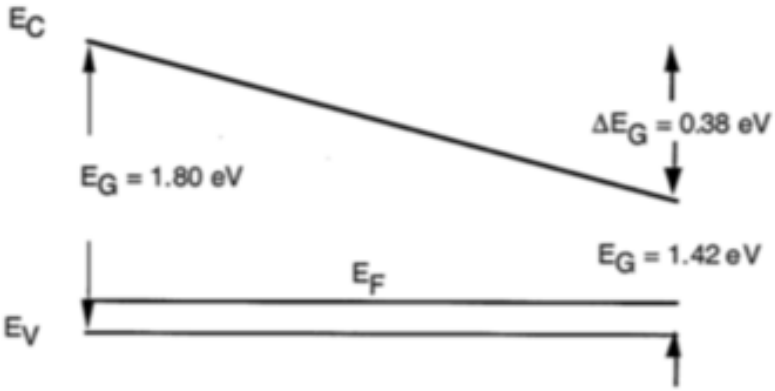

Band Diagrams for Polar Heterostructures

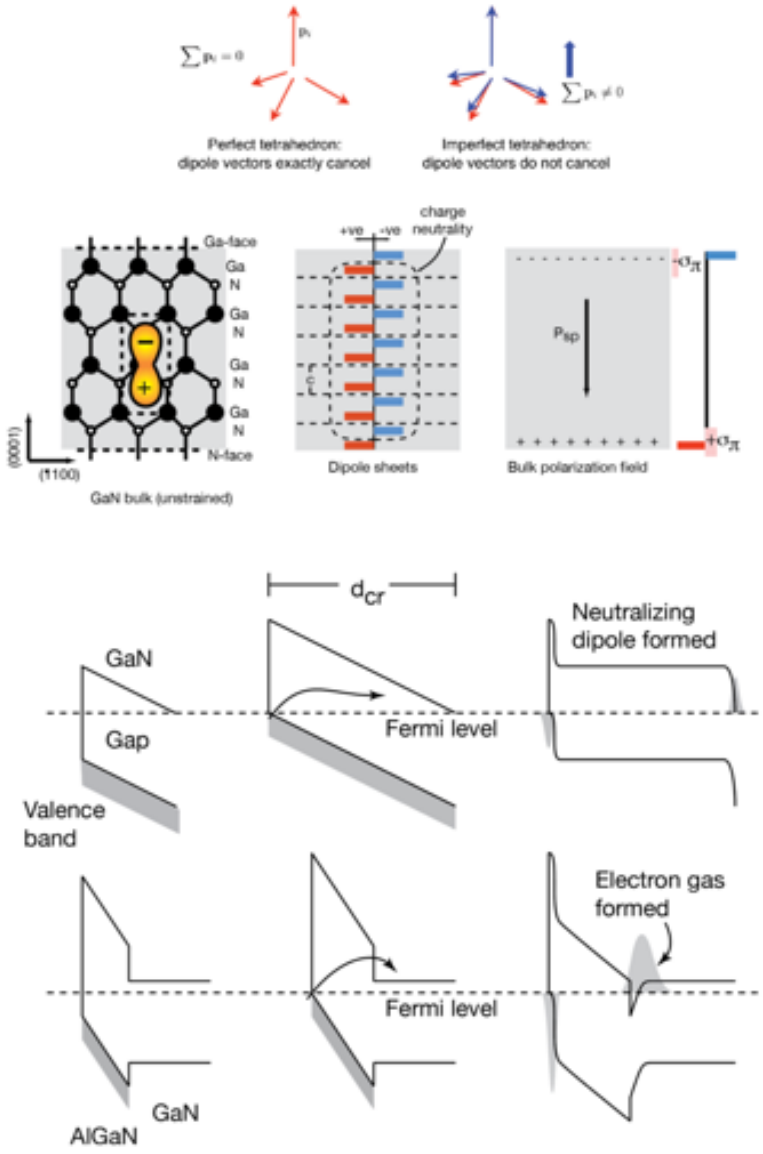

Fig. 14.15 Energy band diagrams of polar heterostructures such as GaN/AlGaN heterjunctions. because of the presence of internal electric charges due to spontaneous and piezoelectric polarization, electric fields and band bending happens *even in the absence* of donor or acceptor doping.

Charge Transport: Drift

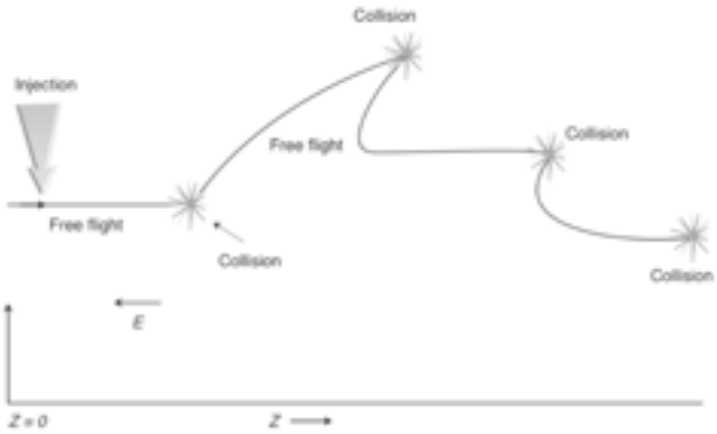

CHARGE TRANSPORT - DRIFT + DIFFUSION

Drift: $v_d = \mu F$ ← electric field

Drift velocity

Mobility $= \frac{e\tau}{m^*}$ ← scattering time, order $\sim 10^{-12}$ s = ps

$J_{drift} = e n v_d = e n \mu F$

flux

v_d - F not always linear; v_d - F plots saturate.

μ → depends on — Temperature (Phonons)
— Doping densities
— Impurities

$l = v_d \tau$ = "mean free path"

Table 1.6 Effective Mass and Mobility for Various Semiconductors

	Material	Effective Mass			Mobility	
		m_e^*	$m_p h^*$	$m_p l^*$	μ_e	μ_h
IV	Si	0.26	0.55	0.24	1350	475
	Ge	0.56	0.37	-	3800	1900
III-V	GaP	0.12	0.86	0.14	200	120
	GaAs	0.065	0.45	0.082	8500	420
	GaSb	0.049	0.33	0.056	7700	1400
	InP	0.077	0.56	0.12	6060	150
	InAs	0.027	0.41	0.024	33000	460
	InSb	0.0135	0.438	0.016	78000	1700
II-VI	ZnS	0.28	1.4		140	5
	ZnSe	0.17	~0.7		530	28
	ZnTe	0.122	0.42	0.17	340	110
	CdS	0.171	~5		350	15
	CdSe	0.112	>1.0		650	
	CdTe	0.0963	0.62	0.092	1050	80

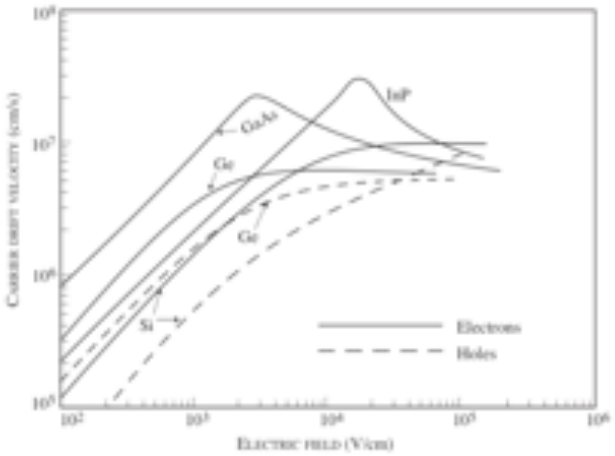

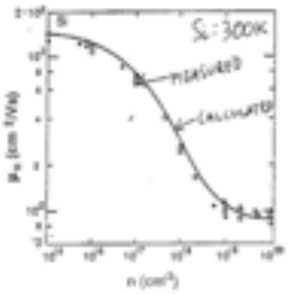

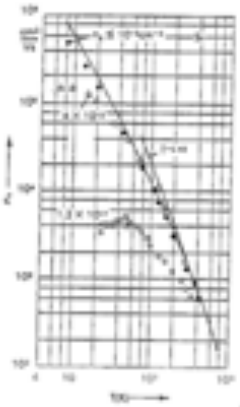

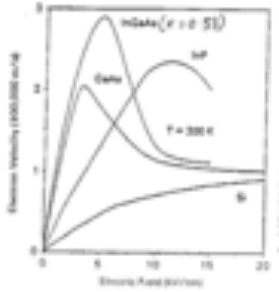

High-Field Transport: Electron Velocity Saturation

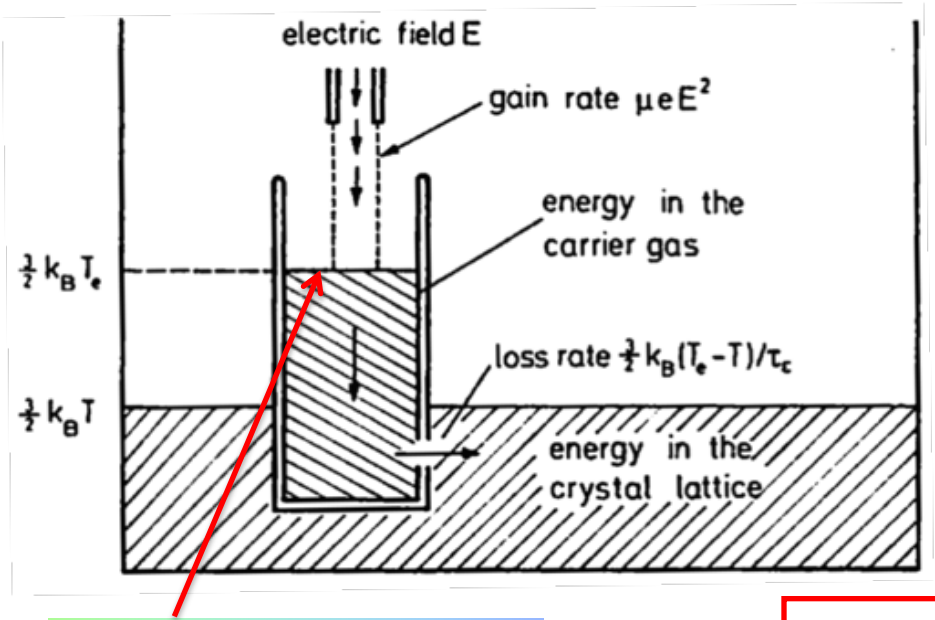

Hot-electron temperature: models non-equilibrium

$$f = \frac{1}{1 + \exp\left[(\mathscr{E} - \zeta)/kT_e\right]}$$

Hot-electron temperature

$$\frac{\partial E}{\partial t} = (-eF)v_d - \frac{\hbar\omega_{LO}}{\tau_E(T_e)},$$

Energy balance eqn.

$$\frac{\partial v_d}{\partial t} = \frac{-eF}{m_e} - \frac{v_d}{\tau_m(T_e)},$$

Momentum balance eqn.

Steady state

$$v_d = v_0\sqrt{\tau_m/\tau_E}$$

$$v_0 = \sqrt{\hbar\omega_{LO}/m_e}$$

Ensemble saturation velocity ~ $(E_{op}/m^*)^{1/2}$

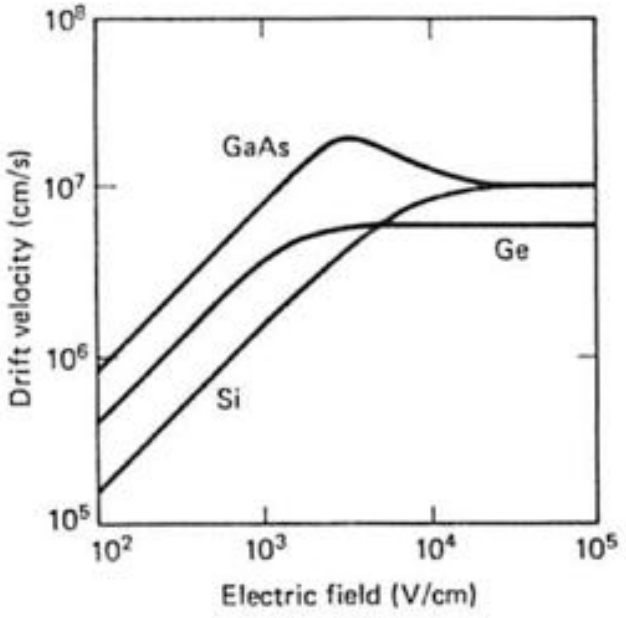

Effective Mass Approximation

- 2D (Quantum Wells)

$$V(x,y,z) = 0, z < 0$$
$$V(x,y,z) = 0, z > W$$
$$V(x,y,z) = -\Delta E_c, 0 \leq z \leq W.$$

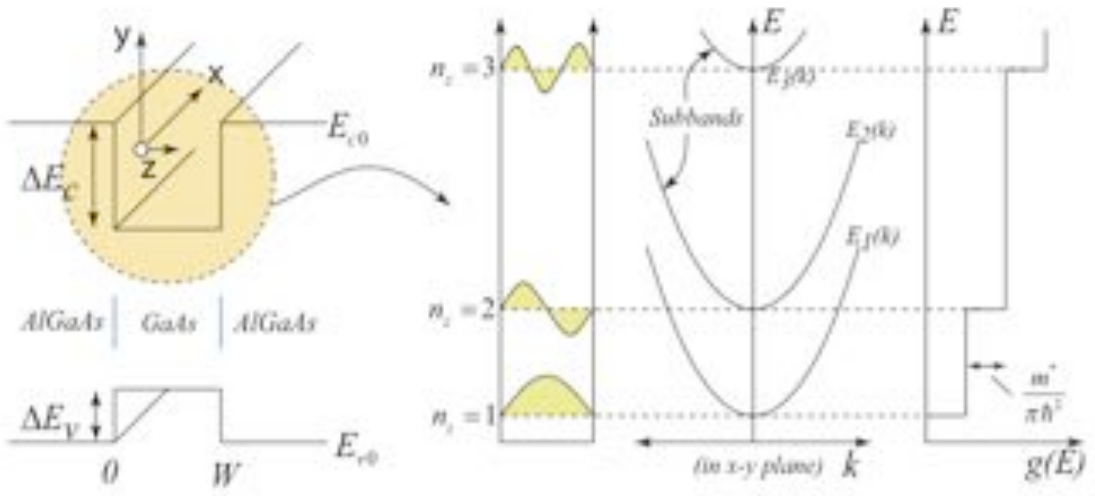

Figure 2: Bandstructure, and DOS of realistic heterostructure quantum wells

$$k_{n_z} = \frac{\pi}{W} n_z$$

$$C_{n_z}(x,y,z) = \phi(x,y)\chi_{n_z}(z) = [\frac{1}{\sqrt{A}} e^{i(k_x x + k_y y)}] \cdot [\chi_{n_z}(z)]$$

$$\chi_{n_z}(z) = \sqrt{\frac{2}{W}} \sin \frac{\pi n_z z}{W}$$

$$E(k) = E_{c0} + \underbrace{\frac{\hbar^2}{2}(\frac{k_x^2}{m_{xx}^\star} + \frac{k_y^2}{m_{yy}^\star})}_{E_{2D}(k_x,k_y} + \underbrace{\frac{\hbar^2}{2m_{zz}^\star}(\frac{\pi n_z}{W})^2}_{E_{1D}(n_z)}$$

$$n_{2D} = \int_0^\infty dE f_{FD}(E) g_{2D}(E) = \underbrace{\frac{m^\star k_B T}{\pi \hbar^2}}_{N_C^{2D}} \ln(1 + e^{\frac{E_F - E_1}{k_B T}})$$

$$n_{2D} = \sum_j n_j = N_c^{2D} \sum_j \ln(1 + e^{\frac{E_F - E_j}{k_B T}})$$

$$g_{QW}(E) = \frac{m^\star}{\pi \hbar^2} \sum_{n_z} \theta(E - E_{n_z})$$

Effective Mass Approximation

- 1D (Quantum Wires)

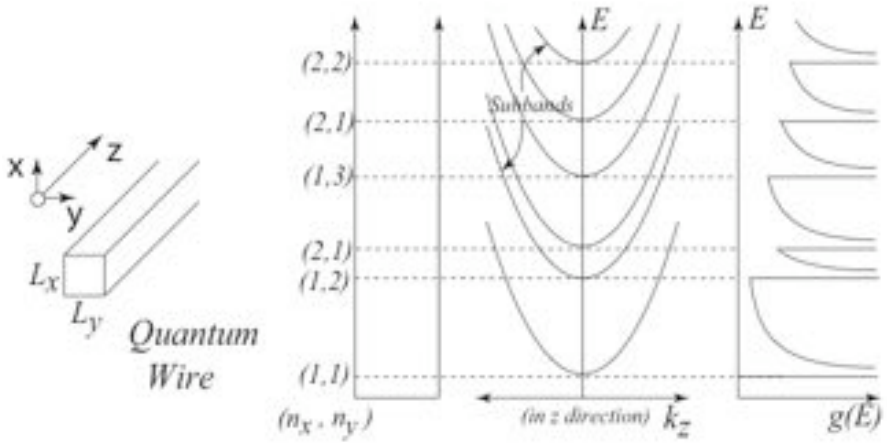

Figure 3: Bandstructure, and DOS of realistic quantum wires.

$$k_{n_x} = \frac{\pi}{L_x} n_x,$$
$$k_{n_y} = \frac{\pi}{L_y} n_y,$$

$$C(x,y,z) = \chi_{n_x}(x) \cdot \chi_{n_y}(y) \cdot (\frac{1}{\sqrt{L_z}} e^{ik_x x})$$

$$E(n_x, n_y, k_z) = E(n_x, n_y) + \frac{\hbar^2 k_k^2}{2m^\star_{zz}}$$

$$C_{n_x,n_y}(x,y,z) = [\sqrt{\frac{2}{L_x}} \sin(\frac{\pi n_x}{L_x} x)] \cdot [\sqrt{\frac{2}{L_y}} \sin(\frac{\pi n_y}{L_y} y)] \cdot [\frac{1}{\sqrt{L_z}} e^{ik_x x}]$$

$$E(n_x, n_y, k_z) = \underbrace{[\frac{\hbar^2}{2m_{xx}} (\frac{\pi n_x}{L_x})^2] + [\frac{\hbar^2}{2m_{yy}} (\frac{\pi n_y}{L_y})^2]}_{E(n_x,n_y)} + \frac{\hbar^2 k_z^2}{2m^\star_{zz}}$$

$$g_{1D}(E) = \frac{1}{\pi} \sqrt{\frac{2m^\star}{\hbar^2}} \frac{1}{\sqrt{E - E_1}}$$

$$g_{QWire}(E) = \frac{1}{\pi} \sqrt{\frac{2m^\star}{\hbar^2}} \sum_{n_x,n_y} \frac{1}{\sqrt{E - E(n_x, n_y)}}$$

Effective Mass Approximation

- 0D (Quantum Dots)

$$C(x,y,z) = [\sqrt{\frac{2}{L_x}}\sin(\frac{\pi n_x}{L_x})] \cdot [\sqrt{\frac{2}{L_y}}\sin(\frac{\pi n_y}{L_y})] \cdot [\sqrt{\frac{2}{L_z}}\sin(\frac{\pi n_z}{L_z})]$$

$$E(n_x,n_y,n_z) = \frac{\hbar^2}{2m_{xx}}(\frac{\pi n_x}{L_x})^2 + \frac{\hbar^2}{2m_{yy}}(\frac{\pi n_y}{L_y})^2 + \frac{\hbar^2}{2m_{zz}}(\frac{\pi n_z}{L_z})^2$$

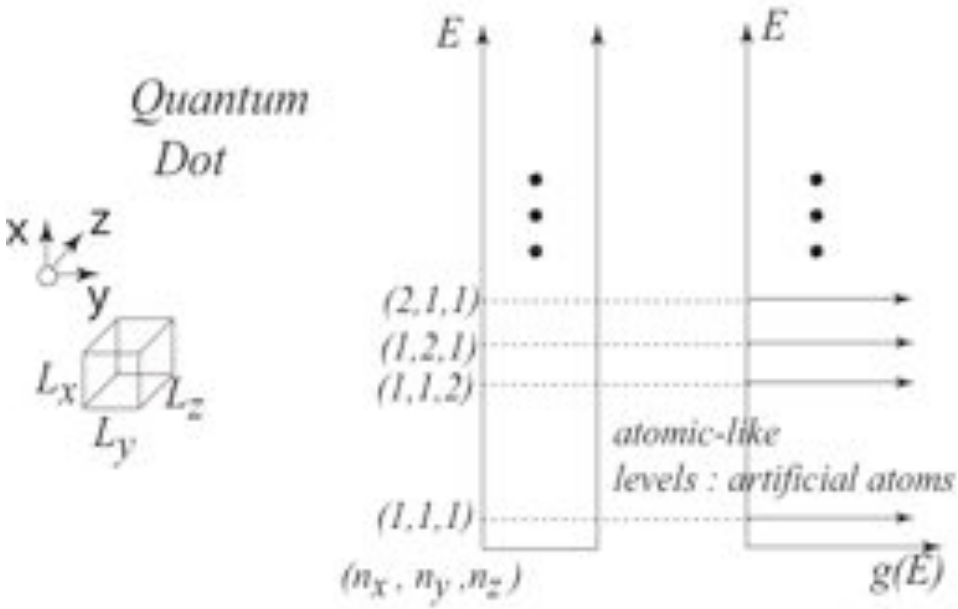

Figure 4: Energy levels and DOS of quantum dots.

$$g_{QDot} = \sum_{n_x,n_y,n_z} \delta(E - E_{n_x,n_y,n_z})$$

Effective Mass Approximation @ Heterojunctions

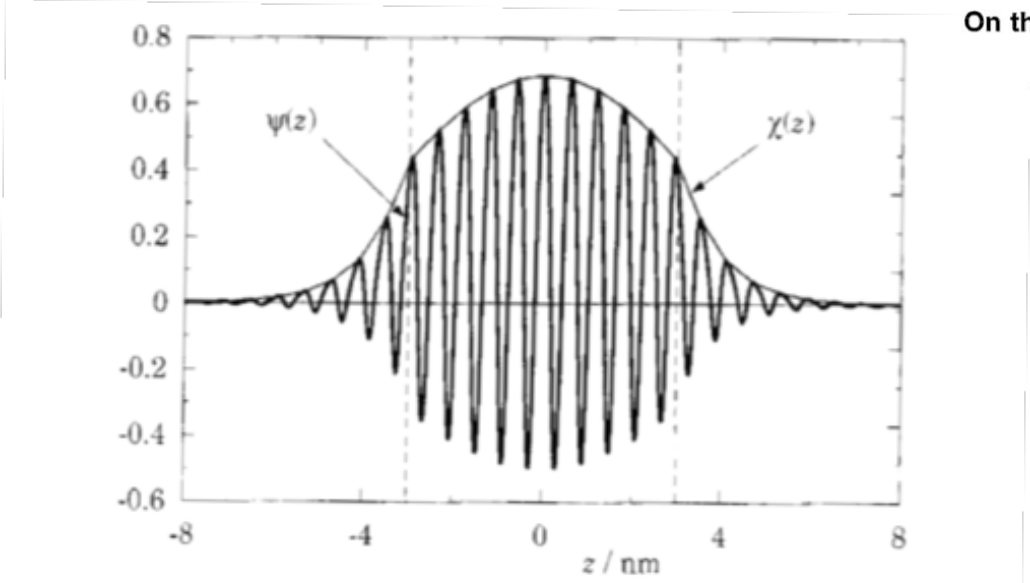

FIGURE 3.22. Wave function for the lowest state in a 6 nm quantum well in a heterostructure, including the Bloch functions. The thin curve is an approximate envelope function joining the peaks of the full wave function. [Redrawn from Burt (1994).]

• Effective Mass Theory works even at sharp heterojunctions, and it works amazingly well! Quantum cascade lasers are designed using this theory.

Proof presented in:
Burt, APL 65 717 (1994)

On the validity and range of applicability of the particle in a box model

M. G. Burt
BT Laboratories, Martlesham Heath, Ipswich IP5 7RE, United Kingdom

(Received 24 February 1994; accepted for publication 27 May 1994)

$$\left(E_c^A - \frac{\hbar^2}{2m_A m_0}\frac{d^2}{dz^2}\right)\chi(z) = E\chi(z), \tag{3.16}$$

$$\left(E_c^B - \frac{\hbar^2}{2m_B m_0}\frac{d^2}{dz^2}\right)\chi(z) = E\chi(z). \tag{3.17}$$

The difference in the bottoms of the conduction bands behaves like a step potential with material B higher by $\Delta E_c = E_c^B - E_c^A$. If the materials were the same we would simply match the value and derivative of the wave function at the interface, giving the usual conditions

$$\chi(0_A) = \chi(0_B), \qquad \left.\frac{d\chi(z)}{dz}\right|_{z=0_A} = \left.\frac{d\chi(z)}{dz}\right|_{z=0_B}, \tag{3.18}$$

where 0_A means the side of the interface in material A and so on. This simple condition is not correct for a heterojunction where the two effective masses are different, and we shall see in Section 5.8 that equation (3.18) does not conserve current. A correct set of matching conditions is

$$\chi(0_A) = \chi(0_B), \qquad \frac{1}{m_A}\left.\frac{d\chi(z)}{dz}\right|_{z=0_A} = \frac{1}{m_B}\left.\frac{d\chi(z)}{dz}\right|_{z=0_B}. \tag{3.19}$$

The condition for matching the derivative now includes the effective mass. Since the derivative is essentially the momentum operator, equation (3.19) requires the velocity to be the same on both sides to conserve current. The envelope function gains a kink at the interface if $m_A \neq m_B$.

Example: Exciton in an InN Nanowire

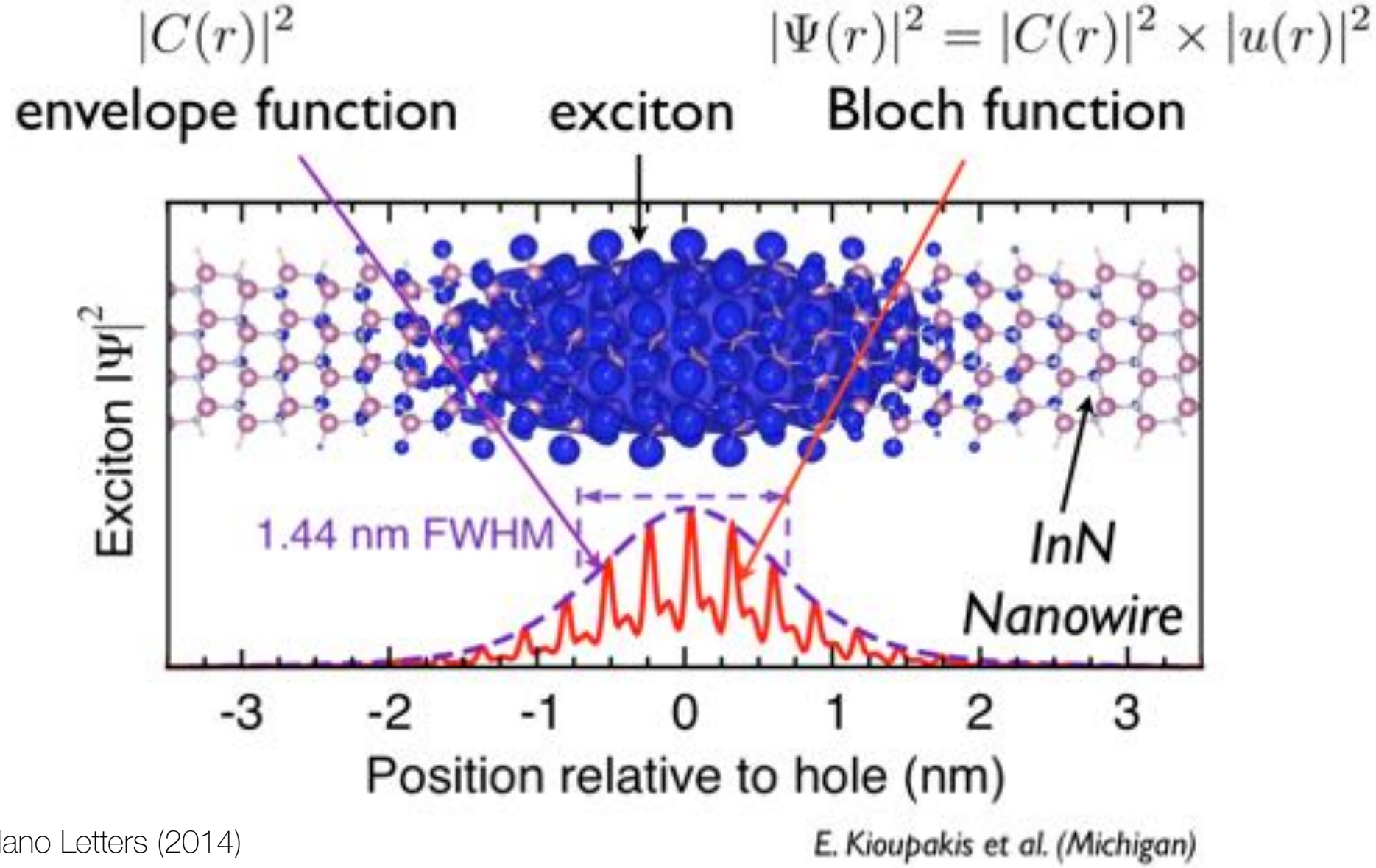

Nano Letters (2014)

E. Kioupakis et al. (Michigan)

Infinitely Deep Quantum Wells

$$[-\frac{\hbar^2}{2m^\star}\frac{d^2}{dx^2} + V(x)]\psi(x) = E\psi(x)$$

$$V(x) = 0 \text{ for } -L \le x \le +L$$

$$V(x) = \infty \text{ for } |x| \ge L$$

$$\psi(x) = Ae^{ikx} + Be^{-ikx}$$

$$k = \frac{2\pi}{\lambda} = \sqrt{\frac{2m^\star(E-V)}{\hbar^2}}$$

$$\psi(+L) = \psi(-L) = 0 \rightarrow k_n = \frac{n\pi}{2L}$$

$$\psi_{even}(x) = A_n \cos(\frac{n\pi}{2L}x) \text{ for } n = \pm 1, \pm 2, \ldots$$

$$\psi_{odd}(x) = A_n \sin(\frac{n\pi}{2L}x) \text{ for } n = \pm 2, \pm 4, \ldots$$

$$E_1^\infty = \frac{\pi^2\hbar^2}{8m^\star L^2} = \frac{\pi^2\hbar^2}{2m^\star L_w^2}$$

$$E_1^\infty = \frac{3.76}{(\frac{m^\star}{m_0})(\frac{L_w}{10 \text{ nm}})^2} \text{ meV}$$

$$E_n = n^2 E_1^\infty$$

The particle in a box problem

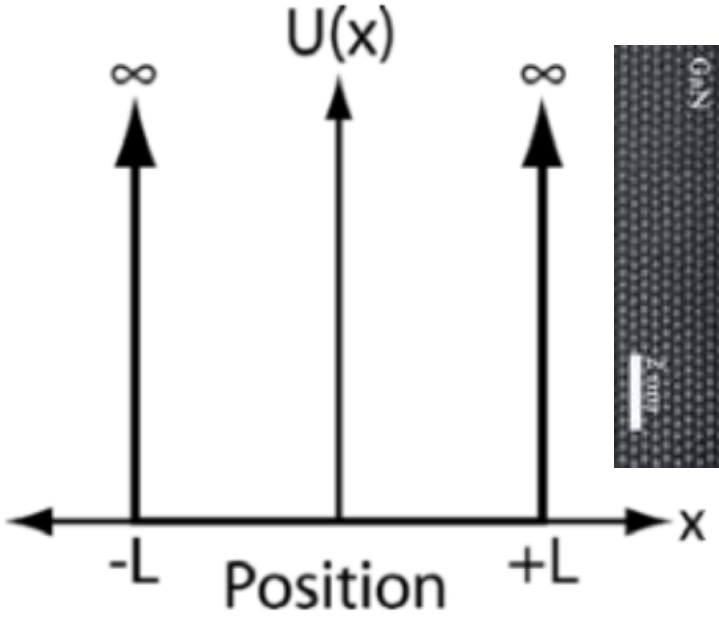

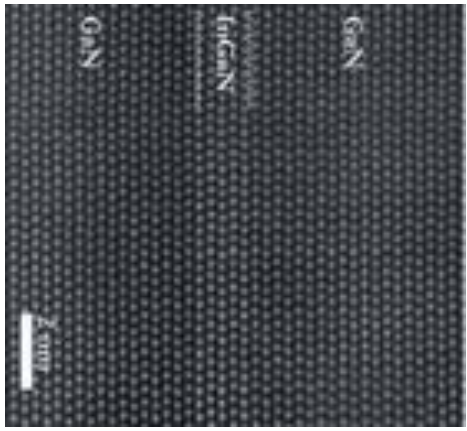

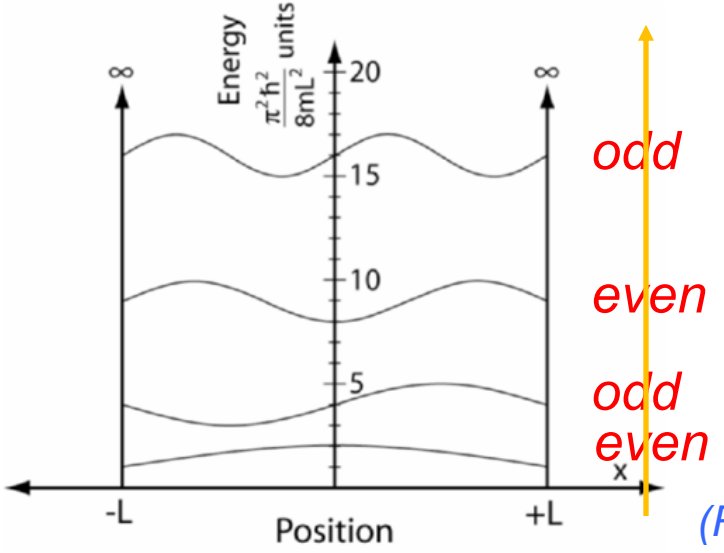

(Rockett)

Finite Quantum Wells

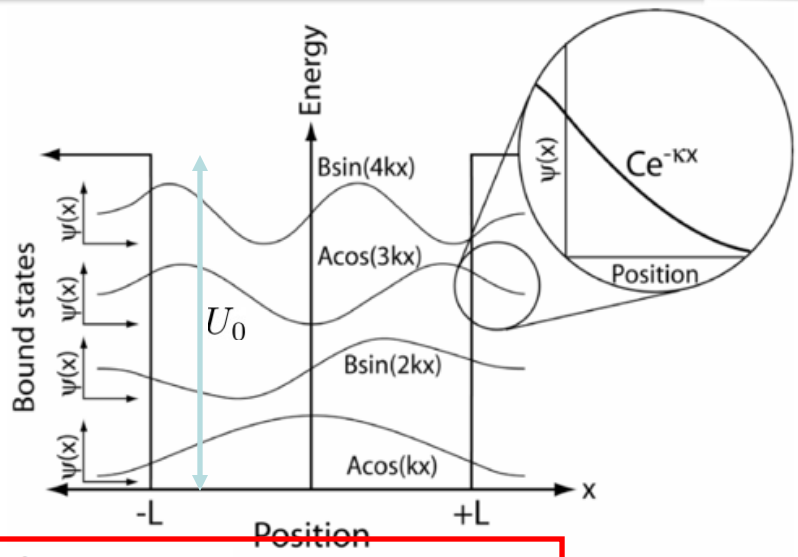

$$\frac{d^2\psi}{dx^2} + \kappa^2\psi = 0$$

$$\kappa^2 = \frac{2mE}{\hbar^2}$$

$$\psi(x) = Ce^{\kappa x} \qquad x < -L$$
$$\psi(x) = A\cos(kx) + B\sin(kx) \qquad -L < x < +L$$
$$\psi(x) = De^{-\kappa x} \qquad x > +L$$

$$k^2 = -\frac{2m}{\hbar^2}(U_0 + |E|) > 0$$

$$\sqrt{\frac{2mU_0}{\hbar^2 k^2} - 1} = \begin{cases} \tan(kL) \\ -\cot(kL) \end{cases} \quad \begin{matrix} \text{Even solutions} \\ \text{Odd solutions} \end{matrix}$$

The particle in a box problem

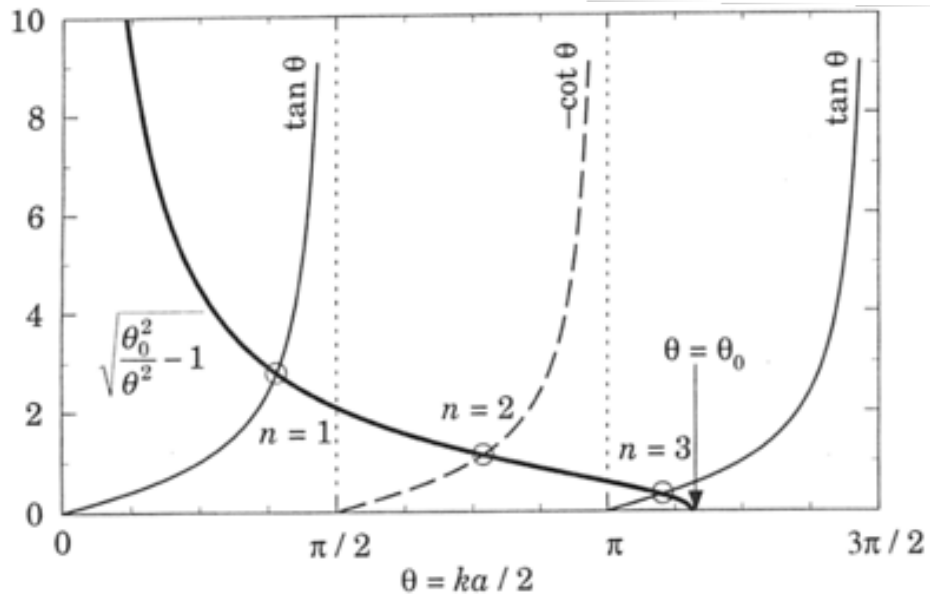

FIGURE 4.2. Graphical solution of equation (4.12) for a square well in GaAs with depth $V_0 = 0.3$ eV and width $a = 10$ nm, giving $\theta_0^2 = 13.2$. There are three bound states.

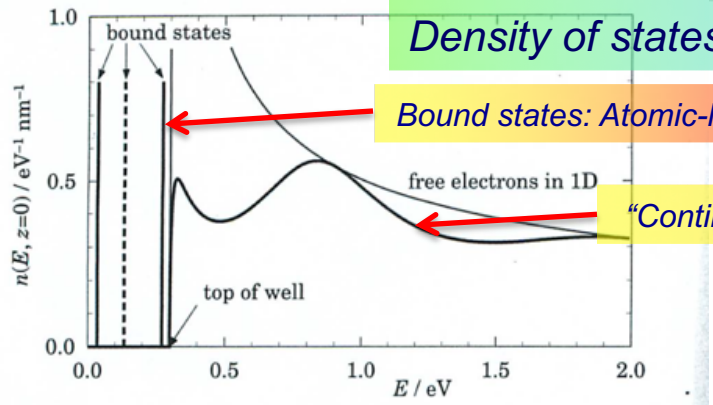

FIGURE 4.3. Local density of states $n(E, z = 0)$ in the middle of a square well in GaAs of width 10 nm and depth 0.3 eV. The result for free electrons, proportional to $E^{-1/2}$, is shown for comparison.

Density of states for a 1D quantum well

Bound states: Atomic-like

"Continuum" states: Free-electron-like

(Rockett/Davies)

Transitions in Semiconductor Quantum Wells

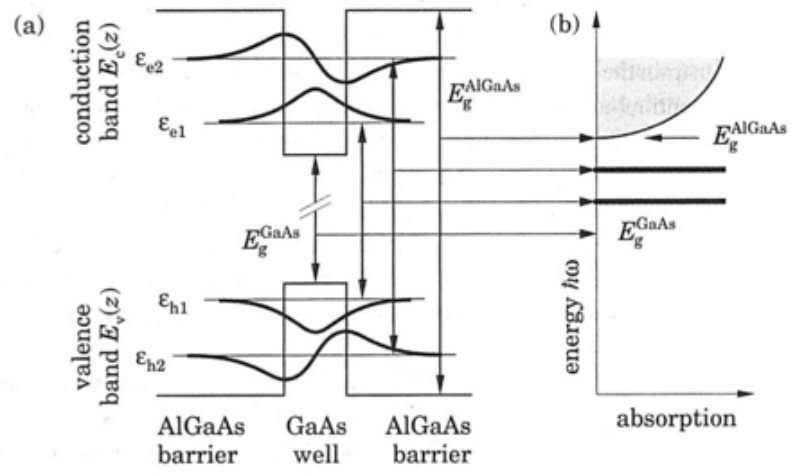

FIGURE 1.3. Optical absorption in a quantum well formed by a layer of GaAs surrounded by AlGaAs. (a) Potential well in conduction and valence band, showing two bound states in each; the energy gap of GaAs is really much larger than this diagram implies. (b) Transitions between states in the quantum well produce absorption lines between the band gaps of the GaAs well and AlGaAs barrier.

Quasi-2D systems: Quantum Wells

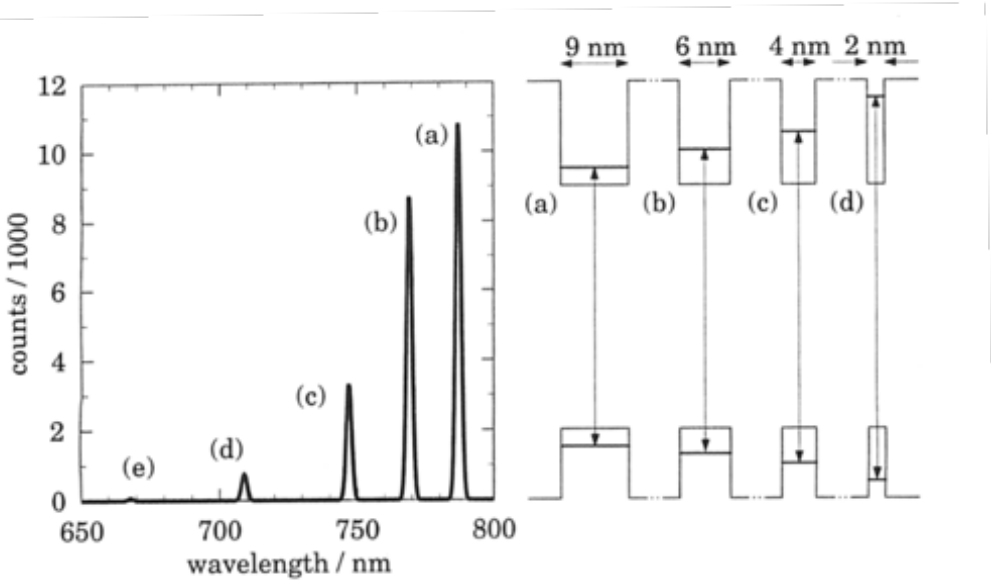

FIGURE 1.4. Photoluminescence as a function of wavelength for a sample with four quantum wells of different widths, whose conduction and valence bands are shown on the right. The barriers between the wells are much thicker than drawn. [Data kindly supplied by Prof. E. L. Hu, University of California at Santa Barbara.]

Photoluminescence spectra of quantum wells

(Davies)

Designing the Transitions in Quantum Wells

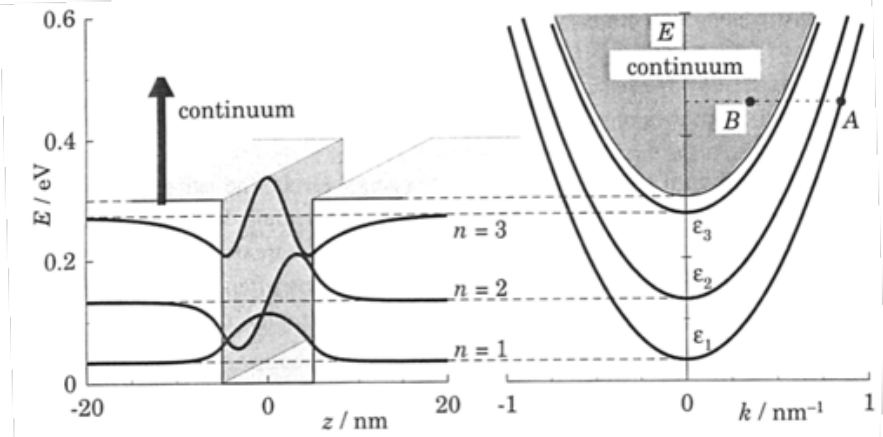

FIGURE 4.9. Quasi-two-dimensional system in a potential well of finite depth. Electrons with the same total energy can be bound in the well (*A*) or free (*B*).

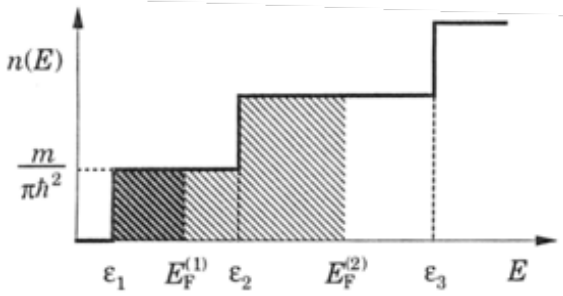

FIGURE 4.8. Occupation of steplike density of states for a quasi-two-dimensional system. Only one subband is occupied if the Fermi energy takes the lower value $E_F^{(1)}$, but two are occupied at the higher value $E_F^{(2)}$.

Rectangular quantum wells

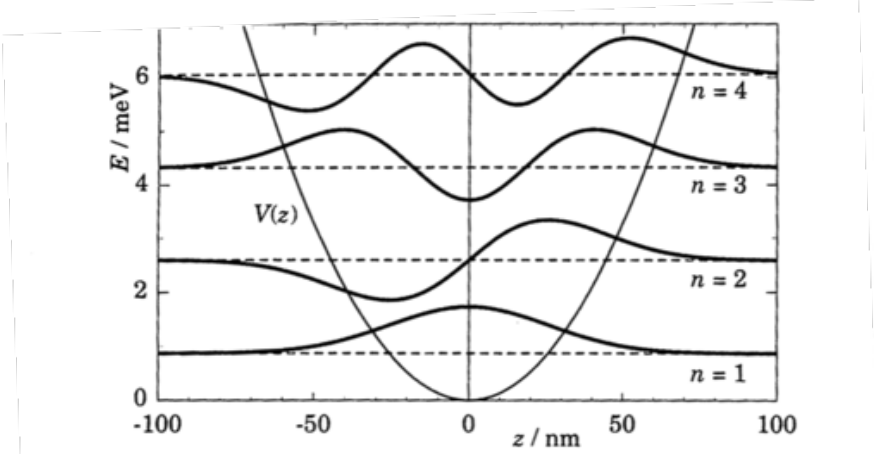

FIGURE 4.4. Potential well $V(z)$, energy levels, and wave functions of a harmonic oscillator. The potential is generated by a magnetic field of 1 T acting on electrons in GaAs.

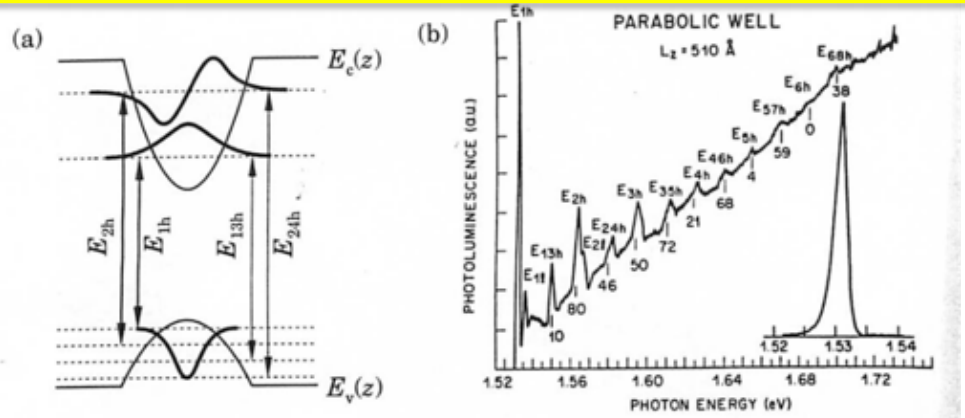

FIGURE 4.5. (a) Parabolic potential in both conduction and valence bands grown into GaAs by a graded composition of $Al_xGa_{1-x}As$. The band gap has been reduced in this sketch, and only heavy holes are shown. (b) Photoluminescence in parabolic wells. [From Miller et al. (1984).]

Parabolic quantum wells: Harmonic Oscillator States! *(Davies)*

Multiple Coupled Quantum Wells

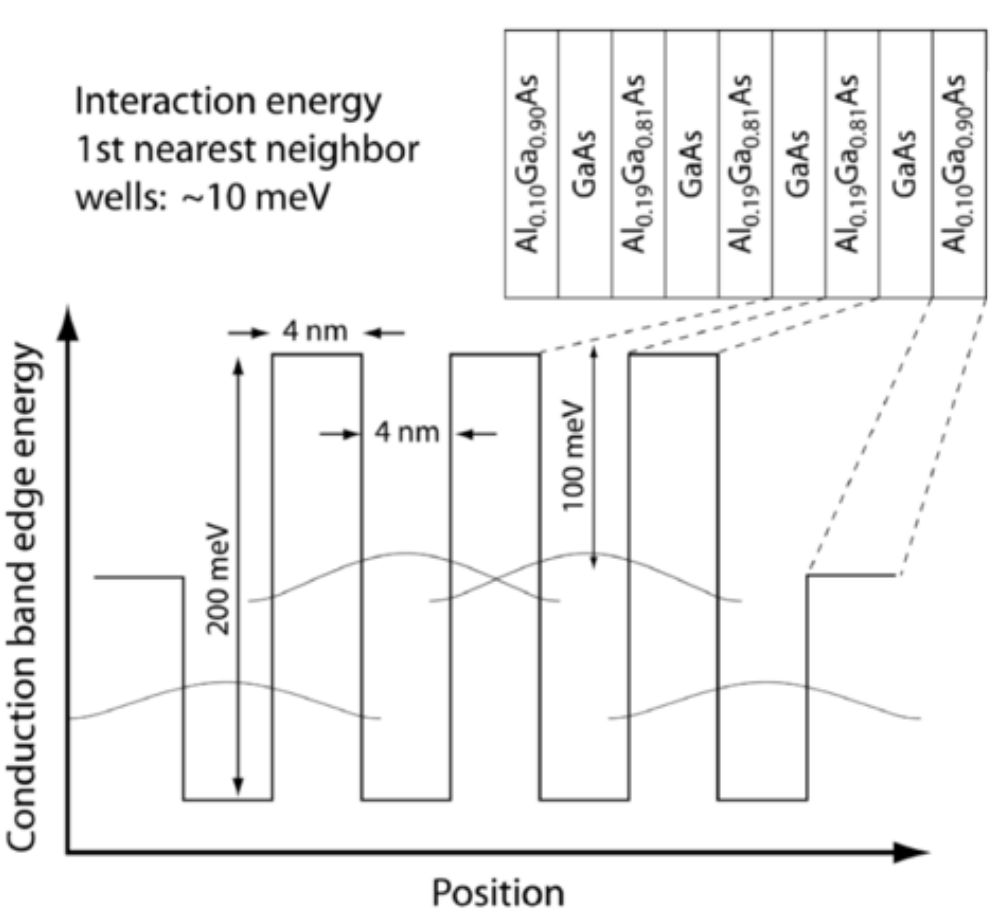

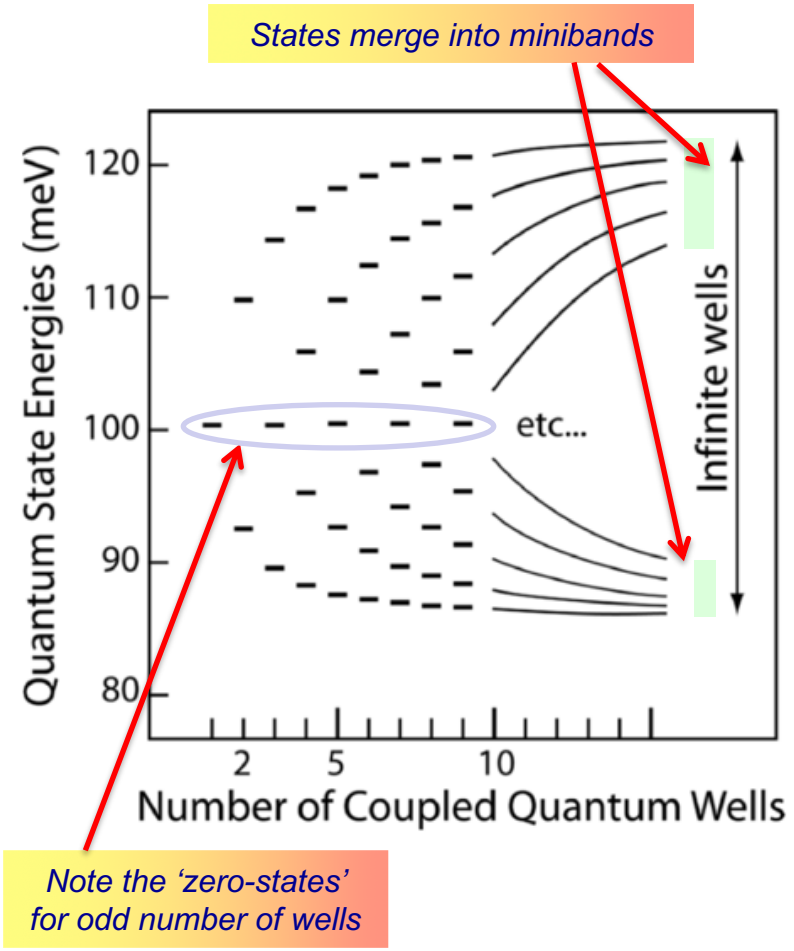

(Rockett)

Designer Quantum Structures

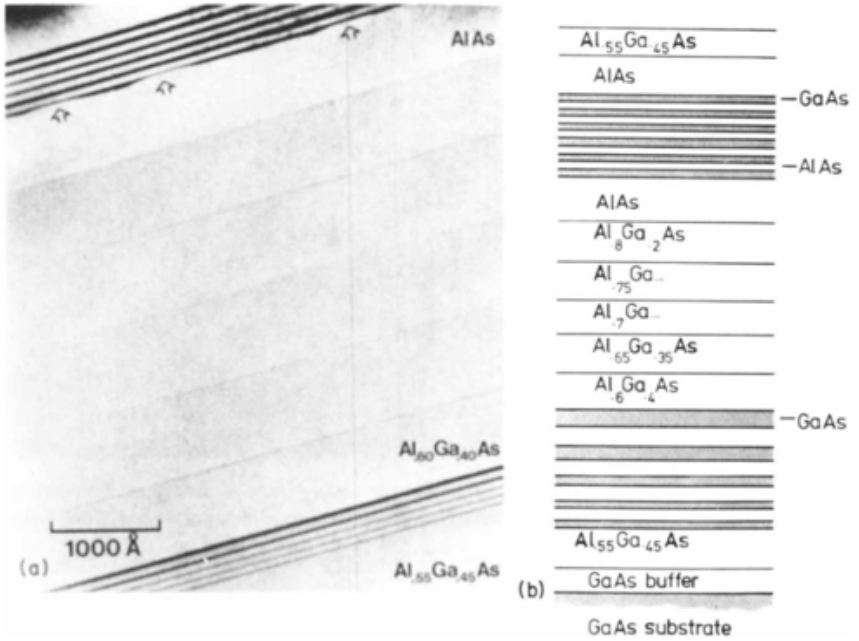

FIG. 3. (a) TEM characterization of a test sample grown by MOCVD. The growth sequence and the structure are shown in (b). The remarkable features are the sharpness of the very narrow GaAs layers (minimum ≈ 25 Å) appearing at the lower right-hand side corner, the interface roughness showing up at the uppermost interface of the AlAs layer, and the subsequent smoothing of this roughness by the multilayer growth (upper left-hand side corner) (after Leys *et al.*[61]).

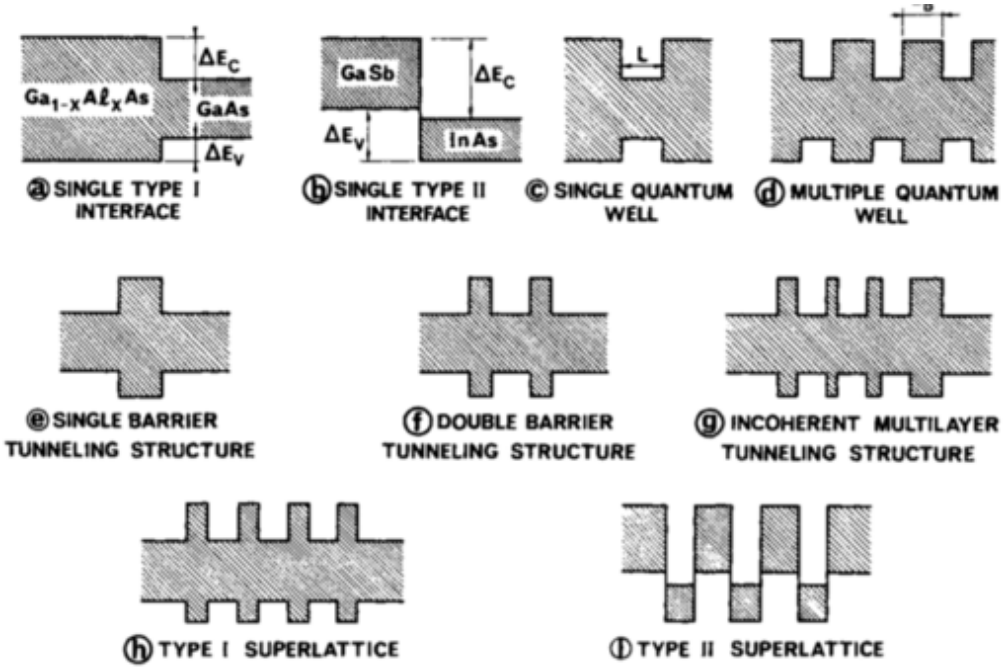

(Weisbuch/Vinter)

Heterostructure Superlattices

SUPERLATTICES

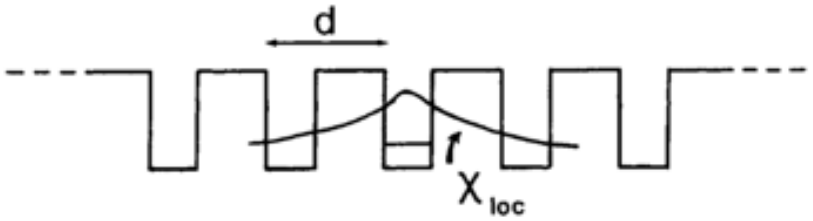

N WELLS

N-DEGENERATE GROUND STATE

TIGHT-BINDING APPROXIMATION

$$\Psi_q(z) = \frac{1}{N^{1/2}} \Sigma\, e^{iqnd}\, X_{loc}(z-nd)$$

$$\boxed{E = E_1 + S + 2T\cos qd}$$

$$S = \int X_{loc}(z-d)\,V(z)\,X_{loc}(z-d)\,dz$$

$$T = \int X_{loc}(z-d)\,V(z)\,X_{loc}(z)\,dz$$

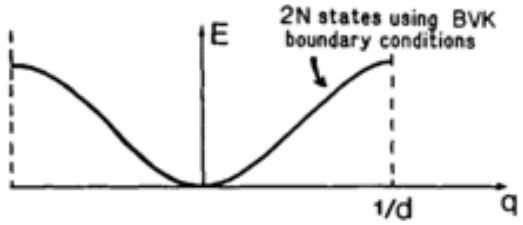

FIG. 15. Tight-binding model of superlattices.

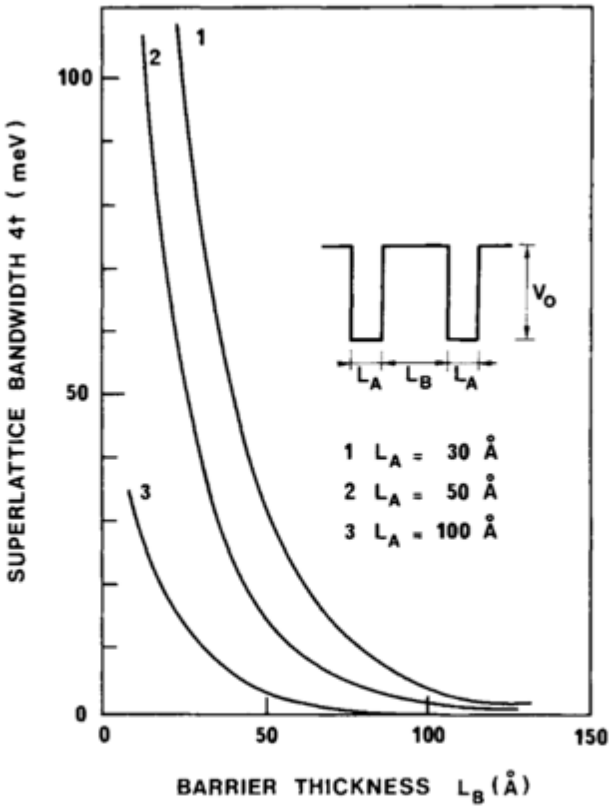

FIG. 16. Tight-binding model of GaAs/GaAlAs superlattices: Variation of the fundamental state bandwidth [$4t_i$ of Eq. (30)] in the tight-binding model as a function of barrier thickness for three different well thicknesses. $X = 0.2$; $V_0 = 212$ meV (after Bastard[125]).

(Weisbuch/Vinter)

Heterostructure Superlattices

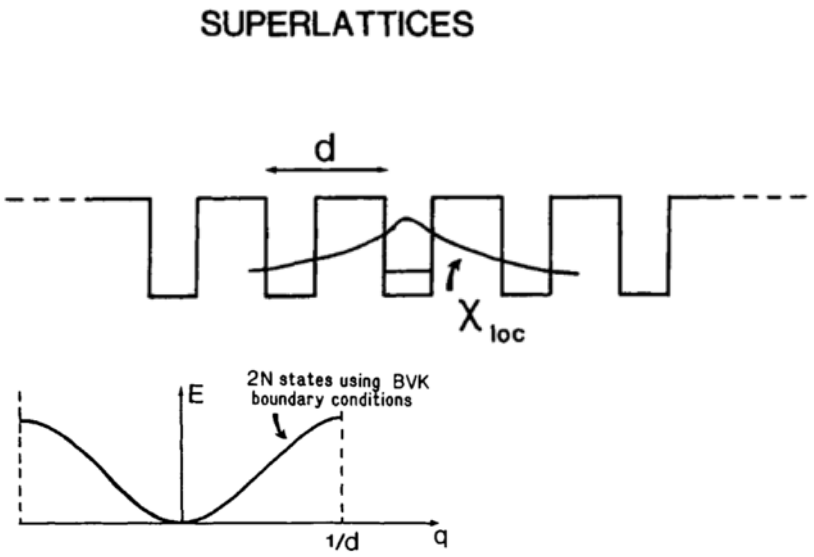

FIG. 15. Tight-binding model of superlattices.

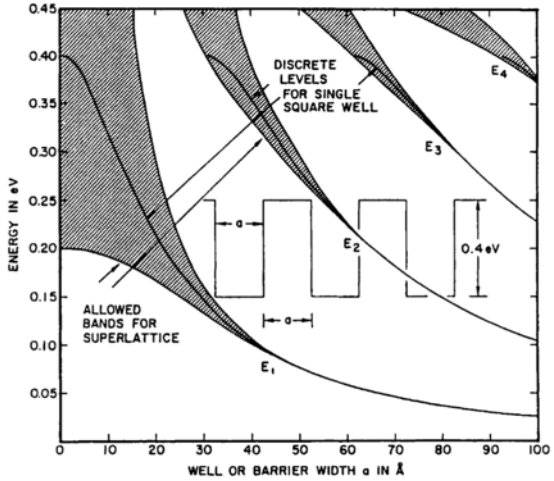

FIG. 18c. Allowed energy bands E_1, E_2, E_3, and E_4 (hatched) calculated as a function of well or barrier width ($L_z = L_B = a$) in a superlattice with a barrier potential $V = 0.4$ V. Note the existence of forbidden gaps even above the barrier potential (Reprinted with permission from World Scientific Pub. Co., L. Esaki, "Recent Topics in Semiconductor Physics" (H. Kamimura and Y. Toyozawce, eds.), 1983.)

$$E = E_1 + S + 2T\cos qd$$

$$\varepsilon_{n*}(q, k_\perp) = \hbar^2 k_\perp^2 / 2m + \varepsilon_n(q)$$

$$\rho_n(\varepsilon) = N \frac{m^*}{\pi\hbar^2} \arccos\left(\frac{\varepsilon_i - E_i - S_i}{2t_i}\right)$$

Density of states of a superlattice

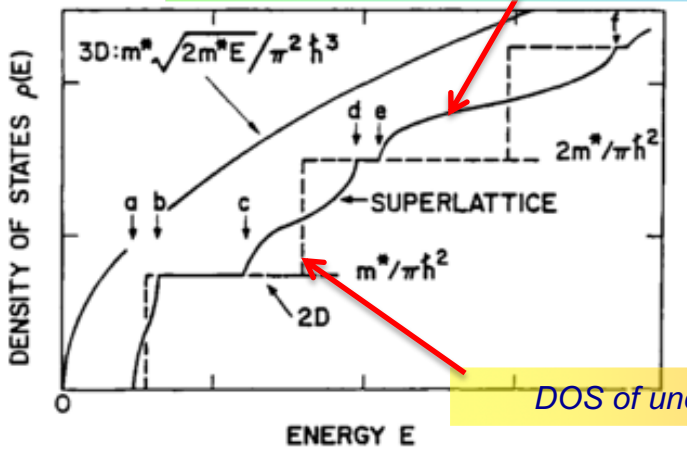

DOS of uncoupled 2D wells

FIG. 17. Comparison of the DOS of a superlattice with that of a 2D system (——) and a 3D isotropic system. Note the broadening of the superlattice band with band index as the overlap of wave functions increases with energy E in the tight-binding description, increasing the transfer matrix element t_i (Reprinted with permission from World Scientific Pub. Co., L. Esaki, "Recent Topics in Semiconductor Physics" (H. Kamimura and Y. Toyozawa, eds.), 1983.)

(Weisbuch/Vinter)

Semiconductor Physics Summary

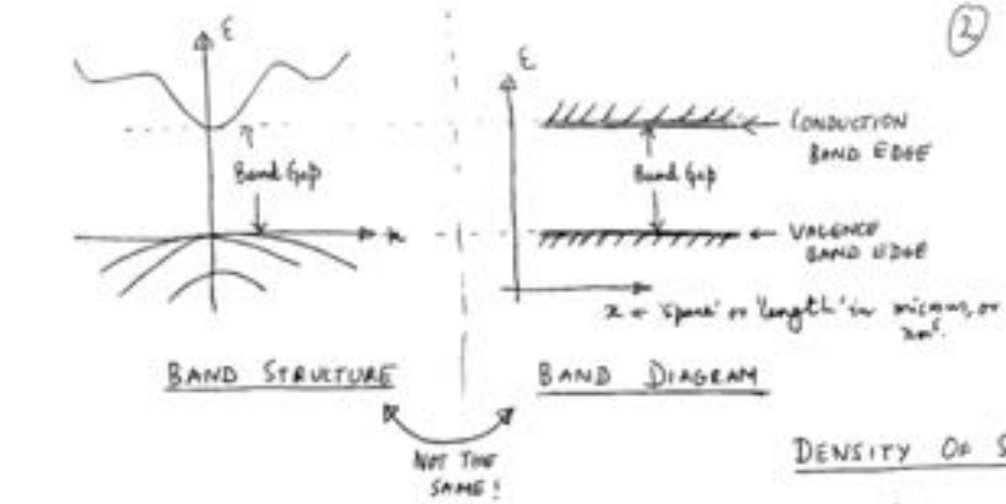

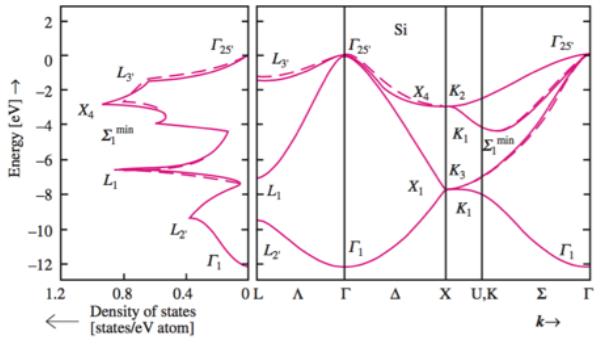

Fig. 2.24. The valence band structure and density of states (see Sect. 4.3.1 for definition) of Si calculated by the tight-binding method (*broken curves*) and by the empirical pseudopotential method (*solid lines*) [2.25]

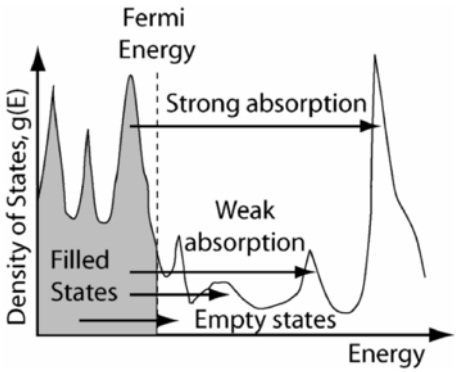

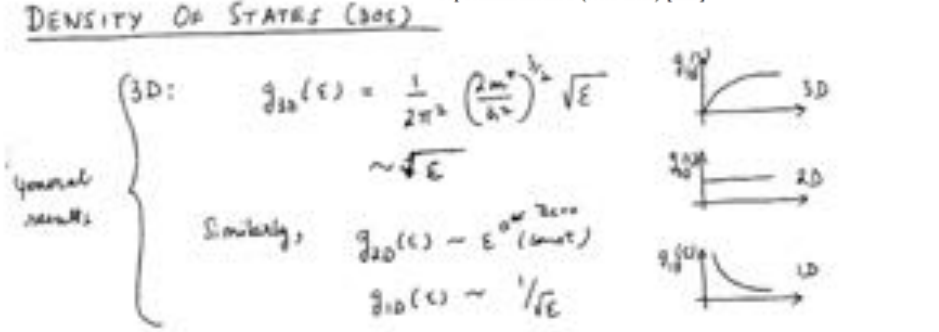

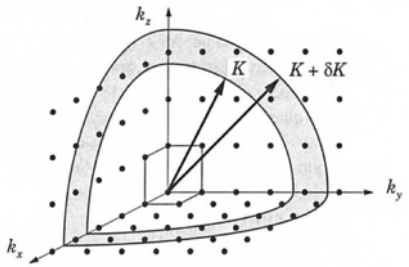

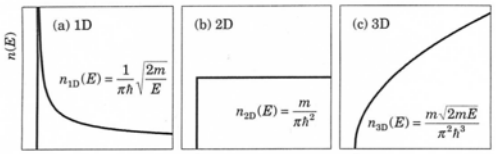

FIGURE 1.9. Densities of states for free electrons in one, two, and three dimensions.

Semiconductor Physics Summary

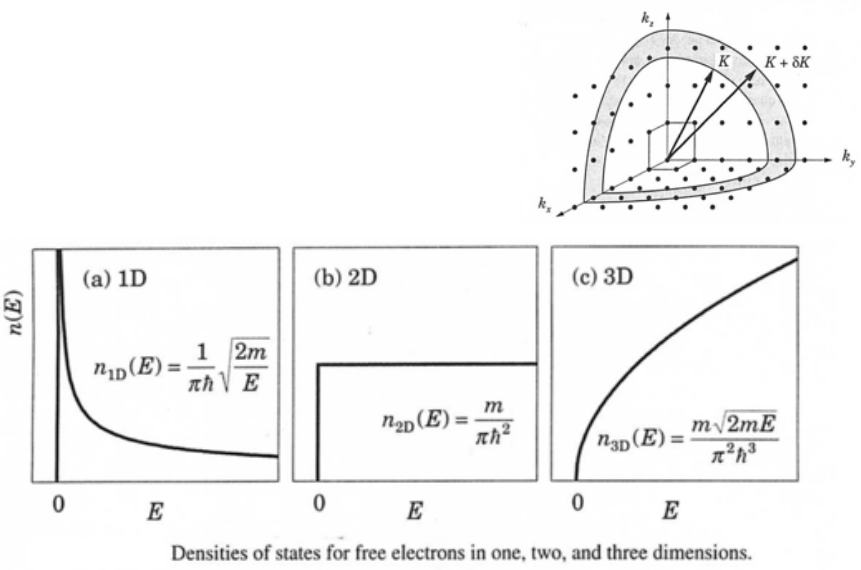

Densities of states for free electrons in one, two, and three dimensions.

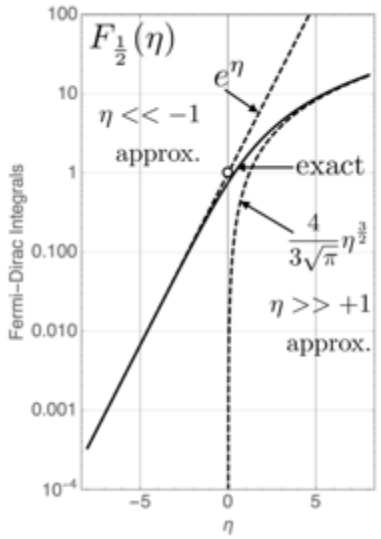

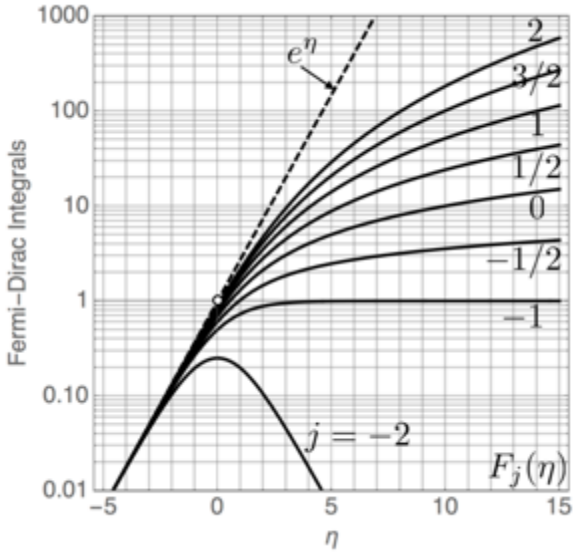

	0 Dimension	1 Dimension	2 Dimensions	3 Dimensions	d Dimensions
Conduction Bandstructure	E_c	$E_c + \frac{\hbar^2 k^2}{2m}$	$E_c + \frac{\hbar^2}{2m}(k_x^2 + k_y^2)$	$E_c + \frac{\hbar^2}{2m}(k_x^2 + k_y^2 + k_z^2)$	$E_c + \frac{\hbar^2}{2m}(\sum_{i=1}^{d} k_i^2)$
Conduction Band DOS $g_c^d(E)$	$g_c(E) = N_c^0 \delta(E - E_{min})$	$g_c(E) = \frac{N_c^0}{2}\left(\frac{2m}{\hbar^2}\right)^{\frac{1}{2}} \frac{1}{\sqrt{E - E_c}}$	$g_c(E) = \frac{N_c^0}{2\pi}\left(\frac{2m}{\hbar^2}\right) H(E - E_c)$	$g_c(E) = \frac{N_c^0}{2\pi^2}\left(\frac{2m}{\hbar^2}\right)^{\frac{3}{2}} \sqrt{E - E_c}$	$g_c(E) = \frac{N_c^0}{\Gamma(\frac{d}{2}+1)}\left(\frac{2m}{\hbar^2}\right)^{\frac{d}{2}} (E - E_c)^{\frac{d-2}{2}}$
Conduction Band-Edge Effective DOS N_c^0	$g_c(E_{min}) = N_c^0$	$g_c(E_{min}) = \frac{N_c^0}{2}\left(\frac{2m}{\hbar^2}\right)^{\frac{1}{2}}$	$g_c(E_{min}) = \frac{N_c^0}{2\pi}\left(\frac{2m}{\hbar^2}\right)$	$g_c(E_{min}) = \frac{N_c^0}{2\pi^2}\left(\frac{2m}{\hbar^2}\right)^{\frac{3}{2}}$	$g_c(E_{min}) = \frac{N_c^0}{\Gamma(\frac{d}{2}+1)}\left(\frac{2m}{\hbar^2}\right)^{\frac{d}{2}}$
Electron Density n_d	–	$N_c^0 \mathcal{F}_{-\frac{1}{2}}\left(\frac{E_F - E_c}{kT}\right)$	$N_c^0 \mathcal{F}_0\left(\frac{E_F - E_c}{kT}\right)$	$N_c^0 \mathcal{F}_{\frac{1}{2}}\left(\frac{E_F - E_c}{kT}\right)$	$N_c^0 \mathcal{F}_{\frac{d-2}{2}}\left(\frac{E_F - E_c}{kT}\right)$
Source Fermi Level E_{Fs} under bias V	–	$n_{1d} = \frac{1}{2}N_c^0 \mathcal{F}_{-\frac{1}{2}}\left(\frac{E_F - E_c}{kT}\right) + \mathcal{F}_{-\frac{1}{2}}\left(\frac{E_c - qV - E_{Fs}}{kT}\right)$	$n_{2d} = \frac{1}{2}N_c^0 \mathcal{F}_0\left(\frac{E_F - E_c}{kT}\right) + \mathcal{F}_0\left(\frac{E_c - qV - E_{Fs}}{kT}\right)$	$n_{3d} = \frac{1}{2}N_c^0 \mathcal{F}_{\frac{1}{2}}\left(\frac{E_F - E_c}{kT}\right) + \mathcal{F}_{\frac{1}{2}}\left(\frac{E_c - qV - E_{Fs}}{kT}\right)$	$n_d = \frac{1}{2}N_c^0 \mathcal{F}_{\frac{d-2}{2}}\left(\frac{E_F - E_c}{kT}\right) + \mathcal{F}_{\frac{d-2}{2}}\left(\frac{E_c - qV - E_{Fs}}{kT}\right)$
Ballistic Electron Current Density J_d at voltage V	–	$\frac{q}{2} \cdot N_c^0 \cdot \frac{kT}{2} \cdot \left[\mathcal{F}_{\frac{1}{2}}\left(\frac{E_F - E_c}{kT}\right) - \mathcal{F}_{\frac{1}{2}}\left(\frac{E_c - qV - E_{Fs}}{kT}\right)\right]$	$\frac{q}{2} \cdot N_c^0 \cdot \frac{kT}{2} \cdot \left[\mathcal{F}_1\left(\frac{E_F - E_c}{kT}\right) - \mathcal{F}_1\left(\frac{E_c - qV - E_{Fs}}{kT}\right)\right]$	$\frac{q}{2} \cdot N_c^0 \cdot \frac{kT}{2} \cdot \left[\mathcal{F}_{\frac{3}{2}}\left(\frac{E_F - E_c}{kT}\right) - \mathcal{F}_{\frac{3}{2}}\left(\frac{E_c - qV - E_{Fs}}{kT}\right)\right]$	$\frac{q}{2} \cdot N_c^0 \cdot \frac{kT}{2} \cdot \left[\mathcal{F}_{\frac{d}{2}}\left(\frac{E_F - E_c}{kT}\right) - \mathcal{F}_{\frac{d}{2}}\left(\frac{E_c - qV - E_{Fs}}{kT}\right)\right]$
Valence Bandstructure	E_v	$E_v - \frac{\hbar^2 k^2}{2m}$	$E_v - \frac{\hbar^2}{2m}(k_x^2 + k_y^2)$	$E_v - \frac{\hbar^2}{2m}(k_x^2 + k_y^2 + k_z^2)$	$E_v - \frac{\hbar^2}{2m}(\sum_{i=1}^{d} k_i^2)$
Valence Band DOS $g_v^d(E)$	$g_v(E) = N_v^0 \delta(E - E_{max})$	$g_v(E) = \frac{N_v^0}{2}\left(\frac{2m}{\hbar^2}\right)^{\frac{1}{2}} \frac{1}{\sqrt{E_v - E}}$	$g_v(E) = \frac{N_v^0}{2\pi}\left(\frac{2m}{\hbar^2}\right) H(E_v - E)$	$g_v(E) = \frac{N_v^0}{2\pi^2}\left(\frac{2m}{\hbar^2}\right)^{\frac{3}{2}} \sqrt{E_v - E}$	$g_v(E) = \frac{N_v^0}{\Gamma(\frac{d}{2}+1)}\left(\frac{2m}{\hbar^2}\right)^{\frac{d}{2}} (E_v - E)^{\frac{d-2}{2}}$
Valence Band-Edge Effective DOS N_v^0	–	$g_v(E_{max}) = N_v^0$	$g_v(E_{max}) = \frac{N_v^0}{2\pi}\left(\frac{2m}{\hbar^2}\right)$	$g_v(E_{max}) = \frac{N_v^0}{2\pi^2}\left(\frac{2m}{\hbar^2}\right)^{\frac{3}{2}}$	$g_v(E_{max}) = \frac{N_v^0}{\Gamma(\frac{d}{2}+1)}\left(\frac{2m}{\hbar^2}\right)^{\frac{d}{2}}$
Hole Density p_d	–	$N_v^0 \mathcal{F}_{-\frac{1}{2}}\left(\frac{E_v - E_F}{kT}\right)$	$N_v^0 \mathcal{F}_0\left(\frac{E_v - E_F}{kT}\right)$	$N_v^0 \mathcal{F}_{\frac{1}{2}}\left(\frac{E_v - E_F}{kT}\right)$	$N_v^0 \mathcal{F}_{\frac{d-2}{2}}\left(\frac{E_v - E_F}{kT}\right)$
Source Fermi Level E_{Fs} under bias V	–	$p_{1d} = \frac{1}{2}N_v^0 \mathcal{F}_{-\frac{1}{2}}\left(\frac{E_v - E_F}{kT}\right) + \mathcal{F}_{-\frac{1}{2}}\left(\frac{E_{Fs} + qV - E_v}{kT}\right)$	$p_{2d} = \frac{1}{2}N_v^0 \mathcal{F}_0\left(\frac{E_v - E_F}{kT}\right) + \mathcal{F}_0\left(\frac{E_{Fs} + qV - E_v}{kT}\right)$	$p_{3d} = \frac{1}{2}N_v^0 \mathcal{F}_{\frac{1}{2}}\left(\frac{E_v - E_F}{kT}\right) + \mathcal{F}_{\frac{1}{2}}\left(\frac{E_{Fs} + qV - E_v}{kT}\right)$	$p_d = \frac{1}{2}N_v^0 \mathcal{F}_{\frac{d-2}{2}}\left(\frac{E_v - E_F}{kT}\right) + \mathcal{F}_{\frac{d-2}{2}}\left(\frac{E_{Fs} + qV - E_v}{kT}\right)$
Ballistic Hole Current Density J_d	–	$\frac{q}{2} \cdot N_v^0 \cdot \frac{kT}{2} \cdot \left[\mathcal{F}_{\frac{1}{2}}\left(\frac{E_v - E_F}{kT}\right) - \mathcal{F}_{\frac{1}{2}}\left(\frac{E_{Fs} + qV - E_v}{kT}\right)\right]$	$\frac{q}{2} \cdot N_v^0 \cdot \frac{kT}{2} \cdot \left[\mathcal{F}_1\left(\frac{E_v - E_F}{kT}\right) - \mathcal{F}_1\left(\frac{E_{Fs} + qV - E_v}{kT}\right)\right]$	$\frac{q}{2} \cdot N_v^0 \cdot \frac{kT}{2} \cdot \left[\mathcal{F}_{\frac{3}{2}}\left(\frac{E_v - E_F}{kT}\right) - \mathcal{F}_{\frac{3}{2}}\left(\frac{E_{Fs} + qV - E_v}{kT}\right)\right]$	$\frac{q}{2} \cdot N_v^0 \cdot \frac{kT}{2} \cdot \left[\mathcal{F}_{\frac{d}{2}}\left(\frac{E_v - E_F}{kT}\right) - \mathcal{F}_{\frac{d}{2}}\left(\frac{E_{Fs} + qV - E_v}{kT}\right)\right]$

Physics of Semiconductor Nanostructures Summary

Table 1: Quantum Electronic, Photonic, and Statistical Properties of Conduction and Valence Band Electrons in Semiconductor Nanostructures.

- E_c is the band edge, and m_c^* the effective mass of the conduction band. E_v is the band edge, and m_v^* the effective mass of the valence band.
- For low dimensions, E_c and E_v, and the bandgap $E_g = E_c - E_v$ include the quantum confinement energies if present.
- h is Planck's constant, $\hbar = \frac{h}{2\pi}$, k_b is the Boltzmann constant, and q the electron charge.
- g_s is the spin degeneracy, and g_v the valley degeneracy.
- $F_j(\eta) = \frac{1}{\Gamma(j+1)} \int_0^\infty d\varepsilon \frac{\varepsilon^j}{1+e^{\varepsilon-\eta}}$ is the Fermi-Dirac integral of order j, and $\Gamma(...)$ is the Gamma function.
- E_f is the Fermi level at equilibrium. E_{fs} is the source quasi-Fermi level and E_{fd} the drain quasi-Fermi level.
- Similarly, F_n is the conduction band quasi-Fermi level and F_p is the valence band quasi-Fermi level.
- $h\nu$ is the photon energy of frequency ν, and L_x, L_y, L_z are the dimensions of the semiconductor nanostructure.
- A and B are the Einstein A and B coefficients, $\lambda_0 = c/\nu$ the wavelength of the photon in vacuum, and n the refractive index of the semiconductor.
- $f_c(E_2) = 1/[1 + e^{\frac{E_2 - F_n}{k_b T}}]$ is the Fermi-Dirac occupation function of state $E_2 = E_c + \frac{\hbar^2 k^2}{2m_c^*}$ in the conduction band.
- $f_v(E_1) = 1/[1 + e^{\frac{E_1 - F_p}{k_b T}}]$ is the Fermi-Dirac occupation function of state $E_1 = E_v - \frac{\hbar^2 k^2}{2m_v^*}$ in the valence band.
- $E_2 - E_1 = h\nu = E_g + \frac{\hbar^2 k^2}{2m_r^*}$ is the energy of the photon emitted when the electron transitions from $E_2 \to E_1$ radiatively.
- The Einstein A and B coefficients are related by $\frac{A}{B} = \frac{8\pi n^3 \nu^3 h}{c^3}$.
- The photon density is $\rho_\nu = I_\nu/(c/n)$ in eV/cm^3, c/n is the speed of light in a media of refractive index n, and $I_\nu = E_0^2/2\eta$ in W/cm^2 is the Poynting energy density with electric field amplitude E_0 and wave impedance η.

Ballistic Transport in 1 Dimension

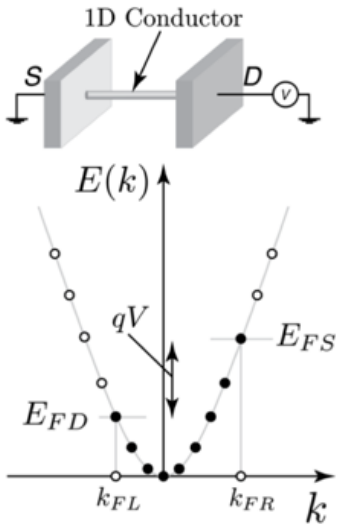

Fig. 5.5 Quantum picture of current flow in the 1D k-space due to a difference in the occupation functions of right-going and left-going eigenstates. The left contact is called the source, and the right contact the drain.

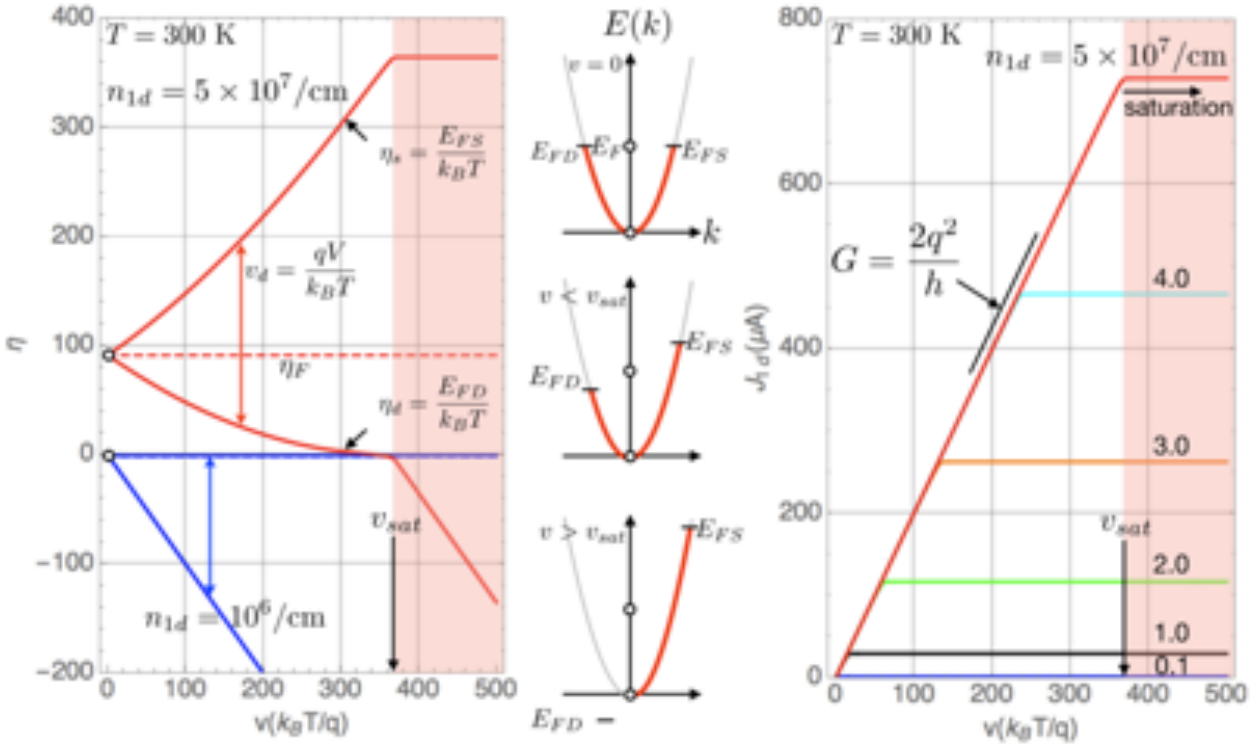

Fig. 5.8 The left plot shows the calcuated normalized Fermi level $\eta_F = E_F/k_BT$ at $V = 0$, and the split normalized Fermi levels η_s and η_d for nonzero normalized voltages $v_d = qV/k_BT$ for two values of 1D electron density at 300 K. The red curves are for $n_{1d} = 5 \times 10^7$/cm, and the blue for $n_{1d} = 10^6$/cm. The right plot shows the resulting quantum mechanical current flowing in response to the voltage for six values of 1D electron densities ranging from $0.1 - 5.0 \times 10^7$/cm. For example, at a 1D electron density of $n_{1d} = 10^7$/cm, the maximum (or saturation) current is ~ 70 μA. The middle $E(k)$ figures show the changes in the corresponding occupied electron states for $n_{1d} = 5 \times 10^7$/cm for three different voltages.

$$\eta_s - \eta_d = v_d, \text{ and } n_{1d} = \frac{1}{2} N_c^{1d}(T)[F_{-\frac{1}{2}}(\eta_s) + F_{-\frac{1}{2}}(\eta_d)]$$

$$J^{1d} = J_R^{1d} - J_L^{1d} = \frac{q g_s g_v}{2\pi\hbar}(k_B T)\ln\left(\frac{1+e^{\eta_s}}{1+e^{\eta_d}}\right).$$

Ballistic Transport in 1, 2, and 3 Dimensions

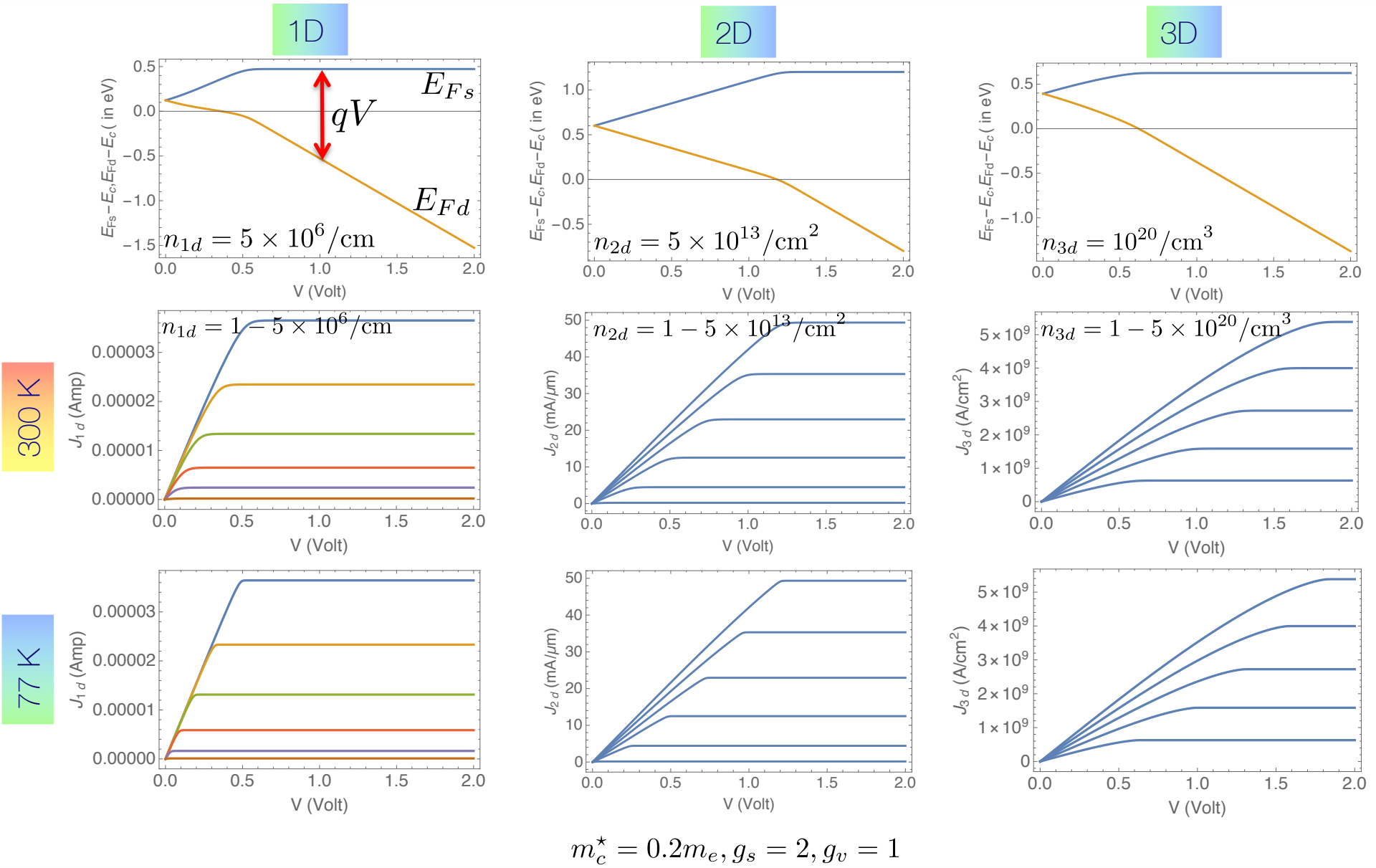

$$m_c^\star = 0.2 m_e, g_s = 2, g_v = 1$$

Ballistic Current in 2 Dimensions

Ballistic metal-oxide-semiconductor field effect transistor

Kenji Natori
Institute of Applied Physics, University of Tsukuba, Tsukuba, Ibaraki 305, Japan

(Received 14 March 1994; accepted for publication 6 July 1994)

J. Appl. Phys. **76** (8), 15 October 1994 0021-8979/94/76(8)/4879/12/$6.00

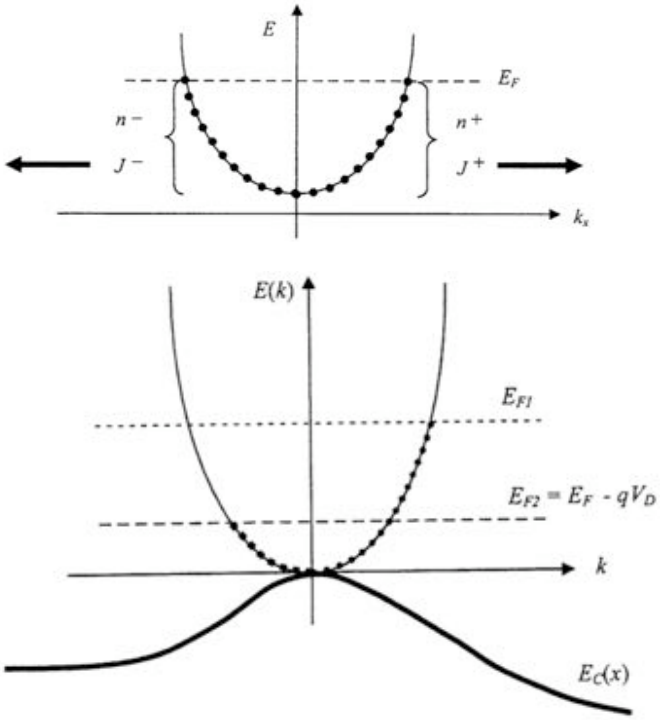

	2 Dimensions
Conduction Bandstructure	$E_c + \frac{\hbar^2}{2m_c^*}(k_x^2 + k_y^2)$
Conduction Band DOS $g_c^d(E)$	$\frac{g_s g_v}{2\pi}(\frac{2m_c^*}{\hbar^2})\theta(E - E_c)$
Conduction Band-Edge Effective DOS N_c^d	$g_s g_v(\frac{2\pi m_c^* k_b T}{\hbar^2})$
Electron Density n_d	$N_c^{2d} F_0(\frac{E_F - E_c}{k_b T})$
Source Fermi Level E_{Fs} under bias V	$n_{2d} = \frac{1}{2} N_c^{2d}[F_0(\frac{E_{Fs} - E_c}{k_b T}) + F_0(\frac{(E_{Fs} - qV) - E_c}{k_b T})]$
Ballistic Electron Current Density J_d at voltage V	$\frac{q^2}{h} \cdot N_c^{1d} \cdot \frac{k_b T}{q} \cdot [F_{\frac{1}{2}}(\frac{E_{Fs} - E_c}{k_b T}) - F_{\frac{1}{2}}(\frac{(E_{Fs} - qV) - E_c}{k_b T})]$

- The physics of a Ballistic FET can be understood by inspecting the carrier distribution in k-space at the source-injection Point.

Ballistic FET

2 Dimensions
$E_c + \frac{\hbar^2}{2m_c^*}(k_x^2 + k_y^2)$
$\frac{g_s g_v}{2\pi}(\frac{2m^*}{\hbar^2})\theta(E - E_c)$
$g_s g_v(\frac{2\pi m_c^* k_b T}{h^2})$
$N_c^{2d} F_0(\frac{E_F - E_c}{k_b T})$
$n_{2d} = \frac{1}{2} N_c^{2d}[F_0(\frac{E_{Fs} - E_c}{k_b T}) + F_0(\frac{(E_{Fs} - qV) - E_c}{k_b T})]$
$\frac{q^2}{h} \cdot N_c^{1d} \cdot \frac{k_b T}{q} \cdot [F_{\frac{1}{2}}(\frac{E_{Fs} - E_c}{k_b T}) - F_{\frac{1}{2}}(\frac{(E_{Fs} - qV) - E_c}{k_b T})]$

$$\frac{q^2 n_s}{C_b} + kT \ln\left(e^{\frac{qn_s}{C_q V_{th}}} - 1\right) = q(V_{gs} - V_T)$$

$$\Longrightarrow \boxed{e^{\frac{qn_s}{C_b V_{th}}}\left(e^{\frac{qn_s}{C_q V_{th}}} - 1\right) = e^{\frac{V_{gs} - V_T}{V_{th}}}}$$

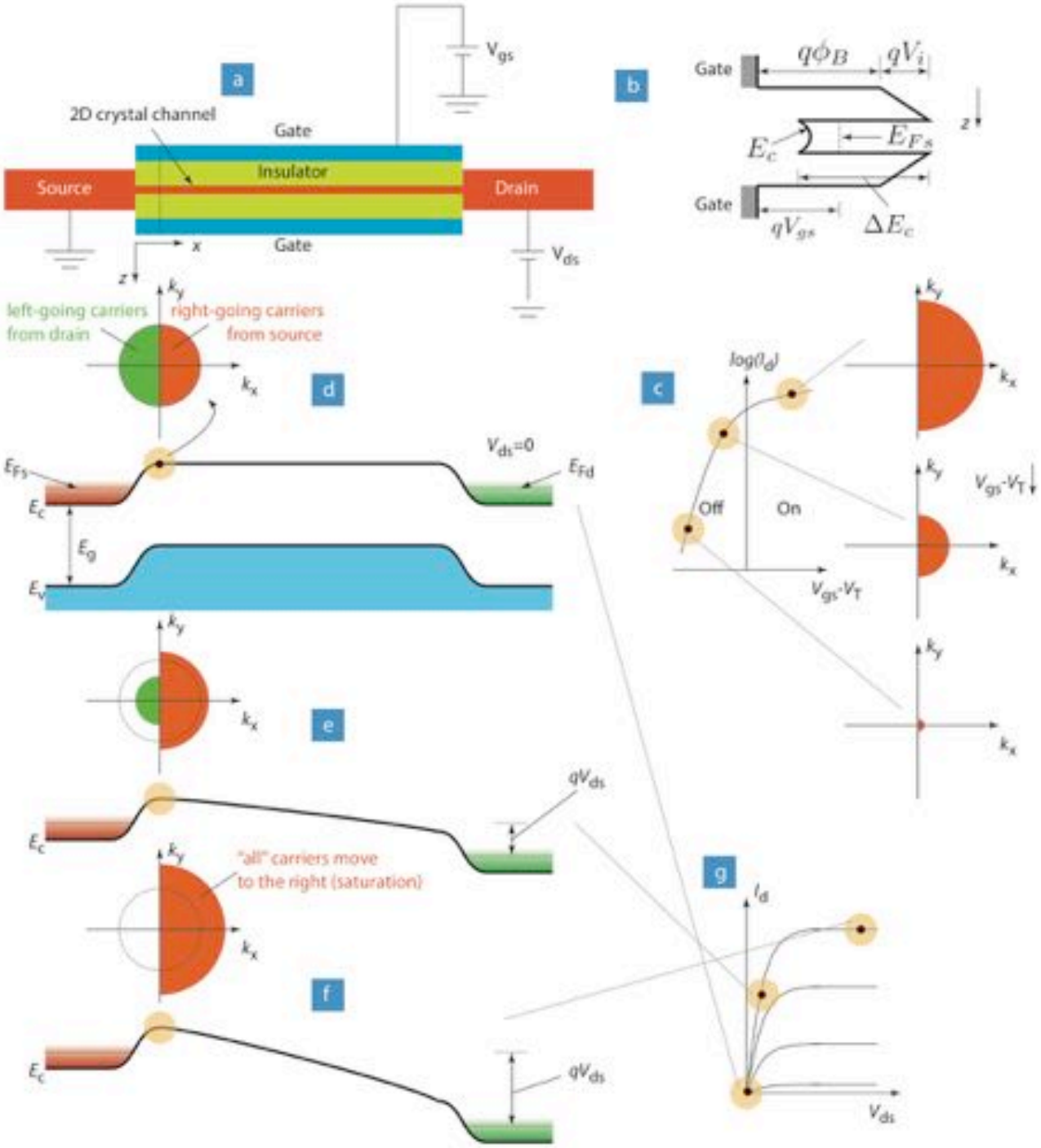

Ballistic FET

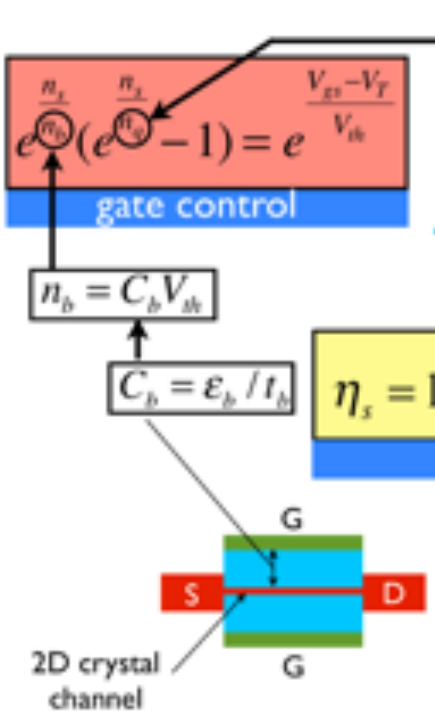

$$n_q = q^2 D_0 V_{th} = C_q V_{th}$$

$$D_0 = g_s \cdot g_v \frac{m_c^*}{2\pi\hbar^2}$$

$$\frac{n_s}{n_0}\left(e^{\frac{n_s}{n_q}} - 1\right) = e^{\frac{V_{gs}-V_T}{V_{th}}}$$

gate control

$$n_b = C_b V_{th}$$

$$C_b = \varepsilon_b / t_b$$

$$\eta_s = \ln\left[\sqrt{(1+e^{\nu_d})^2 + 4e^{\nu_d}\left(e^{2n_s(V_{gs})/n_q} - 1\right)} - (1+e^{\nu_d})\right] - \ln 2$$

drain control

$$J_0 = \frac{q g_s g_v \sqrt{2m_c^*}}{2\pi^2\hbar^2}(kT)^{\frac{3}{2}}$$

$$I_d / W = J_0 [F_{1/2}(\eta_s) - F_{1/2}(\eta_d)]$$

FET output characteristics

$$F_j(\eta) = \frac{1}{\Gamma(j+1)} \int_0^\infty du \frac{u^j}{1+e^{u-\eta}}$$

$$F_j(\eta) \underbrace{\approx}_{\eta<<-1} e^{\eta}$$

$$F_j(\eta) \underbrace{\approx}_{\eta>>1} \frac{\eta^{j+1}}{\Gamma(j+2)}$$

$$\frac{I_d}{W} \sim J_0 e^{\frac{V_{gs}-V_T}{V_{th}}}$$

Subthreshold (off)

$$\frac{I_d}{W} \sim J_0 \left(\frac{V_{gs}-V_T}{V_{th}}\right)^{\frac{3}{2}}$$

On-state

Ballistic FET

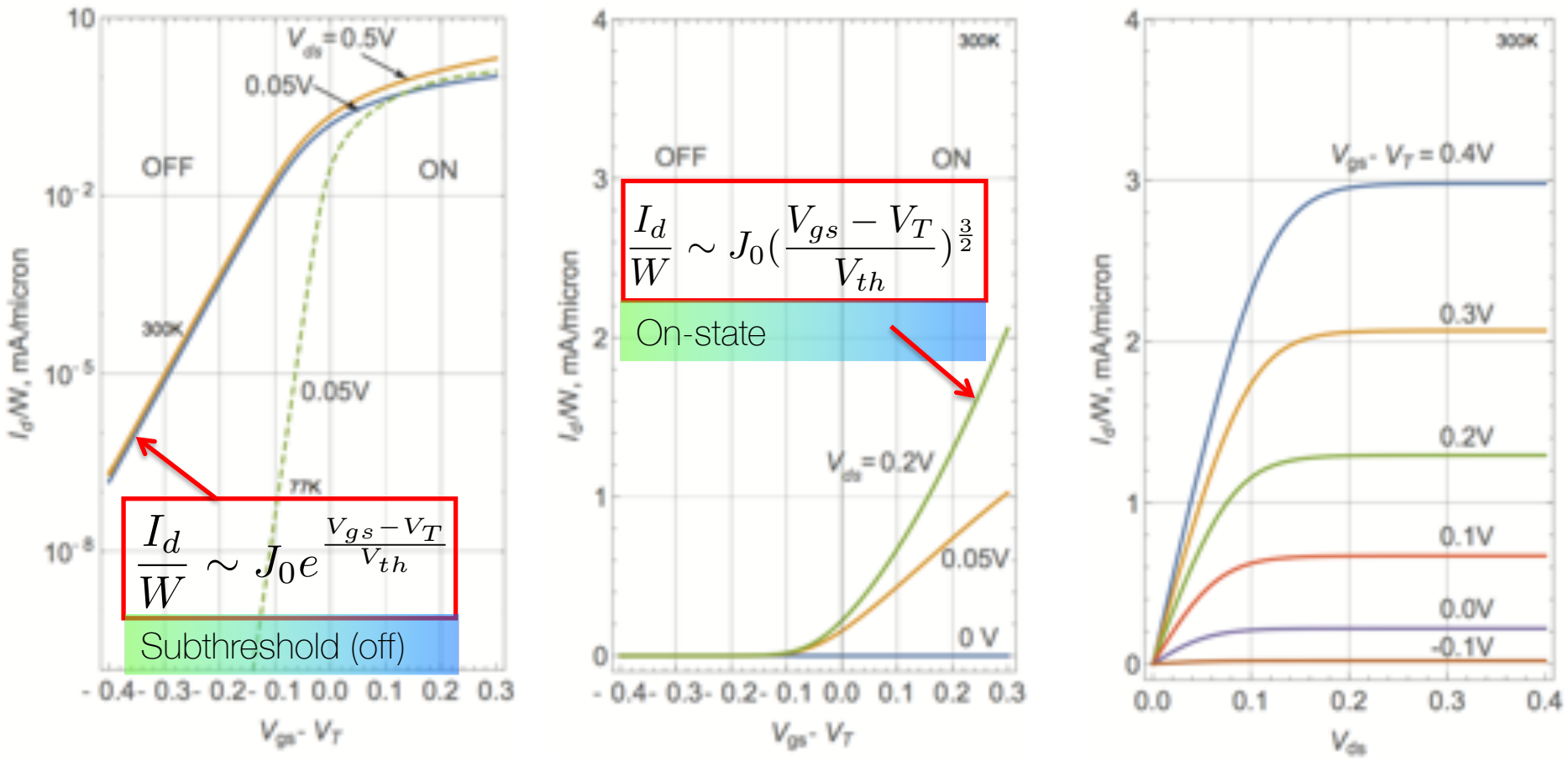

FIGURE 10.4: Ballistic Silicon FET. The device dimensions are $t_b = 1$ nm, $\epsilon_b = 10\epsilon_0$, and for Silicon, $m^* = 0.2m_0$ and $g_v = 2.5$ are used.

- Note the on-off ratio, and the sharper switching at low temperatures. The subthreshold slope is ~(kT/q)ln(10).
- This calculation neglects the contact resistance incurred in injecting carriers from 3D source to 2D channel.

Ballistic FET Limits

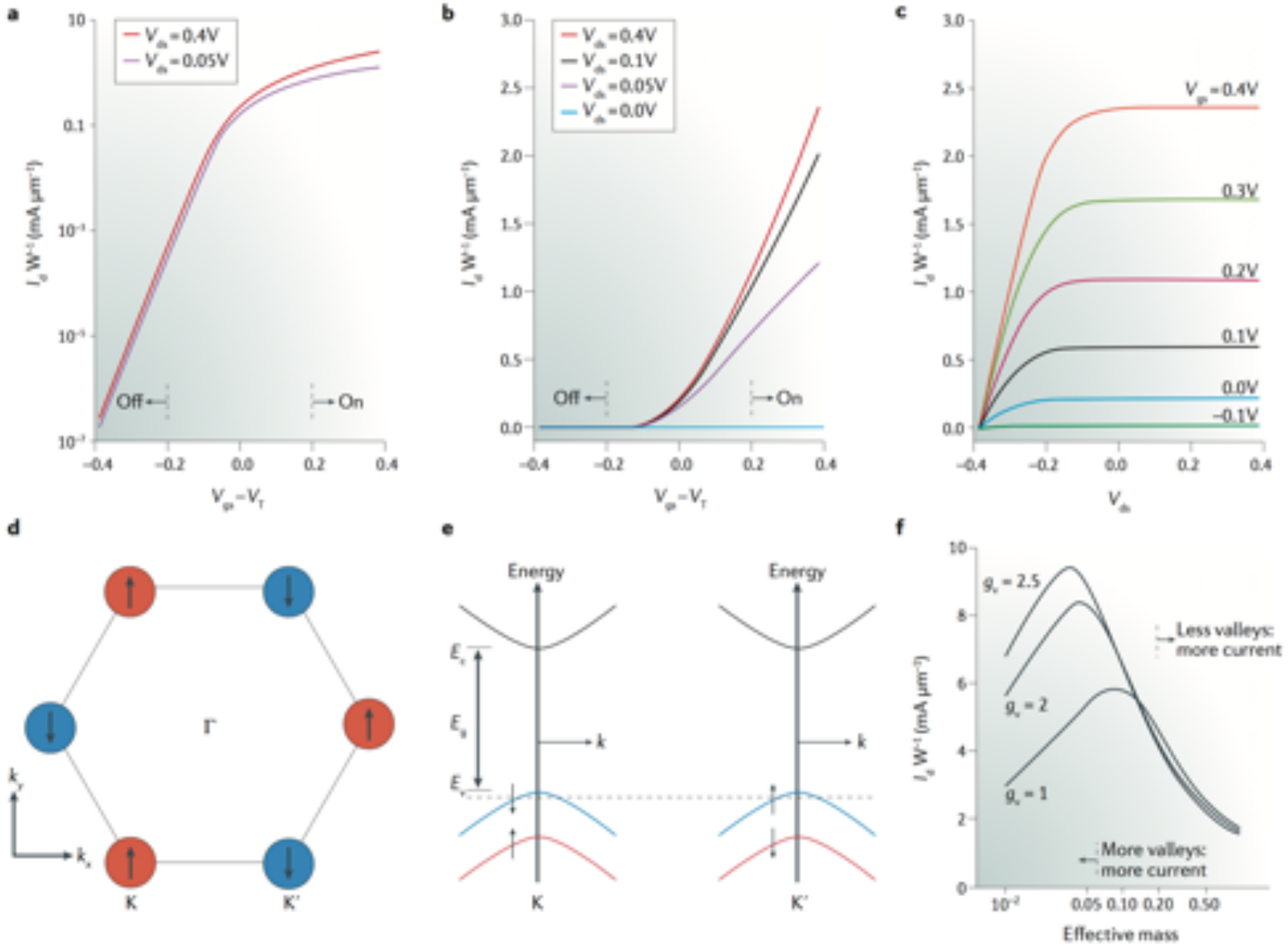

Transistor Applications

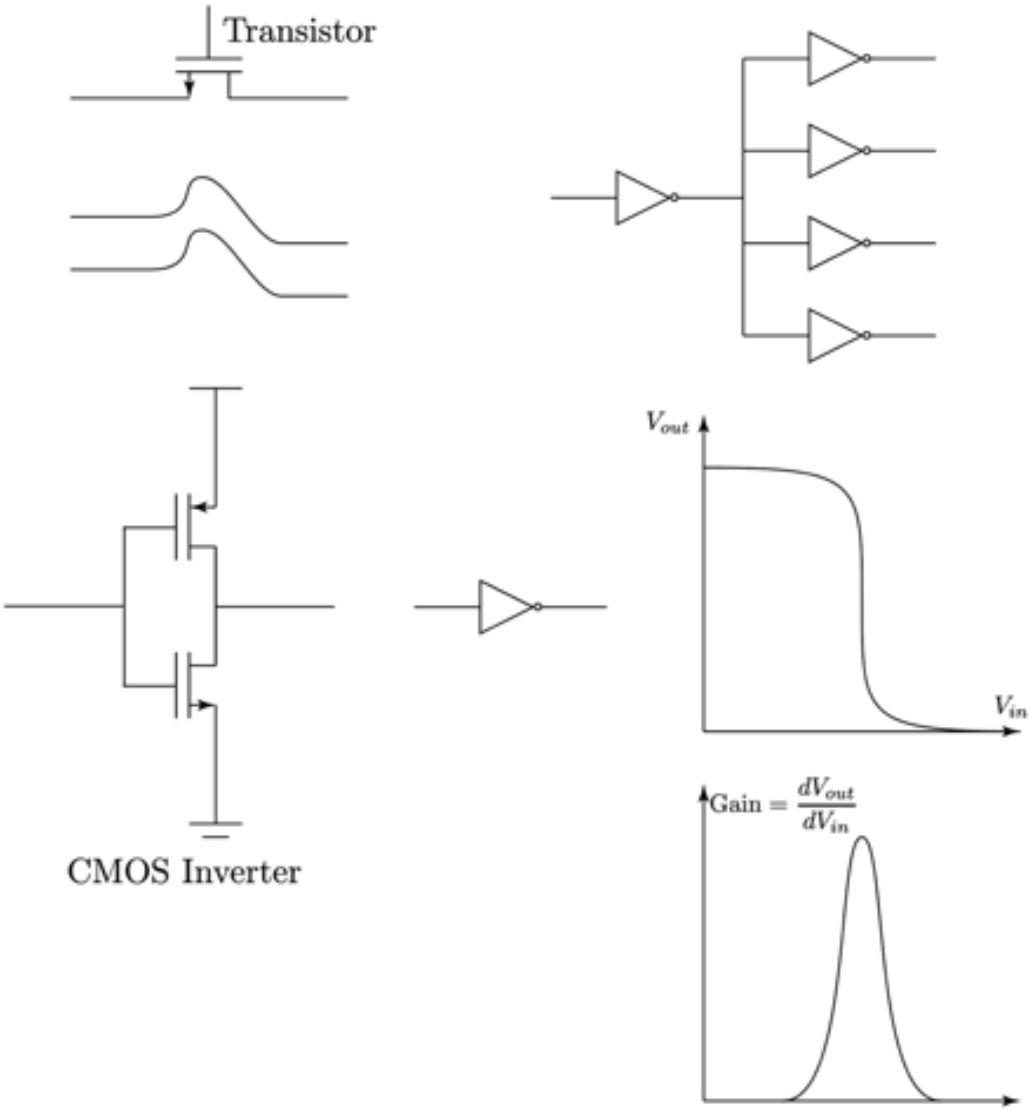

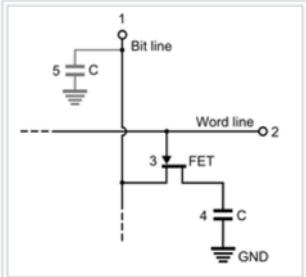

DRAM Cell (1 Transistor and one capacitor)

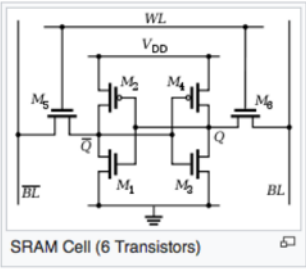

SRAM Cell (6 Transistors)

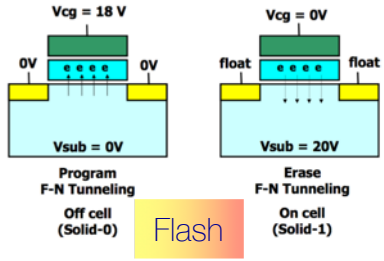

Flash

Memory

Transistor Applications

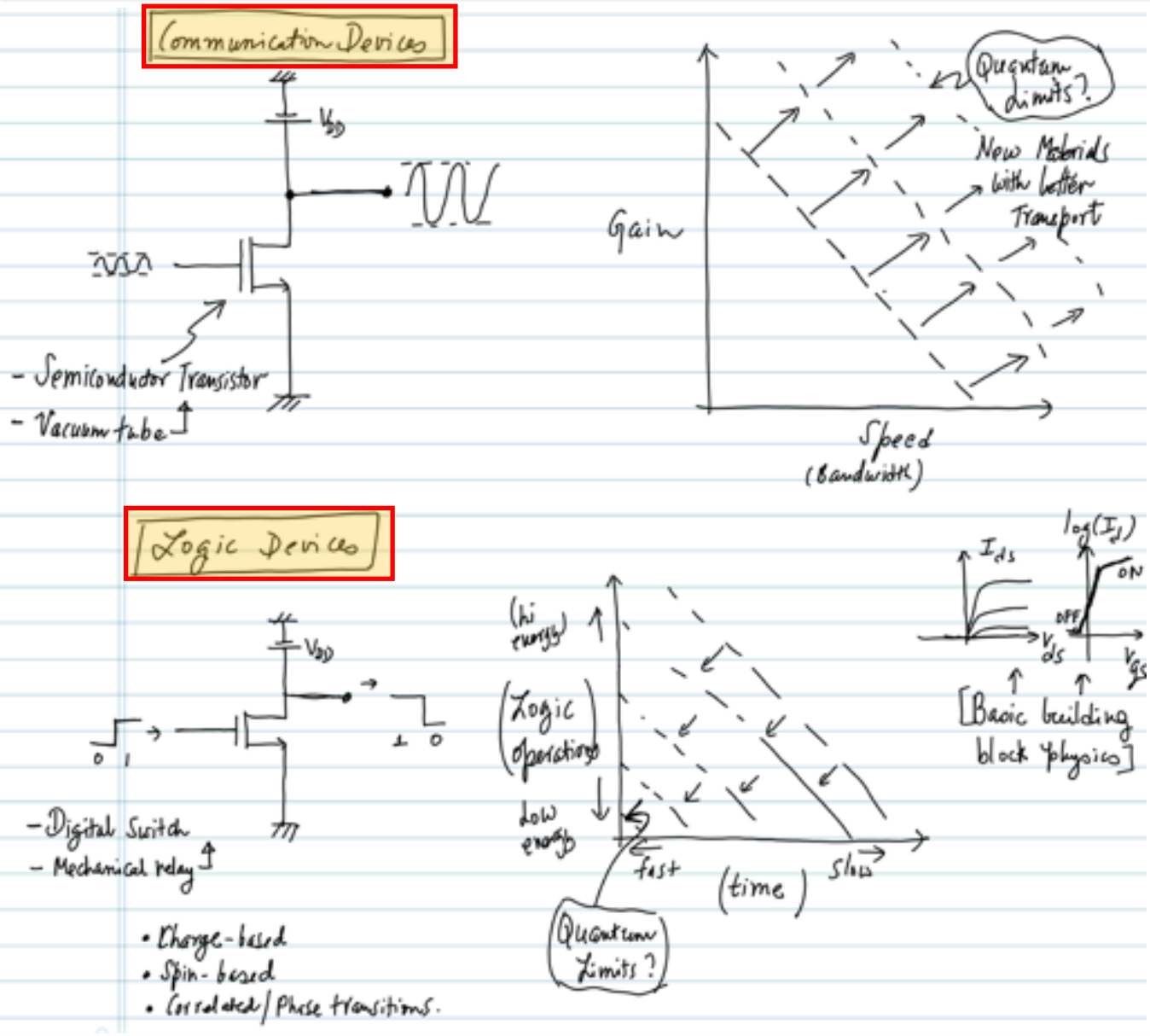

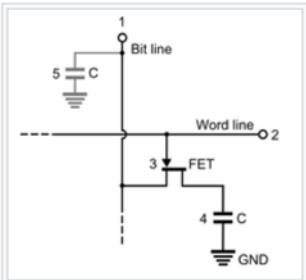

DRAM Cell (1 Transistor and one capacitor)

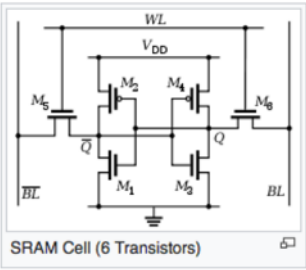

SRAM Cell (6 Transistors)

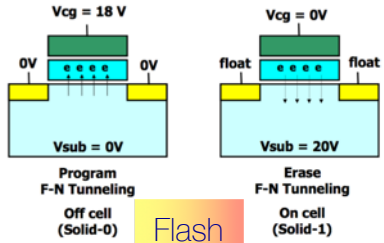

Memory

~Today

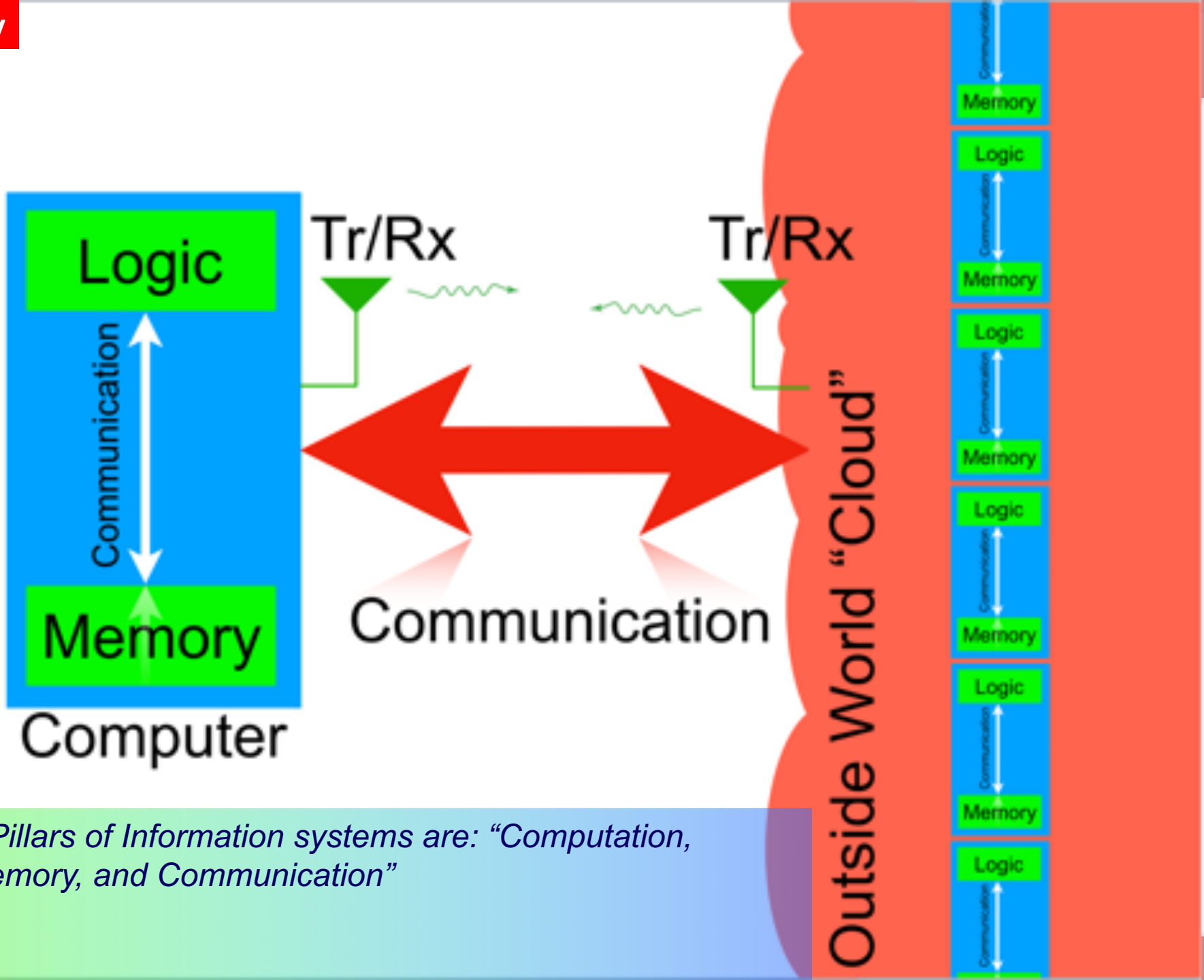

- *3 Pillars of Information systems are: "Computation, Memory, and Communication"*

The "humble" transistor: Many Avatars…

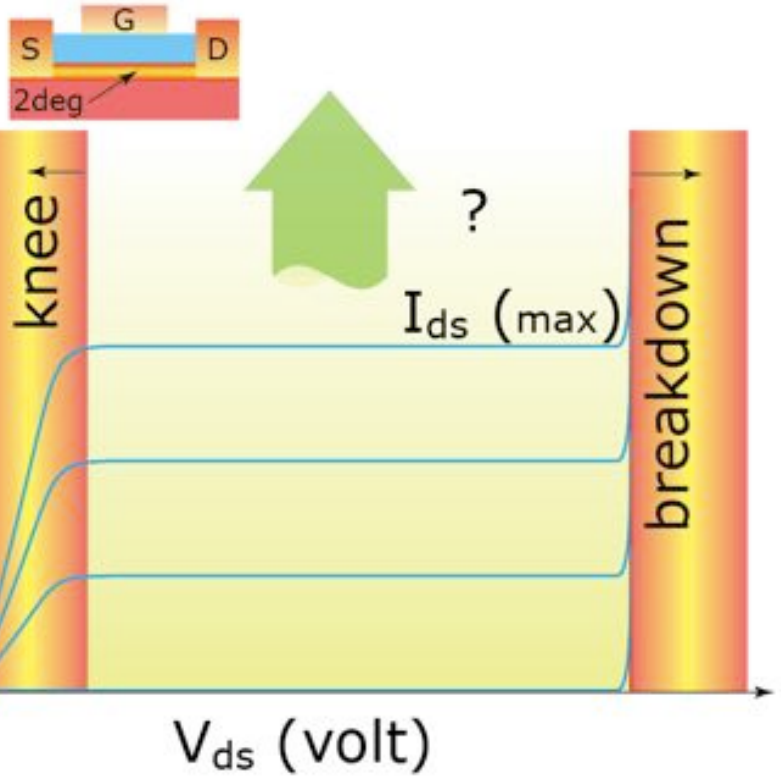

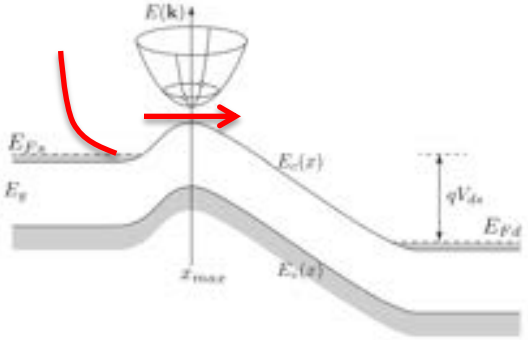

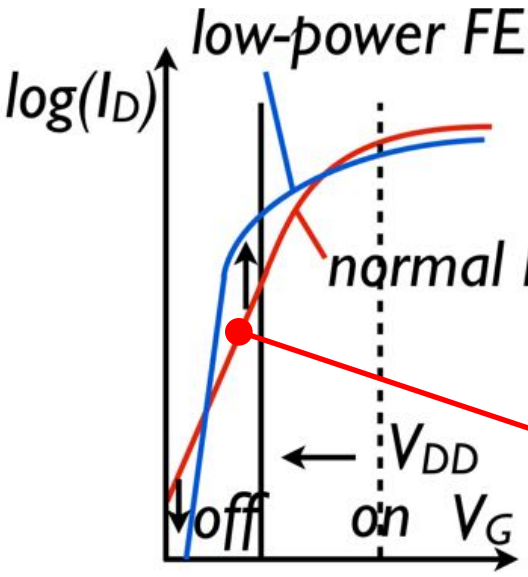

$$I_D \sim e^{\frac{qV_{gs}}{kT}}$$

$$\rightarrow SS \sim \frac{kT}{q}\ln 10$$

$$\sim 60 \frac{\text{mV}}{\text{decade}}$$

- The transistor is an electronic switch
- It is also an amplifier: it has gain
- Gain @ high speed: RF electronics
- Switching @ high voltages: Power electronics

The "humble" transistor: Many Avatars…

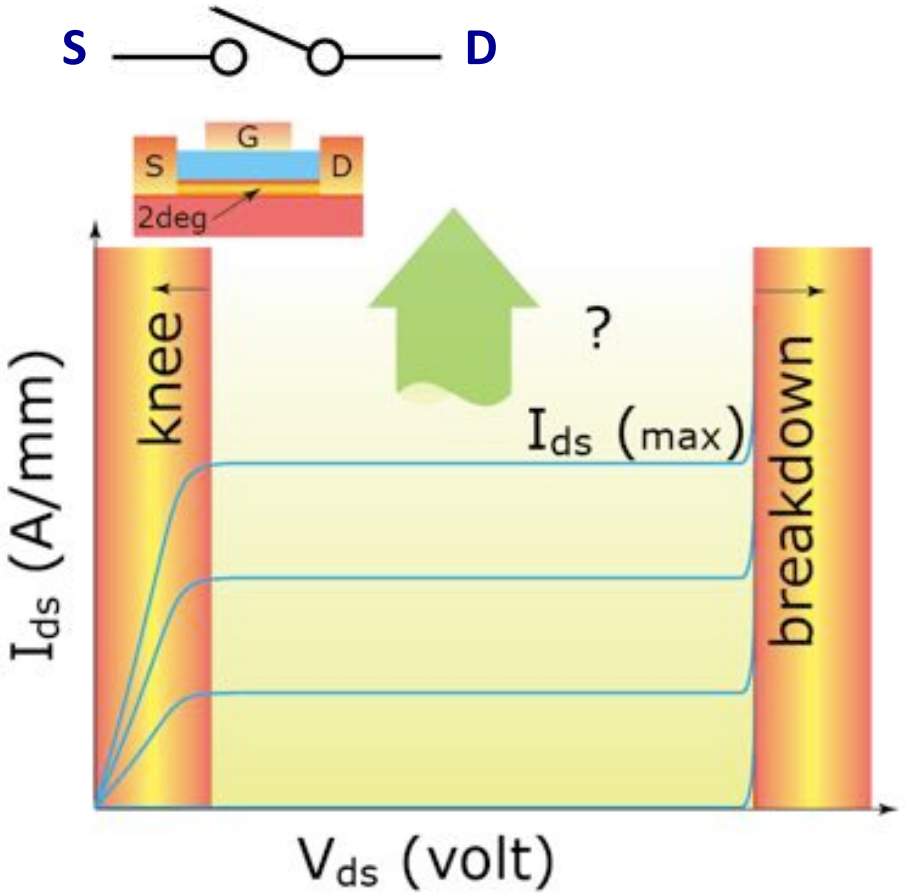

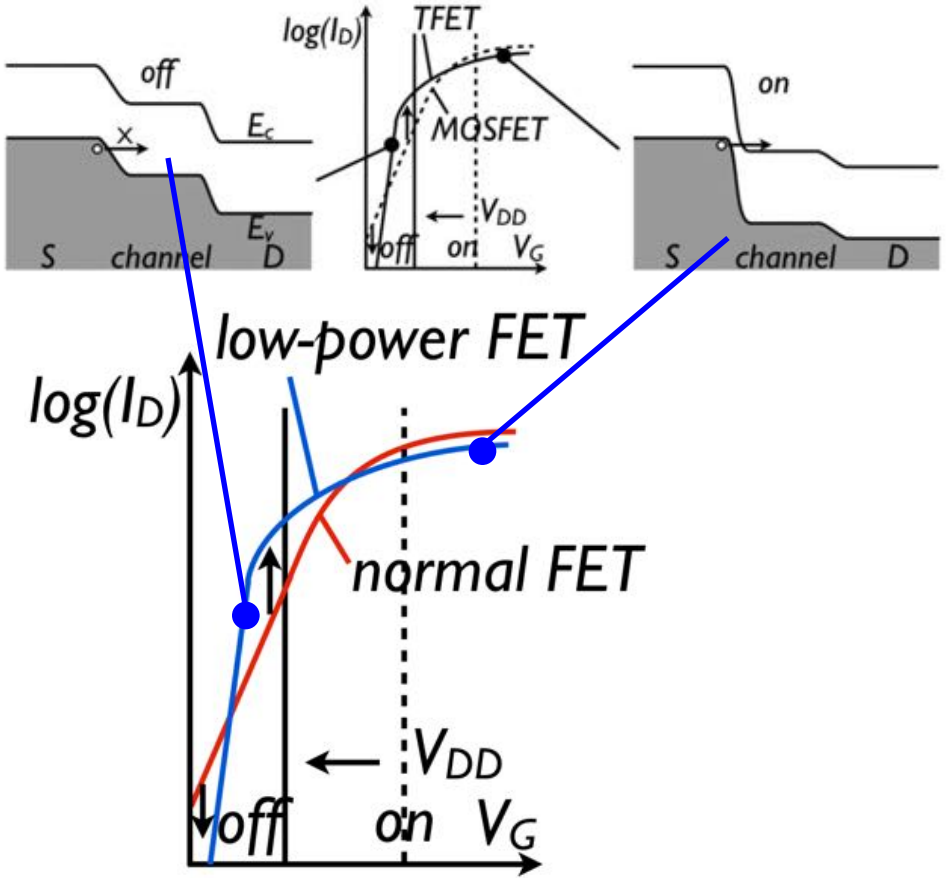

- The transistor is an electronic switch
- It is also an amplifier: it has gain
- Gain @ high speed: RF electronics
- Switching @ high voltages: Power electronics

$$< 60 \frac{\text{mV}}{\text{decade}} \text{possible}$$

Careful what you wish for: you may get it!

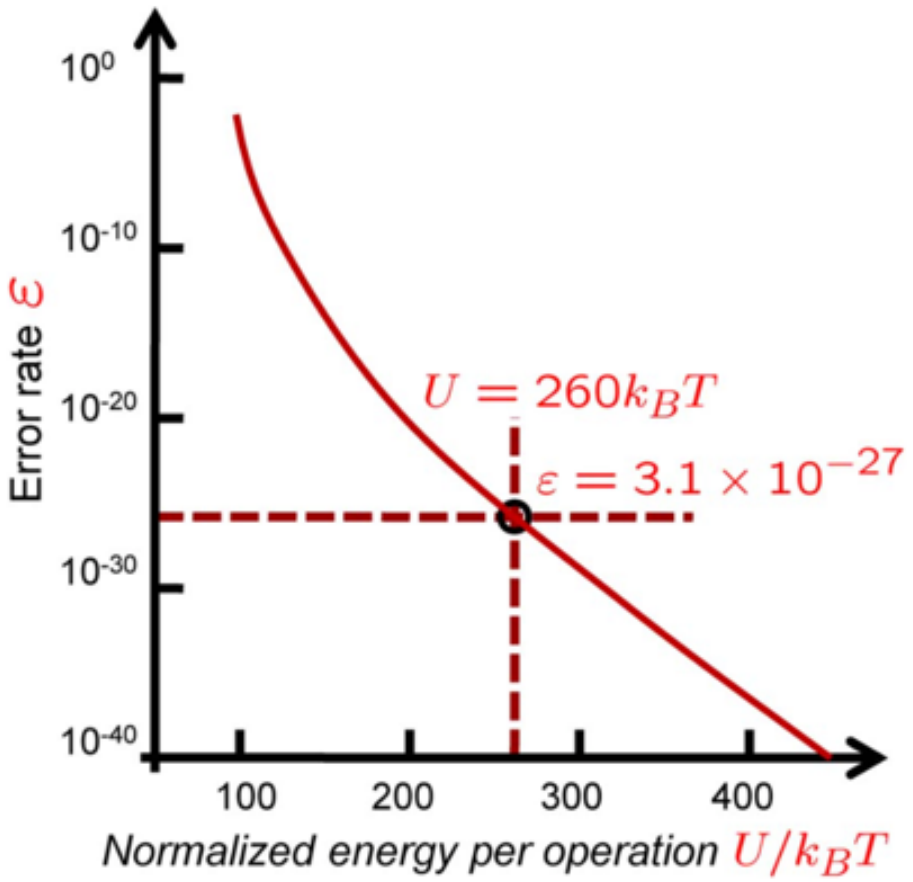

Fig. 2. ***Error-energy relationship for an idealized CMOS gate according to (4) for an ensemble of 10^{10} g = –10 CMOS switches operating at 10% activity factor. For every decade of error improvement, $\approx 15k_BT$ of energy is required in the low error limit.***

Implications of Scales in Processing of Information

The physical form of information processing employing electronics is as a collection of small devices—memories included—beholden to the physics of operation of device and its assembly in achieving desired objectives. This paper reviews and explores these scale connections—of transistors, materials, and the variety of device proposals—internally and in their integration.

By Sandip Tiwari, *Fellow IEEE*

- The "fat" in Boolean logic switching buys us robustness against errors.
- Low power switches will have to figure out a way to be robust to fluctuations.

Transistors old and new

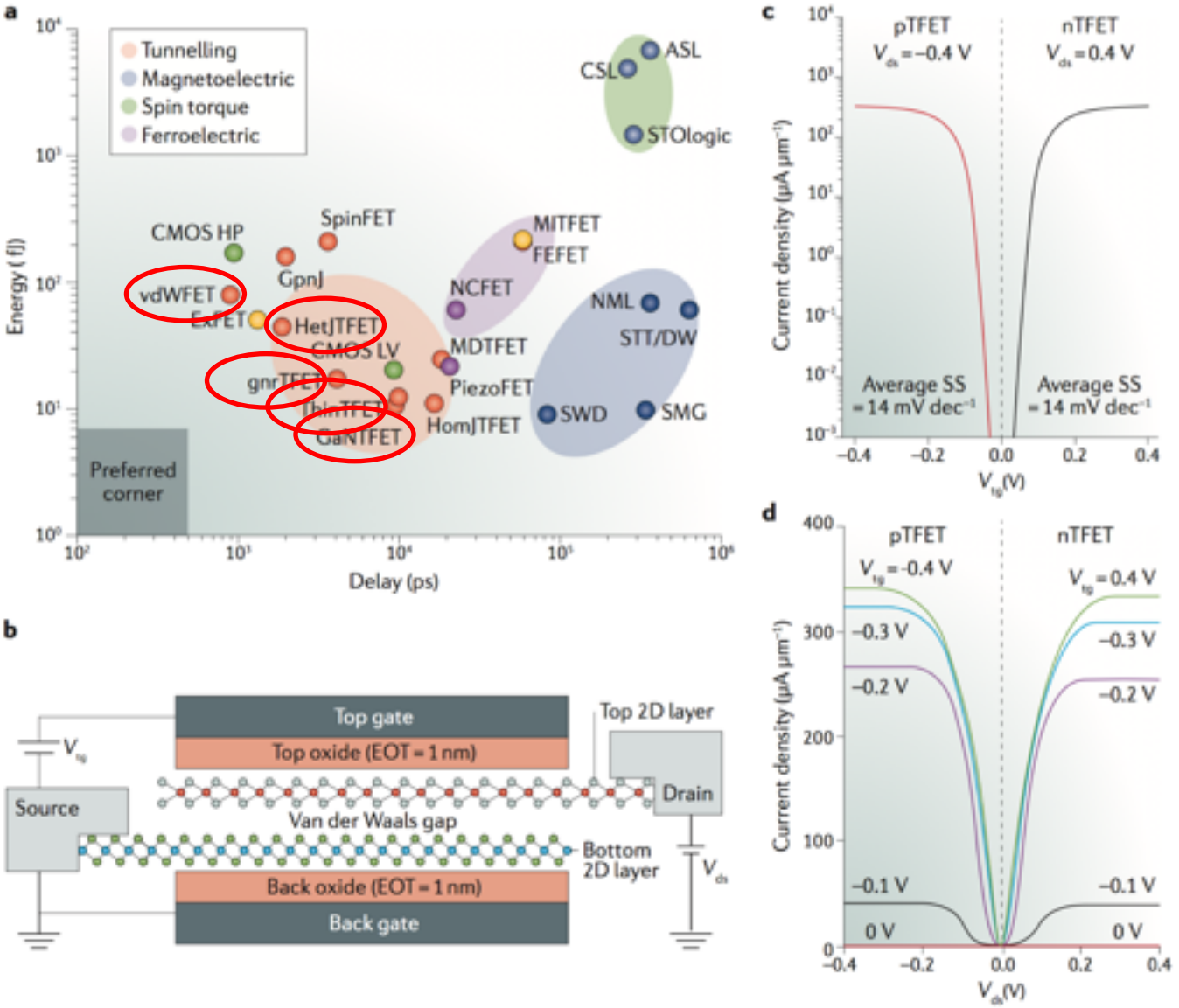

Can Transistors beat the Boltzmann Limit?

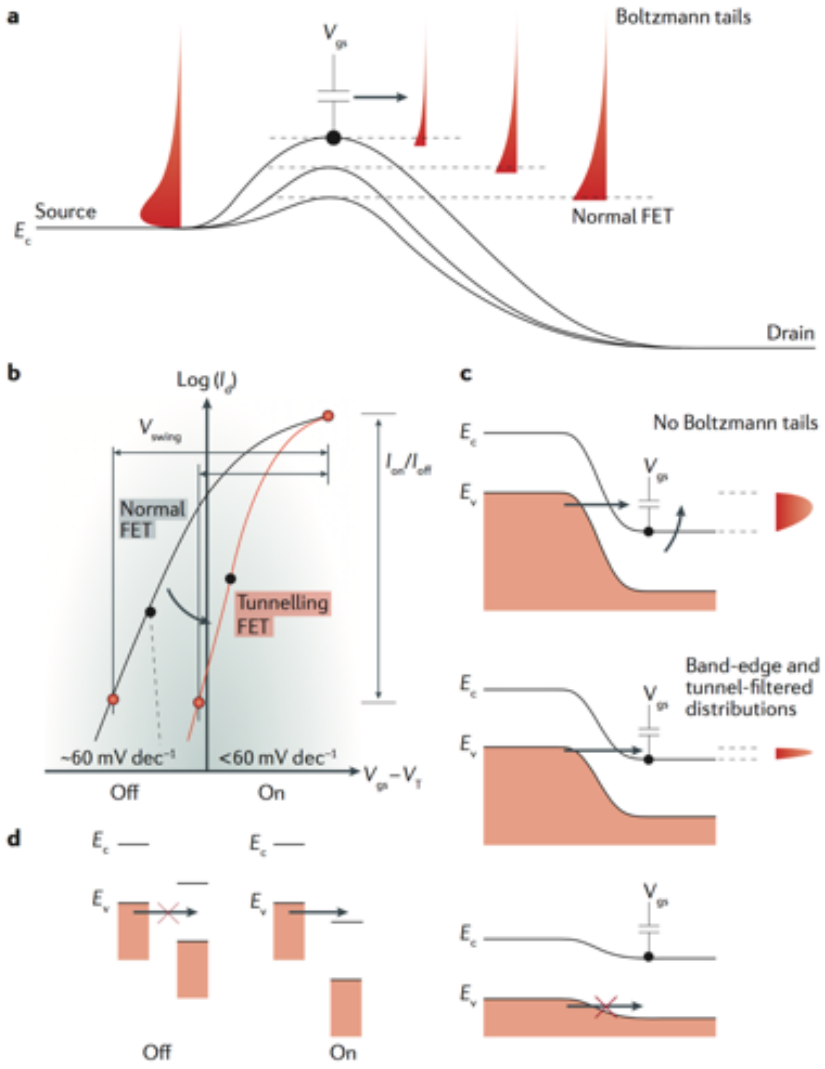

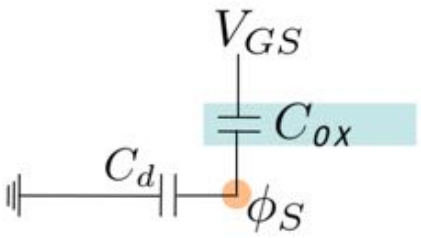

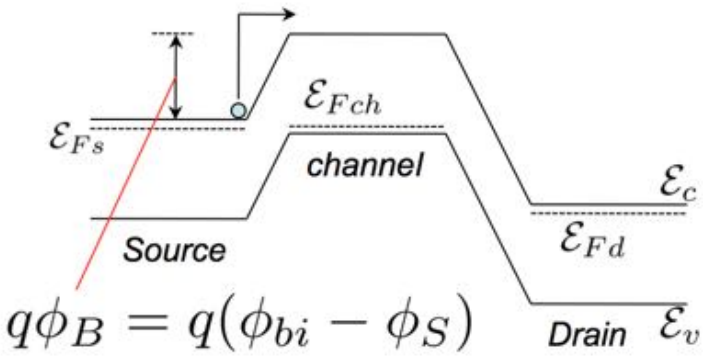

Tunneling FETs (or TFETs)

Negative Capacitance FETs (NCFETs)

The Energy-Delay Switching Bottleneck

$kT\ln(2) \sim 3 \times 10^{-6}$ fJ

$\frac{\hbar}{kT} \sim 3 \times 10^{-2}$ ps

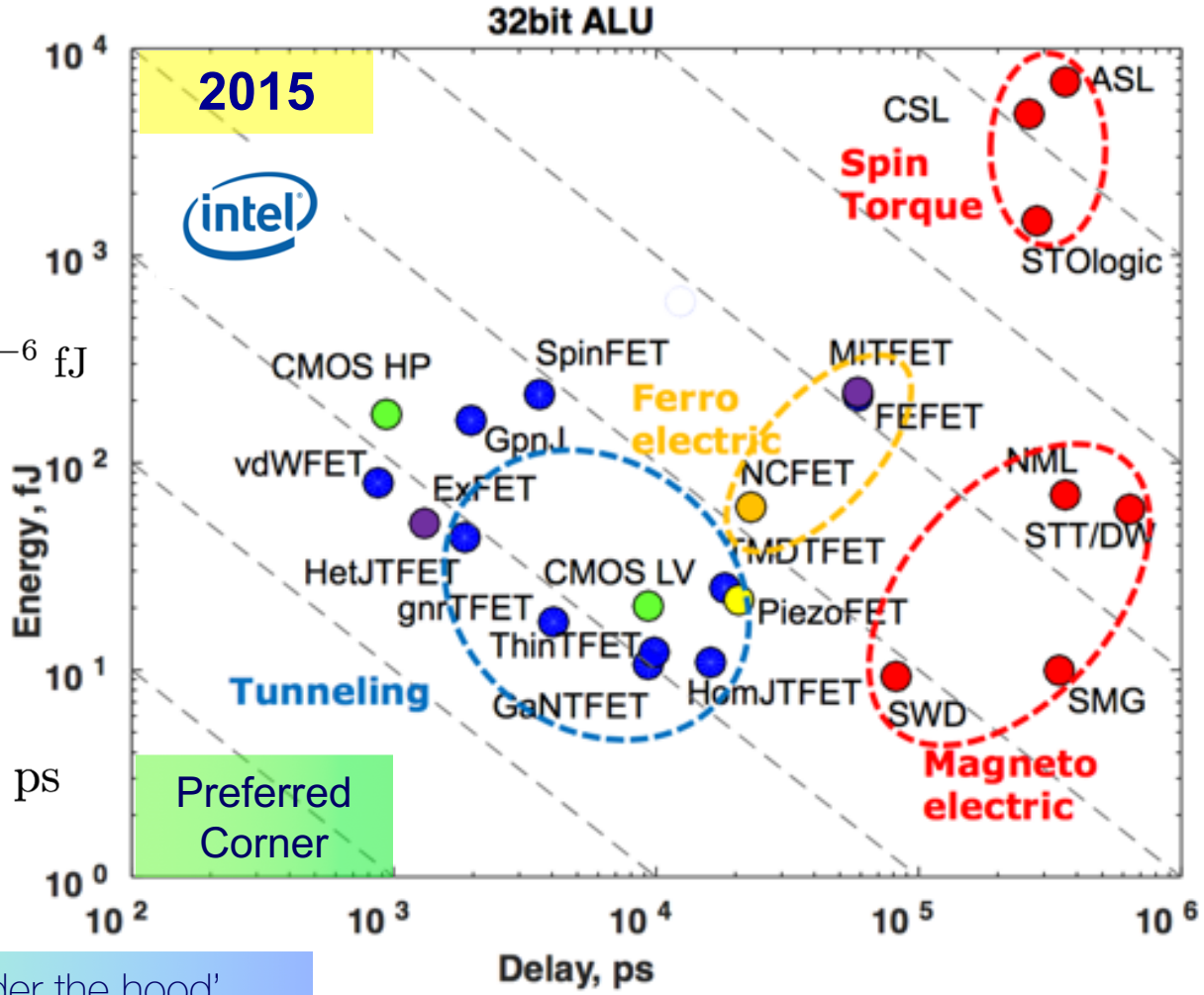

Physics hiding 'under the hood'

$\psi(x_1, x_2) = -\psi(x_2, x_1)$ → $f(E) = \frac{1}{1 + e^{\frac{E - E_F}{kT}}}$ → $F_{mag} \sim F_{el} \cdot \frac{v^2}{c^2}$ → $e^{\frac{qV}{kT}}$ vs. $e^{i\phi}$ logic

New Devices Promise to Do Better

$kT\ln(2) \sim 3 \times 10^{-6}$ fJ

$\frac{\hbar}{kT} \sim 3 \times 10^{-2}$ ps

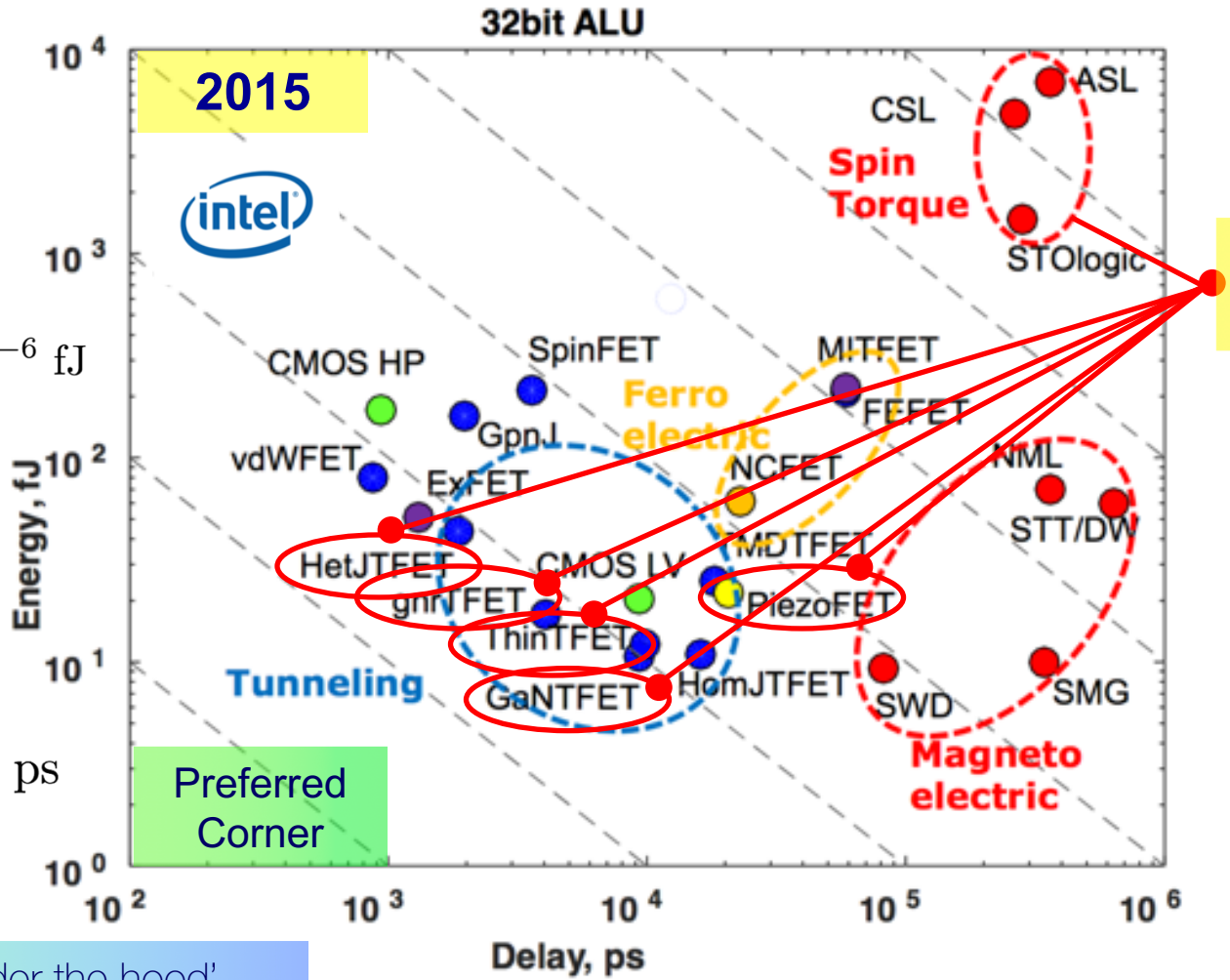

Cornell contributions as new device technologies

Physics hiding 'under the hood'

$\psi(x_1, x_2) = -\psi(x_2, x_1)$ → $f(E) = \frac{1}{1 + e^{\frac{E - E_F}{kT}}}$ → $F_{mag} \sim F_{el} \cdot \frac{v^2}{c^2}$ → $e^{\frac{qV}{kT}}$ vs. $e^{i\phi}$ logic

Tunneling in Semiconductors

TABLE I: Landmarks in the Science of Tunneling

No.	Phenomena	Investigators	Year
1	Observation of field-emission from metals	Lilienfeld[7]	1922
2	Ionization of hydrogen atoms by electron tunneling	Oppenheimer[8]	1928
3	Explanation of Field-emission	Fowler and Nordheim[9]	1928
4	Alpha-decay Theory	Gamow[6], Gurney and Condon[7]	1928
5	Theory of Interband Tunneling in solids	Zener[10]	1934
6	Field Emission Microscope (FEM)	Müller[11]	1937
7	Observation of Zener Breakdown	Chynoweth and McKay[12]	1957
8	Tunneling in Degenerate pn Junctions	Esaki[13]	1958
9	Extension of Zener's Theory to Tunnel Diodes	Keldysh[14], Kane[15], Price et al.[16]	1958-1961
10	Measurement of energy gap of superconductors	Giaever[17]	1960
11	Perturbation Treatment of Tunneling	Bardeen[18]	1961
12	Tunneling of Cooper Particles	Josephson[19]	1962
13	Experimental Verification of Josephson Effect	Anderson[20] et al. Rowell[21] and Fiske[22]	1963–1964
14	Inelastic Tunneling Spectroscopy (IETS)	Jaklevic and Lambe[23]	1966
15	Observation of Tunneling Tails	Lee and Cohen[24], Gadzuk and Plummer[25]	1970–1971
16	Development of Scanning Tunneling Microscope (STM)	Binnig[26]	1981

The Nobel Prize in Physics 1973
Leo Esaki, Ivar Giaever, Brian D. Josephson

Leo Esaki | Ivar Giaever | Brian David Josephson

The Nobel Prize in Physics 1973 was divided, one half jointly to Leo Esaki and Ivar Giaever *"for their experimental discoveries regarding tunneling phenomena in semiconductors and superconductors, respectively"* and the other half to Brian David Josephson *"for his theoretical predictions of the properties of a supercurrent through a tunnel barrier, in particular those phenomena which are generally known as the Josephson effects"*.

Applications:
- *SEMs*
- *TEMs*
- *STMs*
- *Tunnel diodes*
- *Ohmic contacts*
- *RTDs*
- *Quantum Cascade Lasers*
- *TFETs...*

The Nobel Prize in Physics 1986
Ernst Ruska, Gerd Binnig, Heinrich Rohrer

Ernst Ruska | Gerd Binnig | Heinrich Rohrer

The Nobel Prize in Physics 1986 was divided, one half awarded to Ernst Ruska *"for his fundamental work in electron optics, and for the design of the first electron microscope"*, the other half jointly to Gerd Binnig and Heinrich Rohrer *"for their design of the scanning tunneling microscope"*.

Why can electrons tunnel through barriers?

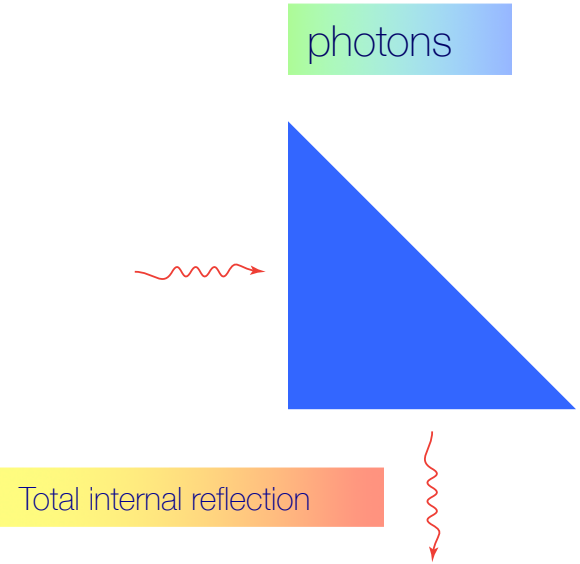

Why can electrons tunnel through barriers?

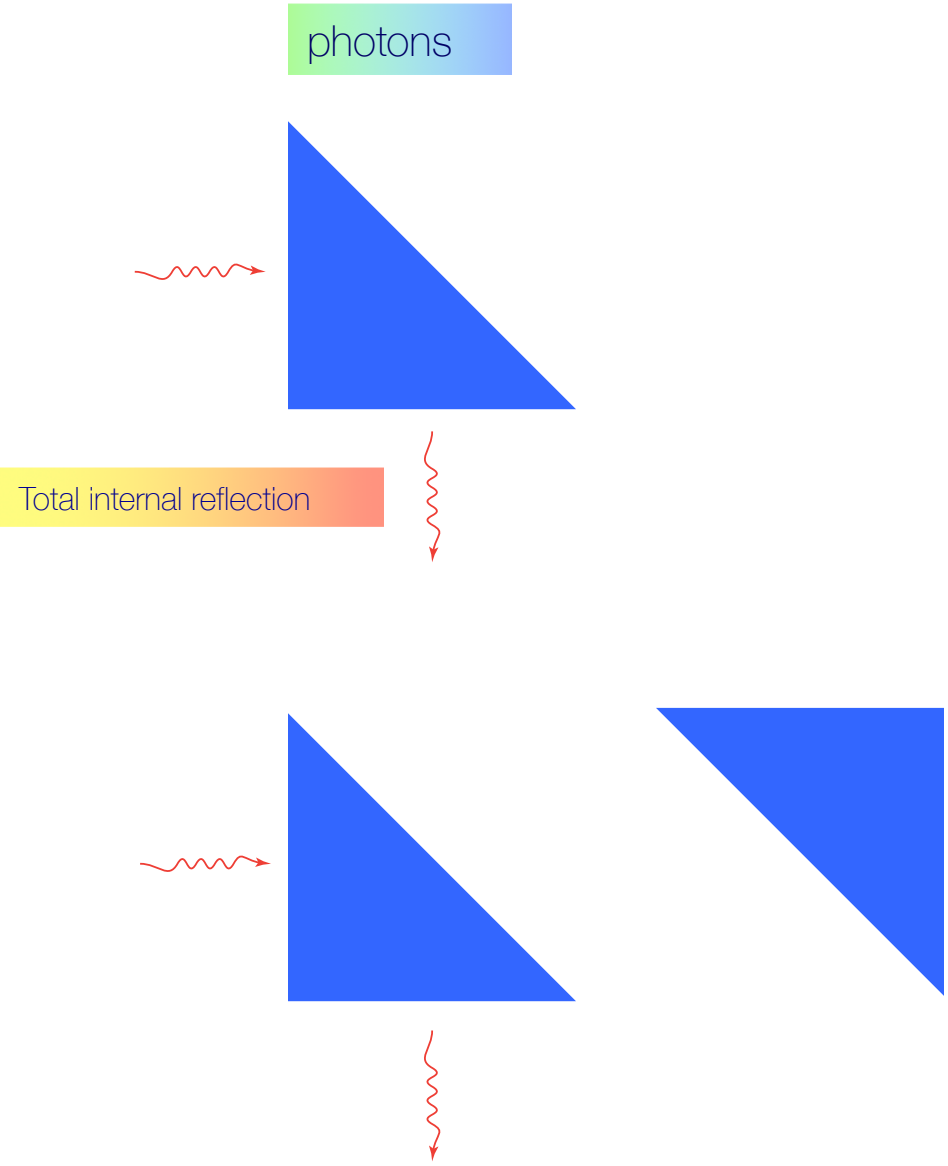

Why can electrons tunnel through barriers?

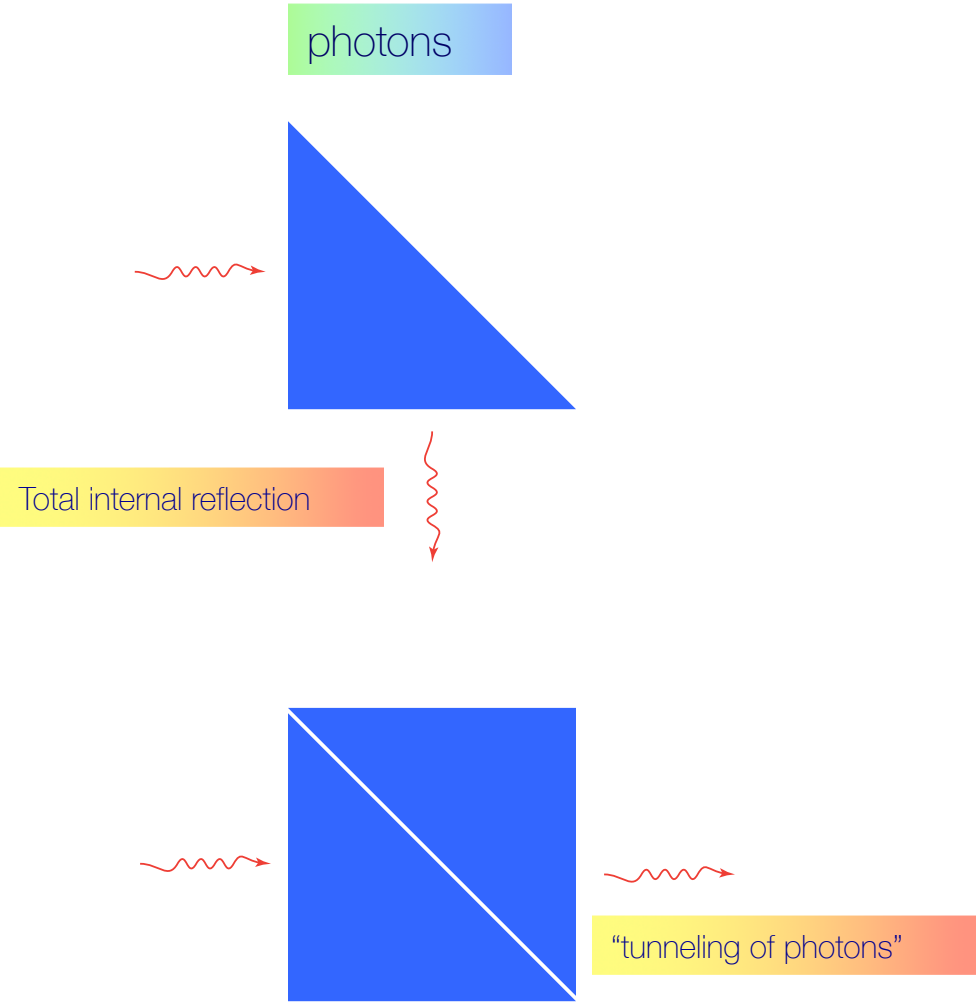

Why can electrons tunnel through barriers?

photons

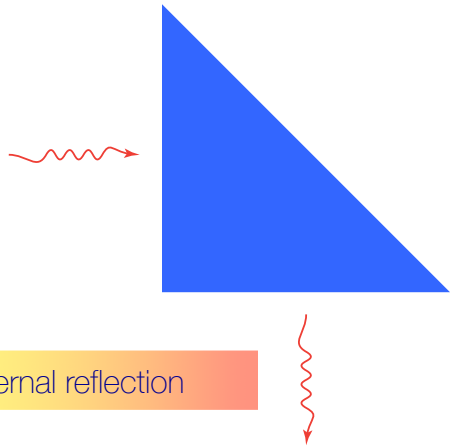

Total internal reflection

“tunneling of photons”

De Broglie

$$\lambda = \frac{h}{mv}$$

electrons

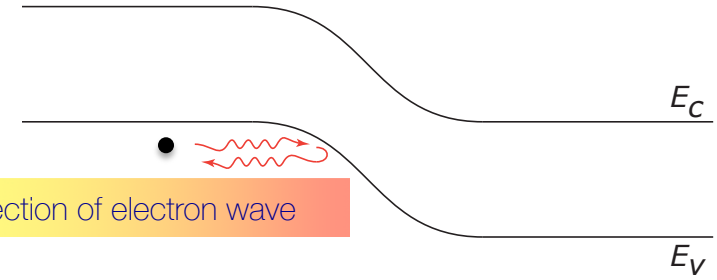

Reflection of electron wave

Why can electrons tunnel through barriers?

photons

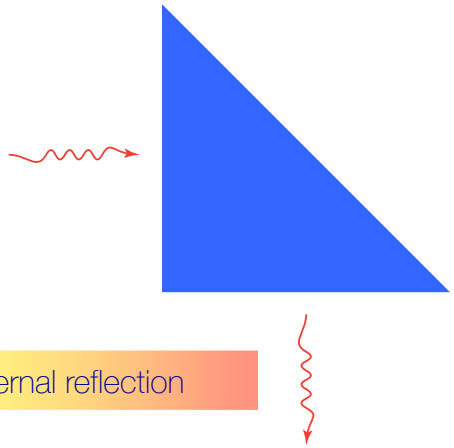

Total internal reflection

“tunneling of photons”

De Broglie

$$\lambda = \frac{h}{mv}$$

electrons

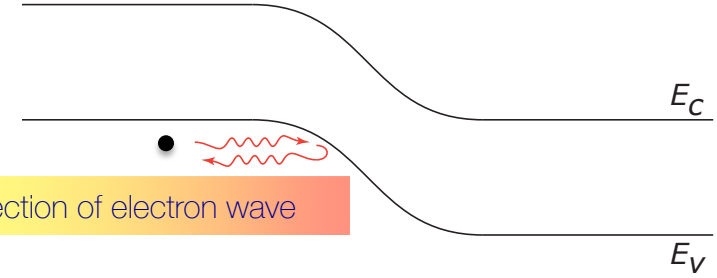

Reflection of electron wave

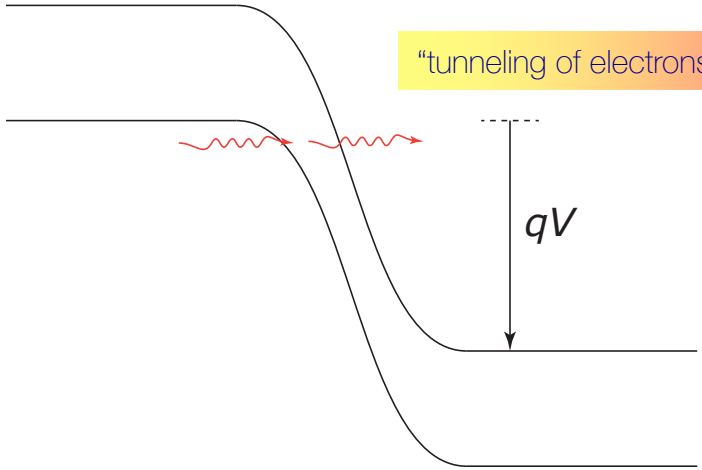

“tunneling of electrons”

Tunneling in Semiconductors

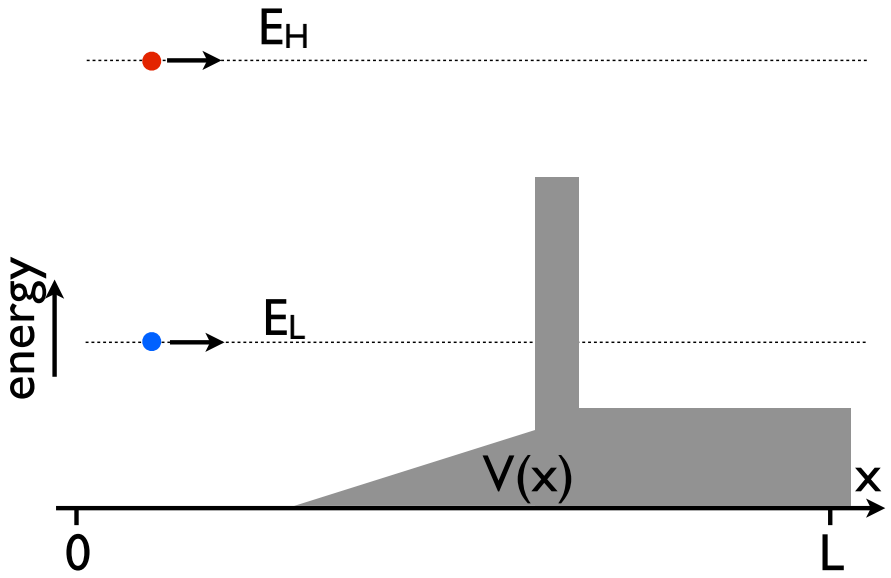

Tunneling in Semiconductors

$$T(E) = \frac{1}{1 + \frac{V_0^2}{4E(E-V_0)} \sin^2(k_b a)}$$

$$k_b = \sqrt{\frac{2m_e}{\hbar^2}(E - V_0)}$$

Kinetic energy

$$E = \frac{\hbar^2 k_b^2}{2m_e} + V_0.$$

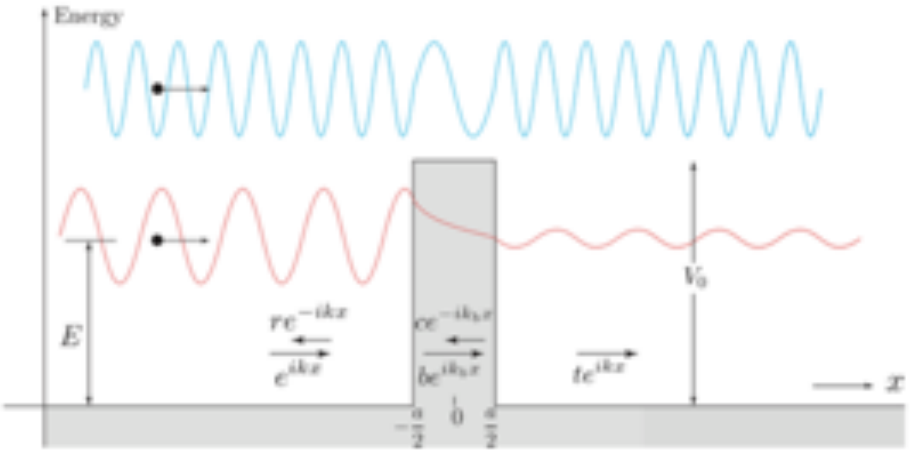

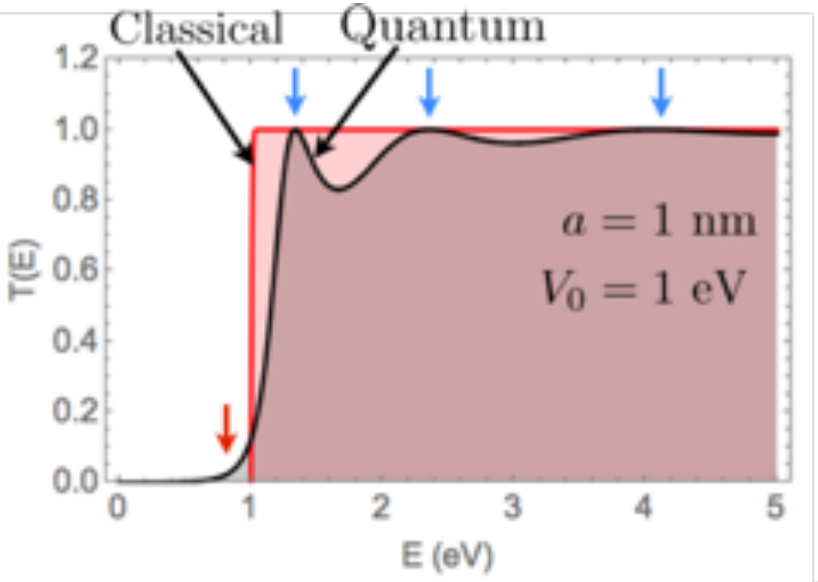

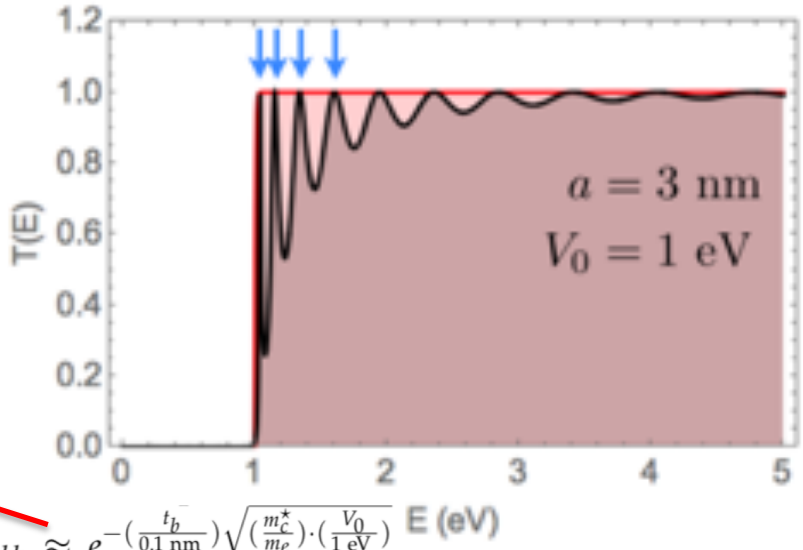

$$\sin(iy) = i\sinh(y)$$

$$T(E) = \frac{1}{1 + \frac{V_0^2}{4E(V_0-E)} \sinh^2(k_b a)} \approx \frac{16E(V_0 - E)}{V_0^2} e^{-2k_b a}$$

$$T_{wkb} \approx e^{-\left(\frac{t_b}{0.1\text{ nm}}\right)\sqrt{\left(\frac{m_c^\star}{m_e}\right)\cdot\left(\frac{V_0}{1\text{ eV}}\right)}}$$

Electron Quantum Transport in Smooth Potentials

Effective Mass Equation for Electron Wavepackets

$$[E_n(-i\nabla)]C(x) = [E - E_c(x)]C(x) \implies \frac{d^2}{dx^2}C(x) = \underbrace{-\frac{2m_c^\star}{\hbar^2}[E - E_c(x)]}_{Q(x)}C(x)$$

$$E_c(-i\nabla) = E_c(x) - \frac{\hbar^2}{2m_c^\star}\frac{d^2}{dx^2}$$

The Effective Mass Approximation For Bands in Semiconductors

The WKB approximation

$$C(x) \approx \frac{K}{Q(x)^{\frac{1}{4}}} e^{\pm \int_a^x du \sqrt{Q(u)}}.$$

$$E > E_c(x), \; Q(x) < 0$$

$$k(x) = \sqrt{\frac{2m_c^\star}{\hbar^2}(E - E_c(x))}$$

$$C(x) \approx \frac{K'}{\sqrt{k(x)}} e^{\pm i \int_a^x duk(u)},$$

$$|C(x)|^2 \propto \frac{1}{k(x)}$$

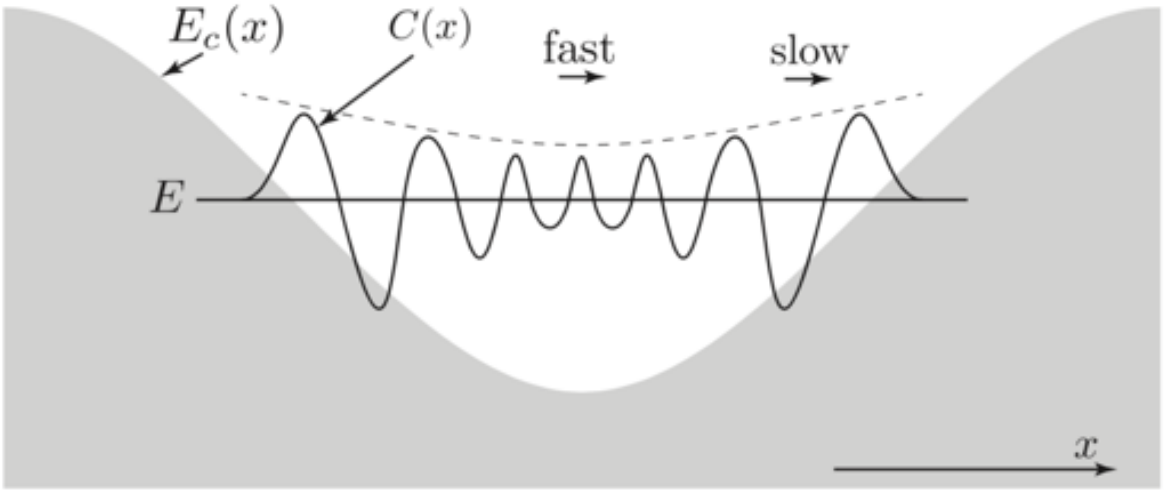

Fig. 18.3 Electron transport and approximate wavefunction in smoothly varying potentials.

Electron Quantum Transport in Smooth Potentials

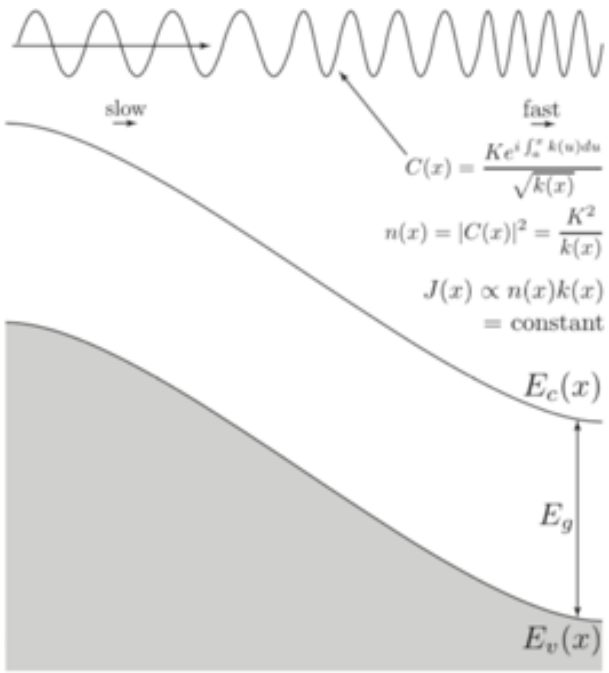

Fig. 18.4 Transport of an effective mass electron wavepacket in the conduction band in a smoothly varying potential. The group velocity $v(x) \sim k(x)$ increases as the kinetic energy increases, but the carrier density $n(x) = |C(x)|^2 \sim 1/k(x)$ decreases, keeping the net current $J(x) \sim n(x)v(x)$ constant.

$$[-\frac{\hbar^2}{2m_e}\frac{d^2}{dx^2} + V(x)]\psi(x,t) = i\hbar\frac{\partial}{\partial t}\psi(x,t) \implies j = \frac{\psi^\star \hat{p}\psi - \psi\hat{p}\psi^\star}{2m_e}$$

$$[-\frac{\hbar^2}{2m_c^\star}\frac{d^2}{dx^2} + E_c(x)]C(x,t) = i\hbar\frac{\partial}{\partial t}C(x,t) \implies j = -\frac{i\hbar}{2m_c^\star}[C^\star\frac{\partial C}{\partial x} - C\frac{\partial C^\star}{\partial x}]$$

$$\boxed{C(x) \approx \frac{K'}{\sqrt{k(x)}}e^{\pm i\int_a^x duk(u)},} \quad |C(x)|^2 \propto \frac{1}{k(x)}$$

$$n(x) = C^\star(x)C(x) = \frac{|K|^2}{k(x)}$$

$$J = \sum_k j_k = qg_sg_v\sum_k v_g(k)|C(x)|^2$$

$$E_c(k) = E_c(x) + \frac{\hbar^2k(x)^2}{2m_c^\star},$$
$$v_g(k) = \frac{1}{\hbar}\frac{\partial E_c(k)}{\partial k} = \frac{\hbar k(x)}{m_c^\star}$$

$$J = qg_sg_v\underbrace{\frac{\hbar k(x)}{m_c^\star}}_{v(x)}\underbrace{|C(x)|^2}_{n(x)} = qg_sg_v\frac{\hbar k(x)}{m_c^\star}\frac{|K|^2}{k(x)} = qg_sg_v\frac{\hbar|K|^2}{m_c^\star}$$

Quantum Current carried by an electron wavepacket in arbitrary potentials

Tunneling of Electrons Through Arbitrary Barriers

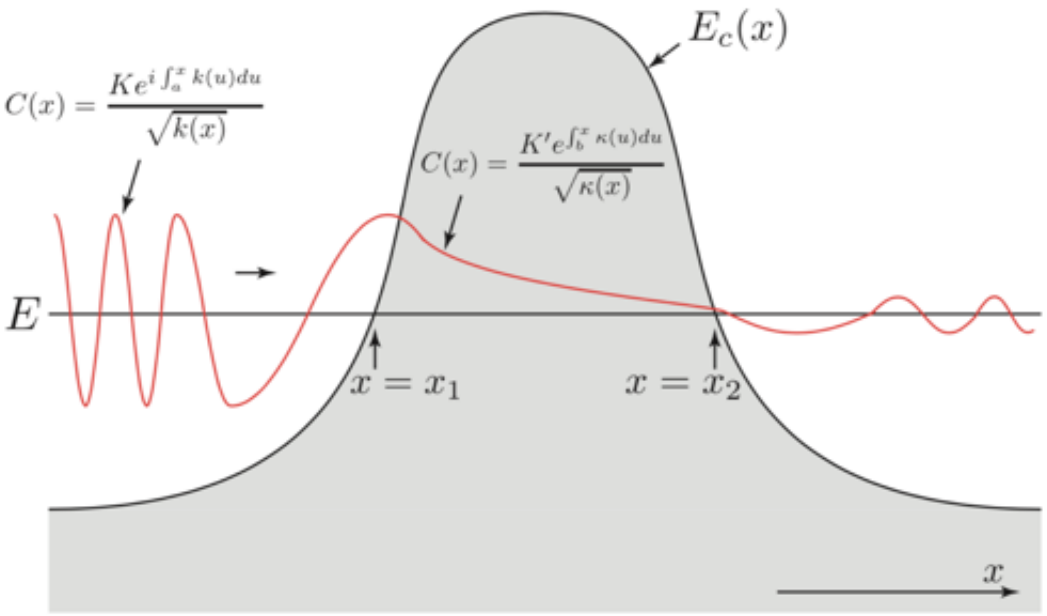

$$C(x) \approx \frac{K'}{\sqrt{k(x)}} e^{\pm i \int_a^x duk(u)},$$

$$k(x) = \sqrt{\frac{2m_c^\star}{\hbar^2}(E - E_c(x))}$$

$$\kappa(x) = -\frac{2m_c^\star}{\hbar^2}(E - E_c(x)) > 0$$

$$C(x) \approx \frac{K}{\sqrt{\kappa(x)}} e^{\pm \int_a^x \kappa(u)du}.$$

$$\frac{C(x_2)}{C(x_1)} \approx \frac{e^{-\int_a^{x_2} \kappa(u)du}}{e^{-\int_a^{x_1} \kappa(u)du}} \approx e^{i\phi} e^{-\int_{x_1}^{x_2} \kappa(u)du}$$

$$\left|\frac{C(x_2)}{C(x_1)}\right|^2 \approx e^{-2\int_{x_1}^{x_2} \kappa(u)du} \Longrightarrow \boxed{T_{wkb} \approx e^{-2\int_{x_1}^{x_2} dx\sqrt{\frac{2m_c^\star}{\hbar^2}[E_c(x)-E]}}}$$

$$T_{wkb} \approx e^{-\left(\frac{t_b}{0.1\text{ nm}}\right)\sqrt{\left(\frac{m_c^\star}{m_e}\right)\cdot\left(\frac{V_0}{1\text{ eV}}\right)}}$$

The WKB Tunneling Probability for tunneling in semiconductors

Tunneling in Homojunctions

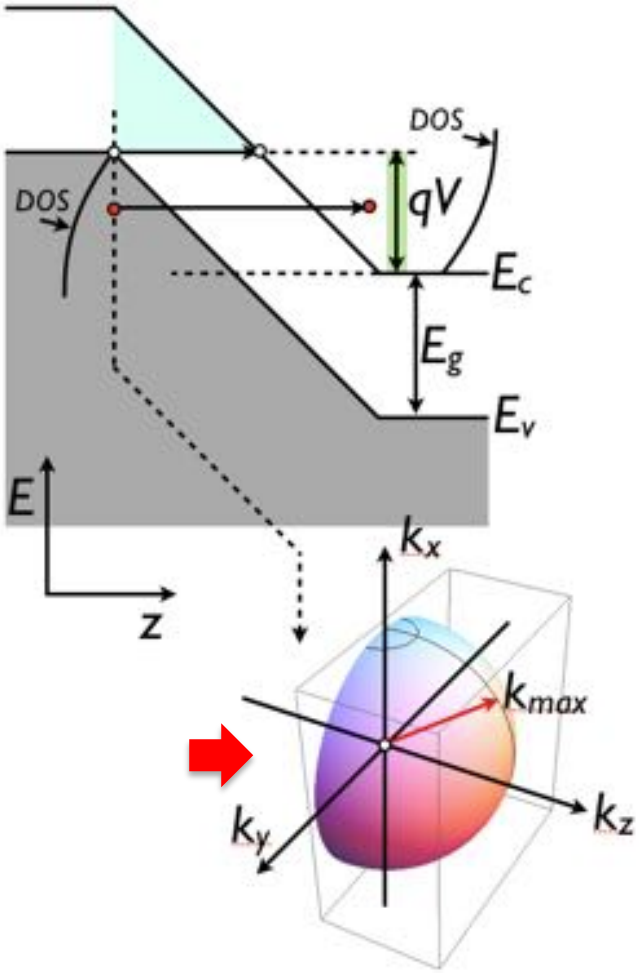

Reverse-bias tunneling current

$$\text{If } qV >> 2\hat{E}_{\parallel},$$

$$J \approx \frac{q^2 m^\star T_0 \hat{E}_{\parallel}}{2\pi^2\hbar^3} V$$

$$\Longrightarrow \sim\text{linear } I - V.$$

$$T_0 = \exp[-\frac{\pi\sqrt{m^\star}E_g^{3/2}}{2\sqrt{2}qF\hbar}]$$

$$\bar{E}_{\parallel} = \frac{\sqrt{2}qF\hbar}{2\pi\sqrt{m^\star}\sqrt{E_g}}$$

Tunneling current depends exponentially on the

- Bandgap
- Effective mass
- Electric field

Tunneling in Homojunctions

A back-of-the envelope evaluation of interband tunneling current in semiconductors

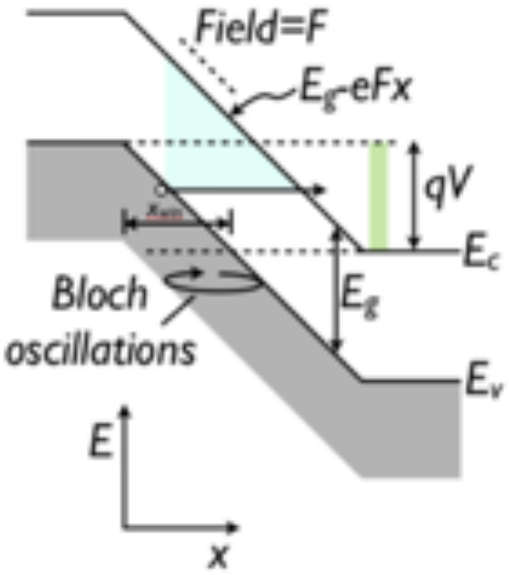

$$T_{WKB} \sim e^{-2S}$$

$$S = \int_{x_1}^{x_2} \sqrt{\tfrac{2m^*}{\hbar^2}(E_g - eFx)}\,dx$$

$$x_1 = 0, x_2 = E_g/eF$$

$$\Longrightarrow \boxed{T_{WKB} \sim \exp[-\tfrac{2^{\frac{5}{2}}\sqrt{m^*}}{3eF\hbar}E_g^{\frac{3}{2}}] = \exp[-F_0/F]}$$

$$\hbar\tfrac{dk}{dt} = eF \Longrightarrow k(t) = k(0) + \tfrac{eF}{\hbar}t$$

$$\Longrightarrow \text{Bloch Osc. period: } T = \tfrac{\hbar G}{eF}$$

***Very** rough estimates! (V=0.2 Volt)*

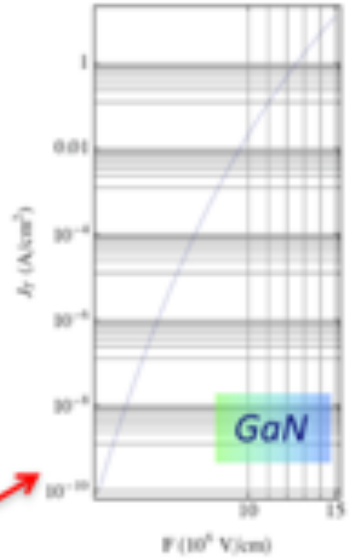

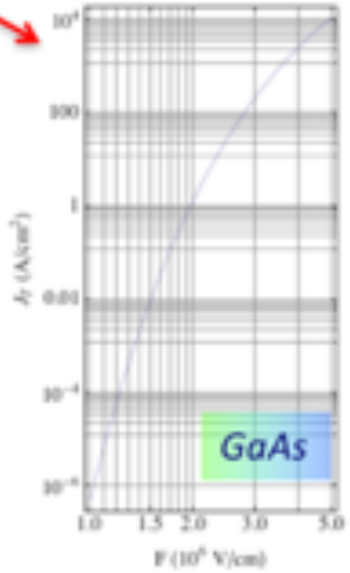

Rate of incidence on band-edge:
$\gamma_{inc} = 1/T = \tfrac{eF}{\hbar G} = \tfrac{a_0 eF}{h}$,
where $G = 2\pi/a_0$ is the reciprocal lattice vector.

Frequency of electron escape:

$$f_{esc} \sim \gamma_{inc} T_{WKB} = \tfrac{a_0 eF}{h} \times \exp[-\tfrac{2^{\frac{5}{2}}\sqrt{m^*}}{3eF\hbar}E_g^{\frac{3}{2}}]$$

Tunneling current density:

$$J_T \sim eN_s f_{esc} = eN_v x_{win} f_{esc} = eN_v(eV/F) f_{esc}$$

Rough estimate: $\Longrightarrow \boxed{J_T \sim \tfrac{e^2}{h} \cdot [a_0 N_v \exp[-\tfrac{2^{\frac{5}{2}}\sqrt{m^*}}{3eF\hbar}E_g^{\frac{3}{2}}]] \cdot V}$

Tunneling in Semiconductor Homojunctions

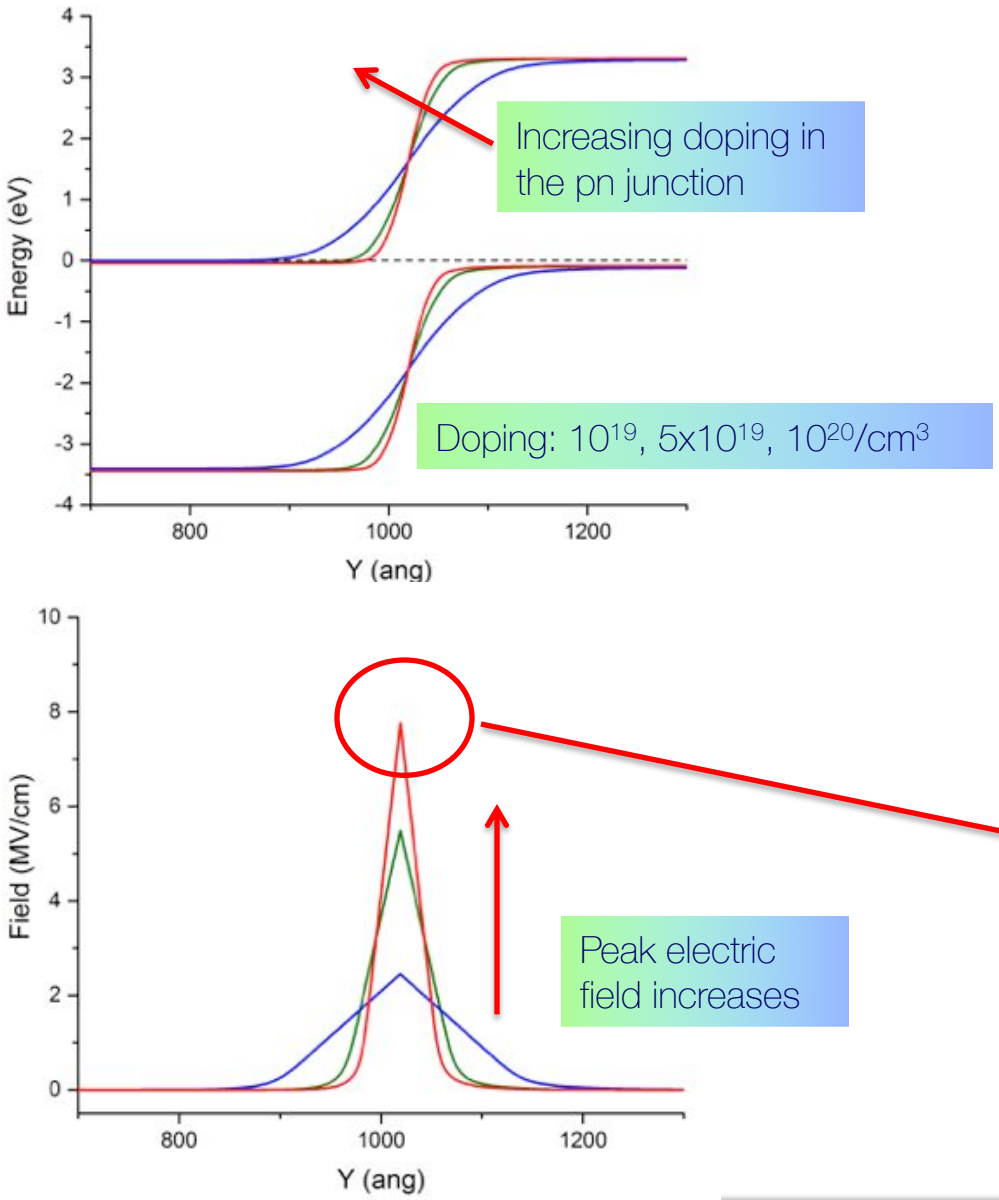

Tunneling in Semiconductor Homojunctions

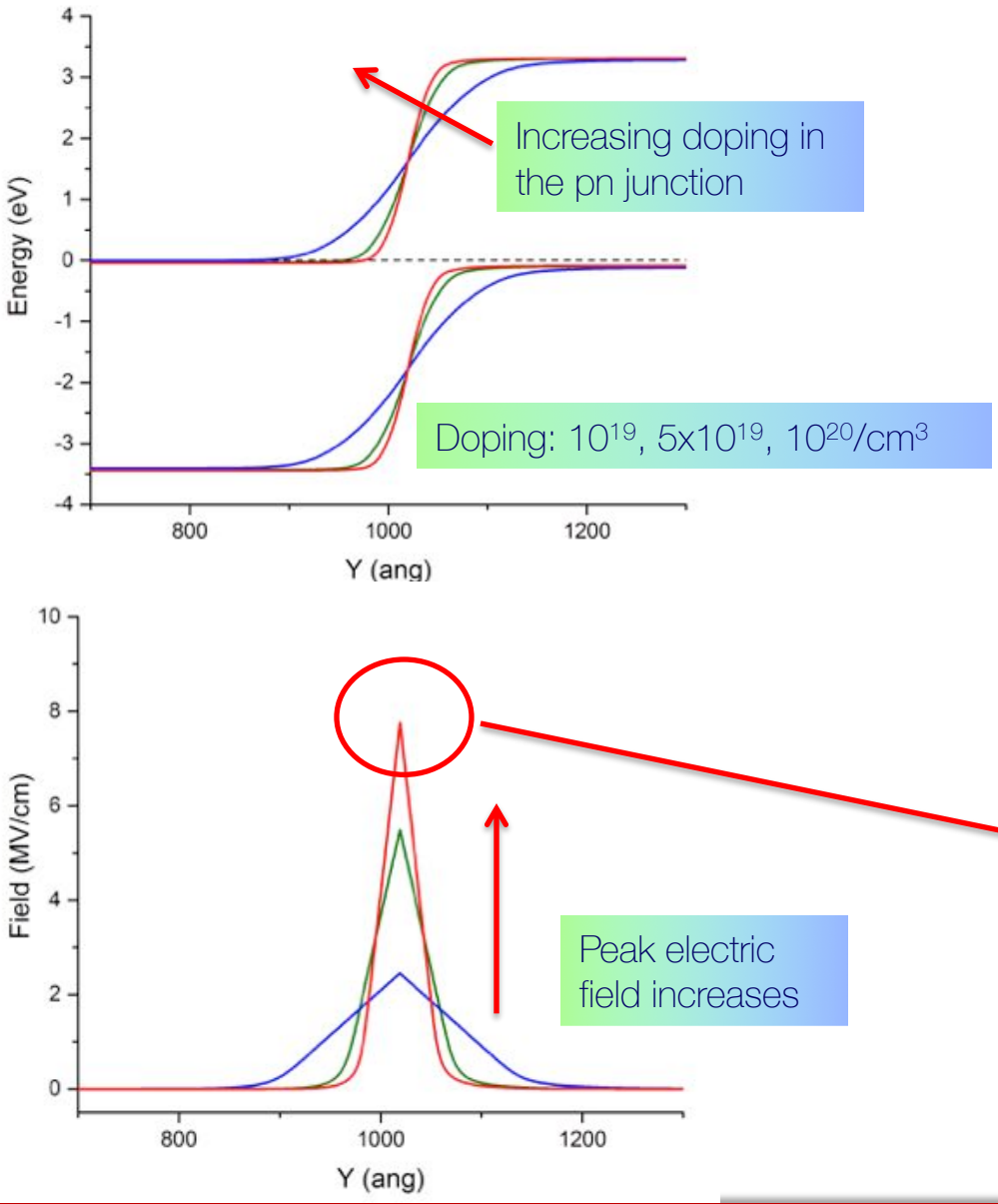

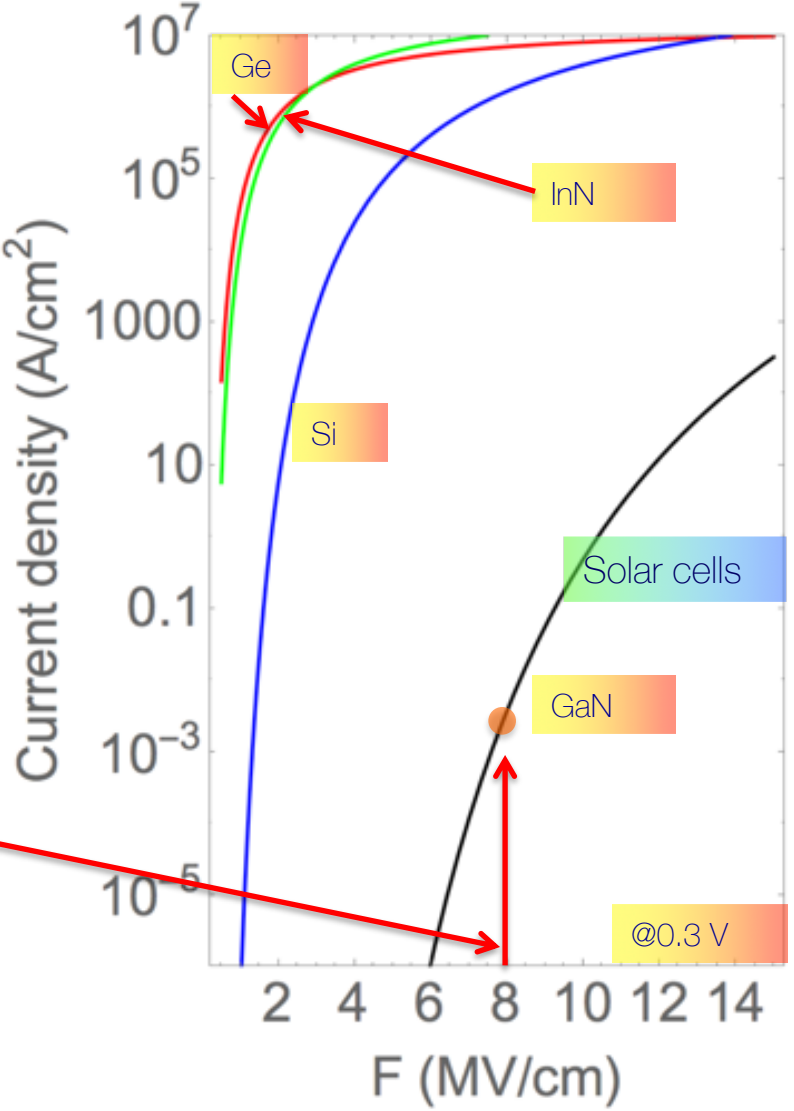

Tunneling in Semiconductor Homojunctions

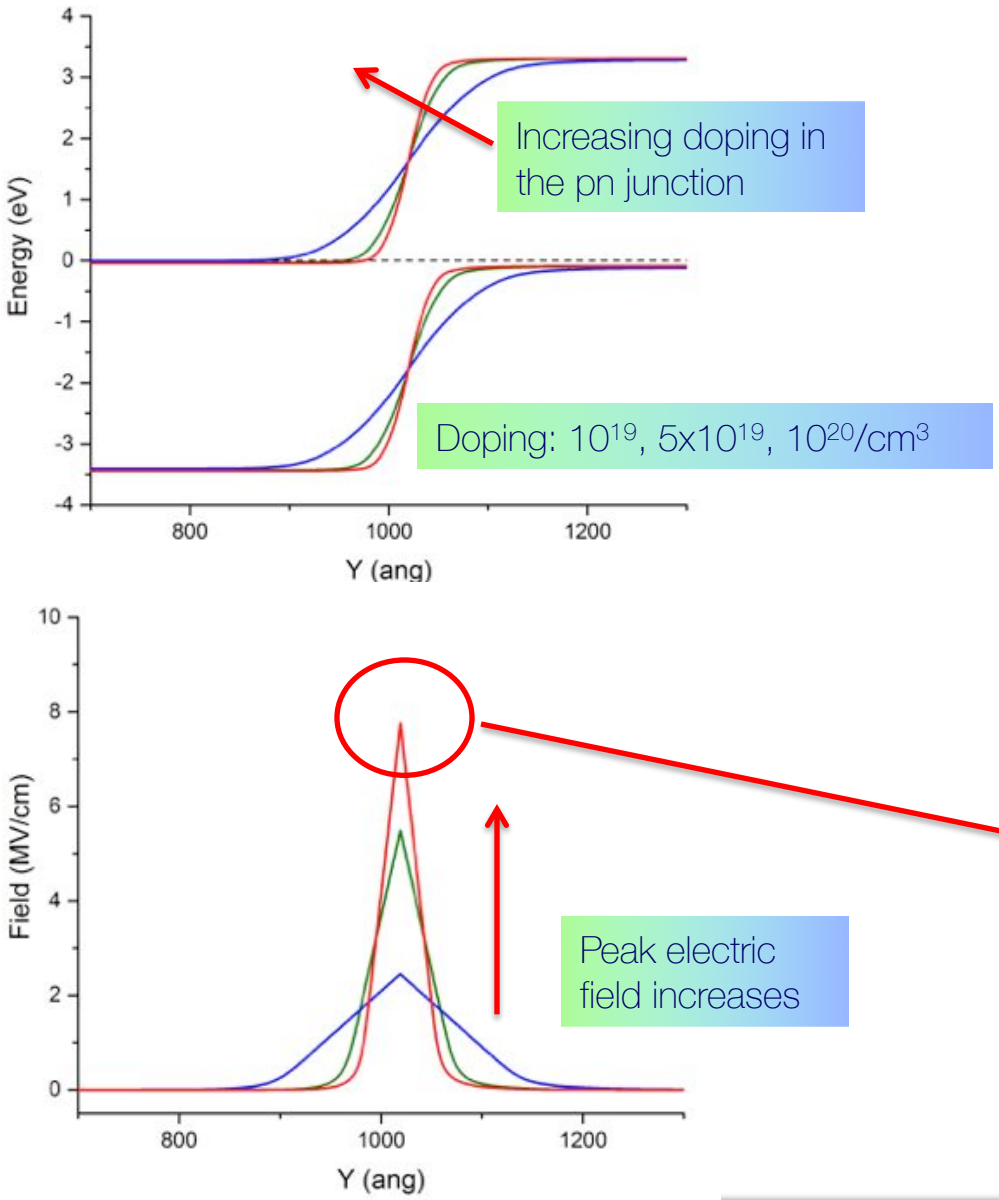

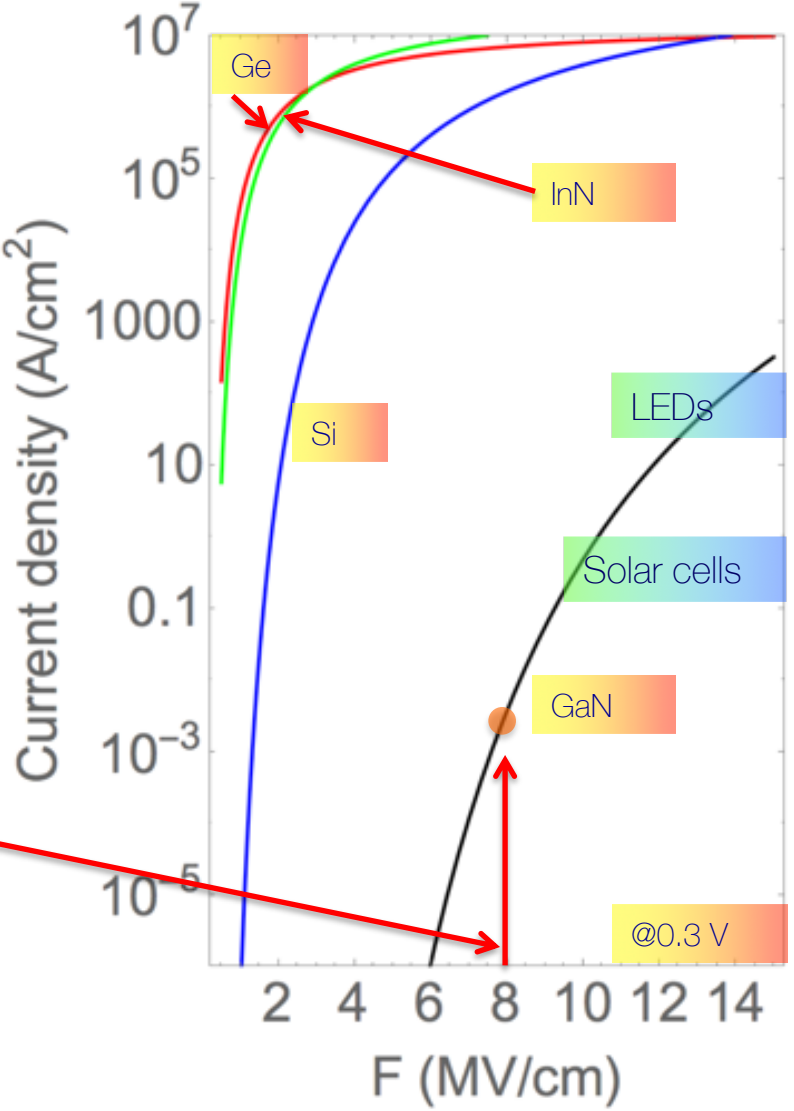

Tunneling in Semiconductor Homojunctions

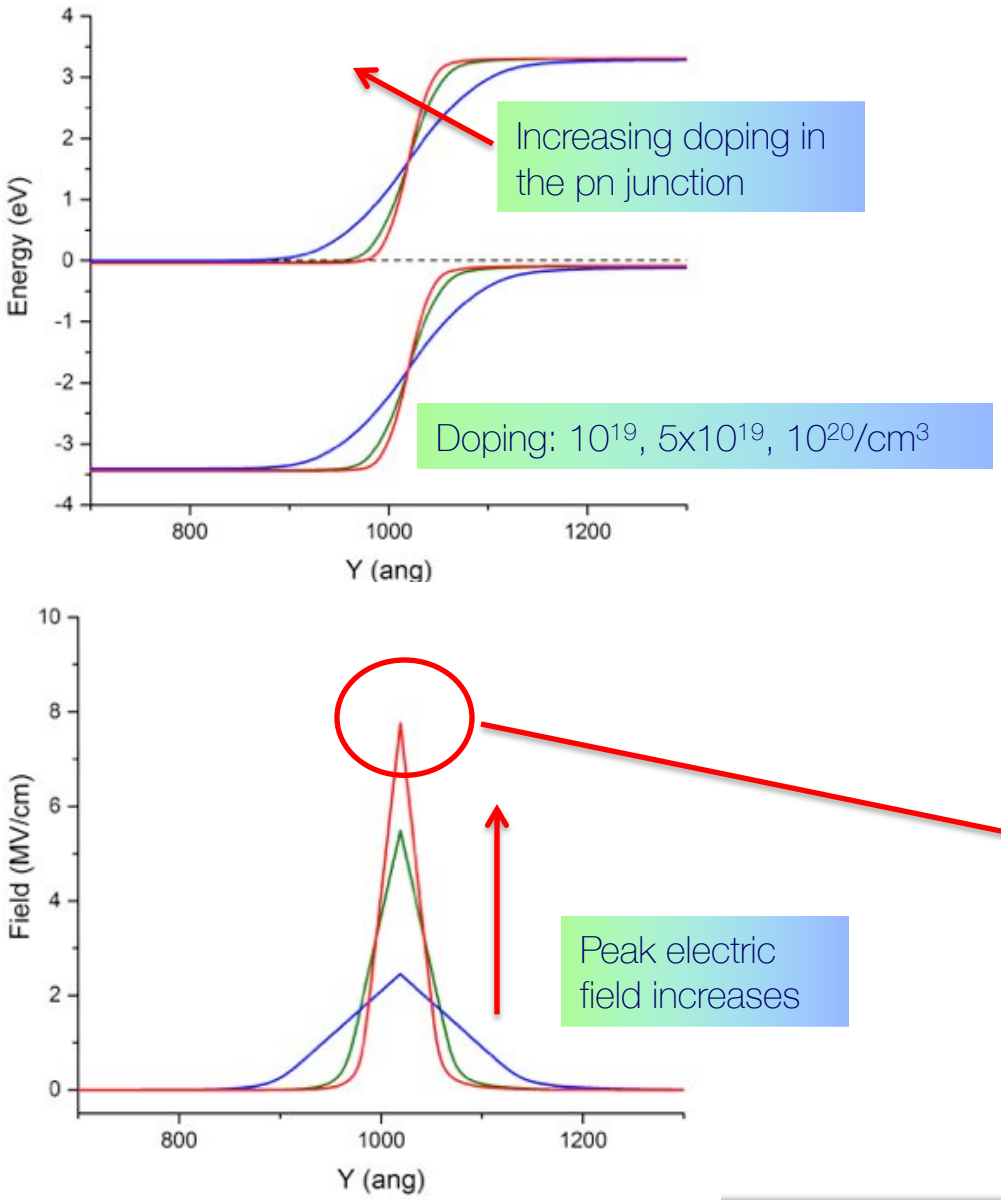

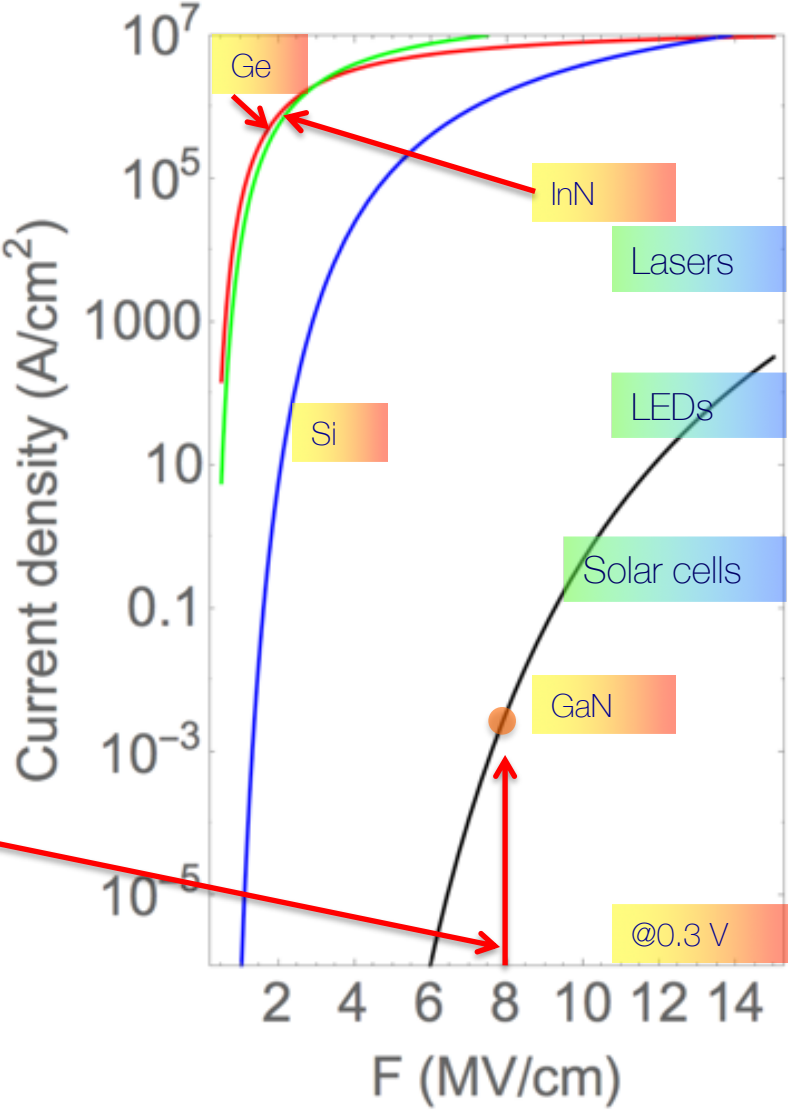

Tunneling in Semiconductor Homojunctions

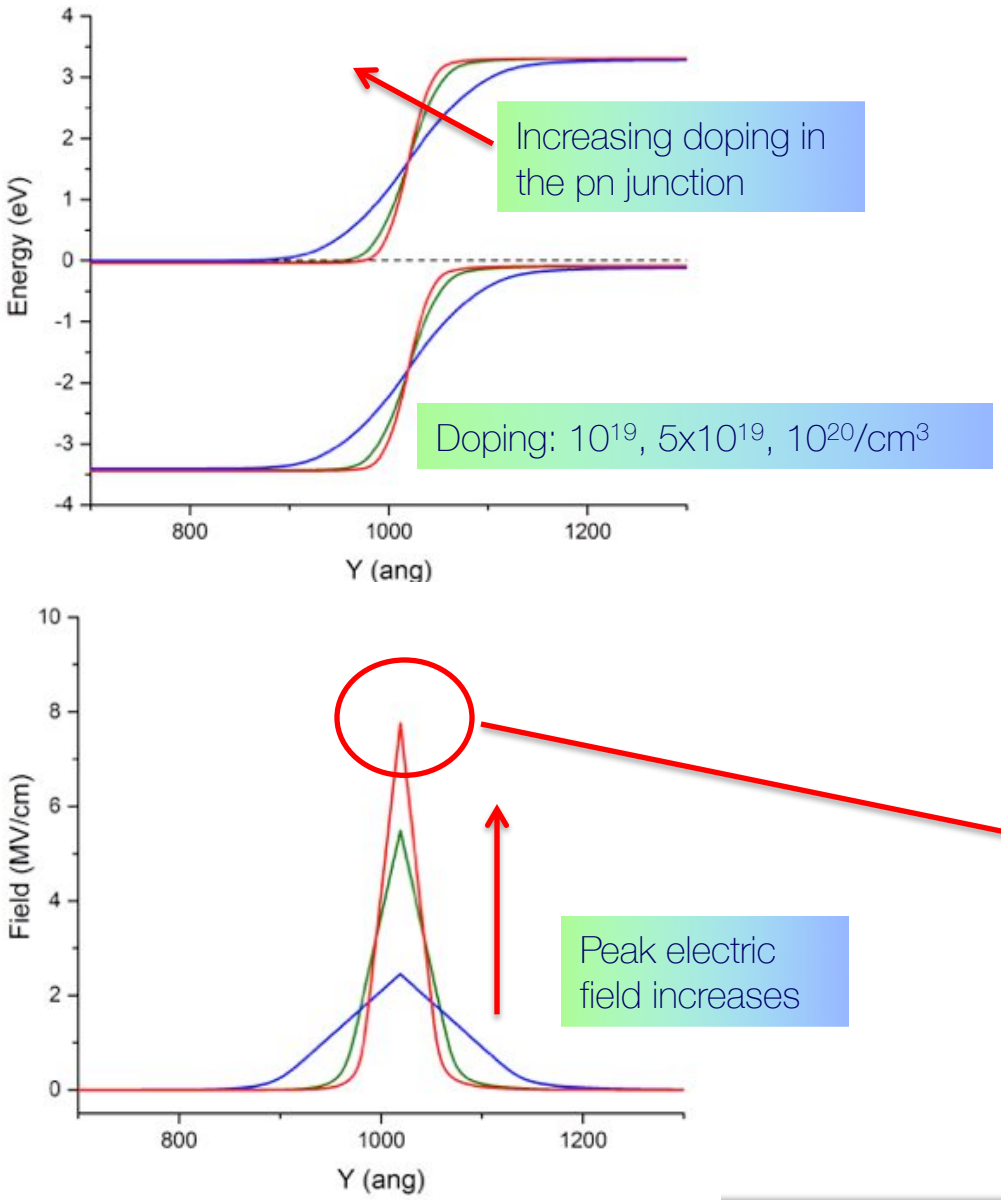

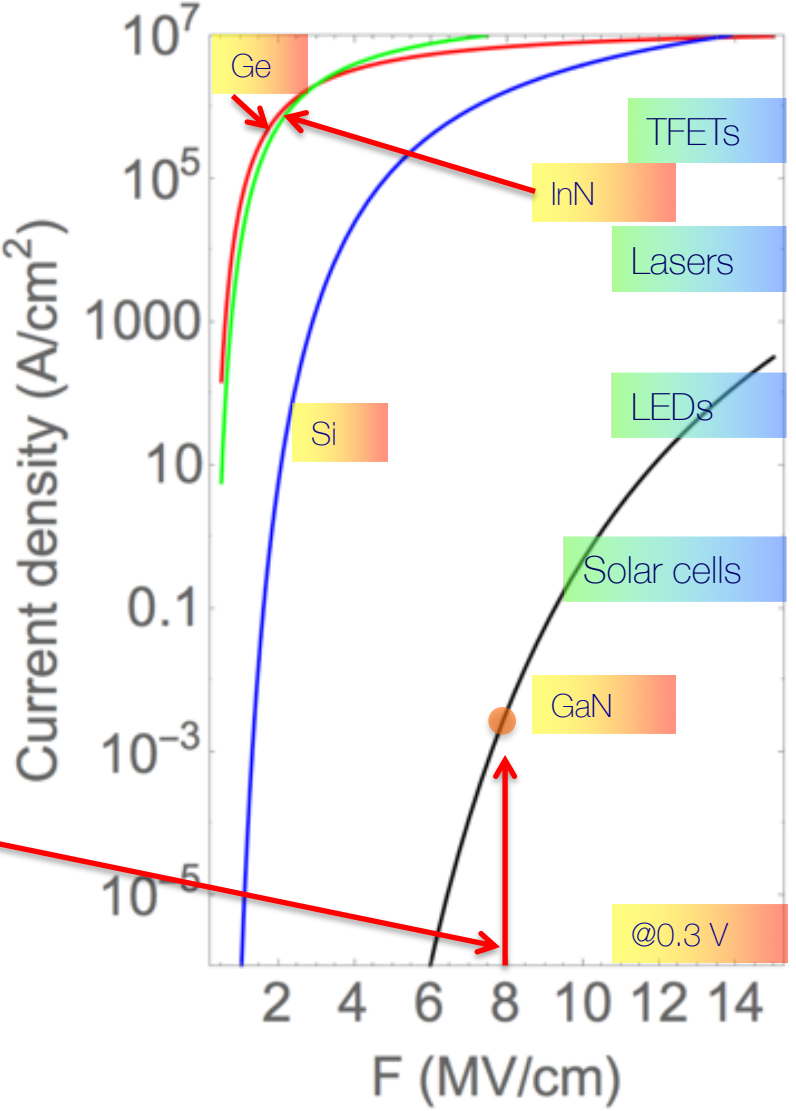

Tunneling in Semiconductor Homojunctions

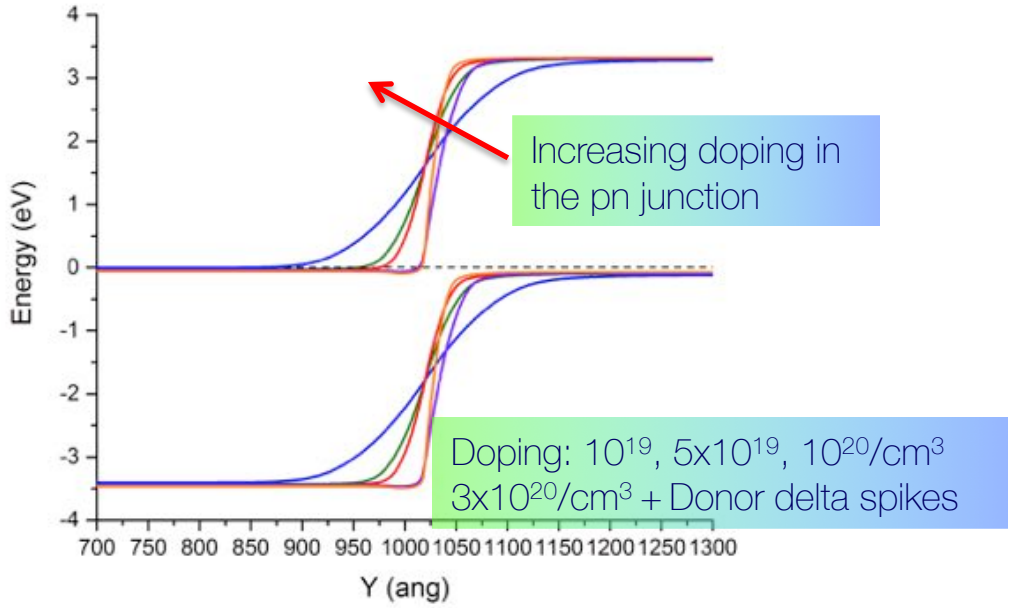

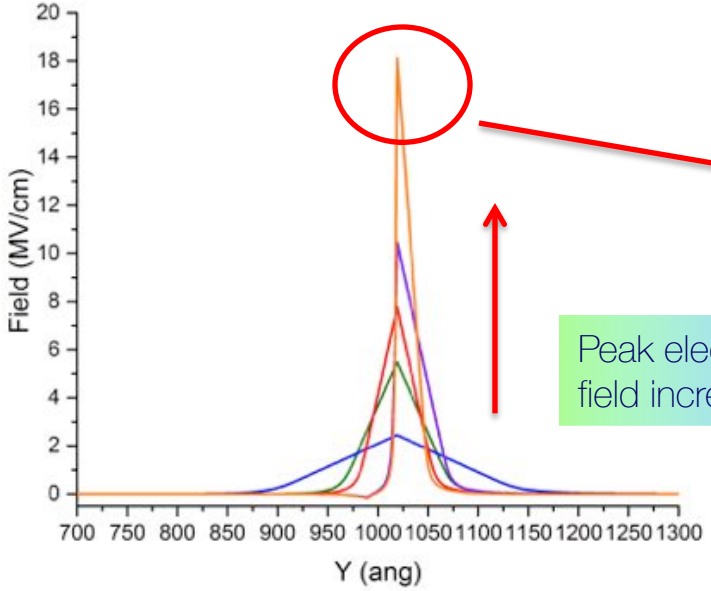

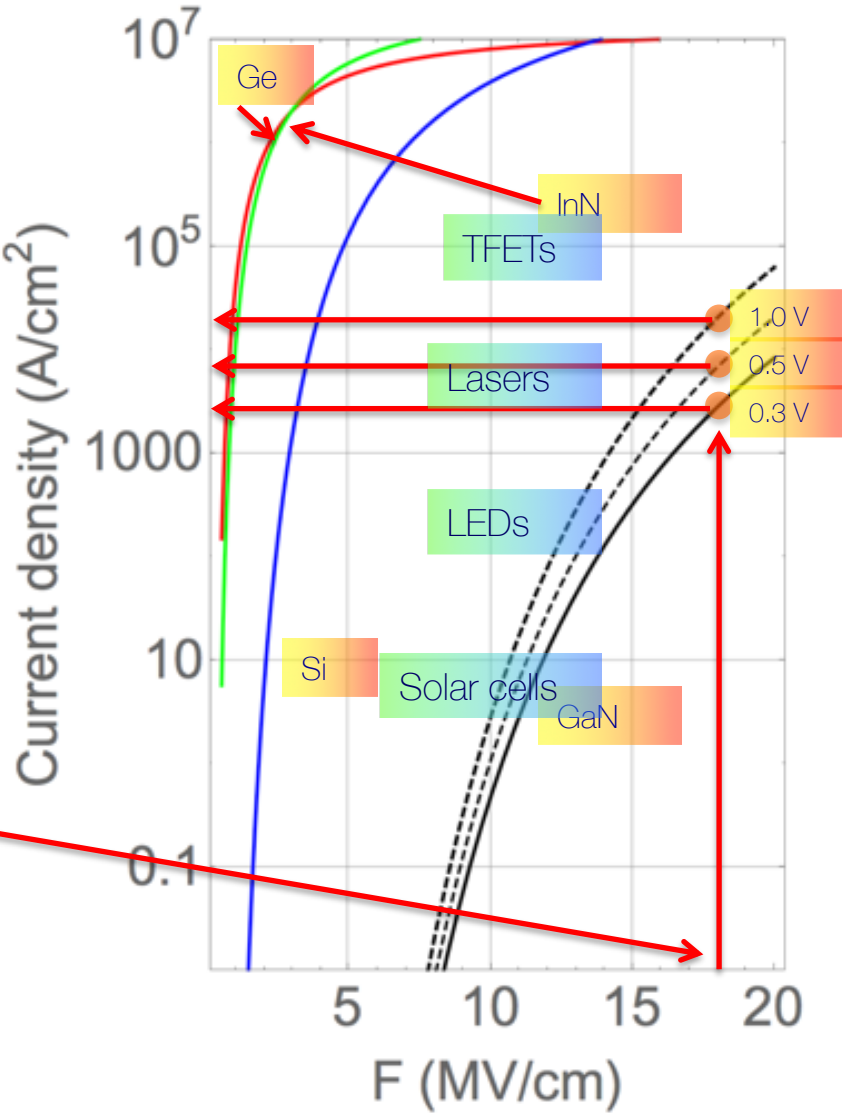

Tunneling in Semiconductors

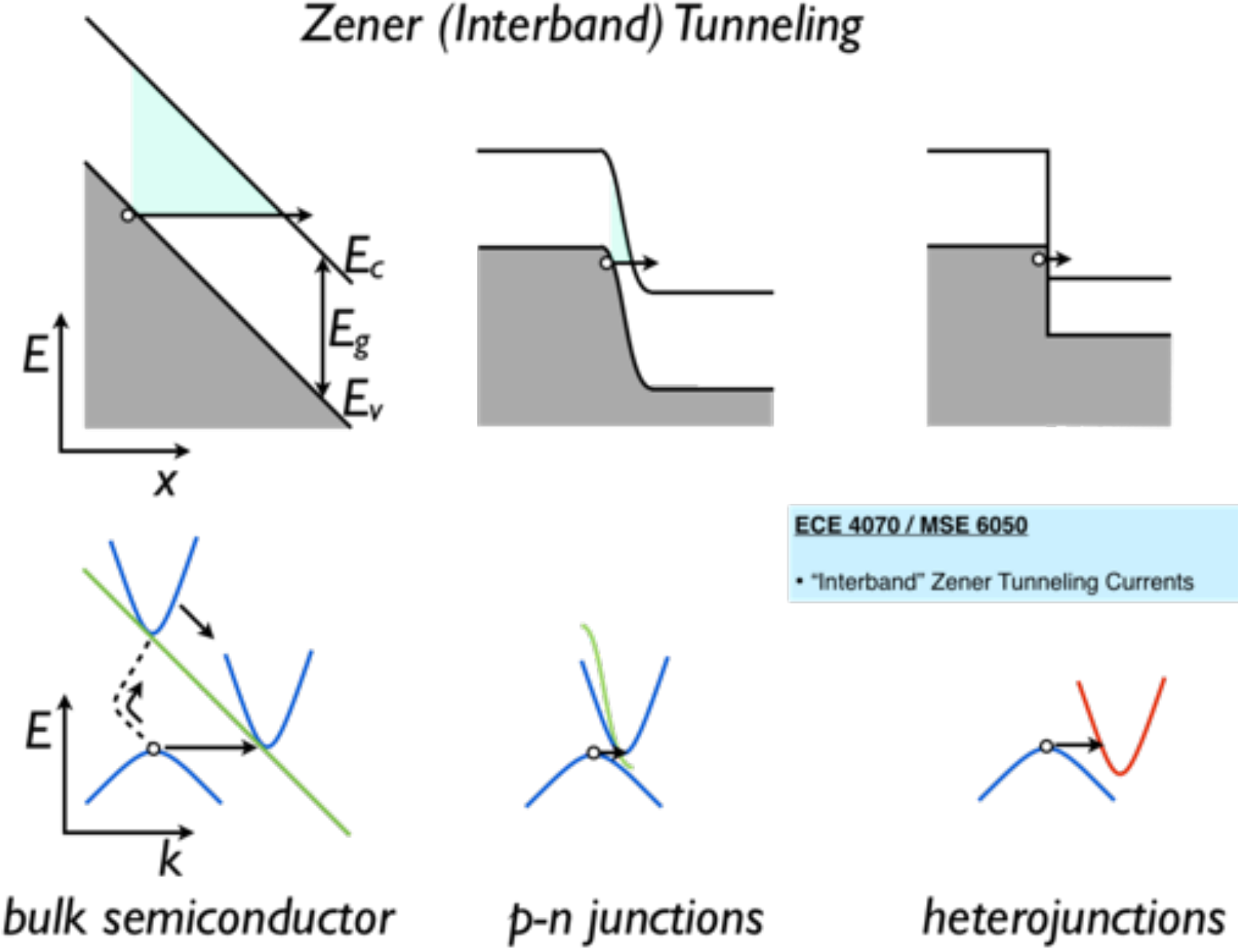

Resonant Tunneling in Semiconductor Nanostructures

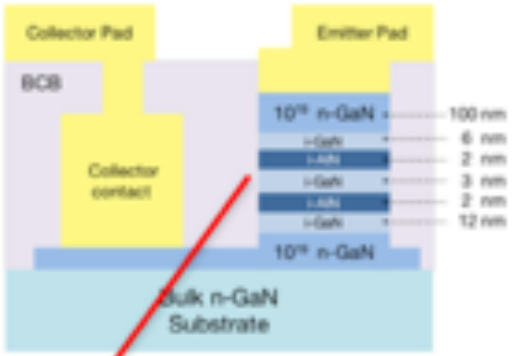

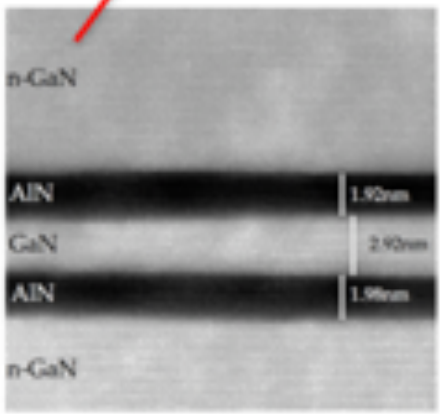

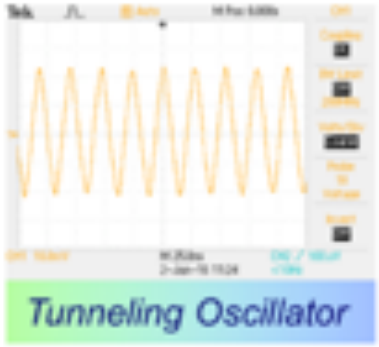

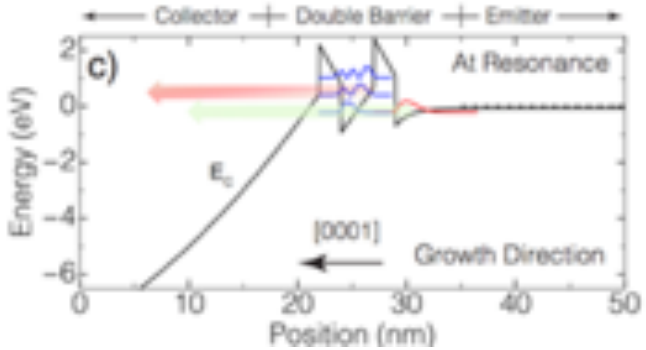

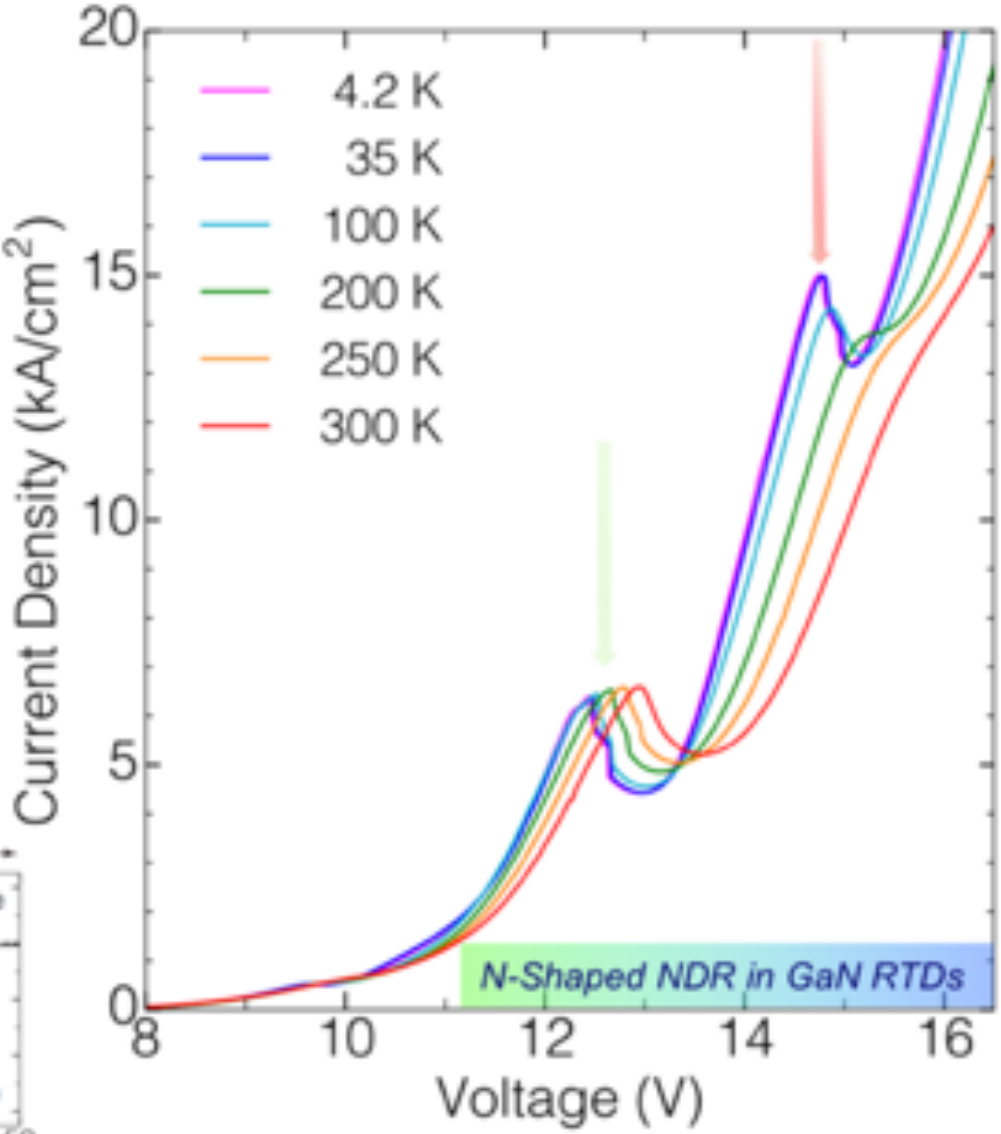

The idea behind "Scattering"

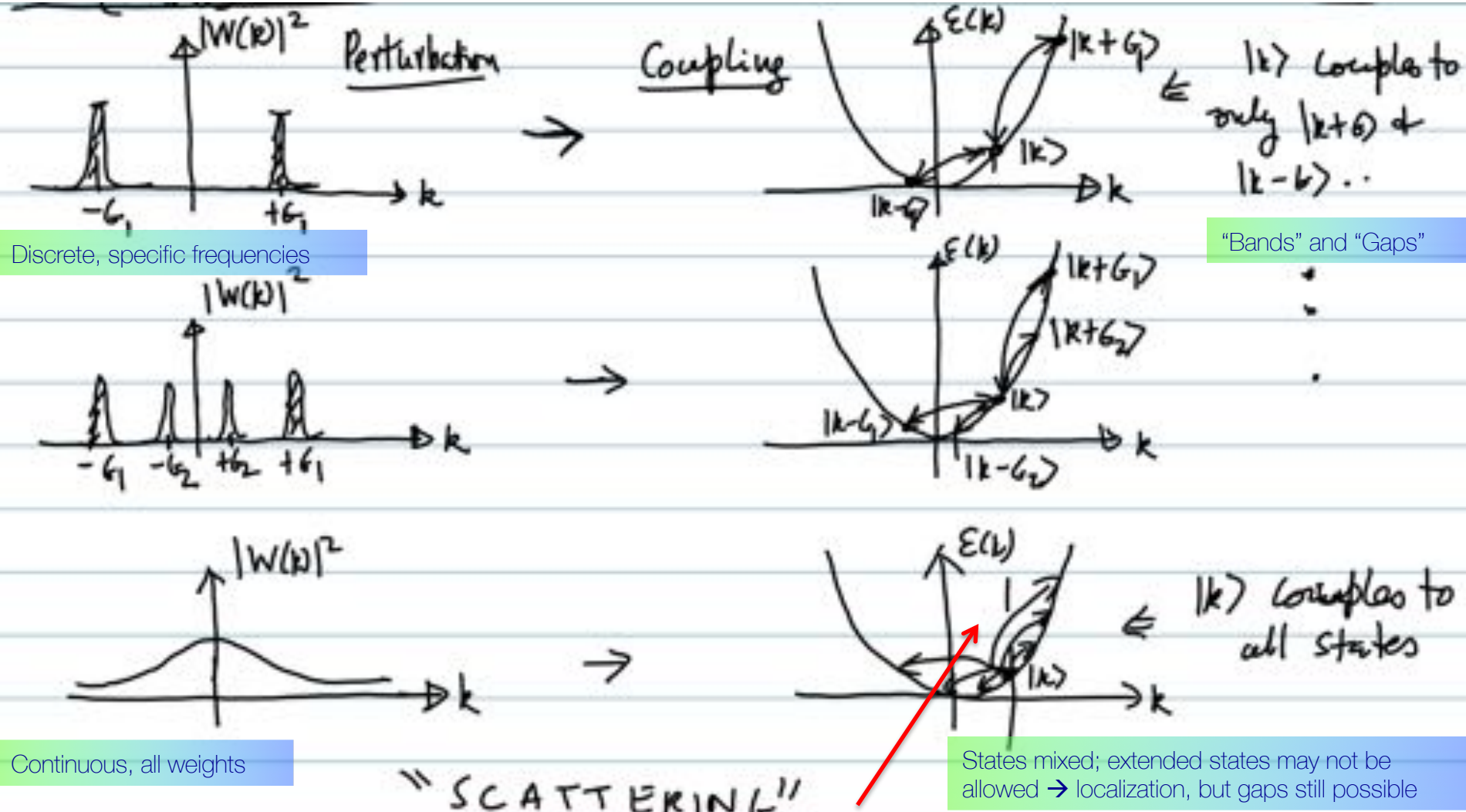

How to find f(k) in the presence of scattering

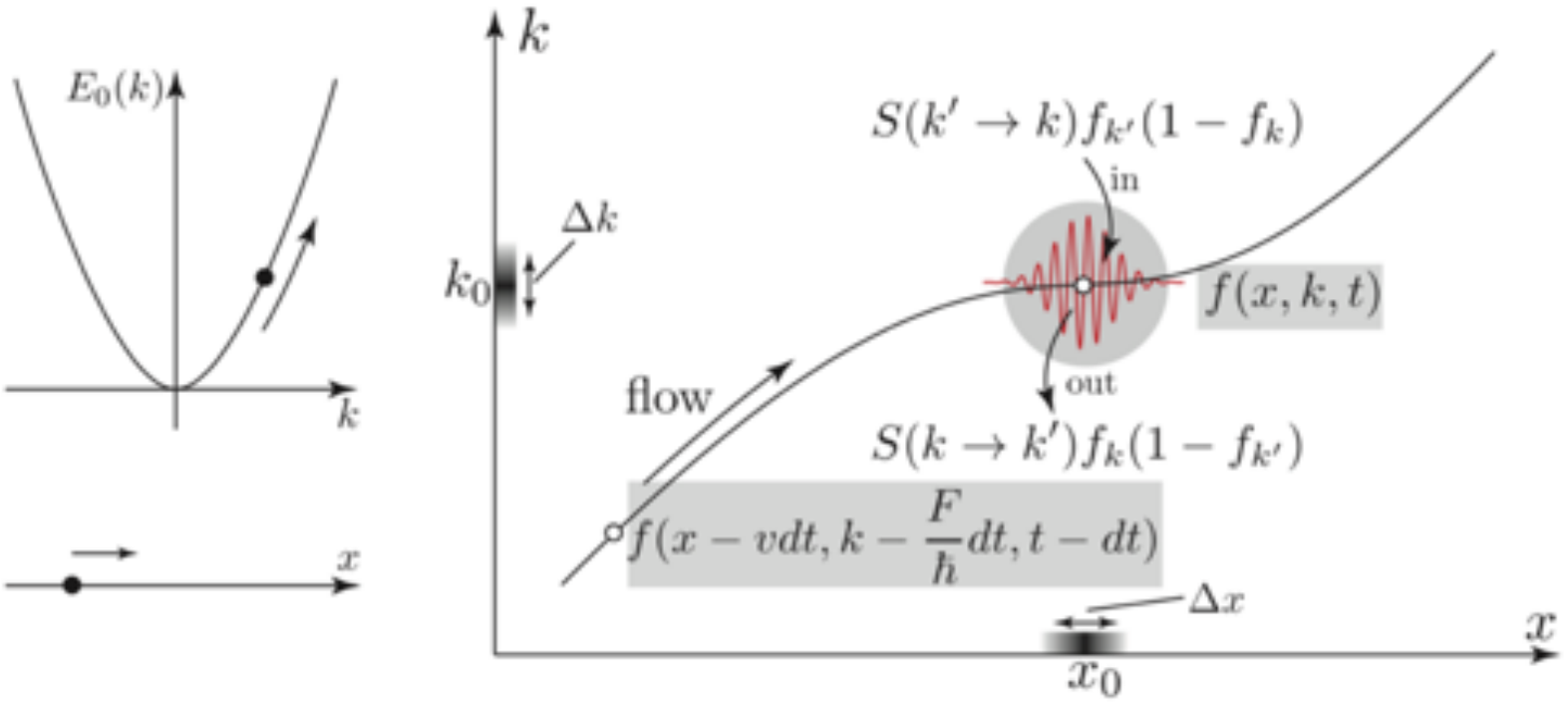

$$\frac{\partial f_k}{\partial t} + \mathbf{v}_k \cdot \nabla_r f_k + \frac{\mathbf{F}}{\hbar} \cdot \nabla_k f_k = \underbrace{\sum_{k'} [S(k' \to k) f_{k'}(1 - f_k) - S(k \to k') f_k(1 - f_{k'})]}_{\text{scattering term, } \hat{C} f_k}.$$

The Boltzmann Transport Equation

$$S(k \to k') = \frac{2\pi}{\hbar} |W_{k,k'}|^2 \delta(E_k - E_{k'} \pm \hbar\omega)$$

Fermi's Golden Rule for Scattering Rates

How to find the quantum current with scattering

$$g_d(\varepsilon) = \frac{1}{2^{d-1}\pi^{\frac{d}{2}}\Gamma(\frac{d}{2})}(\frac{2m^*}{\hbar^2})^{\frac{d}{2}}\varepsilon^{\frac{d}{2}-1}$$

$$n = \int \frac{d^dk}{(2\pi)^d} f(k) = \int d\varepsilon f(\varepsilon) g_d(\varepsilon)$$

$$\mathbf{J} = 2e \int \frac{d^dk}{(2\pi)^d} \mathbf{v} f(\mathbf{k})$$

$$J_i = en \underbrace{\left(-\frac{2e}{dm^*} \frac{\int d\varepsilon \tau_m \varepsilon^{\frac{d}{2}} \frac{\partial f_0}{\partial \varepsilon}}{\int d\varepsilon f_0(\varepsilon) \varepsilon^{\frac{d}{2}-1}}\right)}_{\mu_d} F_i$$

Mobility definition for any dimension

$$f(\mathbf{k}) = f_0(\mathbf{k}) + eF_i\tau(k)v_i\frac{\partial f_0}{\partial \varepsilon}$$

The Boltzmann Transport Equation

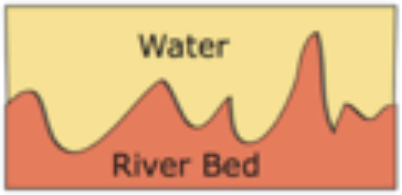

River bed fluctuations 'screened' by water

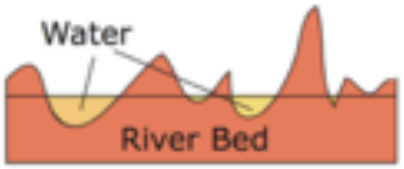

Insufficient water fails to screen fluctuations

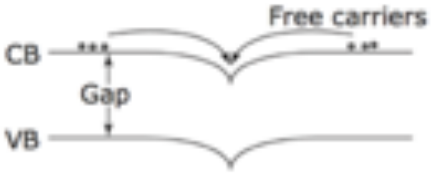

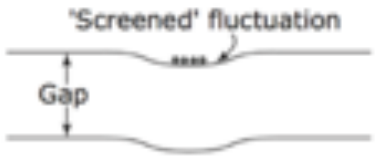

$$U_{sc}(q) = \frac{e^2}{4\pi\epsilon^2 K}\int r^2\sin(\theta)drd\theta d\phi \frac{e^{-\frac{r}{\lambda_D}}}{r} e^{iqr\cos(\theta)}$$

Example of scattering matrix element

$$\mu_I = \frac{2^{\frac{7}{2}}(4\pi\epsilon_s)^2(k_bT)^{\frac{3}{2}}}{\pi^{\frac{3}{2}}Z^2e^3\sqrt{m^*}N_DF(\beta)} \sim \frac{T^{\frac{3}{2}}}{N_D}$$

The Boltzmann Transport Equation gives f(k)

equilibrium

$$f_0(\varepsilon) = \frac{1}{1 + e^{\frac{\varepsilon_{\mathbf{k}} - \mu}{k_B T}}}$$

perturbation

$$f(\mathbf{k}, \mathbf{r}, t)$$

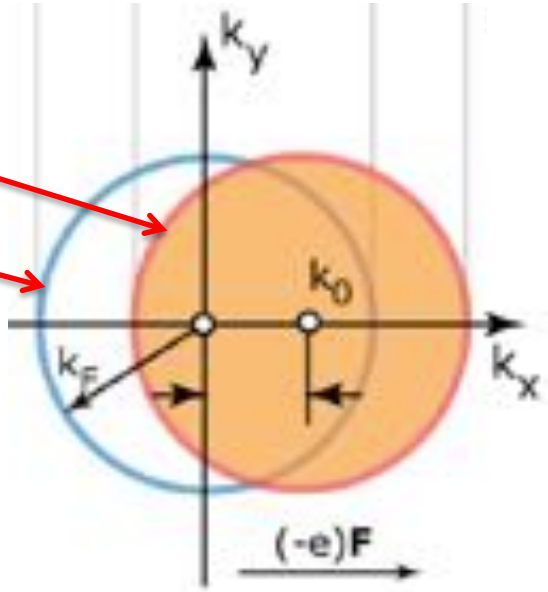

Boltzmann Transport Equation

$$\frac{df}{dt} = \frac{\mathbf{F_t}}{\hbar} \cdot \nabla_{\mathbf{k}} f(\mathbf{k}) + \mathbf{v} \cdot \nabla_{\mathbf{r}} f(\mathbf{k}) + \frac{\partial \mathbf{f}}{\partial \mathbf{t}}$$

Particle number conserved

$$\frac{\partial f}{\partial t} = \frac{\partial f}{\partial t}\Big|_{coll} - \frac{\mathbf{F_t}}{\hbar} \cdot \nabla_{\mathbf{k}} f(\mathbf{k}) - \mathbf{v} \cdot \nabla_{\mathbf{r}} \mathbf{f}(\mathbf{k})$$

$$\left.\frac{\partial f}{\partial t}\right|_c = \frac{-(f - f_0)}{\tau_m}$$

Relaxation time approximation

equilibrium

scattering

$$f = f_0 - \frac{\tau_m}{\hbar} \nabla_k \mathscr{E} \cdot \left(\frac{\partial f}{\partial \mathscr{E}} \mathbf{F} + \nabla_r f \right)$$

bandstructure

applied forces

conc. gradients

The Boltzmann transport equation gives a full-blown treatment of transport properties, and can be solved in several levels of approximation.

Formalism for diffusive charge transport

- Find the perturbation potential due to the defect.
- Use Fermi's Golden rule to evaluate the single-particle scattering rate
- Add up for all allowed states
- Use the solution of Boltzmann equation to find the mobility/conductivity.

$$\mathcal{E}_c(\mathbf{r}) = \mathcal{E}_c^0 + W(\mathbf{r})$$

$$V(\mathbf{q}) = \langle \mathbf{k}' | W(\mathbf{r}) | \mathbf{k} \rangle$$

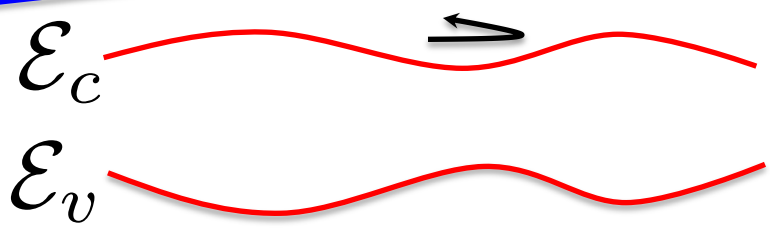

Fermi's golden rule

$$\frac{1}{\tau_{\mathbf{k}\mathbf{k}'}} = \frac{2\pi}{\hbar} |V(\mathbf{q})|^2 \delta[E_{\mathbf{k}'} - (E_{\mathbf{k}} \pm \hbar\omega)]$$

$$f(\mathbf{k}) = f_0(\mathbf{k}) + eF_i \tau(k) v_i \frac{\partial f_0}{\partial \varepsilon}$$

Distribution function: Solution of Boltzmann Transport Equation

$$\mathbf{J} = 2e \int \frac{d^d k}{(2\pi)^d} \mathbf{v} f(\mathbf{k})$$

Current density: Sum over all group velocities `v' in k-space

The Boltzmann Transport Equation

Boltzmann equation →

$$f(k) = f_0(k) + e\tau_m(k)(\mathbf{F}\cdot\mathbf{v})\frac{\partial f_0(k)}{\partial \varepsilon}$$

$$\frac{1}{\tau_m(k)} = \sum_{k'} S(k,k')(1-\cos\theta)$$ - Momentum scattering time $\left(\mu = \frac{e\langle\tau_m(k)\rangle}{m^*}\right)$

$$\frac{1}{\tau_q(k)} = \sum_{k'} S(k,k')$$ - Quantum scattering time

$$S(k,k') = \frac{2\pi}{\hbar}\left|\langle k' \mid \Delta E_c(r) \mid k\rangle\right|^2 \delta(\varepsilon_k - \varepsilon_{k'})$$

Fermi's Golden Rule gives: Scattering rate from state k → k' by perturbation DE_c

Most general expression for 'Current Density' in 'd' dimensions:

$$\mathbf{J_d} = q \times \frac{g_s g_v}{L^d}\sum_k \mathbf{v_g}(k) f(k),$$ where

charge current density (general case)

qv_g may be replaced by other physical quantities:

qv_g → charge current density (electrical cond.)
1 → carrier density
E (k) → heat current density (thermal cond.)
…

Time-dependent perturbation theory

$$i\hbar\frac{\partial}{\partial t}|\Psi_t\rangle = H_0|\Psi_t\rangle$$

Unperturbed problem

$$i\hbar\frac{\partial}{\partial t}|\Psi_t\rangle = [H_0 + W_t]|\Psi_t\rangle$$

Perturbation

Time-dependent perturbation

transformation

$$|\Psi_t\rangle = e^{-i\frac{H_0}{\hbar}t}|\Psi(t)\rangle$$

H_0 is the Hamiltonian *operator*

If the system was in an eigenstate $|\Psi_{t_0}\rangle = |0\rangle$ of energy E_0 at time t_0, then the state at a future time differs from the initial state by a phase factor

$$H_0|\Psi_{t_0}\rangle = E_0|\Psi_{t_0}\rangle \implies |\Psi_t\rangle = e^{-i\frac{E_0}{\hbar}(t-t_0)}|\Psi_{t_0}\rangle.$$

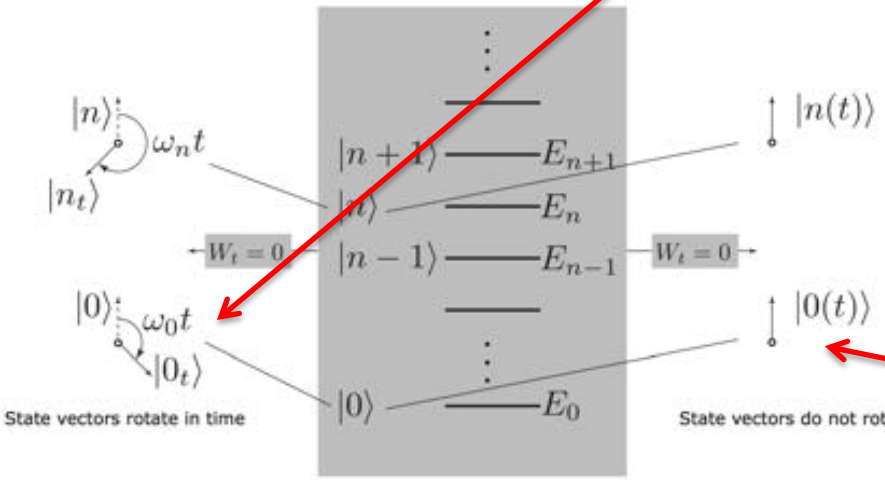

$$i\hbar\frac{\partial}{\partial t}|\Psi(t)\rangle = [e^{+i\frac{H_0}{\hbar}t}W_t e^{-i\frac{H_0}{\hbar}t}]|\Psi(t)\rangle = W(t)|\Psi(t)\rangle$$

Time-dependent evolution in the Interaction picture

$$W_t = 0 \implies W(t) = 0 \implies i\hbar\frac{\partial|\Psi(t)\rangle}{\partial t} = 0$$

$$|\Psi(t)\rangle = |\Psi(t_0)\rangle$$

If W=0, the state vector does not rotate in time in the interaction picture.

$|\Psi_t\rangle$

$$|\Psi_t\rangle = e^{-i\frac{H_0}{\hbar}t}|\Psi(t)\rangle$$

Transformation

$$i\hbar\frac{\partial}{\partial t}|\Psi_t\rangle = [H_0 + W_t]|\Psi_t\rangle$$

Schrodinger picture

$|\Psi(t)\rangle$

$$i\hbar\frac{\partial}{\partial t}|\Psi(t)\rangle = [\underbrace{e^{-i\frac{H_0}{\hbar}t}W_t e^{-i\frac{H_0}{\hbar}t}}_{W(t)}]|\Psi(t)\rangle$$

Interaction picture

FIGURE 24.1: Schrodinger vs. Interaction pictures of time-evolution of quantum state.

$$i\hbar\frac{\partial}{\partial t}|\Psi(t)\rangle = W(t)|\Psi(t)\rangle$$

$$|\Psi(t)\rangle = |\Psi(t_0)\rangle + \frac{1}{i\hbar}\int_{t_0}^{t} dt' W(t')|\Psi(t')\rangle$$

Starting point for time-dependent perturbation theory

Time-dependent perturbation theory

The *probability* of the state making a transition from $|0\rangle$ to $|n\rangle$ at time t is

$$|\langle n|\Psi_t\rangle|^2 = |\langle n|\Psi(t)\rangle|^2 \approx |\langle n|W|0\rangle|^2 \frac{e^{2\eta t}}{(E_0 - E_n)^2 + (\hbar\eta)^2}.$$

The *rate* of transitions from state $|0\rangle \to |n\rangle$ is

$$\frac{1}{\tau_{|0\rangle\to|n\rangle}} = \frac{d}{dt}|\langle n|\Psi(t)\rangle|^2 \approx |\langle n|W|0\rangle|^2 \left(\frac{2\eta}{(E_0 - E_n)^2 + (\hbar\eta)^2}\right) e^{2\eta t}.$$

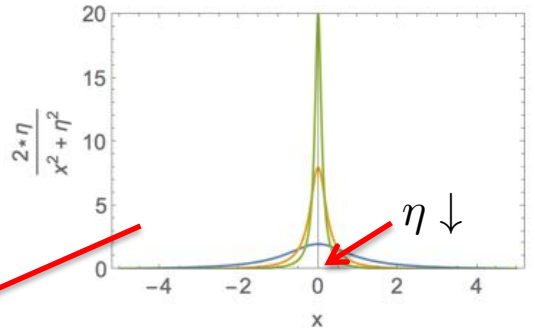

$$\lim_{\eta\to 0^+} \frac{2\eta}{x^2+\eta^2} = \lim_{\eta\to 0^+} \frac{1}{i}\left[\frac{1}{x-i\eta} - \frac{1}{x+i\eta}\right] = 2\pi\delta(x)$$

$$\delta(ax) = \delta(x)/|a|$$

$$\frac{1}{\tau_{|0\rangle\to|n\rangle}} \approx \frac{2\pi}{\hbar}|\langle n|W|0\rangle|^2\delta(E_0 - E_n),$$

Fermi's golden rule for time-varying potentials

$$\theta(\omega) = \int_0^\infty dt e^{i\omega t} = \lim_{\eta\to 0^+}\int_0^\infty dt e^{-\eta t}e^{i\omega t} = \lim_{\eta\to 0^+}\frac{i}{\omega + i\eta} = \frac{i}{\omega^+}$$

Two useful results to be used extensively later!

$$\frac{1}{\omega^+} = P[\frac{1}{\omega}] - i\pi\delta(\omega) \to \int_{-\infty}^{+\infty} d\omega \frac{f(\omega)}{\omega^+} = P[\int_{-\infty}^{+\infty} d\omega \frac{f(\omega)}{\omega}] - i\pi f(0)$$

Here P[…] is the "principal part" of a function

Perturbations oscillating in time

$$W_t = 2We^{\eta t}\cos(\omega t) = e^{\eta t}W(e^{i\omega t} + e^{-i\omega t})$$

$$\langle n|\Psi(t)\rangle \approx \frac{\langle n|W|0\rangle}{i\hbar}\left(\int_{t_0}^t dt' e^{i\left(\frac{E_n - E_0 + \hbar\omega}{\hbar}\right)t'}e^{\eta t'} + \int_{t_0}^t dt' e^{i\left(\frac{E_n - E_0 - \hbar\omega}{\hbar}\right)t'}e^{\eta t'}\right)$$

$$\frac{1}{\tau_{|0\rangle\to|n\rangle}} \approx \frac{2\pi}{\hbar} \times |\langle n|W|0\rangle|^2 \times [\underbrace{\delta(E_0 - E_n + \hbar\omega)}_{\text{absorption}} + \underbrace{\delta(E_0 - E_n - \hbar\omega)}_{\text{emission}}].$$

Fermi's golden rule for oscillating potentials

Scattering rate due to point scatterers

$$W(r) = V_0\delta(\mathbf{r})$$

$$\langle \mathbf{k}'|V_0\delta(\mathbf{r})|\mathbf{k}\rangle = \int d^3\mathbf{r}\left(\frac{e^{-i\mathbf{k}'\cdot\mathbf{r}}}{\sqrt{V}}\right)V_0\delta(\mathbf{r})\left(\frac{e^{+i\mathbf{k}\cdot\mathbf{r}}}{\sqrt{V}}\right) = \frac{V_0}{V}$$

$$\frac{1}{\tau(|\mathbf{k}\rangle \rightarrow |\mathbf{k}'\rangle)} = \frac{2\pi}{\hbar}\left(\frac{V_0}{V}\right)^2\delta(E_\mathbf{k} - E_{\mathbf{k}'})$$

$$\frac{1}{\tau(|\mathbf{k}\rangle)} = \sum_{\mathbf{k}'}\frac{1}{\tau(|\mathbf{k}\rangle \rightarrow |\mathbf{k}'\rangle)} = \frac{2\pi}{\hbar}\left(\frac{V_0}{V}\right)^2\underbrace{\sum_{\mathbf{k}'}\delta(E_\mathbf{k} - E_{\mathbf{k}'})}_{D(E_\mathbf{k})}$$

$$\frac{1}{\tau(E_\mathbf{k})} = \frac{2\pi}{\hbar}\left(\frac{V_0}{V}\right)^2 n_{sc}V\int\frac{d^3\mathbf{k}'}{\frac{(2\pi)^3}{V}}\delta(E_\mathbf{k} - E_{\mathbf{k}'}) = \frac{2\pi}{\hbar}V_0^2 n_{sc}g(E_\mathbf{k})$$

Scattering of Bloch Electron States

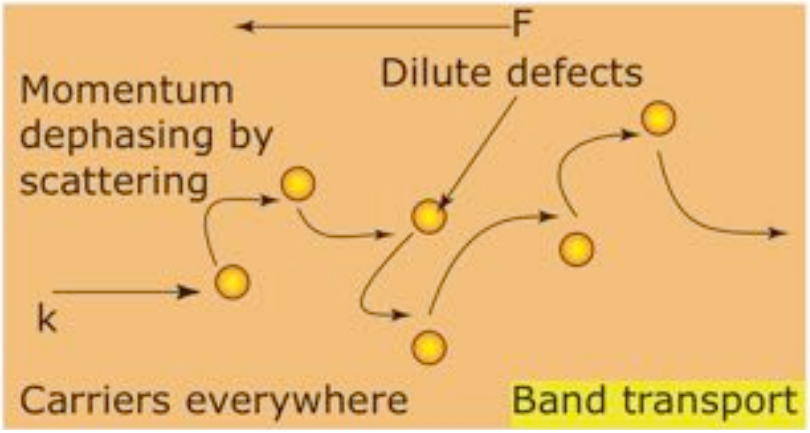

$$\frac{1}{\tau_{\mathbf{k}\mathbf{k}'}} = \frac{2\pi}{\hbar}|V(\mathbf{q})|^2\delta[E_{\mathbf{k}'} - (E_{\mathbf{k}} \pm \hbar\omega)]$$

$$\mathbf{q} = \mathbf{k} - \mathbf{k}'$$

$$V(\mathbf{q}) = \langle \mathbf{k}'|W(\mathbf{r})|\mathbf{k}\rangle$$

Fermi's Golden Rule tells us that the scattering potential is the SUM of ALL the scatterers in the macroscopic crystal.

How do multiple scattering centers add up and contribute to the total scattering rate?

$$= \int_V [\frac{e^{-i\mathbf{k}'\cdot\mathbf{r}}}{\sqrt{V}} u^{\star}_{\mathbf{K}}(\mathbf{r})] \times W(\mathbf{r}) \times [\frac{e^{+i\mathbf{k}\cdot\mathbf{r}}}{\sqrt{V}} u_{\mathbf{K}}(\mathbf{r})] d^3\mathbf{r}$$

$$= \int_V [\frac{e^{i(\mathbf{k}-\mathbf{k}')\cdot\mathbf{r}}}{V}] W(\mathbf{r}) \times [u^{\star}_{\mathbf{K}}(\mathbf{r}) u_{\mathbf{K}}(\mathbf{r})] d^3\mathbf{r}$$

$$\approx \underbrace{\left(\int_V e^{i\mathbf{q}\cdot\mathbf{r}} W(\mathbf{r}) \frac{d^3\mathbf{r}}{V} \right)}_{crystal} \times \underbrace{\left(\int_\Omega u^{\star}_{\mathbf{K}}(\mathbf{r}) u_{\mathbf{K}}(\mathbf{r}) \frac{d^3\mathbf{r}}{\Omega} \right)}_{=1}$$

Fourier Transform of real-space scattering potential!

$$V(\mathbf{q}) \approx \int_V e^{i\mathbf{q}\cdot\mathbf{r}} W(\mathbf{r}) \frac{d^3\mathbf{r}}{V}$$

Scattering by many impurities

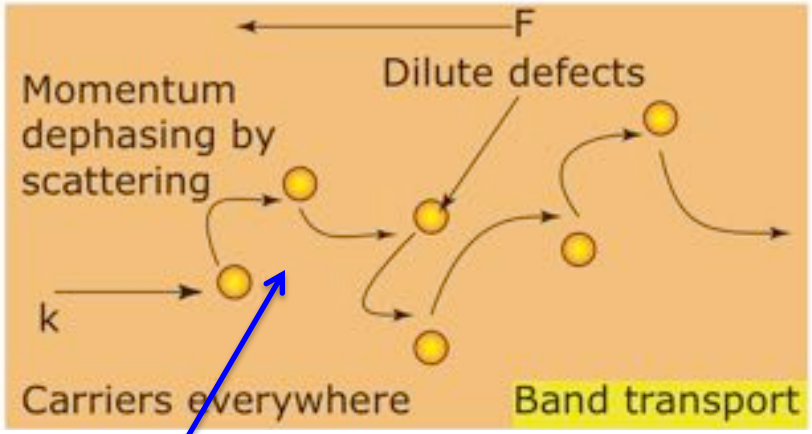

Impurity locations are R_1, R_2, … They are "uncorrelated"

$$W_{total}(\mathbf{r}) = \underbrace{W(\mathbf{r}) + W(\mathbf{r}-\mathbf{R_1}) + W(\mathbf{r}-\mathbf{R_2}) + \ldots}_{`N'_{imp} impurities}$$

$$V_0(\mathbf{q}) \approx \int_V e^{i\mathbf{q}\cdot\mathbf{r}} W(\mathbf{r}) \frac{d^3\mathbf{r}}{V}$$

$$V_{total}(\mathbf{q}) = V_0(\mathbf{q}) + \int_V e^{i\mathbf{q}\cdot\mathbf{r}} W(\mathbf{r}-\mathbf{R_1}) \frac{d^3\mathbf{r}}{V} + \ldots$$

$$V_{total}(\mathbf{q}) = V_0(\mathbf{q}) + V_0(\mathbf{q}) e^{i\mathbf{q}\cdot\mathbf{R_1}} + V_0(\mathbf{q}) e^{i\mathbf{q}\cdot\mathbf{R_2}} \ldots$$

$$V_{total}(\mathbf{q}) = V_0(\mathbf{q}) [\underbrace{1 + e^{i\mathbf{q}\cdot\mathbf{R_1}} + e^{i\mathbf{q}\cdot\mathbf{R_2}} \ldots}_{`N' terms}]$$

$$|V_{total}(\mathbf{q})|^2 = |V_0(\mathbf{q})|^2 [(\underbrace{1 + e^{i\mathbf{q}\cdot\mathbf{R_1}} + e^{i\mathbf{q}\cdot\mathbf{R_2}} \ldots}_{`N'_{imp} terms}) \times (\underbrace{1 + e^{-i\mathbf{q}\cdot\mathbf{R_1}} + e^{-i\mathbf{q}\cdot\mathbf{R_2}} \ldots}_{`N'_{imp} terms})]$$

$$|V_{total}(\mathbf{q})|^2 = |V_0(\mathbf{q})|^2 [N_{imp} + (\underbrace{e^{i\mathbf{q}\cdot(\mathbf{R_1}-\mathbf{R_2})} + e^{i\mathbf{q}\cdot(\mathbf{R_1}-\mathbf{R_3})} \ldots}_{\approx 0 (RPA)})]$$

$$|V_{total}(\mathbf{q})|^2 = N_{imp} |V_0(\mathbf{q})|^2$$

Fourier Transform property:

$$\int e^{iqx} f(x) dx \leftrightarrow F(q)$$

$$\int e^{iqx} f(x+a) dx \leftrightarrow F(q) \times e^{iqa}$$

Effect of multiple scattering

$$\frac{1}{\tau_{\mathbf{k}\mathbf{k}'}(total)} = \frac{2\pi}{\hbar} N_{imp} \times |V_0(\mathbf{q})|^2 \delta[E_{\mathbf{k}'} - (E_{\mathbf{k}} \pm \hbar\omega)]$$

Scattering rate is linearly proportional to impurity density in the dilute uncorrelated limit!

Scattering events in semiconductors

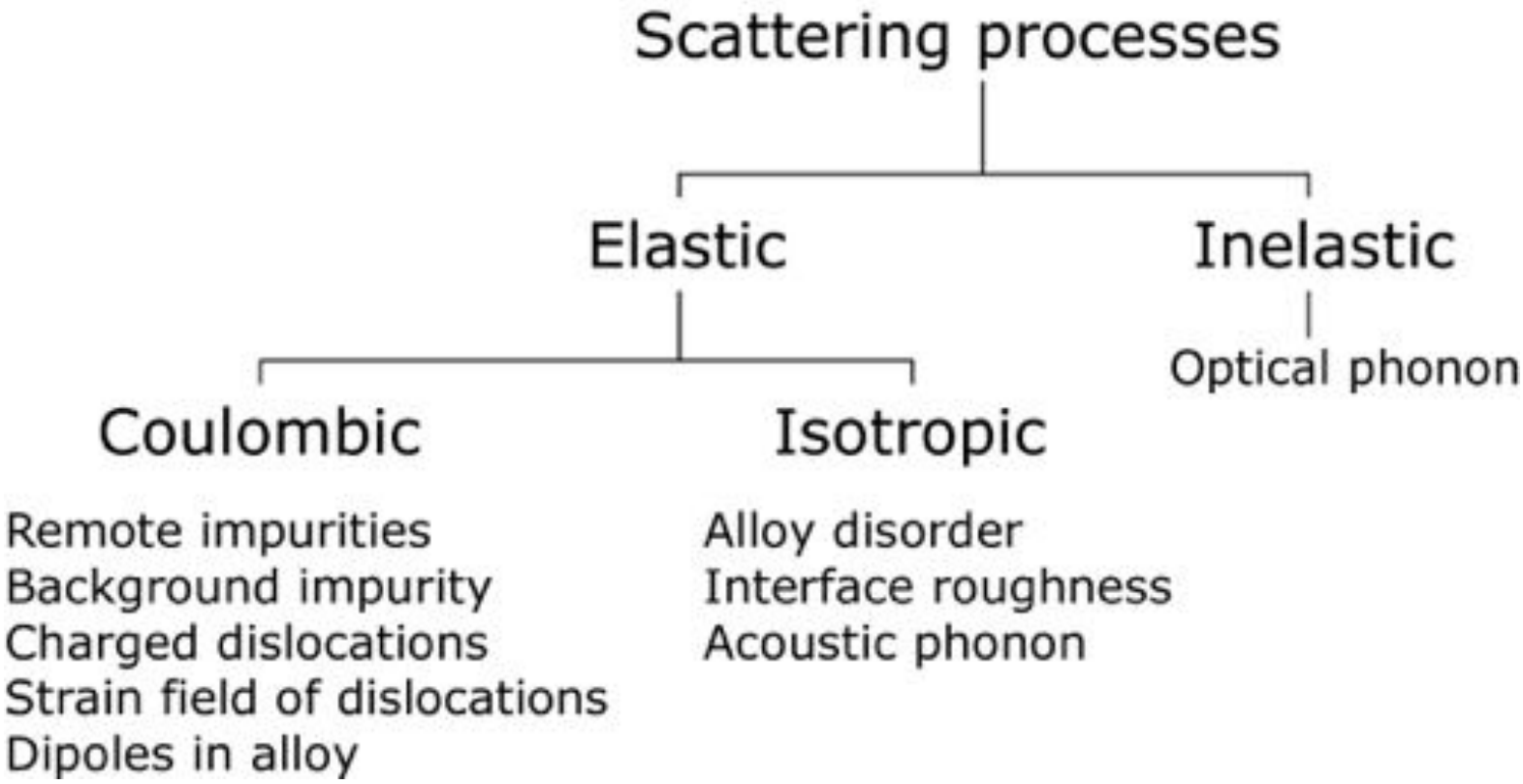

A static periodic potential causes no scattering → every other potential causes scattering!

Periodic 'non-static' potentials: Phonons.
Static non-periodic potentials: Defects & Impurities.

General Nature of Scattering Rates

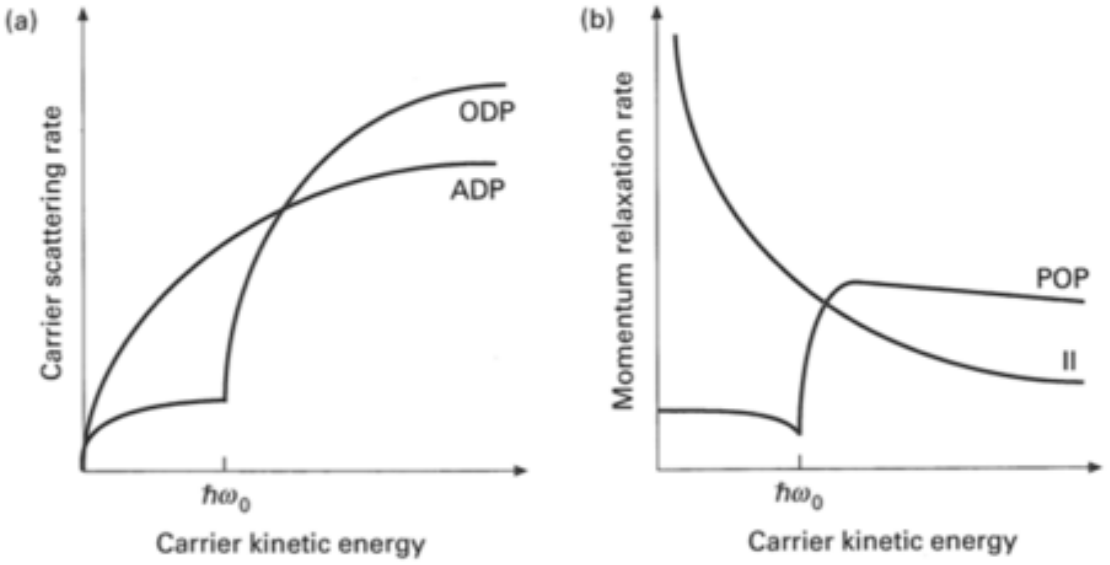

Fig. 2.4 General features of carrier scattering in semiconductors. (a) Nonpolar phonon scattering, acoustic deformation potential (ADP) in the elastic limit and optical deformation potential (ODP). (b) Scattering by electrostatic interactions, ionized impurity (II) and polar optical phonon (POP).

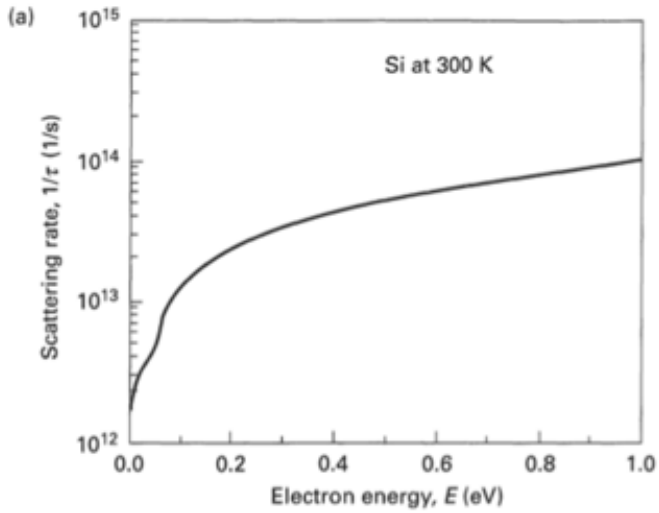

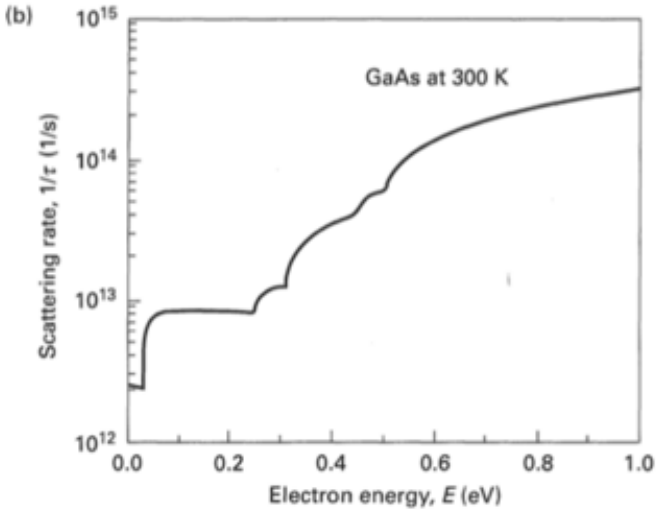

Scattering rates are typically proportional to the density of states

From Lundstrom: Fundamentals of Carrier Transport

Scattering events in semiconductors

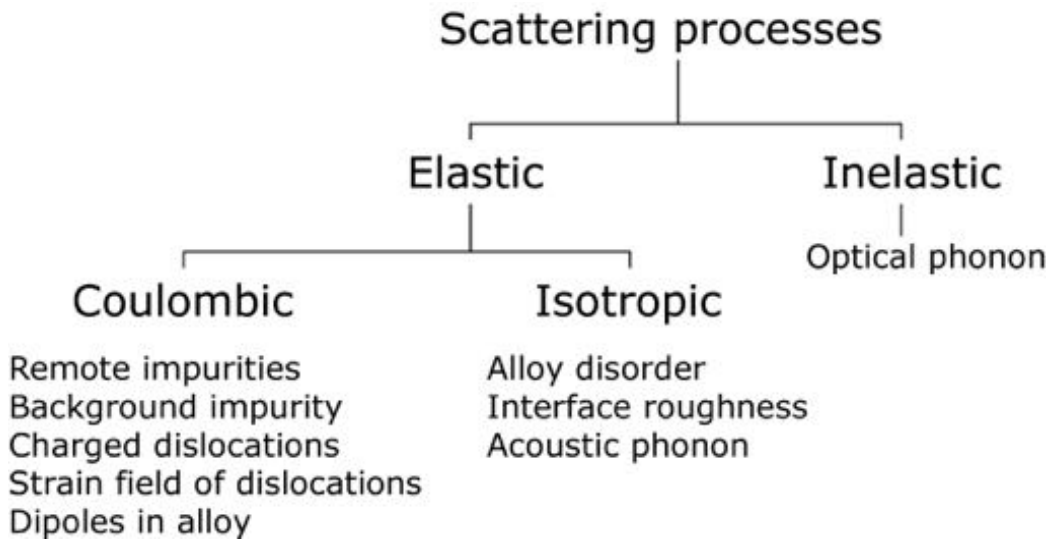

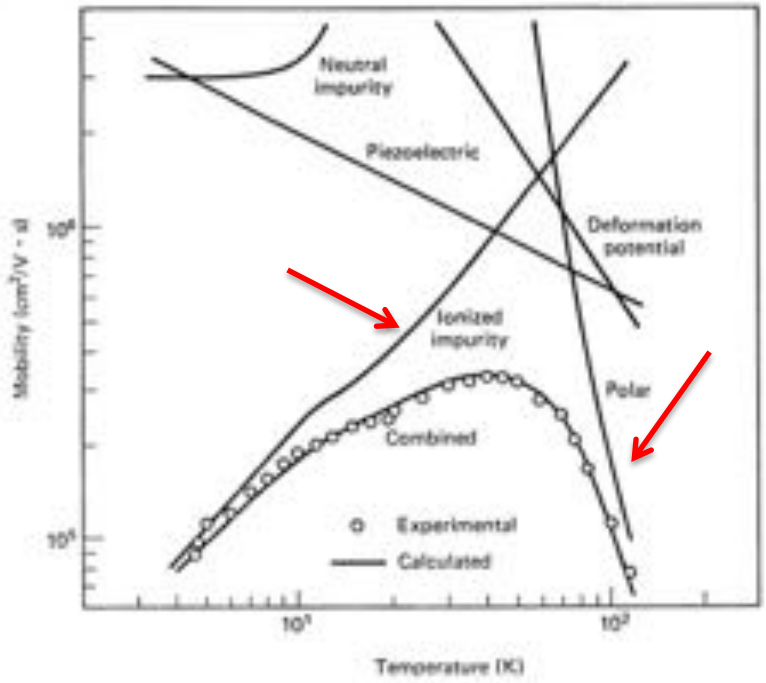

Figure 6.7 Temperature dependence of the mobility for *n*-type GaAs showing the separate and combined scattering processes. [From C. M. Wolfe, G. E. Stillman, and W. T. Lindley, *J. Appl. Phys. 41*, 3088 (1970).]

Scattering by each type of impurity affects the net electron mobility.

- Mobility in a ultra-clean (defect-free) semiconductor is limited by phonon (optical+acoustic) scattering.
- If the scattering rate of defects/impurities exceed that of phonons, then they determine the mobility.
- Method: find the scattering rate due to each type of defect. The total scattering rate is the sum of all.

Scattering by a neutral impurity

$$\mathcal{E}_c(\mathbf{r}) = \mathcal{E}_c^0 + W(\mathbf{r}) \longleftarrow W(r) = W_0\Theta(r - r_0)$$

$$V(\mathbf{q}) = \langle \mathbf{k}'|W(\mathbf{r})|\mathbf{k}\rangle$$

$$\frac{1}{\tau_{\mathbf{k}\mathbf{k}'}} = \frac{2\pi}{\hbar}|V(\mathbf{q})|^2\delta[E_{\mathbf{k}'} - (E_{\mathbf{k}} \pm \hbar\omega)]$$

$$\langle \tau_m \rangle = \frac{2}{3}\frac{\int_0^\infty \tau_m(-\partial f_0/\partial x)x^{3/2}\,dx}{\int_0^\infty f_0 x^{1/2}\,dx}$$

$$\mu_c = \frac{q\langle \tau_m \rangle}{m^*}$$

This & next few slides: material from
- Wolfe/Holonyak/Stillman
- Seeger

From Seeger: Derive your own expression!

$$\mu = \frac{e}{20\,a_B\,\hbar}\,\frac{m/m_0}{\varkappa N^x}$$

which is independent of temperature.

$$\mu = \frac{1.44 \times 10^{22}\ \text{cm}^{-3}}{N^x}\,\frac{m/m_0}{\varkappa}.$$

For example, for electrons in Ge, where $m/m_0 = 0.12$ and $\varkappa = 16$, a mobility of $1.1 \times 10^3\ \text{cm}^2/\text{V s}$ is obtained assuming, e.g., $10^{17}\ \text{cm}^{-3}$ neutral impurities.

Scattering by charged impurities

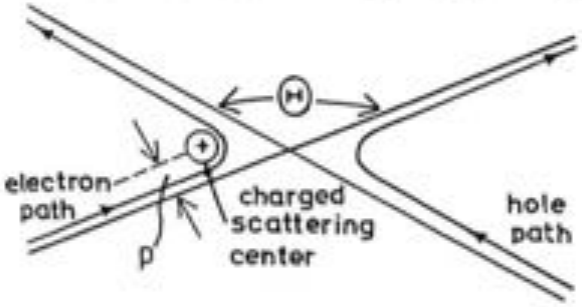

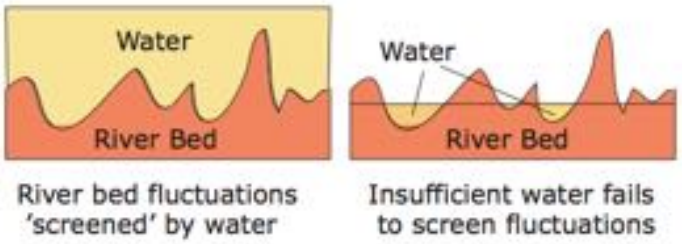

River bed fluctuations 'screened' by water

Insufficient water fails to screen fluctuations

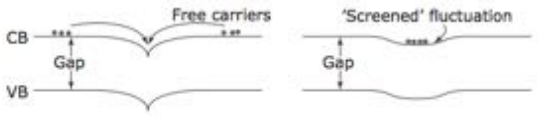

Screened coulomb scattering potential

$$V(r) = -(Z|e|/4\pi\varkappa\varkappa_0 r)\exp(-r/L_D)$$

$$H_{k'k} = -\frac{Ze^2}{V\varkappa\varkappa_0|k-k'|}\int_0^\infty \exp(-r/L_D)\sin(|k-k'|r)\,dr$$

$$= -\frac{Ze^2}{V\varkappa\varkappa_0}\frac{1}{|k-k'|^2+L_D^{-2}} \approx -\frac{Ze^2}{V\varkappa\varkappa_0 4k^2}\frac{1}{\sin^2(\theta/2)+(2k\,L_D)^{-2}}, \quad (6.3.13)$$

$$|k-k'| \approx 2k\sin(\theta/2)$$

$$\beta_{BH} = 2\frac{m}{\hbar}\left(\frac{2}{m}3k_BT\right)^{1/2}L_D$$

$$\beta_{BH} = \left(\frac{\varkappa}{16}\right)^{1/2}\frac{T}{100\text{ K}}\left(\frac{m}{m_0}\right)^{1/2}\left(\frac{2.08\times10^{18}\text{ cm}^{-3}}{n}\right)^{1/2}$$

Brooks-Herring dimensionless factor

The mobility $\mu = (e/m)\langle\tau_m\rangle$ is given by

$$\mu = \frac{2^{7/2}(4\pi\varkappa\varkappa_0)^2(k_BT)^{3/2}}{\pi^{3/2}Z^2e^3m^{1/2}N_I[\ln(1+\beta_{BH}^2)-\beta_{BH}^2/(1+\beta_{BH}^2)]}$$

which in units of $\text{cm}^2/\text{V s}$ is

$$\mu = \frac{3.68\times10^{20}\text{ cm}^{-3}}{N_I}\frac{1}{Z^2}\left(\frac{\varkappa}{16}\right)^2\left(\frac{T}{100\text{ K}}\right)^{1.5}\cdot\frac{1}{(m/m_0)^{1/2}[\log(1+\beta_{BH}^2)-0.434\,\beta_{BH}^2/(1+\beta_{BH}^2)]}$$

and the log is to the base 10.

Phonons in Semiconductors

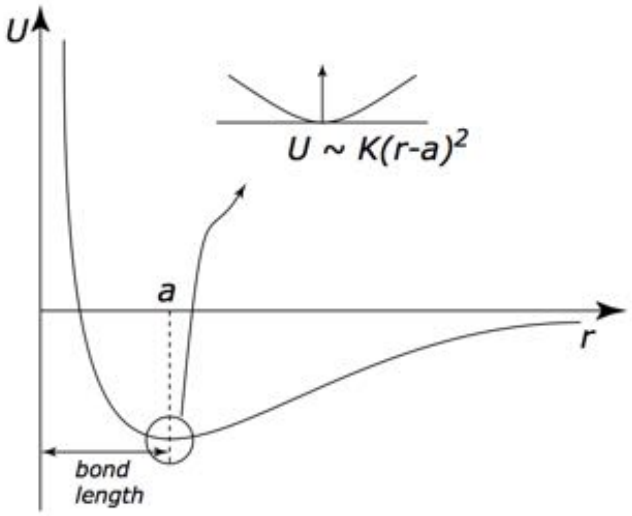

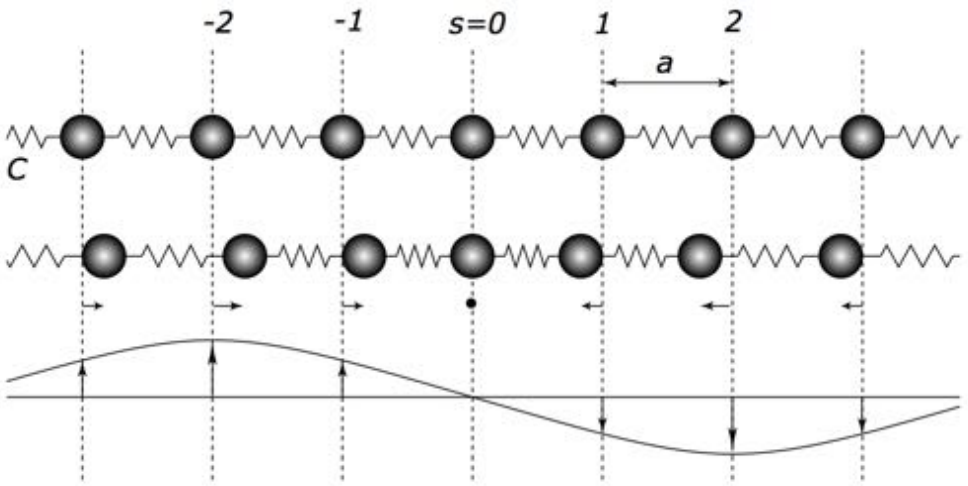

Newton's law for mass-spring chain

$$F = M\frac{d^2u_s}{dt^2} = C(u_{s+1} - u_s) + C(u_{s-1} - u_s)$$

$$u_s = u_0 e^{i(qsa-\omega t)}$$

Vibrations form a wave

$$\omega^2(q) = \frac{2C}{M}(1 - \cos qa)$$

Acoustic phonon dispersion

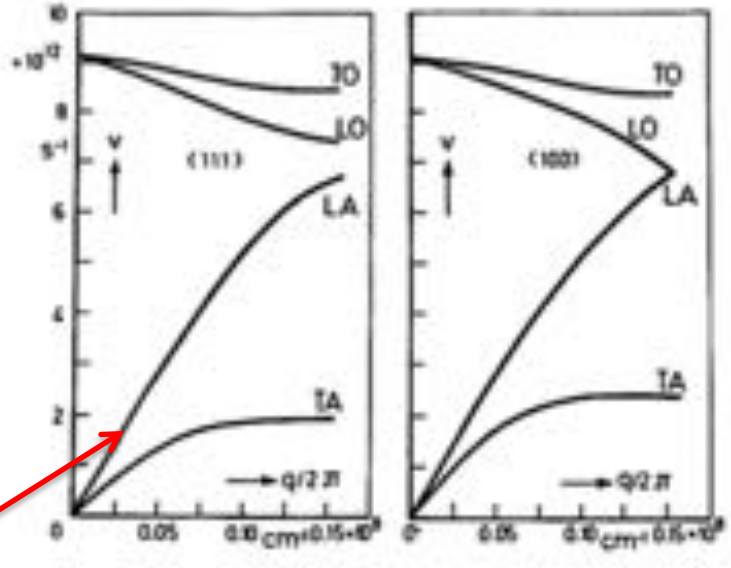

Phonons in Semiconductors

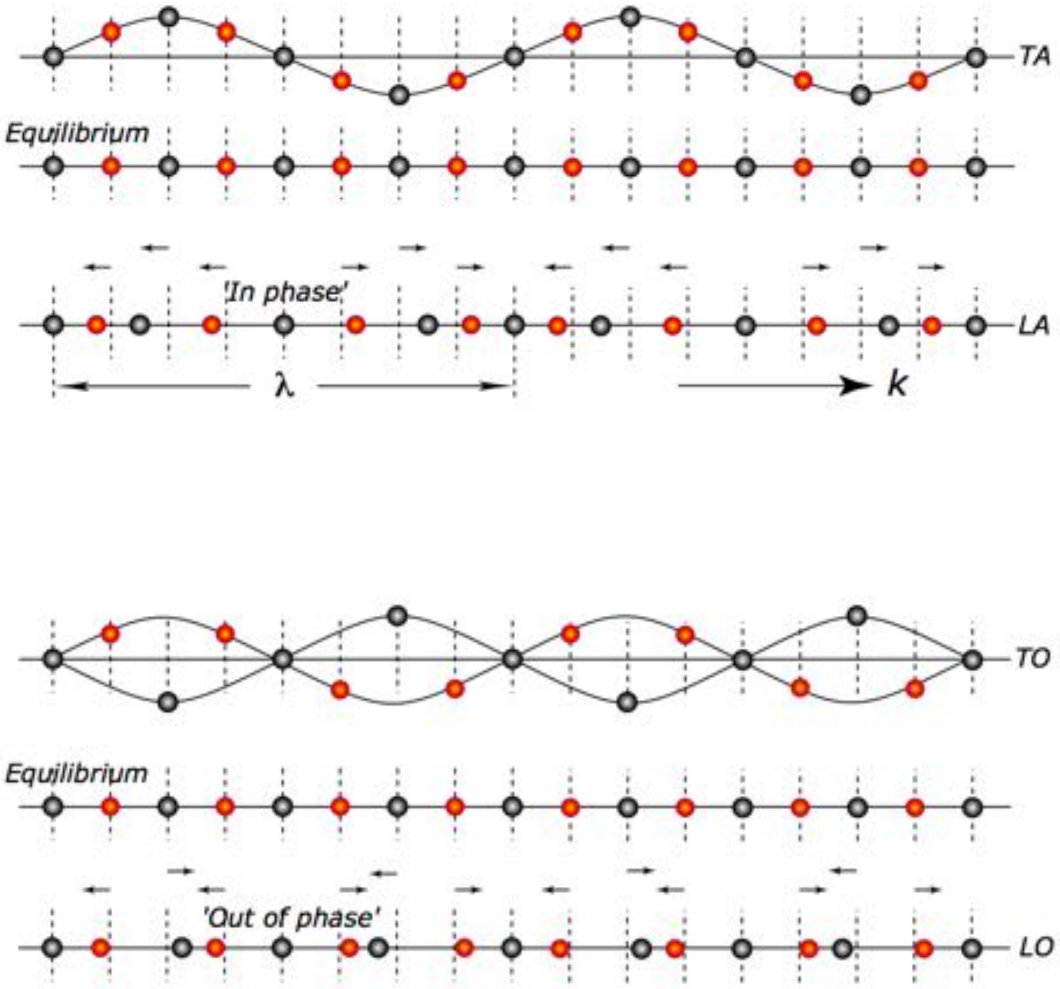

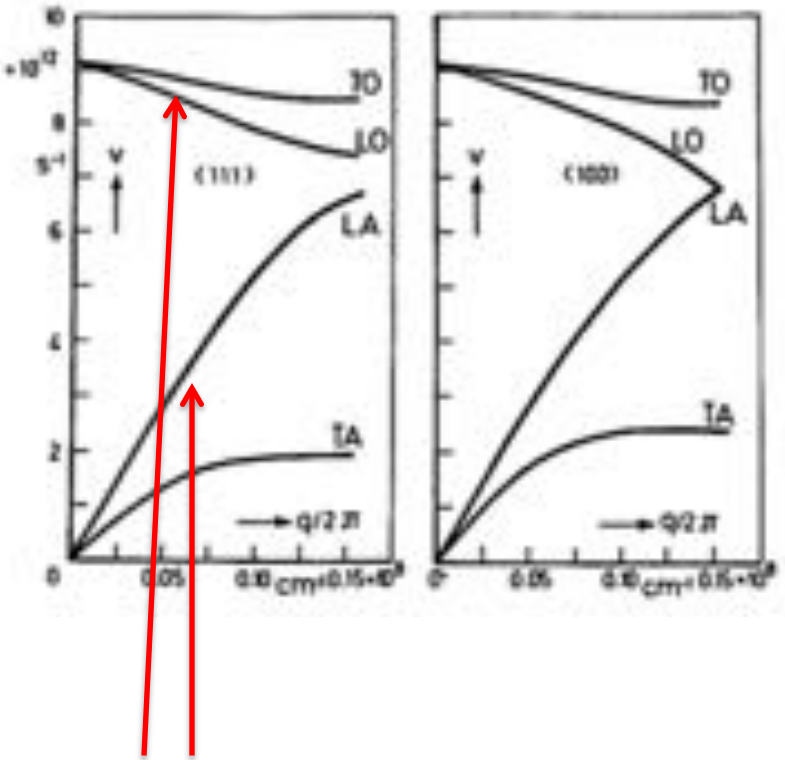

Acoustic and optical phonon dispersion

$$\omega_{\pm}^2(k) = \frac{C}{M_r}\left[1 \pm \sqrt{1 - \frac{2M_r}{M_1 + M_2}(1 - \cos ka)}\right]$$

Phonons in Semiconductors

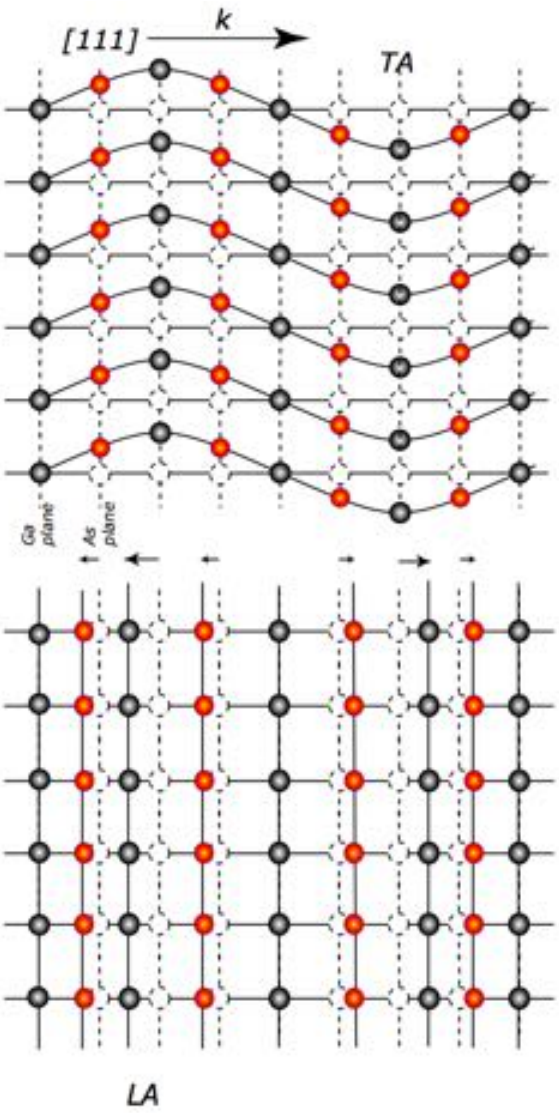

Difference in energies of longitudinal and optical acoustic phonons

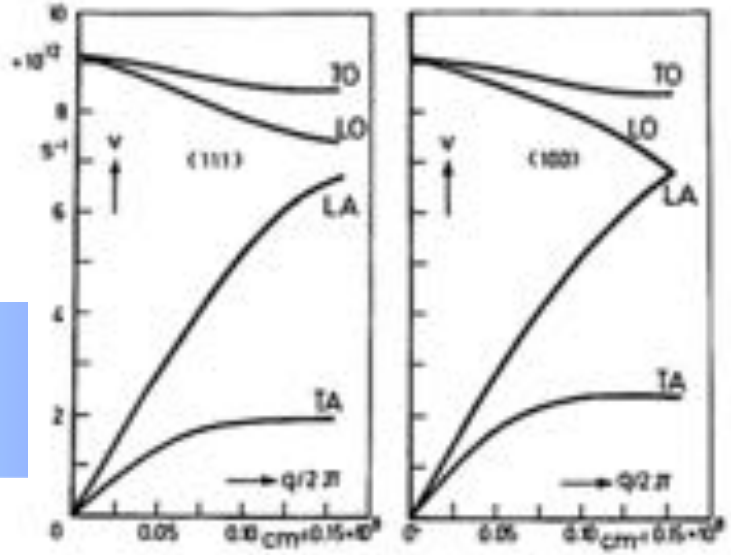

Typical phonon spectra of semiconductors

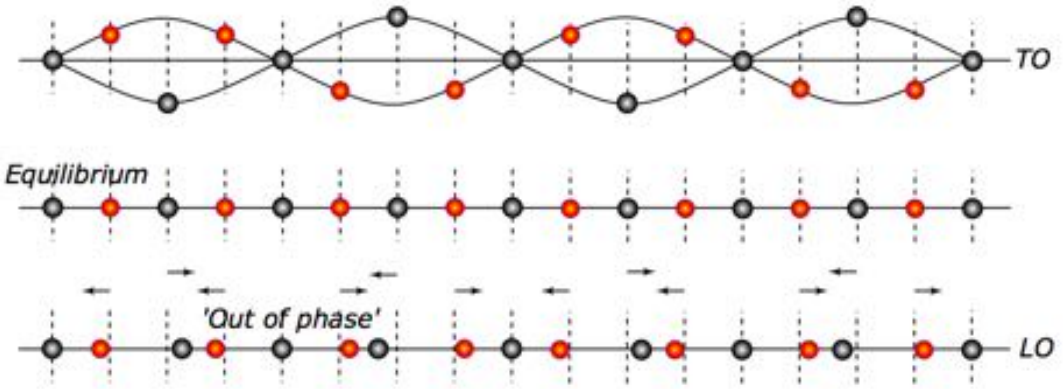

Electron-Def. Pot. Acoustic Phonon interaction

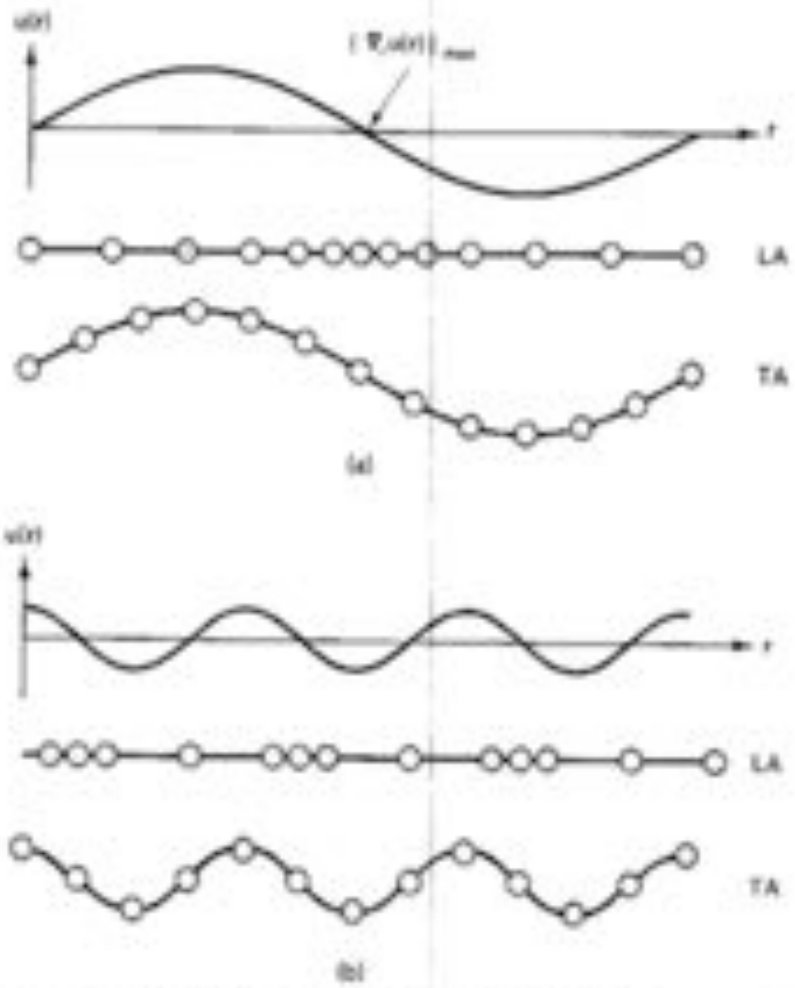

Figure 6.2 Displacements of a diatomic chain for LA and TA phonons at (a) the center and (b) the edge of the Brillouin zone. The lighter mass atoms are indicated by open circles. For zone edge acoustic phonons only the heavier atoms are displaced.

Deformation Potential Acoustic Phonon Scattering Potential

$$\mathbf{u}(\mathbf{r}, t) = \mathbf{a}u(\mathbf{r}, t) \tag{6.4}$$

where

$$u(\mathbf{r}, t) = u \exp\left[i(\mathbf{q}_s \cdot \mathbf{r} - \omega_s t)\right] \tag{6.5}$$

In these equations $\mathbf{a}$ is the displacement direction, and u is the amplitude. The strain associated with the displacement is

$$\nabla \cdot \mathbf{u}(\mathbf{r}, t) = \mathbf{a} \cdot \nabla u(\mathbf{r}, t) \tag{6.6}$$

$$\nabla \cdot \mathbf{u}(\mathbf{r}, t) = i\mathbf{q}_s \cdot \mathbf{a}u(\mathbf{r}, t) \tag{6.7}$$

Equation (6.7) indicates that for the transverse components of a phonon where the displacement and the wavevector are orthogonal, $\mathbf{q}_s \cdot \mathbf{a} = 0$, and no strain is produced. The scattering potential for the longitudinal component is, therefore,

$$\Delta U(\mathbf{r}, t) = \mathcal{E}_A \nabla \cdot \mathbf{u}(\mathbf{r}, t) \tag{6.8}$$

where the *deformation potential*, $\mathcal{E}_A$, in units of energy, is defined as the proportionality constant between the scattering potential (units of energy) and the strain.

Electron-Piezoelectric Acoustic Phonon interaction

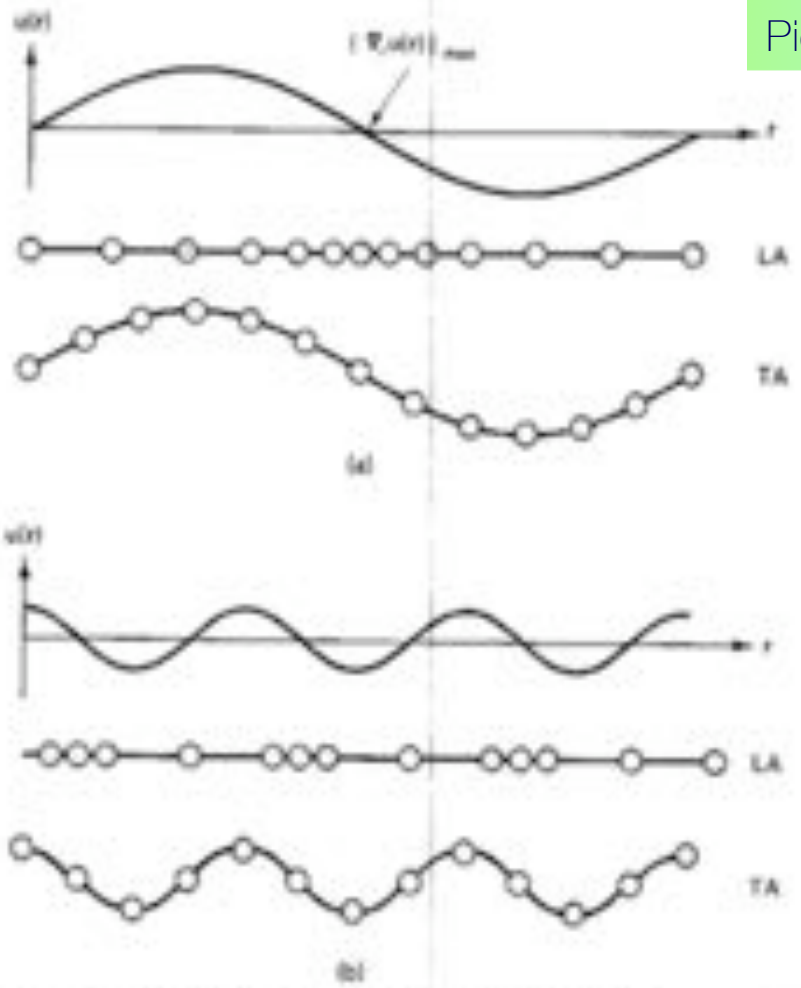

Figure 6.2 Displacements of a diatomic chain for LA and TA phonons at (a) the center and (b) the edge of the Brillouin zone. The lighter mass atoms are indicated by open circles. For zone edge acoustic phonons only the heavier atoms are displaced.

Piezoelectric Acoustic Phonon Scattering Potential

$$\Delta U(\mathbf{r}, t) = -q\phi(\mathbf{r}, t)$$

$$\phi(\mathbf{r}, t) = -\int \mathbf{E}(\mathbf{r}, t)\cdot d\mathbf{r}$$

$$\mathbf{D}(\omega) = \epsilon(\omega)\mathbf{E} = \epsilon_0\mathbf{E} + \mathbf{P}(\omega)$$

$$\mathbf{D}(0) = \epsilon(0)\mathbf{E} = \epsilon_0\mathbf{E} + \mathbf{P}(0)$$

Piezo charge

$$\mathbf{D}(0) = \epsilon(0)\mathbf{E}(\mathbf{r}, t) + e_{pz}\nabla u(\mathbf{r}, t)$$

$$\mathbf{E}(\mathbf{r}, t) = -\frac{e_{pz}}{\epsilon(0)}\nabla u(\mathbf{r}, t)$$

$$\Delta U(\mathbf{r}, t) = \frac{-qe_{pz}}{\epsilon(0)}u(\mathbf{r}, t)$$

$$\Delta U(\mathbf{r}, t) = \frac{iqe_{pz}}{\epsilon(0)q_z}\nabla\cdot\mathbf{u}(\mathbf{r}, t)$$

Electron-Def. Pot. Optical Phonon interaction

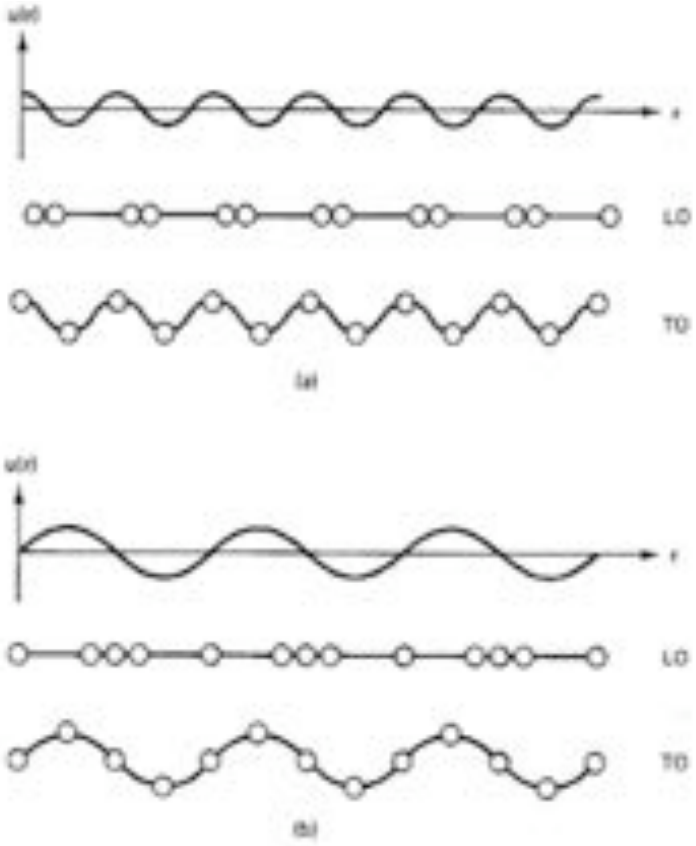

Figure 6.3 Displacements of a diatomic chain for LO and TO phonons at (a) the center and (b) the edge of the Brillouin zone. The lighter mass atoms are indicated by open circles. For zone edge optical phonons only the lighter atoms are displaced.

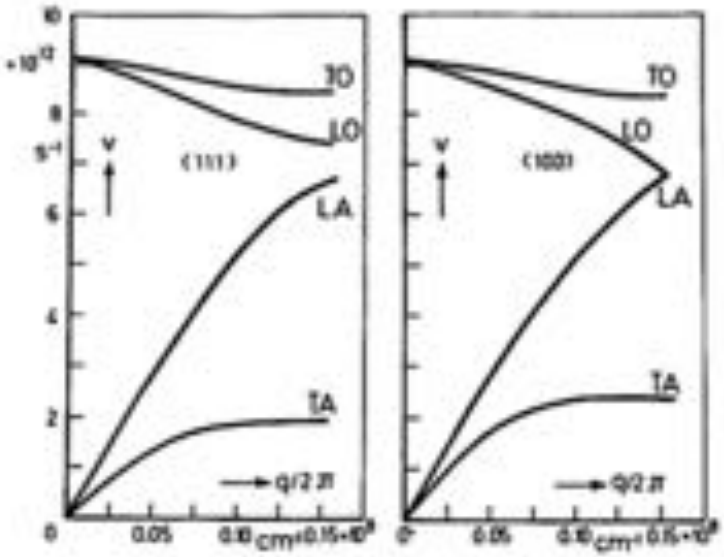

Typical phonon spectra of semiconductors

$$\delta u(\mathbf{r}, t) = u_1(\mathbf{r}, t) - u_2(\mathbf{r}, t) \tag{6.17}$$

where $u_1(\mathbf{r}, t)$ and $u_2(\mathbf{r}, t)$ have the form given by (6.4) and (6.5). The scattering potential due to modulation of the conduction and valence edges must then be proportional to this relative displacement and

$$\Delta U(\mathbf{r}, t) = D\,\delta u(\mathbf{r}, t) \tag{6.18}$$

where

$$\delta u(\mathbf{r}, t) = \mathbf{a}\,\delta u(\mathbf{r}, t) \tag{6.19}$$

Optical Deformation Potential scattering potential D~10^8 eV/cm

Electron-Polar Optical Phonon interaction

$$\mathbf{D}(0) = \epsilon(0)\mathbf{E} = \epsilon_\infty \mathbf{E} + \mathbf{P}(0)$$

$$\mathbf{D}(\infty) = \epsilon(\infty)\mathbf{E} = \epsilon_\infty \mathbf{E} + \mathbf{P}(\infty)$$

$$\mathbf{P}(0) = \mathbf{P}(\infty) + \mathbf{P}_i \tag{6.22}$$

Using (6.22) in (6.20) and subtracting (6.21), we obtain

$$\epsilon(0)\mathbf{E} = \epsilon(\infty)\mathbf{E} + \mathbf{P}_i \tag{6.23}$$

or

$$\mathbf{D}(0) = \epsilon(\infty)\mathbf{E} + \mathbf{P}_i \tag{6.24}$$

From (6.24) we can determine the internal fields induced by the optical phonon polarization of the unit cell.

The polarization of a unit cell, $\mathbf{P}_i(\mathbf{r}, t)$, is determined by the relative displacement of the ions in a unit cell, $\delta\mathbf{u}(\mathbf{r}, t)$, and the effective ionic charge, e^*, such that

$$\mathbf{P}_i(\mathbf{r}, t) = \frac{e^*}{\Omega}\delta\mathbf{u}(\mathbf{r}, t) \tag{6.25}$$

In this equation $\Omega = V/N$ is the volume of the N primitive or Wigner–Seitz unit cells and e^* is the Born effective charge given by

$$e^* = \left[\Omega\omega_{LO}^2\epsilon(\infty)\rho^{1/2}\left[\frac{1}{\epsilon(\infty)} - \frac{1}{\epsilon(0)}\right]\right]^{1/2} \tag{7.174}$$

where ρ is the mass density. This equation is derived in Chapter 7. Assuming no space or surface charges, (6.24) and (6.25) give an internal field,

$$\mathbf{E}(\mathbf{r}, t) = -\frac{e^*}{\Omega\epsilon(\infty)}\delta\mathbf{u}(\mathbf{r}, t) \tag{6.26}$$

Using (6.9), (6.10), and (6.26), the scattering potential for polar mode scattering is

$$\Delta U(\mathbf{r}, t) = \frac{-qe^*}{\Omega\epsilon(\infty)}\int \delta u(\mathbf{r}, t)\,d\mathbf{r} \tag{6.27}$$

or with (6.5) and (6.19),

$$\Delta U(\mathbf{r}, t) = \frac{iqe^*}{\Omega\epsilon(\infty)q_x}\delta u(\mathbf{r}, t) \tag{6.28}$$

A comparison of (6.18) and (6.28) shows that the scattering potentials for deformation potential and polar mode scattering by optical phonons are out of phase by 90° and are thus independent.

Polar optical phonon scattering potential

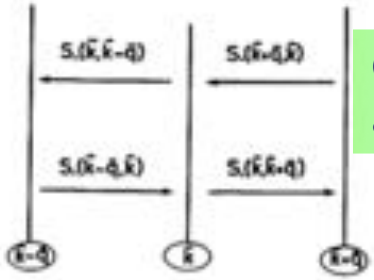

Optical phonon absorption and emission processes

Fig. 6.12. Schematic representation of electron transitions involving phonon emission and phonon absorption

Frohlich interaction

$$\frac{\epsilon_r(0)}{\epsilon_r(\infty)} = \left(\frac{\omega_{LO}}{\omega_{TO}}\right)^2$$

as the Lyddane–Sachs–Teller relation

$$[-\partial f(k)/\partial t]_{\text{coll}} = V(2\pi)^{-3}\int d^3q\,[S_-(k, k-q)\,f(k)\,[1-f(k-q)] + S_+(k, k+q)\,f(k)\,[1-f(k+q)] - S_-(k+q, k)\,f(k+q)\,[1-f(k)] - S_+(k-q, k)\,f(k-q)\,[1-f(k)]]\,. \tag{6.9.1}$$

Amplitude of Phonon Vibrations

$$u_s(x,t) = u_0 e^{i(\beta x - \omega t)} + u_0 e^{-i(\beta x - \omega t)}$$

$$|u_s|^2 = 4u_0^2 \cos(\beta x - \omega t)$$

$$\text{KE} = \frac{1}{2} M (\frac{du_s}{dt})^2 = 2M\omega^2 u_0^2 \sin^2(\beta x - \omega t)$$

$$\text{PE} = \frac{1}{2} K u_s^2 = 2K u_0^2 \cos^2(\beta x - \omega t)$$

$$\text{but}\ldots \omega^2 = \frac{K}{M} \rightarrow$$

$$\text{KE} + \text{PE} = 2M\omega^2 u_0^2 = N_\omega \cdot \hbar\omega \rightarrow$$

$$\text{since}\ldots M = \rho V,$$

$$\boxed{u_0^2 = \frac{\hbar}{2\omega\rho V} \cdot N_\omega}$$

$$\boxed{N_\omega(T) = \frac{1}{e^{\frac{\hbar\omega}{kT}} - 1}}$$

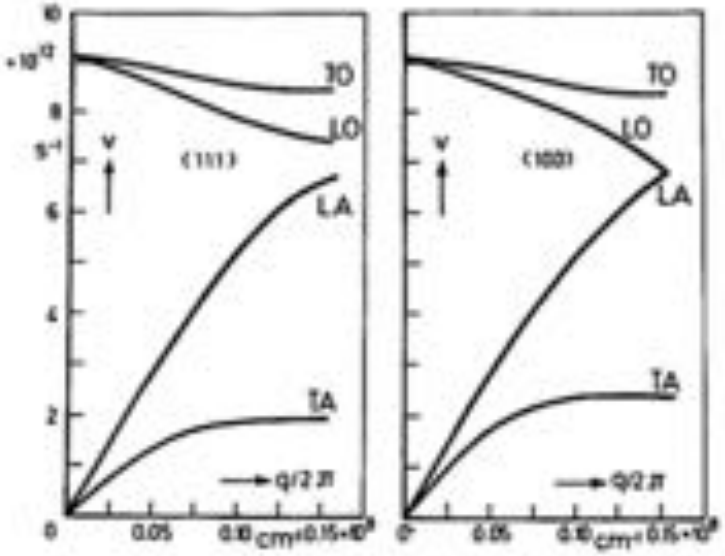

Typical phonon spectra of semiconductors

Vibration amplitude as a function of the temperature: Quantum-Classical connection of the phonon harmonic oscillator

Electron-Phonon Scattering Rates

Polar optical phonon

$$D = \epsilon_0 E + \frac{q^\star u}{\Omega}$$

$$E(x,t) = -\frac{qq^\star u}{\epsilon_0 \Omega}$$

$$W(r,t) = -q\int dx E(x,t) = \frac{q}{i\beta\epsilon_0}\cdot\frac{q^\star}{\Omega}\cdot u_0 e^{i(\boldsymbol{\beta}\cdot\mathbf{r}-\omega t)}$$

$$\left(\frac{q^\star}{\Omega}\right)^2 = \rho\epsilon_0\omega_0^2\left(\frac{1}{\epsilon_s^\infty}-\frac{1}{\epsilon_s^0}\right)$$

$$W(r,t) = -q\int dx E(x,t) = \frac{q\omega_0\sqrt{\rho}}{i\beta}\sqrt{\frac{1}{\epsilon_s^\infty}-\frac{1}{\epsilon_s^0}}\cdot u_0 e^{i(\boldsymbol{\beta}\cdot\mathbf{r}-\omega t)}$$

Piezoelectric acoustic phonon

$$D = \epsilon_0\epsilon_s E + e_{pz}\frac{\partial u}{\partial x}$$

$$E(x,t) = -\frac{e_{pz}}{\epsilon_0\epsilon_s}\frac{\partial u}{\partial x}$$

$$W(r,t) = -q\int dx E(x,t) = \frac{qe_{pz}}{\epsilon_0\epsilon_s}u_0 e^{i(\boldsymbol{\beta}\cdot\mathbf{r}-\omega t)}$$

$$\frac{K^2}{1-K^2} = \frac{e_{pz}^2}{\epsilon_0\epsilon_s v_s}$$

$$S(k\to k') = \frac{2\pi}{\hbar}|W(q_s)|^2\frac{\hbar}{2\rho\Omega\omega_{q_s}}[N(\omega_{q_s})+\frac{1}{2}\mp\frac{1}{2}]\delta[\pm\cos(\theta)+\frac{q_s}{2k}\mp\frac{\omega_{q_s}}{vq_s}]$$

Deformation potential acoustic phonon

$$W(x,t) = D_{ac}\frac{\partial u}{\partial x}$$

$$W(r,t) = D_{ac}(\nabla\cdot\mathbf{u}) = iD_{ac}\beta u_0 e^{i(\boldsymbol{\beta}\cdot\mathbf{r}-\omega t)}$$

Deformation potential optical phonon

$$W(r,t) = D_{op}u = D_{op}u_0 e^{i(\boldsymbol{\beta}\cdot\mathbf{r}-\omega t)}$$

Momentum conservation

$$\hbar\mathbf{k}' = \hbar\mathbf{k}\pm\hbar\boldsymbol{\beta}$$

Energy conservation

$$E_{\mathbf{k}'} = E_{\mathbf{k}}\pm\hbar\omega_{\boldsymbol{\beta}}$$

$$k'^2 = k^2+\beta^2\pm 2k\beta\cos\theta$$

Energy conservation

$$\beta^2\pm 2\beta k\cos\theta\mp\frac{2m^\star\hbar\omega_\beta}{\hbar^2} = 0$$

For acoustic phonons, $\hbar\omega_\beta = \hbar v_s\beta$, and we get

Allowed angles for acoustic phonon scattering events

$$\beta = 2k(\mp\cos\theta\pm\frac{m^\star v_s}{\hbar k}) = 2k(\mp\cos\theta\pm\frac{v_s}{v_k})$$

For optical phonons, we get

Allowed angles for optical phonon scattering events

$$\beta = \mp k\cos\theta\pm\sqrt{k^2\cos^2\theta\pm\frac{2m^\star\hbar\omega_\beta}{\hbar^2}}$$

Electron-Acoustic Phonon interaction: Mobility

$\delta r = A_l \exp[\pm i(q_l \cdot r)]$

Acoustic phonon scattering

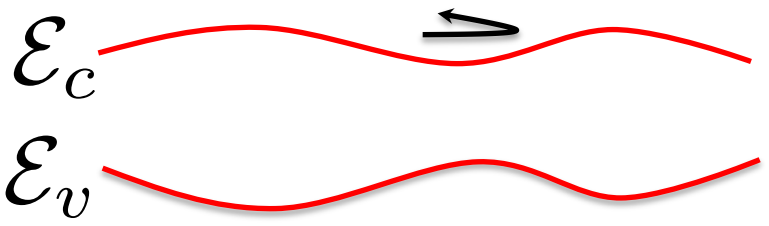

$$|H_{k'k}| = \frac{\varepsilon_{ac} q_l A_l}{V} \left| \int \exp[i(k - k' \pm q_l) \cdot r] \, d^3r \right|$$

$k' = k \pm q_l$

$$2M\omega^2 u_0^2 \approx N_{ph} \times \hbar\omega$$

$|H_{k'k}| = \varepsilon_{ac} q_l A_l .$

$$A_l \to \left| \int \psi^*_{N\pm1} \, x \, \psi_N \, d^3r \right| = \begin{cases} (N\hbar/2M\omega_l)^{1/2} & \text{for } N \to N-1 \\ ((N+1)\hbar/2M\omega_l)^{1/2} & \text{for } N \to N+1 \end{cases}$$

SHO: |amplitude|^2 ~ number of phonons

$$N \to N_q = [\exp(\hbar\omega_l / k_B T) - 1]$$

$$S \approx \frac{2\pi}{\hbar} |H_{k'k}|^2 [\delta(\varepsilon(k') - \varepsilon(k) + \hbar\omega_l) + \delta(\varepsilon(k') - \varepsilon(k) - \hbar\omega_l)]$$

$$\approx 2\frac{2\pi}{\hbar} |H_{k'k}|^2 \delta[\varepsilon(k') - \varepsilon(k)] .$$

absorption~emission

$|H_{k\pm q,k}| = \varepsilon_{ac} q_l [(N_q + 1/2 \mp 1/2)\hbar/2\varrho V\omega_l]^{1/2} .$

$c_l = \rho v_s^2$

$|H_{k'k}| = \varepsilon_{ac} q_l [k_B T/2\varrho V\omega_l^2]^{1/2} = \varepsilon_{ac} [k_B T/2Vc_l]^{1/2}$

Deformation potential

$$\Delta U(\mathbf{r}, t) = \mathcal{E}_A \nabla \cdot \mathbf{u}(\mathbf{r}, t)$$

$$\mu = \frac{2\sqrt{2\pi}}{3} \frac{e\hbar^4 c_l}{m^{5/2}(k_B)^{3/2}\varepsilon_{ac}^2} T^{-3/2}$$

which in units of cm^2/V s is given by

$$\mu = 3.06 \times 10^4 \frac{c_l/10^{12} \text{ dyn cm}^{-2}}{(m/m_0)^{5/2}(T/100 \text{ K})^{3/2}(\varepsilon_{ac}/\text{eV})^2} \propto T^{-3/2} .$$

Piezoelectric

$$\Delta U(\mathbf{r}, t) = \frac{iqe_{pz}}{\epsilon(0)q^2} \nabla \cdot \mathbf{u}(\mathbf{r}, t)$$

$$\mu = \frac{16\sqrt{2\pi}}{3} \frac{\hbar^2 \varkappa \varkappa_0}{m^{3/2} e K^2 (k_B T)^{1/2}} \propto T^{-1/2}$$

and in units of cm^2/V s

$$\mu = 2.6 \frac{\varkappa}{(m/m_0)^{3/2} K^2 (T/100 \text{ K})^{1/2}} .$$

$$K^2 = \frac{e_{pz}^2/c_l}{\varkappa\varkappa_0 + e_{pz}^2/c_l} .$$

Coupling K ~10^{-3}

Electron-Optical Phonon Scattering Rates, Mobility

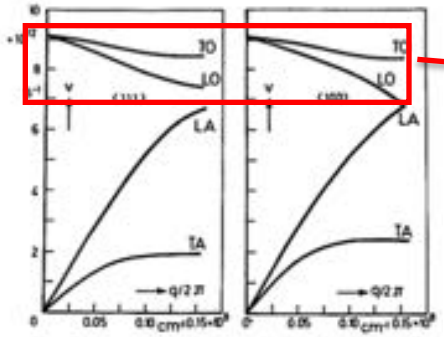

$\hbar\omega_0 = k_B\Theta$.

Θ is known as the *Debye temperature*

Deformation potential Optical Phonon

$$\mu_0 = \frac{4\sqrt{2\pi}\, e\hbar^2 \varrho (k_B\Theta)^{1/2}}{3m^{5/2} D^2} f(T/\Theta).$$

The function $f(T/\Theta)$ is given by

$$f(T/\Theta) = (2z)^{5/2}(e^{2z}-1)\int_0^\infty \frac{y^{3/2} e^{-2zy}\, dy}{\sqrt{y+1} + e^{2z}\,\mathrm{Re}\{\sqrt{y-1}\}},$$

where $z = \Theta/2T$ and $y = \varepsilon/k_B\Theta$. The function is shown

Its numerical value in units of $cm^2/V\,s$ is given by

$$\mu = 2.04\times 10^3 \frac{(\varrho/\mathrm{g\,cm^{-3}})(\Theta/400\ \mathrm{K})^{1/2}}{(m/m_0)^{5/2}(D/10^8\ \mathrm{eV\,cm^{-1}})^2} f(T/\Theta)$$

Polar Optical Phonon Scattering

$$\alpha = \frac{\hbar |e| E_0}{2^{1/2} m^{1/2} (\hbar\omega_0)^{3/2}} = \frac{1}{137}\sqrt{\frac{mc^2}{2k_B\Theta}}\left(\frac{1}{x_{opt}} - \frac{1}{x}\right)$$

$$= 397.4\sqrt{\frac{m/m_0}{\Theta/\mathrm{K}}}\left(\frac{1}{x_{opt}} - \frac{1}{x}\right)$$

The mobility is simply $(e/m)\,\tau_m$:

$$\mu = [|e|/(2m\,\alpha\,\omega_0)]\exp(\Theta/T)$$

which in units of $cm^2/V\,s$ is given by

$$\mu = 2.6\times 10^5 \frac{\exp(\Theta/T)}{\alpha(m/m_0)(\Theta/\mathrm{K})} \quad \text{for} \quad T \ll \Theta$$

For example, in n-type GaAs where $\Theta = 417$ K, $m/m_0 = 0.072$, $\alpha = 0.067$, we calculate a mobility at 100 K of $2.2\times 10^5\ cm^2/V\,s$. This is of the order of magnitude of the highest mobilities observed in this material. At this and

Electron-Photon Interactions

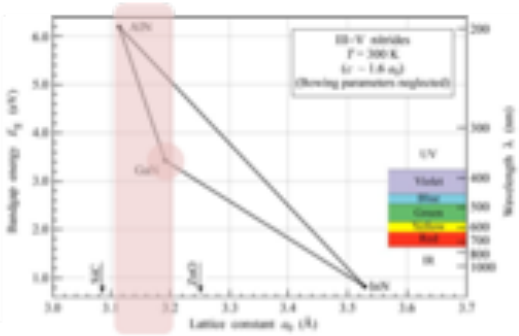

Fig. 12.12. Bandgap energy versus lattice constant of III-V nitride semiconductors at room temperature.

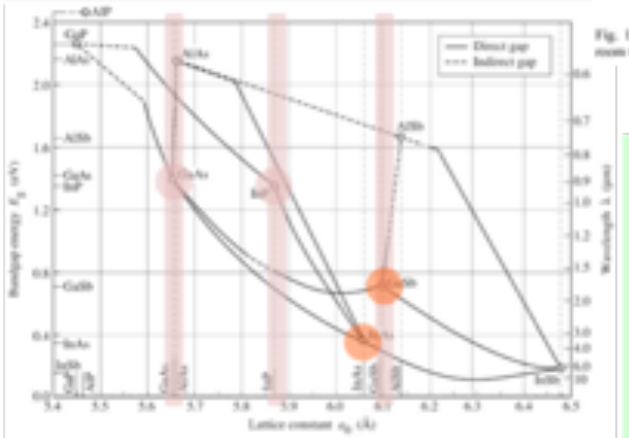

Fig. 7.6. Bandgap energy and lattice constant of various III-V semiconductors at room temperature (adapted from Tien, 1988).

Major III-V Semiconductor families:

- *GaAs-based (AlGaAs/GaAs) (strain-free, or pseudomorphic)*
- *InP based (InGaAs channels)*
- *6.1 Angstrom/narrow gap channels (generally grown metamorphically on GaAs)*
- *GaN-based (InGaN/GaN and AlGaN/GaN) (typically pseudomorphic)*

Electron-Photon Interactions

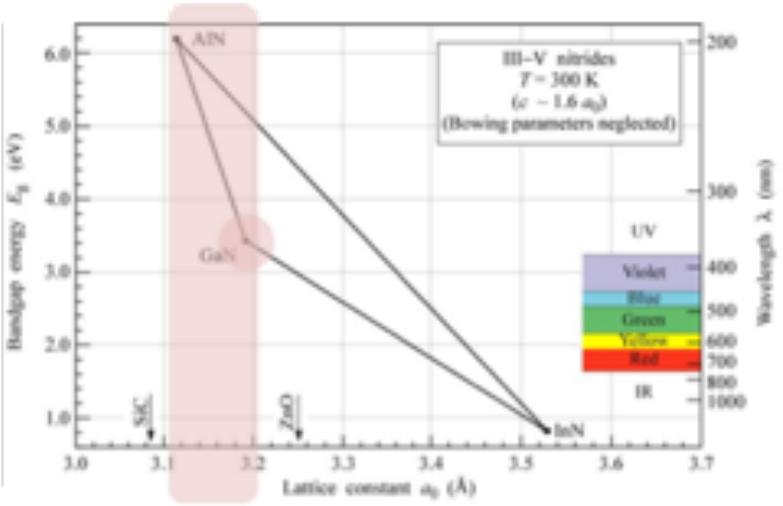

Fig. 12.12. Bandgap energy versus lattice constant of III–V nitride semiconductors at room temperature.

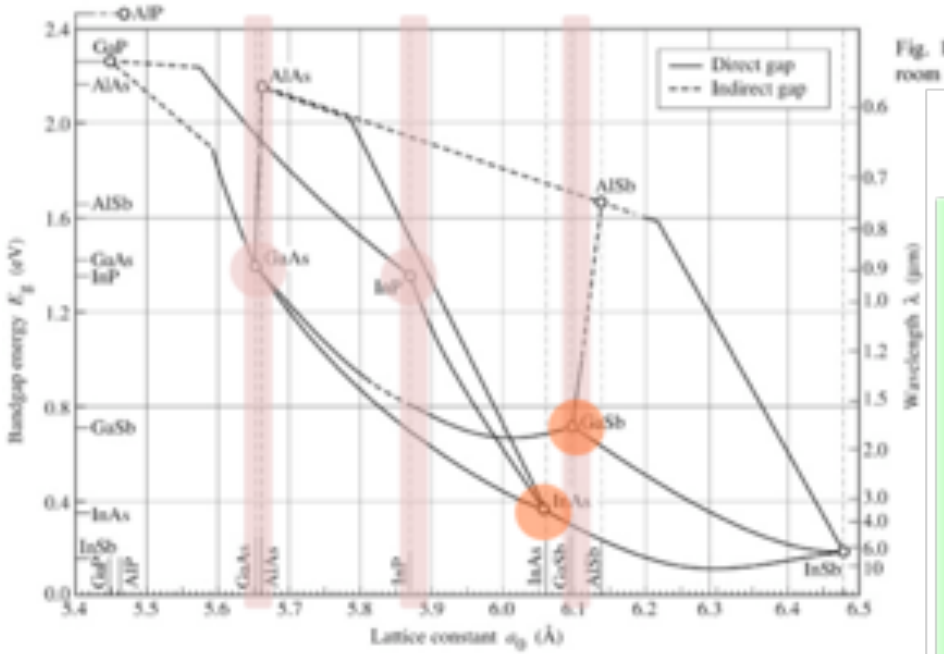

Fig. 7.6. Bandgap energy and lattice constant of various III-V semiconductors at room temperature (adopted from Tien, 1988).

Major III-V Semiconductor families:

- *GaAs-based (AlGaAs/GaAs) (strain-free, or pseudomorphic)*
- *InP based (InGaAs channels)*
- *6.1 Angstrom/narrow gap channels (generally grown metamorphically on GaAs)*
- *GaN-based (InGaN/GaN and AlGaN/GaN) (typically pseudomorphic)*

How to make white light with semiconductors

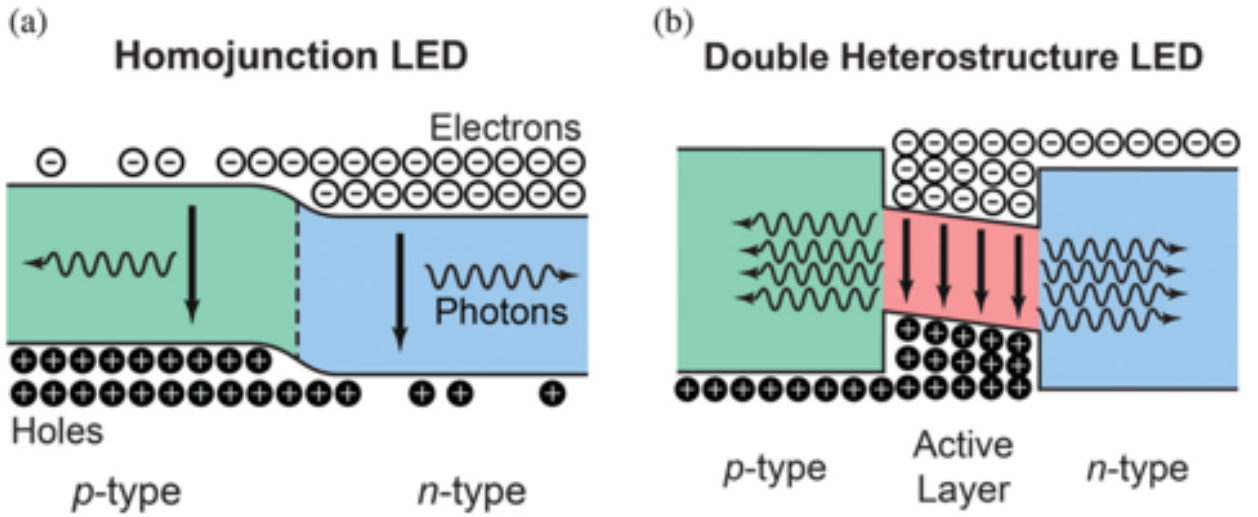

$$\text{IQE} = \frac{\text{Light generated}}{\text{Electrons injected}} = \frac{R_{\text{radiative}}}{R_{\text{radiative}} + R_{\text{nonradiative}}} = \frac{Bn^2}{An + Bn^2 + Cn^3}.$$

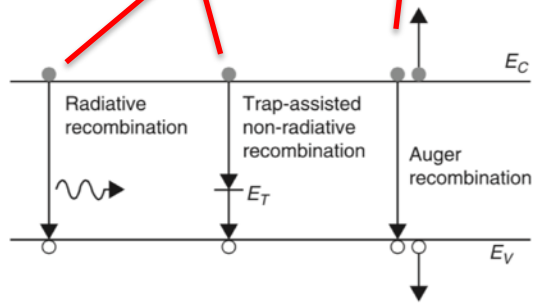

LED Blue + **Phosphor** Blue → Yellow = **White Light** Blue + Yellow & **White LED**

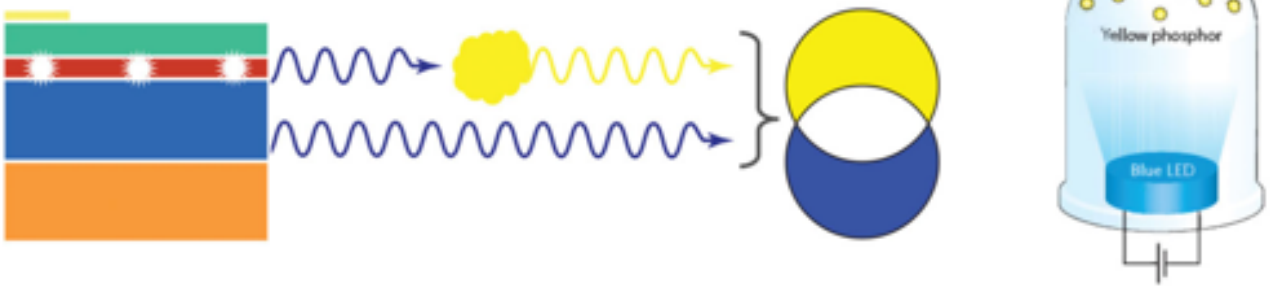

Electron-Photon Interactions

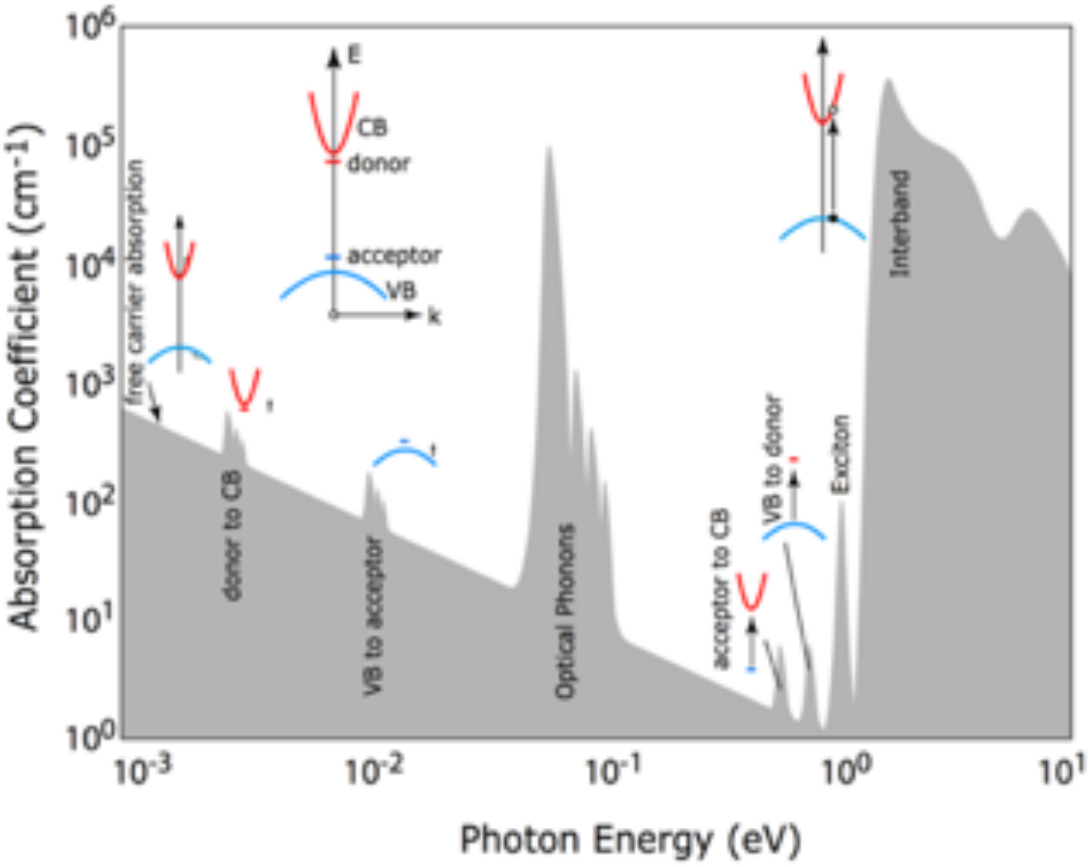

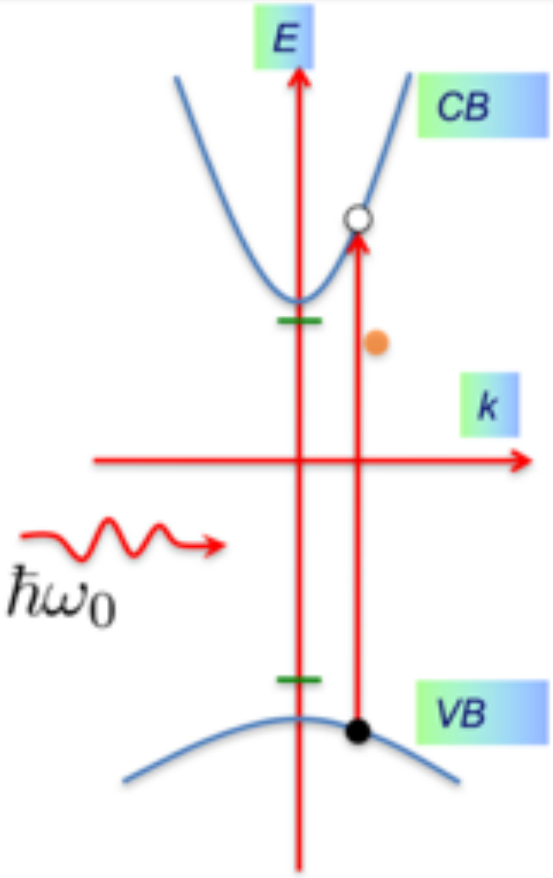

FIGURE 26.1: Schematic absorption spectrum $\alpha(\hbar\omega)$ of bulk semiconductors. The insets depict various state transitions upon absorption of photons.

- *Absorption power is Quantified by "Absorption Coefficient"*
- *A negative absorption coefficient is equivalent to optical gain!*

- *Adapted from: Wolfe/Holonyak/Stillman Physical Properties of Semiconductors*

Absorption Coefficient of Compound Semiconductors

$$\alpha(\hbar\omega) = \frac{\text{Number of photons absorbed per unit volume per second}}{\text{Number of photons incident per unit area per second}}$$

$$\alpha(\hbar\omega) = \frac{R}{S/\hbar\omega}$$

Number of photons incident per unit area per second:

Vector potential:

$$\mathbf{A}(\mathbf{r},\mathbf{t}) = \hat{e}A_0\cos(\mathbf{k_{op}}\cdot\mathbf{r}-\omega t)$$

Electric Field:

$$\mathbf{E}(\mathbf{r},t) = -\frac{\partial}{\partial t}\mathbf{A}(\mathbf{r},t) = -\hat{e}\omega A_0\sin(\mathbf{k_{op}}\cdot\mathbf{r}-\omega t)$$

Magnetic Field:

$$\mathbf{H}(\mathbf{r},t) = \frac{1}{\mu}\nabla\times\mathbf{A}(\mathbf{r},t) = -\frac{1}{\mu}\mathbf{k_{op}}\times\hat{e}A_0\sin(\mathbf{k_{op}}\cdot\mathbf{r}-\omega t)$$

Poynting Vector:

$$\mathbf{S}(\mathbf{r},t) = \mathbf{E}(\mathbf{r},t)\times\mathbf{H}(\mathbf{r},t) = \mathbf{k_{op}}\frac{\omega A_0^2}{\mu}\sin^2(\mathbf{k_{op}}\cdot\mathbf{r}-\omega t)$$

$$\langle\mathbf{S}(\mathbf{r},t)\rangle = \frac{\omega A_0^2}{2\mu}\mathbf{k_{op}}$$

Incident energy per unit area per second:

$$S = |\langle\mathbf{S}(\mathbf{r},t)\rangle| = \frac{\omega A_0^2}{2\mu}k_{op} = \frac{n_r c\epsilon_0\omega^2 A_0^2}{2}$$

- Incident photon number per unit area per second: |Poynting vector|/ photon energy
- Goes as square of the amplitude of vector potential (or electric field, or magnetic field)

Absorption Spectra of Compound Semiconductors

$$E_c(\mathbf{k}) = E_g + \frac{\hbar^2 k^2}{2m_e^*}$$

$$E_v(\mathbf{k}) = -\frac{\hbar^2 k^2}{2m_h^*}$$

$$E_c(\mathbf{k}) - E_v(\mathbf{k}) = E_g + \frac{\hbar^2 k^2}{2m_r^*}$$

$$\frac{1}{m_r^*} = \frac{1}{m_e^*} + \frac{1}{m_h^*}$$

first assume $f_v(k)=1$, $f_c(k)=0$

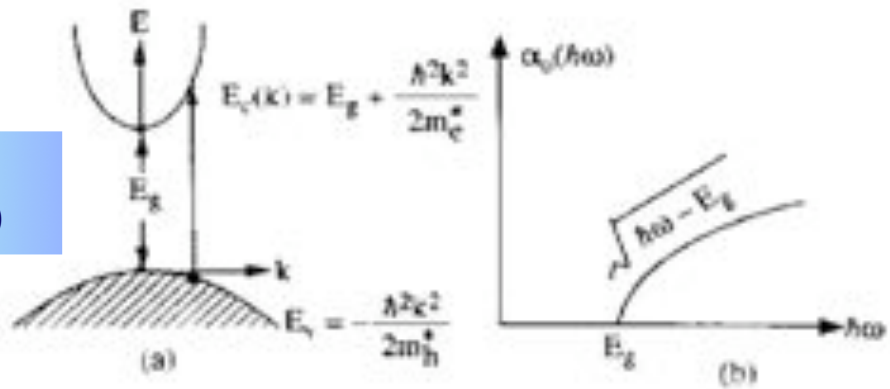

Figure 9.5 (a) Optical absorption in a direct-band-gap semiconductor (b) The absorption spectrum due to the interband transitions

$$\alpha_0(\hbar\omega) = C_0|\hat{e}\cdot\mathbf{p_{cv}}|^2 \times (g_s g_v) \times \int_{\mathbf{k}} \frac{d^3\mathbf{k}}{(2\pi)^3}\delta[E_c(\mathbf{k}) - (E_v(\mathbf{k}) + \hbar\omega)]$$

$$\gamma_{abs} = \frac{2\pi}{\hbar}|\langle b|W(\mathbf{r})|a\rangle|^2\delta[E_b - (E_a + \hbar\omega)]$$

$$\gamma_{em} = \frac{2\pi}{\hbar}|\langle a|W(\mathbf{r})|b\rangle|^2\delta[E_a - (E_b - \hbar\omega)]$$

Fermi's Golden Rule

$$\alpha_0(\hbar\omega) = C_0|\hat{e}\cdot\mathbf{p_{cv}}|^2 \cdot \rho_r(\hbar\omega - E_g)$$

$$\rho_r(u) = g_s g_v \cdot \frac{1}{(2\pi)^2}\cdot\left(\frac{2m_r^\star}{\hbar^2}\right)^{\frac{3}{2}}\cdot\sqrt{u}$$

$$C_0 = \frac{\pi e^2}{n_r c\varepsilon_0 m_0^2\omega}$$

Optical absorption coeff. of bulk semiconductor (general form applicable to quantum wells, etc…)

"Joint" density of states of (VB,CB)

This and next few slides:
From: S. L. Chuang (Photonic Devices)

Loss Coefficient of Semiconductors

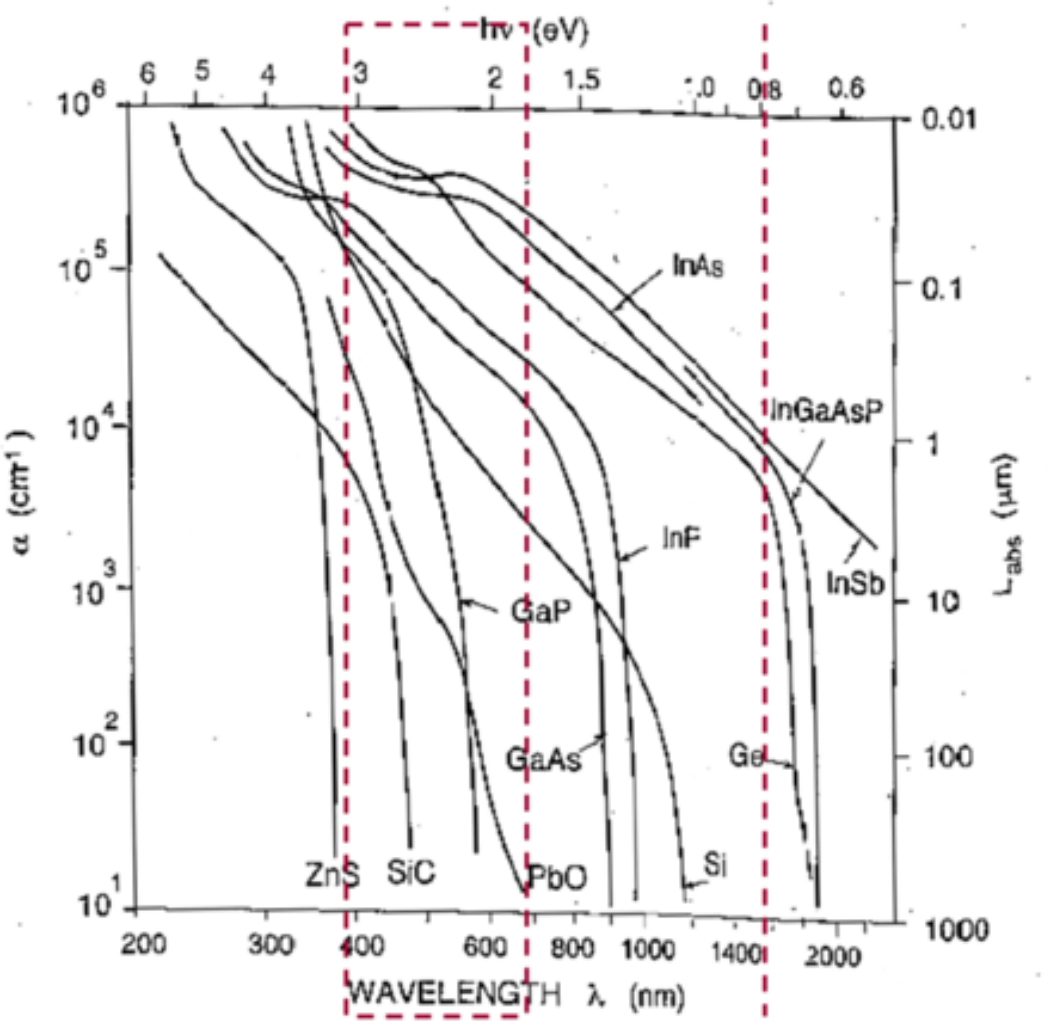

Optical Matrix Elements for Transitions

$$\alpha_0(\hbar\omega) = \frac{2.64\times10^5}{\eta_r} \cdot \underbrace{\frac{2|\hat{e}\cdot\mathbf{p_{cv}}|^2/m_0}{\hbar\omega}}_{`oscillator strength'} \cdot \underbrace{\left(\frac{2m_r^\star}{m_0}\right)^{\frac{3}{2}} \cdot \sqrt{\hbar\omega - E_g}}_{\propto reduced DOS} \ \mathrm{cm}^{-1}$$

Absorption spectrum of a general III-V semiconductor at equilibrium

Momentum matrix elements for bulk & quantum well structures

$$M_b^2 = \frac{1}{3}P_x^2 = \frac{m_0^2}{3\hbar^2}P^2$$

$$= \left(\frac{m_0}{m_e^*} - 1\right)\frac{m_0 E_g(E_g+\Delta)}{6\left(E_g+\frac{2}{3}\Delta\right)}$$

Table 9.1 Summary of the Momentum Matrix Elements in Parabolic Band Model ($|\hat{e}\cdot\mathbf{p}_{cv}|^2 = |\hat{e}\cdot\mathbf{M}|^2$)

Bulk $|\hat{x}\cdot\mathbf{p}_{cv}|^2 = |\hat{y}\cdot\mathbf{p}_{cv}|^2 = |\hat{z}\cdot\mathbf{p}_{cv}|^2 = M_b^2 = \frac{m_0}{6}E_p$

Quantum Well

TE Polarization ($\hat{e} = \hat{x}$ or $\hat{y}$)

$\langle|\hat{e}\cdot\mathbf{M}_{c-hh}|^2\rangle = \frac{3}{4}(1+\cos^2\theta)M_b^2$

$\langle|\hat{e}\cdot\mathbf{M}_{c-lh}|^2\rangle = (\frac{5}{4}-\frac{3}{4}\cos^2\theta)M_b^2$

TM Polarization ($\hat{e} = \hat{z}$)

$\langle|\hat{e}\cdot\mathbf{M}_{c-hh}|^2\rangle = \frac{3}{2}\sin^2\theta M_b^2$

$\langle|\hat{e}\cdot\mathbf{M}_{c-lh}|^2\rangle = \frac{1}{2}(1+3\cos^2\theta)M_b^2$

Conservation Rule

$\langle|\hat{x}\cdot\mathbf{M}_{c-h}|^2\rangle + \langle|\hat{y}\cdot\mathbf{M}_{c-h}|^2\rangle + \langle|\hat{z}\cdot\mathbf{M}_{c-h}|^2\rangle = 3M_b^2$, ($h$ = hh or lh)

$\langle|\hat{e}\cdot\mathbf{M}_{c-hh}|^2\rangle + \langle|\hat{e}\cdot\mathbf{M}_{c-lh}|^2\rangle = 2M_b^2$

Optical Gain in Semiconductors

- We have looked at light absorption by a semiconductor (useful for photodetectors & solar cells)
- But LEDs and LASERs are electrically injected light emitters
- The same theory that explains absorption explains emission under electrical injection as well

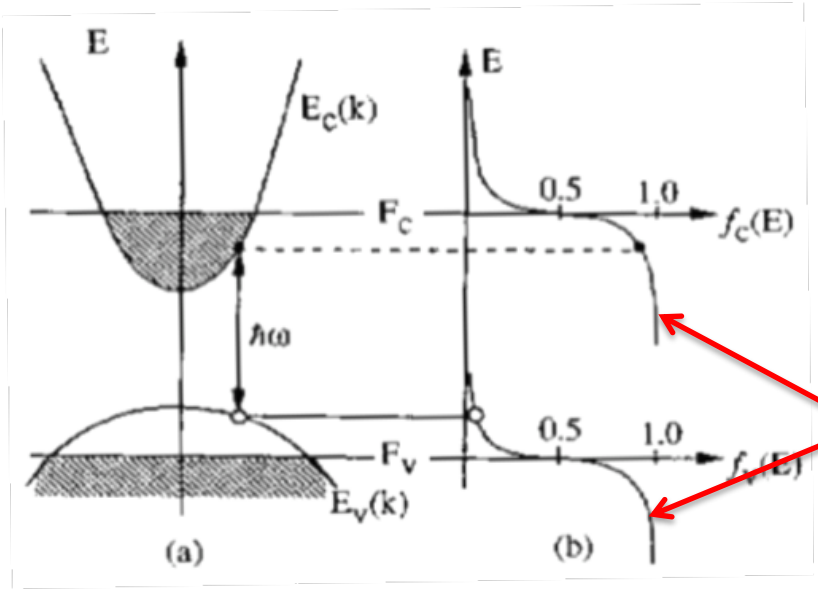

Non-equilibrium Fermi-Dirac functions with electron quasi-Fermi levels (note: not necessary to talk about holes here)
F_C: Conduction Band quasi-Fermi level
F_V: Valence Band quasi-Fermi level

$$f_v(\mathbf{k}) = \frac{1}{1 + e^{(E_v(\mathbf{k}) - F_v)/k_B T}}$$

$$f_c(\mathbf{k}) = \frac{1}{1 + e^{(E_c(\mathbf{k}) - F_c)/k_B T}}$$

$$\alpha(\hbar\omega) = C_0 |\hat{e} \cdot \mathbf{p_{cv}}|^2 \times (g_s g_v) \times \int_{\mathbf{k}} \frac{d^3\mathbf{k}}{(2\pi)^3} \delta\left[E_g + \frac{\hbar^2 k^2}{2m_r^*} - \hbar\omega\right] \times [f_v(\mathbf{k}) - f_c(\mathbf{k})]$$

Non-equilibrium absorption coefficient

$$\alpha(\hbar\omega) = \alpha_0(\hbar\omega) \times [f_v(k_0) - f_c(k_0)]$$

$$k_0 = \sqrt{\frac{2m_r^*}{\hbar^2}(\hbar\omega - E_g)}$$

Fundamental result for understanding LEDs and LASERs

Optical Gain in Non-Equilibrium Conditions

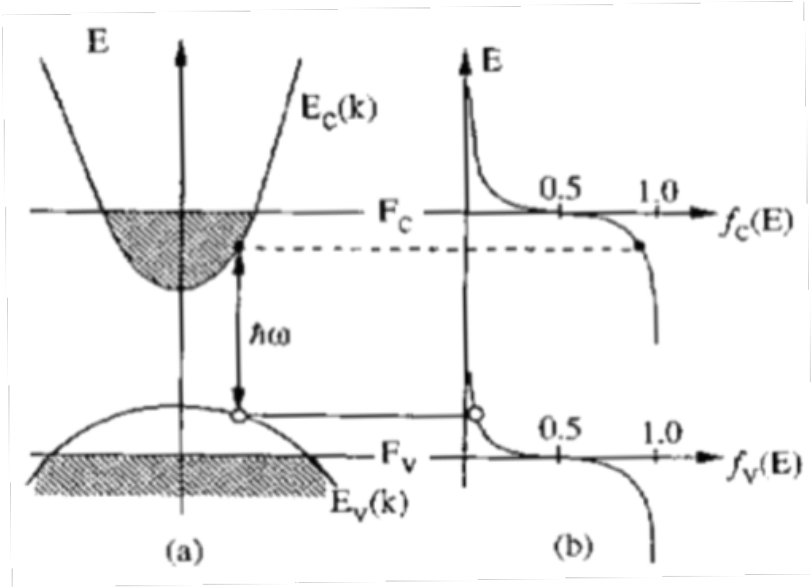

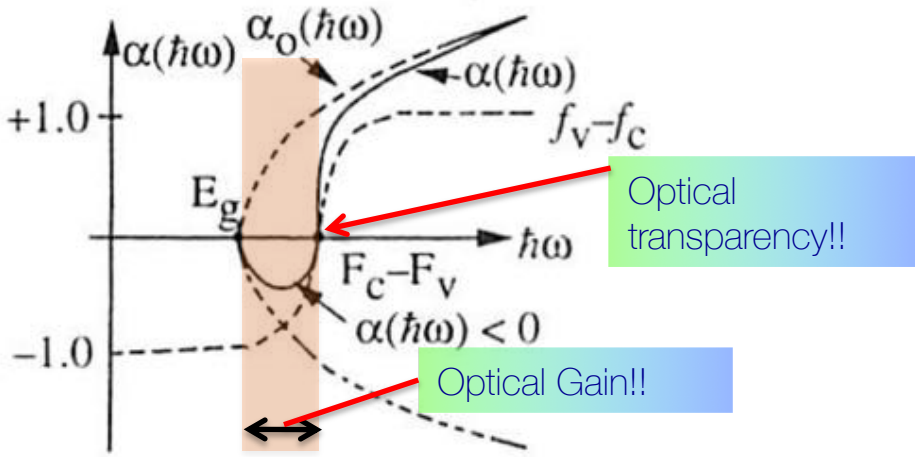

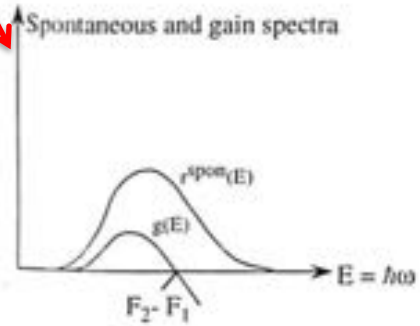

$$\alpha(\hbar\omega) = \alpha_0(\hbar\omega) \times [f_v(k_0) - f_c(k_0)] \qquad k_0 = \sqrt{\frac{2m_r^*}{\hbar^2}(\hbar\omega - E_g)}$$

$$f_v(k_0) - f_c(k_0) = \frac{\exp\left(\frac{E_c - F_c}{kT}\right) - \exp\left(\frac{E_v - F_v}{kT}\right)}{\left[1 + \exp\left(\frac{E_v - F_v}{kT}\right)\right]\left[1 + \exp\left(\frac{E_c - F_c}{kT}\right)\right]} < 0 \rightarrow$$

$$\exp\left(\frac{E_c - F_c}{kT}\right) < \exp\left(\frac{E_v - F_v}{kT}\right)$$

$$F_c - F_v > E_c - E_v = \hbar\omega$$

Bernard-Duraffourg inversion condition

The inversion conditions can be achieved by
- Optical pumping (gas lasers), or
- Electrical pumping (semiconductor LEDs & Lasers)

A laser requires a light emitter to be placed in a high-finesse (hi-Q) optical cavity to amplify a specific mode.

Absorption Coefficient/Optical Gain in Quantum Wells

$$\psi_v(r) = u_v(\mathbf{r}) \times [\frac{1}{\sqrt{A}} e^{i\mathbf{k_t}\cdot\rho}] \times V(n_v, z)$$

$$\psi_c(r) = u_c(\mathbf{r}) \times [\frac{1}{\sqrt{A}} e^{i\mathbf{k_t'}\cdot\rho}] \times C(n_c, z)$$

Effective-mass functions!!

$$\mathbf{p_{ba}} = \langle \psi_c|\mathbf{p}|\psi_v\rangle \approx \langle\ u_c|\mathbf{p}|u_v\rangle \times \delta_{\mathbf{k_t},\mathbf{k_t'}} \times I^{c,n_c}_{v,n_v}$$

$$I^{en}_{hm} = \int_{\infty}^{+\infty} dz C^{\star}(n_c, z) V(n_v, z)$$

Determines selection rules

General form of absorption coefficient:

$$\alpha_0(\hbar\omega) = C_0|\hat{e}\cdot\mathbf{p_{cv}}|^2 \cdot \rho_r(\hbar\omega - E_g)$$

$$C_0 = \frac{\pi e^2}{n_r c \varepsilon_0 m_0^2 \omega} \qquad \rho_r^{2D} = \frac{m_r}{\pi\hbar^2 L_z}$$

$$\frac{\alpha_0(\hbar\omega)}{C_0|\hat{e}\cdot\mathbf{p}_{c_1}|^2} = \begin{cases} \frac{m_r}{\pi\hbar^2 L_z} & \text{for } E_{h1}^{e1} < \hbar\omega < E_{h2}^{e2} \\ 2\frac{m_r}{\pi\hbar^2 L_z} & \text{for } E_{h2}^{e2} < \hbar\omega < E_{h3}^{e3} \\ 3\frac{m_r}{\pi\hbar^2 L_z} & \text{for } E_{h3}^{e3} < \hbar\omega < E_{h4}^{e4} \\ \text{etc.} \end{cases}$$

Interband and Intersubband Optical Transitions in QWs

Using effective-mass theory, optical matrix elements in quantum wells:

$$M \propto |\langle f|\mathbf{r}\cdot\eta|i\rangle| = \int \chi_e(z) e^{i(\mathbf{k}_{e\perp}\cdot\mathbf{r}_\perp)} u_{ck_e}(\mathbf{r})\,\eta\cdot\mathbf{r}\,\chi_h(z) e^{i(\mathbf{k}_{h\perp}\cdot\mathbf{r}_\perp)} u_{vk_h}(\mathbf{r})\,d\mathbf{r}$$

For INTERBAND transitions:

$$M \simeq \sum_{R_i} \chi_e(\mathbf{R}_i)\,\chi_n(\mathbf{R}_i)\, e^{i(\mathbf{k}_{h\perp}-\mathbf{k}_{e\perp})\cdot\mathbf{R}_i} \int_{\text{cell}} u_{ck_e}(\mathbf{r})\,\eta\cdot\mathbf{r}\,u_{vk_h}(\mathbf{r})\,d\mathbf{r}$$

$M_{interband} \sim a_0$, dipole length $\sim$ lattice constant

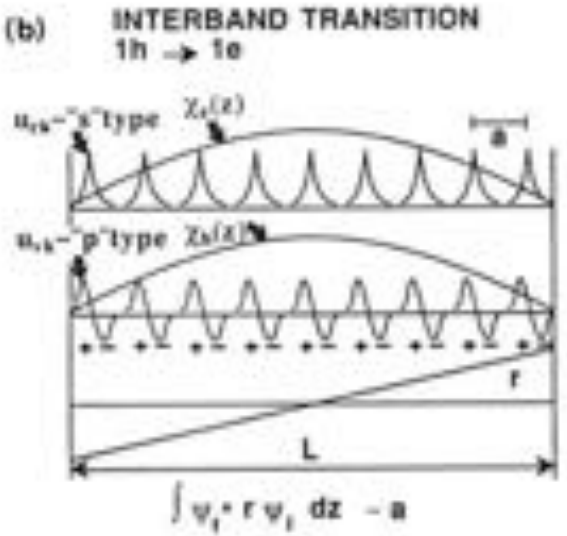

For INTERSUBBAND (intra-band) transitions:

$$M \sim \int_{\text{crystal}} \chi_e(z)\,\eta\cdot\mathbf{r}\,\chi'_e(z)\,dr \int_{\text{cell}} u_{cke}(\mathbf{r})\,u^*_{cke}(\mathbf{r})\,d^3r$$

$M_{intersubband} \sim L_{well}$, dipole length $\sim$ Quantum Well Width (giant dipole effect!!)

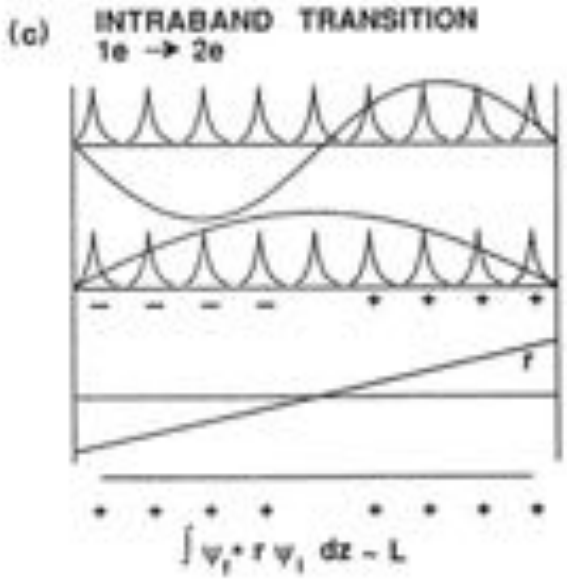

Optical Gain in Quantum Wells

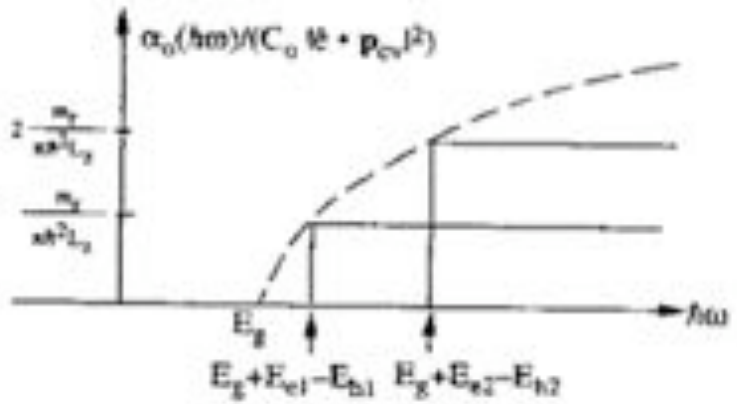

$$\frac{\alpha_0(\hbar\omega)}{C_0|\hat{e}\cdot\mathbf{p}_{cv}|^2} = \begin{cases} \dfrac{m_r}{\pi\hbar^2 L_z} & \text{for } E_{h1}^{e1} < \hbar\omega < E_{h2}^{e2} \\ 2\dfrac{m_r}{\pi\hbar^2 L_z} & \text{for } E_{h2}^{e2} < \hbar\omega < E_{h3}^{e3} \\ 3\dfrac{m_r}{\pi\hbar^2 L_z} & \text{for } E_{h3}^{e3} < \hbar\omega < E_{h4}^{e4} \\ \text{etc.} \end{cases}$$

Figure 9.7. The stepwise absorption spectrum for a quantum-well structure.

Equilibrium absorption coefficient in QW is proportional to the joint DOS and has 2D subband features

$$\alpha(\hbar\omega) = \alpha_0(\hbar\omega)\left[f_c^m(E_t = \hbar\omega - E_{hm}^{en}) - f_c^n(E_t = \hbar\omega - E_{hm}^{en})\right]$$

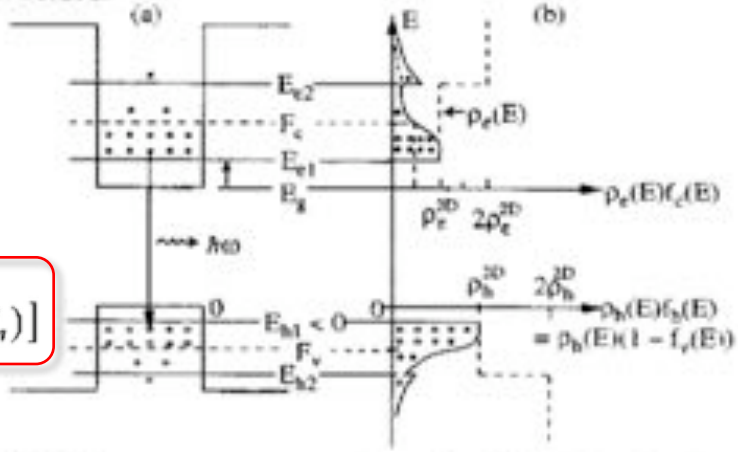

Figure 9.8. (a) Population inversion in a quantum well such that $F_c - F_v > \hbar\omega > E_g + E_{e1} - E_{h1}$. Here F_v is measured from the valence band edge where the energy level is chosen to be zero. (b) The products of the density of states and the occupation probability for electrons in the conduction band $\rho_e(E)f_c(E)$ and holes in the valence band $\rho_h(E)f_h(E) = \rho_h(E)[1 - f_v(E)]$ are plotted vs the energy E in the vertical scale.

Compound Semiconductor Heterojunction LEDs

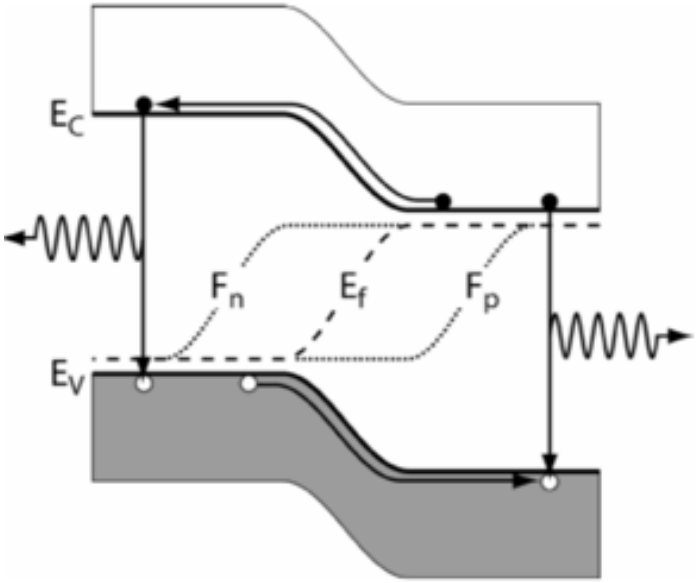

$$R_{radiative} = npv_{th}S_R/2\eta^2$$

$$S_R \approx 5x10^{-25}\eta^2 E_{gap}^2 \alpha \left(m_e^* m_h^*\right)^{-3/2} \left(300/T\right)^{5/2} cm^2$$

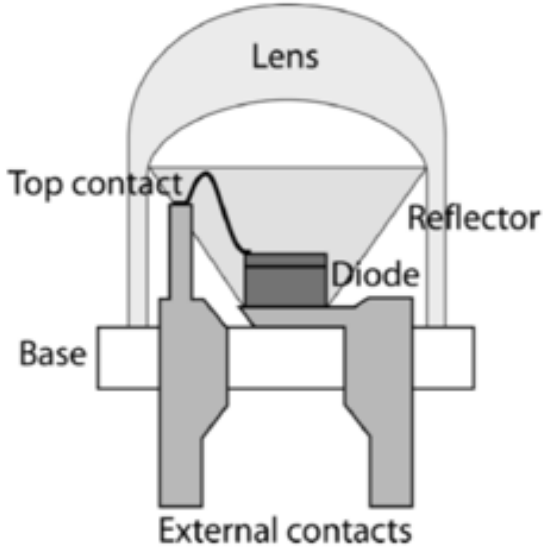

(Rockett)

Measured Gain Spectra in III-V Quantum Wells

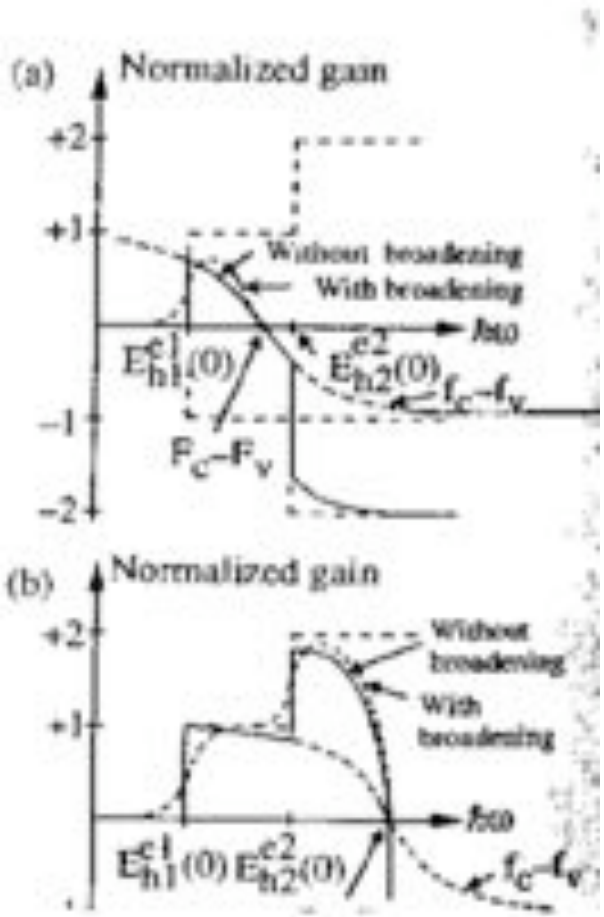

Gain spectrum in QWs follows the equilibrium JDOS modulated by the Fermi Dirac functions in accordance with the Bernard-Duraffourg condition.

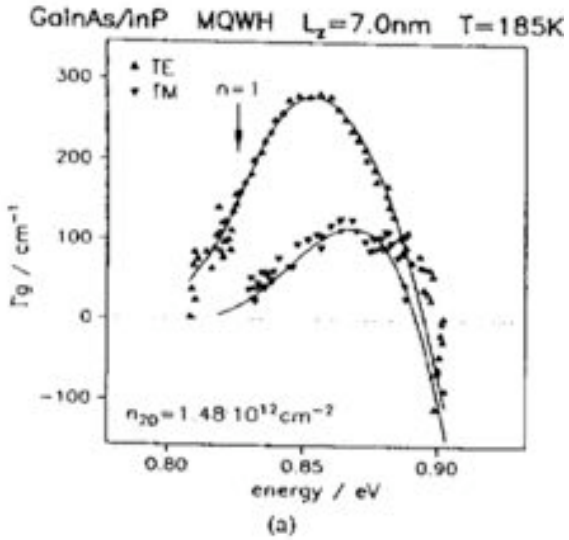

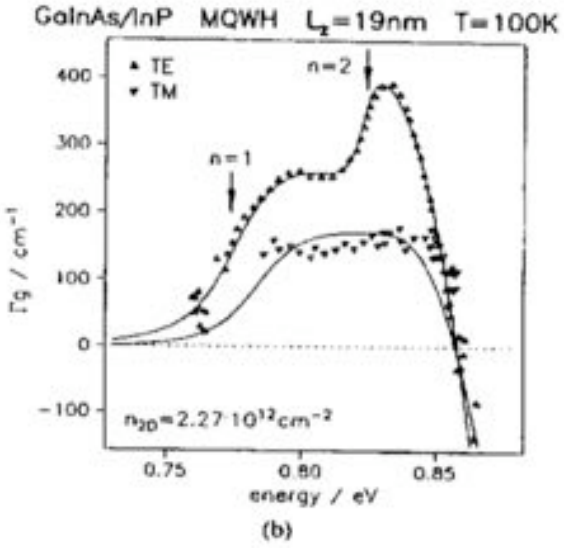

Compound Semiconductor Heterojunction Devices

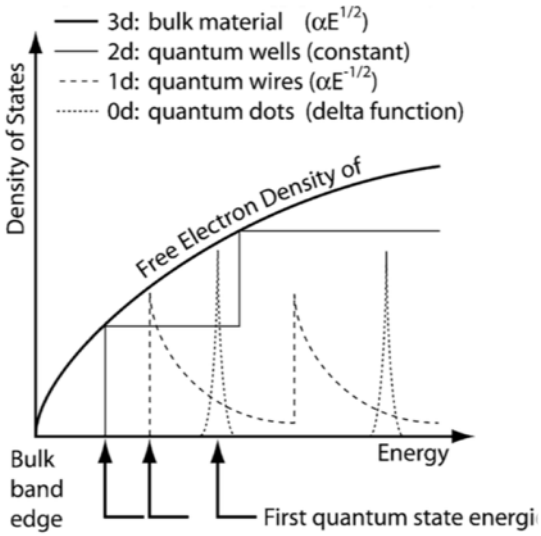

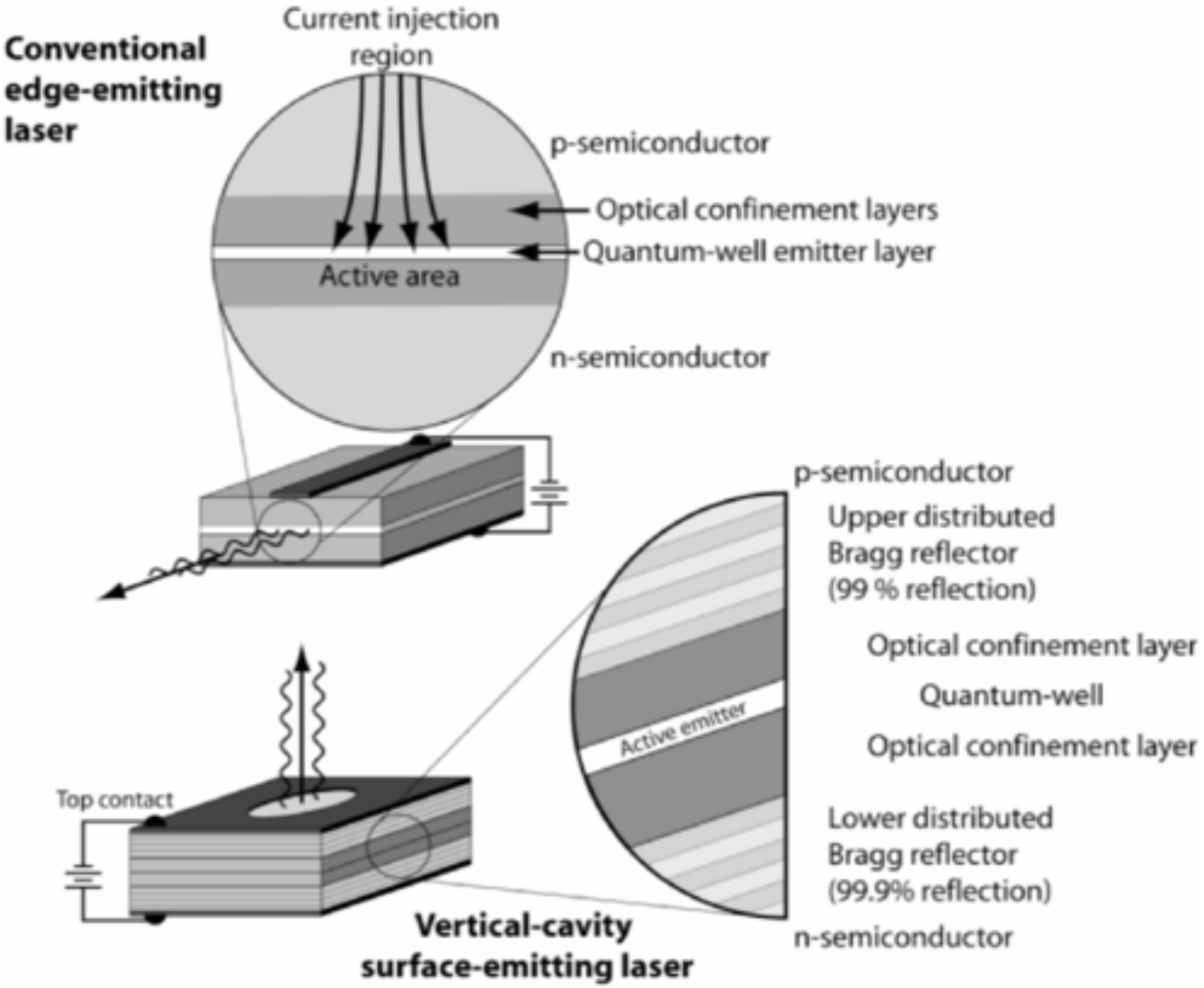

(Rockett)

Compound Semiconductor Heterojunction Devices

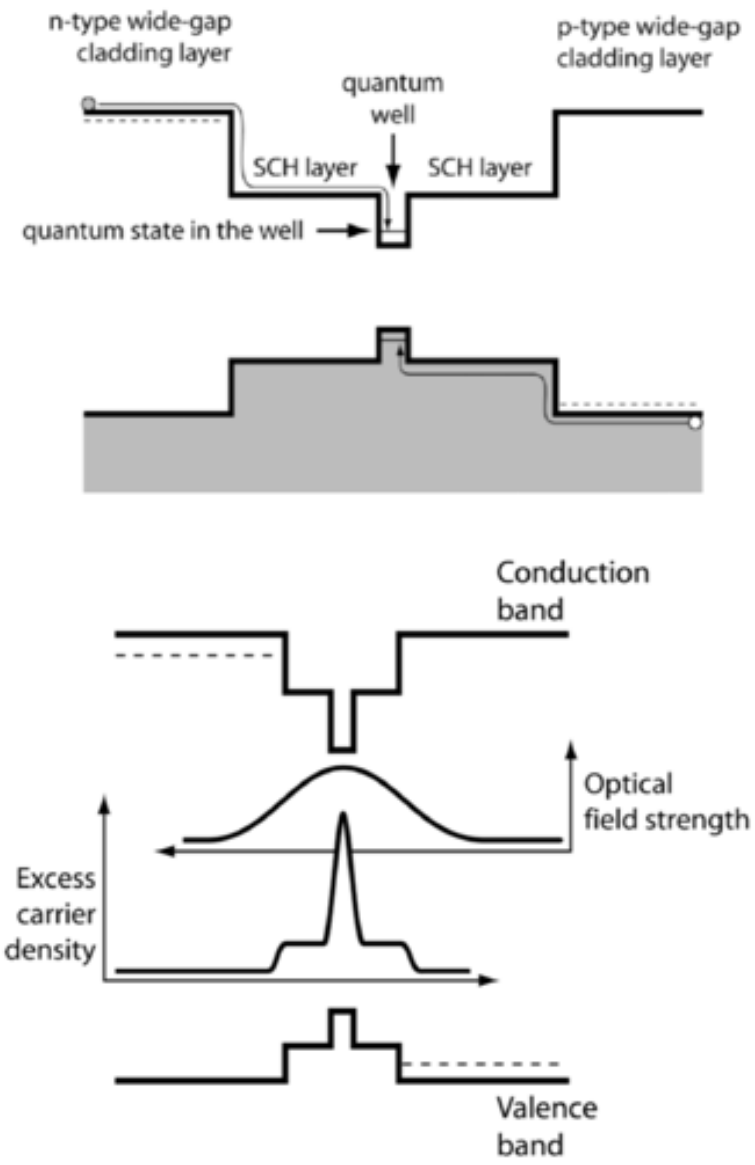

(Rockett)

Applications: The Double-Heterostructure Laser

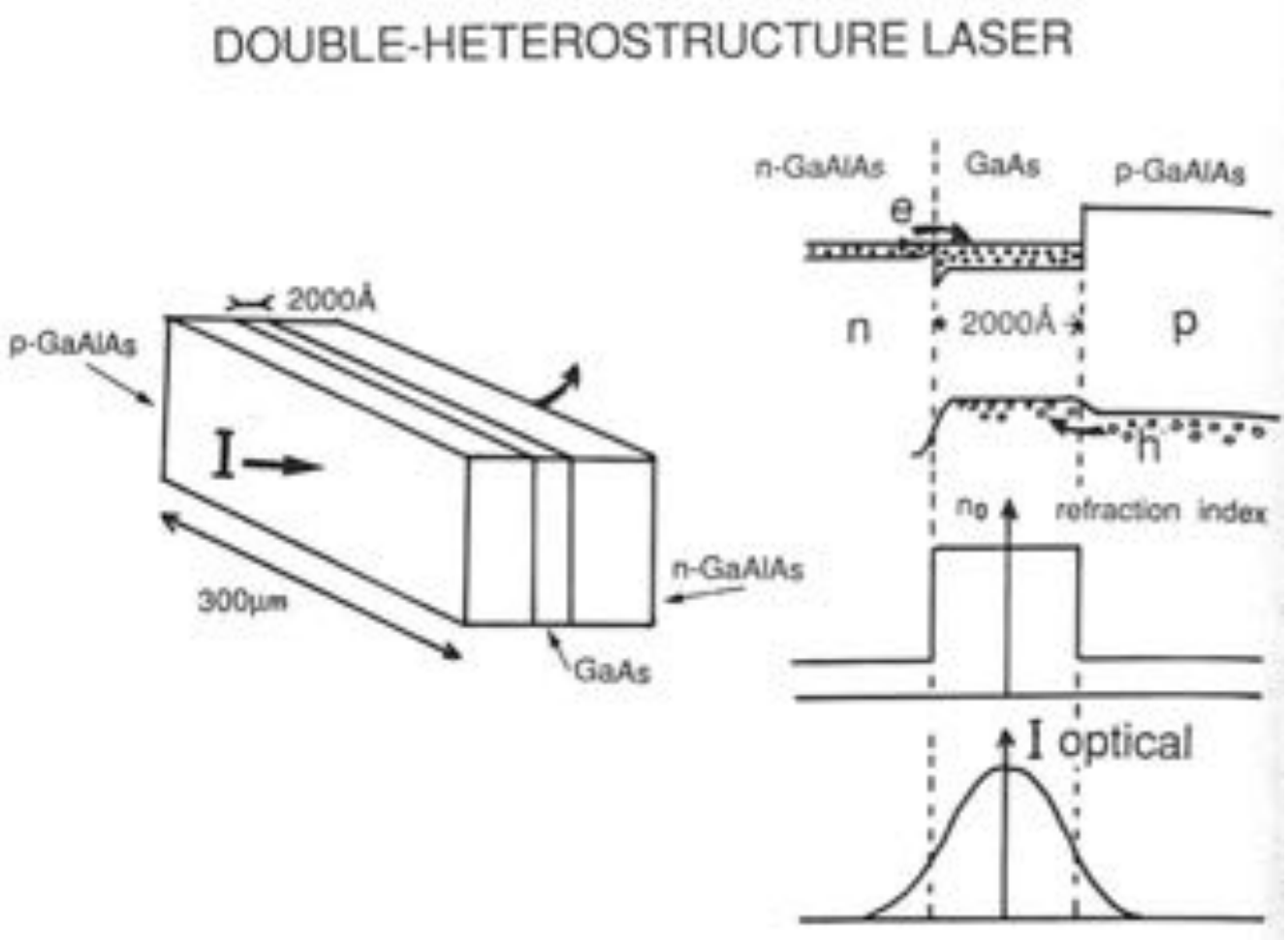

Compound Semiconductor Laser Designs

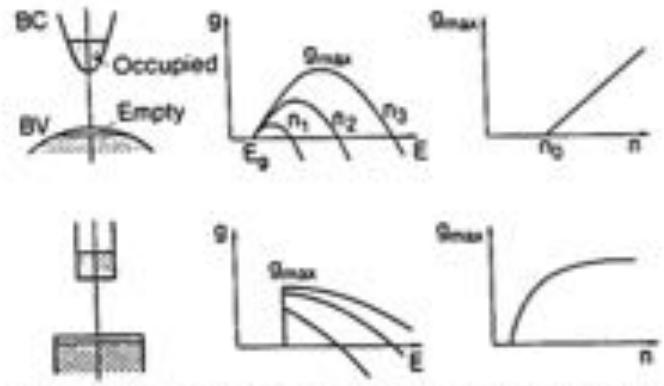

FIG. 91. Schematics of the gain formation in DH lasers (top) and QW lasers (bottom).

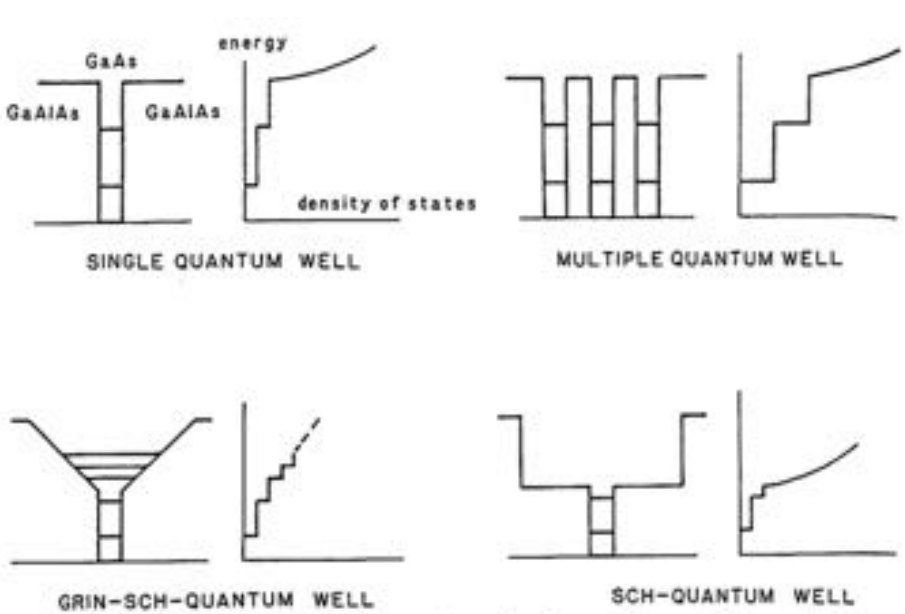

FIG. 93. The various QW structures used as active layers in lasers and the associated density of states.

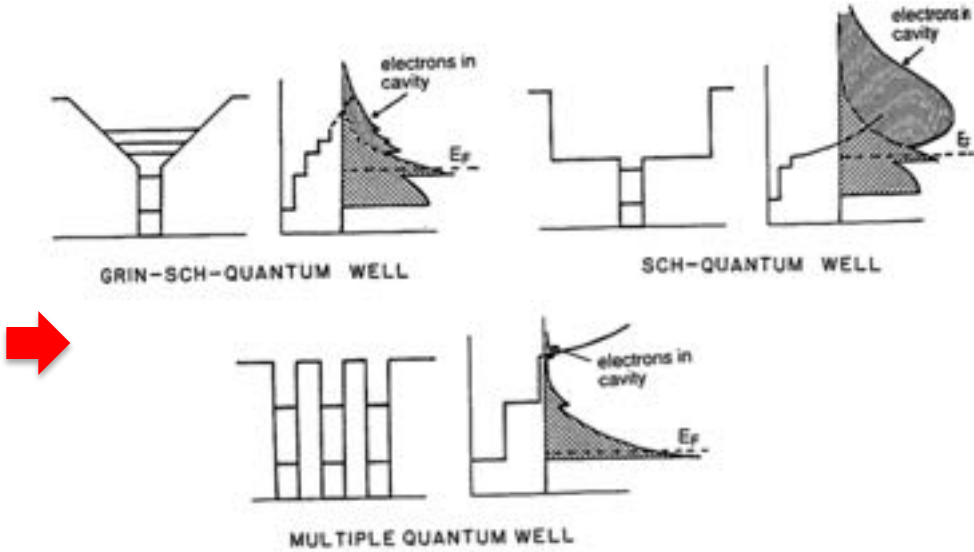

FIG. 96. Schematics of GRIN-SCH and SCH structures, and corresponding density-of-states and occupied states.

(Weisbuch/Vinter)

Compound Semiconductor Laser Designs

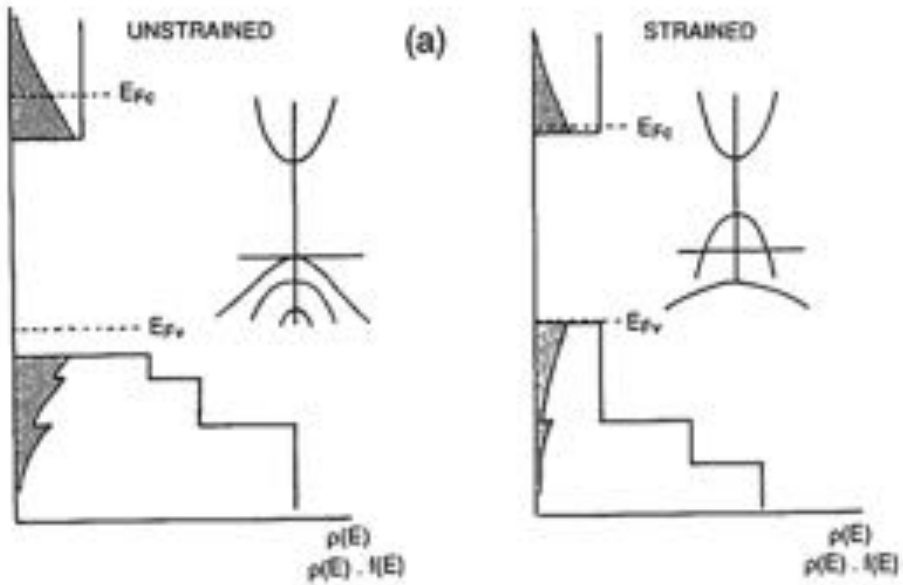

FIG. 100a. Schematics of band-filling for conduction and valence band states for equal numbers of injected electrons and holes in unstrained (left) and strained (right) QW active layers.

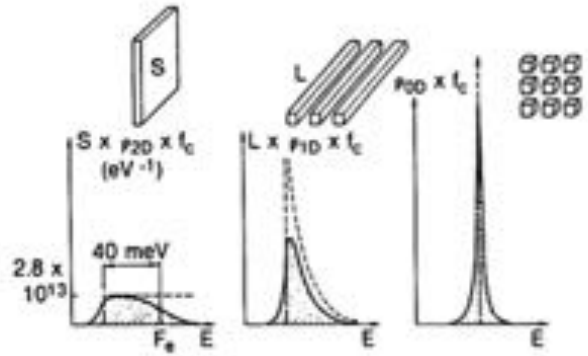

FIG. 113. Schematics of gain curves in 2D, 1D, and 0D structures. Similar numbers of electrons and holes are being injected above transparency, yielding equal integrated gain. (From Nagle and Weisbuch.[465])

When $L \gg a_B$, (but still well-separated, confined energy levels), a "giant" oscillator strength situation develops, which yields a transition matrix element[575-7]

$$f \approx f_{at} \cdot (V_{box}/V_{exc}) \qquad (112)$$

where V_{box} and V_{exc} are the QB and exciton volume, respectively. The enhancement of the oscillator strength originates in the coherent excitation of the QB volume (somewhat analogous to the intersubband giant dipole matrix element of Eq. (54e)), which yields an increased dipole moment.

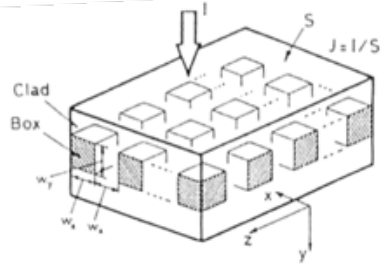

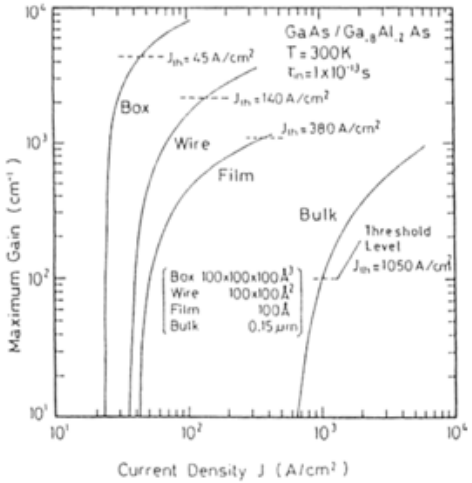

FIG. 114. Schematics of quantum box structure and gain curves 3D, 2D, 1D, 0D lasers, with optimized optical confinement in each case. (Adapted from M. Asada, Y. Miyamoto, and Y. Suematsu, IEEE *J. Quantum Electron.* **QE-22**, 1915, © 1986 IEEE.)

(Weisbuch/Vinter)

Reduction of lasing threshold current density

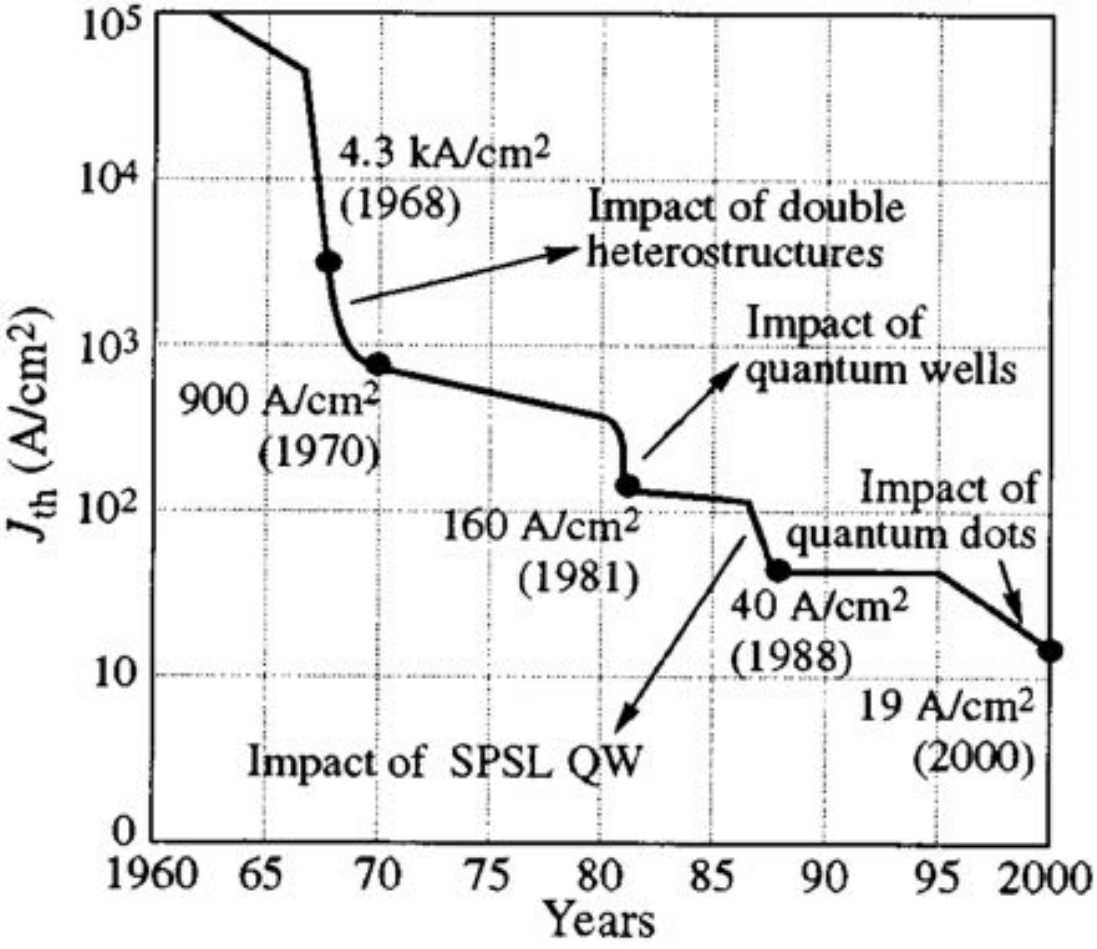

Alferov Nobel Lecture 2000

Intersubband Optical Transitions

Optical transitions for intersubband processes

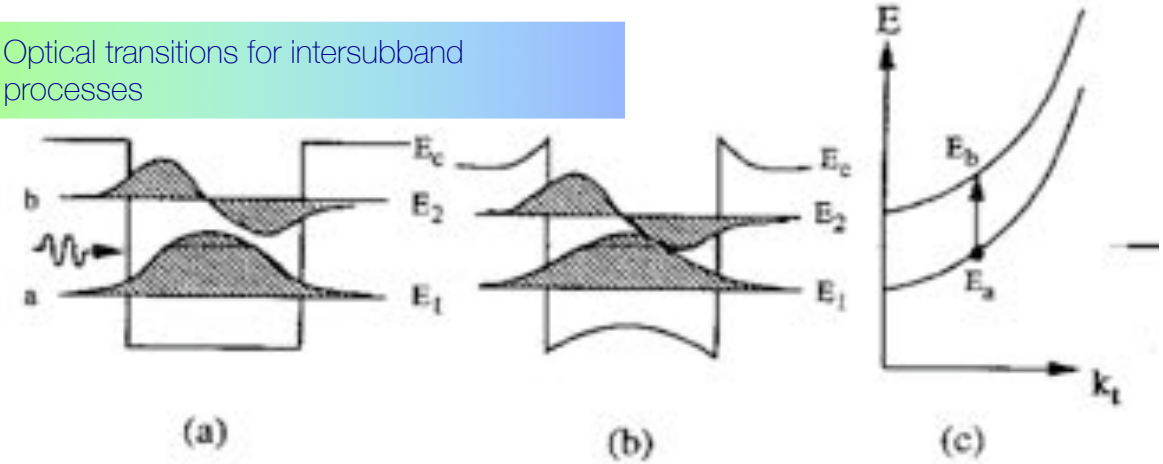

Figure 9.11. (a) A simple quantum well with a small doping concentration. (b) A modulation-doped quantum well with a significant amount of screening due to a large doping concentration. (c) The subband energy diagram in the k_t space. A direct vertical transition occurs because of the k-selection rule in the plane of quantum wells.

$$\psi_a(r) = u_c(\mathbf{r}) \times [\frac{1}{\sqrt{A}} e^{i\mathbf{k_t}\cdot\rho}] \times \phi_1(z)$$

$$\psi_b(r) = u_c(\mathbf{r}) \times [\frac{1}{\sqrt{A}} e^{i\mathbf{k_t'}\cdot\rho}] \times \phi_2(z)$$

$$\mu_{\mathbf{ba}} = \langle\psi_b|e\mathbf{e}|\psi_a\rangle \approx \langle\ u_c|u_c\rangle \times \langle \frac{1}{\sqrt{A}} e^{i\mathbf{k_t}\cdot\rho}|e\mathbf{r}|\frac{1}{\sqrt{A}} e^{i\mathbf{k_t'}\cdot\rho}\rangle$$

$$\approx \delta_{\mathbf{k_t},\mathbf{k_t'}} \langle\phi_2|ez|\phi_1\rangle\hat{z} \approx \delta_{\mathbf{k_t},\mathbf{k_t'}} \times e\mathbf{z_{12}}$$

For INTERSUBBBAND (intra-band) transitions:

$$M \sim \int_{\text{crystal}} \chi_e(z)\boldsymbol{\eta}\cdot\mathbf{r}\chi_e'(z)\,dr \int_{\text{cell}} u_{cke}(\mathbf{r})u_{cke}^*(\mathbf{r})\,d^3r$$

$M_{intersubband} \sim L_{well}$, dipole length $\sim$ Quantum Well Width (giant dipole effect!!)

Intersubband Optical Transitions

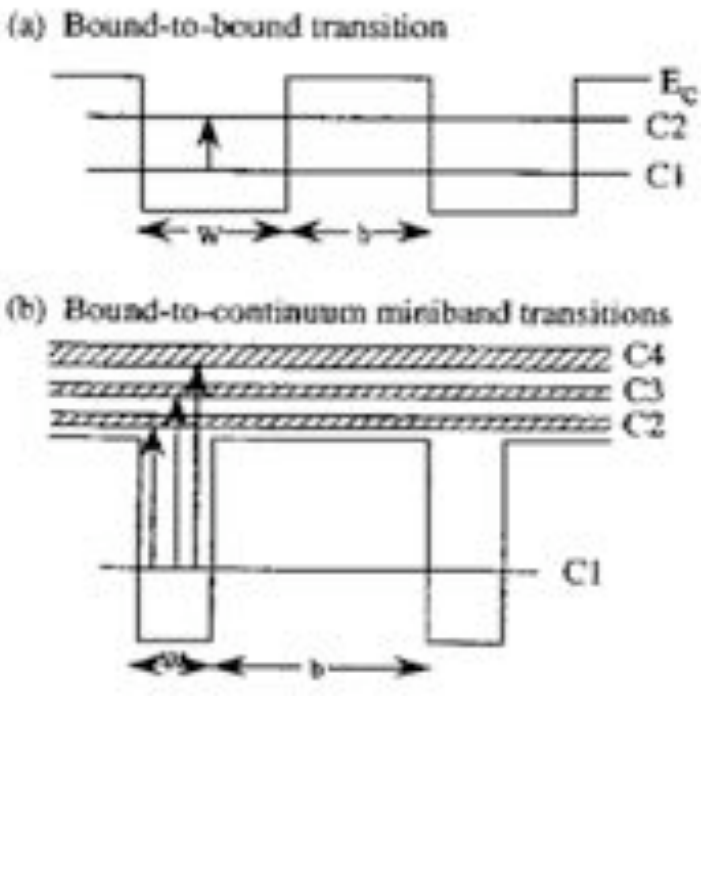

$$\alpha(\hbar\omega) = \left(\frac{\omega}{n_r c \varepsilon_0}\right) \frac{|\mu_{21}|^2 (\Gamma/2)}{(E_2 - E_1 - \hbar\omega)^2 + (\Gamma/2)^2} \left(\frac{m_c^* k_B T}{\pi \hbar^2 L}\right) \ln\left(\frac{1 + e^{(E_F - E_1)/k_B T}}{1 + e^{(E_F - E_2)/k_B T}}\right)$$

Figure 9.15. A period of a quantum cascade laser [27] using intersubband transition between E_2 and E_1. The barriers are $Al_{0.48}In_{0.52}As$ and the wells are $In_{0.7}Ga_{0.3}As$ materials. The calculated values are $E_3 - E_2 = 295$ meV and $E_2 - E_1 = 30$ meV.

Applications of ISB transitions: In Quantum Cascade Lasers

Electron-Photon Interactions

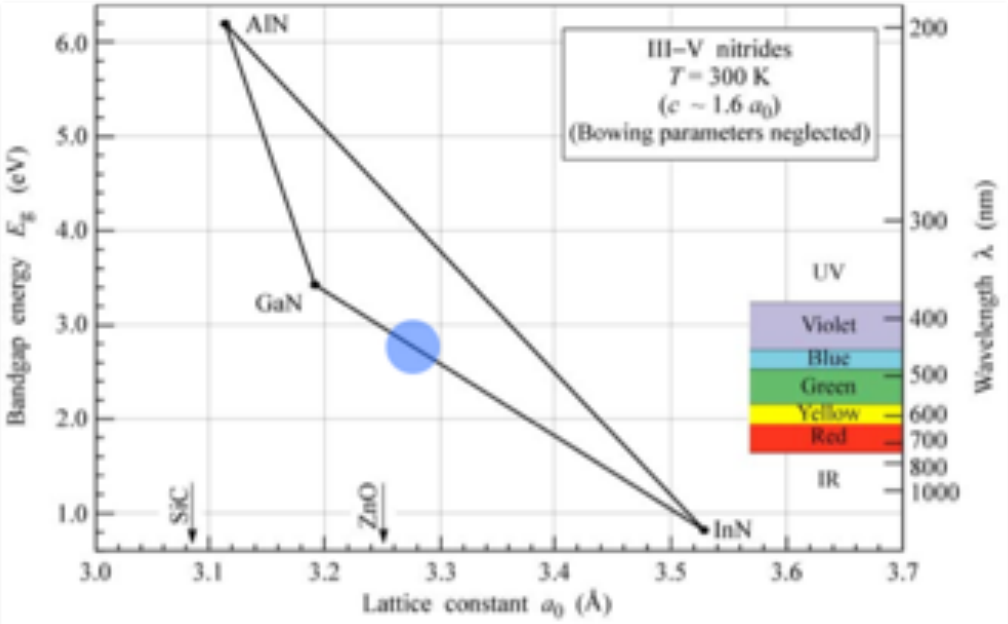

Fig. 12.12. Bandgap energy versus lattice constant of III–V nitride semiconductors at room temperature.

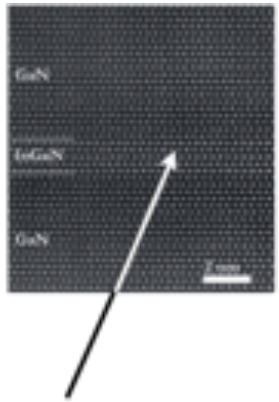

Semiconductor "Nanostructures": A Quantum Well

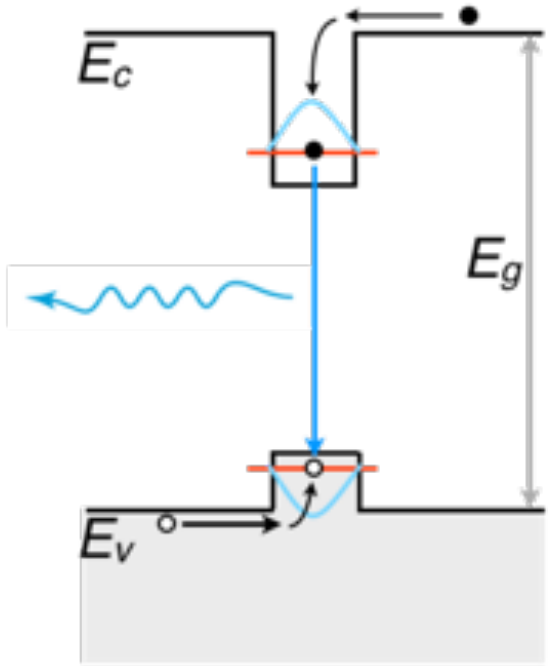

ECE 4070 / MSE 6050

- Design of a quantum well blue laser diode

Electron-Photon Interactions

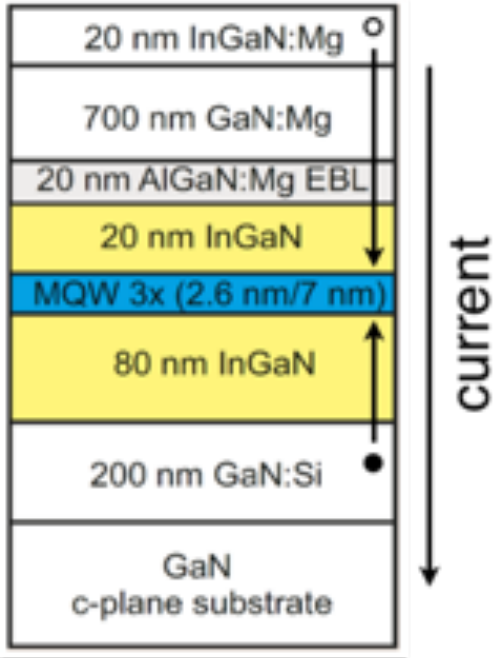

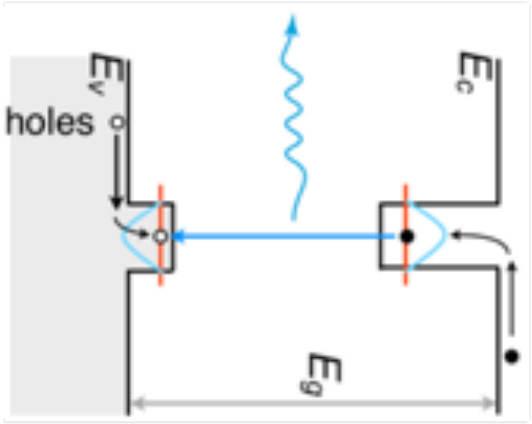

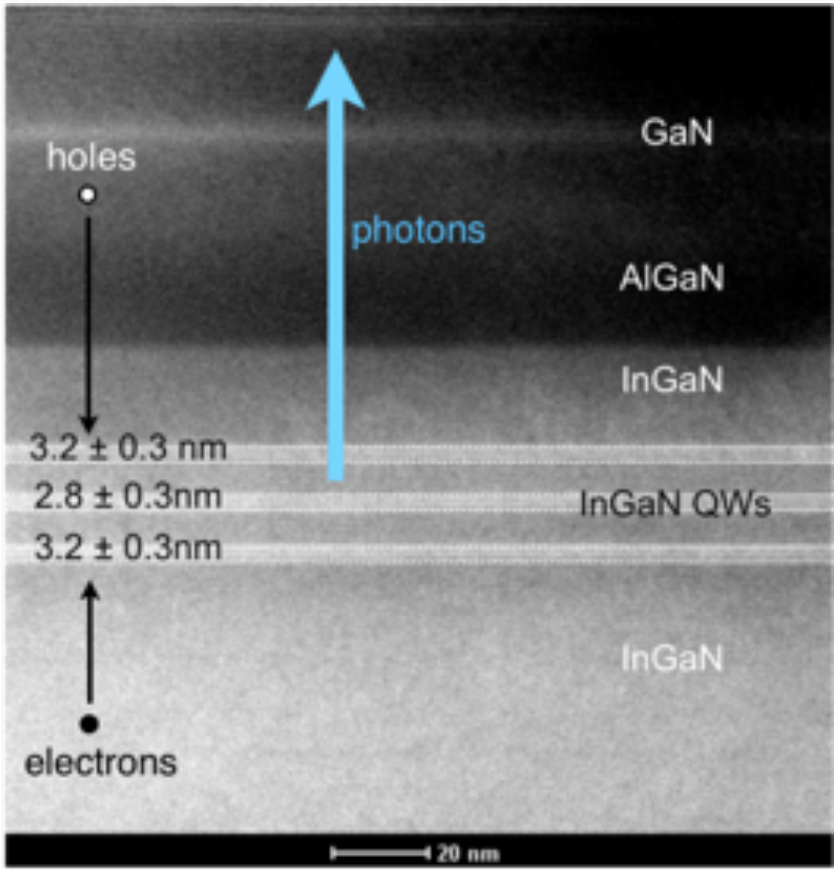

Quantum well Heterostructures grown by MBE
(Henryk Turski)

ECE 4070 / MSE 6050

- Demonstration of a GaN/InGaN/GaN Quantum Well Laser Diode

Electron-Photon Interactions

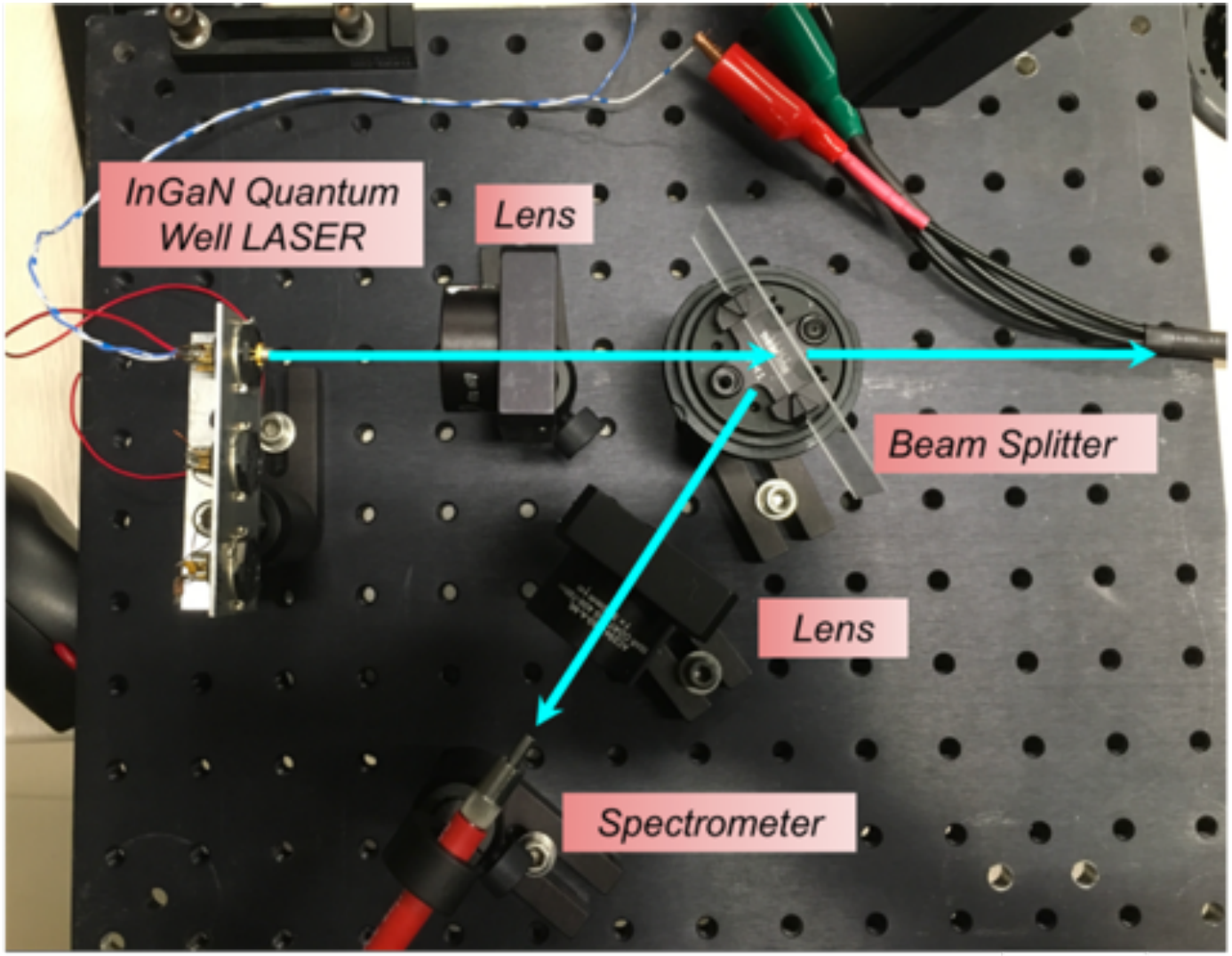

ECE 4070 / MSE 6050

- Demonstration of a GaN/InGaN/GaN Quantum Well Laser Diode

Electron-Photon Interactions

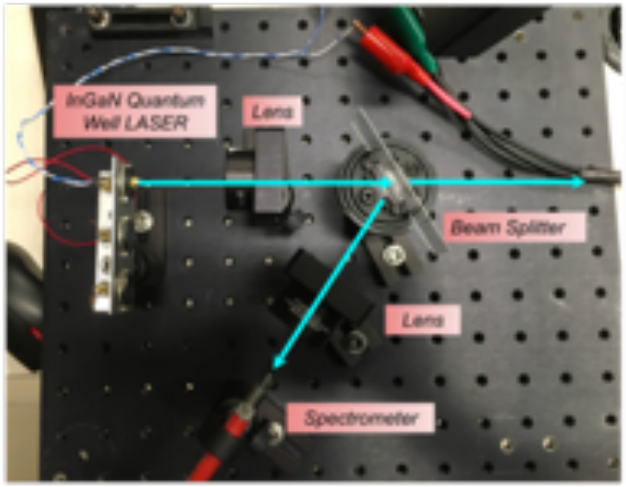

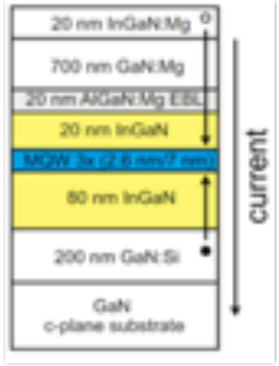

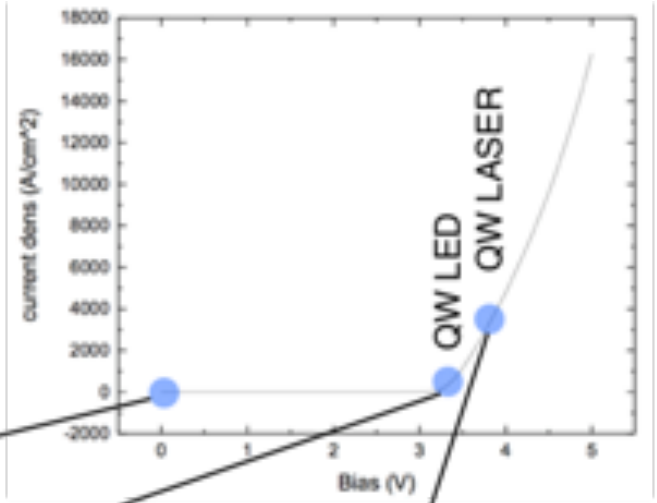

@0 V

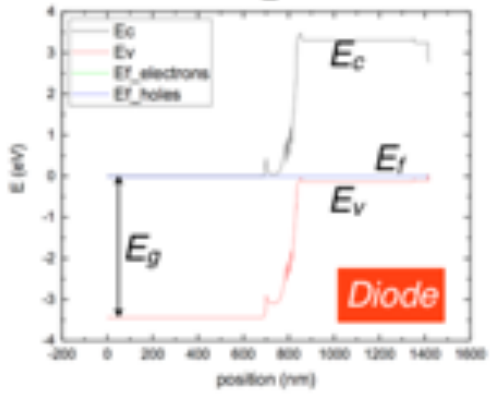

$E_{fn} < E_c$

$E_{fp} > E_v$

@3 V

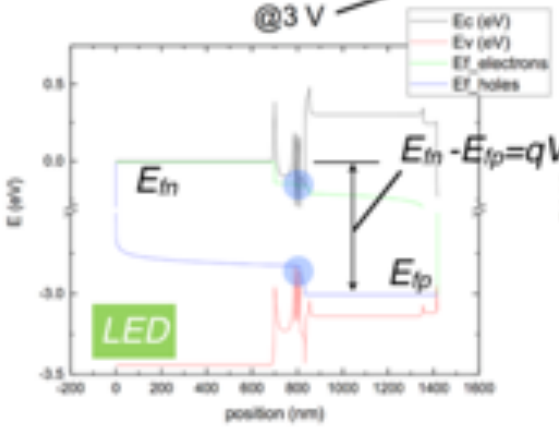

$E_{fn} > E_c$

$E_{fp} > E_v$

@3.5 V

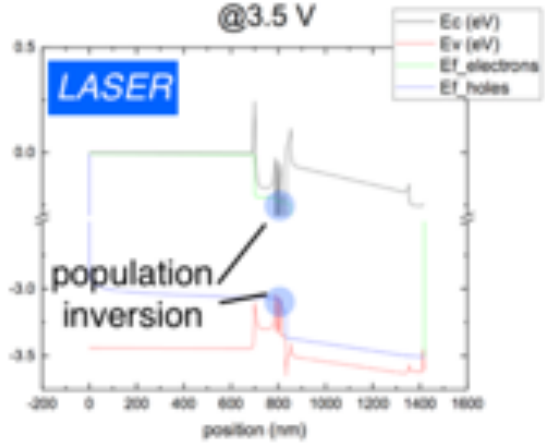

$E_{fn} > E_c$

$E_{fp} < E_v$

ECE 4070 / MSE 6050

- Demonstration of a GaN/InGaN/GaN Quantum Well Laser Diode

End